Table of Contents

2.0 PRINCIPAL DESIGN CRITERIA 2-1

2.1 Spent Fuel To Be Stored 2.1-1
- 2.1.1 PWR Fuel Evaluation 2.1.1-1
- 2.1.2 BWR Fuel Evaluation 2.1.2-1
- 2.1.3 Site Specific Spent Fuel 2.1.3-1
  - 2.1.3.1 Maine Yankee Site Specific Spent Fuel 2.1.3-1

2.2 Design Criteria for Environmental Conditions and Natural Phenomena 2.2-1
- 2.2.1 Tornado and Wind Loadings 2.2-1
  - 2.2.1.1 Applicable Design Parameters 2.2-1
  - 2.2.1.2 Determination of Forces on Structures 2.2-2
  - 2.2.1.3 Tornado Missiles 2.2-2
- 2.2.2 Water Level (Flood) Design 2.2-3
  - 2.2.2.1 Flood Elevations 2.2-3
  - 2.2.2.2 Phenomena Considered in Design Load Calculations 2.2-3
  - 2.2.2.3 Flood Force Application 2.2-3
  - 2.2.2.4 Flood Protection 2.2-4
- 2.2.3 Seismic Design 2.2-4
  - 2.2.3.1 Input Criteria 2.2-4
  - 2.2.3.2 Seismic - System Analyses 2.2-4
- 2.2.4 Snow and Ice Loadings 2.2-5
- 2.2.5 Combined Load Criteria 2.2-6
  - 2.2.5.1 Load Combinations and Design Strength -Vertical Concrete Cask 2.2-6
  - 2.2.5.2 Load Combinations and Design Strength - Canister and Basket 2.2-6
  - 2.2.5.3 Design Strength - Transfer Cask 2.2-7
- 2.2.6 Environmental Temperatures 2.2-7

Table of Contents (Continued)

2.3 Safety Protection Systems 2.3-1
2.3.1 General 2.3-1
2.3.2 Protection by Multiple Confinement Barriers and Systems 2.3-2
2.3.2.1 Confinement Barriers and Systems 2.3-2
2.3.2.2 Cask Cooling 2.3-3
2.3.3 Protection by Equipment and Instrumentation Selection 2.3-3
2.3.3.1 Equipment 2.3-4
2.3.3.2 Instrumentation 2.3-5
2.3.4 Nuclear Criticality Safety 2.3-5
2.3.4.1 Control Methods for Prevention of Criticality 2.3-5
2.3.4.2 Error Contingency Criteria 2.3-7
2.3.4.3 Verification Analyses 2.3-7
2.3.5 Radiological Protection 2.3-7
2.3.5.1 Access Control 2.3-7
2.3.5.2 Shielding 2.3-8
2.3.5.3 Ventilation Off-Gas 2.3-8
2.3.5.4 Radiological Alarm Systems 2.3-9
2.3.6 Fire and Explosion Protection 2.3-10
2.3.6.1 Fire Protection 2.3-10
2.3.6.2 Explosion Protection 2.3-10
2.3.7 Ancillary Structures 2.3-10

2.4 Decommissioning Considerations 2.4-1

2.5 References 2.5-1

List of Figures

Figure 2.1.3.1-1 Preferential Loading Diagram for Maine Yankee Site Specific Spent Fuel 2.1.3-8

List of Tables

Table 2-1 Summary of Universal Storage System Design Criteria 2-2
Table 2.1.1-1 PWR Fuel Assembly Characteristics 2.1.1-2
Table 2.1.1-2 Loading Table for PWR Fuel 2.1.1-3
Table 2.1.2-1 BWR Fuel Assembly Characteristics 2.1.2-2
Table 2.1.2-2 Loading Table for BWR Fuel 2.1.2-3
Table 2.1.3.1-1 Maine Yankee Site Specific Fuel Population 2.1.3-9
Table 2.1.3.1-2 Maine Yankee Fuel Can Design and Fabrication Specification Summary 2.1.3-10
Table 2.1.3.1-3 Major Physical Design Parameters of the Maine Yankee Fuel Can 2.1.3-11
Table 2.1.3.1-4 Loading Table for Maine Yankee Fuel without Nonfuel Material 2.1.3-12
Table 2.1.3.1-5 Loading Table for Maine Yankee Fuel Containing a CEA 2.1.3-14
Table 2.2-1 Load Combinations for the Vertical Concrete Cask 2.2-9
Table 2.2-2 Load Combinations for the Transportable Storage Canister 2.2-10
Table 2.2-3 Structural Design Criteria for Components Used in the Transportable Storage Canister 2.2-11
Table 2.3-1 Safety Classification of Universal Storage System Components 2.3-12
Table 2.4-1 Activity Concentration Summary for the Concrete Cask - PWR Design Basis Fuel (Ci/m^3) 2.4-3
Table 2.4-2 Activity Concentration Summary for the Canister - PWR Design Basis Fuel (Ci/m^3) 2.4-3
Table 2.4-3 Activity Concentration Summary for the Concrete Cask - BWR Design Basis Fuel (Ci/m^3) 2.4-4
Table 2.4-4 Activity Concentration Summary for the Canister - BWR Design Basis Fuel (Ci/m^3) 2.4-4

2.0 PRINCIPAL DESIGN CRITERIA

The Universal Storage System is a canister-based spent fuel dry storage cask system that is designed to be compatible with the Universal Transportation System. It is designed to store a variety of intact PWR and BWR fuel assemblies. This chapter presents the design bases, including the principal design criteria, limiting load conditions, and operational parameters of the Universal Storage System. The principal design criteria are summarized in Table 2-1.

Table 2-1 Summary of Universal Storage System Design Criteria

Parameter	Criteria
Design Life	50 years
Design Code - Confinement	ASME Code, Section III, Subsection NB [1] for confinement boundary
Design Code - Nonconfinement	
Basket	ASME Code, Section III, Subsection NG [2] and NUREG/CR-6322 [3]
Vertical Concrete Cask	ACI-349 [4], ACI-318 [5]
Transfer Cask	ANSI N14.6 [6] and NUREG-0612 [7]
Maximum Weight:	
Canister with Design Basis PWR Fuel Assembly (dry, including inserts) (Class 2)	72,900 lbs.
Canister with Design Basis BWR Fuel (dry) (Class 5)	75,600 lbs.
Vertical Concrete Cask (loaded) (Class 5)	323,900 lbs.
Transfer Cask (Class 3)	121,500 lbs.
Thermal:	
Maximum Fuel Cladding Temperature:	
PWR Fuel	752°F (400°C) for Normal and Transfer [25] 1058°F (570°C) Off-Normal and Accident [21]
BWR Fuel	752°F (400°C) for Normal and Transfer [25] 1058°F (570°C) Off-Normal and Accident [21]
Ambient Temperature:	
Normal (average annual ambient)	76°F
Off-Normal (extreme cold; extreme hot)	-40°F; 106°F
Accident	133°F
Concrete Temperature:	
Normal Conditions	≤ 150°F (bulk); ≤ 300°F (local) [24]
Off-Normal/Accident Conditions	≤ 350°F local/ surface [4]
Cavity Atmosphere	Helium

Table 2-1 Summary of Universal Storage System Design Criteria (Continued)

Radiation Protection/Shielding	Criteria
Concrete Cask Side Wall Contact Dose Rate	< 50 mrem/hr. (avg)
Concrete Cask Top Lid Contact Dose Rate	< 50 mrem/hr. (avg)
Concrete Cask Air Inlet/Outlet Dose Rate	< 100 mrem/hr. (avg)
Owner Controlled Area Boundary Dose [11]	
Normal/Off-Normal Conditions	25 mrem (Annual Whole Body)
Accident Whole Body Dose	5 rem (Whole Body)

THIS PAGE INTENTIONALLY LEFT BLANK

2.1 Spent Fuel To Be Stored

The Universal Storage System is designed to safely store up to 24 PWR spent fuel assemblies, or up to 56 BWR spent fuel assemblies, contained within a Transportable Storage Canister. On the basis of fuel assembly length and cross-section, the fuel assemblies are grouped into three classes of PWR fuel assemblies and two classes of BWR fuel assemblies. The class of the fuel assemblies is shown in Tables 6.2-1 and 6.2-2 for PWR and BWR fuel, respectively, and is based primarily on overall length.

The PWR and BWR fuel having the parameters shown in Tables 2.1.1-1 and 2.1.2-1, respectively, may be stored in the Universal Storage System. As shown in Table 2.1.1-1, the evaluation of PWR fuel includes fuel having thimble plugs and burnable poison rods in guide tube positions. As shown in Table 2.1.2-1, the BWR fuel evaluation includes fuel with a Zircaloy channel. Any empty fuel rod position must be filled with a solid filler rod fabricated from either Zircaloy or Type 304 stainless steel, or may be solid neutron absorber rods inserted for in-core reactivity control prior to reactor operation.

In addition to the design basis fuel, fuel that is unique to a reactor site, referred to as site specific fuel, is also evaluated. Site specific fuel consists of fuel assemblies that are configured differently, or have different parameters (such as enrichment or burnup), than the design basis fuel assemblies.

Site specific fuel is described in Section 2.1.3.

Site specific fuel is shown to be bounded by the fuel parameters shown in Tables 2.1.1-1 or 2.1.2-1, or it is separately evaluated.

The minimum initial enrichment limits are shown in Tables 2.1.1-2 and 2.1.2-2 for PWR and BWR fuel, respectively. The minimum enrichment limits exclude the loading of fuel assemblies enriched to less than 1.9 wt.% ^{235}U, including unenriched fuel assemblies, into the Transportable Storage Canister. However, fuel assemblies with unenriched axial end-blankets may be loaded into the canister.

THIS PAGE INTENTIONALLY LEFT BLANK

2.1.1 PWR Fuel Evaluation

The parameters of the PWR fuel assemblies that may be loaded in the transportable storage canister (canister) are shown in Table 2.1.1-1. The maximum initial enrichment limit represents the maximum fuel rod enrichment limit for variably enriched PWR assemblies. Each canister may contain up to 24 intact PWR fuel assemblies.

The design of the Universal Storage System is based on certain reference fuel assemblies that maximize the source terms used for the shielding and criticality evaluation, and that maximize the weight used in the structural evaluation. These reference fuel assemblies are described in the chapters appropriate to the condition being evaluated. The principal characteristics and parameters of a reference fuel, such as fuel volume, initial enrichment, cool time and burnup, do not represent limiting or bounding values. Bounding values for a fuel class are established based primarily on how principal parameters are combined and on the loading conditions or restrictions established for a class of fuel based on its parameters.

The maximum decay heat load for the storage of all types of PWR fuel assemblies is 23.0 kW (0.958 kW/assembly), except in cases where preferential loading is employed.

The minimum cool time is based on the maximum decay heat load (23.0 kW) and the dose rate limits for the concrete and transfer casks and is presented in Section 5.5. PWR fuel must be loaded in accordance with Table 2.1.1-2.

Site specific fuel that does not meet the enrichment and burnup limits of this section and Table 2.1.1-1 is separately evaluated in Section 2.1.3 to establish loading limits.

Table 2.1.1-1 PWR Fuel Assembly Characteristics

Fuel Class[1, 2]	14 × 14	14 × 14	15 × 15	15 × 15	15 × 15	16 × 16	17 × 17
Fissile Isotopes	UO_2	UO_2	UO_2	UO_2	UO_2	UO_2	UO_2
Max Initial Enrichment (wt % ^{235}U)[3]	5.0	5.0	4.6	4.4	4.2	4.8	4.3
Max Initial Enrichment (wt % ^{235}U)[4]	5.0	5.0	5.0	5.0	5.0	5.0	5.0
Number of Fuel Rods	176	179	204	208	216	236	264
Number of Water Holes	5	17	21	17	9	5	25
Max Assembly Average Burnup (MWD/MTU)	45,000	45,000	45,000	45,000	45,000	45,000	45,000
Min Cool Time (years)	5	5	5	5	5	5	5
Min Average Enrichment (wt % ^{235}U)	1.9	1.9	1.9	1.9	1.9	1.9	1.9
Cladding Material	Zircaloy	Zircaloy	Zircaloy	Zircaloy	Zircaloy	Zircaloy	Zircaloy
Non-Fuel Hardware[5]	FM, T, BPR	FM, T, BPR	FM, T, BPR	FM, T, BPR	FM, T, BPR	FM, T, BPR	FM, T, BPR
Max Weight (lb) per Storage Location[6]	1,602	1,602	1,602	1,602	1,602	1,602	1,602
Max Decay Heat (Watts) per Storage Location[7]	958.3	958.3	958.3	958.3	958.3	958.3	958.3
Fuel Condition	Intact	Intact	Intact	Intact	Intact	Intact	Intact

General Notes:

1. Fuel, except Maine Yankee fuel, must be loaded in accordance with Table 2.1.1-2.
2. Maine Yankee fuel must be loaded in accordance with Tables 2.1.3.1-4 and 2.1.3.1-5, as appropriate.
3. Maximum initial enrichment without boron credit. Represents the maximum fuel rod enrichment for variably enriched assemblies. Assemblies meeting this limit may contain a flow mixer (FM), an ICI thimble (T), or a burnable poison rod insert (BPR).
4. Maximum initial enrichment with taking credit for a minimum soluble boron concentration of 1000 ppm in the spent fuel pool water. Represents the maximum fuel rod enrichment for variably enriched assemblies. Assemblies meeting this limit may contain a flow mixer.
5. Assemblies may not contain control element assemblies, except as permitted for site specific fuel.
6. Weight includes the weight of non-fuel bearing components.
7. Maximum decay heat may be higher for site specific fuel configurations, which control fuel loading position.

Table 2.1.1-2 Loading Table for PWR Fuel

Minimum Initial Enrichment	Burnup ≤30 GWD/MTU Minimum Cooling Time [years]				30< Burnup ≤35 GWD/MTU Minimum Cooling Time [years]			
wt % ^{235}U (E)	14×14	15×15	16×16	17×17	14×14	15×15	16×16	17×17
1.9 ≤ E < 2.1	5	5	5	5	7	7	5	7
2.1 ≤ E < 2.3	5	5	5	5	7	6	5	6
2.3 ≤ E < 2.5	5	5	5	5	6	6	5	6
2.5 ≤ E < 2.7	5	5	5	5	6	6	5	6
2.7 ≤ E < 2.9	5	5	5	5	6	5	5	5
2.9 ≤ E < 3.1	5	5	5	5	5	5	5	5
3.1 ≤ E < 3.3	5	5	5	5	5	5	5	5
3.3 ≤ E < 3.5	5	5	5	5	5	5	5	5
3.5 ≤ E < 3.7	5	5	5	5	5	5	5	5
3.7 ≤ E < 3.9	5	5	5	5	5	5	5	5
3.9 ≤ E < 4.1	5	5	5	5	5	5	5	5
4.1 ≤ E < 4.3	5	5	5	5	5	5	5	5
4.3 ≤ E < 4.5	5	5	5	5	5	5	5	5
4.5 ≤ E < 4.7	5	5	5	5	5	5	5	5
4.7 ≤ E < 4.9	5	5	5	5	5	5	5	5
E ≥ 4.9	5	5	5	5	5	5	5	5

Minimum Initial Enrichment	35< Burnup ≤40 GWD/MTU Minimum Cooling Time [years]				40< Burnup ≤45 GWD/MTU Minimum Cooling Time [years]			
wt % ^{235}U (E)	14×14	15×15	16×16	17×17	14×14	15×15	16×16	17×17
1.9 ≤ E < 2.1	10	10	7	10	15	15	11	15
2.1 ≤ E < 2.3	9	9	6	9	14	13	9	13
2.3 ≤ E < 2.5	8	8	6	8	12	12	8	12
2.5 ≤ E < 2.7	8	7	6	7	11	11	7	11
2.7 ≤ E < 2.9	7	7	6	7	10	10	7	10
2.9 ≤ E < 3.1	7	6	6	7	9	9	7	9
3.1 ≤ E < 3.3	6	6	6	6	9	8	7	8
3.3 ≤ E < 3.5	6	6	6	6	8	8	7	8
3.5 ≤ E < 3.7	6	6	6	6	7	8	7	7
3.7 ≤ E < 3.9	6	6	6	6	7	8	7	7
3.9 ≤ E < 4.1	6	6	6	6	7	7	7	7
4.1 ≤ E < 4.3	5	6	6	6	6	7	7	7
4.3 ≤ E < 4.5	5	6	6	6	6	7	7	7
4.5 ≤ E < 4.7	5	6	5	6	6	7	6	7
4.7 ≤ E < 4.9	5	6	5	6	6	7	6	7
E ≥ 4.9	5	6	5	6	6	7	6	7

THIS PAGE INTENTIONALLY LEFT BLANK

2.1.2 BWR Fuel Evaluation

The parameters of the BWR fuel assemblies that may be loaded in the transportable storage canister (canister) are shown in Table 2.1.2-1. Each canister may contain up to 56 intact BWR fuel assemblies.

The design of the Universal Storage System is based on certain reference fuel assemblies that maximize the source terms used for the shielding and criticality evaluation, and that maximize the weight used in the structural evaluation. These reference fuel assemblies are described in the chapters appropriate to the condition being evaluated. The principal characteristics and parameters of a reference fuel, such as fuel volume, initial enrichment, cool time and burnup, do not represent limiting or bounding values. Bounding values for a fuel class are established based primarily on how principal parameters are combined and on the loading conditions or restrictions established for a class of fuel based on its parameters.

The maximum canister decay heat load for the storage of all types of BWR fuel assemblies is 23.0 kW (0.411 kW/assembly).

The minimum cooling time determination is based on the maximum decay heat load (23.0 kW) and the dose rate limits for the concrete and transfer casks and is presented in Section 5.5. BWR fuel must be loaded in accordance with Table 2.1.2-2.

Table 2.1.2-1 BWR Fuel Assembly Characteristics

Fuel Class[1]	**7 × 7**	**7 × 7**	**8 × 8**	**8 × 8**	**8 × 8**	**9 × 9**	**9 × 9**
Fissile Isotopes	UO_2	UO_2	UO_2	UO_2	UO_2	UO_2	UO_2
Max Initial Enrichment (wt % ^{235}U)[1]	4.5	4.7	4.5	4.7	4.8	4.5	4.6
Number of Fuel Rods	48	49	60	62	63	74	79
Number of Water Holes	1[4]	0	1/4[5]	2	4	2/7[5]	2
Max Assembly Average Burnup (MWD/MTU)	45,000	45,000	45,000	45,000	45,000	45,000	45,000
Min Cool Time (years)	5	5	5	5	5	5	5
Min Average Enrichment (wt % ^{235}U)	1.9	1.9	1.9	1.9	1.9	1.9	1.9
Cladding Material	Zircaloy	Zircaloy	Zircaloy	Zircaloy	Zircaloy	Zircaloy	Zircaloy
Nonfuel Hardware[2]	Channel	Channel	Channel	Channel	Channel	Channel	Channel
Max Channel Thickness (mil)	120	120	120	120	120	120	120
Max Weight (lb) per Storage Location[3]	702	702	702	702	702	702	702
Max Decay Heat (Watts) per Storage Location	410.7	410.7	410.7	410.7	410.7	410.7	410.7
Fuel Condition	Intact	Intact	Intact	Intact	Intact	Intact	Intact

General Notes:

1. Fuel must be loaded in accordance with Table 2.1.2-2.
2. Each BWR fuel assembly may have a Zircaloy channel or be unchanneled, but cannot have a stainless steel channel.
3. Weight includes the weight of the channel.
4. Solid fill or water rod.
5. Water rods may occupy more than one fuel lattice location.

Table 2.1.2-2 Loading Table for BWR Fuel

Minimum Initial Enrichment wt % ^{235}U (E)	Burnup ≤30 GWD/MTU Minimum Cooling Time [years]			30< Burnup ≤35 GWD/MTU Minimum Cooling Time [years]		
	7×7	8×8	9×9	7×7	8×8	9×9
1.9 ≤ E < 2.1	5	5	5	8	7	7
2.1 ≤ E < 2.3	5	5	5	6	6	6
2.3 ≤ E < 2.5	5	5	5	6	5	6
2.5 ≤ E < 2.7	5	5	5	5	5	5
2.7 ≤ E < 2.9	5	5	5	5	5	5
2.9 ≤ E < 3.1	5	5	5	5	5	5
3.1 ≤ E < 3.3	5	5	5	5	5	5
3.3 ≤ E < 3.5	5	5	5	5	5	5
3.5 ≤ E < 3.7	5	5	5	5	5	5
3.7 ≤ E < 3.9	5	5	5	5	5	5
3.9 ≤ E < 4.1	5	5	5	5	5	5
4.1 ≤ E < 4.3	5	5	5	5	5	5
4.3 ≤ E < 4.5	5	5	5	5	5	5
4.5 ≤ E < 4.7	5	5	5	5	5	5
4.7 ≤ E < 4.9	5	5	5	5	5	5
E ≥ 4.9	5	5	5	5	5	5

Minimum Initial Enrichment wt % ^{235}U (E)	35< Burnup ≤40 GWD/MTU Minimum Cooling Time [years]			40< Burnup ≤45 GWD/MTU Minimum Cooling Time [years]		
	7×7	8×8	9×9	7×7	8×8	9×9
1.9 ≤ E < 2.1	16	14	15	26	24	25
2.1 ≤ E < 2.3	13	12	12	23	21	22
2.3 ≤ E < 2.5	11	9	10	20	18	19
2.5 ≤ E < 2.7	9	8	8	18	16	17
2.7 ≤ E < 2.9	8	7	7	15	13	14
2.9 ≤ E < 3.1	7	6	6	13	11	12
3.1 ≤ E < 3.3	6	6	6	11	10	10
3.3 ≤ E < 3.5	6	5	6	9	8	9
3.5 ≤ E < 3.7	6	5	6	8	7	7
3.7 ≤ E < 3.9	6	5	5	7	6	7
3.9 ≤ E < 4.1	5	5	5	7	6	7
4.1 ≤ E < 4.3	5	5	5	7	6	6
4.3 ≤ E < 4.5	5	5	5	6	6	6
4.5 ≤ E < 4.7	5	5	5	6	6	6
4.7 ≤ E < 4.9	5	5	5	6	6	6
E ≥ 4.9	5	5	5	6	6	6

THIS PAGE INTENTIONALLY LEFT BLANK

2.1.3 Site Specific Spent Fuel

This section describes site specific spent fuel, i.e., fuel assemblies that are configured differently or that have different fuel parameters, such as enrichment or burnup, than the fuel assemblies considered in the design basis. The site specific fuel configurations result from conditions that occurred during reactor operations, participation in research and development programs, testing programs intended to improve reactor operations or from the insertion of control components or other items within the fuel assembly.

Site specific spent fuel configurations are either shown to be bounded by the design basis fuel analysis or are separately evaluated. Unless specifically excepted, site specific spent fuel must also meet the conditions specified for the fuel considered in the design basis that is described in Sections 2.1.1 and 2.1.2.

2.1.3.1 Maine Yankee Site Specific Spent Fuel

The standard Maine Yankee site specific fuel is a Combustion Engineering PWR 14×14 assembly that is included in those fuel assemblies considered in the design basis fuel parameters described in Table 2.1.1-1. Maine Yankee spent fuel assemblies are categorized as intact (undamaged) or damaged as defined in Table 1-1. All damaged fuel and certain undamaged fuel configurations are placed in a Maine Yankee fuel can for storage in the Transportable Storage Canister. Each canister may contain up to 24 Maine Yankee assemblies, including up to 4 Maine Yankee Fuel Cans.

The estimated Maine Yankee site specific spent fuel inventory is shown in Section B2.0 of Appendix B. As noted, certain fuel configurations are preferentially loaded to take advantage of the design features of the Transportable Storage Canister and basket to allow the loading of fuel that does not specifically conform to the design basis spent fuel. Loading positions are shown in Figure 2.1.3.1-1.

The evaluated fuel includes those standard fuel assemblies modified by the installation or removal of fuel or nonfuel-bearing components. The three principal types of modifications are:

- The removal of fuel rods without replacement.
- The replacement of removed fuel rods or burnable poison rods with rods of another material, such as stainless steel, or with fuel rods of a different enrichment.
- The insertion of control elements, nonfuel items including start-up sources, or instrument or plug segments, in guide tube positions.

Site specific spent fuel also includes fuel assemblies that are uniquely designed to support reactor physics. These fuel assemblies include those that are variably enriched or that are variably enriched with annular axial blankets. Generally, these fuel assemblies (described in Sections 6.6.1.2.2 and 6.6.1.2.3) are bounded by the evaluation of the design basis fuel.

As described in Section 2.1.3.1.6, certain of the site-specific spent fuel configurations, including damaged and consolidated fuel loaded in Maine Yankee fuel cans, must be preferentially loaded in corner positions of the fuel basket. A fuel assembly with a burnup between 45,000 and 50,000 MWD/MTU must be preferentially loaded in a peripheral fuel position in the basket.

2.1.3.1.1 Damaged Fuel Lattices

There are two lattices for damaged fuel rods in the current Maine Yankee fuel inventory, designated CF1 and CA3, that are loaded in Maine Yankee fuel cans. CF1 is a lattice having roughly the same dimensions as a standard fuel assembly. It is a 9×9 array of tubes, some of which contain damaged fuel rods. CA3 is a previously used fuel assembly lattice that has had all of the rods removed, and into which, damaged fuel rods have been inserted. The CF1 and CA3 lattices are placed in a Maine Yankee fuel can for storage. No credit is taken for the lattice structures in the criticality, structural, or thermal analysis.

2.1.3.1.2 Maine Yankee Consolidated Fuel

The Maine Yankee fuel inventory includes two consolidated fuel lattices, which house intact fuel rods taken from three fuel assemblies. Each lattice is a 17×17 array formed using stainless steel grids and top and bottom stainless steel end fittings. Four solid stainless steel connector rods connect the end fittings. The top end fitting is designed so that the lattice can be handled by the standard fuel assembly lifting fixture (grapple). These lattices were not used in the reactor and the stainless steel hardware is not activated.

One of these lattices contains 283 fuel rods and 2 rod position vacancies. The other contains 172 fuel rods, with the 76 stainless steel dummy rods in the outer periphery of the lattice.

The consolidated fuel is placed in a Maine Yankee fuel can for storage. No credit is taken for the lattice structures in the criticality, structural, or thermal analysis.

2.1.3.1.3 Maine Yankee Spent Fuel with Inserted Integral Hardware or Non-Fuel Items

Certain Maine Yankee fuel assemblies have either a Control Element Assembly or an Instrument Segment inserted in the fuel assembly. These components add to the gamma radiation source term of the standard fuel assembly.

A Maine Yankee Control Element Assembly (CEA) consists of five control rods mounted on a Type 304 stainless steel spider assembly. The five control rods are inserted in the fuel assembly guide tubes when the CEA is inserted in the fuel assembly. When fully inserted, the control element spider rests on the fuel assembly upper end fitting. The rods are fabricated from Inconel 625 or stainless steel and encapsulate B_4C as the primary neutron poison material. Fuel assemblies with a control element installed must be loaded into a Class 2 canister because of the additional height that the control element spider adds to the fuel assembly overall length. A CEA plug may also be inserted in a fuel rod. The CEA plug installs in the same position on the top of the fuel assembly, but the plug rods are only about 10 inches in length. These plugs are used to control water flow in the guide tubes. Fuel assemblies with CEA plugs installed must be loaded in a Class 2 canister.

Some standard fuel assemblies have an in-core instrument (ICI) thimble inserted in the center guide tube of the fuel assembly. The detector material and lead wire have been removed from the ICI assembly. The thimble top end and tube are primarily Zircaloy. When installed, the instrument thimble does not add to the overall fuel assembly length. Consequently, fuel assemblies with ICI thimbles are loaded in the Class 1 canister.

The non-fuel inventory includes a segment of an ICI instrument thimble approximately 24 inches long. This segment is loaded in the corner guide tube position of an intact fuel assembly. The fuel assembly with the ICI segment installed must have a CEA flow plug installed to close the top of the corner guide tube, capturing the segment between the CEA flow plug and the bottom end plate of the fuel assembly. The ICI segment may be installed in a fuel assembly that also holds CEA finger tips in other corner guide tube positions. Because of the CEA fuel plug, the fuel assembly must be installed in a Class 2 canister.

The non-fuel inventory also includes five startup sources. One of the startup sources is unirradiated.

The startup sources include three Pu-Be sources and two Sb-Be sources that are installed in the center guide tubes of fuel assemblies that subsequently must be loaded in one of the four corner fuel positions of the basket. Each source is designed to fit in the center guide tube of an assembly, and only one startup source may be loaded in any fuel assembly. All five of these startup sources contain Sb-Be pellets, which are 50% Be by volume. One of the three Pu-Be sources is unirradiated and evaluation of this source is based on a "fresh" source material assumption.

2.1.3.1.4 Maine Yankee Spent Fuel with Unique Design

Certain Maine Yankee fuel assemblies were uniquely designed to accommodate reactor physics. These assemblies incorporate variable radial enrichment and axial blankets.

Two batches of fuel used at Maine Yankee contain variably enriched fuel rods. The maximum fuel rod enrichment of one batch is 4.21 wt % ^{235}U with the variably enriched rods enriched to 3.5 wt % ^{235}U. The maximum planar average enrichment of this batch is 3.99 wt % ^{235}U. For the other batch, the maximum fuel rod enrichment is 4.0 wt % ^{235}U, with the variably enriched rods enriched to 3.4 wt % ^{235}U. The maximum planar average enrichment of this batch is 3.92 wt % ^{235}U.

One batch of variably enriched fuel also incorporates axial end blankets with fuel pellets that have a center hole, referred to as annular fuel pellets. Annular fuel pellets are used in the top and bottom 5% of the active fuel length of each fuel rod in this batch.

2.1.3.1.5 Maine Yankee Fuel Can

Fuel assemblies classified as damaged that exceed the limits for loading as intact fuel and certain undamaged fuel configurations are loaded in a Maine Yankee fuel can, which is shown in Drawings 412-501 and 412-502. The fuel can may be loaded only in a corner position (positions numbered 3, 6, 19 and 22 in Figure 2.1.3.1-1) in the basket of a Class 1 canister. The fuel can analysis assumes the failure of 100% of the fuel rods held in the fuel can.

The fuel can is sized to accommodate a fuel assembly and must be loaded in a corner position of the fuel basket. As shown in the drawings, the can is provided in two configurations. Both cans are 162.8 inches in length and, in the top 4.5 inches, have an external square dimension of 8.8 inches. One configuration of the fuel can body has an internal square dimension of 8.52 inches and an external square dimension of 8.62 inches. The corresponding dimensions of the second configuration are 8.3 and 8.4 inches, respectively. The smaller cross-section allows the use of the fuel can in a basket in which the corner fuel loading positions of the bottom weldment are not enlarged. The fuel cans are closed on the bottom end by a 0.63-inch thick plate that is welded to the can shell. The plate has drilled holes in each corner to allow water to drain from the can. A screen covers the holes to preclude the release of gross particulates from the fuel can. A lid having an overall depth dimension of 2.38 inches closes the can. The lid is not secured to the can shell, but is held in place when the shield lid is installed in the canister. The lid also has four drilled and screened holes. The damaged fuel is inserted in the fuel can and the lid is installed. Slots in the can shell allow the loaded can to be lifted and installed in the basket. Alternately, the fuel can may be inserted in a basket corner position before the damaged fuel assembly is inserted in the fuel can. Since the fuel can lid is held in place by the canister shield lid, the fuel can may be used only in the Class 1 canister.

A Maine Yankee fuel can containing fuel debris with greater than 20 Curies of plutonium, requires double containment for transport conditions in accordance with 10 CFR 71.63 (b).

The Maine Yankee fuel can design and fabrication specification summary is provided in Table 2.1.3.1-2. The major physical design parameters of the Maine Yankee fuel can are provided in Table 2.1.3.1-3. The structural evaluation of the Maine Yankee site specific fuel configurations is provided in Section 3.6.1

2.1.3.1.6 Maine Yankee Site Specific Spent Fuel Preferential Loading

The estimated Maine Yankee site specific spent fuel inventory is shown in Table 2.1.3.1-1. (Note that the population of fuel in a given configuration may change based on future spent fuel inspection or survey.) As shown in this table, certain fuel configurations are preferentially loaded to take advantage of the design features of the Transportable Storage Canister and basket to allow the loading of fuel that does not specifically conform to the design basis spent fuel. The designated preferential loading positions are shown in Figure 2.1.3.1-1.

Fuel with missing fuel rods, fuel with fuel rods that have been replaced by rods of other material, consolidated fuel lattices and damaged fuel are preferentially loaded in corner positions of the basket, numbered 3, 6, 19 and 22 in Figure 2.1.3.1-1. The requirements for preferential loading schemes using the corner positions result primarily from shielding or criticality evaluations of the designated fuel configurations.

Preferential loading is also used for spent fuel having a burnup between 45,000 and 50,000 MWD/MTU. This fuel is assigned to peripheral basket locations, which are the outer 12 fuel loading positions shown in Figure 2.1.3.1-1. Locating the high burnup fuel in the peripheral basket locations reduces the maximum temperatures of these assemblies.

High burnup fuel (45,000 – 50,000 MWD/MTU) may be loaded as intact fuel provided that ISG-11, Rev. 2 temperature limits are met. The 752°F (400°C) ISG-11, Rev. 2 fuel temperature limit is met as shown in Table 4.1-4.

Fuel assemblies with a control element inserted will be loaded in a Class 2 canister and basket for storage and transport due to the increased length of the assembly with the control element installed. However, these assemblies are not restricted as to loading position within the basket.

Fuel assemblies with a startup source in the center guide tube position must be loaded in one of the basket corner positions. A fuel assembly may not hold more than one startup source.

The loading position of fuel assemblies holding the CEA finger tips and/or the ICI segment in a fuel assembly corner guide tube position is not controlled; however, these fuel assemblies must have a CEA flow plug to ensure these items are captured within the guide tube(s).

2.1.3.1.7 Maine Yankee High Burnup Fuel

There are ninety (90) Maine Yankee fuel assemblies that have achieved a burnup between 45,000 and 50,000 MWD/MTU. As described in Section 2.1.3.1.6, these fuel assemblies are preferentially loaded in the 12 peripheral fuel loading positions in the basket. The high burnup assemblies are similar to the other Maine Yankee fuel planned to be placed in dry storage (i.e., those with burnup less than 45,000 MWD/MTU), but have design differences that support the high burnup objective.

Figure 2.1.3.1-1 Preferential Loading Diagram for Maine Yankee Site Specific Spent Fuel

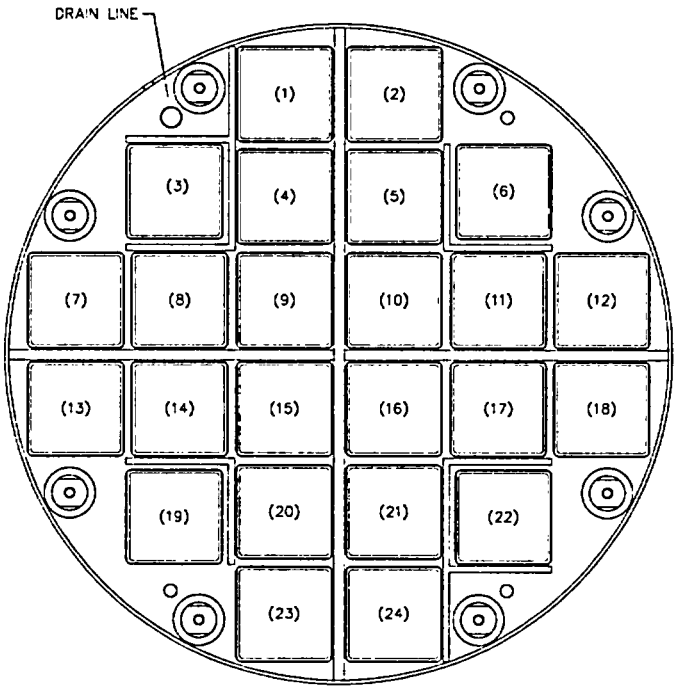

Note: Locations numbered 3, 6, 19 and 22 are corner positions.
Locations numbered 1, 2, 3, 6, 7, 12, 13, 18, 19, 22, 23 and 24 are periphery positions.
Locations numbered 4, 5, 8, 11, 14, 17, 20 and 21 are intermediate positions.
Locations numbered 9, 10, 15 and 16 are center positions.

Table 2.1.3.1-1 Maine Yankee Site Specific Fuel Population

Site Specific Spent Fuel Configurations[1]	Est. Number of Assemblies[2]
Standard Fuel	1,434
Inserted Control Element Assembly (CEA)	168
Inserted In-Core Instrument (ICI) Thimble	138
Consolidated Fuel	2
Fuel Rod Replaced by Rod Enriched to 1.95 wt %	3
Fuel Rod Replaced by Stainless Steel Rod or Zircaloy Rod	18
Fuel Rods Removed	10
Variable Enrichment	72
Variable Enrichment and Axial Blanket	68
Burnable Poison Rod Replaced by Hollow Zircaloy Rod	80
Damaged Fuel in Maine Yankee Fuel Can	12
Burnup between 45,000 and 50,000 MWD/MTU	90
Maine Yankee Fuel Can	As Required
Inserted Startup Source	5
Inserted CEA Fingertips or ICI String Segment	1

1. The loading of the site- specific fuel is controlled by the requirement of Appendix B, Section B 2.0, of the Amendment 3 Technical Specifications.
2. The number of fuel assemblies in some categories may vary depending on future fuel inspections.

Table 2.1.3.1-2 Maine Yankee Fuel Can Design and Fabrication Specification Summary

Design

- The Maine Yankee Fuel Can shall be designed in accordance with ASME Code, Section III, Subsection NG except for: 1) the noted exceptions of Table B3-1 for fuel basket structures; and 2) the Maine Yankee Fuel Can may deform under accident conditions of storage.
- The Maine Yankee Fuel Can will have screened vents in the lid and base plate. Stainless steel meshed screens (250×250) shall cover all openings.
- The Maine Yankee Fuel Can shall limit the release of material from damaged fuel assemblies and fuel debris to the canister cavity.
- The Maine Yankee Fuel Can lifting structure and lifting tool shall be designed with a minimum factor of safety of 3.0 on material yield strength.

Materials

- All material shall be in accordance with the referenced drawings and meet the applicable ASME Code sections.
- All structural materials are ASME SA 240, Type 304 stainless steel.

Welding

- All welds shall be in accordance with the referenced drawings.
- The final surface of all welds (first unit) shall be liquid penetrant examined in accordance with ASME Code Section V, Article 6, with acceptance in accordance with ASME Code Section III, NG-5350. Subsequent units shall be visually examined in accordance with ASME Code Section V, Article 9, with acceptance in accordance with ASME Code Section III, NG-5360.

Fabrication

- All cutting, welding, and forming shall be in accordance with ASME Code Section III, NG-4000.

Acceptance Testing

- The Maine Yankee Fuel Can (first unit) and handling tool shall be load tested and visually inspected at the completion of fabrication.

Quality Assurance

- The Maine Yankee Fuel Can shall be constructed under a quality assurance program that meets 10 CFR 72 Subpart G. The quality assurance program must be accepted by NAC International and the licensee prior to initiation of the work.
- A Certificate of Conformance (or Compliance) shall be issued by the fabricator stating that the component meets the specifications and drawings.

Table 2.1.3.1-3 Major Physical Design Parameters of the Maine Yankee Fuel Can

Parameter	Value
Overall Length (in.)	162.8
Inside Cross Section (in.)	8.5 × 8.5 or 8.3 × 8.3
Outside Cross Section (in.) (1)	8.6 × 8.6 or 8.4 × 8.4
Can Wall Thickness	18 Gauge (0.048 in.)
Internal Cavity Length (in.)	160.0
Empty Weight (nominal) (lbs.)	130

Note (1) The top of the Maine Yankee Fuel Can is located above the top weldment of the fuel basket when it is installed. The outside top cross-section is 8.82 × 8.82 in. at the top 4.5 inches to allow for lid engagement and fuel can lifting.

Table 2.1.3.1-4 Loading Table for Maine Yankee Fuel without Nonfuel Material

Enrichment	Burnup ≤ 30 GWD/MTU - Minimum Cool Time [years] for		
	Standard[1]	Preferential (I)[2]	Preferential (P)[3]
1.9 ≤ E < 2.1	5	5	5
2.1 ≤ E < 2.3	5	5	5
2.3 ≤ E < 2.5	5	5	5
2.5 ≤ E < 2.7	5	5	5
2.7 ≤ E < 2.9	5	5	5
2.9 ≤ E < 3.1	5	5	5
3.1 ≤ E < 3.3	5	5	5
3.3 ≤ E < 3.5	5	5	5
3.5 ≤ E < 3.7	5	5	5
3.7 ≤ E ≤ 4.2	5	5	5
Enrichment	30 < Burnup ≤ 35 GWD/MTU – Minimum Cool Time [years] for		
	Standard[1]	Preferential (I)[2]	Preferential (P)[3]
1.9 ≤ E < 2.1	5	5	5
2.1 ≤ E < 2.3	5	5	5
2.3 ≤ E < 2.5	5	5	5
2.5 ≤ E < 2.7	5	5	5
2.7 ≤ E < 2.9	5	5	5
2.9 ≤ E < 3.1	5	5	5
3.1 ≤ E < 3.3	5	5	5
3.3 ≤ E < 3.5	5	5	5
3.5 ≤ E < 3.7	5	5	5
3.7 ≤ E ≤ 4.2	5	5	5
Enrichment	35 < Burnup ≤ 40 GWD/MTU - Minimum Cool Time [years] for		
	Standard[1]	Preferential (I)[2]	Preferential (P)[3]
1.9 ≤ E < 2.1	7	7	5
2.1 ≤ E < 2.3	6	6	5
2.3 ≤ E < 2.5	6	6	5
2.5 ≤ E < 2.7	5	6	5
2.7 ≤ E < 2.9	5	6	5
2.9 ≤ E < 3.1	5	6	5
3.1 ≤ E < 3.3	5	6	5
3.3 ≤ E < 3.5	5	6	5
3.5 ≤ E < 3.7	5	6	5
3.7 ≤ E ≤ 4.2	5	6	5

1. "Standard" loading pattern: allowable decay heat = 0.958 kW per assembly
2. "Preferential" loading pattern: interior basket locations; allowable heat decay = 0.867 kW per assembly
3. "Preferential" loading pattern: periphery basket locations; allowable heat decay = 1.05 kW per assembly

Table 2.1.3.1-4 Loading Table for Maine Yankee Fuel without Nonfuel Material (continued)

Enrichment	40 < Burnup ≤ 45 GWD/MTU - Minimum Cool Time [years] for[1]		
	Standard[1]	Preferential (I)[2]	Preferential (P)[3]
1.9 ≤ E < 2.1	11	11	6
2.1 ≤ E < 2.3	9	9	6
2.3 ≤ E < 2.5	8	8	6
2.5 ≤ E < 2.7	7	7	6
2.7 ≤ E < 2.9	7	7	6
2.9 ≤ E < 3.1	6	7	6
3.1 ≤ E < 3.3	6	7	5
3.3 ≤ E < 3.5	6	7	5
3.5 ≤ E < 3.7	6	7	5
3.7 ≤ E ≤ 4.2	6	7	5
Enrichment	**45 < Burnup ≤ 50 GWD/MTU - Minimum Cool Time [years] for[1]**		
	Standard[1]	**Preferential (I)[2]**	**Preferential (P)[3]**
1.9 ≤ E < 2.1	Not allowed	Not allowed	7
2.1 ≤ E < 2.3	Not allowed	Not allowed	7
2.3 ≤ E < 2.5	Not allowed	Not allowed	7
2.5 ≤ E < 2.7	Not allowed	Not allowed	7
2.7 ≤ E < 2.9	Not allowed	Not allowed	7
2.9 ≤ E < 3.1	Not allowed	Not allowed	7
3.1 ≤ E < 3.3	Not allowed	Not allowed	7
3.3 ≤ E < 3.5	Not allowed	Not allowed	6
3.5 ≤ E < 3.7	Not allowed	Not allowed	6
3.7 ≤ E ≤ 4.2	Not allowed	Not allowed	6

1. "Standard" loading pattern: allowable decay heat = 0.958 kW per assembly
2. "Preferential" loading pattern: interior basket locations; allowable heat decay = 0.867 kW per assembly
3. "Preferential" loading pattern: periphery basket locations; allowable heat decay = 1.05 kW per assembly

+Table 2.1.3.1-5 Loading Table for Maine Yankee Fuel Containing a CEA

Enrichment	≤ 30 GWD/MTU Burnup - Minimum Cool Time in Years for				
	No CEA (Class 2)	5 Year CEA	10 Year CEA	15 Year CEA	20 Year CEA
1.9 ≤ E < 2.1	5	5	5	5	5
2.1 ≤ E < 2.3	5	5	5	5	5
2.3 ≤ E < 2.5	5	5	5	5	5
2.5 ≤ E < 2.7	5	5	5	5	5
2.7 ≤ E < 2.9	5	5	5	5	5
2.9 ≤ E < 3.1	5	5	5	5	5
3.1 ≤ E < 3.3	5	5	5	5	5
3.3 ≤ E < 3.5	5	5	5	5	5
3.5 ≤ E < 3.7	5	5	5	5	5
3.7 ≤ E ≤ 4.2	5	5	5	5	5
Enrichment	30 < Burnup ≤ 35 GWD/MTU - Minimum Cool Time in Years for				
	No CEA (Class 2)	5 Year CEA	10 Year CEA	15 Year CEA	20 Year CEA
1.9 ≤ E < 2.1	5	5	5	5	5
2.1 ≤ E < 2.3	5	5	5	5	5
2.3 ≤ E < 2.5	5	5	5	5	5
2.5 ≤ E < 2.7	5	5	5	5	5
2.7 ≤ E < 2.9	5	5	5	5	5
2.9 ≤ E < 3.1	5	5	5	5	5
3.1 ≤ E < 3.3	5	5	5	5	5
3.3 ≤ E < 3.5	5	5	5	5	5
3.5 ≤ E < 3.7	5	5	5	5	5
3.7 ≤ E ≤ 4.2	5	5	5	5	5
Enrichment	35 < Burnup ≤ 40 GWD/MTU - Minimum Cool Time in Years for				
	No CEA (Class 2)	5 Year CEA	10 Year CEA	15 Year CEA	20 Year CEA
1.9 ≤ E < 2.1	7	7	7	7	7
2.1 ≤ E < 2.3	6	6	6	6	6
2.3 ≤ E < 2.5	6	6	6	6	6
2.5 ≤ E < 2.7	5	6	5	5	5
2.7 ≤ E < 2.9	5	6	5	5	5
2.9 ≤ E < 3.1	5	6	5	5	5
3.1 ≤ E < 3.3	5	5	5	5	5
3.3 ≤ E < 3.5	5	5	5	5	5
3.5 ≤ E < 3.7	5	5	5	5	5
3.7 ≤ E ≤ 4.2	5	5	5	5	5
Enrichment	40 < Burnup ≤ 45 GWD/MTU - Minimum Cool Time in Years for				
	No CEA (Class 2)	5 Year CEA	10 Year CEA	15 Year CEA	20 Year CEA
1.9 ≤ E < 2.1	11	11	11	11	11
2.1 ≤ E < 2.3	9	9	9	9	9
2.3 ≤ E < 2.5	8	8	8	8	8
2.5 ≤ E < 2.7	7	7	7	7	7
2.7 ≤ E < 2.9	7	7	7	7	7
2.9 ≤ E < 3.1	6	6	6	6	6
3.1 ≤ E < 3.3	6	6	6	6	6
3.3 ≤ E < 3.5	6	6	6	6	6
3.5 ≤ E < 3.7	6	6	6	6	6
3.7 ≤ E ≤ 4.2	6	6	6	6	6

Note: The No CEA (Class 2) column is provided for comparison. Fuel assemblies without a CEA insert may not be loaded in a Class 2 canister.

2.2 Design Criteria for Environmental Conditions and Natural Phenomena

This section presents the design criteria for site environmental conditions and natural phenomena applied in the design basis analysis of the UMS® Universal Storage System. These criteria reflect conditions and phenomena to which the Storage System could be exposed during the period of storage. The system is designed to withstand the loads imposed by these environmental conditions and natural phenomena. Analyses to demonstrate that the design basis system meets the design criteria defined in this section are presented in the appropriate chapters of this Safety Analysis Report.

The use of the UMS® Universal Storage System at a specific site requires that the site either meet the design criteria of this section or be separately evaluated against the site specific conditions to ensure the acceptable performance of the UMS® Universal Storage System. Site specific evaluations are incorporated in designated sections of each chapter of this Safety Analysis Report. Site specific evaluations for environmental conditions and natural phenomena are presented in Section 11.2.15.

2.2.1 Tornado and Wind Loadings

The Vertical Concrete Casks are typically placed outdoors on an unsheltered reinforced concrete storage pad at an ISFSI site. This storage condition exposes the casks to tornado and wind loading.

2.2.1.1 Applicable Design Parameters

The design basis tornado and wind loading is defined based on Regulatory Guide 1.76 [9] Region 1 and NUREG-0800 [10]. The tornado and wind loading criteria are:

Tornado and Wind Condition	Limit
Rotational Wind Speed, mph	290
Translational Wind Speed, mph	70
Maximum Wind Speed, mph	360
Radius of Max. Wind Speed, ft.	150
Pressure Drop, psi	3.0
Rate of Pressure Drop, psi/sec	2.0

2.2.1.2 Determination of Forces on Structures

Tornado wind forces on the Vertical Concrete Cask are calculated by multiplying the dynamic wind pressure by the frontal area of the cask normal to the wind direction. Wind forces are applied to the cask in the wind direction. No streamlining is assumed. The evaluation of wind loading and tornado missile effects on the cask is presented in Section 11.2.11. The total design basis wind loading on the projected area of the cask is determined in Section 11.2.11. The cask is demonstrated to remain stable under design basis tornado wind loading in conjunction with impact from a high energy tornado missile.

2.2.1.3 Tornado Missiles

The design basis tornado missile impacts are defined in Paragraph 4, Subsection III, Section 3.5.1.4 of NUREG-0800 [10]. The design basis tornado is considered to generate three types of missiles that impact the cask at normal incidence:

1. Massive Missile - (Deformable w/high kinetic energy)	Weight = 4,000 lbs Frontal Area = 20 sq.-ft
2. Penetration Missile - (Rigid hardened steel)	Weight = 280 lbs Diameter = 8.0 in
3. Protective Barrier Missile - (Solid steel sphere)	Weight = 0.15 lbs Diameter = 1.0 in

Each missile is assumed to impact the cask at a velocity of 126 miles per hour, horizontal to the ground, which is 35 percent of the maximum wind speed of 360 miles per hour. For missile impacts in the vertical direction, the assumed missile velocity is (0.7)(126) = 88.2 miles per hour.

The detailed analysis of the Vertical Concrete Cask for missile impacts applies the laws of conservation of momentum and conservation of energy to determine the rigid body response of the concrete cask. Each missile impact is evaluated, and all missiles are assumed to impact in a manner that produces the maximum damage to the cask. The tornado and wind driven missile impact evaluation is presented in Section 11.2.11.

2.2.2 Water Level (Flood) Design

The Vertical Concrete Cask may be exposed to a flood during storage on an unsheltered concrete storage pad at an ISFSI site. The source and magnitude of the probable maximum flood depend on specific site characteristics.

2.2.2.1 Flood Elevations

The Vertical Concrete Cask is evaluated in Section 11.2.9 for a maximum flood water depth of 50 feet above the base of the cask. The flood water velocity is assumed to be 15 feet per second. Results of the evaluation show that under design basis flood conditions, the cask does not float, tip, or slide on the storage pad, and that the confinement function is maintained.

2.2.2.2 Phenomena Considered in Design Load Calculations

The occurrence of flooding at an ISFSI site is dependent upon the specific site location and the surrounding geographical features, natural and man-made. Some possible sources of a flood at an ISFSI site are: (1) overflow from a river or stream due to unusually heavy rain, snow-melt runoff, a dam or major water supply line break caused by a seismic event (earthquake); (2) high tides produced by a hurricane; and (3) a tsunami (tidal wave) caused by an underwater earthquake or volcanic eruption.

Flooding at an ISFSI site is highly improbable because of the extensive environmental impact studies that are performed during the selection of a site for a nuclear facility.

2.2.2.3 Flood Force Application

The evaluation of the Universal Storage System for a flood condition determines a maximum allowable flood water current velocity and a maximum allowable flood water depth. The criteria employed in the determination of the maximum allowable values are that a cask sliding or tip-over will not occur, and that the canister material yield strength is not exceeded. The evaluation of the effects of flood conditions on the system is presented in Section 11.2.9.

The force of the flood water current on the cask is calculated as a function of the current velocity by multiplying the dynamic water pressure by the frontal area of the cask that is normal to the current direction. The dynamic water pressure is calculated using Bernoulli's equation relating fluid velocity and pressure. The force of the flood water current is limited such that the overturning moment on the cask will be less than that required to tip the cask over.

2.2.2.4 Flood Protection

The inherent strength of the reinforced concrete cask provides a substantial margin of safety against any permanent deformation of the cask for a credible flood event at an ISFSI site. Therefore, no special flood protection measures for the cask are necessary. The evaluation presented in Section 11.2.9 shows that for the design basis flood, the allowable stresses in the canister are not exceeded.

2.2.3 Seismic Design

An ISFSI site may be subject to seismic events (earthquakes) during its lifetime. The seismic response spectra experienced by the cask depends upon the geographical location of the specific site and the distance from the epicenter of the earthquake. The only significant effect of a seismic event on the Vertical Concrete Cask is a possible tip-over; however, tip-over does not occur during the design basis earthquake. Seismic response of the cask is presented in Section 11.2.8.

2.2.3.1 Input Criteria

The Transportable Storage Canister and Vertical Concrete Cask are designed and analyzed by applying a 0.26g seismic acceleration at the top surface of the ISFSI pad.

2.2.3.2 Seismic - System Analyses

The analysis for the earthquake condition applied to nuclear facilities is provided in Section 11.2.8.2. The evaluation shows that the concrete cask does not tip over or slide in the design basis earthquake. Evaluation of the consequences of a hypothetical tip-over event is provided in Section 11.2.12.

2.2.4 Snow and Ice Loadings

The criterion for determining design snow loads is based on ANSI/ASCE 7-93 [12], Section 7.0. Flat roof snow loads apply and are calculated from the following formula:

$$p_f = 0.7C_eC_tIp_g$$

where:

p_f = flat roof snow load (psf)
C_e = Exposure factor = 1.0
C_t = Thermal factor = 1.2
I = Importance factor = 1.2
p_g = ground snow load, (psf) = 100

The numerical values of C_e, C_t, I and p_g are obtained from Tables 18, 19, 20 and Figure 7, respectively, of ANSI/ASCE 7-93.

The exposure factor, C_e, accounts for wind effects. The site of the Universal Storage System is assumed to be a location typical for siting Category C, which is defined to be "locations in which snow removal by wind cannot be relied on to reduce roof loads because of terrain, higher structures, or several trees nearby."

The thermal factor, C_t, accounts for the importance of buildings and structures in relation to public health and safety. The Universal Storage System is conservatively classified as Category III.

Ground snow loads for the contiguous United States are given in Figures 5, 6 and 7 of ANSI/ ASCE 7-93. A worst case value of 100 lbs per square ft is assumed.

Based on the above, the design criterion for snow and ice loads is:

Flat Roof Snow Load, $p_f = (0.7)\ (1.0)\ (1.2)\ (1.2)\ (100) = 100.8$ psf

This load is bounded by the weight of the loaded transfer cask on the top of the concrete cask shell and by the tornado missile loading on the concrete cask lid. The snow load is considered in the load combinations described in Section 3.4.4.2.2.

2.2.5 Combined Load Criteria

Each normal, off-normal and accident condition has a combination of load cases that defines the total combined loading for that condition. The individual load cases considered include thermal, seismic, external and internal pressure, missile impacts, drops, snow and ice loads, and/or flood water forces.

The load conditions to be evaluated for storage casks are identified in 10 CFR 72[11] and ANSI/ANS-57.9 [13].

2.2.5.1 Load Combinations and Design Strength - Vertical Concrete Cask

The load combinations specified in ANSI/ANS 57.9 for concrete structures are applied to the concrete casks as shown in Table 2.2-1. The live loads are considered to vary from 0 percent to 100 percent to ensure that the worst-case condition is evaluated. In each case, use of 100 percent of the live load produces the maximum load condition. The steel liner of the concrete cask is a stay-in-place form and it provides radiation shielding. The concrete cask is designed to the requirements of ACI 349 [4].

In calculating the design strength of concrete in the Vertical Concrete Cask body, nominal strength values are multiplied by a strength reduction factor in accordance with Section 9.3 of ACI 349.

2.2.5.2 Load Combinations and Design Strength - Canister and Basket

The canister is designed in accordance with the 1995 edition of the ASME Code, Section III, Subsection NB [1] for Class 1 components. The basket structure is designed in accordance with

ASME Code, Section III, Subsection NG [2]. Structural buckling of the basket is evaluated in accordance with NUREG/CR-6322 [3].

The load combinations for all normal, off-normal, and accident conditions and corresponding service levels are shown in Table 2.2-2. The table, therefore, defines the canister design and service loadings. Levels A and D service limits are used for normal and accident conditions, respectively. Levels B and C service limits are used for off-normal conditions. The analysis methods of the ASME Code are employed. Stress intensities caused by pressure, temperature, and mechanical loads are combined before comparing them to ASME code allowables. The Code allowables are listed in Table 2.2-3.

2.2.5.3 Design Strength - Transfer Cask

The transfer cask is a special lifting device. It is designed and fabricated to the requirements of ANSI N14.6 [6] and NUREG 0612 [7] for the lifting trunnions and supports, and ANSI/ANS-57.9 [13] for the remainder of the structure. The criteria are:

1. The combined shear stress or maximum tensile stress during the lift (with 10 percent dynamic load factor) shall be $\leq S_y/6$ and $S_u/10$ for a nonredundant load path, or shall be $\leq S_y/3$ and $S_u/5$ for redundant load paths.

2. The ferritic steel material used for the load bearing members of the transfer cask shall satisfy the material toughness requirements of ANSI N14.6, paragraph 4.2.6.

Load testing of the transfer cask is described in Section 2.3.3.1.

2.2.6 Environmental Temperatures

A normal, long-term annual average design ambient temperature of 76°F is selected to bound most annual average temperatures seen by a cask over its lifetime. This temperature is based on the maximum average annual temperature in the 48 contiguous United States, specifically, Miami, FL., at 75.6°F [14], and is, therefore, used so as to bound existing and potential ISFSI sites.

The 76°F normal temperature is used as the base for thermal evaluations. The evaluation of this environmental condition is discussed along with the thermal analysis models in Chapter 4.0. The thermal stress evaluation for the normal operating conditions is provided in Section 3.4.4. Normal temperature fluctuations are bounded by the severe ambient temperature cases that are evaluated as off-normal and accident conditions.

Off-normal, severe environmental conditions are defined as -40°F with no solar loads and 106°F with solar loads. An extreme environmental condition of 133°F with maximum solar loads is evaluated as an accident case (11.2.7) to show compliance with the maximum heat load case required by ANSI/ANS-57.9. Thermal performance is also evaluated assuming half-blockage of the concrete cask air inlets and the complete blockage of the air inlets and outlets. Thermal analyses for these cases are presented in Sections 11.1.2 and 11.2.13. The evaluation based on ambient temperature conditions is presented in Section 4.4.

The design basis temperatures used in the Universal Storage System analysis are shown below. Solar insolance is as specified in 10 CFR 71.71 [15] and Regulatory Guide 7.8 [16].

Condition	Ambient Temperature	Solar Insolance
Normal	76°F	yes
Off-Normal - Severe Heat	106°F	yes
Off-Normal - Severe Cold	-40°F	no
Accident - Extreme Heat	133°F	yes

Table 2.2-1 Load Combinations for the Vertical Concrete Cask

Load Combination	Condition	Dead	Live	Wind	Thermal	Seismic	Tornado/ Missile	Drop/ Impact	Flood
1	Normal	1.4D	1.7L						
2	Normal	1.05D	1.275L		$1.275T_o$				
3	Normal	1.05D	1.275L	1.275W	$1.275T_o$				
4	Off-Normal and Accident	D	L		T_a				
5	Accident	D	L		T_o	E_{ss}			
6	Accident	D	L		T_o			A	
7	Accident	D	L		T_o				F
8	Accident	D	L		T_o		W_t		

Load Combinations are from ANSI/ANS-57.9 [13] and ACI 349 [4].

D = Dead Load

L = Live Load

W = Wind

T_o = Normal Temperature

F = Flood

T_a = Off- Normal or Accident Temperature

E_{ss} = Design Basis Earthquake

W_t = Tornado/Tornado Missile

A = Drop/Impact

Table 2.2-2 Load Combinations for the Transportable Storage Canister

LOAD		NORMAL			OFF-NORMAL		CONDITIONS			ACCIDENT					
ASME Service Level		A			B		C			D					
Load Combinations		1	2	3	1	2	3	4	5	1	2	3	4	5	6
Dead Weight	Canister with fuel	X	X	X	X	X	X	X	X	X	X	X	X	X	X
Thermal	In Storage Cask 76° F Ambient	X		X				X		X	X	X	X	X	
	In Transfer Cask 76° F Ambient		X		X		X								X
	In Storage Cask -40°F or 106°F Ambient					X			X						
Internal Pressure	Normal	X	X	X			X	X	X	X	X	X	X		
	Off-Normal				X	X									
	Accident													X	X
Handling Load	Normal		X	X	X										
	Off-Normal						X	X	X						
Drop/Impact	Accident									X					
Seismic	Accident										X				
Flood	Accident											X			
Tornado	Accident												X		

Table 2.2-3 Structural Design Criteria for Components Used in the Transportable Storage Canister

	Component	Criteria
1.	Normal Operations: Service Level A Canister: ASME Section III, Subsection NB [1] Basket: ASME Section III, Subsection NG [2] Lifting Devices: ANSI N14.6 [6] and NUREG 0612 [7]	$P_m \leq S_m$ $P_L + P_b \leq 1.5\ S_m$ $P_L + P_b + Q \leq 3S_m$ Redundant load path: combined shear or max. tensile stress $\leq S_u/5$ and $S_y/3$
2.	Off-Normal Operations: Service Level B Canister: ASME Section III, Subsection NB	$P_m < 1.1\ S_m$ and $P_L + P_b < 1.65\ S_m$
3.	Off-Normal Operations: Service Level C Canister: ASME Section III, Subsection NB Basket: ASME Section III, Subsection NG Note: Subsection NB allowables for Service Level C are conservatively applied to the basket.	Subsection NB Allowables: $P_m < 1.2\ S_m$ or S_y (whichever is greater) and $P_L + P_b < 1.8\ S_m$ or $1.5\ S_y$ (whichever is less)
4.	Accident Conditions, Service Level D Canister: ASME Section III, Subsection NB Basket: ASME Section III, Subsection NG	$P_m \leq 2.4\ S_m$ or $0.7\ S_u$ (whichever is less) and $P_L + P_b \leq 3.6\ S_m$ or $1.05\ S_u$ (whichever is less)
5.	Basket Structural Buckling	NUREG/CR-6322 [3]

Symbols:

S_m = material design stress intensity
S_u = material ultimate strength
S_y = material yield strength
P_L = primary local membrane stress
P_m = primary general membrane stress
P_b = primary bending stress

THIS PAGE INTENTIONALLY LEFT BLANK

2.3 Safety Protection Systems

The Universal Storage System relies upon passive systems to ensure the protection of public health and safety, except in the case of fire or explosion. As discussed in Section 2.3.6, fire and explosion events are effectively precluded by site administrative controls that prevent the introduction of flammable and explosive materials. The use of passive systems provides protection from mechanical or equipment failure.

2.3.1 General

The Universal Storage System is designed for safe, long-term storage of spent nuclear fuel. The system will withstand all of the evaluated normal, off-normal, and postulated accident conditions without release of radioactive material or excessive radiation exposure to workers or the general public. The major design considerations that are incorporated in the Universal Storage System to assure safe, long-term fuel storage are:

1. Continued containment in postulated accidents.
2. Thick concrete and steel biological shield.
3. Passive systems that ensure reliability.
4. Inert helium atmosphere to provide corrosion protection for fuel cladding and enhanced heat transfer for the stored fuel.

Each component of the Universal Storage System is classified with respect to its function and corresponding effect on public safety. In accordance with Regulatory Guide 7.10 [17], each system component is assigned a safety classification and then "important to safety" items are further categorized based on importance to safety into Category A, B, or C, as shown in Table 2.3-1. The safety classification is based on review of each component's function and the assessment of the consequences of its failure following the guidelines of NUREG/CR-6407 [18]. The safety classification categories are defined as follows:

- Category A - Components critical to safe operations whose failure or malfunction could directly result in conditions adverse to safe operations, integrity of spent fuel, or public health and safety.

- Category B - Components with major impact on safe operations whose failure or malfunction could indirectly result in conditions adverse to safe operations, integrity of spent fuel, or public health and safety.

- Category C - Components whose failure would not significantly reduce the packaging effectiveness and would not likely result in conditions adverse to safe operations, integrity of spent fuel, or public health and safety.

As discussed in the following sections, the Universal Storage System design incorporates features addressing the above design considerations to assure safe operation during loading, handling, and storage of spent nuclear fuel.

2.3.2 Protection by Multiple Confinement Barriers and Systems

2.3.2.1 Confinement Barriers and Systems

The radioactivity that the Universal Storage System must confine originates from the spent fuel assemblies to be stored and residual contamination that may remain inside the canister as a result of contact with water in the fuel pool where the canister loading is conducted. The system is designed to confine this radioactive material.

The Transportable Storage Canister is closed by welding. The shield lid weld is pressure tested. All of the field-installed shield lid welds are liquid penetrant examined following the root and final weld passes. The shield lid welds are leak tested. The installation of the canister structural lid, which provides a redundant closure over the shield lid and port covers, is accomplished by multi-pass welding that is either: 1) progressively liquid penetrant examined; or 2) ultrasonically examined in conjunction with a liquid penetrant examination of the final weld surface. The longitudinal and girth welds of the canister shell are full penetration welds that are radiographically examined during fabrication. The weld that joins the bottom plate to the canister shell is ultrasonically and liquid penetrant examined during fabrication.

The canister welds are an impenetrable boundary to the release of fission gas products during the period of storage. There are no evaluated normal, off-normal, or accident conditions that result in the breach of the canister and the subsequent release of fission products. The canister is

designed to withstand a postulated drop accident in the UMS® Universal Transport Cask without precluding the subsequent removal of the fuel (i.e., the fuel tubes do not deform such that they bind the fuel assemblies).

Personnel radiation exposure during handling and closure of the canister is minimized by the following steps:

1. Placing the shield lid on the canister while the transfer cask and canister are under water in the fuel pool.
2. Decontaminating the exterior of the transfer cask prior to draining the canister or performing canister closure operations with the transfer cask partially submerged to preserve the shielding benefit of the water.
3. Using temporary shielding.
4. Using a retaining ring on the transfer cask to ensure that the canister is not raised out of the shield provided by the transfer cask.
5. Placing a shielding ring over the annular gap between the transfer cask and the canister.

2.3.2.2 Cask Cooling

The loaded Vertical Concrete Cask is passively cooled. Cool (ambient) air enters at the bottom of the concrete cask through four inlet vents. Heated air exits through the four outlets at the top of the cask. Radiant heat transfer also occurs from the canister shell to the concrete cask liner. Consequently, the liner also heats the convective air flow. Conduction does not play a substantial role in heat removal from the canister surface. This natural circulation of air inside the Vertical Concrete Cask, in conjunction with radiation from the canister surface, maintains the fuel cladding temperature and all of the concrete cask component temperatures below their design limits. The cask cooling system is described in detail in Sections 4.1 and 4.4.

2.3.3 Protection by Equipment and Instrumentation Selection

The Universal Storage System is a passive storage system that does not rely on equipment or instruments to preserve public health or safety and to meet its safety functions in long-term storage. The system employs support equipment and instrumentation to facilitate operations. These items, and the actions taken to assure performance, are described below.

2.3.3.1 Equipment

The equipment that is important-to-safety employed in the use and operation of the Universal Storage System is the transfer cask and the lifting yoke used to lift the transfer cask. The transfer cask is provided in the standard and advanced configurations. The lifting yoke is designed to meet the requirements of ANSI N14.6 and NUREG-0612 and is designed as a special lifting device for critical loads. Both lifting yokes are proof load tested to 300% of design load when fabricated. The lifting yokes have no welds in the lifting load path. Following the load test, the bolted connections are disassembled, and the components are inspected for deformation. Permanent deformation of components is not acceptable. The lifting yoke is inspected for visible defects prior to each use and is inspected annually.

The transfer cask is used to move the empty and loaded Transportable Storage Canister in all of the operations that precede the installation of the loaded canister in the Vertical Concrete Cask. The transfer cask is evaluated as a lifting component. The principal design criteria of the transfer cask are presented in Section 2.2.5.3, above. The transfer cask design meets the requirements of ANSI N14.6 and NUREG-0612. The standard and advanced transfer casks both have two pairs of lifting trunnions. Each pair is designed as a special lifting device for critical loads, but both pairs may be used together in order to provide a redundant load path. Each pair of transfer cask trunnions is load tested to 300% of the maximum calculated service load. The service load includes the transfer cask weight, the loaded canister, and water in the canister. Following the load test, the trunnion welds and other welds in the load path are inspected for indications of cracking or deformation. The principal load bearing welds and the transfer cask lifting trunnions are evaluated in Section 3.4.3.3.

The transfer cask bottom shield doors support the canister from the bottom during handling of the canister. The shield doors are also load tested to 300% of the maximum calculated service load. The service load includes the weight of the loaded canister and water in the canister. Following the load test, the load bearing surface areas of the doors, rails, and attachment welds are examined for evidence of cracking or deformation.

The transfer cask welds are subjected to a liquid penetrant examination, performed in accordance with the ASME Code, Section V, Article 6. Acceptance criteria is in accordance with the ASME Code, Paragraph NF-5350.

Any evidence of permanent deformation, cracking, galling of bearing surfaces, or unacceptable liquid penetrant examination results is cause for rejection. Any identified defects must be repaired and the load test repeated prior to final acceptance.

2.3.3.2 Instrumentation

A remote temperature measuring system is employed to measure the outlet air temperature of the Vertical Concrete Casks in long-term storage. The outlet temperature is recorded daily as a check of the thermal performance of the heat rejection capability of the storage cask. The outlet temperature is expected to increase in the unlikely event that one or more inlets or outlets become blocked. Consequently, visual inspection of the inlets and outlets is required when the temperature differential between the ambient air temperature and the outlet air temperature exceeds 102°F for the PWR configuration or 92°F for the BWR configuration during normal operations. In addition, visual inspection of the inlets and outlets is required following any natural phenomena event, such as an earthquake, that could lead to a reduction in efficiency of the cooling system.

The canister shield lid weld is helium leak tested during closure. The leak detector is checked against a known helium source immediately prior to, and after, use to preclude unknown leak detector failure.

2.3.4 Nuclear Criticality Safety

The Universal Storage System design includes features to ensure that nuclear criticality safety is maintained (i. e., the cask remains subcritical) under normal, off-normal, and accident conditions. The design of the canister and fuel basket is such that, under all conditions, the highest neutron multiplication factor (k_{eff}) is less than 0.95. The criticality evaluation for the design basis fuel is presented in Section 6.4.

2.3.4.1 Control Methods for Prevention of Criticality

Criticality control in the PWR basket is achieved using a neutron flux trap configuration. Individual fuel assemblies are surrounded by four neutron absorber sheets, one on each side of the assembly, that provide absorption of moderated neutrons. The assemblies are separated by a gap that is filled with water during hypothetical accident conditions when the canister is flooded. Fast neutrons escaping one fuel assembly are moderated in the gap between the assemblies and

absorbed by the neutron absorber material surrounding the assemblies. The minimum loading of the neutron absorber sheets is 0.025 g $^{10}B/cm^2$. The sheets are mechanically supported by the fuel tube structure to ensure that the neutron absorber sheets remain in place during the design basis normal, off-normal, and accident events.

Individual fuel assemblies in the BWR basket are separated from adjacent assemblies by a single neutron absorber sheet between fuel assemblies. Of the total 56 fuel tubes, 42 tubes contain neutron absorber sheets on two sides of the tubes, 11 tubes contain neutron absorber sheets on one side, and the remaining 3 tubes contain no neutron absorber sheets. The arrangement of the fuel tubes ensures that there is at least one neutron absorber sheet between adjacent fuel assemblies. Although this configuration of water gaps and neutron absorber sheets does not form a classic neutron flux trap, the design ensures that there is sufficient absorption of moderated neutrons by the neutron absorber to maintain criticality control in the basket ($k_{eff} < 0.95$). The minimum loading of the neutron absorber sheets in the BWR fuel tubes is 0.011 g $^{10}B/cm^2$. The neutron absorber sheets are mechanically supported by the fuel tube structure to ensure that the sheets remain in place during the design basis normal, off-normal, and accident events.

The efficiency of the neutron absorber sheets in preserving nuclear criticality safety is demonstrated by the criticality results presented in Section 6.4.3.

The principal criticality design criterion is that k_{eff} remain below 0.95 under all conditions. Assumptions made in the analyses used to demonstrate conformance to this criterion include:

1. Fuel assembly with maximum ^{235}U loading (95% theoretical density);
2. 75 percent of the nominal ^{10}B loading in the neutron absorber sheet;
3. Infinite array of casks in the X-Y (horizontal) plane;
4. Infinite fuel length with no inclusion of end leakage effects;
5. No credit taken for structural material present in the assembly; and,
6. No credit taken for fuel burnup or for the buildup of fission product neutron poisons.

Use of administrative controls of fuel burnup levels, neutron absorption properties of the burned fuel, and the presence of steel shell of the canister provide further criticality controls in the Universal Storage System.

2.3.4.2 Error Contingency Criteria

The calculated values of k_{eff} include error contingencies and calculation and modeling biases. The standards and regulations of criticality safety require that k_{eff}, including uncertainties, k_s, be less than 0.95. The bias and 95/95 uncertainty are applied to the calculation of k_s by using:

$$k_s = k_{nom} + 0.0052 + [(0.0087)^2 + (2\sigma_{MC})^2]^{1/2} \leq 0.95$$

where:

k_{nom} = the nominal k_{eff} for the cask, and
σ_{MC} = the Monte Carlo uncertainty.

The calculation of error contingencies and uncertainties is presented in Section 6.4.

2.3.4.3 Verification Analyses

The CSAS25 criticality analysis sequence is benchmarked through a series of calculations based on 63 critical experiments. These experiments span a range of fuel enrichments, fuel rod pitches, poison sheet characteristics, shielding materials, and geometries that are typical of light water reactor fuel in a cask. To achieve accurate results, three-dimensional models, as close to the actual experiment as possible, are used to evaluate the experiments. The results of the benchmark calculations are provided in Section 6.5.

2.3.5 Radiological Protection

The Universal Storage System, in keeping with the As Low As Is Reasonably Achievable (ALARA) philosophy, is designed to minimize, to the extent practicable, operator radiological exposure.

2.3.5.1 Access Control

Access to a Universal Storage System ISFSI site is controlled by a peripheral fence to meet the requirements of 10 CFR 72 and 10 CFR 20 [19]. Access to the storage area, and its designation as to the level of radiation protection required, are established by site procedure. The storage

area is surrounded by a fence, having lockable truck and personnel access gates. The fence has intrusion-detection features as determined by the site procedure.

2.3.5.2 Shielding

The Universal Storage System is designed to limit the dose rates as follows:

- external surface dose (gamma and neutron) to less than 50 mrem/hr (average) on the Vertical Concrete Cask sides.
- external surface dose to less than 50 mrem/hr (average) on the Vertical Concrete Cask top.
- a maximum of 100 mrem/hr (average) at the Vertical Concrete Cask air inlets and outlets.
- the supplemental shielding at the top of the canister shield lid reduces personnel exposure during canister closure operations.

Sections 72.104 and 72.106 of 10 CFR 72 set whole body dose limits for an individual located beyond the controlled area at 25 millirems per year (whole body) during normal operations and 5 rems (5,000 millirems) from any design basis accident. The analyses showing the actual Universal Storage System doses, and dose rates, are included in Chapters 5.0, 10.0 and 11.0.

2.3.5.3 Ventilation Off-Gas

The Universal Storage System is passively cooled by radiation and natural convection heat transfer at the outer surface of the concrete cask and in the canister-concrete cask annulus. The bottom of the cask is conservatively assumed to be an adiabatic surface. In the canister-concrete cask annulus, air enters the air inlets, flows up between the canister and concrete cask liner in the annulus, and exits the air outlets. The air flow in the annulus is due to the buoyancy effect created by the heating of the air by the canister and concrete cask liner walls. The details of the passive ventilation system design are provided in Chapter 4.0.

The surface of the canister is exposed to cooling air when the canister is placed in the concrete cask. If the surface is contaminated, the possibility exists that contamination could be carried aloft by the cooling air stream. Therefore, during fuel loading, the spent fuel pool water is excluded from the canister exterior by filling the transfer cask/canister annular gap with clean water as the transfer cask is being lowered into the fuel pool. Clean water is injected into the gap during the entire time the transfer cask is submerged. These steps minimize the potential for the intrusion of contaminated water into the canister annular gap.

Once the transfer cask is removed from the pool, a smear survey is taken of the exterior surface of the canister near the top. While no contamination is expected to be found, it is possible that the surface could be contaminated. The allowable upper limit for surface contamination of the canister and transfer cask is provided in LCO 3.2.1 in Appendix A. As described in LCO 3.2.1, if this limit is exceeded, steps to decontaminate the canister surface must be taken and continued until the contamination is less than the allowable limit.

To facilitate decontamination, the canister is fabricated so that its exterior surface is smooth. There are no corners or pockets that could trap and hold contamination.

There are no radioactive releases during normal operations. Also, there are no credible accidents that cause significant releases of radioactivity from the Universal Storage System and, hence, there are no off-gas system requirements for the system during normal storage operation. The only time an off-gas system is required is during the canister drying phase. During this operation, the reactor off-gas system or a HEPA filter system is used.

2.3.5.4 Radiological Alarm Systems

No radiological alarms are required on the Universal Storage System. Justification for this is provided in Chapter 5.0 (Shielding), 10.0 (Radiological Protection), and 11.0 (Accident Analysis).

Typically, total radiation exposure due to the ISFSI installation is determined by the use of Thermo-Luminescent Detectors (TLDs) mounted at convenient locations on the ISFSI fence. The TLDs are read quarterly to provide a record of boundary dose.

2.3.6 Fire and Explosion Protection

Fire and explosion protection of the Universal Storage System is provided primarily by administrative controls applied at the site, which preclude the introduction of any explosive and any excessive flammable materials into the ISFSI area.

2.3.6.1 Fire Protection

A major ISFSI fire is not considered credible, since there is very little material near the casks that could contribute to a fire. The concrete cask is largely impervious to incidental thermal events. Administrative controls are put in place to ensure that the presence of combustibles is minimized. A hypothetical fire event is evaluated as an accident condition in Section 11.2.6. The fire event evaluated is a 1475°F fire of 8 minutes duration. This condition is considered to be highly conservative.

2.3.6.2 Explosion Protection

The Universal Storage System is analyzed to ensure its proper function under an over-pressure condition. As described in Section 11.2.5, in the evaluated 22 psig over-pressure condition, stresses in the canister remain below allowable limits and there is no loss of confinement. These results are conservative, as the canister is protected from direct over-pressure conditions by the concrete cask.

For the same reasons as for the fire condition, a severe explosion on an ISFSI site is not considered credible. The evaluated over-pressure is considered to bound any explosive over-pressure resulting from an industrial explosion at the boundary of the owner-controlled area.

2.3.7 Ancillary Structures

The loading, transfer and transport of the UMS® System requires the use of auxiliary equipment as described in Section 2.3.3 and may require the use of an ancillary structure, referred to as a "Canister Handling Facility." The Canister Handling Facility is an especially designed and engineered structure separate from the 10 CFR 50 facilities at the site. The Canister Handling Facility, if required, would provide a housing for a lifting crane, service air and water, a radiation control area, auxiliary equipment storage and support services and work areas related to canister

handling and transfer. Transfer operations could include temporary holding of a loaded canister in the transfer cask to allow repair of a concrete cask, transfer of a canister from one concrete cask to another, or transfer from a concrete cask to a transport cask.

The design of the Canister Handling Facility would meet the requirements of the Universal Storage System described in Approved Contents and Design Features presented in Appendix B of the Amendment 3 Technical Specifications, in addition to those requirements established by the site.

The design, analysis, fabrication, operation and maintenance of the Canister Handling Facility would be performed in accordance with the quality assurance program requirements of the site general licensee, or the site-specific licensee of the ISFSI. The Canister Handling Facility would be classified as Important to Safety or Not Important to Safety in accordance with the guidelines of NUREG-6407.

Table 2.3-1 Safety Classification of Universal Storage System Components

Drawing No.	Description	Item No.	Component	Function	Safety Class
790-559	Assembly, Transfer Adapter	17	Cylinder Bolt	Operations	C
		15	Connector Body Bolt	Operations	C
		14	Wear Pad Bolt	Operations	NQ
		13	Wear Pad	Operations	NQ
		12	Connector Body	Operations	C
		10	Cylinder Nut	Operations	C
		8	Door Cylinder	Operations	C
		7	Lift Lug	Operations	C
		6	Support	Operations	C
		5	Side Shield	Operations	C
		3, 4	Door Rail	Operations	C
		2	Locating Ring	Operations	C
		1	Base Plate	Operations	C
790-560	Assembly, Transfer Cask	46	Dowel Pin	Operations	NQ
		45	Fill/Drain Line Pipe	Operations	C
		44	Fill/Drain Line Plate	Operations	C
		43	Shielding Ring	Shielding	B
		42	Transfer Adapter SHCS	Shielding	B
		41	Transfer Cask Extension	Shielding	B
		39	Connector	Operations	C
		38	Retaining Ring Bolt	Operations	B
		37	Scuff Plate	Operations	NQ
		36	Gamma Shield Brick	Shielding	B
		33-34	Neutron Shield Cover Plate	Operations	C
		28-32	Neutron Shield Boundary	Structural	C
		26-27	Bottom Plate	Structural	B
		25	Stainless Steel Sheet	Operations	NQ
		24	Paint	Operations	NQ

Table 2.3-1 Safety Classification of Universal Storage System Components (continued)

Drawing No.	Description	Item No.	Component	Function	Safety Class
790-560 (Continued)	Assembly, Transfer Cask	23	Lead Wool	Operations/Shielding	NQ
		22	Coating	Operations	C
		21	Support Plate	Operations	B
		20	Retaining Ring	Operations	B
		19	Door Lock Bolt	Operations	C
		16	Door Rail	Operations	B
		15	Top Plate	Structural	B
		14	Neutron Shield	Shielding	B
		13	Trunnion Cap	Operations	C
		12	Trunnion	Structural	B
		7-11	Outer Shell	Structural	B
		2-6	Inner Shell	Structural	B
		1	Bottom Plate	Structural	B
790-561	Weldment, Structure, Vertical Concrete Cask	31	Lifting Nut	Operations	NQ
		27-30	Shell	Shielding/Structural	B
		26	Screen Table	Structural	C
		25	Baffle	Heat Transfer	B
		18-24	Outlet (4)	Heat Transfer	B
		20	Shield Plate	Shielding	B
		17	Nelson Stud	Structural	B
		16	Base Plate	Structural	B
		15	Stand	Structural	B
		13-14	Inlet (4)	Heat Transfer	B
		12	Bottom	Structural	B

Table 2.3-1 Safety Classification of Universal Storage System Components (continued)

Drawing No.	Description	Item No.	Component	Function	Safety Class
790-561 (Continued)	Weldment, Structure, Vertical Concrete Cask	11	Shield Ring	Shielding	B
		10	Cover	Operations	B
		4-8	Jack (Leveling)	Operations	NQ
		3	Support Ring	Structural	C
		2	Top Flange	Structural	B
		1	Shell	Structural	B
790-562	Reinforcing Bar And Concrete Placement	32	Base Plate	Structural	B
		31	Lift Lug	Structural	B
		29	Lag Screw	Operations	NQ
		28	Concrete Anchor	Operations	NQ
		25	Outlet Screen	Operations	NQ
		24	Inlet Screen	Operations	NQ
		20-23	Structure Weldment	Shielding/Structural	B
		16-19	Screen/Strip/Screw	Operations	NQ
		15	Concrete Shell	Shielding/ Structural	B
		13	Structure Weldment	Shielding/ Structural	B
		1-11, 33	Reinforcing Bar	Structural	B
790-563	Lid, Vertical Concrete Cask	1	Lid	Structural/Operations	B
790-564	Shield Plug, Vertical Concrete Cask	4	Neutron Shield Cover	Shielding/Operations	B
		3, 5	Neutron Shield	Shielding	B
		2, 6	NS Retaining Ring	Structural	B
		1	Shield Plug	Shielding	B
790-565	Nameplate, Vertical Concrete Cask	1	Nameplate	Operations	NQ

Table 2.3-1 Safety Classification of Universal Storage System Components (Continued)

Drawing No.	Description	Item No.	Component	Function	Safety Class
790-570	BWR Fuel Basket	24	Heat Transfer Disk	Heat Transfer	A
		23	Flat Washer	Structural	C
		22	Split Spacer	Structural	A
		21	Top Spacer	Structural	A
		13-20	Tube	Structural	A
		11-12	Tie Rod	Structural	A
		10	Top Nut	Structural	A
		8-9	Tube (1-Sided)	Structural	A
		7	Spacer	Structural	A
		5-6	Tube (2-Sided)	Structural	A
		4	Drain Tube Sleeve	Operations	C
		3	Support Disk	Structural	A
		2	Top Weldment	Structural	A
		1	Bottom Weldment	Structural	A
790-571	Bottom Weldment, BWR Fuel Basket	3	Support	Structural	A
		2	Pad	Structural	A
		1	Plate	Structural	A
790-572	Top Weldment, BWR Fuel Basket	6	Baffle	Structural	A

Table 2.3-1 Safety Classification of Universal Storage System Components (Continued)

Drawing No.	Description	Item No.	Component	Function	Safety Class
790-573	Support Disk and BWR Basket Details	8	Split Spacer	Structural	A
		7	Top Spacer	Structural	A
		5, 6	Tie Rod	Structural	A
		4	Top Nut	Structural	A
		3	Spacer	Structural	A
		1	Support Disk	Structural	A
790-574	Heat Transfer Disk, BWR		Heat Transfer Disk	Thermal	A
790-575	BWR Fuel Tube	7	Flange	Structural	A
		5-6	Cladding	Criticality Control	A
		3-4	Neutron Absorber	Criticality Control	A
		1-2	Tubing	Structural	A
790-581	PWR Fuel Tube	10	Flange	Structural	A
		7-9	Cladding	Criticality Control	A
		4-6	Neutron Absorber	Criticality Control	A
		1-3	Tubing	Structural	A

Table 2.3-1 Safety Classification of Universal Storage System Components (Continued)

Drawing No.	Description	Item No.	Component	Function	Safety Class
790-582	Canister, Shell	7	Location Lug	Operations	C
		6	Bottom	Structural/Confinement	A
		1-5	Shell	Structural/Confinement	A
790-583	Drain Tube Assembly	7	Metal Boss Seal	Operations	C
		2-6	Tube	Operations	C
		1	Nipple	Operations	C
790-584	Canister Details	8	Key	Operations	C
		7	Spacer Ring	Structural	C
		6	Lid Support Ring	Structural	B
		5	Cover	Confinement/Operations	B
		4	Structural Lid	Structural	A
		3	Metal Boss Seal	Operations	C
		2	Nipple	Operations	C
		1	Shield Lid	Shielding/Confinement	B
790-585	Transportable Storage Canister	24	Dowel Pin	Operations	NQ
		23	Structural Lid Plug	Operations	NQ
		22	Shield Lid Plug	Operations	NQ
		21	Key	Operations	C
		20	Backing Ring	Structural	C
		19	Structural Lid	Structural	A
		18	Cover	Confinement/ Operations	B
		17	Shield Lid Assembly	Shielding	B
		16	Lid Support Ring	Structural	B
		11-15	Drain Tube Assembly	Operations	C

Table 2.3-1 Safety Classification of Universal Storage System Components (Continued)

Drawing No.	Description	Item No.	Component	Function	Safety Class
790-587	Spacer Shim, Canister	1-6	Spacer Shims #1 - #6	Operations	C
790-590	Loaded Vertical Concrete Cask	19	Tab	Operations	NQ
		18	Seal Wire	Operations	C
		17	Security Seal	Operations	C
		16	Seal Tape	Operations	NQ
		15	Cover	Operations	C
		14	Washer (Lid Bolt)	Operations	NQ
		13	Lid Bolt	Operations	B
		12	Cask Lid	Operations	B
		11	Shield Plug	Shielding	B
790-591	Bottom Weldment, PWR Basket	5, 6	Support	Structural	A
		4	Pad	Structural	A
		2, 3	Support	Structural	A
		1	Bottom Disk	Structural	A
790-592	Top Weldment, PWR Basket	7	Baffle	Structural	A
		3-6	Support	Structural	A
		2	Ring	Structural	A
		1	Top Disk	Structural	A
790-593	Support Disk and Details, PWR	8	Top Spacer	Structural	A
		5-7	Tie Rod	Structural	A
		4, 9, 10	Top Nut	Structural	A
		3	Spacer	Structural	A
		2	Split Spacer	Structural	A
		1	Support Disk	Structural	A

Table 2.3-1 Safety Classification of Universal Storage System Components (Continued)

Drawing No.	Description	Item No.	Component	Function	Safety Class
790-594	Heat Transfer Disk, PWR	1	Heat Transfer Disk	Thermal	A
790-595	PWR Fuel Basket	19-20	Top Nut	Structural	A
		17-18	Top Weldment	Structural	A
		16	Top Spacer	Structural	A
		14-15	Tube	Structural	A
		12-13	Tie Rod	Structural	A
		11	Heat Transfer Disk	Heat Transfer	A
		10	Tie Rod	Structural	A
		9	Top Nut	Structural	A
		8	Flat Washer	Structural	C
		7	Split Spacer	Structural	A
		6	Spacer	Structural	A
		4-5	Drain Tube Sleeve/Tube	Operations	C
		3	Support Disk	Structural	A
		2	Top Weldment	Structural	A
		1	Bottom Weldment	Structural	A
790-605	BWR Fuel Tube, Over-Sized	7	Flange	Structural	A
		5-6	Cladding	Criticality Control	A
		3-4	Neutron Absorber	Criticality Control	A
		1-2	Tubing	Structural	A

Table 2.3-1 Safety Classification of Universal Storage System Components (Continued)

Drawing No.	Description	Item No.	Component	Function	Safety Class
790-613	Supplemental Shielding, VCC Inlets	4	Shims	Operations	NQ
		3	Paint	Operations	NQ
		2	Pipe	Shielding	B
		1	Side Plate	Shielding	B
790-617	Door Stop	6	Attachment Screw	Operations	NQ
		5	Lock Pin	Operations	NQ
		4	Handle	Operations	NQ
		3	Back Plate	Operations	NQ
		2	Top Plate	Operations	NQ
		1	Bottom Plate	Operations	NQ
412-502	Maine Yankee (MY) Fuel Can Details, NAC-UMS®	13	Support Ring	Structural/Operations	A
		12	Lift Tee	Structural/Operations	B
		10	Tube Body	Structural/Criticality	A
		9	Side Plate	Structural/Criticality	A
		8	Bottom Plate	Structural/Criticality	A
		7	Backing Screen	Operations	C
		6	Filter Screen	Confinement	B
		4	Wiper	Operations	C
		3	Lid Guide	Operations	C
		2	Lid Plate	Structural/Criticality	A
		1	Lid Collar	Confinement	A

2.4 Decommissioning Considerations

The principal elements of the Universal Storage System are the Vertical Concrete Cask and the Transportable Storage Canister.

The concrete cask provides biological shielding and physical protection for the contents of the canister during long-term storage. The concrete that provides biological shielding is not expected to become contaminated during the period of use, as it does not come into contact with other contaminated objects or surfaces. The concrete cask is not expected to become surface contaminated during use, except through incidental contact with other contaminated surfaces. Incidental contact could occur at the interior surface (liner) of the concrete cask, the top surface that supports the transfer cask during loading and unloading operations, and the base plate of the concrete cask that supports the canister. All of these surfaces are made of carbon steel, and it is anticipated that these surfaces could be decontaminated as necessary for decommissioning.

Activation of the carbon steel liner, concrete, support plates, and reinforcing bar could occur due to neutron flux from the stored fuel. Since the neutron flux rate is low, only minimal activation of carbon steel in the concrete cask is expected to occur. The activity concentrations from activation of storage cask components are listed in Tables 2.4-1 through 2.4-4. Tables 2.4-1 and 2.4-2 provide the activation summaries of the concrete cask and canister for the design-basis PWR fuel, while Tables 2.4-3 and 2.4-4 provide the summaries for the design-basis BWR fuel. These tables include the radiologically significant isotopes, together with a total concentration of all activated nuclides in the respective component. The total concentrations listed include activities of radionuclides, which do not have any substantial contribution to radiation dose and are not specifically identified by 10 CFR 61 waste classification. In particular, the isotope contributing the majority of the carbon steel total curie activity is ^{55}Fe, which decays following electron capture and is not of radiological concern.

Decommissioning of the concrete cask will involve the removal of the canister, and the subsequent disassembly of the concrete cask. It is expected that the concrete will be broken up, and steel components segmented, to reduce volume. Any contaminated or activated items are expected to qualify for near-surface disposal as low specific activity material. The activity concentrations from activation of concrete cask components resulting from the design basis PWR and BWR fuel assemblies are listed in Tables 2.4-1 and 2.4-3, respectively.

The Transportable Storage Canister is designed and fabricated to be suitable for use as part of the waste package for permanent disposal in a deep Mined Geological Disposal System (i.e., it meets the requirements of the DOE MPC Design Procurement Specification [20]). The canister is fabricated from materials having high long-term corrosion resistance, and it contains no paints or coatings that could adversely affect its permanent disposal. Consequently, decommissioning of the canister will occur only if the fuel contained in the canister had to be removed, or if current requirements for disposal were to change. Decommissioning of the canister will require that the closure welds at the canister structural lid, shield lid, and shield lid port covers be cut, so that the spent fuel can be removed. Removal of the contents of the canister will require that the canister be returned to a spent fuel pool or dry unloading facility, such as a hot cell. Closure welds can be cut either manually or with automated equipment, with the procedure being essentially the reverse of that used to initially close the canister.

Following removal of its contents, the canister interior is expected to have significant contamination, and the bottom of the canister may contain "crud" or other residual material. Some effort may be required to remove the surface contamination prior to disposal; however, in practice, it will not be absolutely necessary to decontaminate the canister internals. Since the canister internal contamination will consist only of by-product materials, any contaminated canister and internal components are expected to qualify for near-surface disposal as low specific activity waste without internal contamination. Any required internal decontamination is facilitated, should it become necessary, by the smooth surfaces of the canister and the basket, and by the design that precludes the presence of crud traps. Since the neutron flux rate from the stored fuel is low, only minimal activation of the canister is expected to occur. The activity concentrations from activation of canister components resulting from the design basis PWR and BWR fuel assemblies are listed in Tables 2.4-2 and 2.4-4, respectively.

The unloaded canister can also qualify as a strong, tight container for other waste. In this case, the canister can be filled, within weight limits, with other qualified waste, closed, and transported to a near-surface disposal site. Use of the canister for this purpose can reduce decommissioning costs by avoiding decontamination, segmenting, and repackaging.

The storage pad, fence, and supporting utility fixtures are not expected to require decontamination as a result of use of the Universal Storage System. The design of the cask and canister precludes the release of contamination from the contents over the period of use of the system. Consequently, these items may be reused or disposed of as locally generated clean waste.

Table 2.4-1 Activity Concentration Summary for the Concrete Cask - PWR Design Basis Fuel (Ci/m^3)

Isotope[1]	Concrete Shell	Shell Liner	Shield Plug	Lid	Cover Plate	Bottom	Base Plate
^{14}C	--	--	2.35E-08	--	--	--	--
^{45}Ca	4.62E-06	--	--	--	--	--	--
^{54}Mn	5.13E-08	6.97E-02	1.34E-03	1.63E-04	3.17E-06	5.56E-02	1.88E-02
^{55}Fe	2.30E-05	1.22E+00	2.12E-01	5.49E-02	3.85E-05	7.15E-01	2.27E-01
^{60}Co	1.95E-06	3.43E-04	7.22E-05	1.38E-05	1.54E-05	2.71E-04	8.58E-05
^{63}Ni	--	--	--	--	2.02E-02	--	--
Total	3.09E-05	1.30E+00	2.15E-01	5.54E-02	2.06E-02	7.77E-01	2.48E-01

1. 40-year activation, 1-week cooling.

Table 2.4-2 Activity Concentration Summary for the Canister – PWR Design Basis Fuel (Ci/m^3)

Isotope[1]	Wall	Shield Lid	Structural Lid	Bottom
^{54}Mn	9.94E-05	3.32E-04	4.42E-06	1.00E-04
^{55}Fe	7.94E-04	8.26E-04	3.67E-04	1.05E-03
^{60}Co	3.15E-04	3.31E-04	1.47E-04	4.22E-04
^{59}Ni	3.54E-07	3.67E-07	1.64E-07	4.66E-07
^{63}Ni	4.17E-01	4.33E-01	1.93E-01	5.49E-01
Total	4.27E-01	4.43E-01[2]	1.97E-01[2]	5.63E-01[2]

1. 40-year activation, 1 -week cooling.
2. ^{32}P accounts for most of the unlisted total activity.

Table 2.4-3 Activity Concentration Summary for the Concrete Cask – BWR Design Basis Fuel (Ci/m^3)

Isotope[1]	Concrete Shell	Shell Liner	Shield Plug	Lid	Cover Plate	Bottom	Base Plate
^{14}C	--	--	3.57E-08	--	--	--	--
^{45}Ca	7.91E-06	--	--	--	--	--	--
^{54}Mn	7.74E-08	1.07E-01	1.97E-03	2.39E-04	1.37E-06	7.06E-02	2.40E-02
^{55}Fe	3.93E-05	2.10E00	3.23E-01	8.29E-02	2.08E-05	1.13E-04	3.52E-01
^{60}Co	3.33E-06	5.93E-04	1.10E-04	2.08E-05	8.35E-06	4.26E-04	1.33E-04
^{63}Ni	--	--	--	--	1.09E-02	--	--
Total	5.28E-05	2.22E00	3.27E-01	8.37E-02	1.12E-02	1.21E00	3.79E-01

1. 40-year activation, 1-week cooling.

Table 2.4-4 Activity Concentration Summary for the Canister – BWR Design Basis Fuel (Ci/m^3)

Isotope[1]	Wall	Shield Lid	Structural Lid	Bottom
^{54}Mn	1.53E-04	4.89E-05	6.51E-06	1.26E-04
^{55}Fe	1.39E-03	1.26E-06	5.57E-04	1.68E-03
^{60}Co	5.52E-04	5.04E-04	2.22E-04	6.73E-04
^{59}Ni	6.21E-07	5.60E-07	2.48E-07	7.46E-07
^{63}Ni	7.31E-01	6.60E-01	2.92E-01	8.79E-01
Total	7.49E-01	6.76E-01	2.99E-01	9.00E-01

1. 40-year activation, 1-week cooling.

2.5 References

1. ASME Boiler and Pressure Vessel Code, Division I, Section III, Subsection NB, "Class 1 Components," 1995 Edition with 1995 Addenda.

2. ASME Boiler and Pressure Vessel Code, Division I, Section III, Subsection NG, "Core Support Structures," 1995 Edition with 1995 Addenda.

3. Nuclear Regulatory Commission, "Buckling Analysis of Spent Fuel Basket," NUREG/CR-6322, May 1995.

4. American Concrete Institute, "Code Requirements for Nuclear Safety Related Concrete Structures (ACI 349-85) and Commentary (ACI 349R-85)," March 1986.

5. American Concrete Institute, "Building Code Requirements for Structural Concrete (ACI 318-95) and Commentary (ACI 318R-95), October 1995.

6. ANSI N14.6-1993, "American National Standard for Radioactive Materials - Special Lifting Devices for Shipping Containers Weighing 10,000 Pounds (4,500 kg) or More," American National Standards Institute, Inc., June 1993.

7. Nuclear Regulatory Commission, "Control of Heavy Loads at Nuclear Power Plants," NUREG-0612, July 1980.

8. Levy, et al., Pacific Northwest Laboratory, "Recommended Temperature Limits for Dry Storage of Spent Light-Water Zircalloy Clad Fuel Rods in Inert Gas," PNL-6189, May 1987.

9. Nuclear Regulatory Commission, "Design Basis Tornado for Nuclear Power Plants," Regulatory Guide 1.76, April 1974.

10. Nuclear Regulatory Commission, "Standard Review Plan," NUREG-0800, April 1996.

11. Code of Federal Regulations, "Licensing Requirements for the Independent Storage of Spent Nuclear Fuel and High-Level Radioactive Waste," Part 72, Title 10, January 1996.

12. ANSI/ASCE 7-93 (formerly ANSI A58.1), "Minimum Design Loads for Buildings and Other Structures," American Society of Civil Engineers, May 1994.

13. ANSI/ANS-57.9-1992, "Design Criteria for an Independent Spent Fuel Storage Installation (Dry Type)," American Nuclear Society, May 1992.

14. ASHRAE Handbook, "Fundamentals," American Society of Heating, Refrigeration, and Air Conditioning Engineers, 1993.

15. Code of Federal Regulations, "Packaging and Transportation of Radioactive Materials," Part 71, Title 10, April 1996.

16. Nuclear Regulatory Commission, "Load Combinations for the Structural Analysis of Shipping Casks for Radioactive Material," Regulatory Guide 7.8, March 1989.

17. Nuclear Regulatory Commission, "Establishing Quality Assurance Programs for Packaging Used in the Transport of Radioactive Material," Regulatory Guide 7.10, June 1986.

18. Nuclear Regulatory Commission, "Classification of Transportation Packaging and Dry Spent Fuel Storage System Components According to Importance to Safety," NUREG/CR-6407, February 1996.

19. Code of Federal Regulations, "Standards for Protection Against Radiation," Part 20, Title 10, January 1991.

20. Department of Energy, "Multi-Purpose Canister (MPC) Subsystem Design Procurement Specification," Document No. DBG000000-01717-6300-00001, Rev. 6, June 1996.

21. Johnson, A.B., and Gilbert, E.R., Pacific Northwest Laboratory, "Technical Basis for Storage of Zircaloy-Clad Spent Fuel in Inert Gases," PNL-4835, September, 1983.

22. Garde, M., "Hot Cell Examination of Extended Burnup Fuel from Fort Calhoun," DOE/ET/34030-11, CEND-427A, September 1986.

23. Newman, L. M., "The Hot Cell Examination of Oconee 1 Fuel Rods after Five Cycles of Irradiation," DOE/ET/34212-50, BAW-1874L, October 1986.

24. Nuclear Regulatory Commission, "Standard Review Plan for Dry Cask Storage Systems," NUREG-1536, January 1997.

25. Nuclear Regulatory Commission, "Cladding Considerations for the Transport and Storage of Spent Fuel," Interim Staff Guidance-11, Revision 2.

Table of Contents

3.0 STRUCTURAL EVALUATION 3.1-1

3.1 Structural Design 3.1-1
- 3.1.1 Discussion 3.1-2
- 3.1.2 Design Criteria 3.1-6

3.2 Weights and Centers of Gravity 3.2-1

3.3 Mechanical Properties of Materials 3.3-1
- 3.3.1 Primary Component Materials 3.3-1
- 3.3.2 Fracture Toughness Considerations 3.3-16

3.4 General Standards 3.4.1-1
- 3.4.1 Chemical and Galvanic Reactions 3.4.1-1
  - 3.4.1.1 Component Operating Environment 3.4.1-1
  - 3.4.1.2 Component Material Categories 3.4.1-2
  - 3.4.1.3 General Effects of Identified Reactions 3.4.1-12
  - 3.4.1.4 Adequacy of the Canister Operating Procedures 3.4.1-12
  - 3.4.1.5 Effects of Reaction Products 3.4.1-12
- 3.4.2 Positive Closure 3.4.2-1
- 3.4.3 Lifting Devices 3.4.3-1
  - 3.4.3.1 Vertical Concrete Cask Lift Evaluation 3.4.3-5
  - 3.4.3.2 Canister Lift 3.4.3-28
  - 3.4.3.3 Standard Transfer Cask Lift 3.4.3-35
  - 3.4.3.4 Advanced Transfer Cask Lift 3.4.3-66
- 3.4.4 Normal Operating Conditions Analysis 3.4.4-1
  - 3.4.4.1 Canister and Basket Analyses 3.4.4-1
  - 3.4.4.2 Vertical Concrete Cask Analyses 3.4.4-63
- 3.4.5 Cold 3.4.5-1

3.5 Fuel Rods 3.5-1

Table of Contents (Continued)

3.6 Structural Evaluation of Site Specific Spent Fuel 3.6-1
3.6.1 Structural Evaluation of Maine Yankee Site Specific Spent Fuel for Normal Operating Conditions 3.6-1
3.6.1.1 Maine Yankee Intact Spent Fuel 3.6-1
3.6.1.2 Maine Yankee Damaged Spent Fuel 3.6-2

3.7 References 3.7-1

3.8 Carbon Steel Coatings Technical Data 3.8-1
3.8.1 Carboline 890 ..... 3.8-2
3.8.2 Keeler & Long E-Series Epoxy Enamel 3.8-4
3.8.3 Description of Electroless Nickel Coating 3.8-8
3.8.4 Keeler & Long Kolor-Poxy Primer No. 3200 ..... 3.8-12
3.8.5 Acrythane Enamel Y-1 Series Top Coating 3.8-14

List of Figures

Figure 3.1-1 Principal Components of the Universal Storage System 3.1-7
Figure 3.4.2-1 Universal Storage System Welded Canister Closure 3.4.2-2
Figure 3.4.3-1 Standard Transfer Cask Lifting Trunnion 3.4.3-3
Figure 3.4.3-2 Canister Hoist Ring Design 3.4.3-4

Figure 3.4.3.1-1 Base Weldment Finite Element Model 3.4.3-27
Figure 3.4.3.2-1 Canister Lift Finite Element Model 3.4.3-33
Figure 3.4.3.2-2 Canister Lift Model Stress Intensity Contours (psi) 3.4.3-34
Figure 3.4.3.3-1 Finite Element Model for Standard Transfer Cask Trunnion and Shells 3.4.3-55
Figure 3.4.3.3-2 Node Locations for Standard Transfer Cask Outer Shell Adjacent to Trunnion 3.4.3-56
Figure 3.4.3.3-3 Node Locations for Standard Transfer Cask Inner Shell Adjacent to Trunnion 3.4.3-57
Figure 3.4.3.3-4 Stress Intensity Contours (psi) for Standard Transfer Cask Outer Shell Element Top Surface 3.4.3-58
Figure 3.4.3.3-5 Stress Intensity Contours (psi) for Standard Transfer Cask Outer Shell Element Bottom Surface 3.4.3-59
Figure 3.4.3.3-6 Stress Intensity Contours (psi) for Standard Transfer Cask Inner Shell Element Top Surface 3.4.3-60
Figure 3.4.3.3-7 Stress Intensity Contours (psi) for Standard Transfer Cask Inner Shell Element Bottom Surface 3.4.3-61
Figure 3.4.3.4-1 Advanced Transfer Cask Finite Element Model 3.4.3-83
Figure 3.4.3.4-2 Node Locations for Advanced Transfer Cask Outer Shell Adjacent to Trunnion 3.4.3-84
Figure 3.4.3.4-3 Node Locations for Advanced Transfer Cask Inner Shell Adjacent to Trunnion 3.4.3-85
Figure 3.4.3.4-4 Node Locations for Advanced Transfer Cask Stiffener Plate Above Trunnion 3.4.3-86
Figure 3.4.3.4-5 Stress Intensity Contours (psi) for Advanced Transfer Cask Outer Shell Element Top Surface 3.4.3-87
Figure 3.4.3.4-6 Stress Intensity Contours (psi) for Advanced Transfer Cask Outer Shell Element Bottom Surface 3.4.3-88

List of Figures (Continued)

Figure 3.4.3.4-7 Stress Intensity Contours (psi) for Advanced Transfer Cask Inner Shell Element Top Surface 3.4.3-89
Figure 3.4.3.4-8 Stress Intensity Contours (psi) for Advanced Transfer Cask Inner Shell Element Bottom Surface 3.4.3-90
Figure 3.4.3.4-9 Stress Intensity Contours (psi) for Advanced Transfer Cask Stiffener Plate Element Top Surface 3.4.3-91
Figure 3.4.3.4-10 Stress Intensity Contours (psi) for Advanced Transfer Cask Stiffener Plate Element Bottom Surface 3.4.3-92
Figure 3.4.4.1-1 Canister Composite Finite Element Model 3.4.4-20
Figure 3.4.4.1-2 Weld Regions of Canister Composite Finite Element Model at Structural and Shield Lids 3.4.4-21
Figure 3.4.4.1-3 Bottom Plate of the Canister Composite Finite Element Model 3.4.4-22
Figure 3.4.4.1-4 Locations for Section Stresses in the Canister Composite Finite Element Model 3.4.4-23
Figure 3.4.4.1-5 BWR Fuel Assembly Basket Showing Typical Fuel Basket Components 3.4.4-24
Figure 3.4.4.1-6 PWR Fuel Basket Support Disk Finite Element Model 3.4.4-25
Figure 3.4.4.1-7 PWR Fuel Basket Support Disk Sections for Stress Evaluation (Left Half) 3.4.4-26
Figure 3.4.4.1-8 PWR Fuel Basket Support Disk Sections for Stress Evaluation (Right Half) 3.4.4-27
Figure 3.4.4.1-9 PWR Class 3 Fuel Tube Configuration 3.4.4-28
Figure 3.4.4.1-10 PWR Top Weldment Plate Finite Element Model 3.4.4-29
Figure 3.4.4.1-11 PWR Bottom Weldment Plate Finite Element Model 3.4.4-30
Figure 3.4.4.1-12 BWR Fuel Basket Support Disk Finite Element Model 3.4.4-31
Figure 3.4.4.1-13 BWR Fuel Basket Support Disk Sections for Stress Evaluation (Quadrant I) 3.4.4-32
Figure 3.4.4.1-14 BWR Fuel Basket Support Disk Sections for Stress Evaluation (Quadrant II) 3.4.4-33
Figure 3.4.4.1-15 BWR Fuel Basket Support Disk Sections for Stress Evaluation (Quadrant III) 3.4.4-34
Figure 3.4.4.1-16 BWR Fuel Basket Support Disk Sections for Stress Evaluation (Quadrant IV) 3.4.4-35

List of Figures (Continued)

Figure 3.4.4.1-17 BWR Class 5 Fuel Tube Configuration 3.4.4-36
Figure 3.4.4.1-18 BWR Top Weldment Plate Finite Element Model 3.4.4-37
Figure 3.4.4.1-19 BWR Bottom Weldment Plate Finite Element Model 3.4.4-38
Figure 3.4.4.2-1 Concrete Cask Thermal Stress Model 3.4.4-70
Figure 3.4.4.2-2 Concrete Cask Thermal Stress Model - Vertical and Horizontal Rebar Detail 3.4.4-71
Figure 3.4.4.2-3 Concrete Cask Thermal Stress Model Boundary Conditions 3.4.4-72
Figure 3.4.4.2-4 Concrete Cask Thermal Model Axial Stress Evaluation Locations 3.4.4-73
Figure 3.4.4.2-5 Concrete Cask Thermal Model Circumferential Stress Evaluation Locations 3.4.4-74

List of Tables

Table 3.2-1 Universal Storage System Weights and CGs – PWR Configuration 3.2-2
Table 3.2-2 Universal Storage System Weights and CGs – BWR Configuration 3.2-3
Table 3.2-3 Calculated Under-Hook Weights for the Standard Transfer Cask 3.2-4
Table 3.3-1 Mechanical Properties of SA-240 and A-240, Type 304 Stainless Steel 3.3-3
Table 3.3-2 Mechanical Properties of SA-479, Type 304 Stainless Steel 3.3-4
Table 3.3-3 Mechanical Properties of SA-240, Type 304L Stainless Steel 3.3-5
Table 3.3-4 Mechanical Properties of SA-564 and SA-693, Type 630, 17-4 PH Stainless Steel 3.3-6
Table 3.3-5 Mechanical Properties of A-36 Carbon Steel 3.3-7
Table 3.3-6 Mechanical Properties of A615, Grade 60, A615, Grade 75 and A-706 Reinforcing Steel 3.3-7
Table 3.3-7 Mechanical Properties of SA-533, Type B, Class 2 Carbon Steel 3.3-8
Table 3.3-8 Mechanical Properties of A-588, Type A or B Low Alloy Steel 3.3-9
Table 3.3-9 Mechanical Properties of SA-350/A-350, Grade LF 2, Class 1 Low Alloy Steel 3.3-10
Table 3.3-10 Mechanical Properties of SA-193, Grade B6, High Alloy Steel Bolting Material 3.3-11
Table 3.3-11 Mechanical Properties of 6061-T651 Aluminum Alloy 3.3-12
Table 3.3-12 Mechanical Properties of Concrete 3.3-13
Table 3.3-13 Mechanical Properties of NS-4-FR and NS-3 ..... 3.3-14
Table 3.3-14 Mechanical Properties of SA-516, Grade 70 Carbon Steel 3.3-15
Table 3.4.3.3-1 Top 30 Stresses for Standard Transfer Cask Outer Shell Element Top Surface 3.4.3-62
Table 3.4.3.3-2 Top 30 Stresses for Standard Transfer Cask Outer Shell Element Bottom Surface 3.4.3-63
Table 3.4.3.3-3 Top 30 Stresses for Standard Transfer Cask Inner Shell Element Top Surface 3.4.3-64
Table 3.4.3.3-4 Top 30 Stresses for Standard Transfer Cask Inner Shell Element Bottom Surface 3.4.3-65

List of Tables (Continued)

Table 3.4.3.4-1 Top 30 Stresses for Advanced Transfer Cask Outer Shell Element Top Surface 3.4.3-93
Table 3.4.3.4-2 Top 30 Stresses for Advanced Transfer Cask Outer Shell Element Bottom Surface 3.4.3-94
Table 3.4.3.4-3 Top 30 Stresses for Advanced Transfer Cask Inner Shell Element Top Surface 3.4.3-95
Table 3.4.3.4-4 Top 30 Stresses for Advanced Transfer Cask Inner Shell Element Bottom Surface 3.4.3-96
Table 3.4.3.4-5 Top 30 Stresses for Advanced Transfer Cask Stiffener Plate Element Top Surface 3.4.3-97
Table 3.4.3.4-6 Top 30 Stresses for Advanced Transfer Cask Stiffener Plate Element Bottom Surface 3.4.3-98
Table 3.4.4.1-1 Canister Secondary (Thermal) Stresses (ksi). 3.4.4-39
Table 3.4.4.1-2 Canister Dead Weight Primary Membrane (P_m) Stresses (ksi), $P_{internal}$ = 0 psig 3.4.4-40
Table 3.4.4.1-3 Canister Dead Weight Primary Membrane plus Bending ($P_m + P_b$) Stresses (ksi), $P_{internal}$ = 0 psig 3.4.4-41
Table 3.4.4.1-4 Canister Normal Handling With No Internal Pressure Primary Membrane (P_m) Stresses, (ksi) 3.4.4-42
Table 3.4.4.1-5 Canister Normal Handling With No Internal Pressure Primary Membrane plus Bending ($P_m + P_b$) Stresses (ksi) 3.4.4-43
Table 3.4.4.1-6 Summary of Canister Normal Handling plus Normal Internal Pressure Primary Membrane (P_m) Stresses (ksi). 3.4.4-44
Table 3.4.4.1-7 Summary of Canister Normal Handling, Plus Normal Pressure Primary Membrane plus Bending ($P_m + P_b$) Stresses (ksi). 3.4.4-45
Table 3.4.4.1-8 Summary of Maximum Canister Normal Handling, plus Normal Pressure, plus Secondary (P + Q) Stresses (ksi) 3.4.4-46
Table 3.4.4.1-9 Canister Normal Internal Pressure Primary Membrane (P_m) Stresses (ksi) 3.4.4-47
Table 3.4.4.1-10 Canister Normal Internal Pressure Primary Membrane plus Bending ($P_m + P_b$) Stresses (ksi) 3.4.4-48
Table 3.4.4.1-11 Listing of Sections for Stress Evaluation of PWR Support Disk 3.4.4-49
Table 3.4.4.1-12 $P_m + P_b$ Stresses for PWR Support Disk - Normal Conditions (ksi) 3.4.4-52

List of Tables (Continued)

Table 3.4.4.1-13 $P_m + P_b + Q$ Stresses for the PWR Support Disk - Normal Conditions (ksi) 3.4.4-53
Table 3.4.4.1-14 Listing of Sections for Stress Evaluation of BWR Support Disk 3.4.4-54
Table 3.4.4.1-15 $P_m + P_b$ Stresses for BWR Support Disk - Normal Conditions (ksi) 3.4.4-60
Table 3.4.4.1-16 $P_m + P_b + Q$ Stresses for BWR Support Disk - Normal Conditions (ksi) 3.4.4-61
Table 3.4.4.1-17 Summary of Maximum Stresses for PWR and BWR Fuel Basket Weldments - Normal Conditions (ksi) 3.4.4-62
Table 3.4.4.2-1 Summary of Maximum Stresses for Vertical Concrete Cask Load Combinations 3.4.4-75
Table 3.4.4.2-2 Maximum Concrete and Reinforcing Bar Stresses 3.4.4-76
Table 3.4.4.2-3 Concrete Cask Average Concrete Axial Tensile Stresses 3.4.4-77
Table 3.4.4.2-4 Concrete Cask Average Concrete Hoop Tensile Stresses 3.4.4-77

3.0 STRUCTURAL EVALUATION

This chapter describes the design and analysis of the principal structural components of the Universal Storage System under normal operating conditions. It demonstrates that the Universal Storage System meets the structural requirements for confinement of contents, criticality control, radiological shielding, and contents retrievability required by 10 CFR 72 [1] for the design basis normal operating conditions. Off-normal and accident conditions are evaluated in Chapter 11.0.

3.1 Structural Design

The Universal Storage System includes five configurations to accommodate three classes of PWR and two classes of BWR fuel assemblies. The five classes of fuel are determined primarily by the overall length of the fuel assembly. The allocation of a fuel design to a UMS class is shown in Tables 2.1.1-1 and 2.1.2-1 for PWR and BWR fuel, respectively.

The three major components of the Universal Storage System are the vertical concrete cask; the transportable storage canister (canister), and the transfer cask (see Figure 3.1-1). These components are provided in five different lengths to accommodate the five classes of fuel. They also have different weights, as shown in Table 3.2-1 for the PWR configurations, and in Table 3.2-2 for the BWR configurations. The weight differences reflect the differences in length of components and fuel, and differences in basket design between the PWR and BWR configurations.

The principal structural members of the vertical concrete cask are the reinforced concrete shell and steel liner. The principal structural members of the canister are the structural lid, shell, bottom plate, the welds joining these components, and the fuel basket assembly. For the transfer cask, the trunnions, the inner and outer steel walls, the bottom shield doors, and the shield door support rails, are the principal structural components.

The evaluations presented in this chapter are based on the bounding or limiting configuration of the UMS System for the condition being evaluated. In most cases, the bounding condition evaluates the heaviest configuration of the five classes. For each evaluated condition, the bounding configuration applied is identified. Margins of safety greater than ten are generally stated in the analyses as "+Large." Numerical values are shown for Margins of safety that are less than ten.

3.1.1 Discussion

The transportable storage canister is designed to be transported in the Universal Transport Cask (USNRC Docket Number 71-9270 [2]. Consequently, the canister diameter is same for each of the five configurations. The outside diameter of the vertical concrete cask is established by the shielding requirement for the design basis fuel used for the shielding evaluation. The shielding required for the design basis fuel is conservatively applied to the five concrete cask configurations.

Vertical Concrete Cask

The vertical concrete cask is a reinforced concrete cylinder with an outside diameter of 136 in. and an overall height (including the lid) ranging from 210.68 in. to 227.38 in., depending upon the configuration. The internal cavity of the concrete cask is lined by a 2.5-inch thick carbon steel inner shell having an inside diameter of 74.5 in. The support ring for the concrete cask shield plug at the top of the inner shell limits the available contents diameter to less than 69.5 in. The inner shell thickness is primarily determined by radiation shielding requirements, but is also related to the need to establish a practical limit for the diameter of the concrete shell. The concrete shell is constructed using Type II Portland Cement and has a nominal density of 140 lb/ft^3 and a nominal compressive strength of 4000 psi. The inner and outer rebar assemblies are formed by vertical hook bars and horizontal hoop bars.

A ventilation air-flow path is formed by inlets at the bottom of the cask, the annular space between the cask inner shell and the canister, and outlets near the top of the cask. The passive ventilation system operates by natural convection as cool air enters the bottom inlets, is heated by the canister, and exits from the top outlets.

A shield plug that consists of 4.125 inches of carbon steel and either a 1-inch thick layer of NS-4-FR or a 1.5-inch thick layer of NS-3 neutron shield material enclosed by the carbon steel is installed in the concrete cask cavity above the canister. The plug is supported by a support ring welded to the inner shell. The 1.5-in. thick carbon steel lid provides a cover to protect the canister from adverse environmental conditions and postulated tornado driven missiles. The shield plug and lid provide shielding to reduce the skyshine radiation. When the lid is bolted in place, the shield plug is secured between the lid and the shield plug support ring.

Transportable Storage Canister

The transportable storage canister consists of a cylindrical shell assembly closed at its top end by an inner shield lid and an outer structural lid. The canister forms the confinement boundary for the basket assembly that contains the PWR or BWR spent fuel. Three canister classes accommodate the PWR fuel assemblies (Tables 2.1.1-1) and two canister classes accommodate the BWR fuel assemblies (Table 2.1.2-1). The canister is fabricated from Type 304L stainless steel. The canister shield lid is 7-in. thick, SA-240 Type 304 stainless steel, and the structural lid is 3.0-in. thick SA-240, Type 304L stainless steel. SA-182 Type 304 stainless steel may be substituted for the SA-240 Type 304 stainless steel used in the shield lid, provided that the SA-182 material has yield and ultimate strengths equal to or greater than those of the SA-240 material. Similarly, SA-182 Type 304L stainless steel may be substituted for the SA-240 Type 304L stainless steel used in the structural lid, provided that the SA-182 material has yield and ultimate strengths equal to or greater than those of the SA-240 material. Both lids are welded to the canister shell to close the canister. The minimum weld sizes for the PWR canister are 0.75 inch for the structural lid and 0.375 inch for the shield lid. For analysis purposes, bounding PWR canister results are reported except for the BWR canister tip-over evaluation (Section 11.2.12.3.2). The minimum weld sizes for the BWR canister are 0.875 inch for the structural lid and 0.5 inch for the shield lid. The shield lid is supported by a support ring. The structural lid is supported, prior to welding, by the shield lid. A groove is machined into the structural lid circumference to accept a spacer ring. The spacer ring facilitates welding of the structural lid to the canister shell. The bottom of the canister is a 1.75-in. thick SA-240, Type 304L stainless steel plate that is welded to the canister shell. The canister is also described in Section 1.2.1.1.

The fuel basket assembly is provided in two configurations — one for up to 24 PWR fuel assemblies and one for up to 56 BWR fuel assemblies. The PWR basket is comprised of Type 17-4 PH stainless steel support disks, Type 6061-T651 aluminum alloy heat transfer disks, and Type 304 stainless steel fuel tubes equipped with a neutron absorber and stainless steel cover. The remaining structural components are Type 304 stainless steel. The BWR basket is comprised of SA-533 carbon steel support disks coated with electroless nickel, Type 6061-T651 aluminum alloy heat transfer disks, and fuel tubes constructed of the same materials as the PWR tubes. The remaining structural components of the BWR basket are Type 304 stainless steel. The basket assemblies are more fully described in Section 1.2.1.2.

The fuel basket support disks, heat transfer disks, and fuel tubes, together with the top and bottom weldments, are positioned by tie rods (with spacers and washers) that extend the length of the basket and hold the assembly together. The support disks provide structural support for the fuel tubes. They also help to remove heat from the fuel tubes. The heat transfer disks provide the primary heat removal capability and are not considered to be structural components. The heat transfer disks are sized so that differential thermal expansion does not result in disk contact with the canister shell. The number of heat transfer disks and support disks varies depending upon the length of the fuel to be confined in the basket. The fuel tubes house the spent fuel assemblies. The top and bottom weldments provide longitudinal support for the fuel tubes. The fuel tubes are fabricated from Type 304 stainless steel. No structural credit is taken for the presence of the fuel tubes in the basket assembly analysis. The walls of each PWR fuel tube support a sheet of neutron absorber material that is covered by stainless steel. No structural credit is taken in the basket assembly analysis for the neutron absorber sheet or its stainless steel cover. The PWR assembly fuel tubes have a nominal inside dimension of 8.8-inches square and a composite wall thickness of 0.14 inch. The BWR assembly fuel tubes have a nominal inside dimension of 5.9-inches square and a composite wall thickness of 0.20 inch. Depending upon its location in the basket assembly, an individual BWR fuel tube may support neutron absorber material on one or two sides. Certain fuel tubes located on the outer edge of the basket do not have neutron absorber material. The fuel tubes have been evaluated to ensure that the neutron absorber material remains in place under normal conditions and design basis off-normal and accident events.

Four over-sized fuel storage positions are located on the periphery of the BWR basket to provide additional space for BWR fuel assemblies with channels that have been reused, since reused channels are expected to have increased bowing or bulging. Normal BWR fuel assemblies may also be stored in these locations.

As mentioned above, five classes of transportable storage canisters are provided for the storage of PWR and BWR spent fuel. The analysis is based on the identification of bounding conditions and the application of those conditions to determine the maximum stresses.

The canister is designed to be transported in the Universal Transport Cask. Transport conditions establish the design basis loading, except for lifting, because the hypothetical accident transport conditions produce higher stresses in the canister and basket than do the design basis storage conditions. Consequently, the canister and basket design is conservative with respect to storage conditions. The evaluation of the canister and basket assembly for transport conditions is documented in the Safety Analysis Report for the Universal Transport Cask [2].

Transfer Cask

The transfer cask, with its lifting yoke, is primarily a lifting device used to move the canister. It provides biological shielding when it contains a loaded canister. The transfer cask is provided in the Standard configuration for canisters weighing up to 88,000 lbs, or in the Advanced configuration for canisters weighing up to 98,000 lbs. The transfer cask configurations have identical operational features. The transfer cask is a heavy lifting device that is designed, fabricated and load-tested to the requirements of NUREG-0612 [8] and ANSI N14.6 [9]. The transfer cask design incorporates a top retaining ring, which is bolted in place to prevent a loaded canister from being inadvertently lifted through the top of the transfer cask. The transfer cask has retractable bottom shield doors. During loading operations, the doors are closed and secured by bolts/pins, so they cannot inadvertently open. During unloading, the doors are retracted using hydraulic cylinders to allow the canister to be lowered into the storage or transport cask. The principal design parameters of the transfer casks are shown in Table 1.2-7.

Both transfer cask configurations are provided in five different lengths to accommodate the canisters containing one of the three classes of PWR fuel assemblies or two classes of BWR fuel assemblies.

The transfer cask is used for the vertical transfer of the canister between work stations and the concrete cask, or transport cask. It incorporates a multiwall (steel/lead/NS-4-FR/steel) design to provide radiation shielding.

Component Evaluation

The following components are evaluated in this chapter:

- canister lifting devices,
- canister shell, bottom, and structural lid,
- canister shield lid support ring,
- fuel basket assembly,
- transfer cask trunnions, shells, retaining ring, bottom doors, and support rails,
- vertical concrete cask body, and
- concrete cask steel components (reinforcement, inner shell, lid, bottom plate, bottom, etc.).

Other Universal Storage System components shown on the license drawings in Chapter 1 are included as loads in the evaluation of the components listed above, as appropriate.

The structural evaluations in this chapter demonstrate that the Universal Storage System components meet their structural design criteria and are capable of safely storing the design basis PWR or BWR spent fuel.

3.1.2 Design Criteria

The Universal Storage System structural design criteria are described in Section 2.2. Load combinations for normal, off-normal, and accident loads are evaluated in accordance with ANSI/ANS 57.9 [3] and ACI-349 [4] for the concrete cask (see Table 2.2-1), and in accordance with the ASME Code, Section III, Division I, Subsection NB [5] for Class 1 components of the canister (see Table 2.2-2). The basket is evaluated in accordance with ASME Code, Section III, Subsection NG [6], and NUREG-6322 [7]. The transfer cask and the lifting yoke are lifting devices that are designed to NUREG-0612 [8] and ANSI N14.6 [9].

Figure 3.1-1 Principal Components of the Universal Storage System

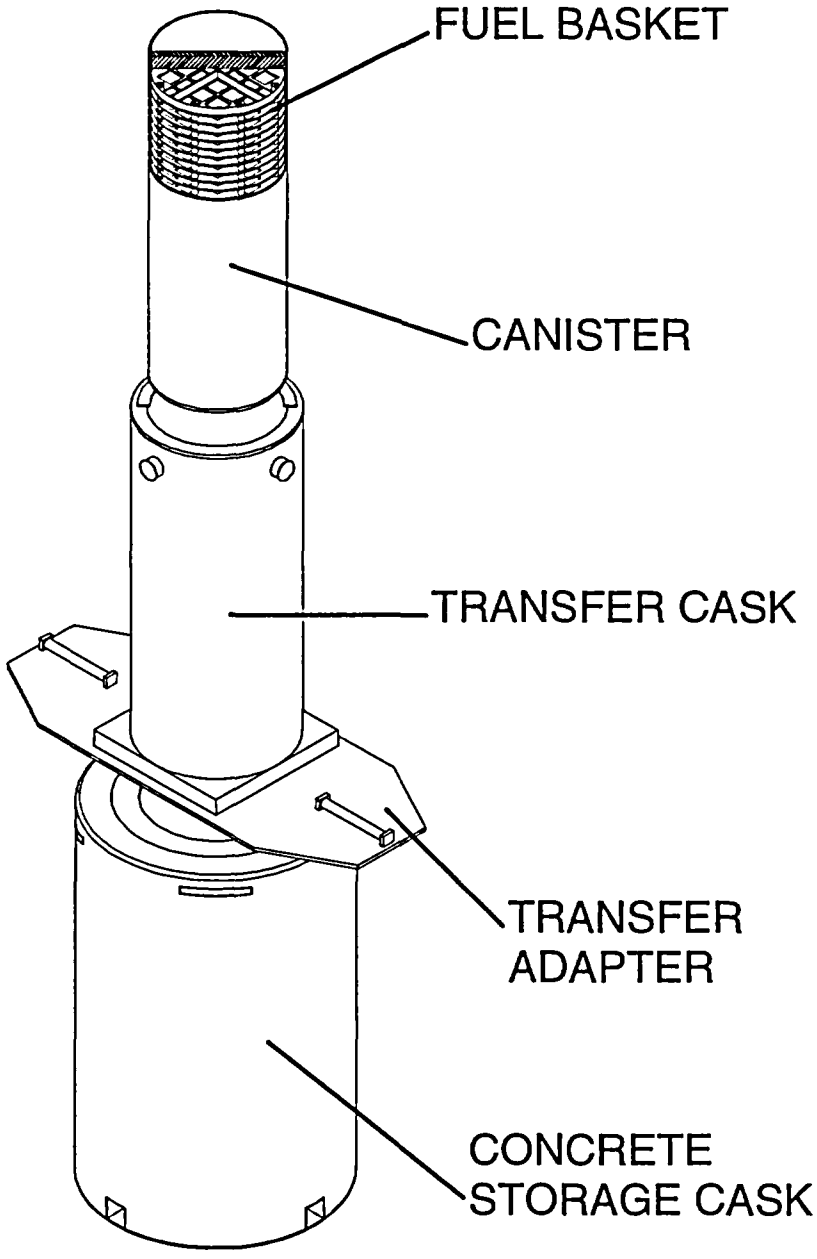

Note: Standard transfer cask shown.

THIS PAGE INTENTIONALLY LEFT BLANK

3.2 Weights and Centers of Gravity

The weights and centers of gravity (CGs) for the Universal Storage System PWR configuration and components are summarized in Table 3.2-1. Those for the BWR configuration are summarized in Table 3.2-2. The weights and CGs presented in this section are calculated on the basis of nominal design dimensions.

Table 3.2-1 Universal Storage System Weights and CGs – PWR Configuration

Description	Class 1		Class 2		Class 3	
	Calculated Weight (lb)	Center of Gravity[1]	Calculated Weight (lb)	Center of Gravity[1]	Calculated Weight (lb)	Center of Gravity[1]
Fuel Contents (including inserts)	37,700	—	38,500	—	35,600	—
Poison Rods (Inserts)	(1,400)	—	(1,400)	—	—	—
Concrete Cask Lid	2,500	—	2,500	—	2,500	—
Concrete Cask Shield Plug	4,900	—	4,900	—	4,900	—
Canister (empty, w/o lids)	8,400	—	8,700	—	9,000	—
Canister Structural Lid	3,000	—	3,000	—	3,000	—
Canister Shield Lid	7,000	—	7,000	—	7,000	—
Transfer Adapter Plate	11,200	—	11,200	—	11,200	—
Transfer Cask Lifting Yoke[4]	6,000	—	6,000	—	6,000	—
Water in Canister	14,000	—	14,800	—	15,800	—
Basket	14,900	—	16,000	—	16,500	—
Canister (with basket, without fuel or lids)	23,300	—	24,700	—	25,500	—
Canister (with fuel, and shield and structural lids)	70,600	—	72,900	—	70,800	—
Concrete Cask (empty, with shield plug and lid; includes optional lift lugs) – 140 pcf concrete	223,500	—	232,300	—	239,700	—
Concrete Cask (with loaded Canister and lids; includes optional lift lugs)[2] – 140 pcf concrete	294,100	108.8	305,100	113.1	310,400	117.1
Concrete Cask with Lift Anchors (empty, with shield plug and lid) – 148 pcf concrete	232,600	—	241,700	—	249,400	—
Concrete Cask with Lift Anchors (with loaded Canister and lids)[2] – 148 pcf concrete	303,300	108.7	314,600	112.9	320,200	117.0
Transfer Cask (empty)[3]	112,300	—	117,300	—	121,500	—
Transfer Cask and Canister, basket (empty, without lids)[3]	135,500	—	141,900	—	146,900	—
Transfer Cask and Canister (with fuel, water and shield lid)[3]	193,900	—	201,900	—	205,000	—
Transfer Cask and Canister (with fuel, dry with lids)[3]	182,900	—	190,100	—	192,200	—

General Note: All weights are rounded up. Therefore, assembly weights cannot be computed using rounded value of component weights.

1. Weights and CGs are calculated from nominal design dimensions.
2. Center of gravity is measured from the bottom of the concrete cask.
3. Standard or Advanced Transfer Cask.
4. Transfer cask lifting yoke weight for specific sites may vary from listed weight. The site-specific yoke weight should be used for site-specific applications.

Table 3.2-2 Universal Storage System Weights and CGs – BWR Configuration

Item Description	Class 4		Class 5	
	Calculated Weight (lb)	Center of Gravity[1]	Calculated Weight (lb)	Center of Gravity[1]
Fuel Contents (Including channels)	39,400	—	39,400	—
Concrete Cask Lid	2,500	—	2,500	—
Concrete Cask Shield Plug	4,900	—	4,900	—
Canister (empty, w/o lids)	8,800	—	9,000	—
Canister Structural Lid	3,000	—	3,000	—
Canister Shield Lid	7,000	—	7,000	—
Transfer Adapter Plate	11,200	—	11,200	—
Transfer Cask Lifting Yoke[4]	6,000	—	6,000	—
Water in Canister	15,100	—	15,200	—
Basket	17,200	—	17,600	—
Canister (with basket, without fuel or lids)	25,900	—	26,500	—
Canister (with fuel, and shield and structural lids)	75,000	—	75,600	—
Concrete Cask (empty, with shield plug and lid, includes optional lift lugs) – 140 pcf concrete	233,700	—	238,400	—
Concrete Cask (with loaded Canister and lids, includes optional lift lug)[2] – 140 pcf concrete	308,700	113.7	313,900	115.8
Concrete Cask (empty, with shield plug and lid, includes optional lift lugs) – 148 pcf concrete	243,200	—	248,000	—
Concrete Cask (with loaded Canister and lids, includes optional lift lug)[2] – 148 pcf concrete	319,000	113.6	323,900	115.7
Transfer Cask (empty)[3]	118,000	—	120,700	—
Transfer Cask and Canister (empty, without lids)[3]	143,900	—	147,200	—
Transfer Cask and Canister (with fuel, water and shield lid)[3]	205,100	—	208,400	—
Transfer Cask and Canister (with fuel, dry with lids)[3]	193,000	—	196,200	—

General Note: All weights are rounded up. Therefore, assembly weights cannot be computed using rounded values of component weights.

1. Weights and CGs are calculated from nominal design dimensions.
2. Center of gravity is measured from the bottom of the concrete cask.
3. Standard or Advanced Transfer Cask
4. Transfer cask lifting yoke weight for specific sites may vary from listed weight. The site-specific yoke weight should be used for site-specific applications.

Table 3.2-3 Calculated Under-Hook Weights for the Standard Transfer Cask

Configuration	PWR Class 1	PWR Class 2	PWR Class 3	BWR Class 4	BWR Class 5
Transfer cask (empty)	112,300	117,300	121,500	118,000	120,700
Transfer cask, canister (empty, without lids) and yoke[1]	141,400	147,800	152,700	149,800	153,000
Transfer cask; loaded canister wet (fuel, water and shield lid); and yoke[1]	199,800	207,800	210,900	211,000	214,300
Transfer cask, loaded canister dry (fuel and lids) and yoke[1]	188,700	196,000	198,000	198,900	202,100

General Note: All weights are rounded to the next 100 lb.

1. Transfer cask lifting yoke weight for specific sites may vary from listed weight. The site-specific yoke weight should be used for site-specific applications.

3.3 Mechanical Properties of Materials

The mechanical properties of steels used in the fabrication of the Universal Storage System components are presented in Tables 3.3-1 through 3.3-10. The primary steels, Type 304 and Type 304L stainless steel, were selected because of their high strength, ductility, resistance to corrosion and brittle fracture, and metallurgical stability for long-term storage.

3.3.1 Primary Component Materials

The steels and aluminum alloy used in the fabrication of the canister and basket are:

Canister shell	ASME SA-240, Type 304L stainless steel
Canister bottom plate	ASME SA-240, Type 304L stainless steel
Canister shield lid	ASME SA-240, Type 304 stainless steel
Canister structural lid	ASME SA-240, Type 304L stainless steel
Support disks	
PWR basket	ASME SA-693, Type 630, 17-4 PH stainless steel
BWR basket	ASME SA-533, Type B class 2 carbon steel
Heat transfer disks	ASME SB-209, Type 6061-T651 aluminum alloy
Spacers	ASME SA-312, Type 304 stainless steel
Tie rods	ASME SA-479, Type 304 stainless steel
Basket end weldments	ASME SA-240, Type 304 stainless steel
Fuel tubes	ASTM A240, Type 304 stainless steel

SA-182 Type 304 stainless steel may be substituted for SA-240 Type 304 stainless steel for the shield lid provided that the SA-182 material has yield and ultimate strengths greater than or equal to those of the SA-240 material. SA-182 Type 304L stainless steel may be substituted for SA-240 Type 304L stainless steel for the structural lid provided that the SA-182 material has yield and ultimate strengths greater than or equal to those of the SA-240 material.

Steels used in the fabrication of the vertical concrete cask are:

Inner shell	ASTM A36 carbon steel
Pedestal and base	ASTM A36 carbon steel
Reinforcing bar	ASTM A615, Grade 60 carbon steel
	ASTM A615, Grade 75 carbon steel
	ASTM A706 carbon steel

The steels used in the fabrication of the transfer cask are:

Inner shell	ASTM A588 low alloy steel
Outer shell	ASTM A588 low alloy steel
Bottom plate	ASTM A588 low alloy steel
Top plate	ASTM A588 low alloy steel
Retaining ring	ASTM A588 low alloy steel
Trunnions	ASTM A350, LF2 low alloy steel
Shield doors and rails	ASTM A350, LF2 low alloy steel
Retaining ring bolts	ASTM A193, Grade B6 high alloy steel

The mechanical properties of the 6061-T651 aluminum heat transfer disks in the fuel basket are shown in Table 3.3-11. The mechanical properties of the concrete are listed in Table 3.3-12. Table 3.3-13 provides the mechanical properties of NS-4-FR and NS-3. The mechanical properties of carbon steel (SA-516, Grade 70) are shown in Table 3.3-14.

Table 3.3-1 Mechanical Properties of SA-240 and A-240, Type 304 Stainless Steel

Property	Value									
Temperature (°F)	-40	-20	70	200	300	400	500	750	800	900
Ultimate strength, S_u (ksi)*	75.0	75.0	75.0	71.0	66.0	64.4	63.5	63.1	62.7	61.0
Yield strength, S_y (ksi)*	30.0	30.0	30.0	25.0	22.5	20.7	19.4	17.3	16.8	16.2
Design Stress Intensity, S_m (ksi)*	20.0	20.0	20.0	20.0	20.0	18.7	17.5	15.6	15.2	—
Modulus of Elasticity, E ($\times 10^3$ ksi)*	28.7	28.7	28.3	27.6	27.0	26.5	25.8	24.4	24.1	23.5
Alternating Stress @ 10 cycles (ksi)**	718.0	718.0	708.0	690.5	675.5	663.0	645.5	610.4	—	—
Alternating Stress @ 10^6 cycles (ksi)**	28.7	28.7	28.3	27.6	27.0	26.5	25.8	24.4	—	—
Coefficient of Thermal Expansion, α ($\times 10^{-6}$ in/in/°F)*	8.13	8.19	8.46	8.79	9.00	9.19	9.37	9.76	9.82	—
Poisson's Ratio*	0.31									
Density*	503 lbm/ft^3 (0.291 lbm/in^3)									

General Note: SA-182, Type 304 stainless steel may be substituted for SA-240, Type 304 stainless steel provided that the SA-182 material yield and ultimate strengths are equal to or greater than those of the SA-240 material. The SA-182 forging material and the SA-240 plate material are both Type 304 austenitic stainless steels. Austenitic stainless steels do not experience a ductile-to-brittle transition for the range of temperatures considered in this Safety Analysis Report. Therefore, fracture toughness is not a concern.

* ASME Code, Section II, Part D [10].

** ASME Code, Appendix I [11].

Table 3.3-2 Mechanical Properties of SA-479, Type 304 Stainless Steel

Property	Value							
Temperature (°F)	-40	-20	70	200	300	400	500	750
Ultimate strength, S_u, (ksi) ***	—	75.0	75.0	71.0	66.0	64.4	63.5	63.1
Yield strength, S_y, (ksi) ***	—	30.0	30.0	25.0	22.5	20.7	19.4	17.3
Design Stress Intensity, S_m,(ksi) *	20.0	20.0	20.0	20.0	20.0	18.7	17.5	15.6
Modulus of Elasticity ($\times 10^3$ ksi) *	28.8	28.7	28.3	27.6	27.0	26.5	25.8	24.4
Alternating Stress @ 10 cycles (ksi) **	720	718	708	683	675	663	645	610
Alternating Stress @ 10^6 cycles (ksi) **	28.8	28.7	28.3	27.6	27.0	26.5	25.8	24.4
Coefficient of Thermal Expansion, α ($\times 10^{-6}$ in/in/°F) *	—		8.46	8.79	9.00	9.19	9.37	9.76
Poisson's Ratio*	0.31							
Density*	503 lbm/ft^3 (0.291 lbm/in^3)							

* ASME Code, Section II, Part D [10].

** ASME Code, Appendix I [11].

*** Calculated based on Design Stress Intensity:

$$\left(\frac{S_{m-temp}}{S_{m70°}}\right)S_{u70} = S_{u-temp}$$

Table 3.3-3 Mechanical Properties of SA-240, Type 304L Stainless Steel

Property	Value							
Temperature (°F)	-40	-20	70	200	300	400	500	750
Ultimate strength, S_u, (ksi) *	70.0	70.0	70.0	66.2	60.9	58.5	57.8	55.9
Yield strength, S_y, (ksi) *	25.0	25.0	25.0	21.4	19.2	17.5	16.4	14.7
Design Stress Intensity, S_m,(ksi) *	16.7	16.7	16.7	16.7	16.7	15.8	14.8	13.3
Modulus of Elasticity ($\times 10^3$ ksi) *	28.7	28.7	28.3	27.6	27.0	26.5	25.8	24.4
Alternating Stress @ 10 cycles (ksi) **	718.0	718.0	708.0	690.5	675.5	663.0	645.5	610.4
Alternating Stress @ 10^6 cycles (ksi) **	28.7	28.7	28.3	27.6	27.0	26.5	25.8	24.4
Coefficient of Thermal Expansion, α ($\times 10^{-6}$ in/in/°F) **	8.13	8.19	8.46	8.79	9.00	9.19	9.37	9.76
Poisson's Ratio*	0.31							
Density*	503 lbm/ft^3(0.291 lbm/in^3)							

General Note: SA-182, Type 304L stainless steel may be substituted for SA-240 Type 304L stainless steel provided that the SA-182 material yield and ultimate strengths are equal to or greater than those of the SA-240 material. The SA-182 forging material and the SA-240 plate material are both Type 304L austenitic stainless steels. Austenitic stainless steels do not experience a ductile-to-brittle transition for the range of temperatures considered in this Safety Analysis Report. Therefore, fracture toughness is not a concern.

* ASME Code, Section II, Part D [10].

** ASME Code, Appendix I [11].

Table 3.3-4 Mechanical Properties of SA-564 and SA-693, Type 630, 17-4 PH Stainless Steel

Property	Value								
Temperature (°F)	-40	-20	70	200	300	400	500	650	800
Ultimate strength, S_u, (ksi) *	135.0	135.0	135.0	135.0	135.0	131.4	128.5	125.7	105.3***
Yield strength, S_y, (ksi) *	105.0	105.0	105.0	97.1	93.0	89.8	87.0	83.6	77.7***
Design Stress Intensity, S_m,(ksi) *	45.0	45.0	45.0	45.0	45.0	43.8	42.8	41.9	35.1
Modulus of Elasticity ($\times 10^3$ ksi) *	28.7	28.7	28.3	27.6	27.0	26.5	25.8	25.1	24.1
Alternating Stress @ 10 cycles (ksi) **	401.8	401.8	396.2	386.4	378.0	371.0	361.2	341.6	--
Alternating Stress @ 10^6 cycles (ksi) **	19.1	19.1	18.9	18.4	18.0	17.7	17.2	16.3	--
Coefficient of Thermal Expansion, α ($\times 10^{-6}$ in/in/°F) **	—		5.89	5.90	5.90	5.91	5.91	5.93	5.96
Poisson's Ratio*	0.31								
Density*	503 lbm/ft^3 (0.291 lbm/in^3)								

* ASME Code, Section II, Part D [10].

** ASME Code, Appendix I [11].

*** MIL-HDBK-5G [15].

Table 3.3-5 Mechanical Properties of A-36 Carbon Steel

Property	Value							
Temperature (°F)	100	200	300	400	500	600	650	700
Ultimate strength, S_u, (ksi) ***	58.0	58.0	58.0	58.0	—	—	—	—
Yield strength, S_y, (ksi) *	36.0	32.8	31.9	30.8	29.1	26.6	26.1	25.9
Design Stress Intensity, S_m,(ksi) *	19.3	19.3	19.3	19.3	19.3	17.7	17.4	17.3
Modulus of Elasticity, E ($\times 10^3$ ksi) *	29.0	28.8	28.3	27.7	27.3	26.7	26.1	25.5
Coefficient of Thermal Expansion, α ($\times 10^{-6}$ in/in/°F) *	5.53	5.89	6.26	6.61	6.91	7.17	7.30	7.41
Poisson's Ratio*	0.31							
Density**	0.284 lbm/in^3							

* ASME Code, Section II, Part D [10].

** Metallic Materials Specification Handbook [12].

*** ASME Code Case, Nuclear Components, N-71-17 [13].

Table 3.3-6 Mechanical Properties of A615, Grade 60, A615, Grade 75 and A706 Reinforcing Steel

Property	A615, Grade 60	A615, Grade 75	A706
Ultimate Strength ** (ksi)	90.0	100.0	80.0
Yield Strength ** (ksi)	60.0	75.0	60.0
Coefficient of Thermal Expansion,* α (in/in/° F)	6.1×10^{-6}	6.1×10^{-6}	6.1×10^{-6}
Density [12] lbm/in^3	0.284	0.284	0.284

* Metallic Materials Specification Handbook [12].

** Annual Book of ASTM Standards [14].

Table 3.3-7 Mechanical Properties of SA-533, Type B, Class 2 Carbon Steel

Property	Value							
Temperature (°F)	-20	70	200	300	400	500	750	800
Ultimate strength S_u, (ksi) *	90.0	90.0	90.0	90.0	90.0	90.0	87.2	81.8
Yield strength, S_y, (ksi) *	70.0	70.0	65.5	64.5	63.2	62.3	59.3	58.3
Design Stress Intensity, S_m,(ksi) *	30.0	30.0	30.0	30.0	30.0	30.0	—	—
Modulus of Elasticity E, ($\times 10^3$ ksi) *	29.9	29.2	28.5	28.0	27.4	27.0	24.6	23.9
Alternating Stress @ 10 cycles (ksi) **	465.0	465.0	453.8	435.0	436.3	429.9	391.7	—
Alternating Stress @ 10^6 cycles (ksi) **	15.8	15.8	15.4	15.2	14.8	14.6	13.3	—
Coefficient of Thermal Expansion, α ($\times 10^{-6}$ in/in/°F) *	—	7.02	7.25	7.43	7.58	7.70	8.00	8.05
Poisson's Ratio *	0.31							
Density *	503 lbm/ft^3(0.291 lbm/in^3)							

* ASME Code, Section II, Part D [10].

** ASME Code, Section III, Appendix I [11].

Table 3.3-8 Mechanical Properties of A-588, Type A or B Low Alloy Steel

Property	Value							
Temperature (°F)	100	200	300	400	500	600	650	700
Ultimate strength, S_u, (ksi) ***	70.0	70.0	70.0	70.0	70.0	70.0	70.0	70.0
Yield strength, S_y, (ksi) ***	50.0	47.5	45.6	43.0	41.8	39.9	38.9	37.9
Design Stress Intensity, S_m, (ksi) ***	23.3	23.3	23.3	23.3	23.3	23.3	23.3	23.3
Modulus of Elasticity E, ($\times 10^3$ ksi) *	29.0	28.8	28.3	27.7	27.3	26.7	26.1	25.5
Coefficient of Thermal Expansion, α ($\times 10^{-6}$ in/in/°F) *	5.53	5.89	6.26	6.61	6.91	7.17	7.30	7.41
Poisson's Ratio*	0.31							
Density **	0.284 lbm/in^3							

* ASME Code, Section II, Part D [10].

** Metallic Materials Specification Handbook [12].

*** ASME Code Cases, Nuclear Components, NC-71-17, Tables 1, 2, 3, 4, and 5 for material thickness ≤ 4 inches [13].

Table 3.3-9 Mechanical Properties of SA-350/A-350, Grade LF 2, Class 1 Low Alloy Steel

Property	Value					
Temperature (°F)	70	200	300	400	500	700
Ultimate strength, S_u, (ksi) *	70.0	70.0	70.0	70.0	70.0	70.0
Yield strength, S_y (ksi) *	36.0	32.8	31.9	30.8	29.1	25.9
Design Stress Intensity, S_m (ksi) *	23.3	21.9	21.3	20.6	19.4	17.3
Modulus of Elasticity, E, ($\times 10^3$ ksi) *	29.2	28.5	28.0	27.4	27.0	25.3
Coefficient of Thermal Expansion α ($\times 10^{-6}$ in/in/°F) *	—	5.89	6.26	6.61	6.91	7.41
Alternating Stress at 10^6 cycles (ksi) **	12.5	12.2	11.9	11.7	11.5	10.8
Alternating Stress at 10 cycles (ksi) **	580.0	566.0	556.1	544.2	536.3	502.5
Poisson's Ratio *	0.31					
Density *	0.279 lbm/in^3					

* ASME Code, Section II, Part D [10].

** ASME Code, Appendix I [11].

Table 3.3-10 Mechanical Properties of SA-193, Grade B6, High Alloy Steel Bolting Material

Property	Value							
Temperature (°F)	-40	-20	70	200	300	400	500	600
Ultimate Stress, S_u (ksi) *, ***	No Value Given	110.0	110.0	104.9	101.5	98.3	95.6	92.9
Yield Stress, S_y (ksi) *, ***	No Value Given	85.0	85.0	81.1	78.1	76.0	73.9	71.8
Design Stress Intensity, S_m (ksi) *	28.3	28.3	28.3	27.0	26.1	25.3	24.6	23.9
Modulus of Elasticity, E (ksi) *	30.1E+ 03	30.1E+ 03	29.2E+ 03	28.5E+ 03	27.9E+ 03	27.3E+ 03	26.7E+ 03	26.1E+03
Alternating Stress @ 10 cycles (ksi) **	1104.4	1100.0	1085.0	1058.0	1035.0	1015.0	989.0	935.3
Alternating Stress @ 10^6 cycles (ksi) **	13.0	12.9	12.7	12.4	12.2	11.9	11.6	11.0
Coefficient of Thermal Expansion, α (in/in/°F) *	5.73E-06	5.76E-06	5.92E-06	6.15E-06	6.30E-06	6.40E-06	6.48E-06	6.53E-06
Poisson's Ratio *	← 0.31 →							
Density *	← 503 lbm/ft^3(0.291 lbm/in^3) →							

* ASME Code, Section II, Part D [10].

** ASME Code, Appendix I [11].

*** Calculated based on Design Stress Intensity:

$$\left(\frac{S_{m-temp}}{S_{m70^\circ}}\right)S_{u70} = S_{u-temp}$$

Table 3.3-11 Mechanical Properties of 6061-T651 Aluminum Alloy

Property	Value								
Temperature (°F)	70	100	200	300	400	500	600	700	750
Ultimate strength, S_u (ksi) **	42.0	40.7	38.2	31.5	17.2	6.7	3.4	2.1	--
Yield strength, Sy (ksi) **	35.0	33.9	32.2	26.9	14.0	5.3	2.5	1.4	1.4
Design Stress Intensity S_m (ksi) *	10.5	10.5	10.5	8.4	4.4	--	--	--	--
Modulus of Elasticity, E ($\times 10^3$ ksi) *	10.0	9.9	9.6	9.2	8.7	8.1	7.0	--	--
Coefficient of Thermal Expansion, α ($\times 10^{-6}$ in/in/°F) *	—	12.6	12.91	13.22	13.52	13.7	14.3	--	--
Poisson's Ratio *	0.33								
Density *	0.098 lbm/in^3								

* ASME Code, Section II, Part D [10].

** Military Handbook MIL-HDBK-5G [15].

Table 3.3-12 Mechanical Properties of Concrete

Property	**Value**					
Temperature (°F)	70	100	200	300	400	500
Compressive Strength (psi) *	4000	4000	4000	3800	3600	3400
Modulus of Elasticity, ($\times 10^3$ ksi) *	—	3.64	3.38	3.09	3.73	3.43
Coefficient of Thermal Expansion, α ($\times 10^{-6}$ in/in/°F) *	5.5					
Density *	140 lbm/ft^3					

* Handbook of Concrete Engineering [16].

Table 3.3-13 Mechanical Properties of NS-4-FR and NS-3

NS-4-FR	Temperature (°F)			
Property (units) *	**86**	**158**	**212**	**302**
Coefficient of Thermal Expansion (in/in/°F)	2.22E-5	4.72E-5	5.88E-5	5.74E-5
Compressive Modulus of Elasticity (ksi)	561			
Density (lbm/in^3)	0.0607			

NS-3	
Property (units) *	**Value**
Coefficient of Thermal Expansion (in/in/°F) at 150°F	7.78×10^{-6}
Compressive Modulus of Elasticity (ksi)	163
Density (lbm/in^3)	0.0636

* GESC Product Data [17].

Table 3.3-14 Mechanical Properties of SA-516, Grade 70 Carbon Steel

Property	Value						
Temperature (°F)	70	200	300	400	500	700	800
Ultimate Tensile Stress S_u (ksi) *	70.0	70.0	70.0	70.0	70.0	70.0	64.3
Yield Stress, S_y (ksi) *	38.0	34.6	33.7	32.6	30.7	27.4	25.3
Design Stress Intensity, S_m (ksi) *	23.3	23.1	22.5	21.7	20.5	18.3	—
Modulus of Elasticity (ksi) *	29.5E+3	28.8E+3	28.3E+3	27.7E+3	27.3E+3	25.5E+3	24.2E+3
Alternating Stress @ 10 cycles (ksi) **	580.0	552.8	543.0	531.5	523.7	477.0	—
Alternating Stress @ 10^6 cycles (ksi) **	12.5	11.9	11.7	11.5	11.3	10.3	—
Coefficient of Thermal Expansion, α (in/in/ °F) *	—	5.89E-6	6.26E-6	6.61E-6	6.91E-6	7.41E-6	7.59E-6
Thermal Conductivity (BTU/hr-in°F) *	1.9	2.0	2.0	2.0	2.0	1.9	1.8
Poisson's Ratio*	0.31						
Density*	482 lbm/ft^3 (0.279 lbm/in^3)						

* ASME Code, Section II, Part D [10].

** ASME Code, Appendix I [11].

3.3.2 Fracture Toughness Considerations

The primary structural materials of the NAC-UMS® Transportable Storage Canister and basket are a series of stainless steels. These stainless steel materials do not undergo a ductile-to-brittle transition in the temperature range of interest for the NAC-UMS® System. Therefore, fracture toughness is not a concern for these materials.

The optional lift anchors for the NAC-UMS® Vertical Concrete Cask are fabricated from A-537, Class 2, and A-706 ferritic steels. Since there are eight rebars (A-706) for each lift anchor, the rebars are not considered fracture-critical components because multiple, redundant load paths exist, in the same manner that bolted systems are considered in Section 5 of NUREG/CR-1815. Therefore, brittle fracture evaluation of the rebar material is not required. The lifting lug and base plate of the lift anchors are designed as 2-inch thick, A 537 Class 2, steel plates in accordance with ANSI N14.6. Applying the fracture toughness requirements of ASME Code Section III, Subsection NF-2311(b)13 and Figure NF-2311(b)-1, the minimum allowable design metal temperature is –5°F (Curve D, 2-inch nominal thickness). The Vertical Concrete Cask lift anchors are restricted to be used only when the surrounding air temperatures are greater than, or equal to, 0°F (Section 12(B 3.4)(9)), so impact testing of the material is not required.

The NAC-UMS® BWR basket support disks are 0.625-inch thick, SA 533, Type B, Class 2, ferritic steel plate. Per ASME Code Section III, Subsection NG-2311(a)(1), impact testing of material with a nominal section thickness of 5/8 inch (16 mm) and less is not required. To provide added assurance of the fracture toughness of the BWR support disk material, Charpy V-notch (C_v) impact testing is specified on Drawing No. 790-573 for each plate of material in the heat treated condition in accordance with ASME Code Section III, Subsection NG-2320. Acceptance values shall be per ASTM A-370, Section 26.1, with a minimum average value of 20 Mils lateral expansion at a Lowest Service Temperature of - 40°F.

3.4 General Standards

3.4.1 Chemical and Galvanic Reactions

The materials used in the fabrication and operation of the Universal Storage System are evaluated to determine whether chemical, galvanic or other reactions among the materials, contents, and environments can occur. All phases of operation — loading, unloading, handling, and storage — are considered for the environments that may be encountered under normal, off-normal, or accident conditions. Based on the evaluation, no potential reactions that could adversely affect the overall integrity of the vertical concrete cask, the fuel basket, the transportable storage canister or the structural integrity and retrievability of the fuel from the canister have been identified. The evaluation conforms to the guidelines of NRC Bulletin 96-04 [18].

3.4.1.1 Component Operating Environment

Most of the component materials of the Universal Storage System are exposed to two typical operating environments: 1) an open canister containing fuel pool water or borated water with a pH of 4.5 and spent fuel or other radioactive material; or 2) a sealed canister containing helium, but with external environments that include air, rain water/snow/ice, and marine (salty) water/air. Each category of canister component materials is evaluated for potential reactions in each of the operating environments to which those materials are exposed. These environments may occur during fuel loading or unloading, handling or storage, and include normal, off-normal, and accident conditions.

The long-term environment to which the canister's internal components are exposed is dry helium. Both moisture and oxygen are removed prior to sealing the canister. The helium displaces the oxygen in the canister, effectively precluding chemical corrosion. Galvanic corrosion between dissimilar metals in electrical contact is also inhibited by the dry environment inside the sealed canister. NAC's operating procedures provide two helium backfill cycles in series separated by a vacuum-drying cycle during the preparation of the canister for storage. Therefore, the sealed canister cavity is effectively dry and galvanic corrosion is precluded.

The control element assembly, thimble plugs and nonfuel components—including start-up sources and instrument segments—are nonreactive with the fuel assembly. By design, the control components and nonfuel components are inserted in the guide tubes of a fuel assembly. During reactor operation, the control and nonfuel components are immersed in acidic water

having a high flow rate and are exposed to significantly higher neutron flux, radiation and pressure than will exist in dry storage. The control and nonfuel components are physically placed in storage in a dry, inert atmosphere in the same configuration as when used in the reactor. Therefore, there are no adverse reactions, such as gas generation, galvanic or chemical reactions or corrosion, since these components are nonreactive with the Zircaloy guide tubes and fuel rods. There are no aluminum or carbon steel parts, and no gas generation or corrosion occurs during prolonged water immersion (20 – 40 years). Thus, no adverse reactions occur with the control and nonfuel components over prolonged periods of dry storage.

3.4.1.2 Component Material Categories

The component materials are categorized in this section for their chemical and galvanic corrosion potential on the basis of similarity of physical and chemical properties and component functions. The categories are stainless steels, nonferrous metals, carbon steel, coatings, concrete, and criticality control materials. The evaluation is based on the environment to which these categories could be exposed during operation or use of the canister.

The canister component materials are not reactive among themselves, with the canister's contents, nor with the canister's operating environments during any phase of normal, off-normal, or accident condition, loading, unloading, handling, or storage operations. Since no reactions will occur, no gases or other corrosion by-products will be generated.

The control component and nonfuel component materials are those that are typically used in the fabrication of fuel assemblies, i.e., stainless steels, Inconel 625, and Zircaloy, so no adverse reactions occur in the inert atmosphere that exists in storage. The control element assembly, thimble plugs and nonfuel components—including start-up sources or instrument segments to be inserted into a fuel assembly—are nonreactive among themselves, with the fuel assembly, or with the canister's operating environment for any storage condition.

3.4.1.2.1 Stainless Steels

No reaction of the canister component stainless steels is expected in any environment except for the marine environment, where chloride-containing salt spray could potentially initiate pitting of the steels if the chlorides are allowed to concentrate and stay wet for extended periods of time

(weeks). Only the external canister surface could be so exposed. The corrosion rate will, however, be so low that no detectable corrosion products or gases will be generated. The Universal Storage System has smooth external surfaces to minimize the collection of such materials as salts.

Galvanic corrosion between the various types of stainless steels does not occur because there is no effective electrochemical potential difference between these metals. No coatings are applied to the stainless steels. An electrochemical potential difference does exist between austenitic (300 series) stainless steel and aluminum. However, the stainless steel becomes relatively cathodic and is protected by the aluminum.

The canister confinement boundary uses Type 304L stainless steel for all components, except the shield lid, which is made of Type 304 stainless steel. Type 304L resists chromium-carbide precipitation at the grain boundaries during welding and assures that degradation from intergranular stress corrosion will not be a concern over the life of the canister. Fabrication specifications control the maximum interpass temperature for austenitic steel welds to less than 350°F. The material will not be heated to a temperature above 800°F, other than by welding thermal cutting. Minor sensitization of Type 304 stainless steel that may occur during welding will not affect the material performance over the design life because the storage environment is relatively mild.

Based on the foregoing discussion, no potential reactions associated with the stainless steel canister or basket components are expected to occur.

3.4.1.2.2 Nonferrous Metals

Aluminum is used as a heat transfer component in the Universal Storage System spent fuel basket, and aluminum components in electrical contact with austenitic stainless steel could experience corrosion driven by electrochemical Electromotive Force (EMF) when immersed in water. The conductivity of the water is the dominant factor. BWR fuel pool water is demineralized and is not sufficiently conductive to promote detectable corrosion for these metal couples. PWR pool water, however, does provide a conductive medium. The only aluminum components that will be in contact with stainless steel and exposed to the pool water are the alloy 6061-T651 heat transfer disks in the fuel basket.

Aluminum produces a thin surface film of oxidation that effectively inhibits further oxidation of the aluminum surface. This oxide layer adheres tightly to the base metal and does not react readily with the materials or environments to which the fuel basket will be exposed. The volume of the aluminum oxide does not increase significantly over time. Thus, binding due to corrosion product build-up during future removal of spent fuel assemblies is not a concern. The borated water in a PWR fuel pool is an oxidizing-type acid with a pH on the order of 4.5. However, aluminum is generally passive in pH ranges down to about 4 [19]. Data provided by the Aluminum Association [20] shows that aluminum alloys are resistant to aqueous solutions (1-15%) of boric acid (at 140°F). Based on these considerations and the very short exposure of the aluminum in the fuel basket to the borated water, oxidation of the aluminum is not likely to occur beyond the formation of a thin surface film. No observable degradation of aluminum components is expected as a result of exposure to BWR or PWR pool water at temperatures up to 200°F, which is higher than the permissible fuel pool water temperature.

Aluminum is high on the electromotive potential table, and it becomes anodic when in electrical contact with stainless or carbon steel in the presence of water. BWR pool water is demineralized and is not sufficiently conductive to promote detectable corrosion for these metal couples. PWR pool water is sufficiently conductive to allow galvanic activity to begin. However, exposure time of the aluminum components to the PWR pool environment is short. The long-term storage environment is sufficiently dry to inhibit galvanic corrosion.

From the foregoing discussion, it is concluded that the initial surface oxidation of the aluminum component surfaces effectively inhibits any potential galvanic reactions.

Heat transfer disks fabricated from 6061-T651 aluminum alloy are used in the NAC-UMS® Universal Storage System PWR and BWR fuel baskets to augment heat transfer from the spent fuel through the basket structure to the canister exterior. Vendor and Nuclear Regulatory Commission safety evaluations of the NUHOMS Dry Spent Fuel Storage System (Docket No. 72-1004) have concluded that combustible gases, primarily hydrogen, may be produced by a chemical reaction and/or radiolysis when aluminum or aluminum flame-sprayed components are immersed in spent fuel pool water. The evaluations further concluded that it is possible, at higher temperatures (above 150 - 160°F), for the aluminum/water reaction to produce a hydrogen concentration in the canister that approaches or exceeds the Lower Flammability Limit (LFL) for hydrogen of 4 percent. The NRC Inspection Reports No. 50-266/96005 and 50-301/96005 dated July 01, 1996, for the Point Beach Nuclear Plant concluded that hydrogen generation by radiolysis was insignificant relative to other sources.

Thus, it is reasonable to conclude that small amounts of combustible gases, primarily hydrogen, may be produced during UMS® Storage System canister loading or unloading operations as a result of a chemical reaction between the 6061-T6 aluminum heat transfer disks in the fuel basket and the spent fuel pool water. The generation of combustible gases stops when the water is removed from the cask or canister and the aluminum surfaces are dry.

A galvanic reaction may occur at the contact surfaces between the aluminum disks and the stainless steel tie rods and spacers in the presence of an electrolyte, like the pool water. The galvanic reaction ceases when the electrolyte is removed. Each metal has some tendency to ionize, or release electrons. An EMF associated with this release of electrons is generated between two dissimilar metals in an electrolytic solution. The EMF between aluminum and stainless steel is small and the amount of corrosion is directly proportional to the EMF. Loading operations generally take less than 24 hours, a large portion of which has the canister immersed in and open to the pool water after which the electrolyte (water) is drained and the cask or canister is dried and back-filled with helium, effectively halting any galvanic reaction.

The potential chemical or galvanic reactions do not have a significant detrimental effect on the ability of the aluminum heat transfer disks to perform their function for all normal and accident conditions associated with dry storage.

Loading Operations

After the canister is removed from the pool and during canister closure operations, an air space is created inside the canister beneath the shield lid by the drain-down of the water in the canister so that the shield-lid-to-canister-shell weld can be performed. The resulting air space is at least 3 inches in depth. As there is some clearance between the inside diameter of the canister shell and the outside diameter of the shield lid, it is possible that gases released from a chemical reaction inside the canister could accumulate beneath the shield lid. A bare aluminum surface oxidizes when exposed to air, reacts chemically in an aqueous solution, and may react galvanically when in contact with stainless steel in the presence of an aqueous solution.

The reaction of aluminum in water, which results in hydrogen generation, proceeds as:

$$2\ Al + 3\ H_20 \Rightarrow Al_2O_3 + 3\ H_2$$

The aluminum oxide (Al_2O_3) produces the dull, light gray film that is present on the surface of bare aluminum when it reacts with the oxygen in air or water. The formation of the thin oxide film is a self limiting reaction as the film isolates the aluminum metal from the oxygen source acting as a barrier to further oxidation. The oxide film is stable in pH neutral (passive) solutions, but is soluble in borated PWR spent fuel pool water. The oxide film dissolves at a rate dependent upon the pH of the water, the exposure time of the aluminum in the water, and the temperatures of the aluminum and water.

PWR spent fuel pool water is a boric acid and demineralized water solution. BWR spent fuel pool water does not contain boron and typically has a neutral pH (approximately 7.0). The pH, water chemistry, and water temperature vary from pool to pool. Since the reaction rate is largely dependent upon these variables, it may vary considerably from pool to pool. Thus, the generation rate of combustible gas (hydrogen) that could be considered representative of spent fuel pools in general is very difficult to accurately calculate, but the reaction rate would be less in the neutral pH BWR pool.

The BWR basket configuration incorporates carbon steel support plates that are coated with electroless nickel. The coating protects the carbon steel during the comparatively short time that the canister is immersed in, or contains, water. The coating is described in Section 3.8.3. The coating is non-reactive with the BWR pool water and does not off-gas or generate gases as a result of contact with the pool water. Consequently, there are no flammable gases that are generated by the coating. A coating is not used in PWR basket configurations.

To ensure safe loading and/or unloading of the UMS® transportable storage canister, the loading and unloading procedures defined in Chapter 8 are revised to provide for the monitoring of hydrogen gas before and during the welding operations joining the shield lid to the canister shell. The monitoring system shall be capable of detecting hydrogen at 60% of the lower flammability limit for hydrogen (i.e. 0.6 × 4.0 = 2.4%). The hydrogen detector shall be mounted so as to detect hydrogen prior to initiation of the weld, and continuously during the welding operation. Detection of hydrogen in a concentration exceeding 2.4% shall be cause for the welding operation to stop. If hydrogen gas is detected at concentrations above 2.4% at any time, the hydrogen gas shall be removed by flushing ambient air into the region below the shield lid. To

remove hydrogen from below the shield lid, the vacuum pump is attached to the vent port and operated for a sufficient period of time to remove at least five times the air volume of the space below the lid by drawing ambient air through the gap between the shield lid and the canister shell, thus removing or diluting any combustible gas concentrations.

The vacuum pump shall exhaust to a system or area where hydrogen flammability is not an issue. Once the root pass weld is completed, there is no further likelihood of a combustible gas burn because the ignition source is isolated from the combustible gas. Once welding of the shield lid has been completed, the canister is drained, vacuum dried and backfilled with helium.

No hydrogen is expected to be detected prior to, or during, the welding operations. During the completion of the shield lid to canister shell root pass, the hydrogen gas detector is attached to the vent port and continuously operates. During operation, the detector maintains a negative pressure in the canister, drawing air into the canister at the circumference of the shield lid. This ensures that hydrogen gas does not enter the weld area. The mating surfaces of the support ring and inner lid are machined to provide a good level fit-up, but are not machined to provide a metal-to-metal seal. Consequently, additional exit paths for the combustible gases exist at the circumference of the shield lid. Once the canister is dry, no combustible gases form within the canister.

Unloading Operations

It is not expected that the canister will contain a measurable quantity of combustible gases during the time period of storage. The canister is vacuum dried and backfilled with helium immediately prior to being welded closed. There are only minor mechanisms by which hydrogen is generated after the canister is dried and sealed.

As shown in Section 8.3, the principal steps in opening the canister are the removal of the structural lid, the removal of the vent and drain port covers, and the removal of the shield lid. These steps are expected to be performed by cutting or grinding. The design of the canister precludes monitoring for the presence of combustible gases prior to the removal of the structural lid and the vent or drain port covers. Following removal of the vent port cover, a vent line is connected to the vent port quick disconnect. The vent line incorporates a hydrogen gas detector which is capable of detecting hydrogen at a concentration of 2.4% (60% of its lower flammability limit of 4%). The pressurized gases (expected to be greater than 96% helium) in the canister are expected to carry combustible gases out of the vent port. If the exiting gases in the vent line contain no hydrogen at concentrations above 2.4%, the drain port cover weld is cut and the cover removed. If levels of hydrogen gas above 2.4% concentration are detected in the vent line, then the vacuum system is used to remove all residual gas prior to removal of the drain port cover. During the removal of the drain port cover, the hydrogen gas detector is attached to the vent port to ensure that the hydrogen gas concentration remains below 2.4%. Following removal of the drain port cover, the canister is filled with water using the vent and drain ports. Prior to cutting the shield lid weld, 50 gallons of water are removed from the canister to permit the removal of the shield lid. Monitoring for hydrogen would then proceed as described for the loading operations.

3.4.1.2.3 Carbon Steel

Carbon steel support disks are used in the BWR basket configuration. There is a small electrochemical potential difference between carbon steel (SA-533) and aluminum and stainless steel. When in contact in water, these materials exhibit limited electrochemically-driven corrosion. BWR pool water is demineralized and is not sufficiently conductive to promote detectable corrosion for these metal couples. In addition, the carbon steel support disks are coated with electroless nickel to protect the carbon steel surface during exposure to air or to spent fuel pool water, further reducing the possibility of corrosion. Once the canister is loaded, the water is drained from the cavity, the air is evacuated, and the canister is backfilled with helium and sealed. Removal of the water and the moisture eliminates the catalyst for galvanic corrosion. The canister operating procedures (see Chapter 8) provide two backfill cycles in series separated by a vacuum drying cycle during closing of the canister. The displacement of oxygen by helium effectively inhibits corrosion.

The transfer cask structural components are fabricated primarily from ASTM A-588 and A-36 carbon steel. The exposed carbon steel components are coated with either Keeler & Long E-

Series Epoxy Enamel or Carboline 890 to protect the components during in-pool use and to provide a smooth surface to facilitate decontamination.

The concrete shell of the vertical concrete cask contains an ASTM A36 carbon steel liner, as well as other carbon steel components. The exposed surfaces of the base of the concrete cask and the liner are coated with Keeler & Long Y-1-Series Acrylic Urethane Enamel to provide protection from weather-related moisture and direct sunlight.

No potential reactions associated with the BWR basket carbon steel disks, the transfer cask components or vertical concrete cask components are expected to occur.

3.4.1.2.4 Coatings

The exposed carbon steel surfaces of the transfer cask and the transfer cask adapter plate are coated with either Carboline 890 or Keeler & Long E-Series Epoxy Enamel. The technical specifications for these coatings are provided in Sections 3.8.1 and 3.8.2, respectively. These coatings are approved for Nuclear Service Level 2 use. Load bearing surfaces (i.e., the bottom surface of the trunnions and the contact surfaces of the transfer cask doors and rails) are not painted, but are coated with an appropriate nuclear grade lubricant, such as Neolube®. The exposed metal surfaces of the vertical concrete cask are coated with Keeler & Long Kolor-Poxy Primer No. 3200 and Acrythane Enamel Y-1 Series top coating. The technical specifications for these coatings are provided in Sections 3.8.4 and 3.8.5, respectively.

Carbon steel support disks used in the BWR canister basket are coated with electroless nickel. The coating is applied in accordance with ASTM B733-SC3, Type V, Class 1[37]. As described in Section 3.8.3, the electroless nickel coating process uses a chemical reducing agent in a hot aqueous solution to deposit nickel on a catalytic surface. The deposited nickel coating is a hard alloy of uniform thickness of 25 μm (0.001 inch), containing from 4% to 12% phosphorus. Following its application, the nickel coating combines with oxygen in the air to form a passive oxide layer that effectively eliminates free electrons on the surface that would be available to cathodically react with water to produce hydrogen gas. Consequently, the production of hydrogen gas in sufficient quantities to facilitate combustion is highly unlikely.

3.4.1.2.5 Concrete

The vertical concrete storage cask is fabricated of 4000 psi, Type 2 Portland cement that is reinforced with vertical and circumferential carbon steel rebar. Quality control of the proportioning, mixing, and placing of the concrete, in accordance with the NAC fabrication specification, will make the concrete highly resistant to water. The concrete shell is not expected to experience corrosion, or significant degradation from the storage environment through the life of the cask.

3.4.1.2.6 Criticality Control Material

The criticality control material is boron carbide mixed in an aluminum alloy matrix. Sheets of this material are affixed to one or more sides of the designated fuel tubes and enclosed by a welded stainless steel sheet. The material resists corrosion similar to aluminum, and is protected by an oxide layer that forms shortly after fabrication and inhibits further interaction with the stainless steel. Consequently, no potential reactions associated with the aluminum-based criticality control material are expected.

3.4.1.2.7 Neutron Shielding Material

The neutron shielding materials, NS-3 and NS-4-FR, consist primarily of aluminum, carbon, oxygen and hydrogen. NS-4-FR is used in the transfer cask and either NS-3 or NS-4-FR may be used in the shield plug of the vertical concrete storage cask to provide radiation shielding. The acceptable performance of the materials has been demonstrated by use and testing. The materials have been used for over 10 years in licensed storage casks in the United States and in licensed casks in Japan, Spain and the United Kingdom. There are no reports that the shielding effectiveness of the materials has degraded in these applications, demonstrating the long-term reliability for the purpose of shielding neutrons from personnel and the environment. There are no potential reactions associated with the polymer structure of the materials and the stainless steel or carbon steel in which it is encapsulated during use.

The chemistry of the materials (e.g., the way the elements are bonded to one another) contributes significantly to the fire-retardant capability. Approximately 90% of the off-gassing that does occur consists of water vapor.

The thermal performance of NS-4-FR has been demonstrated by long-term functional stability tests of the material at temperatures from -40°F to 338°F. These tests included specimens open to the atmosphere and enclosed in a cavity at both constant and cyclic thermal loads. The tests evaluated material loss though off-gassing and material degradation. The results of the tests demonstrate that, in the temperature range of interest, the NS-4-FR does not exhibit loss of material by off-gassing, does not generate any significant gases, and does not suffer degradation or embrittlement. Further, the tests demonstrated that encased material, as it is used in the NAC-UMS®, performed significantly better than exposed material. Consequently, the formation of flammable gases is not a concern.

Radiation exposure testing of NS-4-FR in reactor pool water demonstrated no physical deterioration of the material and no significant loss of hydrogen (less than 1%). The tests also demonstrated that the NS-4-FR retains its neutron shield capability over the cask's 50-year design life with substantial margin. The radiation testing has shown that detrimental embrittlement and loss of hydrogen from the material do not occur at dose rates (9×10^{14} n/cm^2) that exceed those that would occur assuming the continuous storage of design basis fuel for a 50-year life (estimated to be 1.7×10^{12} cm^2/yr). Consequently, detrimental deterioration or embrittlement due to radiation flux does not occur.

Since the NS-4-FR in the NAC-UMS® transfer cask is sandwiched between the shell and the lead shield and enclosed within a welded steel shell where the shell seams are welded to top and bottom plates with full penetration or fillet welds, it will maintain its form over the expected lifetime of the transfer cask's radiation exposure. The material's placement between the lead shield and the outer shell does not allow the material to redistribute within the annulus.

The NS-3 and NS-4-FR shield material is similarly enclosed in the storage cask shield plug, since a disk of NS-3 or NS-4-FR is captured in a cavity formed by a carbon steel ring and two carbon steel plates. This material cannot redistribute within this volume.

3.4.1.3 General Effects of Identified Reactions

No potential chemical, galvanic, or other reactions have been identified for the Universal Storage System. Therefore, no adverse conditions, such as the generation of flammable or explosive quantities of combustible gases or an increase in neutron multiplication in the fuel (criticality) because of boron precipitation, can result during any phase of canister operations for normal, off-normal, or accident conditions.

3.4.1.4 Adequacy of the Canister Operating Procedures

Based on this evaluation, which results in no identified reactions, it is concluded that the Universal Storage System operating controls and procedures presented in Chapter 8.0 are adequate to minimize the occurrence of hazardous conditions.

3.4.1.5 Effects of Reaction Products

No potential chemical, galvanic, or other reactions have been identified for the Universal Storage System. Therefore, the overall integrity of the canister and the structural integrity and retrievability of the spent fuel are not adversely affected for any operations throughout the design basis life of the canister. Based on the evaluation, no change in the canister or fuel cladding thermal properties is expected, and no corrosion of mechanical surfaces is anticipated. No change in basket clearances or degradation of any safety components, either directly or indirectly, is likely to occur since no potential reactions have been identified.

3.4.2 Positive Closure

The Universal Storage System employs a positive closure system composed of multi-pass welds to join the canister shield lid and the canister structural lid to the shell. The penetrations to the canister cavity through the shield lid are sealed by welded port covers. The welded canister closure system (see Figure 3.4.2-1) precludes the possibility of inadvertent opening of the canister.

The top of the vertical concrete cask is closed by a bolted lid that weighs approximately 2,500 lbs. The weight of the lid, its inaccessibility, and the presence of the bolts effectively preclude inadvertent opening of the lid. In addition, a security seal is provided between two of the lid bolts to detect tampering with the closure lid.

Figure 3.4.2-1 Universal Storage System Welded Canister Closure

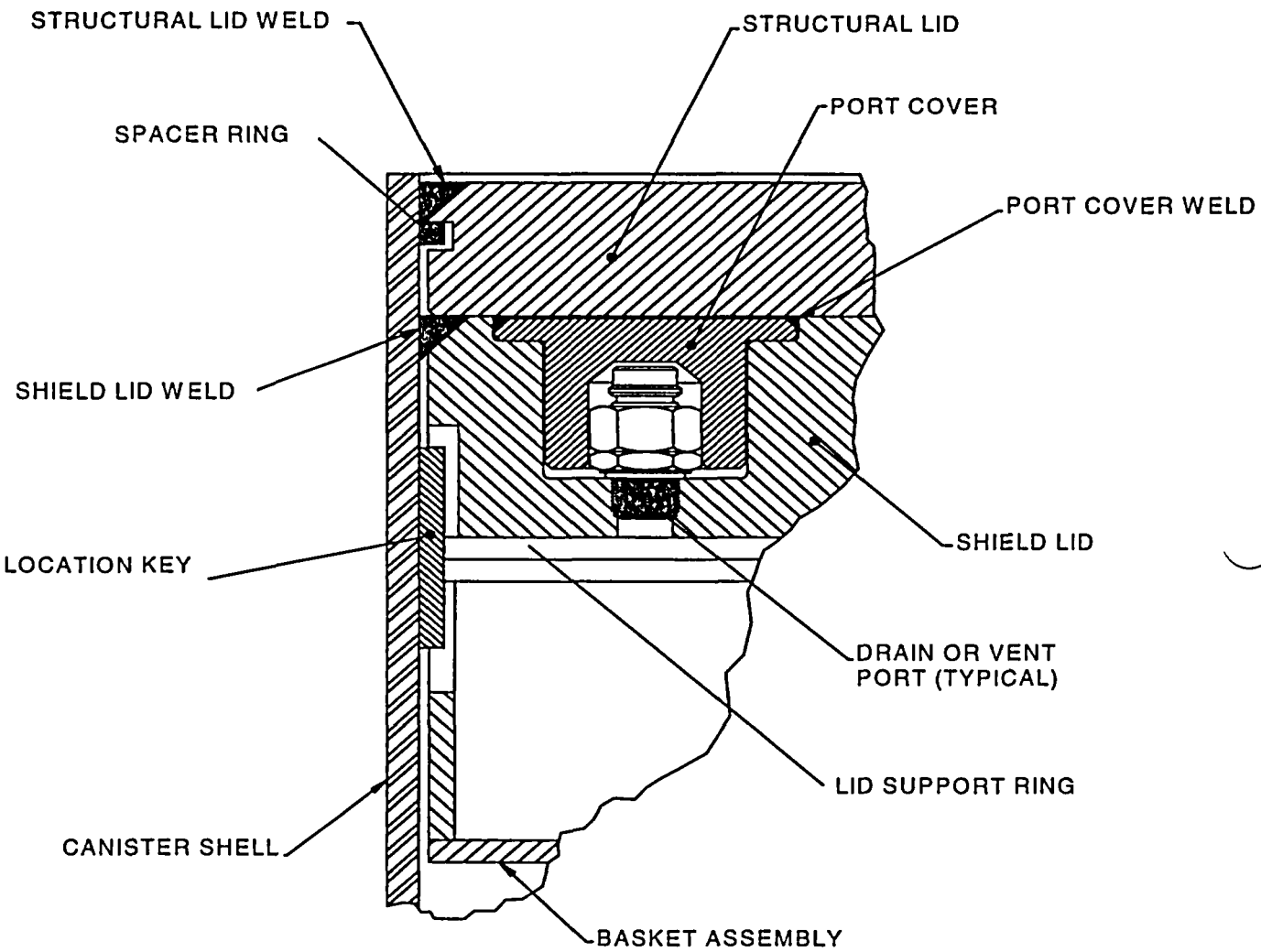

3.4.3 Lifting Devices

To provide more efficient handling of the Universal Storage System, different methods of lifting are designed for each of the components. The transfer cask, the transportable storage canister, and the concrete cask, are handled using trunnions, hoist rings, and a system of jacks and air pads, respectively.

The designs of the UMS® Universal Storage System and Universal Transport System components address the concerns identified in U.S. NRC Bulletin 96-02, "Movement of Heavy Loads Over Spent Fuel, Over Fuel in the Reactor Core, or Over Safety-Related Equipment" (April 11, 1996) as follows:

(1) The UMS® lifting and handling components satisfy the requirements of NUREG-0612 and ANSI N14.6 for safety factors on redundant or nonredundant load paths as described in this chapter.

(2) Transfer or transport cask lifting in the spent fuel pool or cask loading pit or transfer or transport cask lifting and movement above the spent fuel pool operating floor will be addressed on a plant-specific basis.

The transfer cask is provided in either the Standard configuration for canisters weighing up to 88,000 lbs or in the Advanced configuration for canisters weighing up to 98,000 lbs. The two configurations have identical operating features. The transfer casks are lifted by trunnions located near the top of each cask. The Standard transfer cask trunnions are attached by full-penetration welds to both the inner and the outer shells (Figure 3.4.3-1). The Advanced transfer cask trunnions are similarly attached, but incorporate a trunnion support plate at each trunnion for the additional load. The transfer casks are each designed as a heavy-lifting device that satisfies the requirements of NUREG-0612 and ANSI N14.6 for lifting the fully loaded canister of fuel and water, together with the shield lid, which is the maximum weight of the transfer cask during a lifting operation with a given configuration.

The transportable storage canister remains within the transfer cask during all preparation, loading, canister closure, and transfer operations. The canister is equipped with six hoist rings threaded into the structural lid to lift the loaded canister and to lower it into the concrete cask after the shield doors are opened. The hoist rings, shown in Figure 3.4.3-2, are also used for any subsequent lifting of the loaded dry canister.

The vertical concrete cask is moved by means of a system of air pads. The cask is raised approximately 4 inches. by four lifting jacks placed at the jacking pads located near the end of each air inlet. A system consisting of 4 air pads is then inserted under the concrete cask. The cask is lowered onto the uninflated air pads, the jacks are removed, and the air pads are inflated to lift the concrete cask and position it as required on the storage pad or transport vehicle. When positioning is complete, the jacks are used to support the cask as the air pads are removed.

As an option, the loaded concrete cask may also be lifted and moved using lifting lugs at the top of the cask. The top lifting lugs are described in Section 3.4.3.1.3.

The structural evaluations in this section consider the bounding conditions for each aspect of the analysis. Generally, the bounding condition for lifting devices is represented by the heaviest component, or combination of components, of each configuration. The bounding conditions used in this section are:

Section	Evaluation	Bounding Condition	Configuration
3.4.3.1	Concrete Cask Lifting Jacks	Heaviest loaded Concrete Cask + 10% dynamic load factor	BWR Class 5
	Pedestal Loading	Heaviest loaded Canister + 10% dynamic load factor	BWR Class 5
	Concrete Cask Air Pads (Lifting)	Heaviest loaded Concrete Cask	BWR Class 5
	Concrete Cask Top Lifting Lugs (Lifting)	Heaviest loaded Concrete Cask + 10% dynamic load factor	BWR Class 5
3.4.3.2	Canister Lift	Heaviest loaded Canister + 10% dynamic load factor	BWR Class 5
3.4.3.3	Standard Transfer Cask Lift	Heaviest loaded Transfer Cask + 10% dynamic load factor	BWR Class 5
3.4.3.3.4	Standard Transfer Cask Shield Doors and Rails	Heaviest loaded Canister + water, shield doors and 10% dynamic load factor	BWR Class 5

Figure 3.4.3-1 Standard Transfer Cask Lifting Trunnion

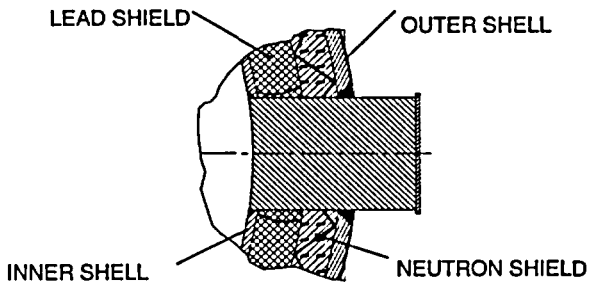

TRUNNION REGION DETAIL

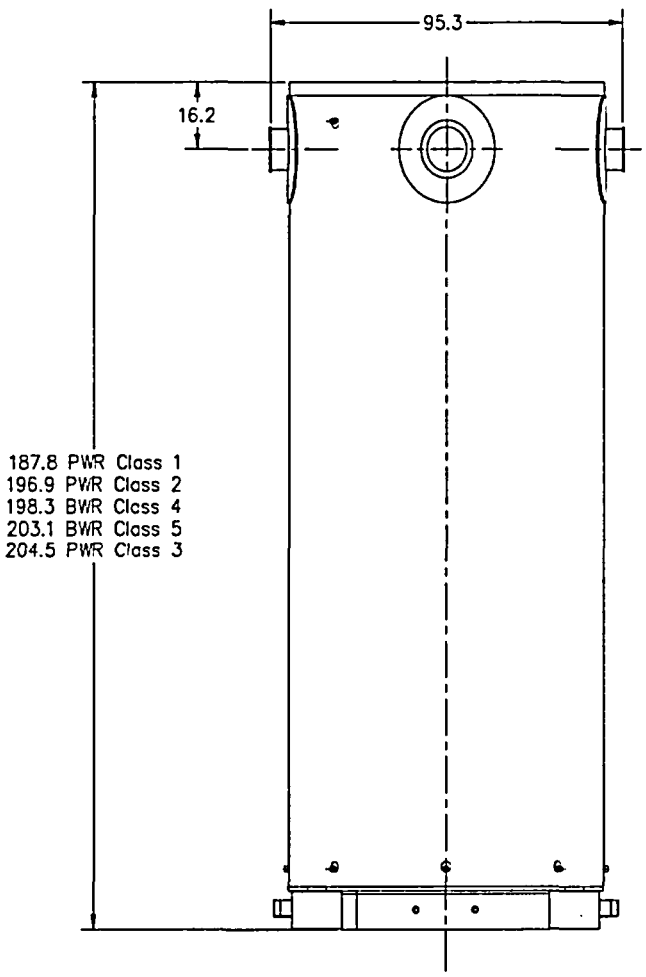

Dimensions in inches

Figure 3.4.3-2 Canister Hoist Ring Design

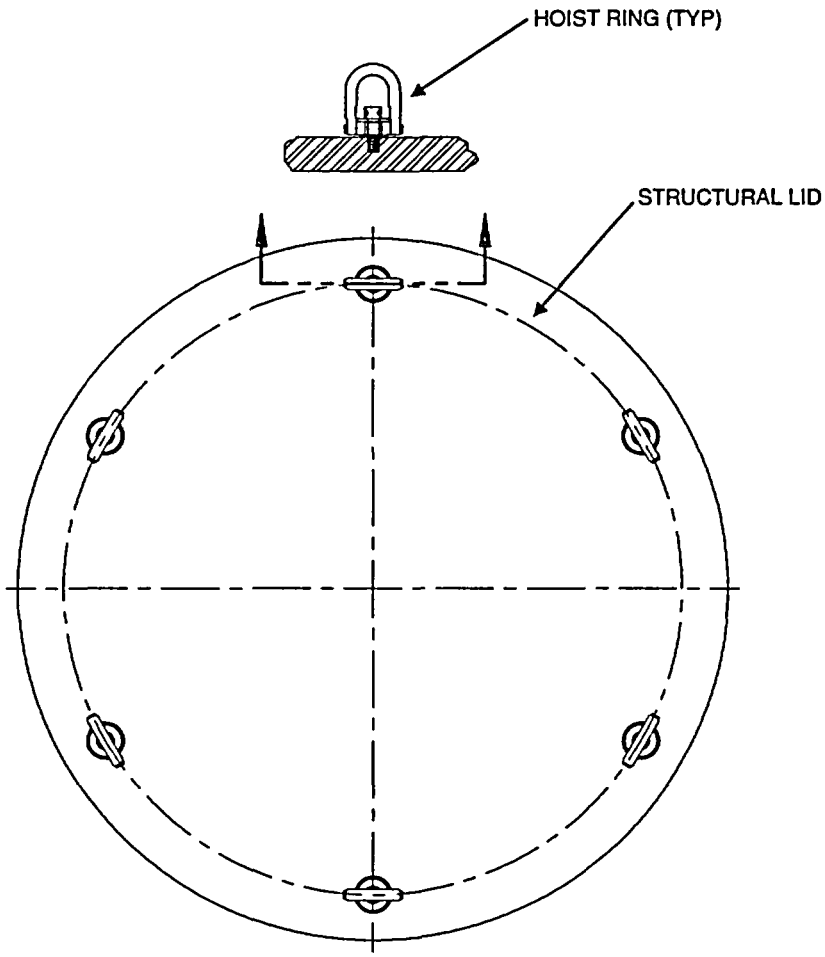

3.4.3.1 Vertical Concrete Cask Lift Evaluation

The vertical concrete cask may be lifted and moved using an air pad system under the base of the cask or four lifting lugs provided at the top of the cask.

Lifting jacks installed at jacking points in the air inlet channels are used to raise the cask so that the air pads can be inserted under the cask. The lifting jacks use a synchronous lifting system to equally distribute the hydraulic pressure among four hydraulic jack cylinders. The calculated weight of the heaviest, loaded concrete cask to be lifted by the jacking system, the BWR Class 5 configuration, is 323,900 pounds with loaded canister and lids (center of gravity is measured from the bottom of the concrete cask). A bounding weight of 330,000 pounds is used for the evaluation in this section.

The lifting lugs are analyzed in accordance with ANSI N14.6 and ACI-349.

3.4.3.1.1 Bottom Lift By Hydraulic Jack

To ensure that the concrete bearing stress at the jack locations due to lifting the cask does not exceed the allowable stress, the area of the surface needed to adequately spread the load is determined in this section. The allowable bearing capacity of the concrete at each jack location is:

$$U_b = \phi f_c' A = \frac{(0.7)(4{,}000)\pi d^2}{4} = 2{,}199.1\ d^2,$$

where:

ϕ = 0.7 strength reduction factor for bearing,
f_c' = 4,000 psi concrete compressive strength,
$A = \frac{\pi d^2}{4}$, concrete bearing area (d = bearing area diameter).

The concrete bearing strength must be greater than the cask weight multiplied by a load reduction factor, $L_f = 1.4$.

$$2{,}199.1\ d^2 > \frac{L_f \times W}{n} = \frac{1.4(330{,}000\ \text{lb})}{4} \Rightarrow d > 7.25\ \text{in.},$$

where:

n = the number of jacks, 4
W = the weight of the vertical concrete cask, 330,000 lb.
L_f = the load factor, 1.4

The diameter obtained in the above equation corresponds to the minimum permissible area over which the load must be distributed. The force exerted by the jack is applied through the 2.25-in. - thick steel air inlet top plate. This increases the effective diameter of the load acting on the concrete surface from a 4.125-in. diameter jack cylinder to about 8.625 in., assuming a 45° angle for the cone of influence.

The bearing stress at each jack location with a bearing area of $\frac{\pi \times 8.625^2}{4} \approx 58.4\ \text{in}^2$ is:

$$\sigma = \frac{P}{A} = \frac{(1.4)(330{,}000\ \text{lb})}{4(58.4\ \text{in}^2)} = 1{,}978\ \text{psi}$$

The allowable bearing stress is:

$$\sigma = \phi f_c = (0.7)(4{,}000\ \text{psi}) = 2{,}800\ \text{psi}$$

The Margin of Safety is:

$$MS = \frac{2{,}800}{1{,}978} - 1 = +0.42$$

Bottom Plate Flexure

During a bottom lift of the concrete cask, the weight of the loaded canister, the pedestal, and the air inlet system are transferred to the bottom plate. As the load is applied, the bottom plate flexes, tending to separate from the concrete. Nelson studs are used to tie the concrete to the bottom plate and prevent separation.

Thirty-two 3/4 in. diameter × 6 3/16-in. long Nelson studs are used in the concrete cask. The shear capacity of each stud is about 23.9 kips [21]. The total load capacity of the studs is:

Capacity = 32 studs × 23.86 kips/stud = 763.5 kips.

The allowable load, P_u, with a load factor of 2.0, as specified in the manufacturer's design data [21], is:

$$P_u = \frac{763.5 \text{ kips}}{2.0} = 381.8 \text{ kips}$$

The total calculated load applied to the concrete cask bottom plate is 75,600 pounds.

Loaded Canister + Pedestal Assembly = 95,000* + 11,000 = 106,000 lb

*Note a conservative value of 95,000 lb. is used for evaluation.

The total load applied to the storage cask bottom plate (including a 10% dynamic load factor) is:

106,000 × 1.1 = 116,600 lb

Therefore, the margin of safety is:

$$MS = \frac{381.8 \text{ kip}}{116.6 \text{ kip}} - 1 = +2.3$$

Base Weldment

This analysis evaluates a bounding configuration of the standard design of the pedestal support structure for static loads. The analysis conservatively assumes a loaded canister with a bounding weight of 95,000 pounds. The pedestal assembly weight is 11,000 pounds. The base plate is modeled with a thickness of 2 inches, the stand (pedestal ring) is 2 inches thick, and the baffle is 1/4 inch thick. To bound the maximum pedestal weight, the densities of the base plate and baffle are increased to simulate a 4-inch plate and 2-inch plate, respectively.

A half-symmetry model of the base weldment (pedestal) is built using the ANSYS preprocessor (see Figure 3.4.3.1-1). The model is constructed of 8-node brick elements (SOLID45). Symmetry conditions (UY=0) are applied along the plane of symmetry (X-Z plane). The total load is simulated by increasing the density of the base plate. The total pressure applied to the model is:

$$F = 95{,}000 \text{ lb} \times 1.1 \text{ g},$$

where, a 10% dynamic load factor is applied to account for handling loads.

To determine the baffle assembly's contribution to the support of the pedestal, gap elements (CONTAC52) are added between the upper truncated cone and the base plate. Two analyses are performed. The first assumes that a gap of 1/4 inch exists between the truncated cone and base plate. The second analysis assumes zero gap.

The following table provides a summary of maximum nodal stresses compared to the allowable stresses for SA-36 carbon steel. For conservatism, the nodal stress (membrane + bending) is compared to the membrane allowable (S_m).

Stress Location	Maximum Nodal Stress (psi)	Allowable, S_m (psi)	Margin of Safety
	1/4-inch Gap		
Pedestal Ring	10214.3	19300.0	0.89
Baffle	107.3	19300.0	>10
Base Plate	1021.4	19300.0	>10
	Zero Gap		
Pedestal Ring	8225.5	19300.0	1.35
Baffle	6283.0	19300.0	2.07
Base Plate	790.8	19300.0	>10

As shown in the table, the maximum nodal stress occurs in the pedestal ring when the gap is set to 1/4-inch and does not close. When the gap is set to zero, a portion of the load is distributed to the baffle. In all cases, the maximum nodal stress is less than the allowable.

3.4.3.1.2 Bottom Support by Air Pads

The concrete cask is supported by air pads in each of 4 quadrants during transport. The layout of the air pads (four 60 in. × 60 in. or 48 in. × 48 in. square pads) are designed to clear the air inlet locations by approximately 4 inches to allow for hydraulic jack access.

The air pad system maximum height is 6.0 in. (3-in. maximum lift, plus 3.0-in. overall height when deflated). The air pad system has a rated lift capacity of 560,000 pounds for the 60 in. × 60 in. pads and 360,000 pounds for the 48 in. × 48 in. pads. The air pads must supply sufficient force to overcome the weight of the concrete cask under full load plus a lift load factor of 1.1. The weight of the heaviest storage configuration, the BWR class 5 system, is about 313,900 pounds. The air pad evaluation uses a conservative weight of 320,000 pounds. The required lift load is 1.1 × (320,000 lb) = 352,000 pounds. Since the available lift force is greater than the load, the air pads are adequate to lift the concrete cask. Considering the minimum air pad capacity of 360,000 pounds, the lifting force margin of safety is:

$$MS = (360{,}000 / 352{,}000) - 1 = +0.02.$$

3.4.3.1.3 Top Lift By Lifting Lugs

A set of four lifting lugs is provided at the top of the vertical concrete cask so that the cask, with a loaded transportable storage canister, may be lifted from the top end. Similar to the bottom lift, the BWR Class 5 configuration maximum weight is used in the analysis of the lifting lugs.

The steel components of the lifting lugs are analyzed in accordance with ANSI N14.6. The development length of the rebar embedded in the concrete is analyzed in accordance with ACI-349-85[4].

Lifting Lug Axial Load

The maximum loaded concrete cask weight is about 324,000 pounds. A bounding weight of 325,000 pounds is used in this analysis. Assuming a 10% dynamic load factor, the load (P) on each lug is:

$$P = \frac{325{,}000(1.1)}{4} = 89{,}375 \text{ lb}$$

For the analysis, P is taken as 89,500 pounds. The lugs are evaluated for adequate strength under a uniform axial load in accordance with the method described in Section 9.3 of AFFDL-TR-69-42 [32].

The bearing stresses and loads for lug failure involving bearing, shear-tearout, and hoop tension are determined using an allowable load coefficient (K). Actual lug failures may involve more than one failure mode, but such interaction effects are accounted for in the value of K.

The allowable lug yield bearing stress (F_{byL}) is:

$$F_{byL} = K\frac{a}{D}(F_y) \quad \text{(for e/D < 1.5)}$$

$$= 43.13 \text{ ksi}$$

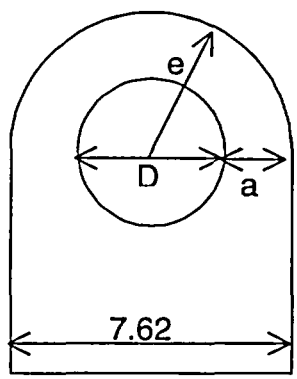

Lifting lug

where:

K = allowable axial load coefficient [32]
=1.65 for e/D = 0.94

e = 7.6/2 = 3.8 in

D = 4.063 in

e /D = 3.8/4.063 = 0.94 (< 1.5)

$a = e - \frac{D}{2} = 1.77$ in

F_y = 60 ksi = lug yield tensile strength for ASME SA537, Class 2 carbon steel

The lug yield bearing load (P_{byL}) for lug failure in bearing, shear-out, or hoop tension is:

$$P_{byL} = F_{byL} \times D \times t$$

$$= 350.47 \text{ kips}$$

where:

t = lug thickness = 2.0 in

The lug yield load capacity (350.47 kips) divided by the lug maximum load (89.5 kips) is:

$$FS_y = \frac{350.47}{89.5} = 3.92 > 3$$

Therefore, the design criterion of a minimum factor of safety (FS) of 3 on the basis of material yield strength is met.

The lug allowable ultimate bearing load (P_{buL}) for lug failure in bearing, shear-out, or hoop tension is:

$$P_{buL} = 1.304 \times F_{byL} \times D \times t \qquad (\text{if } F_u > 1.304\ F_y)$$

$$= 457.02 \text{ kips}$$

where:

$$\frac{F_u}{F_y} = \frac{80 \text{ ksi}}{60 \text{ ksi}} = 1.33 > 1.304$$

t = lug thickness = 2.0 in

F_u = lug ultimate tensile strength = 80 ksi for ASME SA537, Class 2 carbon steel

The lug ultimate load capacity (457.02 kips) divided by the lug maximum load (89.5 kips) is:

$$FS_u = \frac{457.02}{89.5} = 5.11 > 5$$

Therefore, the design criterion of a minimum factor of safety (FS) of 5 on the basis of material yield strength is met.

The tensile stress (σ) in the net cross-sectional area is:

$$\sigma = \frac{P}{A} = \frac{89.5 \text{ kips}}{7.08 \text{ in.}^2} = 12.64 \text{ ksi}$$

where:

P = the load on each lug
A = the net cross sectional area ($2 \times a \times t = 7.08$ in.^{2})

The factor of safety based on material yield strength $(FS_y)_t$ is:

$$(FS_y)_t = \frac{F_y}{\sigma} = \frac{60 \text{ ksi}}{12.64 \text{ ksi}} = 4.75 > 3$$

Therefore, the design criterion of a minimum factor of safety (FS) of 3 on the basis of material yield strength is met.

The factor of safety based on material ultimate strength $(FS_u)_t$ is:

$$(FS_u)_t = \frac{F_u}{\sigma} = \frac{80 \text{ ksi}}{12.64 \text{ ksi}} = 6.33 > 5$$

Therefore, the design criterion of a minimum factor of safety (FS) of 5 on the basis of material ultimate strength is met.

Embedded Plate

The load path from the lugs through the embedded plate and to the embedded reinforcing steel is symmetrical, with the edges of the lifting lugs being very near the axial center line of the reinforcing steel. Therefore, no significant bending moments are introduced into the embedded plate. The embedded plate cross-sectional area is more than double that of the lugs; therefore, the tensile strength of the plate is adequate by inspection.

Concrete Anchors

Each embedded plate has two lifting lugs, therefore, the load (P_{pl}) on each embedded plate is 2 × 89,500 lb or

$$P_{pl} = 179{,}000 \text{ lbs}$$

Four alternate configurations are provided for the anchorage of the lifting lugs to concrete:

Lift Anchor Configuration A – Welded Rebar (ASTM A706)

The required cross-sectional area of reinforcing steel (A_s) on the basis of yield strength ($S_y = 60$ ksi) is:

$$A_s = \frac{P_{pl}}{S_y} = \frac{179\text{kips}}{60\text{ksi}} = 2.98 \text{ in}^2$$

Eight #11 reinforcing steel bars are selected to anchor the embedded plate to the concrete cask concrete shell. The cross-sectional area for each #11 bar is 1.56 in^2 [41]. Therefore, the total area (A_t) resisting the tensile load is:

$$A_t = 8 \times 1.56 \text{ in}^2 = 12.48 \text{ in}^2$$

The reinforcing steel actual cross-sectional area (12.48 in.^{2}) divided by the required cross-sectional area (2.98 in^2) is:

$$FS = \frac{12.48}{2.98} = 4.19 > 3$$

Therefore, the design criterion of a minimum factor of safety (FS) of 3 on the basis of material yield strength is met.

The required cross-sectional area of reinforcing steel (A_s) on the basis of ultimate strength (S_u = 80 ksi) is:

$$A_s = \frac{P_{pl}}{S_u} = \frac{179\text{kips}}{80\text{ksi}} = 2.24 \text{ in}^2$$

The reinforcing steel actual cross-sectional area (12.48 in.^{2}) divided by the required cross-sectional area (2.24 in^2) is:

$$FS = \frac{12.48}{2.24} = 5.57 > 5$$

Therefore, the design criterion of a minimum factor of safety (FS) of 5 on the basis of material ultimate strength is met.

<u>Lift Anchor Configuration B – Threaded Rebars (ASTM A615)</u>

The required cross-sectional area of reinforcing steel (A_s) on the basis of yield strength for Grade 75 is:

$$A_s = \frac{P_{pl}}{S_y}$$

$$= 2.39 \text{ in}^2$$

where:

P_{pl} = 179 kips

$S_y = 75$ ksi

Eight #11 reinforcing steel bars are selected to anchor the embedded plate to the concrete cask concrete shell. The bars are to be threaded 1-3/8 (6 UNC 2A). The tensile stress area for each #11 threaded bar is 1.155 in^2 [40]. Therefore, the total area (A_t) resisting the tensile load is:

$$A_t = 8 \times 1.155 \text{ in.}^2 = 9.24 \text{ in}^2$$

The reinforcing steel actual cross-sectional area divided by the required cross-sectional area is:

$$FS = \frac{9.24}{2.39} = 3.87 > 3$$

Therefore, the design criterion of a minimum factor of safety (FS) of 3 on the basis of material yield strength is met.

The required cross-sectional area of reinforcing steel (A_s) on the basis of ultimate strength for Grade 75 is:

$$A_s = \frac{P_{pl}}{S_u}$$

$$= 1.79 \text{ in}^2$$

where:

$P_{pl} = 179$ kips

$S_u = 100$ ksi

The reinforcing steel actual cross-sectional area divided by the required cross-sectional area is:

$$FS = \frac{9.24}{1.79} = 5.16 > 5$$

Therefore, the design criterion of a minimum factor of safety (FS) of 5 on the basis of material ultimate strength is met.

Thread Engagement

Based on the Machinery's Handbook [40], the shear area of the 1-3/8 (6 UNC 2A) bolt hole internal threads (A_n) is calculated as:

$$A_n = 3.1416 n L_e D_s \min\left[\frac{1}{2n} + 0.57735(D_s \min - E_n \max)\right] = 6.53 \text{ in}^2$$

and the shear area for the external threads of the plate, A_s, is calculated as:

$$A_s = 3.1416 n L_e K_n \max\left[\frac{1}{2n} + 0.57735(E_s \min - K_n \max)\right] = 4.68 \text{ in}^2$$

where:

n = 6, threads per inch

L_e = plate thickness (= 2.0 in),

but not less than bolt thread engagement length

$$= \frac{2A_t}{3.1416 K_n \max[0.5 + 0.57735 n(E_s \min - K_n \max\}]}$$

= 1.0 in (Use L_e = 2.0 in)

$D_s \min$ = 1.3544 in, minimum major diameter–external thread

$E_n \max$ = 1.2771 in, maximum pitch diameter–internal thread

$K_n \max$ = 1.225 in, maximum minor diameter–internal thread

$E_s \min$ = 1.2563 in, minimum pitch diameter–external thread

A_t = 1.155 in^2, tensile stress area

The minimum shear area of 4.68 in^2 controls. Hence, the shear stress, τ, in the bolt hole threads is:

$$\tau = \frac{W/n}{A_s} = 4.78 \text{ ksi}$$

where:

$W = 179.0$ kips

n = number of rebar = 8

$A_s = 4.68 \text{ in}^2$

The factors of safety for ASTM A615 (Grade 75) rebar allowables (S_y = 75 ksi, S_u = 100 ksi), which meet the NUREG criteria for redundant systems, are:

$$FS_y = \frac{0.6S_y}{\tau} = 9.41 > 3$$

$$FS_u = \frac{0.5S_u}{\tau} = 10.46 > 5$$

Lift Anchor Configuration C – Williams All-Thread-Bars

The required cross-sectional area of reinforcing steel (A_s) on the basis of yield strength (S_y = 120 ksi) is:

$$A_s = \frac{P_{pl}}{S_y} = 1.49 \text{ in}^2$$

where $P_{pl} = 179.0$ kips

$S_y = 120.0$ ksi

Six 1-1/4" Grade-150 Williams All-Thread-Bar are selected to anchor the embedded plate to the concrete cask shell. The cross-sectional area for each bar is 1.25 in^2. Therefore, the total area (A_t) resisting the tensile load is:

$A_t = 6 \times 1.25 \text{ in}^2 = 7.5 \text{ in}^2$

The reinforcing steel actual cross-sectional area (7.5 in^2) divided by the required cross-sectional area on the basis of yield strength, (1.49 in^2) is:

$$FS_{yield} = \frac{A_t}{A_s} = 5.03 > 3$$

Therefore, the design criterion of a minimum factor of safety (FS) of 3 on the basis of material yield strength is met.

The required cross-sectional area of reinforcing steel (A_s) on the basis of ultimate strength (S_u = 150 ksi) is:

$$A_s = \frac{P_{pl}}{S_u} = 1.19 \text{ in}^2$$

where $P_{pl} = 179.0$ kips

$S_u = 150.0$ ksi

The reinforcing steel actual cross-sectional area (7.5 in^2) divided by the required cross-sectional area on the basis of yield strength, (1.19 in^2) is:

$$FS_{ultimate} = \frac{A_t}{A_s} = 6.30 > 5$$

Therefore, the design criterion of a minimum factor of safety (FS) of 5 on the basis of material ultimate strength is met.

Thread Engagement

Based on the Machinery's Handbook [40], the shear area for the internal threads of the 1-1/4" nut, A_n, is calculated as:

$$A_n = 3.1416 n L_e D_s \min\left[\frac{1}{2n} + 0.57735\left(D_s \min - E_n \max\right)\right] = 6.30 \text{ in}^2$$

and the shear area for the external threads of the rebar, A_s, is calculated as:

$$A_s = 3.1416 n L_e K_n \max\left[\frac{1}{2n} + 0.57735\left(E_s \min - K_n \max\right)\right] = 5.54 \text{ in}^2$$

where

n = 4, number of threads per inch,

L_e = 2.5 in (overall height of hex nut),

but not less than the thread engagement length

$$= \frac{2A_t}{3.1416 K_n \max[0.5 + 0.57735 n(E_s \min - K_n \max)]}$$

= 1.19 in (Use L_e = 2.5 inches)

A_t = 1.32 in^2, tensile stress area (non-standard),

$D_s$min = 1.399 in, minimum major diameter – external thread (rebar),

$E_n$max = 1.3674 in, maximum pitch diameter – internal thread (nut),

$K_n$max = 1.2898 in, maximum minor diameter – internal thread (nut), and

$E_s$min = 1.31 in, minimum pitch diameter – external thread (rebar)

The minimum shear area of 5.54 in^2 controls. Hence, the shear stress, τ, in the bolt hole threads is:

$$\tau = \frac{W/n}{A_s} = 5.38 \text{ ksi}$$

where:

W = 179.0 kips
n = number of rebar = 6
$A_s = 5.54\ in^2$

The factor of safety for the rebar based on the yield strength (120.0 ksi) is:

$$FS_{yield} = \frac{0.6S_y}{\tau} = 13.38 > 3$$

The factor of safety for the bar based on the ultimate strength (150.0 ksi) is:

$$FS_{ultimate} = \frac{0.5S_u}{\tau} = 13.94 > 5$$

Development Length of Welded Bars, Threaded Bars, and Williams All-Thread-Bars (Configurations A, B, and C)

The development length (l_d) is the length of embedded reinforcing steel required to develop the design strength of the reinforcing steel at a critical section. The required reinforcing steel development length (l_d) for bars in tension in accordance with Section 12.2 of the ASME Code, Code Cases – Nuclear Components [13] shall be:

$$l_d = \text{larger of } \frac{0.04A_bS_y}{\sqrt{f_c'}} \text{ or } 0.0004d_bS_y \text{ or 12 inches}$$

where

d_b = diameter of rebar (1.41 inch for # 11, 1.411 inch for Williams)

A_b = tensile stress area of rebar (1.56 in^2 for # 11, 1.32 in^2 for Williams)

S_y = yield strength of the reinforcing steel (60 ksi for A706, 75 ksi for A615, 120 ksi for Williams)

$f_c^{'}$ = concrete design strength = 4,000 psi

The development lengths for the different diameter and strength rebars are given in the following table:

Development Lengths

S_y	Reinforcing Steel Bar	$l_d = \frac{0.04A_bS_y}{\sqrt{f_c^{'}}}$	$l_d = 0.0004d_bS_y$	l_d =12 in	Max. l_d
60 ksi	# 11 (A706)	59.2	33.8	12.0	59.2
75 ksi	# 11 (A615)	74.0	42.3	12.0	74.0
120 ksi	Williams	100.2	67.7	12.0	100.2

The actual length of the regular reinforcing steel provided is 185.5 inches and that of the Williams threaded bars is 102 inches. These lengths are greater than the maximum required length given in the preceding table.

Lift Anchor Configuration D – Steel Plates

Each vertical plate has one lifting lug; therefore, the load on each vertical plate is 89,500 pounds. The required cross-sectional area of vertical steel plates on the basis of yield (60 ksi) and ultimate (80 ksi) strengths is:

$A_{yield} = 89.5/60 = 1.49\ in^2$

$A_{ultimate} = 89.5/80 = 1.12\ in^2$

The vertical steel plates are welded to the embedded base plate, which acts as an anchor to the vertical concrete cask shell. The actual tensile stress area of the vertical steel plates is 15.2 in^2 (7.6x2.0).

The factors of safety measured as the actual plate areas divided by the required plate areas on the basis of yield and ultimate strengths are given as:

$$\text{FS (yield)} = \frac{15.2}{1.49} = 10.2 > 3$$

$$\text{FS (ultimate)} = \frac{15.2}{1.12} = 13.6 > 5$$

Therefore, the design criteria of a minimum Factor of Safety of 3 on the basis of material yield strength and a minimum Factor of Safety of 5 on the basis of material ultimate strength are met.

The depth of the shear area of the concrete section in tension is evaluated according to Sections 11.1 and 11.3 of ACI 349-85 [4] as follows.

Conservatively, using the shear plane at the edge of the base plate and discounting the face of the plate towards the outer surface of the vertical concrete cask (see the following figure), the shear perimeter is:

$$P = 2\times(11.4\text{-}2)+(9.6\text{-}2) + 2\times\sqrt{2} = 29.23 \text{ inch}$$

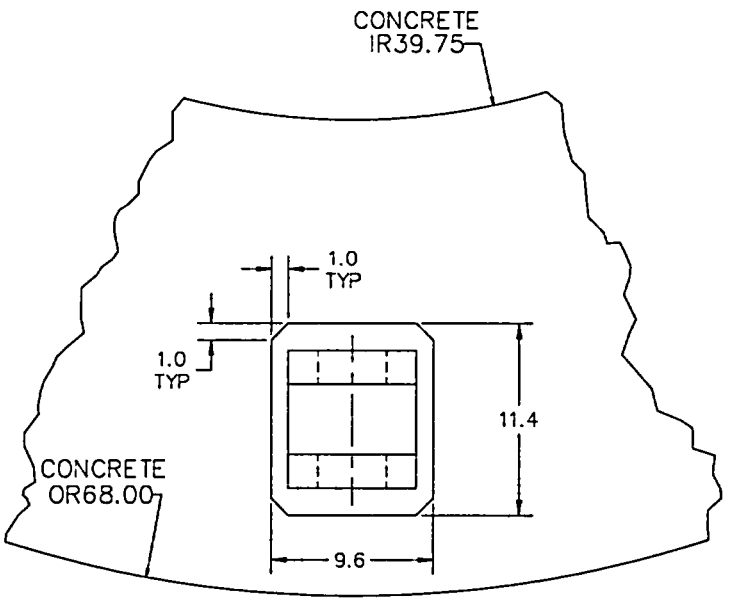

The maximum applied load is W = 89.5×2 = 179 kips. The effective shear area is $A_{shear} = P \times D$ (D is the depth of the shear area). The shear strength provided by concrete (V_n) is conservatively taken as $2\sqrt{f_c'}\,A_{shear}$. Using the relationship $V_u \leq \Phi V_n$ ($\Phi = 0.85$ for shear [13], and V_u is the applied load), the required depth of the shear area (D) is determined as:

$$D = \frac{W}{\Phi 2\sqrt{f_c'}P} = 57.0 \text{ inch} < 61.5 \text{ inch}$$

Where $f_c' = 4{,}000$ psi.

The actual depth of the shear area (61.5 inch) is adequate since it is greater than the required depth calculated above.

Welds

The lifting lugs are welded to the embedded plate with full penetration welds developing the full strength of the attached lugs.

The vertical plate is welded to the base plate with full penetration welds developing the full strength of the vertical plate.

Therefore, all welds are adequate.

Nelson Studs

During a top end lift, the weight of the canister and pedestal applies a tensile load to the Nelson studs. Using the BWR Class 5 configuration, 75,600-pound canister weight (77,000 pounds used in this analysis), an ANSYS finite element model is used to obtain the maximum load on the Nelson studs. The model, shown in the following figure, represents one-eighth of the pedestal. The weight of the canister is applied as a pressure load to the top of the 2-inch base plate. The load is reacted through the Nelson studs and gap elements between the pedestal and the concrete. Using a 10% dynamic load factor, the maximum load on a Nelson stud is 13,467 pounds.

In accordance with ACI-349-85 [4], the design pullout strength of the concrete (P_d) for any embedment is based on a uniform tensile stress acting on an effective stress area which is defined by the projected area of stress cones radiating toward the attachment from the bearing edge of the anchor heads. The effective area shall be limited by overlapping stress cones, by the intersection of the cones with concrete surfaces, by the bearing area of anchor heads, and by the overall thickness of the concrete. A 45° inclination angle is used for the stress cones.

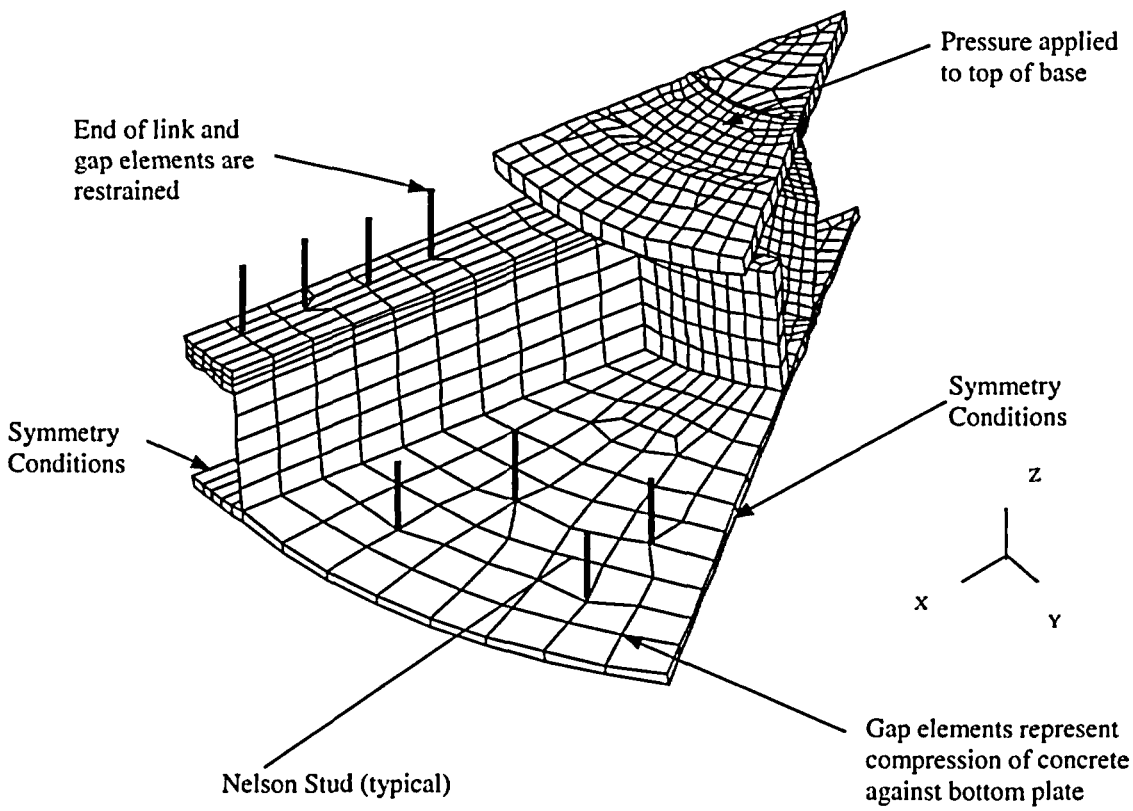

Pedestal Finite Element Model

The maximum pullout strength of the concrete (P_d) is defined by the equation

$$P_d = 4 \times \phi \times \sqrt{f_c^{'}} \times A_{cp}$$

where:

ϕ - strength reduction factor = 0.85

$f_c^{'}$ - concrete compression strength = 4,000 psi

A_{cp} - projected surface area of stress cones for Nelson studs

The maximum load occurs in the eight Nelson studs located on the top of the air inlet. A_{cp} for the eight Nelson studs equals 471.63 inch^2. Therefore, P_d equals:

$$P_d = 4 \times 0.85 \times \sqrt{4000} \times 471.63 = 101{,}417 \text{ lb.}$$

The total load on the eight Nelson studs is 27,379 pounds.

The margin of safety for the concrete is:

$$MS = \frac{101{,}415}{27{,}379} - 1 = +2.70$$

For a single stress cone, the maximum load is 13,467 pounds. The corresponding pull-out strength is 117.86 inch^2.

$$P_d = 4 \text{ x } 0.85 \text{ x } 117.86 \text{ x } \sqrt{4{,}000} = 25{,}344 \text{ lbs.}$$

where the projected surface area for a single stress cone (Acp) of a single Nelson stud is 117.86.

The margin of safety for a single Nelson stud is:

$$MS = \frac{25{,}344}{13{,}467} - 1 = +0.88$$

The cross-sectional area of the Nelson studs is:

$$A_s = \frac{\pi}{4} \times 0.75^2 = 0.44 \text{ in}^2$$

The allowable load per stud is:

$$P_s = 0.44 \times 55{,}000 = 24{,}200 \text{ lbs}$$

where 55,000 psi is the ultimate tensile strength for ASTM A108 Grade 1010 through 1020 low carbon steel [14].

The margin of safety for the Nelson stud is:

$$MS = \frac{24{,}200}{13{,}467} - 1 = +0.80$$

Vertical Concrete Cask Pedestal

Using the same ANSYS Finite Element Model that was used for the Nelson Stud analysis, an analysis of the pedestal was performed. The maximum nodal stress intensity for the pedestal is 5,785 psi. From Tables 4.1-4 and 4.1-5, the maximum canister temperature is 376°F. For A36 steel, the allowable stress (S_m) is 19,300 psi. The margin of safety is, conservatively:

$$MS = \frac{19{,}300}{5{,}785} - 1 = +2.34$$

Figure 3.4.3.1-1 Base Weldment Finite Element Model

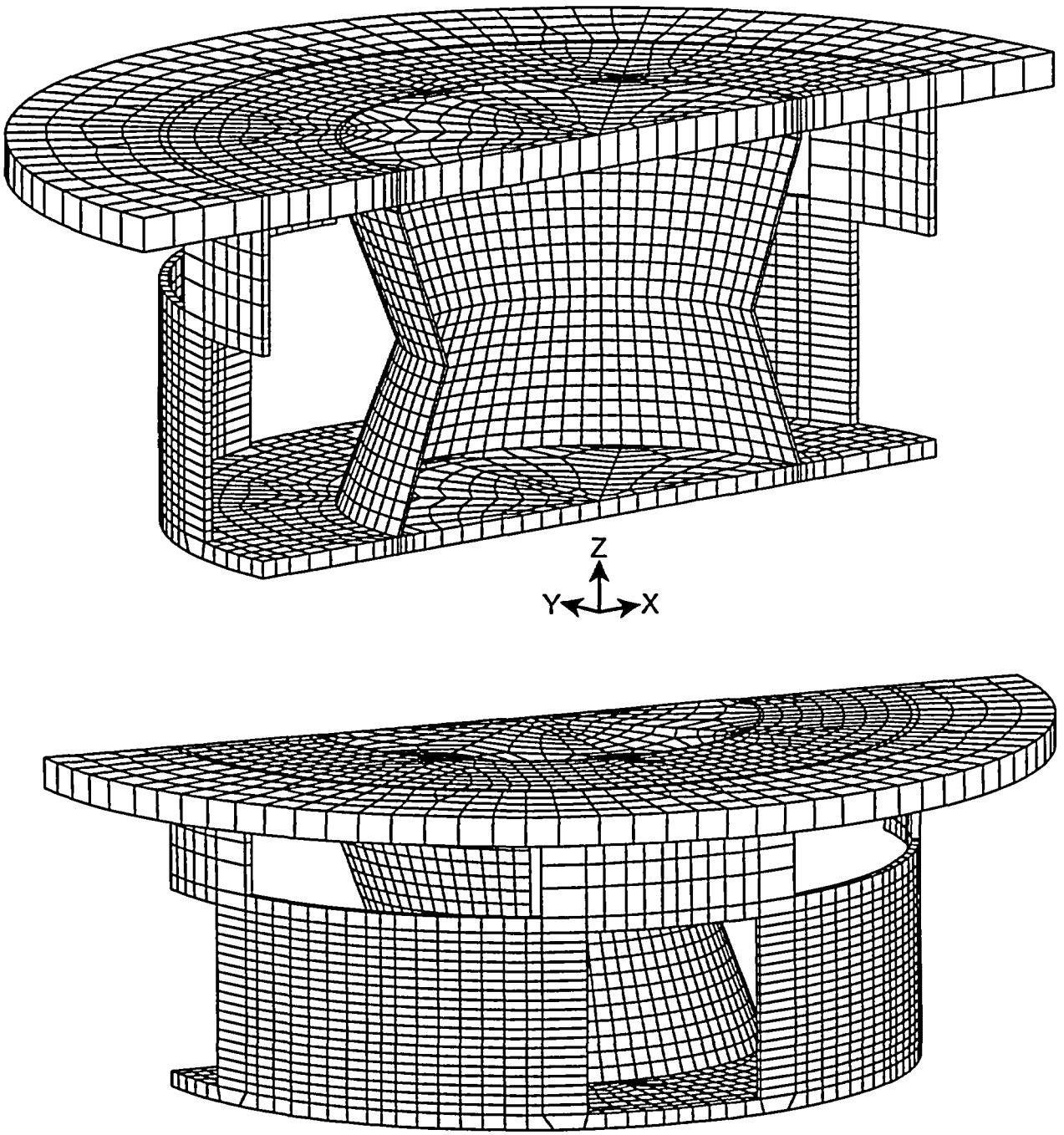

3.4.3.2 Canister Lift

The adequacy of the canister lifting devices is demonstrated by evaluating the hoist rings, the canister structural lid, and the weld that joins the structural lid to the canister shell against the criteria in NUREG-0612 [8] and ANSI N14.6 [9]. The lifting configuration for the PWR and BWR canisters consists of six hoist rings threaded into the structural lid at equally spaced angular intervals. The hoist rings are analyzed as a redundant system with two three-legged lifting slings. For redundant lifting systems, ANSI N14.6 requires that load-bearing members be capable of lifting three times the load without exceeding the tensile yield strength of the material and five times the load without exceeding the ultimate tensile strength of the material. The canister lid is evaluated for lift conditions as a redundant system that demonstrates a factor of safety greater than three based on yield strength and a factor of safety greater than five based on ultimate strength. The canister lift analysis is based on a load of 76,000 lb, which bounds the weight of the heaviest loaded canister configuration, plus a dynamic load factor of 10 %.

The canister lifting configuration is shown in the following figure, where: x is the distance from the canister centerline to the hoist ring center line (29.5 inches); F_y is the vertical component of force on the hoist ring; F_x is the horizontal component of force on the hoist ring; R is the sling length; and, F_R is the maximum allowable force on the hoist ring (30,000 lbs.). The angle θ is the angle from vertical to the sling. The vertical load, F_y, assuming a 10% dynamic load factor, is:

$$F_y = \frac{76{,}000 \text{ lbs x } 1.1}{3 \text{ lift points}} = 27{,}867 \text{ lbs}$$

The hoist rings are American Drill Bushing Company, Model 23200 Safety Engineered Hoist Rings, rated at 30,000 lbs., (or comparable ring from an alternative manufacture) with a safety factor of 5 on ultimate strength.

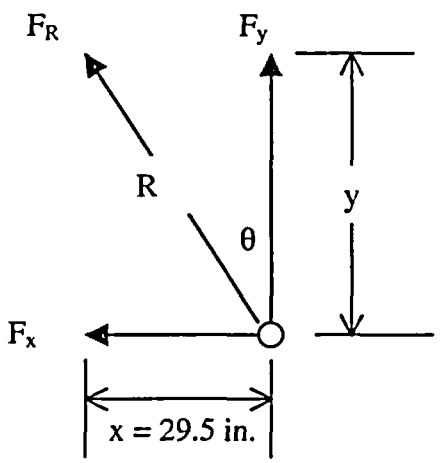

Calculating the maximum angle, θ, that will limit F_R to 30,000 lb:

$$\theta = \cos^{-1}\left(\frac{F_y}{F_R}\right) = \cos^{-1}\left(\frac{27{,}867}{30{,}000}\right) = 21.7 \text{ deg}$$

The minimum sling length, R, is

$$R = \frac{x}{\sin\theta} = \frac{29.5}{\sin 21.7^\circ} = 79.8 \text{ in.}$$

An 80-in. sling places the master link about 75 in. above the top of the canister (y = R cos θ = 80 cos 21.7° = 74.3 inches).

A minimum distance of 75 inches between the master link and the top of the canister is specified in Sections 8.1.2 and 8.2.

From the Machinery's Handbook [24], The shear area, A_n, in the structural lid bolt hole threads is calculated as

$$A_n = 3.1416\, n\, L_e\, D_s\min\left[\frac{1}{2n} + 0.57735\left(D_s\min - E_n\max\right)\right]$$

$$= 3.1416(4.5)(2.0 \text{ in.})(1.9751 \text{ in.})\left[\frac{1}{2(4.5)} + 0.57735(1.9751 \text{ in.} - 1.8681 \text{ in.})\right]$$

$$= 9.654 \text{ in}^2$$

where:

n	=	4.5 threads per in,
L_e	=	2.0-in. bolt thread engagement length
$D_s$min	=	1.9751 in., minimum major diameter of class 2A bolt threads
$E_n$max	=	1.8681 in., maximum pitch diameter of class 2B lid threads

The shear stress, τ, in the structural lid bolt hole threads is calculated as:

$$\tau = \frac{F_y}{A_n} = \frac{27{,}867 \text{ lb}}{9.654 \text{ in}^2} = 2{,}887 \text{ psi}$$

The canister structural lid is constructed of SA240, Type 304L stainless steel. Using shear allowables of 0.6 S_y and 0.5 S_u at a temperature of 300°F, the shear stress of 2,887 psi results in factors of safety of:

$$(F.S.)_y = \frac{0.6 \text{ x } 19{,}200 \text{ psi}}{2{,}887 \text{psi}} = 4.0 > 3$$

$$(F.S.)_u = \frac{0.5 \text{ x } 60{,}900 \text{ psi}}{2{,}887 \text{psi}} = 10.5 > 5$$

The criteria of NUREG-0612 and ANSI N14.6 for a redundant systems are met. Therefore, the 2.0-inch length of thread engagement is adequate.

The total weight of the heaviest loaded transfer cask (Class 5 BWR) is approximately 208,400 pounds. Three (3) times the design weight of the loaded canister is (3 × 76,000) 228,000 lbs, which is greater than the weight of the heaviest loaded transfer cask. Consequently, the preceding analysis bounds the inadvertently lifting of the transfer cask by the canister, since the canister lid and the hoist rings do not yield.

The structural adequacy of the canister structural lid and weld is evaluated using a finite element model of the upper portion of the canister. As shown in Figure 3.4.3.2-1, the model represents one-half of the upper section of the canister, including the structural and shield lids. The model uses gap/spring elements to simulate contact between adjacent components. Specifically, contact between the canister structural and shield lids is modeled using COMBIN40 combination elements in the axial (UY) degree of freedom. Simulation of the spacer ring is accomplished using a ring of COMBIN40 gap/spring elements connecting the shield lid and the canister in the axial direction at the lid lower outside radius. CONTAC52 elements are used to model the interaction between the structural lid and canister shell and the shield lid and canister shell just below the respective lid weld joints. The size of the CONTAC52 gaps was determined from nominal dimensions of contacting components. The COMBIN40 elements used between the structural and shield lids, and for the spacer ring, were assigned small gap sizes of 1×10^{-8} in. All gap/spring elements are assigned a stiffness of 1×10^{8} lb/in.

Boundary conditions were applied to enforce symmetry at the cut boundary of the model (in the x-y plane). All nodes on the x-y symmetry plane were restrained perpendicular to the symmetry

plane (UZ). In addition, the nodes in the x-z plane at the bottom of the model were restrained in the axial direction (UY).

The lifting configuration for the canister consists of six hoist rings bolted to the structural lid at equally spaced angular intervals. To simulate the lifting of the canister, point loads equal to one-sixth of the total loaded canister weight plus a dynamic loading factor of 10% were applied to the model as forces at the lift locations while restraining the model at its base in the axial direction. Because of the symmetry conditions of the model, the forces applied to nodes on the symmetry plane were one-half of that applied at the other locations. The nodal point forces applied to the model as depicted in Figure 3.4.3.2-1 are calculated (including a dynamic load factor of 10%) as

$$W/6 = (76{,}000 \text{ lb} \times 1.1)/6 = 13{,}934 \text{ lb}$$

$$W/12 = (76{,}000 \text{ lb} \times 1.1)/12 = 6{,}967 \text{ lb}$$

To evaluate the canister lid welds during lift conditions, linearized sectional stresses are taken across the weld. The sections are shown in Figure 3.4.3.2-1. Stress results are compared to material allowables at a temperature of 300°F. For conservatism, the weld allowable is taken as the base material. The following table is a summary of the weld stress results.

Section	Component Description	Material	Stress Intensity $P_m + P_b$ (psi)	Factor of Safety on Yield	Factor of Safety on Ultimate
1	Structural Lid Weld	304L SS	1,678	11.4	36.3
2	Canister shell	304L SS	3,083	6.2	19.8
3	Shield Lid Weld	304 SS	1,794	10.7	33.9
4	Canister shell	304L SS	2,491	7.7	24.4
5	Canister shell	304L SS	1,305	14.7	46.7

The maximum nodal stress intensity outside the weld region of 2,608 psi occurs in the structural lid. The nodal stress results are presented graphically in Figure 3.4.3.2-2. The corresponding factors of safety are:

$$(\text{F.S.})_{\text{yield}} = \frac{\text{yield strength}}{\text{maximum nodal stress intensity}} = \frac{19{,}200 \text{ psi}}{2{,}608 \text{ psi}} = 7.4 \ (> 6)$$

$$(F.S.)_{ultimate} = \frac{\text{ultimate strength}}{\text{maximum nodal stress intensity}} = \frac{60{,}900\,\text{psi}}{2{,}608\,\text{psi}} = 23.4\ (>10)$$

Therefore, the canister meets the criteria of NUREG-0612 and ANSI N14.6 for nonredundant systems.

Figure 3.4.3.2-1 Canister Lift Finite Element Model

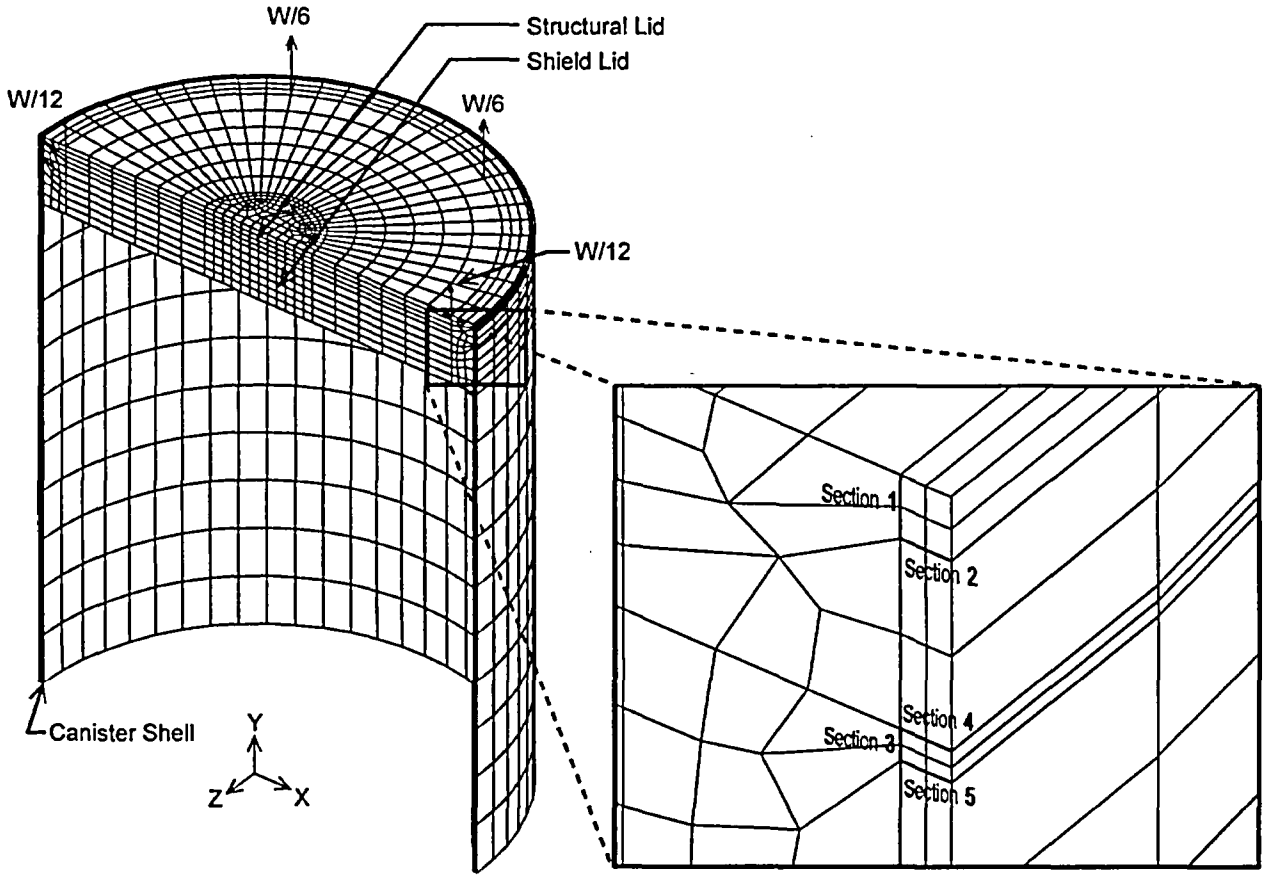

Figure 3.4.3.2-2 Canister Lift Model Stress Intensity Contours (psi)

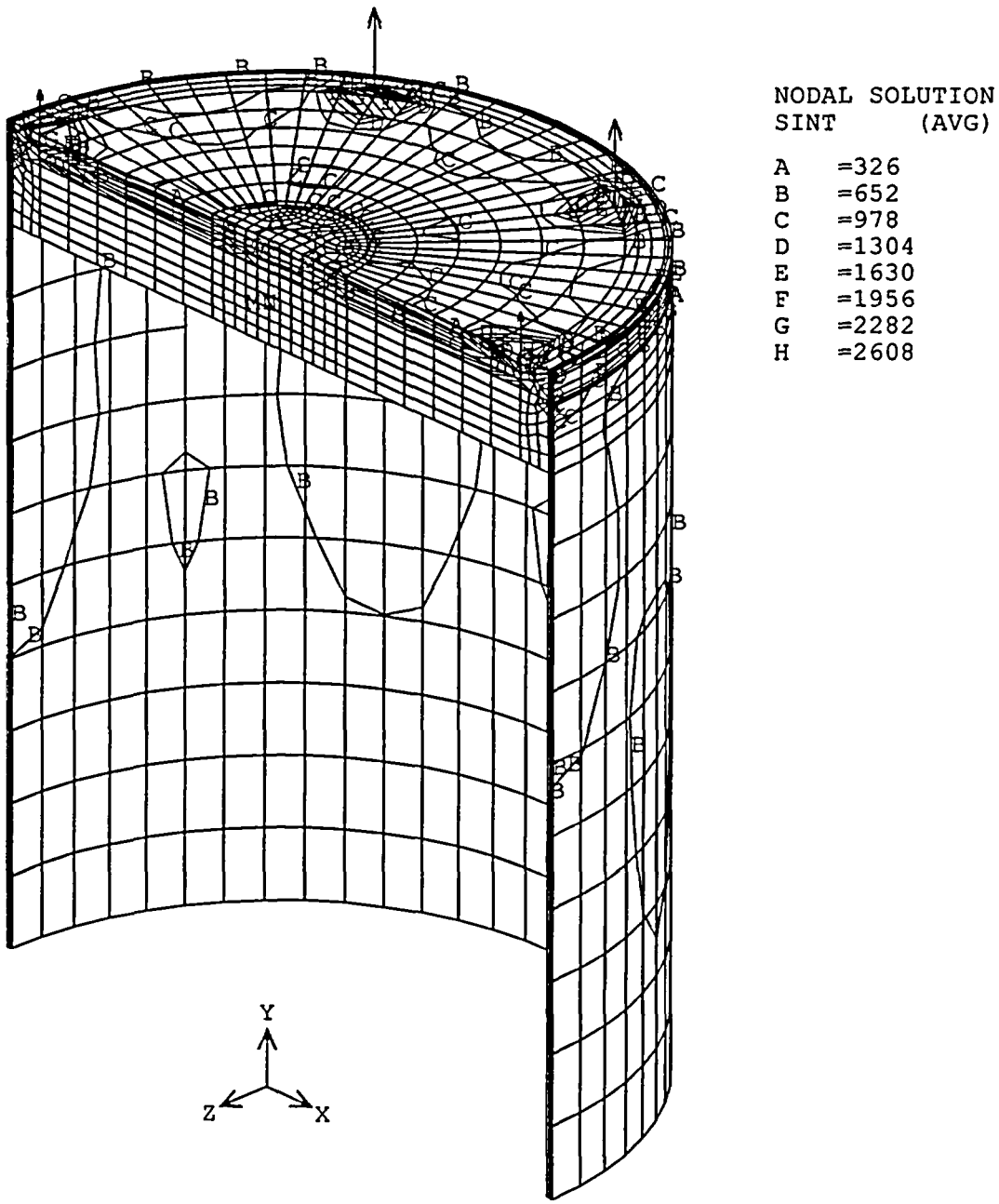

3.4.3.3 Standard Transfer Cask Lift

The evaluation of the standard transfer cask presented here shows that the design meets NUREG-0612 [8] and ANSI N14.6 [9] requirements for nonredundant lift systems. The adequacy of the standard transfer cask is shown by evaluating the stress levels in all of the load-path components against the NUREG-0612 criteria.

3.4.3.3.1 Standard Transfer Cask Shell and Trunnion

The adequacy of the trunnions and the cask shell in the region around the trunnions during lifting conditions is evaluated in this section in accordance with NUREG-0612 and ANSI N14.6.

A three-dimensional finite element model is used to evaluate the lifting of a fully loaded standard transfer cask. Because of symmetry, it was necessary to model only one-quarter of the standard transfer cask, including the trunnions and the shells at the trunnion region. Note that the optional stiffener plates above the trunnions (between the two shells) are not included in the model. The model represents the bounding configuration without the stiffener plates. The lead and the NS-4-FR between the inner and outer shells of the standard transfer cask are neglected, since they are not structural components. SOLID95 (20 noded brick element) and SHELL93 (8 noded shell element) elements are used to model the trunnion and shells, respectively. Due to the absence of rotation degrees of freedom for the SOLID95 elements, BEAM4 elements perpendicular to the shells are used at the interface of the trunnion and the shells to transfer moments from the SOLID95 elements to SHELL93 elements. The finite element model is shown in Figure 3.4.3.3-1.

The total weight of the heaviest loaded standard transfer cask (Class 5 BWR) is calculated at approximately 208,400 pounds. A conservative load of 210,000 lb., plus a 10% dynamic load factor, is used in the model. The load used in the quarter-symmetry model is $(210{,}000 \times 1.1)/4 = 57{,}750$ lb. The load is applied upward at the trunnion as a "surface load" whose location is determined by the lifting yoke dimensions. The model is restrained along two planes of symmetry with symmetry boundary conditions. Vertical restraints are applied to the bottom of the model to resist the force applied to the trunnion.

The maximum temperature in the standard transfer cask shell/trunnion region is conservatively evaluated as 300°F. For the ASTM A-588 shell material, the yield strength, S_y, is 45.6 ksi, and the ultimate strength, S_u, is 70 ksi. The trunnions are constructed of ASTM A-350 carbon steel, Grade LF2, with a yield stress of 31.9 ksi and an ultimate stress of 70 ksi. The standard impact test

temperature for ASTM A-350, Grade LF2 is -50°F. The NDT temperature range is -70°F to -10°F for ASTM A-588 with a thickness range of 0.625 in. to 3 in. [25]. Therefore, the minimum service temperature for the trunnion and shells is conservatively established as 0°F (50°F higher than the NDT test temperature, in accordance with Section 4.2.6 of ANSI N14.6 [9].

Table 3.4.3.3-1 through Table 3.4.3.3-4 provide summaries of the top 30 maximum stresses for both surfaces of the outer shell and inner shell (see Figure 3.4.3.3-2 and Figure 3.4.3.3-3 for node locations for the outer shell and inner shell, respectively). Stress contour plots for the outer shell are shown in Figure 3.4.3.3-4 and Figure 3.4.3.3-5. Stress contours for the inner shell are shown in Figure 3.4.3.3-6 and Figure 3.4.3.3-7. As shown in Table 3.4.3.3-1 through Table 3.4.3.3-4, all stresses, except local stresses, meet the NUREG-0612 and ANSI N14.6 criteria. That is, a factor of safety of 6 applies on material yield strength and 10 applies on material ultimate strength. The high local stresses, as defined in ASME Code Section III, Article NB-3213.10, which are relieved by slight local yielding, are not required to meet the 6 and 10 safety factor criteria [see Ref. 9, Section 4.2.1.2].

The localized stresses occur at the interfaces of the trunnion with the inner and outer shells. The size of the areas are less than 4.1 inches and 4.0 inches for the inner and outer shell, respectively. In accordance with ASME Code, Article NB-3213.10, the area of localized stresses cannot be larger than:

$$1.0\sqrt{Rt}$$

where:

R is the minimum midsurface radius
t is the minimum thickness in the region considered

Based on this formula, the size limitations for local stress regions are 5.1 inches (>4.06 inches) and 7.3 inches (>4.00 inches) for the inner and outer shells, respectively.

For the trunnion, the maximum tensile bending stress and average shear stresses occur at the interface with the outer shell. The linearized stresses through the trunnion are 3,377 psi in bending and 1,687 psi in shear. Comparing these stresses to the material allowable yield and ultimate strength (A350, Grade LF2), the factor of safety on yield strength is 9.4 (which is >6) and on ultimate strength is 20.7 (which is >10).

3.4.3.3.2 Retaining Ring and Bolts

The standard transfer cask uses a retaining ring bolted to the top flange to prevent inadvertent lifting of the canister out of the transfer cask, which could increase the radiation exposure to nearby workers. In the event that the loaded transfer cask is inadvertently lifted by attaching to the canister eyebolts instead of the transfer cask trunnions, the retaining ring and bolts have sufficient strength to support the weight of the heaviest transfer cask, plus a 10% dynamic load factor.

Retaining Ring

To qualify the retaining ring, the equations for annular rings are used (Roark [26], Table 24, Case 1e). The retaining ring is represented as shown in the sketch below. The following sketch assists in defining the variables used to calculate the stress in the retaining ring and bolts. The model assumes a uniform annular line load *w* applied at radius r_o.

The boundary conditions for the model are outer edge fixed, inner edge free with a uniform annular line load w at radius r_o.

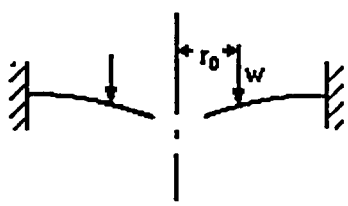

The material properties and parameters for the analysis are:

Plate dimensions:	
thickness:	$t = 0.75$ in
outer radius (bolt circle):	$a = 37.28$ in
outer radius (outer edge):	$c = 38.52$ in
inner radius:	$b = 32.37$ in
Weight of bounding transfer cask:	$wt = 124{,}000 \text{ lb} \times 1.1$
Radial location of applied load:	$r_o = 33.53$ in
Material:	ASTM A-588
Modulus of elasticity:	$E = 28.3 \times 10^6$ psi
Poisson's ratio:	$\nu = 0.31$
Number of bolts:	$Nb = 32$
Radial length of applied load:	$L_r = 2\pi r_o$
	$L_r = 210.675$ in
Applied unit load:	$w \equiv \frac{wt}{L_r}$
	$w = -647.44$ psi

The shear modulus is:

$$G = \frac{E}{2 \cdot (1 + v)}$$

$$G = 1.08 \times 10^7 \text{ psi}$$

D is a plate constant used in determining boundary values; it is also used in the general equations for deflection, slope, moment and shear. K_{sb} and K_{sro} are tangential shear constants used in determining the deflection due to shear:

$$D = \frac{E \cdot t^3}{12 \cdot (1 - v^2)}$$

$$D = 1.101 \times 10^6 \text{ lb-in}$$

Tangential shear constants, K_{sb} and K_{sro}, are used in determining the deflection due to shear:

$$K_{sb} = K_{sro} = -1.2 \cdot \frac{r_o}{a} \cdot \ln\left(\frac{a}{r_o}\right)$$

$$= -0.114$$

Radial moment M_{rb} and M_{ra} at points b and a (inner and outer radius, respectively) are:

M_{rb} (b,0) = 0 lb-in/in

M_{ra} (a,0) = 2207.86 lb-in/in

Transverse moment M_{tb} and M_{ta}, at points b and a (inner and outer radius, respectively) due to bending are:

M_{tb} (b,0) = -122.64 lb-in./in.

M_{ta} (a,0) = 684.44 lb-in./in.

The calculated shear stresses, τ_b and τ_a, at points b and a (inner and outer radius, respectively) are:

$$\tau_b = 0 \text{ psi}$$

$$\tau_a = \frac{wt}{2\pi At}$$

$$\tau_a = -776.42 \text{ psi}$$

The calculated radial bending stresses, σ_{rb} and σ_{ra}, at points b and a (inner and outer radius) are:

$$\sigma_{r(i)} = \frac{6M_{r(i)}}{t^2}$$

$$\sigma_{rb} = 0 \text{ psi}$$

$$\sigma_{ra} = 23{,}550 \text{ psi}$$

The calculated transverse bending stresses, σ_{tb} and σ_{ta}, at points b and a (inner and outer radius) are:

$$\sigma_{t(i)} = \frac{6M_{t(i)}}{t^2}$$

$$\sigma_{tb} = -1308.2 \text{ psi}$$

$$\sigma_{ta} = 7{,}300.7 \text{ psi}$$

The principal stresses at the outer radius are:

$$\sigma_{1a} = 23{,}590 \text{ psi}$$

$$\sigma_{2a} = 7{,}263.6 \text{ psi}$$

$$\sigma_{3a} = 0 \text{ psi}$$

The stress intensity, SI_a, at the outer radius ($P_m + P_b$) is:

$$SI_a = \sigma_{1a} - \sigma_{3a}$$

$$SI_a = 23{,}590 \text{ psi}$$

The principal stresses at the inner radius are:

$$\sigma_{1b} = 0 \text{ psi}$$

$$\sigma_{2b} = -1308.2 \text{ psi}$$

$$\sigma_{3b} = 0 \text{ psi}$$

The stress intensity, SI_b, at the inner radius ($P_m + P_b$) is:

$$SI_b = \sigma_{1b} - \sigma_{2b}$$
$$SI_b = 1308.2 \text{ psi}$$

The maximum stress intensity occurs at the outer radius of the retaining ring. For the off-normal condition, the allowable stress intensity is equal to the lesser of 1.8 S_m and 1.5 S_y. For ASTM A-588, the allowable stress intensity at 300°F is 1.8(23.3) = 41.94 ksi. The calculated stress of 23.59 ksi is less than the allowable stress intensity and the margin of safety is:

$$MS = \frac{41.94}{23.59} - 1 = 0.78$$

Retaining Ring / Canister Bearing

The bearing stress, S_{brg}, between the retaining ring and canister is calculated as:

Weight of Transfer Cask (TFR) = 124,000 × 1.1 = 136,400 lbs.
Area of contact between retaining ring and canister:

$$A = \pi\left(33.53^2 - 32.37^2\right) = 240 \text{ in}^2$$

$$S_{brg} = \frac{136{,}400}{240} = 568 \text{ psi}$$

Bearing stress allowable is S_y. For ASTM A-588, the allowable stress at 300°F is 45.6 ksi. The calculated bearing stress is well below the allowable stress with a large margin of safety.

Shearing stress of Retaining Plate under the Bolt Heads

The shearing stress of the retaining plate under the bolt head is calculated as:

Outside diameter of bolt head d_b = 1.125 in.

Total shear area under bolt head $= \pi\,(1.125) \times 32 \times 0.75$

$= 84.82 \text{ in}^2$.

Shear stress of retaining plate, τ_p, under bolt head is:

$$\tau_p = \frac{136{,}400}{84.82} = 1608\,\text{psi}$$

Conservatively, the shear allowable for normal conditions is used.

$$\tau_{allowable} = (0.6)\,(S_m) = (0.6)\,(23.3\text{ ksi}) = 13.98\text{ ksi}$$

The Margin of Safety is: $\frac{13{,}980}{1{,}608} - 1 = +\text{large}$

Bolt Edge Distance

Using Table J3.5 "Minimum Edge Distance, in." of Section J3 from "Manual of Steel Construction Allowable Stress Design,"[23] the required saw-cut edge distance for a 0.75 inch bolt is 1.0 inch. As shown below, the edge distance for the bolts meets the criteria of the Steel Construction Manual.

$$\frac{77.04 - 74.56}{2} = 1.24\,\text{in} > 1.0\,\text{in}$$

Retaining Ring Bolts

The load on a single bolt, F_F, due to the reactive force caused by inadvertently lifting the canister, is:

$$F_F = \frac{wt}{N_b} = 4{,}262\text{ lb}$$

where:

N_b = number of bolts, 32, and

wt = the weight of the cask, plus a 10% load factor, 124,000 lb × 1.1 = 136,400 lb.

The load on each bolt, F_M, due to the bending moment, is:

$$F_M = \left(\frac{2 \cdot \pi \cdot a}{N_b}\right) \cdot \left(\frac{\sigma \cdot t^2}{6 \cdot L}\right)$$

$$F_M = 12{,}929 \text{ lb}$$

where:

a = the outer radius of the bolt circle, 37.28 in.,

t = the thickness of the ring, 0.75 in.,

σ = the radial bending stress at point *a*, σ_{ra} = 23,550 psi, and

L = the distance between the bolt center line and ring outer edge, c - a = 1.25 in.

The total tension, F, on each bolt is

$$F = F_F + F_M = 17{,}191 \text{ lb}$$

Knowing the bolt cross-sectional area, A_b, the bolt tensile stress is calculated as:

$$\sigma_t = \frac{F}{A_b} = 38{,}912 \text{ psi}$$

where:

$A_b = 0.4418 \text{ in}^2$

For off-normal conditions, the allowable primary membrane stress in a bolt is $2S_m$. The allowable stress for SA-193 Grade B6 bolts is 54 ksi at 120°F, the maximum temperature of the transfer cask top plate. The margin of safety for the bolts is

$$MS = \frac{54{,}000}{38{,}912} - 1 = +0.38$$

Since the SA-193 Grade B6 bolts have higher strength than the top plate, the shear stress in the threads of the top plate is evaluated. The yield and ultimate strengths for the top plate ASTM A-588 material at a temperature of 120°F are:

S_y = 49.5 ksi

S_u = 70.0 ksi

From Reference 27, the shear area for the internal threads of the top plate, A_n, is calculated as:

$$A_n = 3.1416\, n\, L_e\, D_s\min\left[\frac{1}{2n} + 0.57735\left(D_s\min - E_n\max\right)\right] = 1.525\ \text{in}^2$$

where:

D = 0.7482 in., basic major diameter of bolt threads,
n = 10, number of bolt threads per inch,
$D_s\min$ = 0.7353 in., minimum major diameter of bolt threads,
$E_n\max$ = 0.6927 in., maximum pitch diameter of lid threads, and
L_e = 1.625-0.74=0.885 in., minimum thread engagement.

The shear stress (τ_n) in the top plate is:

$$\tau_n = \frac{F}{A_n} = \frac{17{,}191\ \text{lb}}{1.525\ \text{in}^2} = 11{,}273\ \text{psi}$$

Where the total tension, F, on each bolt is

$$F = F_F + F_M = 17{,}191\ \text{lb}$$

The shear allowable for normal conditions is conservatively used:

$$\tau_{allowable} = (0.6)\ (S_m) = (0.6)\ (23.3\ \text{ksi}) = 13.98\ \text{ksi}$$

The Margin of Safety is: $\frac{13{,}980}{11{,}273} - 1 = +0.24$

Therefore, the threads of the top plate will not fail in shear.

3.4.3.3.3 Bottom Plate Weld Analysis

The bottom plate is connected to the outer and inner shell of the transfer cask by full penetration welds. The weight of a loaded canister along with the shield door rail structure is transmitted

from the bottom plate to the shell via the full penetration weld. For conservatism, only the length of the weld directly under the shell is considered effective in transmitting a load.

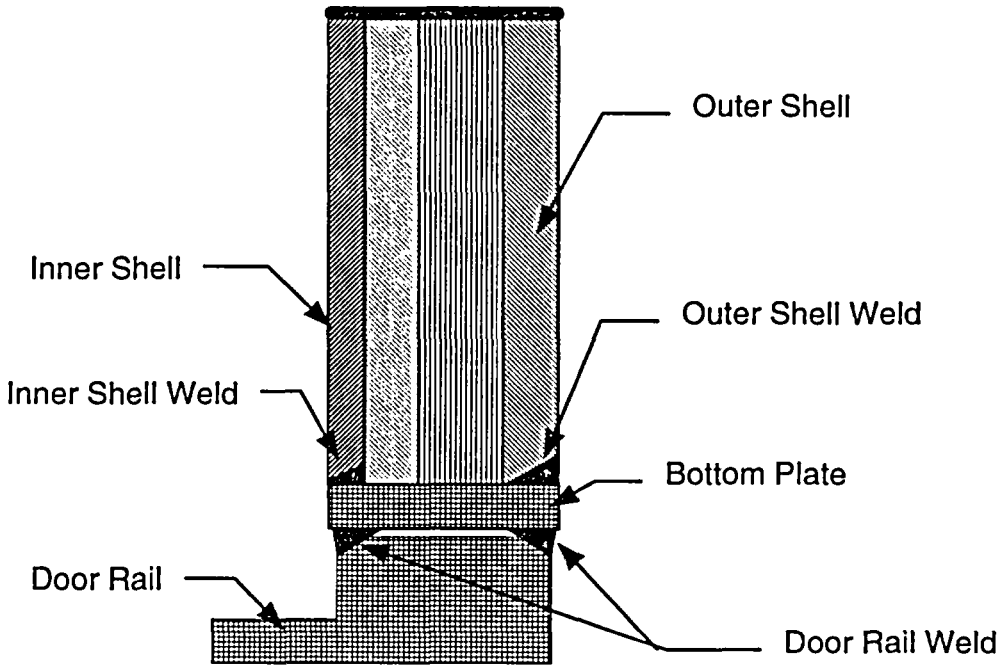

The weld connecting the outer and inner shell to the bottom plate has a length of approximately

$$l_w = (27.33 \text{ in.} + 46.0 \text{ in.})/2 \text{ in.} = 36.66 \text{ in.}$$

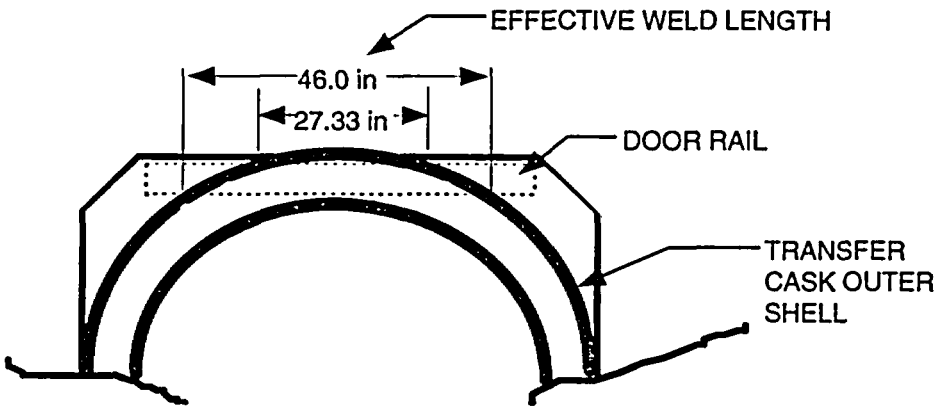

Stresses occurring in the outer shell to bottom plate weld are evaluated using a weight, W = 131,800 lb × 1.1 = 145,000 lb, which bounds the weight of the heaviest loaded canister, the weight of the water, and the weight of the shield doors and rails, with a 10% dynamic load factor.

The door rail structure and canister load will be transmitted to both the inner and outer shell via full penetration welds. The thickness of the two shells and welds are different; however, for conservatism, this evaluation assumes both shell welds are 0.75 in. groove welds.

Weld effective area = (36.66 in.)(0.75 in. + 0.75 in.) = 54.99 in^2

$$\sigma_{axial} = \frac{P}{A} = \frac{(145{,}000\,lb)/(2)}{54.99\,in^2} = 1{,}318\,psi$$

For the bottom plate material (ASTM A-588) at a bounding temperature of 400°F, the yield and ultimate stresses are:

S_y = 43.0 ksi

S_u = 70.0 ksi

$$FS_{yield} = \frac{43.0}{1.32} = +32.6 > 6$$

$$FS_{ultimate} = \frac{70.0}{1.32} = +53.0 > 10$$

Thus, the welds in the bottom plate meet the ANSI N14.6 and NUREG-0612 criteria for nonredundant systems.

3.4.3.3.4 Standard Transfer Cask Shield Door Rails and Welds

This section demonstrates the adequacy of the transfer cask shield doors, door rails, and welds in accordance with NUREG-0612 and ANSI N14.6, which require safety factors of 6 and 10 on material yield strength and ultimate strength, respectively, for nonredundant lift systems.

The shield door rails support the weight of a wet, fully loaded canister and the weight of the shield doors themselves. The shield doors are 9.0-in. thick plates that slide on the door rails. The rails are 9.38 in. deep × 6.5 in. thick and are welded to the bottom plate of the transfer cask. The doors and the rails are constructed of A-588 and A-350 Grade LF 2 low alloy steel, respectively.

The design weight used in this evaluation, W = 131,800 × 1.1 ≈ 145,000 pounds, is an assumed value that bounds the weight of the heaviest loaded canister, the weight of the water in the canister and the weight of the shield doors and rails. A 10% dynamic load factor is included to ensure that the evaluation bounds all normal operating conditions. This evaluation shows that the door rail structures and welds are adequate to support the design input.

Allowable stresses for the material are taken at 400°F, which bounds the maximum temperature at the bottom of the transfer cask under normal conditions. The material properties of A-588 and A-350 Grade LF 2 low alloy steel are provided in Tables 3.3-8 and 3.3-9, respectively. The standard impact test temperature for ASTM A-350, Grade LF2 is -50°F. The NDT temperature range is -70°F to -10°F for ASTM A-588 with a thickness range of 0.625 in. to 3 in. [28]. Therefore, the minimum service temperature for the trunnion and shells is conservatively established as 0°F (50°F higher than the NDT test temperature, in accordance with Section 4.2.6 of ANSI N14.6 [9]. For conservatism, the stress allowables for A-350 Grade LF 2 are used for all stress calculations.

Stress Evaluation for Door Rail

Each rail is assumed to carry a uniformly distributed load equal to 0.5W. The shear stress in each door rail bottom plate due to the applied load, W, is:

$$\tau = \frac{W}{A} = \frac{145{,}000\,\text{lb}}{281.25\,\text{in}^2} = 516\ \text{psi}$$

where:

$$A = 2.5\ \text{in.} \times 56.25\ \text{in. length/rail} \times 2\ \text{rails} = 281.25\ \text{in}^2.$$

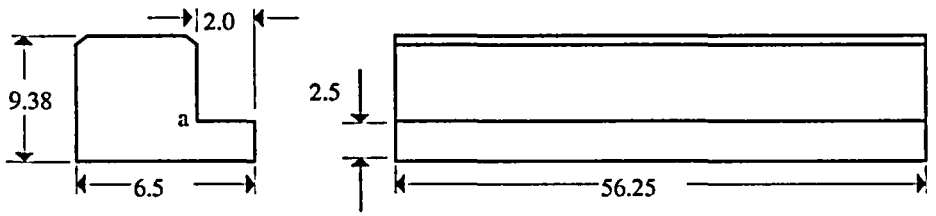

The bending stress in each rail bottom section due to the applied load of W is:

$$\sigma_b = \frac{6M}{bt^2} = \frac{6 \times 86{,}275}{56.25 \times 2.5^2} = 1{,}472 \text{ psi},$$

where:

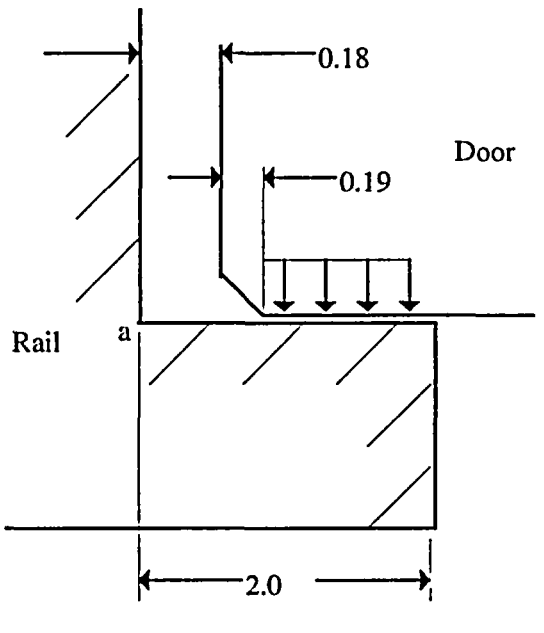

$$M = \text{ moment at } a,$$

$$= \frac{W}{2} \times L = \frac{145{,}000 \text{ lb.}}{2} \times 1.19 \text{ in.}$$

$$= 86{,}275 \text{ in-lb},$$

and,

$$L = 2 - \frac{2-(0.18+0.19)}{2}$$

$$L = 1.19 \text{ in., applied load moment arm.}$$

The maximum principal stress in the bottom section of the rail is:

$$\sigma = \left(\frac{\sigma_b}{2}\right) + \sqrt{\left(\frac{\sigma_b}{2}\right)^2 + \tau^2}$$

$$= 1{,}635 \text{ psi}$$

The acceptability of the rail design is evaluated by comparing the allowable stresses to the maximum calculated stresses, considering the safety factors of NUREG-0612 and ANSI N14.6. For the yield strength criteria:

$$\frac{30{,}800\ \text{psi}}{1{,}635\ \text{psi}} = 18.8 > 6$$

For the ultimate strength criteria,

$$\frac{70{,}000\ \text{psi}}{1{,}635\ \text{psi}} = 42.8 > 10$$

The safety factors meet the criteria of NUREG-0612. Therefore, the rails are structurally adequate.

Stress Evaluation for the Shield Doors

The shield doors consist of a layer of NS-4-FR neutron shielding material sandwiched between low alloy steel plates (Note: steel bars are also welded on the edges of the doors so that the neutron shielding material is fully encapsulated). The door assemblies are 9-inch thick at the center and 6.75-inch thick at the edges, where they slide on the support rails. The stepped edges of the two door leaves are designed to interlock at the center and are, therefore, analyzed as a single plate that is simply supported on two sides.

The shear stress at the edge of the shield door where the door contacts the rail is:

$$\tau = \frac{W}{2 \times A_s} = \frac{145{,}000\ \text{lb}}{2 \times (49.2\ \text{in.} \times 4.75\ \text{in.})} = 310\ \text{psi}$$

where:

A = the total shear area, 4.75 in. thick × 49.2 in. long. Note that the effective thickness at the edge of the doors is taken as 4.75 in. because the neutron shield material and the cover plate are assumed to carry no shear load. The shear stress at the center of the doors approaches 0 psi.

The moment equation for the simply-supported beam with uniform loading is:

$$M = 72{,}500\ X - 2{,}031(X)(0.5\ X) = 72{,}500\ X - 1{,}015\ X^2$$

The maximum bending moment occurs at the center of the doors, X = 35.7 in. The bending moment at this point is:

$$M = 72{,}500 \text{ lb} \times (35.7 \text{ in.}) - 1{,}015 \text{ lb/in.} \times (35.7 \text{ in})^2$$
$$M = 12.95 \times 10^5 \text{ in.-lb.}$$

The maximum bending stress, σ_{max}, at the center of the doors, is

$$\sigma_{ax} = \frac{Mc}{I} = \frac{12.95 \times 10^5 \text{ in.} - \text{lb} \times 5.5 \text{ in.}}{2{,}378 \text{ in.}^4} = 2{,}995 \text{ psi}$$

where:

$$c = \frac{h}{2} = \frac{7 \text{ in.}}{2} + 2 \text{ in.} = 5.5 \text{ in., and}$$

$$I = \frac{bh^3}{12} = \frac{83.2 \text{ in.} \times 7^3 \text{ in}}{12} = 2378 \text{ in}^4.$$

The acceptability of the door design is evaluated by comparing the allowable stresses to the maximum calculated stresses. As shown above, the maximum stress occurs for bending.

For the yield strength criteria,

$$\frac{30{,}800 \text{ psi}}{2{,}995 \text{ psi}} = 10.3 > 6$$

For the ultimate strength criteria,

$$\frac{70{,}000 \text{ psi}}{2{,}995 \text{ psi}} = 23.4 > 10$$

The safety factors satisfy the criteria of NUREG-0612. Therefore, the doors are structurally adequate.

Door Rail Weld Evaluation

The door rails are attached to the bottom of the transfer cask by 0.625-in. partial penetration bevel groove welds that extend the full length of the inside and outside of each rail. If the load is conservatively assumed to act at a point on the inside edge of the rail, the load, P, on each rail is,

$$P = \frac{W}{2} = \frac{145{,}000\ \text{lb}}{2} = 72{,}500\ \text{lb}$$

Summing moments about the inner weld location:

$$0 = P \times a - F_o \times (b) = 72{,}500\ \text{lb} \times 1.19\ \text{in.} - F_o\ (4.5\ \text{in.}),\ \text{or}$$

$$F_o = 19{,}172\ \text{lb}$$

Summing forces:

$$F_i = F_o + P = 19{,}172\ \text{lb} + 72{,}500\ \text{lb} = 91{,}672\ \text{lb}$$

The effective area of the inner weld is $0.625\ \text{in} \times 56.25\ \text{in. long} = 35.16\ \text{in}^2$

The shear stress, τ, in the inner weld is

$$\tau = \frac{91{,}672\ \text{lb}}{35.16\ \text{in}^2} = 2{,}607\ \text{psi}$$

The factors of safety are

$$\frac{30{,}800\ \text{psi}}{2{,}607\ \text{psi}} = 11.8 > 6 \qquad \text{(for yield strength criteria)}$$

$$\frac{70{,}000\ \text{psi}}{2{,}607\ \text{psi}} = 26.8 > 10 \qquad \text{(for ultimate strength criteria)}$$

The safety factors meet the criteria of NUREG-0612.

3.4.3.3.5 PWR Class 1 Standard Transfer Cask with Transfer Cask Extension

The PWR Class 1 standard transfer cask, baseline weight of 112,300 lb. empty, can be equipped with a Transfer Cask extension to accommodate the loading of a PWR Class 2 canister. The purpose of the extended transfer cask configuration is to permit the loading of PWR Class 1 fuel assemblies with Control Element Assemblies inserted into a PWR Class 2 canister; the length of the control element assemblies requires the use of the longer PWR Class 2 canister. The weight of the transfer cask extension is 5,500 pounds. Therefore, the total weight of the PWR Class 1 transfer cask with extension would be:

$$W_{TC} = 112{,}300 + 5{,}500 = 117{,}800 \text{ lbs}$$

Standard Transfer Cask Shell and Trunnion

From the analysis in Section 3.4.3.3.1 for the Transfer Cask Shell and Trunnion, the heaviest loaded transfer cask weight used in the analysis was 210,000 pounds (Class 5 BWR). The total weight of the loaded transfer cask with extension is:

$$W_{TC\text{-}L} = 193{,}900 + 5{,}500 = 199{,}400 \text{ lbs}$$

where:

193,900 lbs = the weight of a PWR Class 1 transfer cask and canister (with fuel, water, and shield lid)

The Class 5 BWR transfer cask configuration bounds the PWR Class 1 transfer cask with extension; therefore, no additional handling analysis is required for the transfer cask shell and trunnions.

Retaining Ring and Bolts

From Section 3.4.3.3.2, the bounding transfer cask weight used was 124,000 pounds. As stated above, the weight of the PWR Class 1 transfer cask with extension is 117,800 pounds; therefore, the existing analysis in Section 3.4.3.3.2 bounds the PWR Class 1 transfer cask with extension and no additional analysis is required.

Standard Transfer Cask Extension Attachment Bolts

The transfer cask extension is attached to the transfer cask by 32 bolts that are identical to the retaining ring bolts with the exception of bolt length. The transfer cask, the top plate, the retaining ring and the extension ring are shown in the following figure. The bolts are only loaded if the transfer cask is accidentally lifted by the retaining ring. In this condition, the only load experienced by the extension bolts is the weight of the transfer cask. The weight of the canister is transferred directly through the lift rig attached to the structural lid.

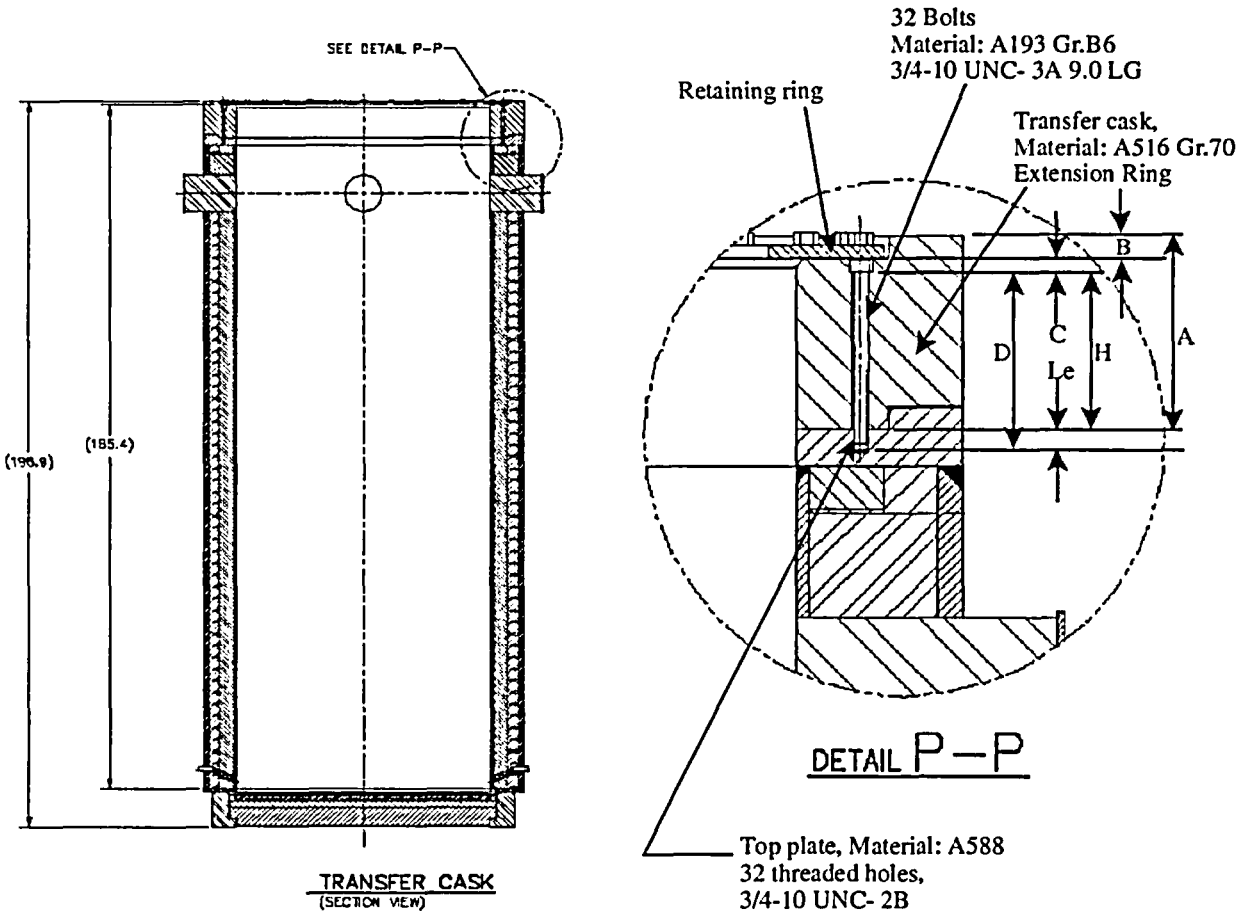

Referring to the preceding figure, the bolt engagement is calculated as follows:

A = 10.3 in. = extension ring thickness
B = 1.2 in = retaining ring seat recess depth
C = 0.81 in. = bolt head counter bore depth
D = 9 in. = bolt body length

The thickness (H) of the extension ring under the bolt head is calculated as:

$$H = A - B - C = 10.3 - 1.2 - 0.81 = 8.29 \text{ in.}$$

The thread engagement length, L_e, in the top plate is:

$$L_e = D - H = 9 - 8.29 = 0.71 \text{ in.}$$

The extension attachment bolts are 9.0 inches long. Since the thickness of the extension ring under the bolt head is 8.29 inches, the prying action is negligible for the transfer cask extension attachment bolts during an inadvertent lift of the transfer cask via the retaining ring during a canister handling operation. The PWR Class 1 Transfer Cask with extension weighs approximately 7,000 pounds less than the bounding analysis weight. A bounding load of 124,000 pounds is conservatively used for this analysis.

The total load (P) applied to each extension bolt is the weight of the transfer cask divided by the number of bolts:

$$P = \frac{(124{,}000)(1.1)}{32} = 4{,}263 \text{ lbs per bolt}$$

The multiplication factor of 1.1 accounts for the dynamic load factor (DLF). From "Machinery's Handbook" [27], the shear area of the external threads (A_s) in the bolt is calculated as:

$$A_s = (3.1416)\, n\, L_e K_n \max\left[\frac{1}{2n} + 0.57735\left(E_s \min - K_n \max\right)\right] = 0.89 \text{ in}^2$$

and the shear area (A_n) for the internal threads of the bolt is calculated as:

$$A_n = (3.1416)\, n\, L_e D_s \min\left[\frac{1}{2n} + 0.57735\left(D_s \min - E_n \max\right)\right] = 1.244 \text{ in}^2$$

where:

K_n max = 0.663 in = maximum minor diameter- internal thread for 3/4 10-UNC-2B

E_s min = 0.6806 in = minimum pitch diameter-external thread for 3/4 10-UNC-3A

D_s min = 0.7371 in = minimum major diameter-external thread for 3/4 10-UNC-3A

E_n max = 0.6927 in = maximum pitch diameter-internal thread for 3/4 10-UNC-2B

L_e = 0.71 in. = length of thread engagement

n = 10 = number of thread per inch

The shear stress (τ_s) on the threads of the bolt is:

$$\tau_s = \frac{4263}{0.89} = 4{,}791 \text{ psi}$$

The allowable stress of ASTM A193 GR B6 at 120°F for pure shear is used.

$$\tau_{allowable} = (0.6)\ (S_m) = (0.6)\ (27.8 \text{ ksi}) = 16.68 \text{ ksi}$$

The margin of safety is $\frac{16.68}{4.79} - 1 = +2.48$

The shear stress (τ_n) on the threads in the bolt hole is:

$$\tau_n = \frac{4263}{1.244} = 3{,}427 \text{ psi}$$

The allowable stress of ASTM A-588 at 120°F for pure shear is used.

$$\tau_{allowable} = (0.6)\ (S_m) = (0.6)\ (23.3 \text{ ksi}) = 13.98 \text{ ksi}$$

The margin of safety is $\frac{13.98}{3.427} - 1 = +3.08$

Figure 3.4.3.3-1 Finite Element Model for Standard Transfer Cask Trunnion and Shells

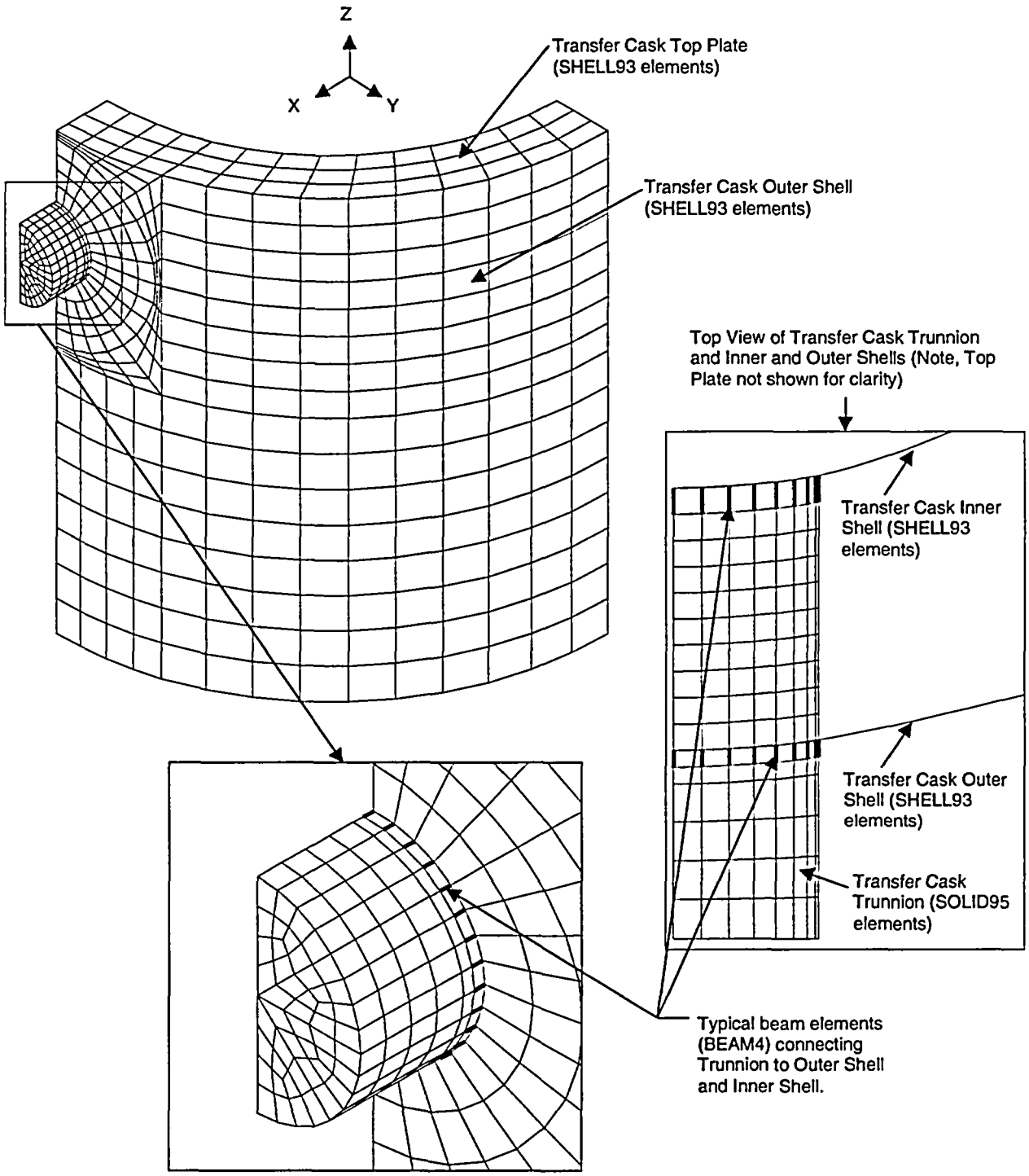

Figure 3.4.3.3-2 Node Locations for Standard Transfer Cask Outer Shell Adjacent to Trunnion

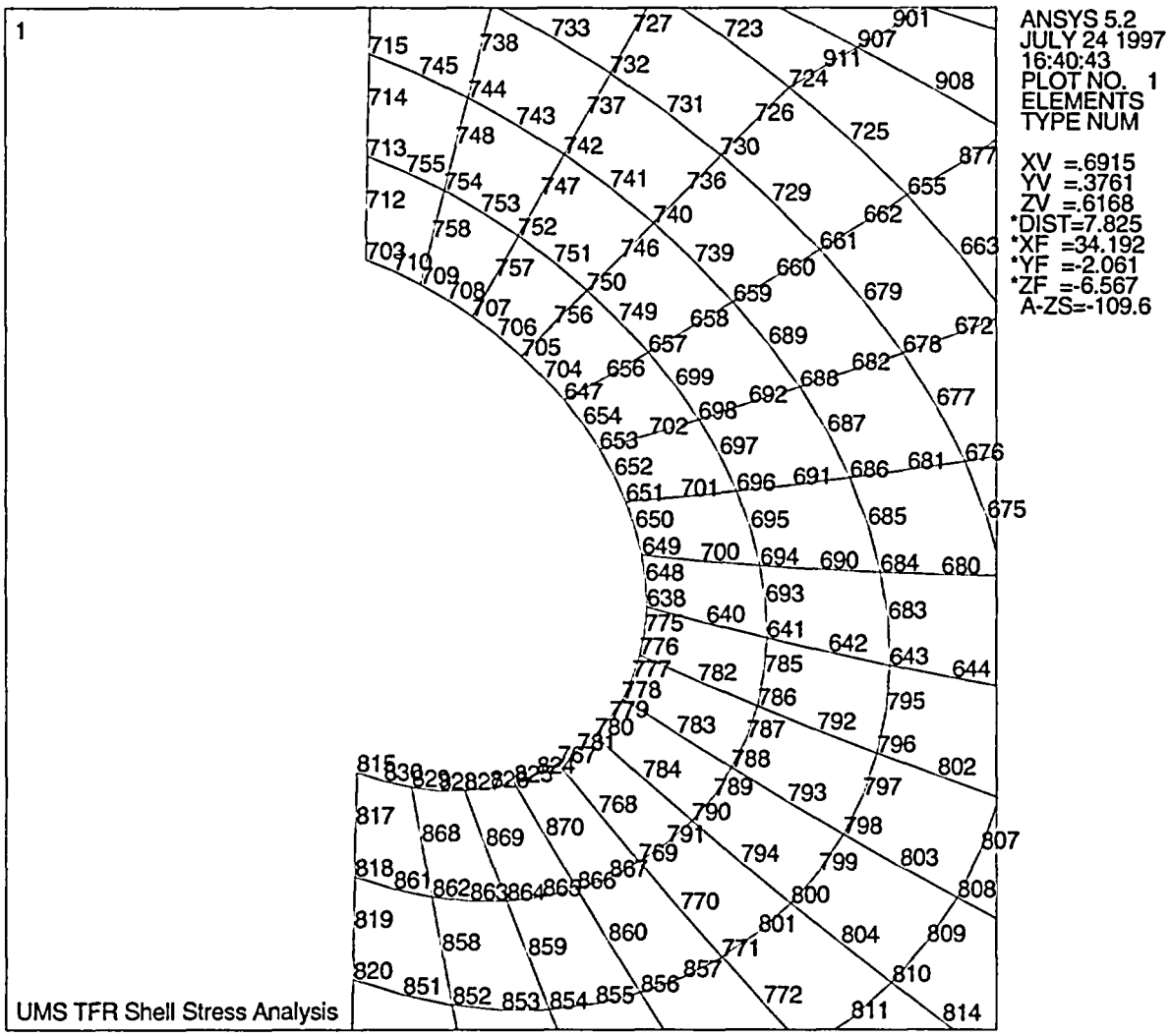

Figure 3.4.3.3-3 Node Locations for Standard Transfer Cask Inner Shell Adjacent to Trunnion

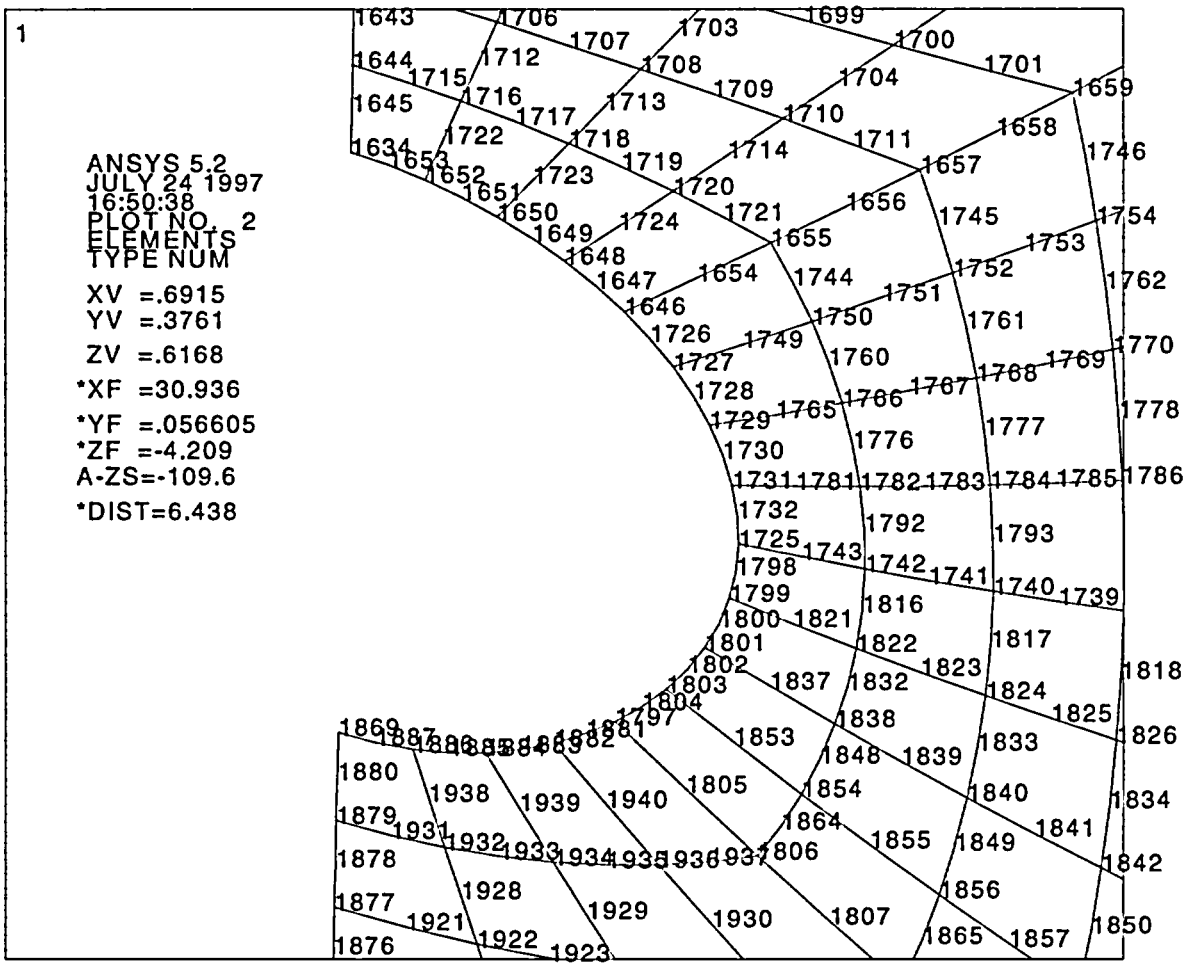

UMS TFR Shell Stress Analysis

Figure 3.4.3.3-4 Stress Intensity Contours (psi) for Standard Transfer Cask Outer Shell Element Top Surface

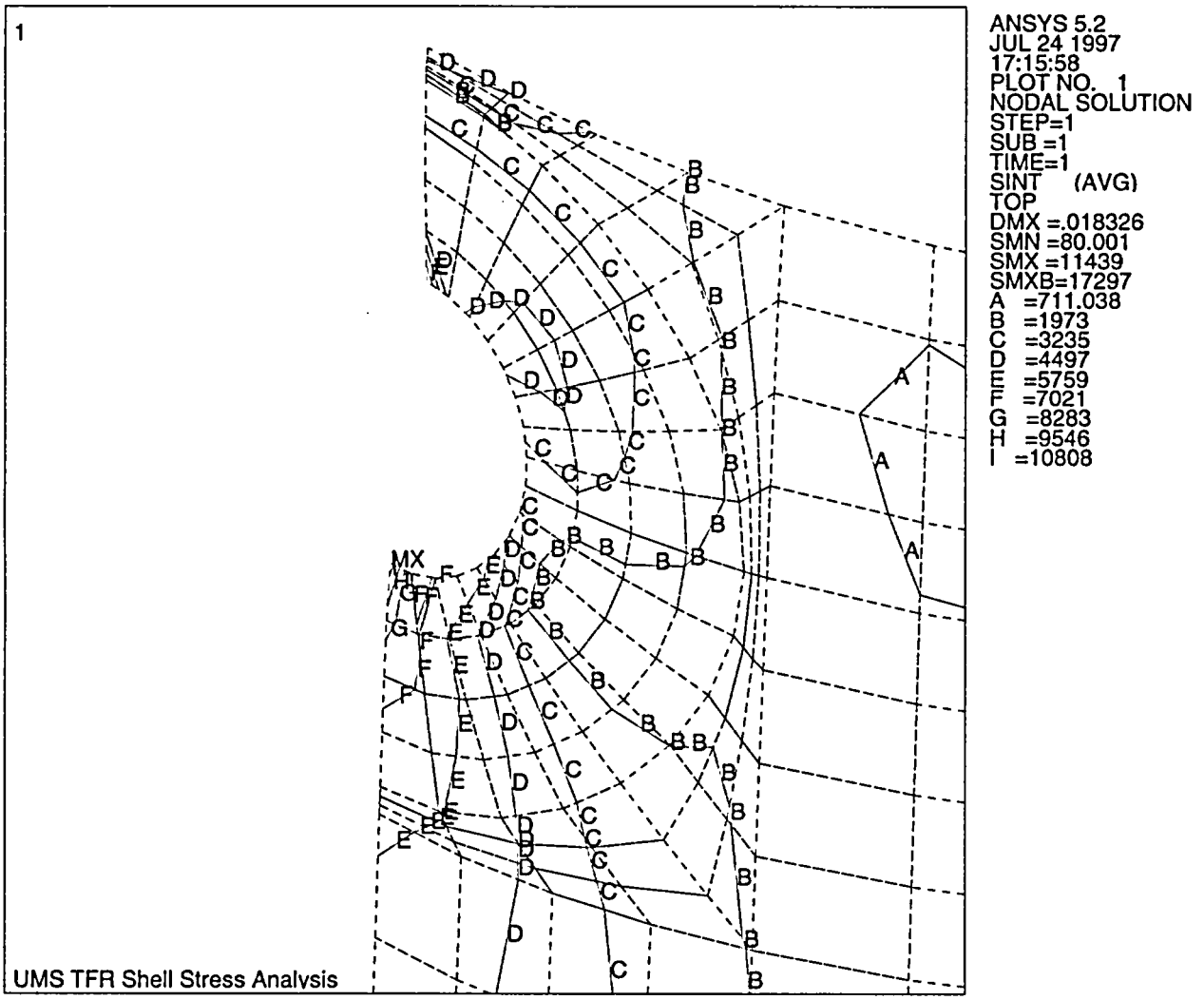

Figure 3.4.3.3-5 Stress Intensity Contours (psi) for Standard Transfer Cask Outer Shell Element Bottom Surface

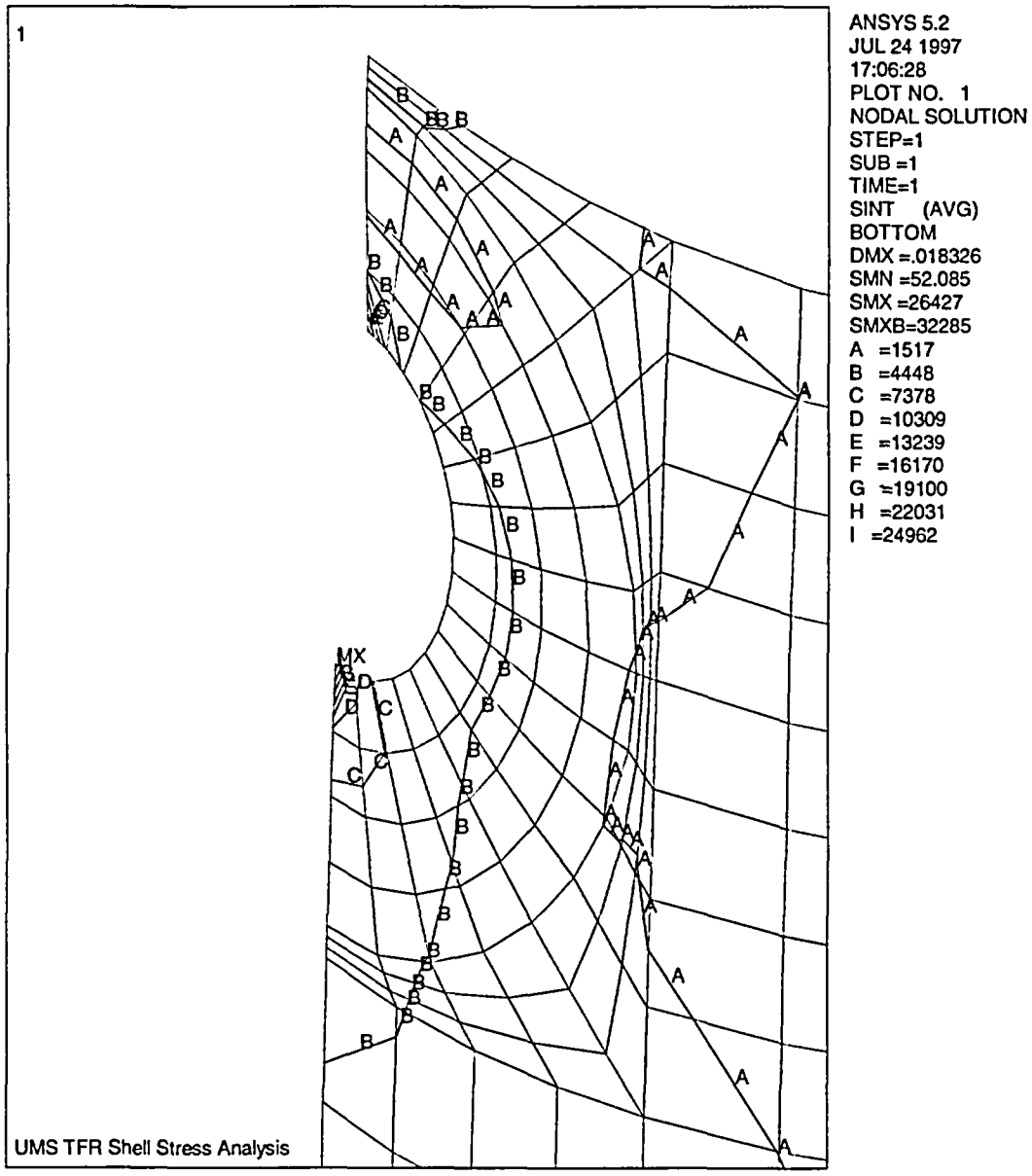

Figure 3.4.3.3-6 Stress Intensity Contours (psi) for Standard Transfer Cask Inner Shell Element Top Surface

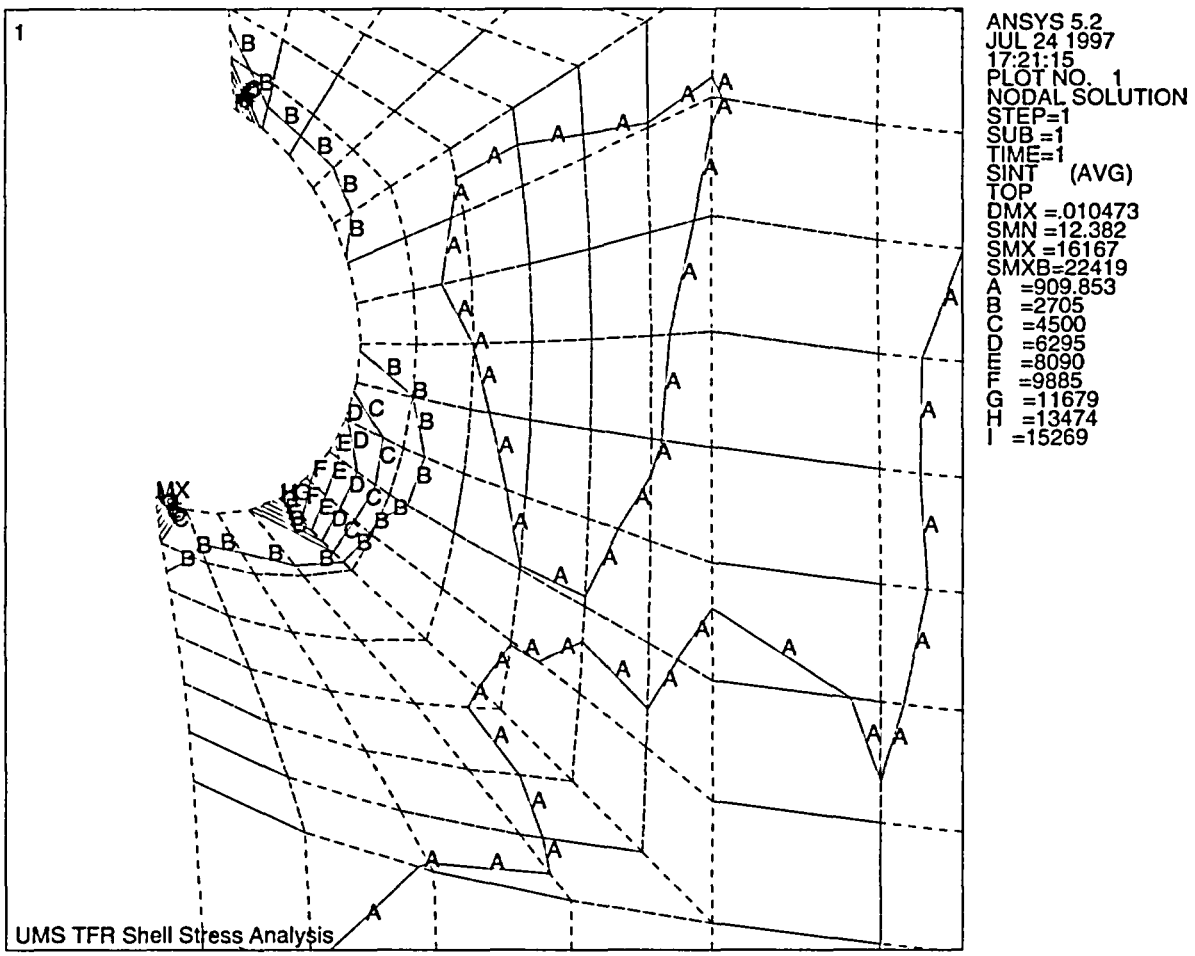

Figure 3.4.3.3-7 Stress Intensity Contours (psi) for Standard Transfer Cask Inner Shell Element Bottom Surface

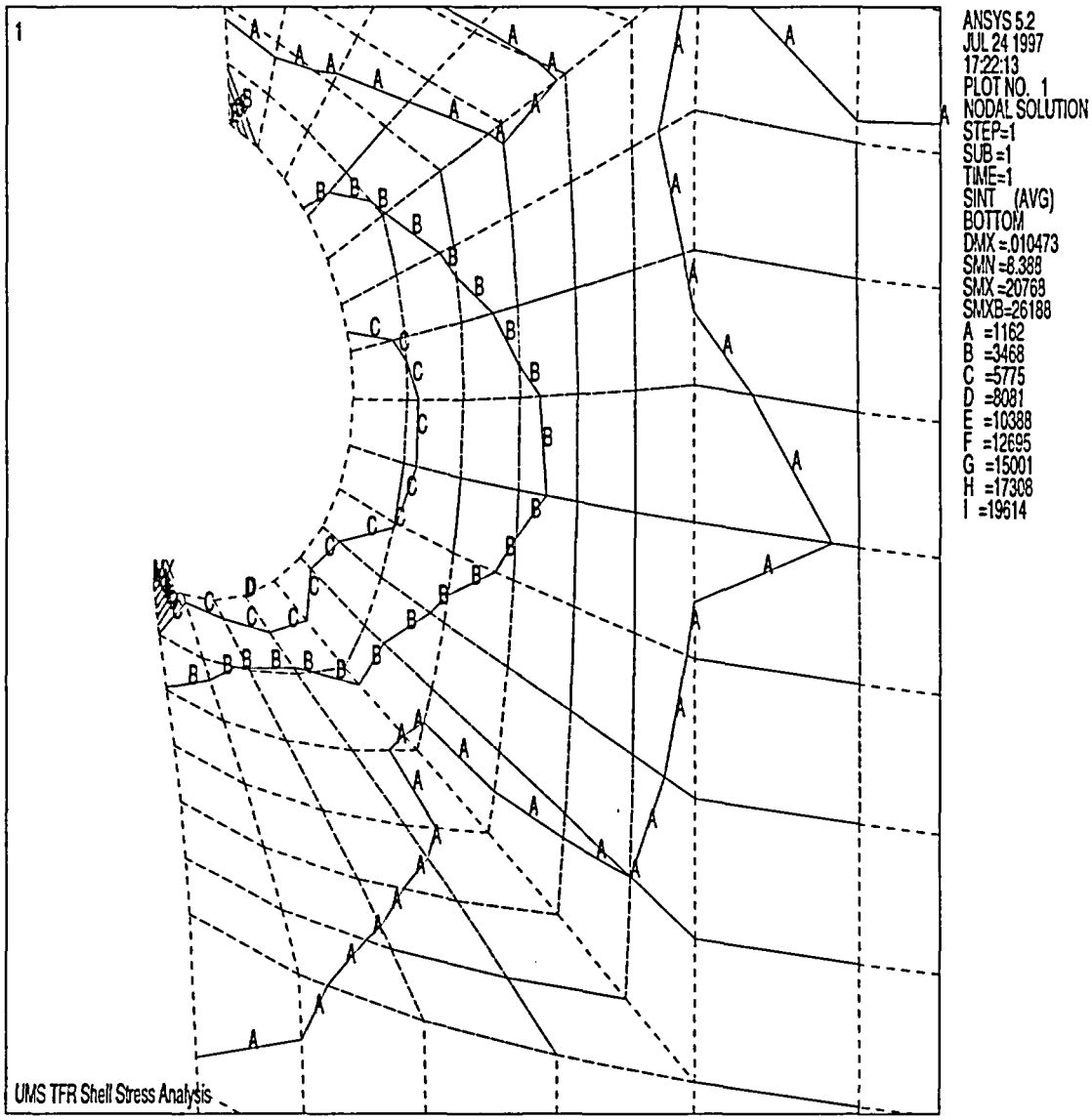

Table 3.4.3.3-1 Top 30 Stresses for Standard Transfer Cask Outer Shell Element Top Surface

Node[1]	Principal Stresses(psi)			Nodal S.I. (psi)	F.S. on Yield S_y/S.I.[2]	F.S. on Ultimate (S_u/S.I.)[2]
	S1	S2	S3			
815	3521.5	-288.8	-7917.2	11439.0	N/A[3]	N/A[3]
818	5092.6	-4.7	-3640.3	8732.9	N/A	N/A
703	7056.8	719.0	-995.8	8052.5	N/A	N/A
820	4315.2	-2.5	-3128.0	7443.2	N/A	N/A
862	4091.0	3.8	-3005.9	7096.9	N/A	N/A
827	4908.7	8.5	-2161.6	7070.3	N/A	N/A
825	4727.4	39.0	-2214.8	6942.2	6.6	10.1
852	4134.8	0.7	-2756.8	6891.6	6.6	10.2
822	3927.3	-0.3	-2788.6	6716.0	6.8	10.4
829	3525.9	-15.5	-3132.6	6658.6	6.8	10.5
767	4010.9	111.0	-2445.3	6456.2	7.1	10.8
842	3806.4	0.2	-2475.5	6281.9	7.3	11.1
816	3607.1	-0.1	-2644.0	6251.1	7.3	11.2
943	3547.6	-0.1	-2638.2	6185.8	7.4	11.3
941	3495.7	-0.1	-2626.5	6122.2	7.4	11.4
2	3430.3	0.0	-2609.0	6039.3	7.6	11.6
832	3497.2	0.2	-2341.5	5838.7	7.8	12.0
964	3412.4	0.3	-2271.0	5683.3	8.0	12.3
864	3625.6	15.6	-2002.0	5627.7	8.1	12.4
854	3683.9	3.6	-1853.7	5537.7	8.2	12.6
954	3335.5	0.3	-2199.9	5535.4	8.2	12.6
8	3251.5	0.1	-2132.4	5383.9	8.5	13.0
780	2941.0	173.8	-2411.8	5352.8	8.5	13.1
871	5250.1	2907.8	-23.4	5273.6	8.6	13.3
47	2848.5	0.0	-2367.8	5216.3	8.7	13.4
844	3470.2	2.3	-1701.8	5172.0	8.8	13.5
657	2272.2	-18.5	-2625.5	4897.7	9.3	14.3
57	2781.3	-0.3	-2093.2	4874.5	9.4	14.4
705	3143.0	-323.9	-1675.6	4818.6	9.5	14.5
834	3227.7	1.9	-1578.1	4805.7	9.5	14.6

Notes:

1. See Figure 3.4.3.3-2 for node locations.
2. S_y = 45,600 psi, S_u = 70,000 psi.
3. Local stresses that are relieved by local material yielding. Therefore, stress design factors of 6 and 10 on material yield and ultimate strength are not applicable (ANSI N14.6, Section 4.2.1.2).

Table 3.4.3.3-2 Top 30 Stresses for Standard Transfer Cask Outer Shell Element Bottom Surface

Node[1]	Principal Stresses(psi)			Nodal S.I. (psi)	F.S. on Yield S_y/S.I.[2]	F.S. on Ultimate (S_u/S.I.)[2]
	S1	S2	S3			
815	26042.0	1368.5	-385.3	26427.0	N/A[3]	N/A[3]
703	433.6	-1196.0	-16049.0	16482.0	N/A	N/A
829	11257.0	4762.2	-25.6	11283.0	N/A	N/A
818	9377.2	1335.4	-11.0	9388.2	N/A	N/A
862	8650.9	2600.4	-13.1	8663.9	N/A	N/A
638	3906.5	-37.6	-3390.4	7296.9	N/A	N/A
864	7245.0	2309.2	-13.3	7258.4	N/A	N/A
776	5054.5	156.6	-1993.6	7048.1	N/A	N/A
649	2372.4	-306.3	-4436.1	6808.5	6.7	10.3
827	6731.4	2737.4	-15.4	6746.9	6.8	10.4
820	6699.0	2463.6	-1.6	6700.6	6.8	10.4
778	5550.7	521.4	-837.7	6388.4	7.1	11.0
852	6375.9	2277.2	-3.5	6379.4	7.1	11.0
709	78.1	-4994.3	-6150.1	6228.2	7.3	11.2
825	6070.4	2367.2	-42.8	6113.2	7.5	11.5
651	1180.6	-998.2	-4879.3	6060.0	7.5	11.6
780	5703.3	1363.7	-312.2	6015.5	7.6	11.6
866	5998.4	1528.3	-1.7	6000.1	7.6	11.7
767	5772.1	2120.8	-131.9	5904.0	7.7	11.9
871	20.8	-416.7	-5855.7	5876.6	7.8	11.9
854	5737.9	1707.3	-4.5	5742.4	7.9	12.2
822	5656.1	1990.6	-0.3	5656.4	8.1	12.4
653	689.6	-2286.6	-4882.7	5572.3	8.2	12.6
842	5453.5	1832.8	-0.8	5454.3	8.4	12.8
873	20.0	-243.1	-5388.0	5408.0	8.4	12.9
769	5322.5	815.7	1.0	5321.5	8.6	13.2
641	3174.6	1.8	-1987.0	5161.6	8.8	13.6
786	3830.7	0.4	-1282.9	5113.5	8.9	13.7
694	2454.1	4.2	-2655.5	5109.6	8.9	13.7
816	5070.5	1851.7	-0.1	5070.6	9.0	13.8

Notes:

1. See Figure 3.4.3.3-2 for node locations.
2. S_y = 45,600 psi, S_u = 70,000 psi.
3. Local stresses that are relieved by local material yielding. Therefore, stress design factors of 6 and 10 on material yield and ultimate strength are not applicable (ANSI N14.6, Section 4.2.1.2).

Table 3.4.3.3-3 Top 30 Stresses for Standard Transfer Cask Inner Shell Element Top Surface

Node[1]	Principal Stresses(psi)			Nodal S.I. (psi)	F.S. on Yield S_y/S.I.[2]	F.S. on Ultimate (S_u/S.I.)[2]
	S1	S2	S3			
1869	1765.2	-503.6	-14402.0	16167.0	N/A[3]	N/A[3]
1797	11044.0	-108.1	-2767.4	13811.0	N/A	N/A
1634	1615.7	-326.8	-12092.0	13708.0	N/A	N/A
1803	10114.0	3278.4	-293.2	10407.0	N/A	N/A
1801	8800.8	3432.8	-213.3	9014.1	N/A	N/A
1799	6238.1	3249.0	-161.2	6399.3	7.1	10.9
1882	728.3	-2351.9	-3701.0	4429.3	10.3	15.8
1633	4070.8	551.7	-1.6	4072.3	11.2	17.2
1879	350.0	-116.5	-3650.0	4000.0	11.4	17.5
1725	3690.7	2859.1	-166.8	3857.5	11.8	18.1
1648	485.8	-261.7	-3244.6	3730.5	12.2	18.8
1652	137.0	-1003.2	-3529.2	3666.2	12.4	19.1
1886	101.9	-2993.0	-3541.1	3643.1	12.5	19.2
1644	962.4	-24.8	-2674.1	3636.5	12.5	19.2
1650	433.9	11.7	-3137.7	3571.6	12.8	19.6
1884	416.6	-1841.5	-3125.6	3542.1	12.9	19.8
1666	3474.7	386.0	-0.3	3475.0	13.1	20.1
1822	3435.6	2108.1	-17.9	3453.6	13.2	20.3
1646	311.6	-945.1	-2960.5	3272.1	13.9	21.4
1838	3148.2	2452.5	-35.3	3183.5	14.3	22.0
1636	3157.0	750.3	-2.3	3159.3	14.4	22.2
1676	2879.2	707.8	-2.4	2881.6	15.8	24.3
1742	2725.1	1367.2	-8.9	2734.0	16.7	25.6
1727	308.8	-540.4	-2300.1	2608.9	17.5	26.8
1668	2486.6	121.0	-10.4	2496.9	18.3	28.0
1854	2393.3	2044.3	-55.4	2448.7	18.6	28.6
1731	2185.5	1530.9	-262.9	2448.4	18.6	28.6
1936	152.0	-126.5	-2235.5	2387.5	19.1	29.3
1638	2372.8	486.1	-2.7	2375.6	19.2	29.5
1120	4.2	-759.8	-2344.0	2348.2	19.4	29.8

Notes:

1. See Figure 3.4.3.3-3 for node locations.
2. S_y = 45,600 psi, S_u = 70,000 psi.
3. Local stresses that are relieved by local material yielding. Therefore, stress design factors of 6 and 10 on material yield and ultimate strength are not applicable (ANSI N14.6, Section 4.2.1.2).

Table 3.4.3.3-4 Top 30 Stresses for Standard Transfer Cask Inner Shell Element Bottom Surface

Node[1]	Principal Stresses(psi)			Nodal S.I. (psi)	F.S. on Yield S_y/S.I.[2]	F.S. on Ultimate (S_u/S.I.)[2]
	S1	S2	S3			
1869	18955.0	554.4	-1812.1	20768.0	N/A[3]	N/A[3]
1634	10094.0	530.6	-887.6	10982.0	N/A	N/A
1882	7550.5	886.3	-631.4	8181.8	N/A	N/A
1797	1147.8	143.2	-5927.0	7074.8	N/A	N/A
1731	2320.8	-75.8	-4368.2	6689.0	6.8	10.5
1884	6149.9	517.9	-483.4	6633.3	6.9	10.6
1725	1242.9	-392.2	-5118.9	6361.8	7.2	11.0
1729	3117.2	52.5	-3023.5	6140.7	7.4	11.4
1803	474.7	-3926.6	-5631.6	6106.3	7.5	11.5
1886	5973.5	2440.1	-81.0	6054.5	7.5	11.6
1801	457.4	-3130.0	-5557.0	6014.4	7.6	11.6
1742	1965.5	-0.9	-4026.8	5992.3	7.6	11.7
1782	2451.4	-0.2	-3512.8	5964.2	7.6	11.7
1799	543.1	-1622.2	-5294.3	5837.4	7.8	12.0
1822	1595.1	4.2	-4233.9	5829.0	7.8	12.0
1766	2666.8	-1.0	-2994.6	5661.4	8.1	12.4
1879	5157.5	127.0	-284.2	5441.6	8.4	12.9
1727	3646.3	282.8	-1615.2	5261.4	8.7	13.3
1838	1426.6	25.3	-3770.7	5197.3	8.8	13.5
1740	2367.5	-2.5	-2661.6	5029.1	9.1	13.9
1784	2285.8	-0.7	-2712.6	4998.4	9.1	14.0
1750	2342.2	-6.7	-2516.2	4858.4	9.4	14.4
1646	3727.5	676.6	-1129.4	4856.9	9.4	14.4
1806	3417.2	95.3	-827.4	4244.6	10.7	16.5
1824	2109.9	-2.3	-2106.6	4216.5	10.8	16.6
1768	1813.3	-0.4	-2337.6	4150.9	11.0	16.9
1854	1304.9	49.1	-2746.8	4051.6	11.3	17.3
1738	2231.7	1.0	-1617.9	3849.6	11.8	18.2
1786	1897.7	0.5	-1860.4	3758.2	12.1	18.6
1932	3722.3	1449.3	-8.2	3730.5	12.2	18.8

Notes:

1. See Figure 3.4.3.3-3 for node locations.
2. S_y = 45,600 psi, S_u = 70,000 psi.
3. Local stresses that are relieved by local material yielding. Therefore, stress design factors of 6 and 10 on material yield and ultimate strength are not applicable (ANSI N14.6, Section 4.2.1.2).

3.4.3.4 Advanced Transfer Cask Lift

The Advanced transfer cask and Standard transfer cask are identical in design, except that the Advanced transfer cask incorporates a 0.75-inch thick support plate positioned above each of the trunnions between the inner shell and the outer shell. The support plate allows the Advanced transfer cask to lifting canisters weighing up to 98,000, whereas the Standard transfer cask is limited to canisters weighing up to 88,000 pounds. The 0.75-inch thick support plate is welded to the inner and outer shells of the Advanced transfer cask, adding significant rigidity to the shell-trunnion juncture to resist the loads applied during the lifting operation of the transfer cask. The welds attaching the support plate to the shells are 0.375-inch double-sided fillet welds at each end of the plate. The support plate is not attached to the trunnion, which prevents any significant shear force from being developed in the welds. The Advanced transfer cask analysis is conservatively based on a transfer cask contents weight of 103,000 pounds.

The evaluation of the Advanced transfer cask presented here shows that the design meets NUREG-0612 [8] and ANSI N14.6 [9] requirements for nonredundant lift systems. The adequacy of the standard transfer cask is shown by evaluating the stress levels in all of the load-path components against the NUREG-0612 criteria.

3.4.3.4.1 Advanced Transfer Cask Shell and Trunnion

The adequacy of the trunnions and the cask shell in the region around the trunnions during lifting conditions is evaluated in this section in accordance with NUREG-0612 and ANSI N14.6.

A three-dimensional finite element model is used to evaluate the lifting of a fully loaded Advanced transfer cask. Because of symmetry, it was necessary to model only one-quarter of the Advanced transfer cask, including the trunnions and the shells at the trunnion region. The stiffener plate above the trunnions (between the two shells) is included in the model. The lead and the NS-4-FR between the inner and outer shells of the Advanced transfer cask are neglected, since they are not structural components. SOLID95 (20 noded brick element) and SHELL93 (8 noded shell element) elements are used to model the trunnion and shells, respectively. Due to the absence of rotational degrees of freedom for the SOLID95 elements, BEAM4 elements perpendicular to the shells are used at the interface of the trunnion and the shells to transfer moments from the SOLID95 elements to SHELL93 elements. The finite element model is shown in Figure 3.4.3.4-1.

The total weight of the heaviest loaded Advanced transfer cask (Advanced Class 3 PWR) is calculated at approximately 217,300 pounds. A conservative load of 225,000 lb., plus a 10% dynamic load factor, is used in the model. The 225,000-pound load corresponds to an assumed transfer cask contents weight of 103,000 pounds. The load used in the quarter-symmetry model is (225,000 × 1.1)/4 = 61,875 pounds. The load is applied upward at the trunnion as a "surface load" whose location is determined by the lifting yoke dimensions. The model is restrained along two planes of symmetry with symmetry boundary conditions. Vertical restraints are applied to the bottom of the model to resist the force applied to the trunnion.

The maximum temperature in the Advanced transfer cask shell/trunnion region is conservatively evaluated as 300°F. For the ASTM A-588 shell material, the yield strength, S_y, is 45.6 ksi, and the ultimate strength, S_u, is 70 ksi. The trunnions are constructed of ASTM A-350 carbon steel, Grade LF2, with a yield stress of 31.9 ksi and an ultimate stress of 70 ksi. The standard impact test temperature for ASTM A-350, Grade LF2 is -50°F. The NDT temperature range is -70°F to -10°F for ASTM A-588 with a thickness range of 0.625 in. to 3 in. [25]. Therefore, the minimum service temperature for the trunnion and shells is conservatively established as -10°F (40°F higher than the NDT test temperature, in accordance with Section 4.2.6 of ANSI N14.6 [9]).

Table 3.4.3.4-1 through Table 3.4.3.4-6 provide summaries of the top 30 maximum combined stresses (Equivalent von Misses stresses) for both surfaces of the outer shell, inner shell, and stiffener plate (see Figure 3.4.3.4-2 through Figure 3.4.3.4-4 for node locations for the outer shell, inner shell, and stiffener plate, respectively). Stress contour plots for the outer shell are shown in Figure 3.4.3.4-5 and Figure 3.4.3.4-6. Stress contours for the inner shell are shown in Figure 3.4.3.4-7 and Figure 3.4.3.4-8. Stress contours for the stiffener plate are shown in Figures 3.4.3.4-9 and 3.4.3.4-10. As shown in Table 3.4.3.4-1 through Table 3.4.3.4-6, all stresses, except local stresses, meet the NUREG-0612 and ANSI N14.6 criteria. That is, a factor of safety of 6 applies on material yield strength and 10 applies on material ultimate strength. The high local stresses, as defined in ASME Code Section III, Article NB-3213.10, which are relieved by slight local yielding, are not required to meet the 6 and 10 safety factor criteria [see Reference 9, Section 4.2.1.2].

The localized stresses occur at the interfaces of the trunnion with the inner and outer shells. In accordance with ASME Code, Article NB-3213.10, the area of localized stresses cannot be larger than:

$1.0\sqrt{Rt}$

where:

R is the minimum midsurface radius

t is the minimum thickness in the region considered

Based on this formula, the maximum distance from the discontinuity to the local high stress is less than 5.1 inches for the inner shell and 7.3 inches for the outer shell.

For the trunnion, the maximum tensile bending stress and average shear stresses occur at the interface with the outer shell. The linearized stresses through the trunnion are 4,260 psi in bending and 1,871 psi in shear. Comparing these stresses to the material allowable yield and ultimate strength (A350, Grade LF2), the factor of safety on yield strength is 7.5 (which is >6) and on ultimate strength is 16.4 (which is >10).

3.4.3.4.2 Advanced Transfer Cask Retaining Ring and Bolts

The Advanced transfer cask uses a retaining ring bolted to the top flange to prevent inadvertent lifting of the canister out of the transfer cask, which could increase the radiation exposure to nearby workers. In the event that the loaded transfer cask is inadvertently lifted by attaching to the canister eyebolts instead of the transfer cask trunnions, the retaining ring and bolts have sufficient strength to support the weight of the heaviest transfer cask, plus a 10% dynamic load factor.

Retaining Ring

To qualify the retaining ring, the equations for annular rings are used (Roark [26], Table 24, Case 1e). The retaining ring is represented as shown in the sketch below. The following sketch assists in defining the variables used to calculate the stress in the retaining ring and bolts. The model assumes a uniform annular line load w applied at radius r_o.

The boundary conditions for the model are outer edge fixed, inner edge free with a uniform annular line load w at radius r_o.

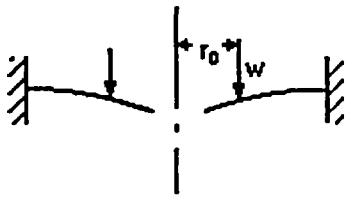

The material properties and parameters for the analysis are:

Plate dimensions:	
thickness:	$t = 0.75$ in
outer radius (bolt circle):	$a = 37.28$ in
outer radius (outer edge):	$c = 38.52$ in
inner radius:	$b = 32.37$ in
Weight of bounding transfer cask:	$wt = 124{,}000$ lb $\times$ 1.1
Radial location of applied load:	$r_o = 33.53$ in
Material:	ASTM A-588
Modulus of elasticity:	$E = 28.3 \times 10^6$ psi
Poisson's ratio:	$v = 0.31$
Number of bolts:	$Nb = 32$
Radial length of applied load:	$L_r = 2\pi r_o$
	$L_r = 210.675$ in
Applied unit load:	$w \equiv \frac{wt}{L_r}$
	$w = 647.44$ psi

The shear modulus is:

$$G = \frac{E}{2 \cdot (1 + v)}$$

$$G = 1.08 \times 10^7 \text{ psi}$$

D is a plate constant used in determining boundary values; it is also used in the general equations for deflection, slope, moment and shear. K_{sb} and K_{sro} are tangential shear constants used in determining the deflection due to shear:

$$D = \frac{E \cdot t^3}{12 \cdot (1 - v^2)}$$

$$D = 1.101 \times 10^6 \text{ lb-in}$$

Tangential shear constants, K_{sb} and K_{sro}, are used in determining the deflection due to shear:

$$K_{sb} = K_{sro} = -1.2 \cdot \frac{r_o}{a} \cdot \ln\left(\frac{a}{r_o}\right)$$

$$= -0.114$$

Radial moment M_{rb} and M_{ra} at point s b and a (inner and outer radius, respectively) are:

M_{rb} (b,0) = 0 lb-in/in

M_{ra} (a,0) = 2207.86 lb-in/in

Transverse moment M_{tb} and M_{ta}, at points b and a (inner and outer radius, respectively) due to bending are:

M_{tb} (b,0) = -122.64 lb-in./in.

M_{ta} (a,0) = 684.44 lb-in./in.

The calculated shear stresses, τ_b and τ_a, at points b and a (inner and outer radius, respectively) are:

$\tau_b = 0$ psi

$$\tau_a = \frac{wt}{2\pi At}$$

$\tau_a = -776.42$ psi

The calculated radial bending stresses, σ_{rb} and σ_{ra}, at points b and a (inner and outer radius) are:

$$\sigma_{r(i)} = \frac{6M_{r(i)}}{t^2}$$

$\sigma_{rb} = 0$ psi

$\sigma_{ra} = 23{,}550$ psi

The calculated transverse bending stresses, σ_{tb} and σ_{ta}, at points b and a (inner and outer radius) are:

$$\sigma_{t(i)} = \frac{6M_{t(i)}}{t^2}$$

$\sigma_{tb} = -1308.2$ psi

$\sigma_{ta} = 7{,}300.7$ psi

The principal stresses at the outer radius are:

$\sigma_{1a} = 23{,}590$ psi
$\sigma_{2a} = 7{,}263.6$ psi
$\sigma_{3a} = 0$ psi

The stress intensity, SI_a, at the outer radius ($P_m + P_b$) is:

$SI_a = \sigma_{1a} - \sigma_{3a}$
$SI_a = 23{,}590$ psi

The principal stresses at the inner radius are:

$\sigma_{1b} = 0$ psi
$\sigma_{2b} = -1308.2$ psi
$\sigma_{3b} = 0$ psi

The stress intensity, SI_b, at the inner radius ($P_m + P_b$) is:

$SI_b = \sigma_{1b} - \sigma_{2b}$
$SI_b = 1308.2$ psi

The maximum stress intensity occurs at the outer radius of the retaining ring. For the off-normal condition, the allowable stress intensity is equal to the lesser of 1.8 S_m and 1.5 S_y. For ASTM A-588, the allowable stress intensity at 300°F is 1.8(23.3) = 41.94 ksi. The calculated stress of 23.59 ksi is less than the allowable stress intensity and the margin of safety is:

$$MS = \frac{41.94}{23.59} - 1 = +0.78$$

<u>Retaining Ring / Canister Bearing</u>

The bearing stress, S_{brg}, between the retaining ring and canister is calculated as:

Weight of Transfer Cask (TFR) = 124,000 × 1.1 = 136,400 lbs.

Area of contact between retaining ring and canister:

$$S_{brg} = \frac{136{,}400}{240} = 568 \text{ psi}$$

$$A = \pi\left(33.53^2 - 32.37^2\right) = 240 \text{ in}^2$$

Bearing stress allowable is S_y. For ASTM A-588, the allowable stress at 300°F is 45.6 ksi. The Calculated bearing stress is well below the allowable stress with a large margin of safety.

Shearing Stress of Retaining Plate under the Bolt Heads

The shearing stress of the retaining plate under the bolt head is calculated as:

Outside diameter of bolt head d_b = 1.125 in.

Total shear area under bolt head = $\pi\,(1.125) \times 32 \times 0.75$

= 84.82 in^2.

$\tau_p = \frac{136{,}400}{84.82} = 1608 \text{ psi}$ Shear stress of retaining plate, τ_p, under bolt head is:

$$\tau_p = \frac{136{,}400}{84.82} = 1{,}608 \text{ psi}$$

Conservatively, the shear allowable for normal conditions is used.

$$\tau_{allowable} = (0.6)\,(S_m) = (0.6)\,(23.3 \text{ ksi}) = 13.98 \text{ ksi}$$

The Margin of Safety is: $\frac{13{,}980}{1{,}608} - 1 = +\text{large}$

Bolt Edge Distance

$\frac{77.04 - 74.56}{2} = 1.24 \text{ in} > 1.0 \text{ in}$ Using Table J3.5 "Minimum Edge Distance, in." of Section J3 from "Manual of Steel Construction Allowable Stress Design,"[23] the required saw-cut edge distance for a 0.75 inch bolt is 1.0 inch. The edge distance for the bolts that meets the criteria of the Steel Construction Manual is:

$$\frac{77.04 - 74.56}{2} = 1.24\,\text{in} > 1.0\,\text{in}$$

Retaining Ring Bolts

The load on a single bolt, F_F, due to the reactive force caused by inadvertently lifting the canister, is:

$$F_F = \frac{wt}{N_b} = 4{,}262\ \text{lb}$$

where:

N_b = number of bolts, 32, and

wt = the weight of the cask, plus a 10% load factor, 124,000 lb × 1.1 = 136,400 lb.

The load on each bolt, F_M, due to the bending moment, is:

$$F_M = \left(\frac{2 \cdot \pi \cdot a}{N_b}\right) \cdot \left(\frac{\sigma \cdot t^2}{6 \cdot L}\right)$$

$$F_M = 12{,}929\ \text{lb}$$

where:

a = the outer radius of the bolt circle, 37.28 in.,

t = the thickness of the ring, 0.75 in.,

σ = the radial bending stress at point *a*, σ_{ra} = 23,550 psi, and

L = the distance between the bolt centerline and ring outer edge, c - a = 1.25 in.

The total tension, F, on each bolt is

$$F = F_F + F_M = 17{,}191\ \text{lb}$$

Knowing the bolt cross-sectional area, A_b, the bolt tensile stress is calculated as:

$$\sigma_t = \frac{F}{A_b} = 38{,}912\ \text{psi}$$

where:

$A_b = 0.4418\ \text{in}^2$

For off-normal conditions, the allowable primary membrane stress in a bolt is $2S_m$. The allowable stress for SA-193 Grade B6 bolts is 54 ksi at 120°F, the maximum temperature of the transfer cask top plate. The margin of safety for the bolts is

$$MS = \frac{54{,}000}{38{,}912} - 1 = +0.38$$

Since the SA-193 Grade B6 bolts have higher strength than the top plate, the shear stress in the threads of the top plate is evaluated. The yield and ultimate strengths for the top plate ASTM A-588 material at a temperature of 120°F are:

S_y = 49.5 ksi
S_u = 70.0 ksi

From Reference 27, the shear area for the internal threads of the top plate, A_n, is calculated as:

$$A_n = 3.1416\, n\, L_e\, D_s\min\left[\frac{1}{2n} + 0.57735\left(D_s\min - E_n\max\right)\right] = 1.525 \text{ in}^2$$

where:

D = 0.7482 in., basic major diameter of bolt threads,
n = 10, number of bolt threads per inch,
$D_s$min = 0.7353 in., minimum major diameter of bolt threads,
$E_n$max = 0.6927 in., maximum pitch diameter of lid threads, and
L_e = 1.625-0.74=0.885 in., minimum thread engagement.

The shear stress (τ_n) in the top plate is:

$$\tau_n = \frac{F}{A_n} = \frac{17{,}191 \text{ lb}}{1.525 \text{ in}^2} = 11{,}273 \text{ psi}$$

Where the total tension, F, on each bolt is

$$F = F_F + F_M = 17{,}191 \text{ lb}$$

The shear allowable for normal conditions is conservatively used:

$$\tau_{allowable} = (0.6)\ (S_m) = (0.6)\ (23.3\ ksi) = 13.98\ ksi$$

The Margin of Safety is:

$$MS = \frac{13{,}980}{11{,}273} - 1 = +0.24$$

Therefore, the threads of the top plate will not fail in shear.

3.4.3.4.3 Advanced Transfer Cask Bottom Plate Weld Analysis

The bottom plate is connected to the outer and inner shell of the transfer cask by full penetration welds. The weight of a loaded canister along with the shield door rail structure is transmitted from the bottom plate to the shell via the full penetration weld. For conservatism, only the length of the weld directly under the shell is considered effective in transmitting a load.

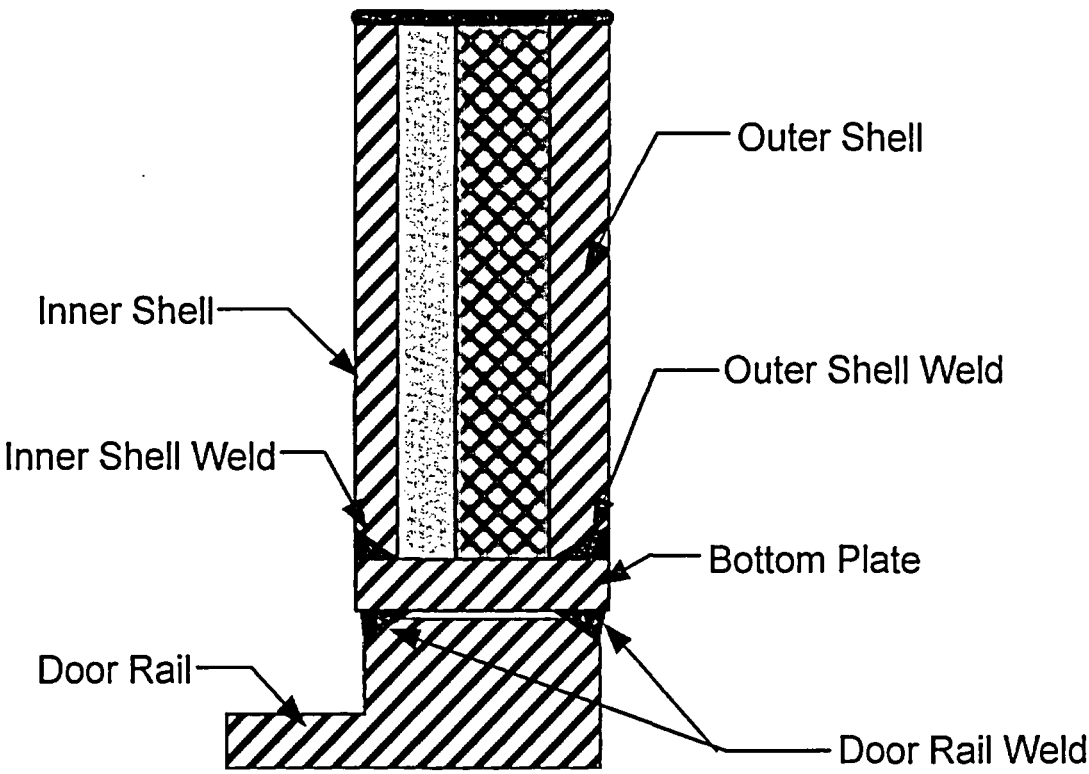

The weld connecting the outer and inner shell to the bottom plate has a length of approximately

l_w = (27.33 in. + 46.0 in.)/2 in. = 36.66 in.

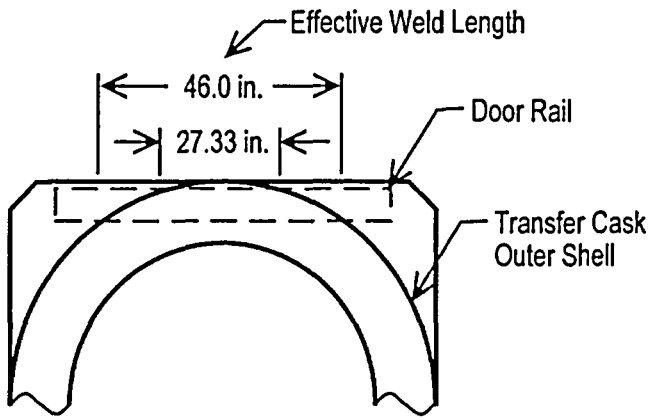

Stresses occurring in the outer shell to bottom plate weld are evaluated using a weight, W = 131,800 lb × 1.1 = 145,000 lb, which bounds the weight of the heaviest loaded canister, the weight of the water, and the weight of the shield doors and rails, with a 10% dynamic load factor.

The door rail structure and canister load will be transmitted to both the inner and outer shell via full penetration welds. The thickness of the two shells and welds are different; however, for conservatism, this evaluation assumes both shell welds are 0.75 in. groove welds.

Weld effective area = (36.66 in.)(0.75 in. + 0.75 in.) = 54.99 in^2

$$\sigma_{axial} = \frac{P}{A} = \frac{(145{,}000\,\text{lb})/(2)}{54.99\,\text{in}^2} = 1{,}318\,\text{psi}$$

For the bottom plate material (ASTM A-588) at a bounding temperature of 400°F, the yield and ultimate stresses are:

$$FS_{yield} = \frac{43.0}{1.32} = +32.6 > 6$$

$$FS_{ultimate} = \frac{70.0}{1.32} = +53.0 > 10$$

where:

S_y = 43.0 ksi

S_u = 70.0 ksi

Thus, the welds in the bottom plate meet the ANSI N14.6 and NUREG-0612 criteria for nonredundant systems.

3.4.3.4.4 Advanced Transfer Cask Shield Door Rails and Welds

This section demonstrates the adequacy of the transfer cask shield doors, door rails, and welds in accordance with NUREG-0612 and ANSI N14.6, which require safety factors of 6 and 10 on material yield strength and ultimate strength, respectively, for nonredundant lift systems.

The shield door rails support the weight of a wet, fully loaded canister and the weight of the shield doors themselves. The shield doors are 9.0-in. thick plates that slide on the door rails. The rails are 9.38 in. deep × 6.5 in. thick and are welded to the bottom plate of the transfer cask. The doors and the rails are constructed of A-588 and A-350 Grade LF 2 low alloy steel, respectively.

The design weight used in this evaluation, $W = 131{,}800 \times 1.1 \approx 145{,}000$ pounds, is an assumed value that bounds the weight of the heaviest loaded canister, the weight of the water in the canister and the weight of the shield doors and rails. A 10% dynamic load factor is included to ensure that the evaluation bounds all normal operating conditions. This evaluation shows that the door rail structures and welds are adequate to support the design input.

Allowable stresses for the material are taken at 400°F, which bounds the maximum temperature at the bottom of the transfer cask under normal conditions. The material properties of A-588 and A-350 Grade LF 2 low alloy steel are provided in Tables 3.3-8 and 3.3-9, respectively. The standard impact test temperature for ASTM A-350, Grade LF2 is -50°F. The NDT temperature range is -70°F to -10°F for ASTM A-588 with a thickness range of 0.625 in. to 3 in. [28]. Therefore, the minimum service temperature for the trunnion and shells is conservatively established as 0°F (50°F higher than the NDT test temperature, in accordance with Section 4.2.6 of ANSI N14.6 [9]. For conservatism, the stress allowables for A-350 Grade LF 2 are used for all stress calculations.

Stress Evaluation for Door Rail

Each rail is assumed to carry a uniformly distributed load equal to 0.5W. The shear stress in each door rail bottom plate due to the applied load, W, is:

$$\tau = \frac{W}{A} = \frac{145{,}000\,\text{lb}}{281.25\,\text{in}^2} = 516\ \text{psi}$$

where:

$$A = 2.5\ \text{in.} \times 56.25\ \text{in. length/rail} \times 2\ \text{rails} = 281.25\ \text{in}^2.$$

The bending stress in each rail bottom section due to the applied load of W is:

$$\sigma_b = \frac{6M}{bt^2} = \frac{6 \times 86{,}275}{56.25 \times 2.5^2} = 1{,}472\ \text{psi},$$

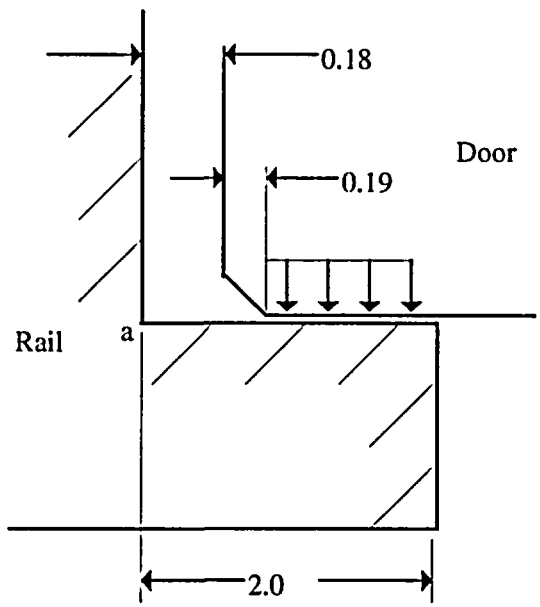

where:

$$M = \text{moment at } a,$$

$$= \frac{W}{2} \times L = \frac{145{,}000\ \text{lb.}}{2} \times 1.19\ \text{in.}$$

$$= 86{,}275\ \text{in-lb},$$

and,

$$L- = 2 - \frac{2-(0.18+0.19)}{2}$$

$$L = 1.19\ \text{in., applied load moment arm.}$$

The maximum principal stress in the bottom section of the rail is:

$$\sigma = \left(\frac{\sigma_b}{2}\right) + \sqrt{\left(\frac{\sigma_b}{2}\right)^2 + \tau^2}$$
$$= 1{,}635 \text{ psi}$$

The acceptability of the rail design is evaluated by comparing the allowable stresses to the maximum calculated stresses, considering the safety factors of NUREG-0612 and ANSI N14.6. For the yield strength criteria:

$$\frac{30{,}800 \text{ psi}}{1{,}635 \text{ psi}} = 18.8 > 6$$

For the ultimate strength criteria,

$$\frac{70{,}000 \text{ psi}}{1{,}635 \text{ psi}} = 42.8 > 10$$

The safety factors meet the criteria of NUREG-0612. Therefore, the rails are structurally adequate.

Stress Evaluation for the Shield Doors

The shield doors consist of a layer of NS-4-FR neutron shielding material sandwiched between low alloy steel plates (Note: steel bars are also welded on the edges of the doors so that the neutron shielding material is fully encapsulated). The door assemblies are 9-inch thick at the center and 6.75-inch thick at the edges, where they slide on the support rails. The stepped edges of the two door leaves are designed to interlock at the center and are, therefore, analyzed as a single plate that is simply supported on two sides.

The shear stress at the edge of the shield door where the door contacts the rail is:

$$\tau = \frac{W}{2 \times A_S} = \frac{145{,}000 \text{ lb}}{2 \times (49.2 \text{ in.} \times 4.75 \text{ in.})} = 310 \text{ psi}$$

where:

A = the total shear area, 4.75 in. thick × 49.2 in. long. Note that the effective thickness at the edge of the doors is taken as 4.75 in. because the neutron shield material and the cover plate are assumed to carry no shear load. The shear stress at the center of the doors approaches 0 psi.

The moment equation for the simply-supported beam with uniform loading is:

$$M = 72{,}500\,X - 2{,}031(X)(0.5\,X) = 72{,}500\,X - 1{,}015\,X^2$$

The maximum bending moment occurs at the center of the doors, X = 35.7 in. The bending moment at this point is:

$$M = 72{,}500 \text{ lb} \times (35.7 \text{ in.}) - 1{,}015 \text{ lb/in.} \times (35.7 \text{ in})^2$$
$$M = 12.95 \times 10^5 \text{ in.-lb.}$$

The maximum bending stress, σ_{max}, at the center of the doors, is

$$\sigma_{ax} = \frac{Mc}{I} = \frac{12.95\times10^5 \text{ in.} - \text{lb}\times5.5 \text{ in.}}{2{,}378 \text{ in.}^4} = 2{,}995 \text{ psi}$$

where:

$$c = \frac{h}{2} = \frac{7 \text{ in.}}{2} + 2 \text{ in.} = 5.5 \text{ in., and}$$

$$I = \frac{bh^3}{12} = \frac{83.2 \text{ in.}\times7^3 \text{ in}}{12} = 2{,}378 \text{ in}^4.$$

The acceptability of the door design is evaluated by comparing the allowable stresses to the maximum calculated stresses. As shown above, the maximum stress occurs for bending.

For the yield strength criteria,

$$\frac{30{,}800 \text{ psi}}{2{,}995 \text{ psi}} = 10.3 > 6$$

For the ultimate strength criteria,

$$\frac{70{,}000\ \text{psi}}{2{,}995\ \text{psi}} = 23.4 > 10$$

The safety factors satisfy the criteria of NUREG-0612. Therefore, the doors are structurally adequate.

Door Rail Weld Evaluation

The door rails are attached to the bottom of the transfer cask by 0.75-in. partial penetration bevel groove welds that extend the full length of the inside and outside of each rail. If the load is conservatively assumed to act at a point on the inside edge of the rail, the load, P, on each rail is,

$$P = \frac{W}{2} = \frac{145{,}000\ \text{lb}}{2} = 72{,}500\ \text{lb}$$

Summing moments about the inner weld location:

$$0 = P \times a - F_o \times (b) = 72{,}500\ \text{lb} \times 1.19\ \text{in.} - F_o\ (4.5\ \text{in.}),\ \text{or}$$

$$F_o = 19{,}172\ \text{lb}$$

Summing forces:

$$F_i = F_o + P = 19{,}172\ \text{lb} + 72{,}500\ \text{lb} = 91{,}672\ \text{lb}$$

The effective area of the inner weld is $0.75\ \text{in} \times .707 \times 56.25\ \text{in. long} = 29.83\ \text{in}^2$

The shear stress, τ, in the inner weld is

$$\tau = \frac{91{,}672\ \text{lb}}{29.83\ \text{in}^2} = 3{,}073\ \text{psi}$$

The factors of safety are

$$\frac{30{,}800\ \text{psi}}{3{,}073\ \text{psi}} = 10.0 > 6 \qquad \text{(for yield strength criteria)}$$

$$\frac{70{,}000\ \text{psi}}{3{,}073\ \text{psi}} = 22.8 > 10 \qquad \text{(for ultimate strength criteria)}$$

The safety factors meet the criteria of NUREG-0612.

Figure 3.4.3.4-1 Advanced Transfer Cask Finite Element Model

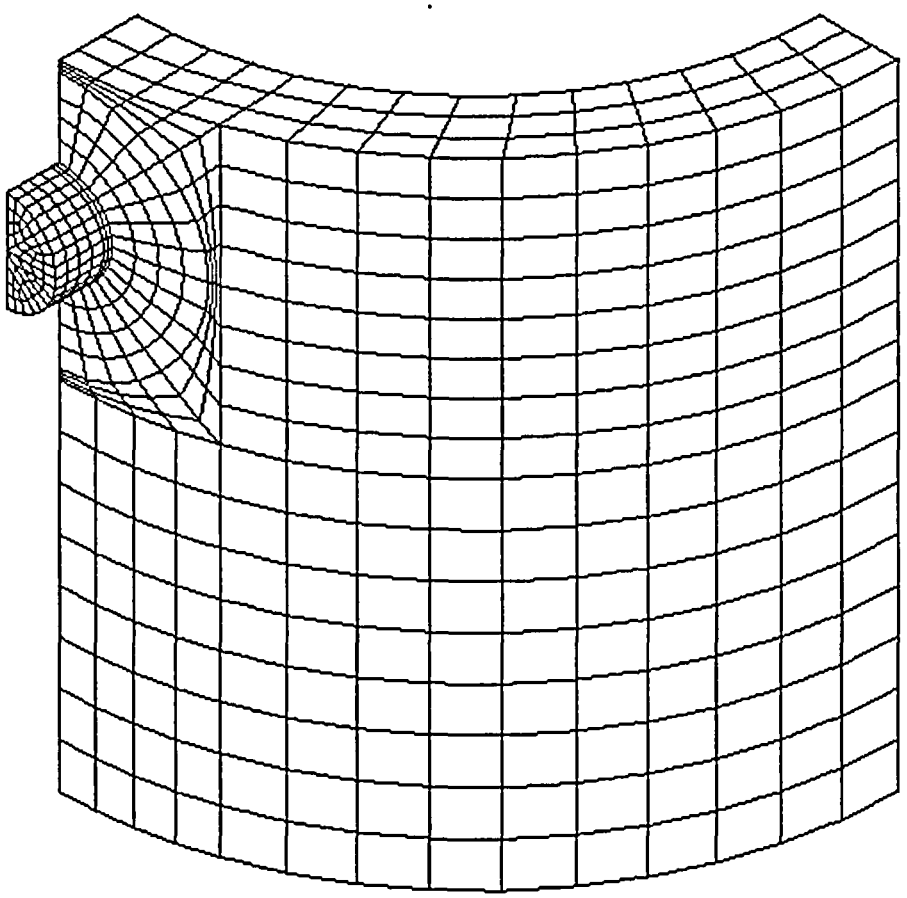

Figure 3.4.3.4-2 Node Locations for Advanced Transfer Cask Outer Shell Adjacent to Trunnion

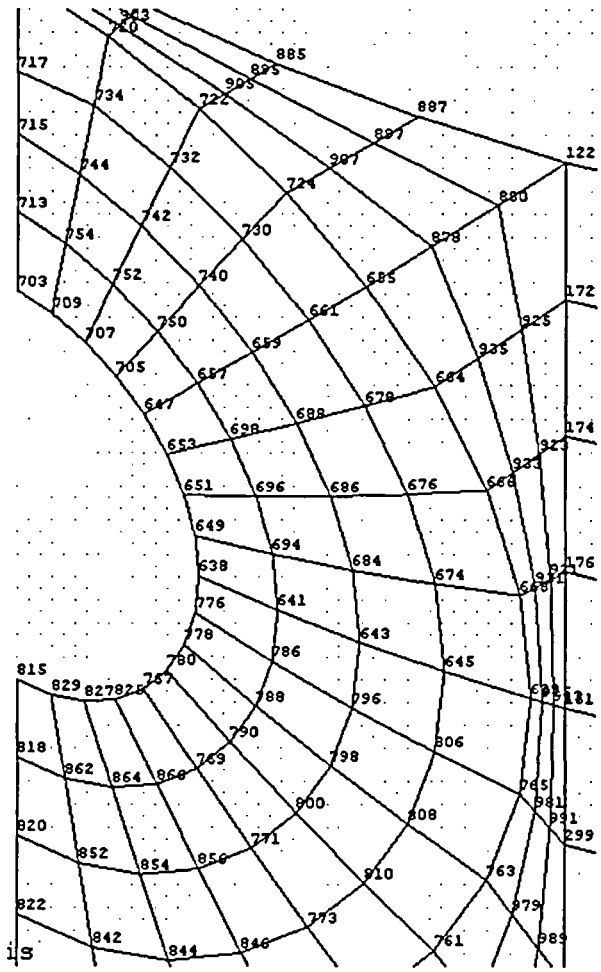

Figure 3.4.3.4-3 Node Locations for Advanced Transfer Cask Inner Shell Adjacent to Trunnion

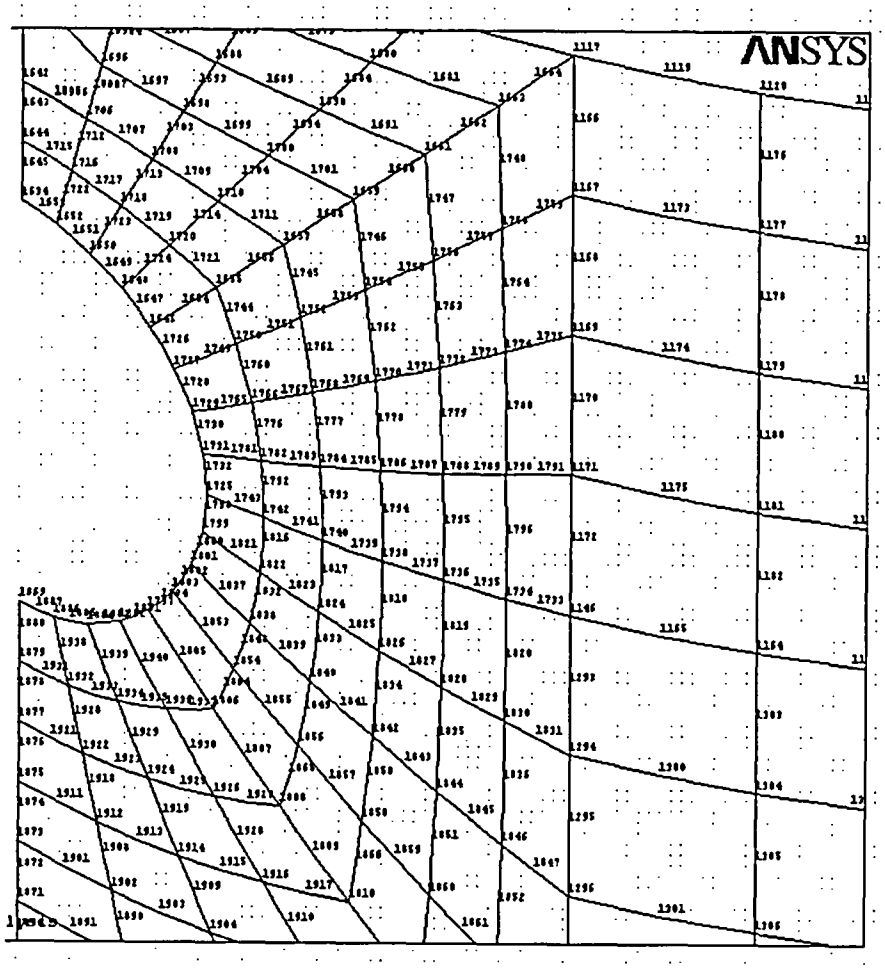

Figure 3.4.3.4-4 Node Locations for Advanced Transfer Cask Stiffener Plate Above Trunnion

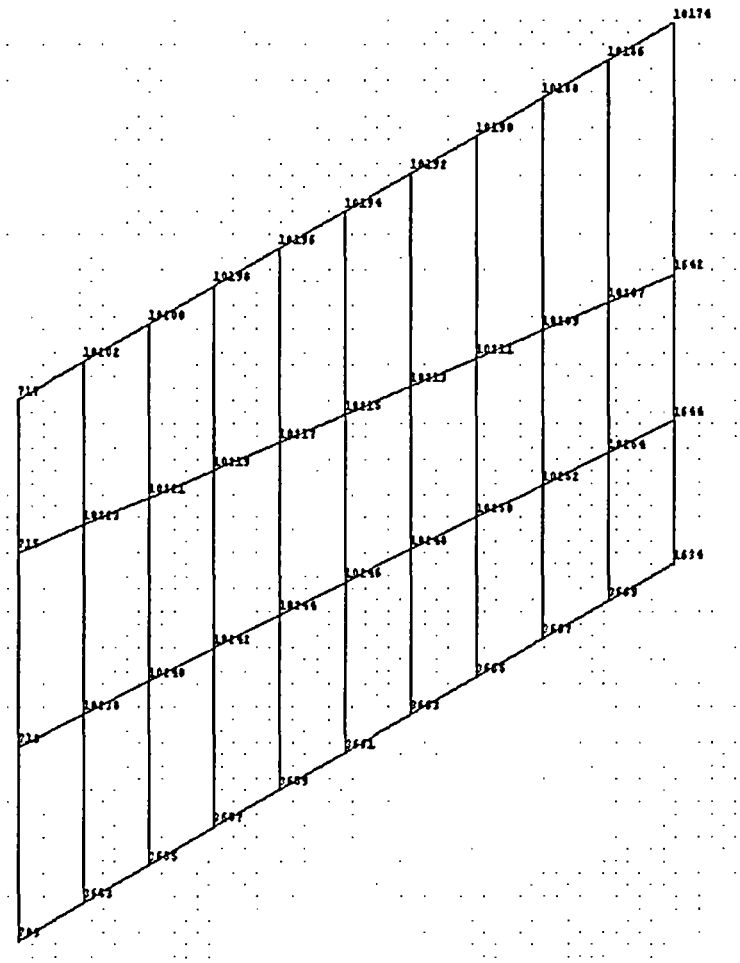

Figure 3.4.3.4-5 Stress Intensity Contours (psi) for Advanced Transfer Cask Outer Shell Element Top Surface

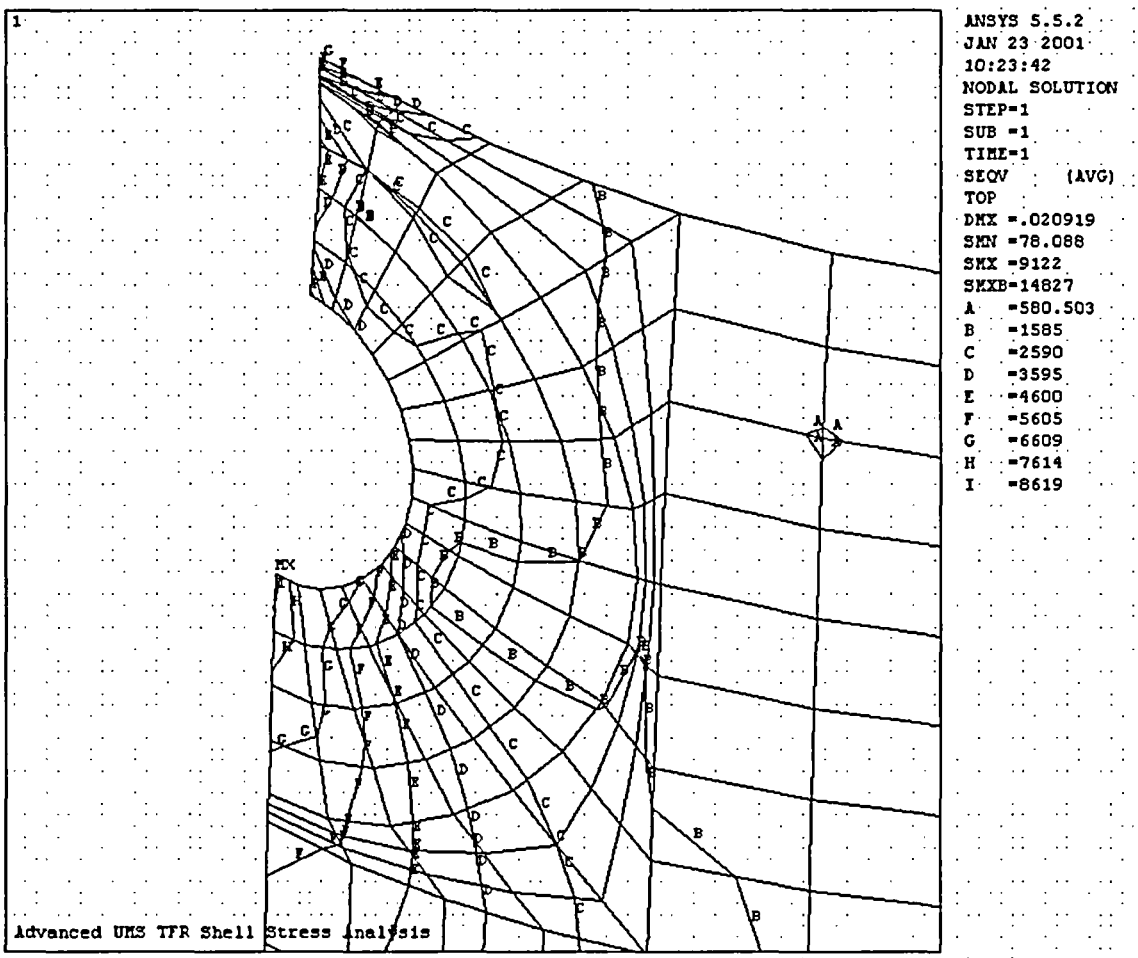

Figure 3.4.3.4-6 Stress Intensity Contours (psi) for Advanced Transfer Cask Outer Shell Element Bottom Surface

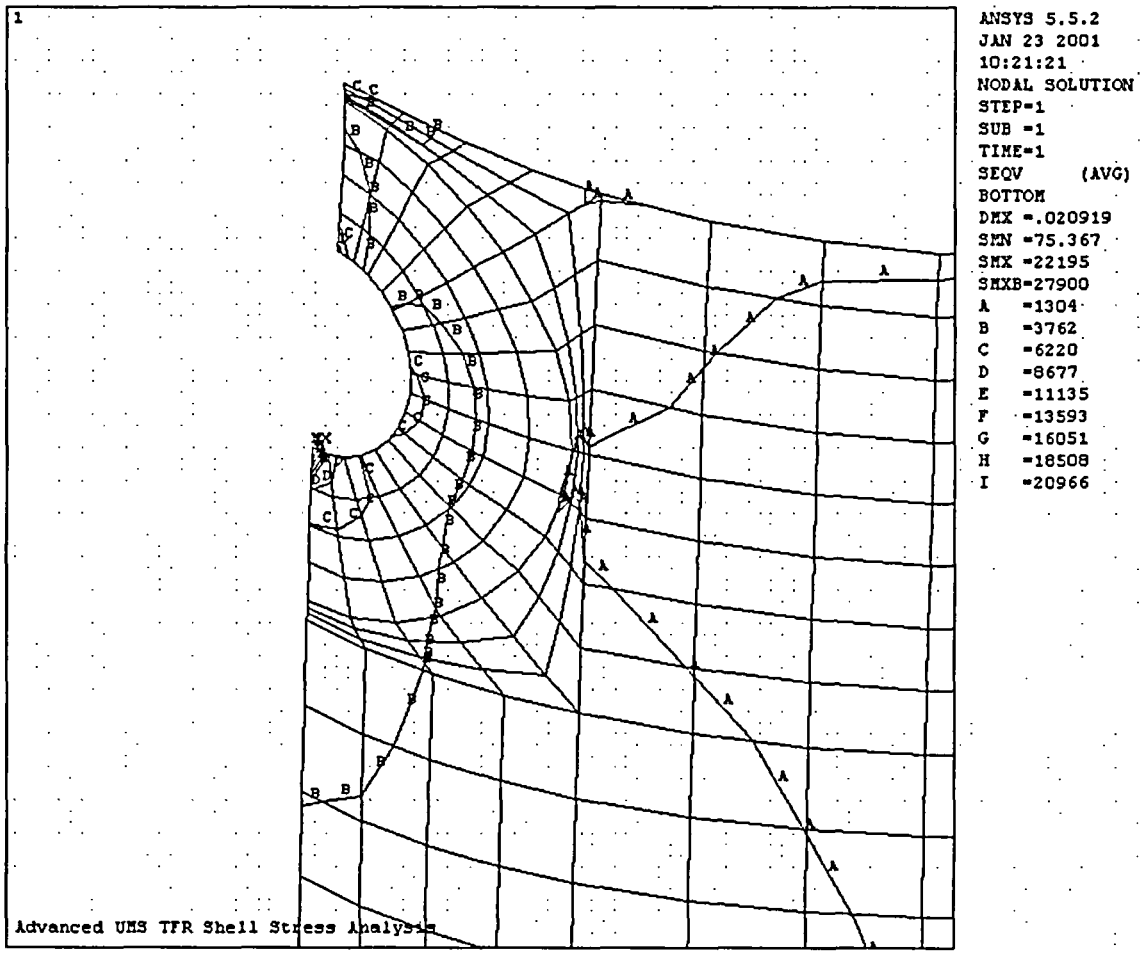

Figure 3.4.3.4-7 Stress Intensity Contours (psi) for Advanced Transfer Cask Inner Shell Element Top Surface

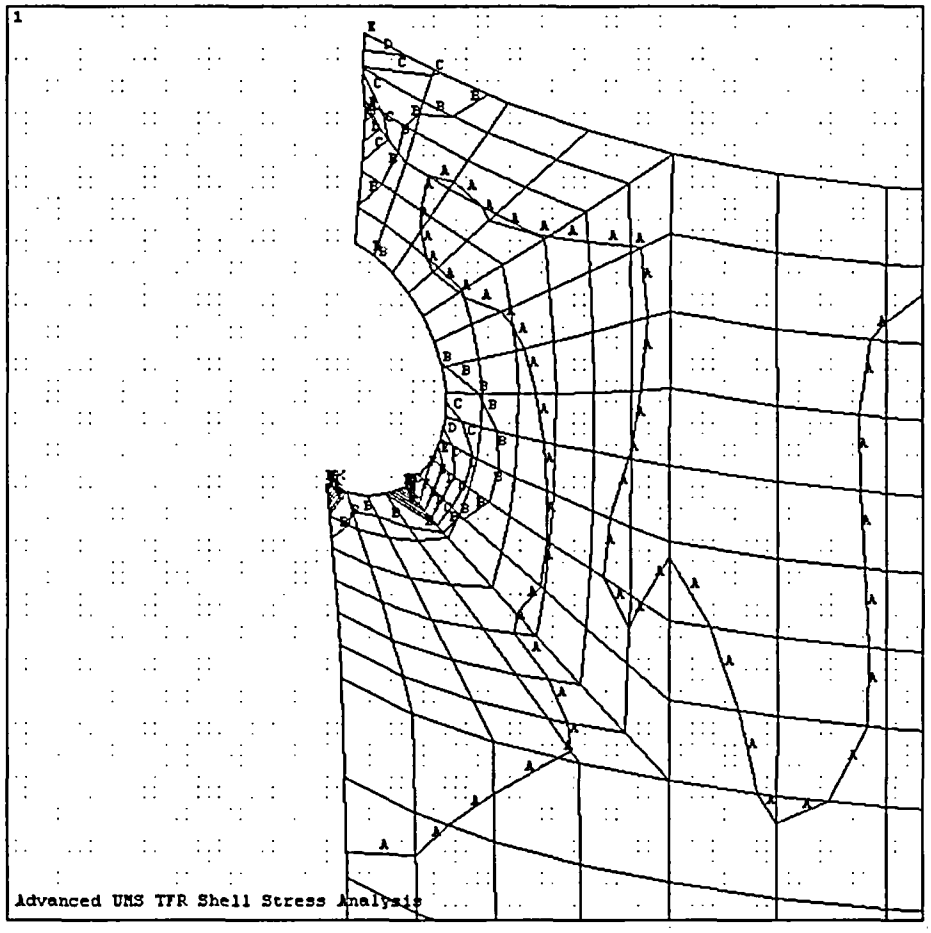

Figure 3.4.3.4-8 Stress Intensity Contours (psi) for Advanced Transfer Cask Inner Shell Element Bottom Surface

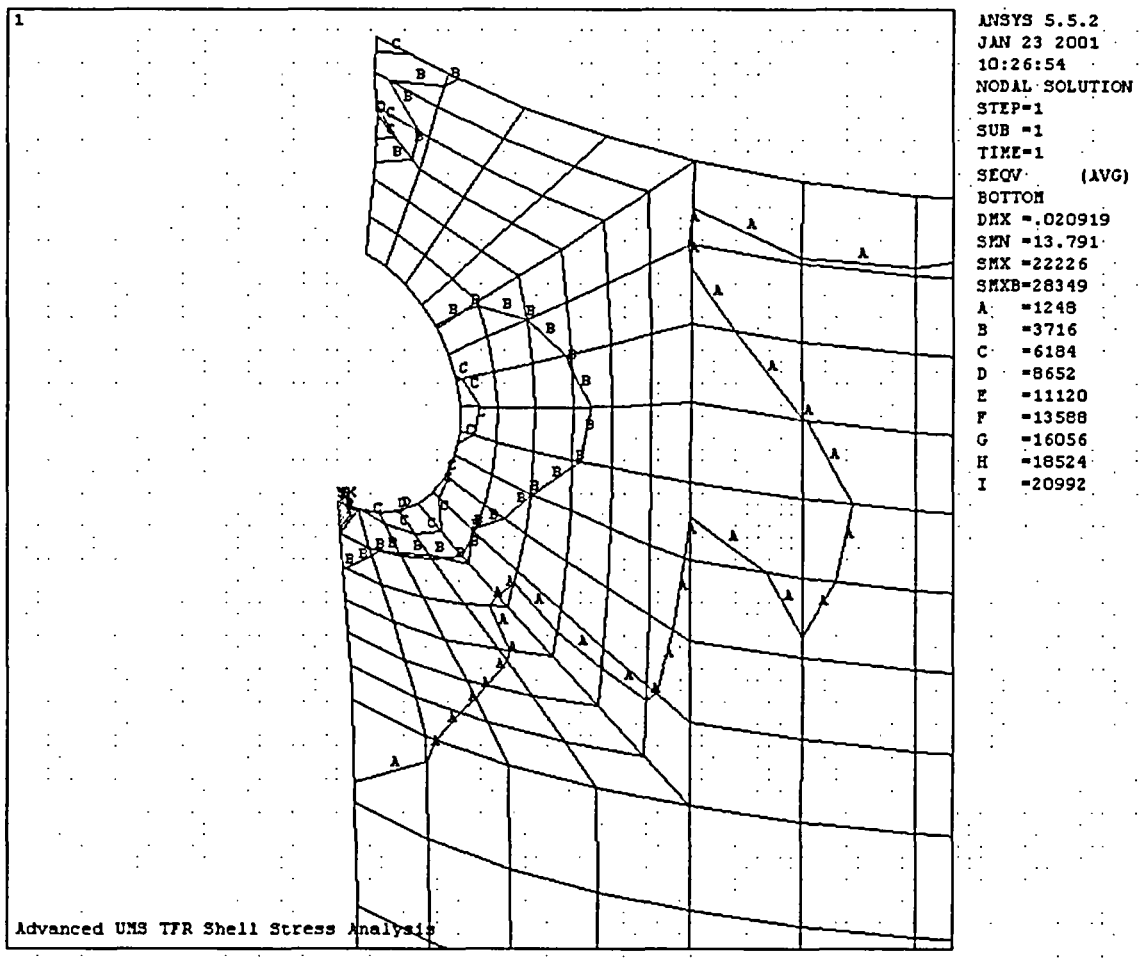

Figure 3.4.3.4-9 Stress Intensity Contours (psi) for Advanced Transfer Cask Stiffener Plate Element Top Surface

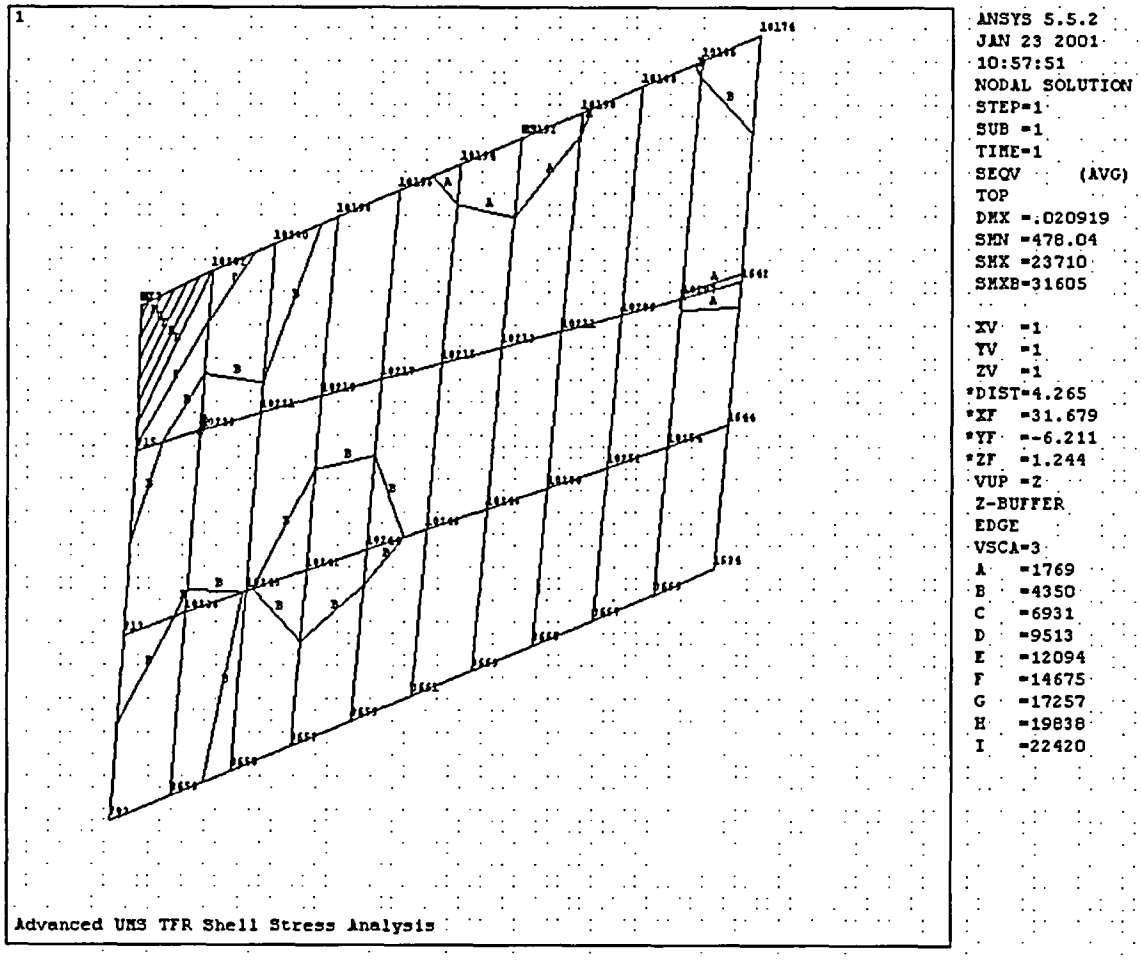

Figure 3.4.3.4-10 Stress Intensity Contours (psi) for Advanced Transfer Cask Stiffener Plate Element Bottom Surface

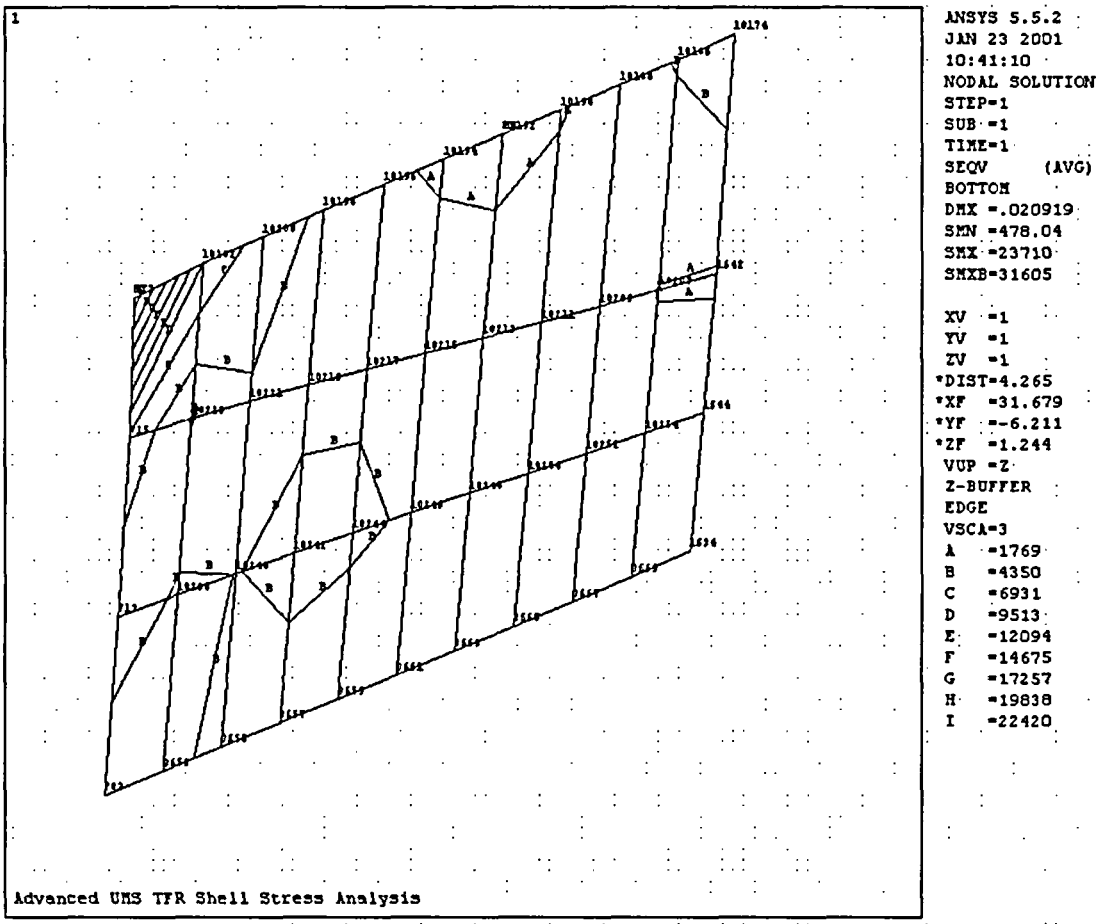

Table 3.4.3.4-1 Top 30 Stresses for Advanced Transfer Cask Outer Shell Element Top Surface

Node[1]	Principal Stresses (psi)			Nodal Von Mises Stresses	FS on Yield $(S_y)^2$	FS on Ultimate $(S_u)^2$
	S1	S2	S3			
815	3826.5	-213.1	-6617.3	9121.6	NA[3]	NA[3]
818	5489.8	-5.1	-4049.8	8293.3	NA	NA
820	4864.3	-1.9	-3634.4	7385.9	6.2	NA
827	5467.3	9.9	-2896.6	7354.7	6.2	NA
862	4847.2	3.3	-3530.7	7285.0	6.3	NA
825	5331.6	46.7	-2843.8	7180.6	6.4	NA
852	4708.0	0.3	-3275.8	6951.2	6.6	10.1
829	4163.6	-32.5	-3761.8	6867.6	6.6	10.2
871	7593.2	2376.9	-104.9	6805.5	6.7	10.3
822	4395.9	-0.3	-3328.5	6710.8	6.8	10.4
767	4460.2	129.3	-3077.8	6552.3	7.0	10.7
842	4289.1	0.2	-3001.4	6346.5	7.2	11.0
816	3994.4	-0.1	-3172.3	6220.2	7.3	11.3
943	3923.2	-0.1	-3167.1	6152.0	7.4	11.4
864	4384.5	9.7	-2590.9	6105.7	7.5	11.5
941	3858.7	-0.1	-3154.5	6083.8	7.5	11.5
2	3777.8	0.0	-3137.0	5997.0	7.6	11.7
832	3896.2	0.2	-2847.8	5864.0	7.8	11.9
854	4294.6	2.8	-2380.3	5858.9	7.8	11.9
703	3796.2	403.9	-2924.7	5820.5	7.8	12.0
964	3797.0	0.3	-2769.6	5710.0	8.0	12.3
873	6270.5	2019.3	-108.3	5625.3	8.1	12.4
954	3706.0	0.2	-2688.5	5561.1	8.2	12.6
844	3986.4	2.1	-2173.4	5410.7	8.4	12.9
8	3604.7	0.0	-2610.7	5405.5	8.4	12.9
780	3173.5	201.6	-3062.0	5402.0	8.4	13.0
47	3082.8	0.0	-2836.0	5127.3	8.9	13.7
717	5482.2	2416.5	-302.7	5012.8	9.1	14.0
834	3658.3	1.9	-2009.6	4977.0	9.2	14.1
866	3876.4	2.7	-1685.2	4939.0	9.2	14.2

Notes:

1. See Figure 3.4.3.4 -2 for node locations.
2. S_y = 45,600 psi, S_u = 70,000 psi.
3. Local stresses that are relieved by local material yielding. Therefore, stress design factors of 6 and 10 on material yield and ultimate strength are not applicable (ANSI N14.6, Section 4.2.1.2).

Table 3.4.3.4-2 Top 30 Stresses for Advanced Transfer Cask Outer Shell Element Bottom Surface

Node[1]Node	Principal Stresses (psi)Principal Stresses (psi)			Nodal Von Mises Stresses	FS on Yield $(S_y)^2$	FS on Ultimate $(S_u)^2$
	S1	S2	S3			
815	23117.0	2218.6	-178.6	22195.0	NA[3]	NA[3]
829	11968.0	5735.9	-18.9	10383.0	NA	NA
703	1423.8	-967.7	-9354.8	9804.1	NA	NA
818	9713.1	2279.0	-6.7	8802.4	NA	NA
871	94.9	-1212.6	-8374.4	7897.2	NA	NA
862	8885.1	3223.8	-10.3	7798.7	NA	NA
638	5557.4	114.7	-2341.4	7001.6	6.5	10.0
827	8016.0	3977.8	-8.5	6949.4	6.6	10.1
776	6510.7	508.4	-1100.0	6947.6	6.6	10.1
873	96.4	-763.0	-7125.6	6833.0	6.7	10.2
864	7722.7	2933.9	-9.0	6759.1	6.7	10.4
778	6789.6	1430.4	-446.1	6503.7	7.0	10.8
649	4028.8	-83.7	-3465.5	6500.5	7.0	10.8
820	7069.8	2942.0	-1.3	6152.4	7.4	11.4
825	7053.3	3670.3	-38.6	6143.9	7.4	11.4
780	6781.3	2682.2	-224.7	6096.5	7.5	11.5
875	100.3	-280.5	-6043.9	5963.0	7.6	11.7
767	6767.8	3530.1	-113.1	5962.5	7.6	11.7
852	6770.6	2764.7	-2.8	5898.5	7.7	11.9
866	6665.5	2211.1	-0.6	5881.0	7.8	11.9
651	2424.8	-291.8	-4029.7	5613.0	8.1	12.5
769	6045.8	1502.0	0.4	5451.9	8.4	12.8
854	6169.1	2215.3	-3.8	5415.8	8.4	12.9
715	42.8	-4696.1	-5838.1	5401.2	8.4	13.0
822	6062.5	2413.7	-0.2	5286.6	8.6	13.2
790	5610.4	835.1	-1.7	5244.1	8.7	13.3
717	356.3	-4113.9	-5392.7	5228.2	8.7	13.4
788	5221.9	112.3	-2.8	5168.2	8.8	13.5
842	5860.1	2239.1	-0.7	5122.3	8.9	13.7
786	4723.6	-2.7	-633.4	5071.1	9.0	13.8

Notes:

1. See Figure 3.4.3.4 -2 for node locations.
2. S_y = 45,600 psi, S_u = 70,000 psi.
3. Local stresses that are relieved by local material yielding. Therefore, stress design factors of 6 and 10 on material yield and ultimate strength are not applicable (ANSI N14.6, Section 4.2.1.2).

Table 3.4.3.4-3 Top 30 Stresses for Advanced Transfer Cask Inner Shell Element Top Surface

Node[1]	Principal Stresses (psi)			Nodal Von Mises Stresses (	FS on Yield $(S_y)^2$	FS on Ultimate $(S_u)^2$
	S1	S2	S3			
1869	2012.7	-552.0	-16137.0	17013.0	NA[3]	NA[3]
1797	13166.0	-115.4	-3089.1	14991.0	NA	NA
1803	12734.0	4058.3	-311.4	11501.0	NA	NA
1801	11627.0	4490.2	-214.9	10327.0	NA	NA
10174	663.9	-6733.1	-10256.0	9653.6	NA	NA
1633	9836.1	2649.9	-31.5	8837.4	NA	NA
1799	8856.4	4640.1	-144.2	7799.9	NA	NA
1638	743.8	-1547.7	-6362.4	6282.1	7.3	11.1
1725	5909.8	4672.1	-118.6	5514.7	8.3	12.7
1666	5438.4	1119.1	-33.4	4996.2	9.1	14.0
1882	783.0	-2383.4	-4495.2	4601.4	9.9	15.2
1636	4276.1	128.5	-576.2	4541.2	10.0	15.4
1822	4908.4	3039.9	-24.4	4313.6	10.6	16.2
1879	385.8	-127.4	-4147.3	4299.6	10.6	16.3
1731	4586.7	3239.6	-100.4	4179.6	10.9	16.7
1642	370.6	-17.7	-3713.0	3904.0	11.7	17.9
1838	4243.3	3272.0	-43.6	3893.2	11.7	18.0
1742	4389.1	2373.4	-14.5	3818.2	11.9	18.3
1886	99.4	-3236.9	-4024.2	3791.7	12.0	18.5
1884	444.8	-1827.8	-3719.9	3611.7	12.6	19.4
1676	3632.1	460.2	-25.6	3440.7	13.3	20.3
1854	3092.7	2724.2	-63.9	2989.4	15.3	23.4
1729	3305.4	1609.1	-110.0	2957.8	15.4	23.7
1652	2282.5	-2.8	-959.2	2884.9	15.8	24.3
1650	1868.2	46.8	-1388.3	2826.8	16.1	24.8
1644	576.4	-30.5	-2481.9	2804.5	16.3	25.0
1782	3124.2	1561.5	-8.7	2713.2	16.8	25.8
1120	4.1	-1046.1	-2882.0	2530.1	18.0	27.7
1648	1619.2	131.3	-1221.8	2461.3	18.5	28.4
1122	3.6	-824.2	-2582.3	2287.2	19.9	30.6

Notes:

1. See Figure 3.4.3.4-3 for node locations.
2. $S_y = 45{,}600$ psi, $S_u = 70{,}000$ psi.
3. Local stresses that are relieved by local material yielding. Therefore, stress design factors of 6 and 10 on material yield and ultimate strength are not applicable (ANSI N14.6, Section 4.2.1.2).

Table 3.4.3.4-4 Top 30 Stresses for Advanced Transfer Cask Inner Shell Element Bottom Surface

Node[1]	Principal Stresses (psi)			Nodal Von Mises Stresses	FS on Yield (S_y)[2]	FS on Ultimate (S_u)[2]
	S1	S2	S3			
1869	21448.0	632.6	-1960.3	22226.0	NA[3]	NA[3]
1882	8980.2	1059.9	-688.5	8923.9	NA	NA
10174	8109.4	7767.7	-819.1	8762.6	NA	NA
1797	1665.5	195.3	-7189.2	8218.8	NA	NA
1633	34.4	-2893.9	-8886.1	7875.8	NA	NA
1884	7160.2	652.9	-518.7	7165.3	6.4	NA
1731	1798.5	-157.2	-5950.2	6979.4	6.5	10.0
1803	501.1	-4651.7	-6891.7	6565.9	6.9	10.7
1725	819.9	-847.5	-6386.4	6534.2	7.0	10.7
1729	2571.3	-23.3	-4710.5	6392.4	7.1	11.0
1801	451.5	-4185.3	-6697.8	6282.0	7.3	11.1
1886	6799.4	2900.0	-79.4	5975.0	7.6	11.7
1879	5957.9	215.5	-205.1	5963.8	7.6	11.7
1638	5833.9	814.9	-647.9	5888.3	7.7	11.9
1799	450.0	-2722.7	-6304.4	5853.1	7.8	12.0
1742	1683.1	-3.7	-4630.1	5661.5	8.1	12.4
1822	1331.5	5.0	-4781.8	5569.8	8.2	12.6
1782	2155.7	-3.5	-4010.0	5418.9	8.4	12.9
1727	2988.1	35.3	-2969.9	5159.9	8.8	13.6
1766	2423.2	-1.0	-3317.9	4992.0	9.1	14.0
1784	2724.4	-2.3	-2938.1	4905.0	9.3	14.3
1838	1172.3	36.4	-4115.5	4821.3	9.5	14.5
1740	2640.2	-5.1	-2772.6	4688.0	9.7	14.9
1768	2402.5	-0.5	-2701.2	4422.5	10.3	15.8
1806	4006.7	141.6	-771.3	4393.2	10.4	15.9
1750	2260.4	0.0	-2725.3	4323.9	10.5	16.2
1666	18.8	-2100.4	-4642.2	4042.1	11.3	17.3
1786	2648.7	1.1	-1951.0	3998.6	11.4	17.5
1636	418.4	-283.5	-3777.7	3892.9	11.7	18.0
1646	2917.4	117.6	-1523.0	3888.9	11.7	18.0

Notes:

1. See Figure 3.4.3.4-3 for node locations.
2. $S_y = 45{,}600$ psi, $S_u = 70{,}000$ psi.
3. Local stresses that are relieved by local material yielding. Therefore, stress design factors of 6 and 10 on material yield and ultimate strength are not applicable (ANSI N14.6, Section 4.2.1.2).

Table 3.4.3.4-5 Top 30 Stresses for Advanced Transfer Cask Stiffener Plate Element Top Surface

Node[1]	Principal Stresses (psi)			Nodal Von Mises Stresses	FS on Yield (S_y)[2]	FS on Ultimate (S_u)[2]
	S1	S2	S3			
717	21871.0	0.0	-3327.1	23710.0	NA[3]	NA[3]
10202	10380.0	2355.3	0.0	9425.9	NA	NA
703	0.0	-2611.0	-7384.1	6485.5	7.0	10.8
715	2540.9	0.0	-4590.8	6260.7	7.3	11.2
10174	0.0	-331.0	-6322.5	6163.7	7.4	11.4
10200	5583.6	0.0	-327.2	5754.1	7.9	12.2
3653	0.0	-234.7	-5162.0	5048.8	9.0	13.9
10238	1540.5	0.0	-3784.2	4745.8	9.6	14.7
10186	0.0	-353.6	-4708.3	4541.8	10.0	15.4
10242	2112.4	0.0	-3100.6	4541.5	10.0	15.4
10244	2350.2	0.0	-2849.7	4510.2	10.1	15.5
10240	1634.9	0.0	-3271.9	4327.5	10.5	16.2
10246	2401.3	0.0	-2507.3	4251.3	10.7	16.5
10217	2848.4	0.0	-2000.3	4220.5	10.8	16.6
10219	3030.0	0.0	-1779.4	4211.7	10.8	16.6
10215	2588.3	0.0	-2137.9	4099.2	11.1	17.1
3657	1182.4	0.0	-3351.0	4073.1	11.2	17.2
10221	3249.6	0.0	-1287.2	4049.6	11.3	17.3
10213	2350.3	0.0	-2163.4	3910.1	11.7	17.9
10198	3889.7	51.5	0.0	3864.2	11.8	18.1
10248	2329.7	0.0	-2066.7	3809.6	12.0	18.4
3659	1493.7	0.0	-2771.5	3748.6	12.2	18.7
3655	0.0	-122.0	-3793.1	3733.6	12.2	18.7
10211	2126.4	0.0	-2015.8	3587.7	12.7	19.5
3661	1862.2	0.0	-2213.6	3534.1	12.9	19.8
3669	3134.7	0.0	-384.7	3343.7	13.6	20.9
3663	2090.4	0.0	-1721.4	3306.3	13.8	21.2
10250	2173.3	0.0	-1540.2	3231.5	14.1	21.7
3665	2305.8	0.0	-1283.8	3150.4	14.5	22.2
10209	1909.7	0.0	-1598.9	3042.5	15.0	23.0

Notes:

1. See Figure 3.4.3.4-4 for node locations.
2. S_y = 45,600 psi, S_u = 70,000 psi.
3. Local stresses that are relieved by local material yielding. Therefore, stress design factors of 6 and 10 on material yield and ultimate strength are not applicable (ANSI N14.6, Section 4.2.1.2).

Table 3.4.3.4-6 Top 30 Stresses for Advanced Transfer Cask Stiffener Plate Element Bottom Surface

Node[1]	Principal Stresses (psi)			Nodal Von Mises Stresses	FS on Yield (S_y)[2]	FS on Ultimate (S_u)[2]
	S1	S2	S3			
717	21871.0	0.0	-3327.1	23710.0	NA[3]	NA[3]
10202	10380.0	2355.3	0.0	9425.9	NA	NA
703	0.0	-2611.0	-7384.1	6485.5	7.0	10.8
715	2540.9	0.0	-4590.8	6260.7	7.3	11.2
10174	0.0	-331.0	-6322.5	6163.7	7.4	11.4
10200	5583.6	0.0	-327.2	5754.1	7.9	12.2
3653	0.0	-234.7	-5162.0	5048.8	9.0	13.9
10238	1540.5	0.0	-3784.2	4745.8	9.6	14.7
10186	0.0	-353.6	-4708.3	4541.8	10.0	15.4
10242	2112.4	0.0	-3100.6	4541.5	10.0	15.4
10244	2350.2	0.0	-2849.7	4510.2	10.1	15.5
10240	1634.9	0.0	-3271.9	4327.5	10.5	16.2
10246	2401.3	0.0	-2507.3	4251.3	10.7	16.5
10217	2848.4	0.0	-2000.3	4220.5	10.8	16.6
10219	3030.0	0.0	-1779.4	4211.7	10.8	16.6
10215	2588.3	0.0	-2137.9	4099.2	11.1	17.1
3657	1182.4	0.0	-3351.0	4073.1	11.2	17.2
10221	3249.6	0.0	-1287.2	4049.6	11.3	17.3
10213	2350.3	0.0	-2163.4	3910.1	11.7	17.9
10198	3889.7	51.5	0.0	3864.2	11.8	18.1
10248	2329.7	0.0	-2066.7	3809.6	12.0	18.4
3659	1493.7	0.0	-2771.5	3748.6	12.2	18.7
3655	0.0	-122.0	-3793.1	3733.6	12.2	18.7
10211	2126.4	0.0	-2015.8	3587.7	12.7	19.5
3661	1862.2	0.0	-2213.6	3534.1	12.9	19.8
3669	3134.7	0.0	-384.7	3343.7	13.6	20.9
3663	2090.4	0.0	-1721.4	3306.3	13.8	21.2
10250	2173.3	0.0	-1540.2	3231.5	14.1	21.7
3665	2305.8	0.0	-1283.8	3150.4	14.5	22.2
10209	1909.7	0.0	-1598.9	3042.5	15.0	23.0

Notes:

1. See Figure 3.4.3.4-4 for node locations.
2. $S_y = 45{,}600$ psi, $S_u = 70{,}000$ psi.
3. Local stresses that are relieved by local material yielding. Therefore, stress design factors of 6 and 10 on material yield and ultimate strength are not applicable (ANSI N14.6, Section 4.2.1.2).

3.4.4 Normal Operating Conditions Analysis

The Universal Storage System is evaluated using individual finite element models for the fuel basket, canister, and vertical concrete cask. Because the individual components are free to expand without interference, the structural finite element models need not be connected.

3.4.4.1 Canister and Basket Analyses

The evaluations presented in this Section are based on consideration of the bounding conditions for each aspect of the analysis. Generally, the bounding condition is represented by the component, or combination of components, of each configuration that is the heaviest. The bounding thermal condition is established by the configuration having the largest thermal gradient in normal use. Some cases require the evaluation of both a PWR and a BWR configuration because of differences in the design of these systems. For reference, the bounding case used in each of the structural evaluations is:

Section	Aspect Evaluated	Bounding Condition	Configuration
3.4.4.1.1	Canister Thermal Stress	Largest temperature gradient	Temperature[a] distribution
3.4.4.1.2	Canister Dead Weight	Heaviest loaded canister	BWR Class 5
3.4.4.1.3	Canister Pressure	Bounding pressure 15 psig, smallest canister	PWR Class 1 BWR Class 4
3.4.4.1.4	Canister Handling	Shortest canister dimensions w/ heaviest canister load [b]	PWR Class 1 BWR Class 5
3.4.4.1.5	Canister Load Combinations	Bounding pressure 15 psig + shortest canister dimensions w/ heaviest loaded canister[b] (handling) + shortest canister dimensions w/ heaviest loaded canister [b] (dead load) largest temperature gradient (thermal)	PWR Class 3 PWR Class 1 BWR Class 5 PWR Class 1 BWR Class 5 Temperature[a] distribution
3.4.4.1.6	Canister Fatigue	Bounding thermal excursions (58°F)	Not Applicable
3.4.4.1.7	Canister Pressure Test	Loaded canister (smallest canister)	PWR Class 1
3.4.4.1.8	PWR Basket Support Disk	Loaded PWR Canister	PWR fuel basket
	BWR Basket Support Disk	Loaded BWR Canister	BWR fuel basket [c]
3.4.4.1.9	PWR Basket Weldment	Loaded PWR Canister	PWR Class 2
	BWR Basket Weldment	Loaded BWR Canister	BWR Class 5
3.4.4.1.10	PWR Fuel Tube	Loaded PWR Canister (Longest)	PWR Class 3
	BWR Fuel Tube	Loaded BWR Canister (Longest)	BWR Class 5
3.4.4.1.11	Canister Closure Weld	Same as 3.4.4.1.5	Same as 3.4.4.1.5

[a] See Section 3.4.4.1.1 for an explanation of the composite temperature distribution used in the analyses. The shortest canister, PWR Class 1, has the fewest number of fuel basket support disks.

[b] When combined with the heaviest fuel assembly/fuel basket weight (BWR Class 5), the load per support disk or weldment disk is maximized.

[c] The evaluation of the BWR basket uses the analysis presented in the UMS Transport SAR [2].

3.4.4.1.1 Canister Thermal Stress Analysis

A three-dimensional finite element model of the canister was constructed using ANSYS SOLID45 elements. By taking advantage of the symmetry of the canister, the model represents one-half (180° section) of the canister including the canister shell, bottom plate, structural lid, and shield lid. Contact between the structural and shield lids is modeled using COMBIN40 combination elements in the axial (UY) degree of freedom. Simulation of the spacer ring is accomplished using a ring of COMBIN40 gap/spring elements connecting the shield lid and the canister in the axial direction at the lid lower outside radius. In addition, CONTAC52 elements are used to model the interaction between the structural lid and the canister shell and between the shield lid and canister shell, just below the respective lid weld joints as shown in Figure 3.4.4.1-2. The size of the CONTAC52 gaps is determined from nominal dimensions of contacting components. The gap size is defined by the "Real Constant" of the CONTAC52 element. Due to the relatively large gaps resulting from the nominal geometry, these gaps remain open during all loadings considered. The COMBIN40 elements used between the structural and shield lids and for the spacer ring are assigned small gap sizes of 1×10^{-8} in. All gap/spring elements are assigned a stiffness of 1×10^{8} lb/in. The three-dimensional finite element model of the canister used in the thermal stress evaluation is shown in Figure 3.4.4.1-1 through Figure 3.4.4.1-3.

The model is constrained in the Z-direction for all nodes in the plane of symmetry. For the stability of the solution, one node at the center of the bottom plate is constrained in the Y-direction, and all nodes at the centerline of the canister are constrained in the X-direction. The directions of the coordinate system are shown in Figure 3.4.4.1-1.

This model represents a "bounding" combination of geometry and loading that envelopes the Universal Storage System PWR and BWR canisters. Specifically, the shortest canister (PWR Class 1) and minimum weld sizes (0.75-inch structural lid weld and 0.375-inch shield lid weld) are modeled in conjunction with the heaviest fuel and fuel basket combination (BWR Class 5). By using the shortest canister (PWR Class 1), which has the fewest number of support disks, in combination with the weight of the heaviest loaded fuel basket, the load per support disk and weldment disk is maximized. Thus, the analysis yields very conservative results relative to the expected performance of the actual canister configurations.

The finite element thermal stress analysis is performed with canister temperatures that envelope the canister temperature gradients for off-normal storage (106°F and -40°F ambient temperatures) and transfer conditions for all canister configurations. Prior to performing the thermal stress analysis, the steady-state temperature distribution is determined using temperature data from the storage and transfer thermal analyses (Chapter 4.0). This is accomplished by converting the SOLID45 structural elements of the canister model to SOLID70 thermal elements and using the material properties from the thermal analyses. Nodal temperatures are applied at six key locations for the steady state heat transfer analysis — top-center of the structural lid, top-outer diameter of the structural lid, bottom-center of the shield lid, bottom-center of the bottom plate, bottom-outer diameter of the bottom plate, and mid-elevation of the canister shell.

Two temperature distributions are used in the structural analyses to envelope the worst-case allowable temperatures and temperature gradients experienced by all PWR and BWR canister configurations under storage and transfer conditions. The temperatures at the key locations are:

Top center of the structural lid	= 160
Top outer diameter of the structural lid	= 150
Bottom center of the shield lid	= 200
Bottom center of the bottom plate	= 300
Bottom outer diameter of the bottom plate	= 200
Mid-elevation of the canister shell	= 600

Temperatures used for determining allowable stress values were selected to envelope the maximum temperatures experienced by the canister components during storage and transfer conditions. Allowable stress values for the structural/shield lid region were taken at 220°F, those for the center of the bottom plate were taken at 300°F, those for the outer radius of the bottom plate at 220°F, and those for the canister shell at 550°F.

The temperatures for all nodes in the canister model are obtained by the solution of the steady state thermal conduction problem. The key temperature differences, ΔT, of the worst-case

PWR and BWR canisters in the radial and axial directions and those used in the canister thermal stress analysis are:

	Maximum ΔT (°F)							
	Top of Structural Lid (Radial)		Bottom Plate (Radial)		Shield and Structural Lid (Axial)		Canister Shell (Axial)	
Condition	PWR	BWR	PWR	BWR	PWR	BWR	PWR	BWR
Storage, Normal 76°F ambient	3	3	3	7	6	8	267	299
Storage, Off-Normal 106°F ambient	4	3	3	7	6	8	266	298
Storage, Off-Normal, -40°F ambient	3	3	4	7	5	7	264	296
Storage, Off-Normal Half Inlets Blocked 76°F	4	3	3	7	6	8	265	296
Transfer, 76°F ambient	10	4	69	64	16	7	396	388
Parameters used for Canister Thermal Stress Analysis	10		100		40		450	

The resulting maximum (secondary) thermal stresses in the canister are summarized in Table 3.4.4.1-1. The sectional stresses at 16 axial locations are obtained for each angular division of the model (a total of 19 angular locations for each axial location). The locations of the stress sections are shown in Figure 3.4.4.1-4. After solving for the canister temperature distribution, the thermal stress analysis was performed by converting the SOLID70 elements back to SOLID45 structural elements.

3.4.4.1.2 Canister Dead Weight Load Analysis

The canister is structurally analyzed for dead weight load using the finite element model described in Section 3.4.4.1.1. The canister temperature distribution discussed in Section 3.4.4.1.1 is used in the dead load structural analysis to evaluate the material properties at temperature. The fuel and fuel basket assembly contained within the canister are not explicitly modeled but are included in the analysis by applying a uniform pressure load representing their combined weight to the top surface of the canister bottom plate. The nodes on the bottom surface of the bottom plate are restrained in the axial direction in conjunction with the constraints described in Section 3.4.4.1.1. The evaluation is based on the weight of the BWR Class 5 canister, which has the highest weight, and the length of the PWR Class 1 canister, which is the shortest configuration and has minimum weld sizes (0.75-inch structural lid weld and 0.375-inch shield lid weld). An acceleration of 1g is applied to the model in the axial direction (Y) to simulate the dead load.

The resulting maximum canister dead load stresses are summarized in Table 3.4.4.1-2 and Table 3.4.4.1-3 for primary membrane and primary membrane plus bending stresses, respectively. The sectional stresses at 16 axial locations are obtained for each angular division of the model (a total of 19 angular locations for each axial location). The locations for the stress sections are shown in Figure 3.4.4.1-4.

The lid support ring is evaluated for the dead load condition using classical methods. The ring, which is made of ASTM A-479, Type 304 stainless steel, is welded to the inner surface of the canister shell to support the shield lid. For conservatism, a temperature of 400°F, which is higher than the anticipated temperature at this location, is used to determine the material allowable stress. The total weight, W, imposed on the lid support ring is conservatively considered to be the weight of the auxiliary shielding and the shield lid. A 10% load factor is also applied to ensure that the analysis bounds all normal operating loads. The stresses on the support ring are the bearing stresses and shear stresses at its weld to the canister shell.

The bearing stress $\sigma_{bearing}$ is:

$$\sigma_{bearing} = \frac{W}{area} = \frac{14{,}200\,\text{lb}}{102.6\,\text{in}^2} = 138\ \text{psi}$$

where:

W = (7,000 lb + 5,890 lb) × 1.1 = 14,179 lb, use 14,200 lb
where the weight of the auxiliary shielding (W_s) can be comprised of three 2-inch-thick stainless steel plates resting on the shield lid, or

W_s = .291 x (π/4) x 65.5^2 x 6 = 5,883 lb, use 5,890 lb

$$A = \frac{\pi}{4}(D^2 - (D-2t)^2)\,in^2 = 102.6\ in^2$$

D = lid support ring diameter = 65.81 in.

t = radial thickness of support ring = 0.5 in.

The yield strength, S_y, for A-479, Type 304 stainless steel = 20,700 psi, and the ultimate allowable tensile stress, S_u = 64,400 psi at 400°F. The allowable bearing stress is 1.0 S_y per ASME Code, Section III, Subsection NB. The acceptability of the support ring design is evaluated by comparing the allowable stresses to the maximum calculated stress:

$$MS = \frac{20{,}700\ psi}{138\ psi} - 1 = +Large$$

Therefore, the support ring is structurally adequate.

The attachment weld for the lid support ring is a 1/8-in. partial penetration groove weld. The total shear force on the weld is considered to be the weight of the shield lid, the structural lid, and the lid support ring. The total effective area of each weld is $A_{eff} = .125 \times \pi \times 65.81$ in. = 25.8 in^2. The average shear stress in the weld is:

$$\sigma_w = \frac{W}{A_{eff}} = \frac{14{,}200\ lb}{25.8\ in^2} = 550\ psi$$

The allowable stress on the weld is 0.30 × the nominal tensile strength of the weld material [Ref.23, Table J2.5]. The nominal tensile strength of E308-XX filler material is 80,000 psi [Ref.28, SFA-5.4, Table 5]. However, for conservatism, S_y and S_u for the base metal, are used. The acceptability of the support ring weld is evaluated by comparing the allowable stress to the maximum calculated stress:

$$MS = \frac{0.3 \times 20{,}700\ psi}{550\ psi} - 1 = +Large$$

Therefore, the support ring attachment weld is structurally adequate.

3.4.4.1.3 Canister Maximum Internal Pressure Analysis

The canister is structurally analyzed for a maximum internal pressure load using the finite element model and temperature distribution and restraints described in Section 3.4.4.1.1. A maximum internal pressure of 15 psig is applied as a surface load to the elements along the internal surface of the canister shell, bottom plate, and shield lid. This pressure bounds the calculated pressure of 7.1 psig that occurs in the smallest canister, PWR Class 1, under normal conditions. The PWR Class 1 canister internal pressure bounds the internal pressures of the other four canister configurations because it has the highest quantity of fission-gas-to-volume ratio.

The resulting maximum canister stresses for maximum internal pressure load are summarized in Table 3.4.4.1-9 and Table 3.4.4.1-10 for primary membrane and primary membrane plus primary bending stresses, respectively. The sectional stresses at 16 axial locations are obtained for each angular division of the model (a total of 19 angular locations for each axial location). The locations of the stress sections are shown in Figure 3.4.4.1-4.

3.4.4.1.4 Canister Handling Analysis

The canister is structurally analyzed for handling loads using the finite element model and conditions described in Section 3.4.4.1.1. Normal handling is simulated by restraining the model at nodes on the structural lid simulating three lift points and applying a 1.1g acceleration, which includes a 10% dynamic load factor, to the model in the axial direction. The canister is lifted at six points; however, a three-point lifting configuration is conservatively used in the handling analysis. Since the model represents a one-half section of the canister, the three-point lift is simulated by restraining two nodes 120° apart (one node at the symmetry plane and a second node 120° from the first) along the bolt diameter at the top of the structural lid in the axial direction. Additionally, the nodes along the centerline of the lids and bottom plate are restrained in the radial direction, and the nodes along the symmetry face are restrained in the direction normal to the symmetry plane.

The maximum stresses during canister handling occur when the heaviest weight canister (BWR class 5) is analyzed with the minimum structural lid weld (PWR class canister with 0.75-inch structural lid weld). Therefore, this analysis bounds all handling configurations.

The resulting maximum stresses in the canister are summarized in Table 3.4.4.1-4 and Table 3.4.4.1-5 for primary membrane and primary membrane plus primary bending stresses, respectively. The sectional stresses at 16 axial locations are obtained for each angular division of the model (a total of 19 angular locations for each axial location). The locations of the stress sections are shown in Figure 3.4.4.1-4.

3.4.4.1.5 Canister Load Combinations

The canister is structurally analyzed for combined thermal, dead, maximum internal pressure, and handling loads using the finite element model and the conditions described in Section 3.4.4.1.1. Loads are applied to the model as discussed in Sections 3.4.4.1.1 through 3.4.4.1.4. A maximum internal pressure of 15.0 psi is used in conjunction with a positive axial acceleration of 1.1g. Two nodes 120° apart (one node at the symmetry plane and a second node 120° from the first) are restrained along the bolt diameter at the top of the structural lid in the axial direction. Additionally, the nodes along the centerline of the lids and bottom plate are restrained in the radial direction, and the nodes along the symmetry face are restrained in the direction normal to the symmetry plane.

The resulting maximum stresses in the canister for combined loads are summarized in Table 3.4.4.1-6, Table 3.4.4.1-7, and Table 3.4.4.1-8, for primary membrane, primary membrane plus primary bending, and primary plus secondary stresses, respectively. The sectional stresses at 16 axial locations are obtained for each angular division of the model (a total of 19 angular locations for each axial location). The locations for the stress sections are shown in Figure 3.4.4.1-4.

As shown in Table 3.4.4.1-6 through Table 3.4.4.1-8, the canister maintains positive margins of safety for the combined load conditions.

3.4.4.1.6 Canister and Basket Fatigue Evaluation

The purpose of this section is to evaluate whether an analysis for cyclic service is required for the Universal Storage System components. The requirements for analysis for cyclic operation of components designed to ASME Code criteria are presented in ASME Section III, Subsection NB-3222.4 [5] for the canister and Subsection NG-3222.4 [6] for the fuel basket. Guidance for components designed to AISC standards is in the Manual of Steel Construction, Table A-K4.1 [23].

During storage conditions, the canister is housed in the vertical concrete cask. The concrete cask is a shielded, reinforced concrete overpack designed to hold a canister during long-term storage conditions. The cask is constructed of a thick inner steel shell surrounded by 28 in. of reinforced concrete. The cask inner shell is not subjected to cyclic mechanical loading. Thermal cycles are limited to changes in ambient air temperature. Because of the large thermal mass of the concrete cask and the relatively minor changes in ambient air temperature (when compared to the steady state heat load of the cask contents), fatigue as a result of cycles in ambient air is not significant, and no further fatigue evaluation of the inner shell is required.

ASME criteria for determining whether cyclic loading analysis is required are comprised of six conditions, which, if met, preclude the requirement for further analysis:

1. Atmospheric to Service Pressure Cycle
2. Normal Service Pressure Fluctuation
3. Temperature Difference — Startup and Shutdown
4. Temperature Difference — Normal Service
5. Temperature Difference — Dissimilar Materials
6. Mechanical Loads

Evaluation of these conditions follows.

Condition 1 — Atmospheric to Service Pressure Cycle

This condition is not applicable. The ASME Code defines a cycle as an excursion from atmospheric pressure to service pressure and back to atmospheric pressure. Once sealed, the canister remains closed throughout its operational life, and no atmospheric to service pressure cycles occur.

Condition 2 — Normal Service Pressure Fluctuation

This condition is not applicable. The condition establishes a maximum pressure fluctuation as a function of the number of significant pressure fluctuation cycles specified for the component, the design pressure, and the allowable stress intensity of the component material. Operation of the canister is not cyclic, and no significant cyclic pressure fluctuation is anticipated.

Condition 3 — Temperature Difference — Startup and Shutdown

This condition is not applicable. The Universal Storage System is a passive, long-term storage system that does not experience cyclic startups and shutdowns.

Condition 4 — Temperature Difference — Normal and Off-Normal Service

The ASME Code specifies that temperature excursions are not significant if the change in ΔT between two adjacent points does not experience a cyclic change of more than the quantity:

$$\Delta T = \frac{S_a}{2E\alpha} = 58°F,$$

where, for Type 304L stainless steel,

S_a = 28,200 psi, the value obtained from the fatigue curve for service cycles $< 10^6$,
E = 26.5×10^6 psi, modulus of elasticity at 400 °F,
α = 9.19×10^{-6} in./in.-°F.

Because of the large thermal mass of the canister and the concrete cask and the relatively constant heat load produced by the canister's contents, cyclic changes in ΔT greater than 58 °F will not occur.

Condition 5 — Temperature Difference Between Dissimilar Materials

The canister and its internal components contain several materials. However, the design of all components considers thermal expansion, thus precluding the development of unanalyzed thermal stress concentrations.

Condition 6 — Mechanical Loads

This condition does not apply. Cyclic mechanical loads are not applied to the vertical concrete cask and canister during storage conditions. Therefore, no further cyclic loading evaluation is required.

The criteria ASME Code Subsections NB-3222.4 and NG-3222.4 are met, and no fatigue analysis is required.

3.4.4.1.7 Canister Pressure Test

The canister is designed and fabricated to the requirements of ASME Code, Subsection NB, to the extent possible. A 35 psia (35 – 14.7 = 20.3 psig) hydrostatic pressure test is performed in accordance with the requirements of ASME Code Subsection NB-6220 [5]. The pressure test is performed after the shield lid to canister shell weld is completed. The test pressure slightly exceeds 1.25 × design pressure (1.25 × 15 psig = 18.75 psig). Considering head pressure for the tallest canister (191.75 × 0.036 = 6.9 psig), the maximum canister pressure developed during the pneumatic pressure test is bounded by using 27.2 psig in the structural evaluation for the canister test pressure.

The ASME Code requires that the pressure test loading comply with the following criteria from Subsection NB-3226:

(a) P_m shall not exceed $0.9S_y$ at test temperature. For convenience, the stress intensities developed in the analysis of the canister due to a normal internal pressure of 15 psig (Tables 3.4.4.1-9 and 3.4.4.1-10) are ratioed to demonstrate compliance with this requirement. From Table 3.4.4.1-9, the maximum primary stress intensity, P_m, is 2.24 ksi. The canister material is ASME SA-240, Type 304L stainless steel, and the test temperature will be less than 200°F for the design basis heat load of 23 kW (Figures 4.4.3-5 and 4.4.3-6). Since yield strength decreases with increasing temperature, for purposes of this calculation, the minimum material yield strength at the bounding canister temperature of 200°F is used for the structural critical limit.

$(P_m)_{test}$ = (27.2/15)(2.24 ksi) = 4.1 ksi, which is < 0.9 S_y = 0.9 (21.4 ksi) = 19.3 ksi

Thus, criterion (a) is met.

(b) For $P_m < 0.67S_y$ (see criterion a), the primary membrane plus bending stress intensity, $P_m + P_b$, shall be $\leq 1.35S_y$. From Table 3.4.4.1-10, $P_m + P_b$ = 7.36 ksi.

$(P_m + P_b)_{test}$ = (27.2/15)×(7.36 ksi) = 13.3 ksi, which is $\leq 1.35S_y$ = 28.9 ksi (1.35×21.4 ksi).

Thus, criterion (b) is met.

(c) The external pressure shall not exceed 135% of the value determined by the rules of NB-3133. The exterior of the canister is at atmospheric pressure at the time the pressure test is conducted. Therefore, this criterion is met.

(d) For the 1.25 Design Pressure pneumatic test of NB-6221, the stresses shall be calculated and compared to the limits of criteria (a), (b), and (c). This calculation and the fatigue evaluation of (e) need not be revised unless the actual hydrostatic test pressure exceeds 1.25 Design Pressure by more than 6%.

The test pressure (20.3 psig) slightly exceeds 1.25 × Design Pressure (18.75). However, the stresses used in this evaluation are ratioed to the test pressure. Thus, the stresses at the test pressure are calculated.

(e) Tests, with the exception of the first 10 hydrostatic tests in accordance with NB-6220, shall be considered in the fatigue evaluation of the component.

The canisters are not reused, and the hydrostatic test will be conducted only once. Thus, the pressure test is not required to be considered in the fatigue analysis.

The canister hydrostatic pressure tests comply with all NB-3226 criteria. These results bound the performance of a pneumatic pressure test performed in accordance with NB-6220, since the pneumatic pressure test pressure is lower (1.2 × the design pressure or 1.2 × 15 psig = 18 psig).

3.4.4.1.8 Fuel Basket Support Disk Evaluation

The PWR and BWR fuel baskets are described in detail in Sections 1.2.1.2.1 and 1.2.1.2.2, respectively. The design of the basket is similar for the PWR and BWR configurations. The major components of the BWR basket are shown in Figure 3.4.4.1-5. The structural evaluation for the PWR and BWR support disks for the normal conditions of storage is presented in the following sections. Note that the canister may be handled in a vertical or horizontal position. The evaluation is performed for the governing configuration in which the canister is handled in a vertical position. During normal conditions, the support disk is subjected to its self-weight only (in canister axial direction) and is supported by the tie rods/spacers at 8 locations for PWR configuration and 6 locations for the BWR configuration. To account for the condition when the canister is handled, a handling load, defined as 10 percent of the dead load, is considered. Finite element analyses using the ANSYS program are performed for the support disk for PWR and BWR configurations, respectively. In addition to the dead load and handling load (10% of dead load), thermal stresses are also considered based on conservative temperatures that envelop those experienced by the support disk during normal, off-normal (106°F and –40°F ambient temperatures) and transfer conditions. The stress criteria is defined according to ASME Code, Section III, Subsection NG. For the normal condition of storage, the Level A allowable stresses from Subsection NG as shown below are used.

Stress Category	Normal (Level A) Allowable Stresses
P_m	S_m
P_m+P_b	$1.5\ S_m$
P+Q	$3.0\ S_m$

3.4.4.1.8.1 PWR Support Disk

As shown in Figure 3.4.4.1-6, a finite element model is generated to analyze the PWR fuel basket support disks. The model is constructed using the ANSYS three-dimensional SHELL63 elements and corresponds to a single support disk with a thickness of 0.5 inch. The only loading on the model is the inertial load (1.1g) that includes the dead load and handling load in the out-of-plane direction (Global Z) for normal conditions of storage. The model is constrained in eight locations in the out-of-plane direction to simulate the supports of the tie rods/spacers.

Note that a full model is generated because this model is also used for the evaluation of the support disk for the off-normal handling condition (Section 11.1.3) in which non-symmetric loading (side load) is present. In addition, this model is used for the evaluation of a support disk for the 24-inch end drop accident condition of the vertical concrete cask (Section 11.2.4).

The model accommodates thermal expansion effects by using the temperature data from the thermal analysis and the coefficient of thermal expansion. Prior to performing the structural analyses, the temperature distribution in the support disk is determined by executing a steady-state thermal conduction analysis. This is accomplished by converting the SHELL63 structural elements to SHELL57 thermal elements. A maximum temperature of 700°F is applied to the nodes at the center slot of the disk model, and a minimum temperature 275°F is applied to the nodes around the outer circumferential edge of the disk, thus providing a bounding temperature delta of 425°F for the support disk. All other nodal temperatures are then obtained by the steady state conduction solution. Note that the applied temperatures are conservatively selected to envelope the maximum temperature, as well as the maximum radial temperature gradient (ΔT) of the disk for all normal, off-normal and accident conditions of storage and for transfer conditions. For normal conditions of storage, the support disk is evaluated using stress allowables at 800°F.

To evaluate the most critical regions of the support disk, a series of cross sections are considered. The locations of these sections on a PWR support disk are shown in Figures 3.4.4.1-7 and

3.4.4.1-8. Table 3.4.4.1-11 lists the cross sections versus Point 1 and Point 2, which spans the cross section of the ligament in the plane of the support disk.

The stress evaluation for the support disk is performed according to ASME Code, Section III, Subsection NG. According to this subsection, linearized stresses of cross sections of the structure are to be compared against the allowable stresses. The stress evaluation results for the support disks for normal condition are presented in Tables 3.4.4.1-12 and 3.4.4.1-13. The tables list the 40 highest P_m+P_b and P+Q stress intensities with large margins of safety. The Level A allowable stresses, $1.5S_m$ and $3S_m$ of the 17-4PH stainless steel at corresponding nodal temperatures, are used for the P_m+P_b and P+Q stresses, respectively. Note that the P_m stresses for the support disk for normal conditions are essentially zero since there are no loads in the plane of the support disk. Stress allowables for the section cuts are taken at 800°F.

3.4.4.1.8.2 BWR Support Disk

Similar to the evaluation for the PWR fuel basket support disk, a finite element model is generated to analyze the BWR fuel basket support disks, as shown in Figure 3.4.4.1-12. The model is constructed using the ANSYS three-dimensional SHELL63 elements and corresponds to a single support disk with a thickness of 5/8 inch. The only loading on the model is the inertial load (1.1g) that includes the dead load and handling load in the out-of-plane direction (Global Z) for normal conditions of storage. The model is constrained in six locations in the out-of-plane direction to simulate the supports of the tie rods/spacers.

The model accommodates thermal expansion effects by using the temperature data from the thermal analysis and the coefficient of thermal expansion. The temperature distribution in the BWR support disk is determined using the same method used in Section 3.4.4.1.8.1 for the PWR support disk. A maximum temperature of 700°F is applied to the nodes at the center of the disk model, and a minimum temperature of 300°F is applied to the nodes around the outer circumferential edge of the disk, thus providing a bounding temperature delta of 400°F for the support disk. All other nodal temperatures are then obtained by the steady state conduction solution. Note that the applied temperatures are conservatively selected to envelope the maximum temperature, as well as the maximum radial temperature gradient (ΔT) of the disk for all normal, off-normal, and accident conditions of storage and for transfer conditions. For normal conditions of storage, the support disk is evaluated using stress allowables at 800°F.

To evaluate the most critical regions of the support disk, a series of cross sections are considered. The locations of these sections on a BWR support disk are shown in Figures 3.4.4.1-13 through 3.4.4.1-16. Table 3.4.4.1-14 lists the cross sections versus Point 1 and Point 2, which spans the cross section of the ligament in the plane of the support disk.

The stress evaluation results for the BWR support disks for normal condition are presented in Tables 3.4.4.1-15 and 3.4.4.1-16. The tables list the 40 highest P_m+P_b and P+Q stress intensities with large margins of safety. The Level A allowable stresses from ASME Code, Section III, Subsection NG, $1.5S_m$ and $3.0S_m$ of the SA533 carbon steel at corresponding nodal temperatures, are used for the P_m+P_b and P+Q stresses, respectively. Note that the P_m stresses for the support disk for normal conditions are essentially zero, since there is no loads in the plane of the support disk.

3.4.4.1.9 Fuel Basket Weldments Evaluation

The PWR and BWR fuel basket weldments are evaluated for normal storage conditions using the finite element method. In addition to the dead load of the weldment, a 10% dynamic load factor is considered to account for handling loads. Therefore, a total acceleration of 1.1g is applied to the weldment model in the out of plane direction. Thermal stresses for the basket weldments are determined using the method presented in Sections 3.4.4.1.8.1 and 3.4.4.1.8.2 for the PWR and BWR support disks, respectively. The temperatures used in the model to establish the weldment temperature gradient are:

Basket Weldment	Temperature at Center of Weldment (°F)	Temperature at Edge of Weldment (°F)
PWR Top	600	275
PWR Bottom	325	175
BWR Top	525	225
BWR Bottom	475	200

These temperatures are conservatively selected to envelop the maximum temperature and the maximum radial temperature gradient of the weldments for all normal and off-normal conditions of storage. The results of the structural analyses for dead load, handling load, and thermal load are summarized in Table 3.4.4.1-17.

3.4.4.1.9.1 PWR Fuel Basket Weldments

The PWR top and bottom weldment plates are 1.25 and 1.0-in. thick Type 304 stainless steel plate, respectively. The weldments support their own weight plus the weight of up to 24 PWR fuel assembly tubes. An ANSYS finite element analysis was prepared for both plates because the support location for each weldment is different. Both models use the SHELL63 elements, which permits out-of-plane loading. The finite element models for the top and bottom weldments are shown in Figures 3.4.4.1-8 and 3.4.4.1-9, respectively. Note that the corner baffles are conservatively omitted in the top weldment model. The load from the fuel tube on the bottom weldment is represented as point forces applied to the nodes at the periphery of the fuel assembly slots. An average point force is applied. The application of the nodal loads at the slot periphery is accurate because the tube weight is transmitted to the edge of the slot, which provides support to the fuel tubes while in the vertical position.

The maximum stress intensity and the margin of safety for the weldments are shown in Table 3.4.4.1-17. Note that the nodal stress intensity is conservatively used for the evaluation. The Pm stresses for the weldments for normal conditions are essentially zero since there are no loads in the plane of the weldments. The weldments satisfy the stress criteria in the ASME Code Section III, Subsection NG [6].

3.4.4.1.9.2 BWR Fuel Basket Weldments

In the BWR fuel basket transport analysis, the responses of the top and bottom weldment plates to normal storage conditions are evaluated in conjunction with the thermal expansion stress. The weldment plates are 1.0-in. thick Type 304 stainless steel. The weldments support their own weight and the weight of up to 56 BWR fuel assembly tubes. A finite element analysis was performed for the top and bottom plates because the support for each weldment differs depending upon the location of the welded ribs for each. Both models use SHELL63 elements, which permit out-of-plane loading. The finite element models for the top and bottom weldments are shown in Figure 3.4.4.1-18 and Figure 3.4.4.1-19, respectively. The load from the fuel tube on the bottom weldment is represented as average point forces applied to the nodes at the periphery of the fuel assembly slots because the tube weight is transmitted to the edge of the slot in the end-impact condition.

The maximum stress intensity and the margin of safety for the weldments are shown in Table 3.4.4.1-17. Note that the nodal stress intensity is conservatively used for the evaluation. The P_m stresses for the weldments for normal conditions are essentially zero since there are no loads in the plane of the weldments. The weldments satisfy the stress criteria in the ASME Code Section III, Subsection NG [6].

3.4.4.1.10 Fuel Tube Analysis

Under normal storage conditions, the fuel tubes, Figure 3.4.4.1-9 (PWR) and Figure 3.4.4.1-17 (BWR), support only their own weight. The fuel assemblies are supported by the canister bottom plate, not by the fuel tubes. Thermal stresses are considered to be negligible since the tubes are free to expand axially and radially. The handling load is taken as 10% of the dead load.

The weight of the fuel tube, with a load of 1.1g (to account for both the dead load and handling load) is carried by the tube cross-section. The cross sectional area of a PWR fuel tube is:

$$\text{Area} = (8.9\text{ in})^2 - (8.9\text{ in.} - 2 \times 0.048\text{ in.})^2 = 1.7\text{ in}^2$$

The bounding weight of the heaviest PWR fuel tube is about 200 pounds. Considering a g-load of 1.1, the maximum compressive and bearing stress in the fuel tube is about 129 psi (200 lb × 1.1 / 1.7 in^2). Limiting the compressive stress level in the tube to the material yield strength ensures the tube remains in position in storage conditions. The yield strength of Type 304 stainless steel is 17,300 psi at a conservatively high temperature of 750°F.

$$\text{MS} = 17{,}300/129 - 1 = +\text{Large}$$

The minimum cross-sectional area of a BWR fuel tube and oversized fuel tube is:

$$\text{Area} = (5.996\text{ in})^2 - (5.9969\text{ in.} - 2 \times 0.048\text{ in.})^2 = 1.14\text{ in}^2$$

The bounding weight of the heaviest BWR fuel tube and oversized fuel tube is about 100 pounds. Considering a g-load of 1.1, the maximum compressive and bearing stress in the fuel tube is about 96 psi (100 lb × 1.1 / 1.14 in.^{2}). Limiting the compressive stress level in the tube to the material yield strength ensures the tube remains in position in storage conditions. The yield strength of Type 304 stainless steel is 17,300 psi at a conservatively high temperature of 750°F.

Margin of Safety = 17,300/96 - 1 = +Large

Thus, the tubes are structurally adequate under normal storage and handing conditions.

3.4.4.1.11 Canister Closure Weld Evaluation

The minimum closure weld for the canister is a 0.75-inch groove weld between the structural lid and the canister shell. The evaluation of this weld incorporates a 0.8 stress reduction factor in accordance with NRC Interim Staff Guidance (ISG) No. 15, Revision 0. The use of this factor is in accordance with ISG No. 15, since the strength of the weld material (E308) is greater than that of the base material (Type 304 or 304L stainless steel).

The stresses for the canister closure weld are evaluated using sectional stresses as permitted by Subsection NB of the ASME Code. The location of the section for the canister closure weld evaluation is shown in Figure 3.4.4.1-4 and corresponds to Section 13. The governing P_m, P_m+ P_b, and P + Q stress intensities for Section 13, and the associated allowables, are listed in Table 3.4.4.1-6, Table 3.4.4.1-7, and Table 3.4.4.1-8, respectively. The factored allowables, incorporating the 0.8 stress reduction factor, and the resulting controlling Margins of Safety are shown below.

This evaluation confirms that the canister closure weld is acceptable for normal operation conditions.

Stress Category	Analysis Stress Intensity (ksi)	0.8 × Allowable Stress (ksi)	Margin of Safety
P_m	1.90	13.36	6.03
$P_m + P_b$	2.67	20.04	6.51
P + Q	6.93	40.08	4.78

Critical Flaw Size for the Canister Closure Weld

The closure weld for the canister is comprised of multiple weld beads using a compatible weld material for Type 304L stainless steel. An allowable (critical) flaw evaluation has been performed to determine the critical flaw size in the weld region. The result of the flaw evaluation is used to define the minimum flaw size, which must be identifiable in the nondestructive examination of the weld. Due to the inherent toughness associated with Type 304L stainless steel, a limit load analysis is used in conjunction with a J-integral/tearing modulus approach.

The safety factor used in this evaluation is that defined in Section XI of the ASME Code.

The stress component used in the evaluation for the critical flaw size is the radial stress component in the weld region of the structural lid. For the normal operation condition, in accordance with ASME Code Section XI, a safety factor of 3 is required. For the purpose of identifying the stress for the flaw evaluation, the weld region corresponding to Section 13 in Figure 3.4.4.1-4 is considered. The radial stress corresponds to SX in Tables 3.4.4.1-1 through 3.4.4.1-10. The maximum reported radial tensile stress is 1.55 ksi.

To perform the flaw evaluation, a 10 ksi stress is conservatively used, resulting in a significantly larger actual safety factor than the required safety factor of 3. Using a 10 ksi stress as the basis for the evaluation of the structural lid weld, the critical flaw size is 0.44 inch for a flaw that extends 360 degrees around the circumference of the structural lid weld. Stress components for the circumferential (Z) and axial (Y) directions are also reported in Tables 3.4.4.1-1 through 3.4.4.1-10, which would be associated with flaws oriented in the radial or horizontal directions, respectively. As shown in Table 3.4.4.1-7 at Section No. 13 (the structural lid weld), the maximum tensile stress reported for these components (SY and SZ) is 1.8 ksi, which is also enveloped by the value of 10 ksi used in the critical flaw evaluation for stresses in the radial direction.

The 360-degree flaw employed for the circumferential direction is considered to be bounding with respect to any partial flaw in the weld, which could occur in the radial and horizontal directions. Therefore, using a minimum detectable flaw size of 0.375 inch is acceptable, since it is less than the very conservatively determined 0.44-inch critical flaw size.

The Type 304L stainless steel structural lid may be forged (SA-182 material), or fabricated from plate (SA-240 material). Since the forged material is required to have ultimate and yield strengths that are equal to, or greater than, the plate material, the critical flaw size determination is applicable to both materials.

Figure 3.4.4.1-1 Canister Composite Finite Element Model

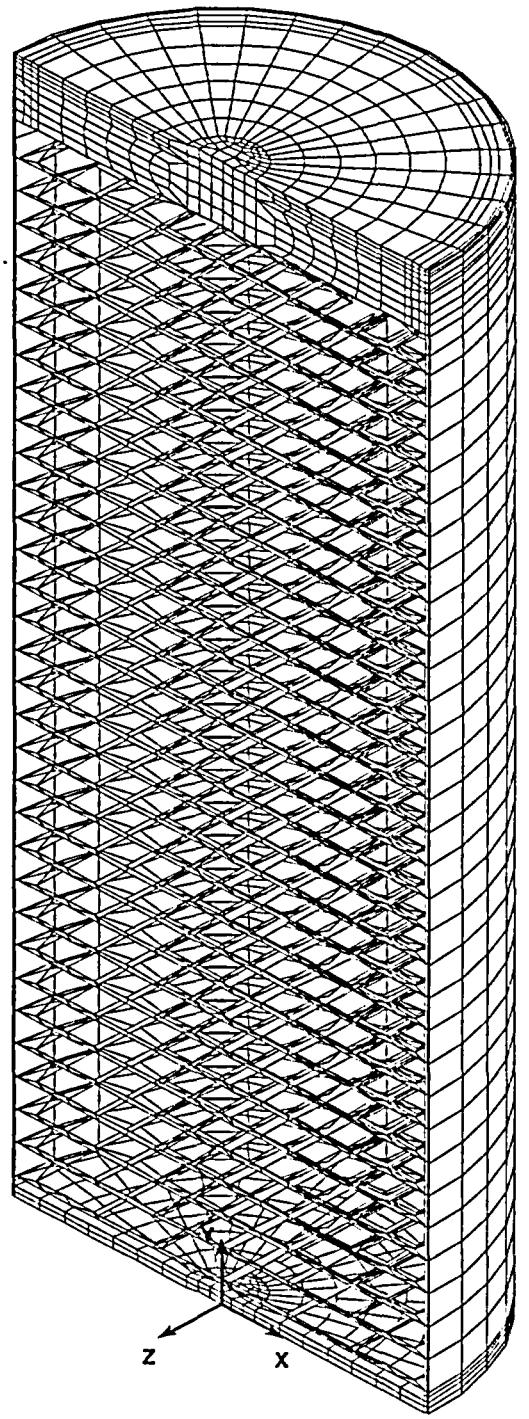

Figure 3.4.4.1-2 Weld Regions of Canister Composite Finite Element Model at Structural and Shield Lids

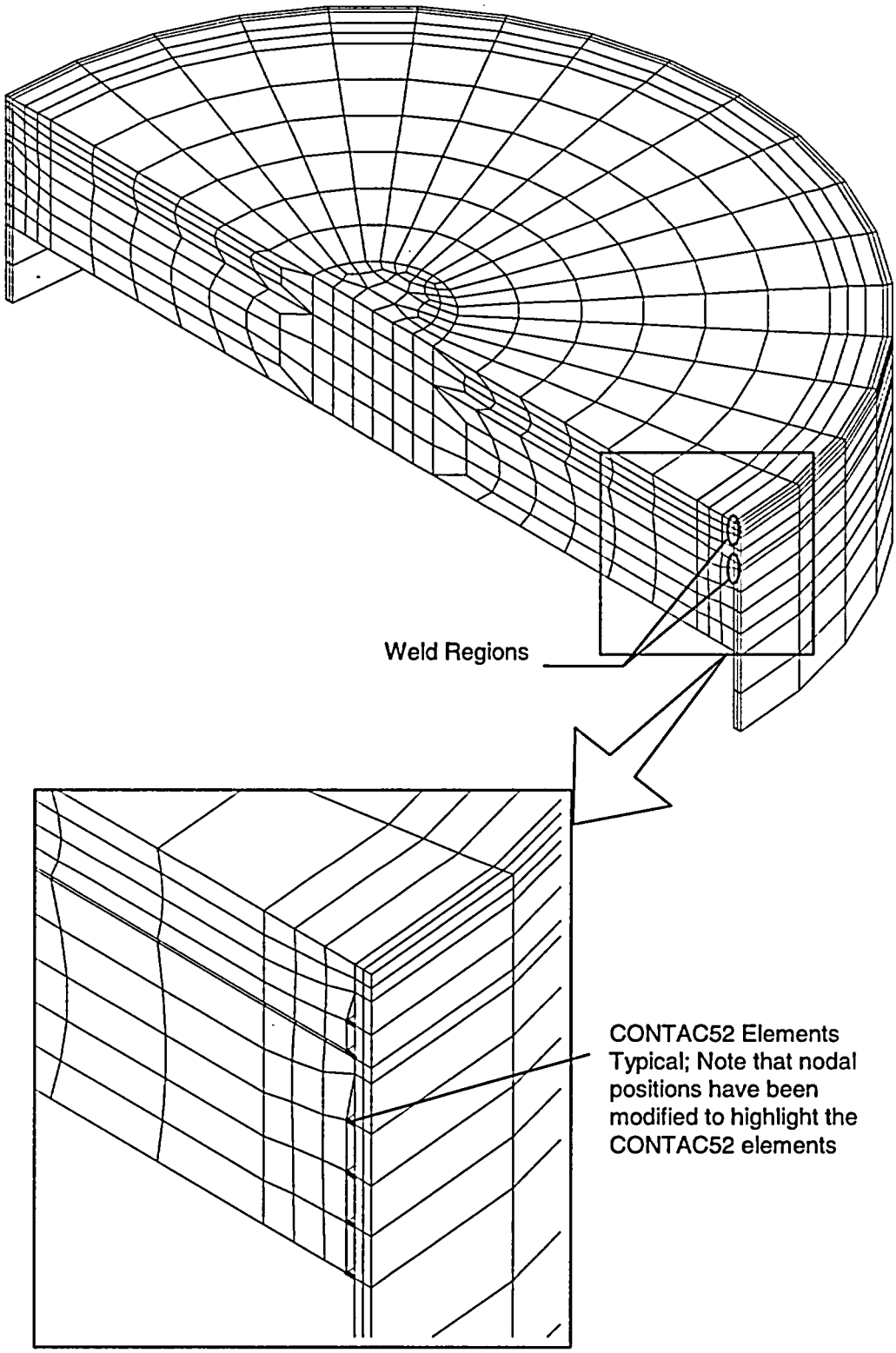

Figure 3.4.4.1-3 Bottom Plate of the Canister Composite Finite Element Model

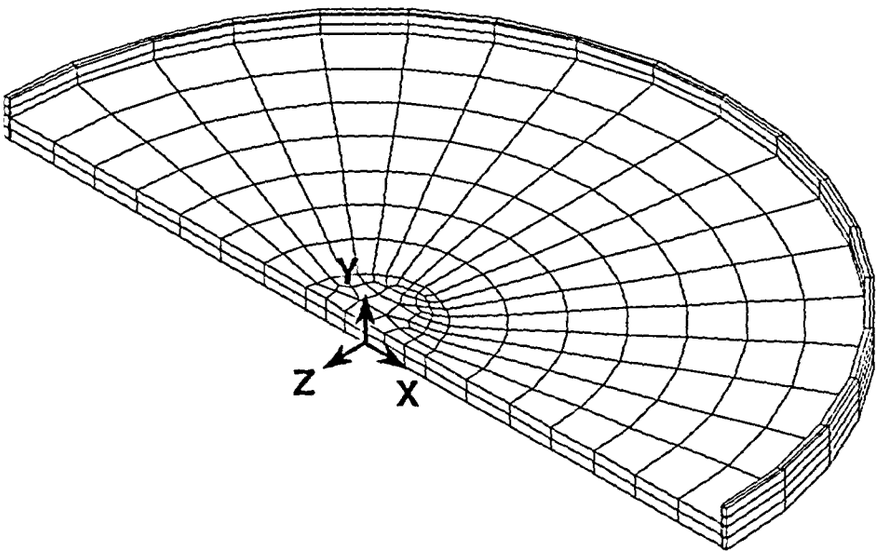

Figure 3.4.4.1-4 Locations for Section Stresses in the Canister Composite Finite Element Model

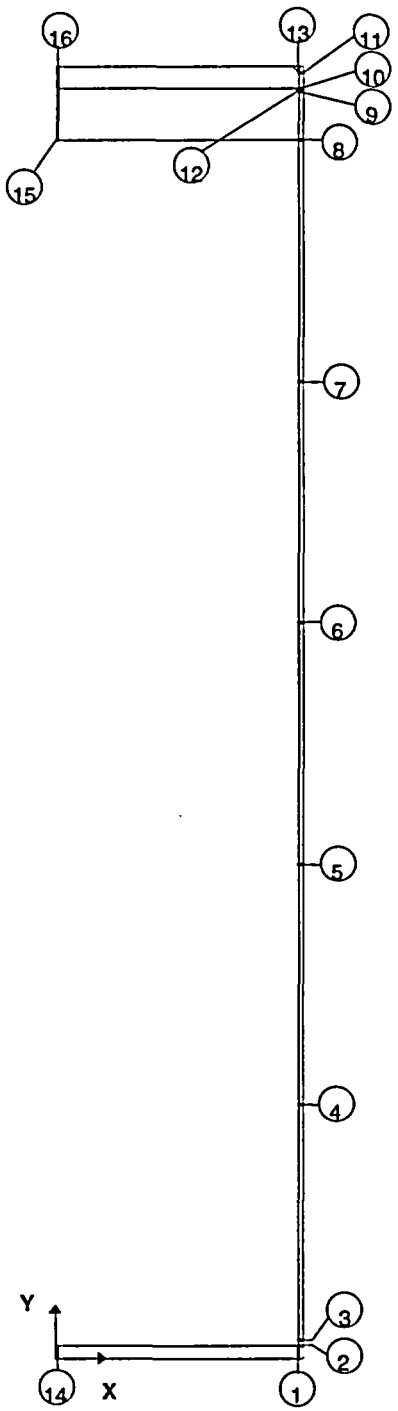

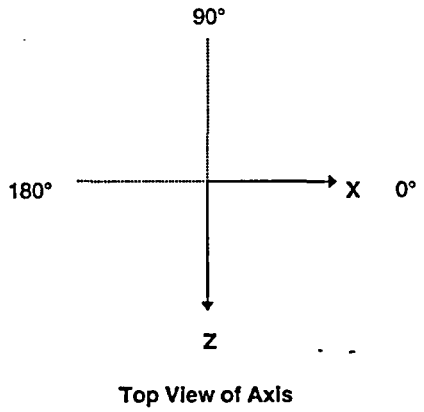

Section Coordinates at Z=0 and X>0

Axial Section	Node 1		Node 2	
	X	Y	X	Y
1	32.905	0.0	32.905	1.75
2	32.905	1.75	33.53	1.75
3	32.905	2.50	33.53	2.50
4	32.905	34.45	33.53	34.45
5	32.905	67.15	33.53	67.15
6	32.905	99.85	33.53	99.85
7	32.905	132.55	33.53	132.55
8	32.905	165.25	33.53	165.25
9	32.905	171.75	33.53	171.75
10	32.905	172.25	33.53	172.25
11	32.905	174.37	33.53	174.37
12	32.905	171.75	32.905	172.25
13	32.905	174.37	32.905	175.25
14	0.1	0.0	0.1	1.75
15	0.1	165.25	0.1	172.25
16	0.1	172.25	0.1	175.25

Figure 3.4.4.1-5 BWR Fuel Assembly Basket Showing Typical Fuel Basket Components

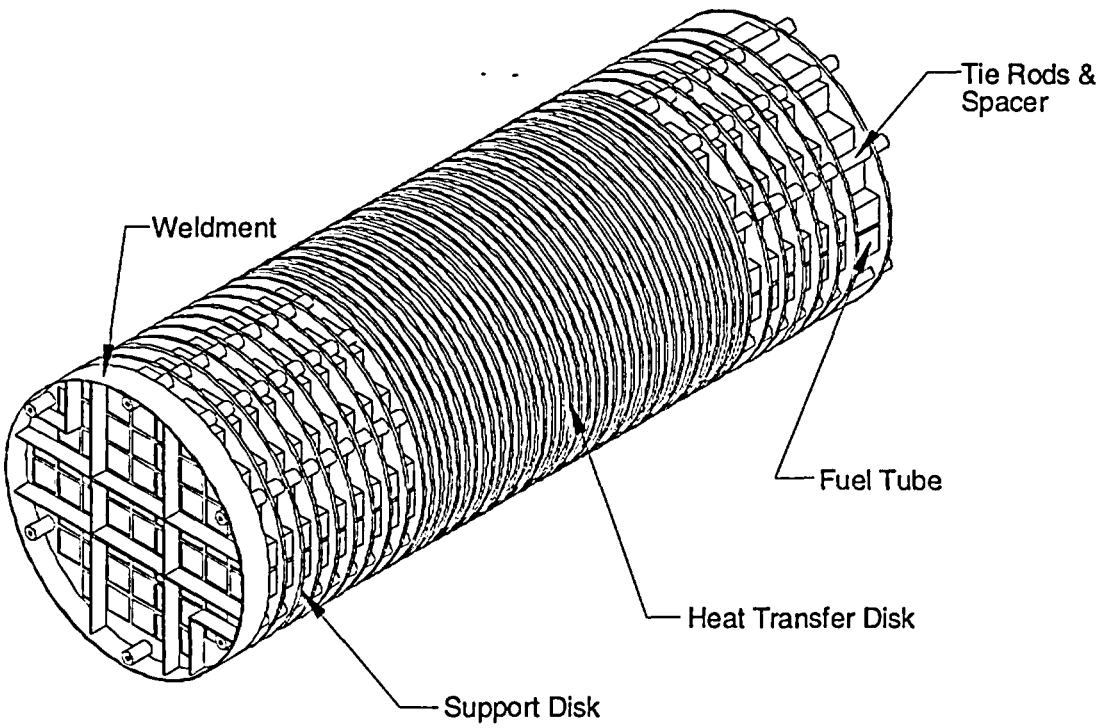

Figure 3.4.4.1-6 PWR Fuel Basket Support Disk Finite Element Model

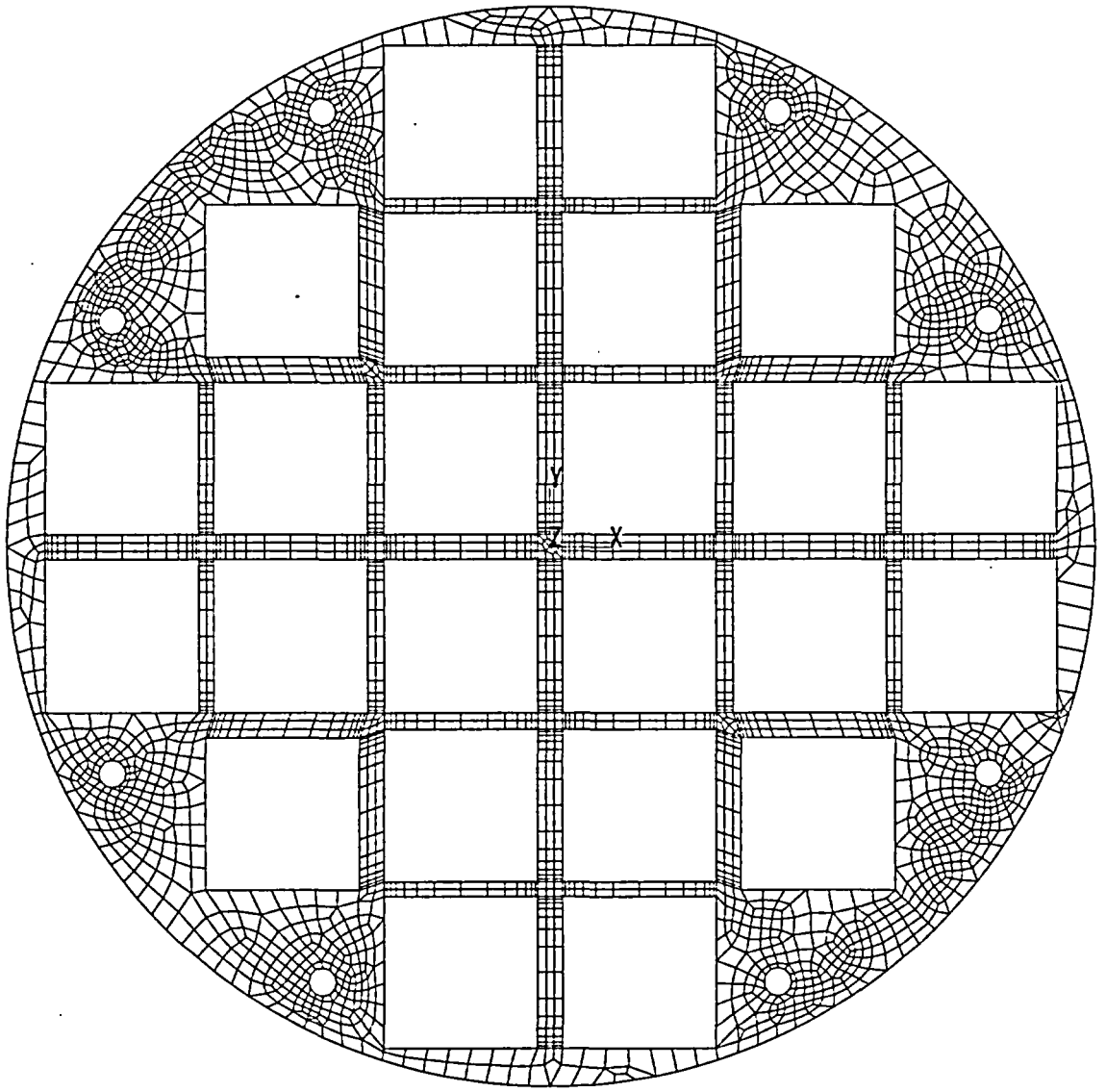

Figure 3.4.4.1-7 PWR Fuel Basket Support Disk Sections for Stress Evaluation (Left-Half)

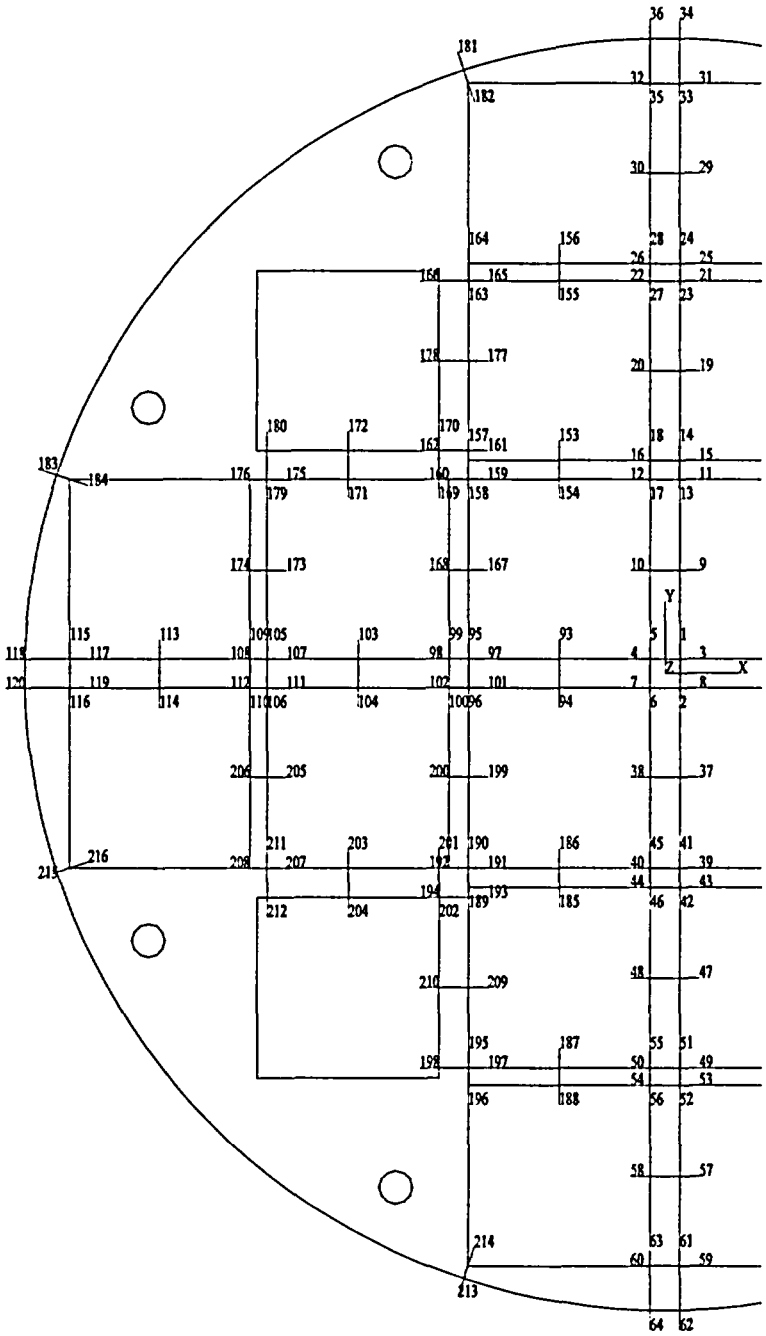

Figure 3.4.4.1-8 PWR Fuel Basket Support Disk Sections for Stress Evaluation (Right-Half)

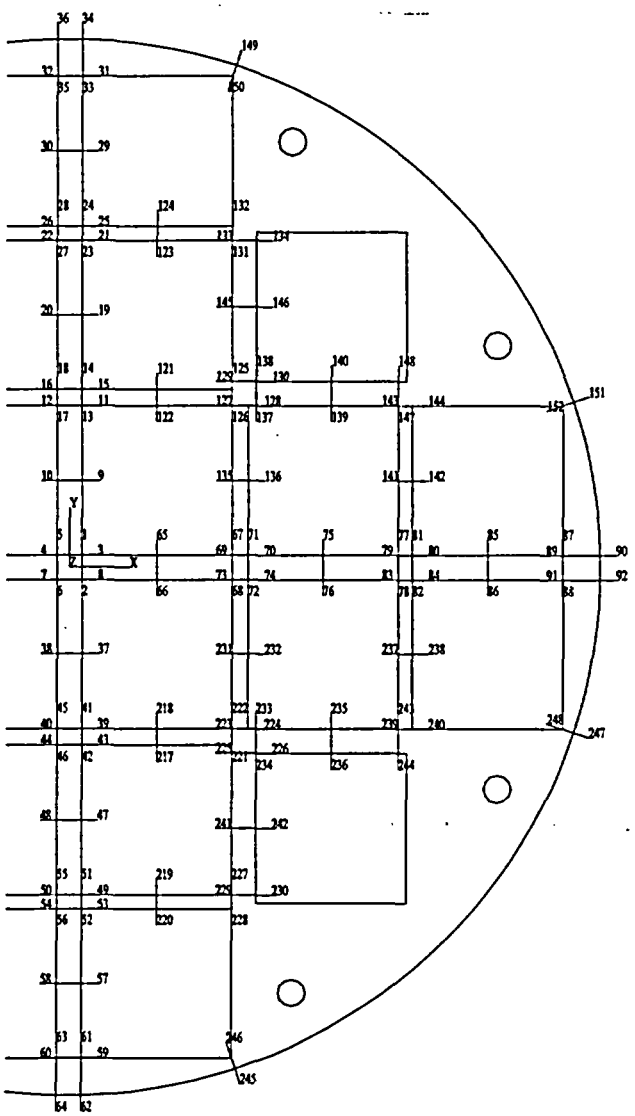

Figure 3.4.4.1-9 PWR Class 3 Fuel Tube Configuration

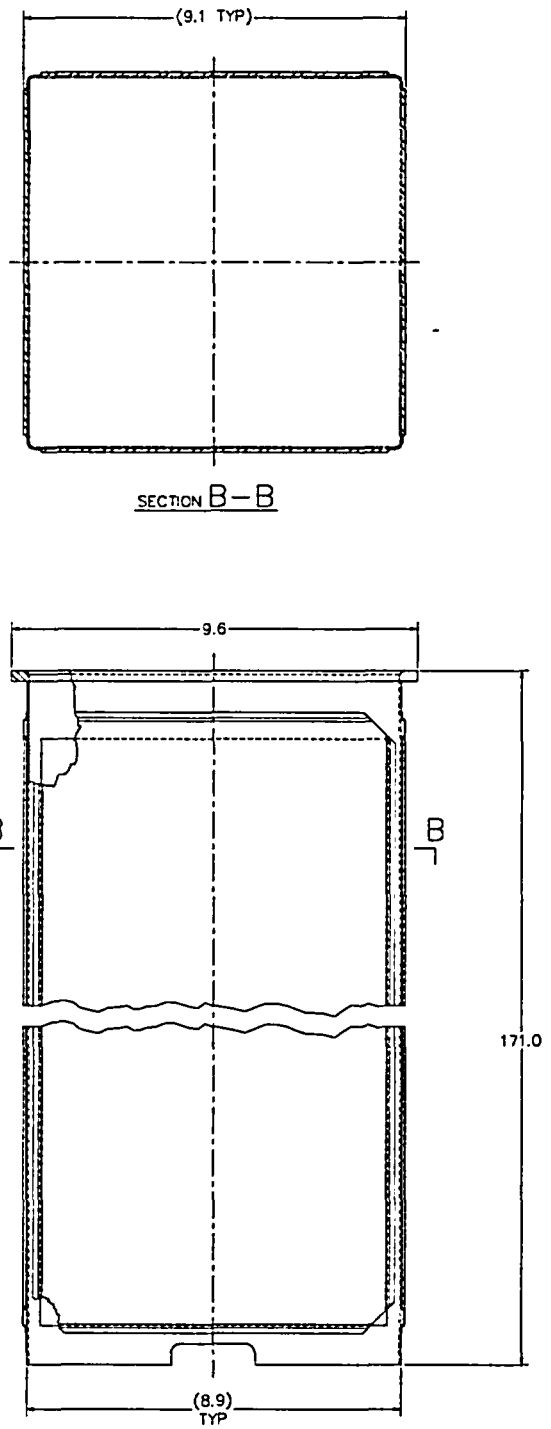

Figure 3.4.4.1-10 PWR Top Weldment Plate Finite Element Model

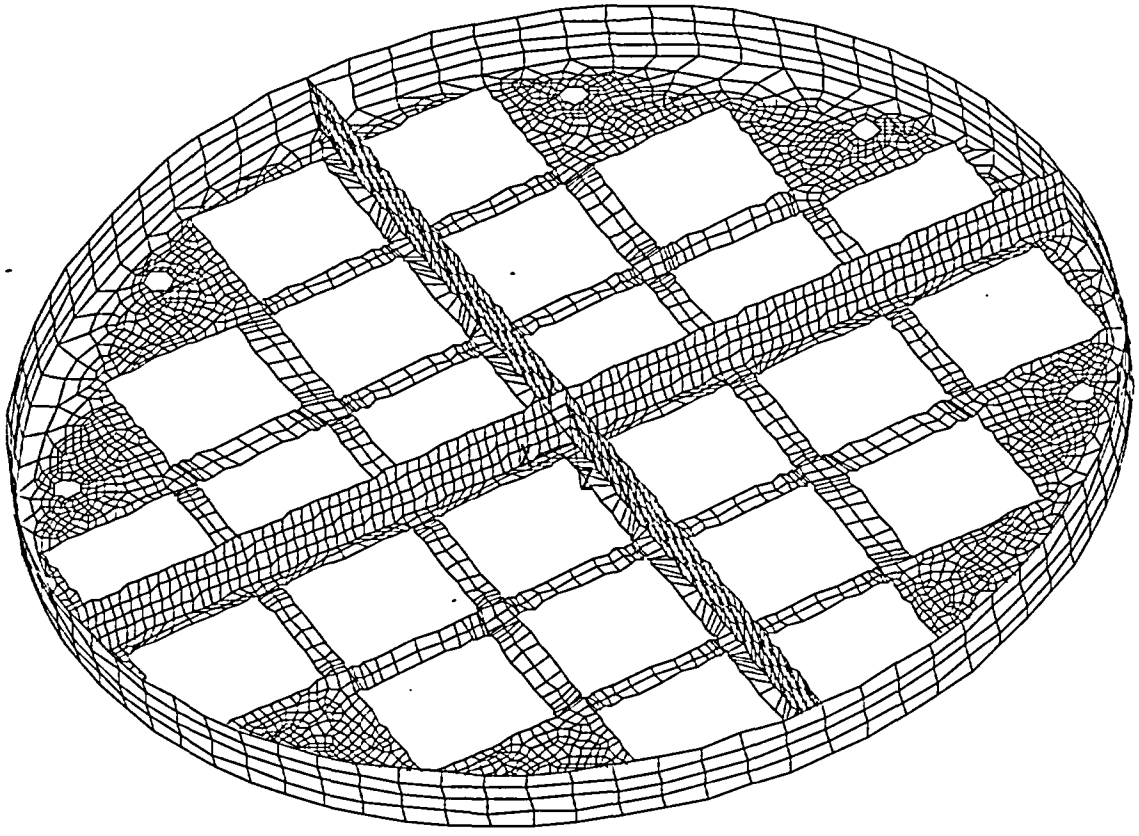

Figure 3.4.4.1-11 PWR Bottom Weldment Plate Finite Element Model

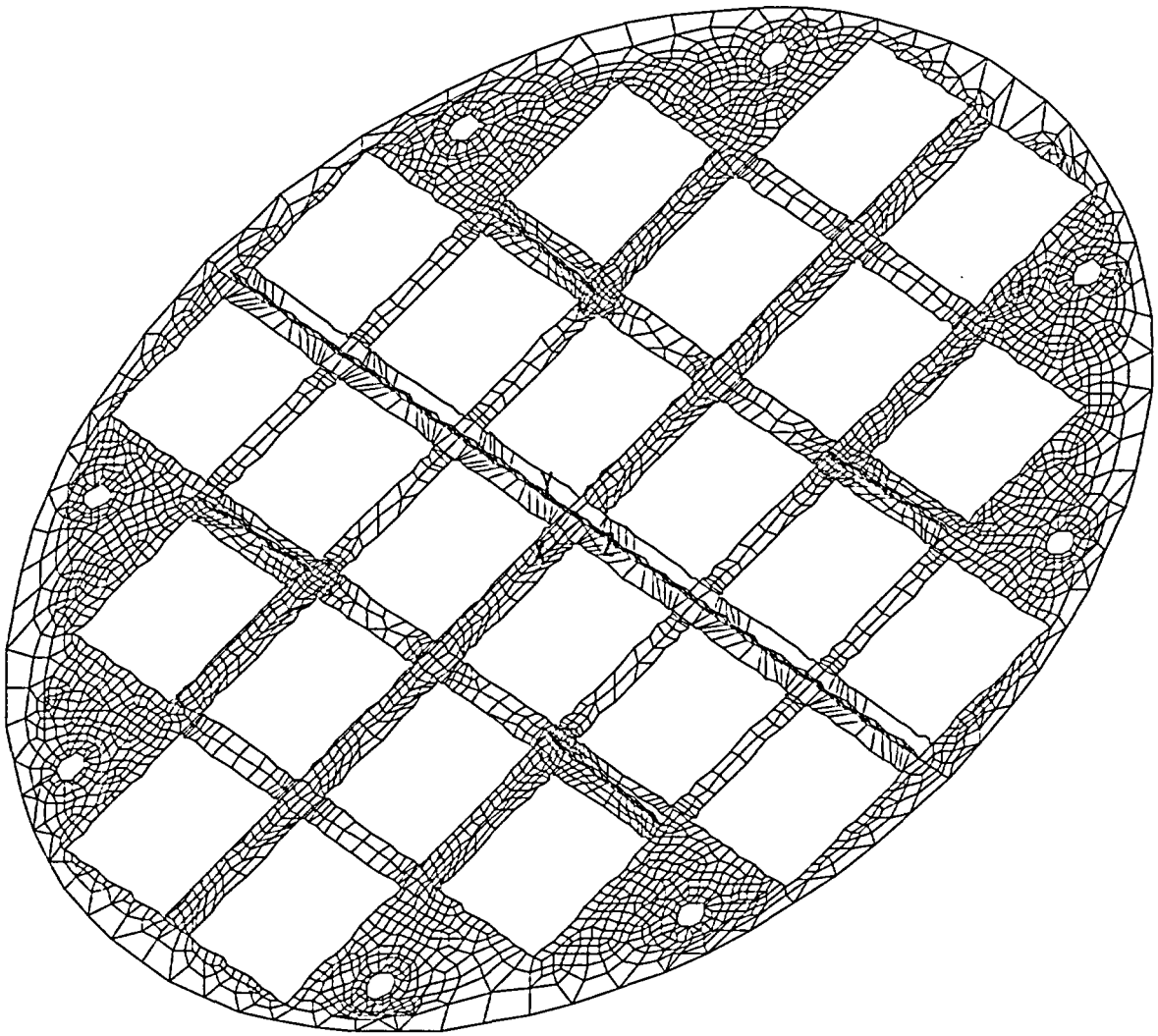

Figure 3.4.4.1-12 BWR Fuel Basket Support Disk Finite Element Model

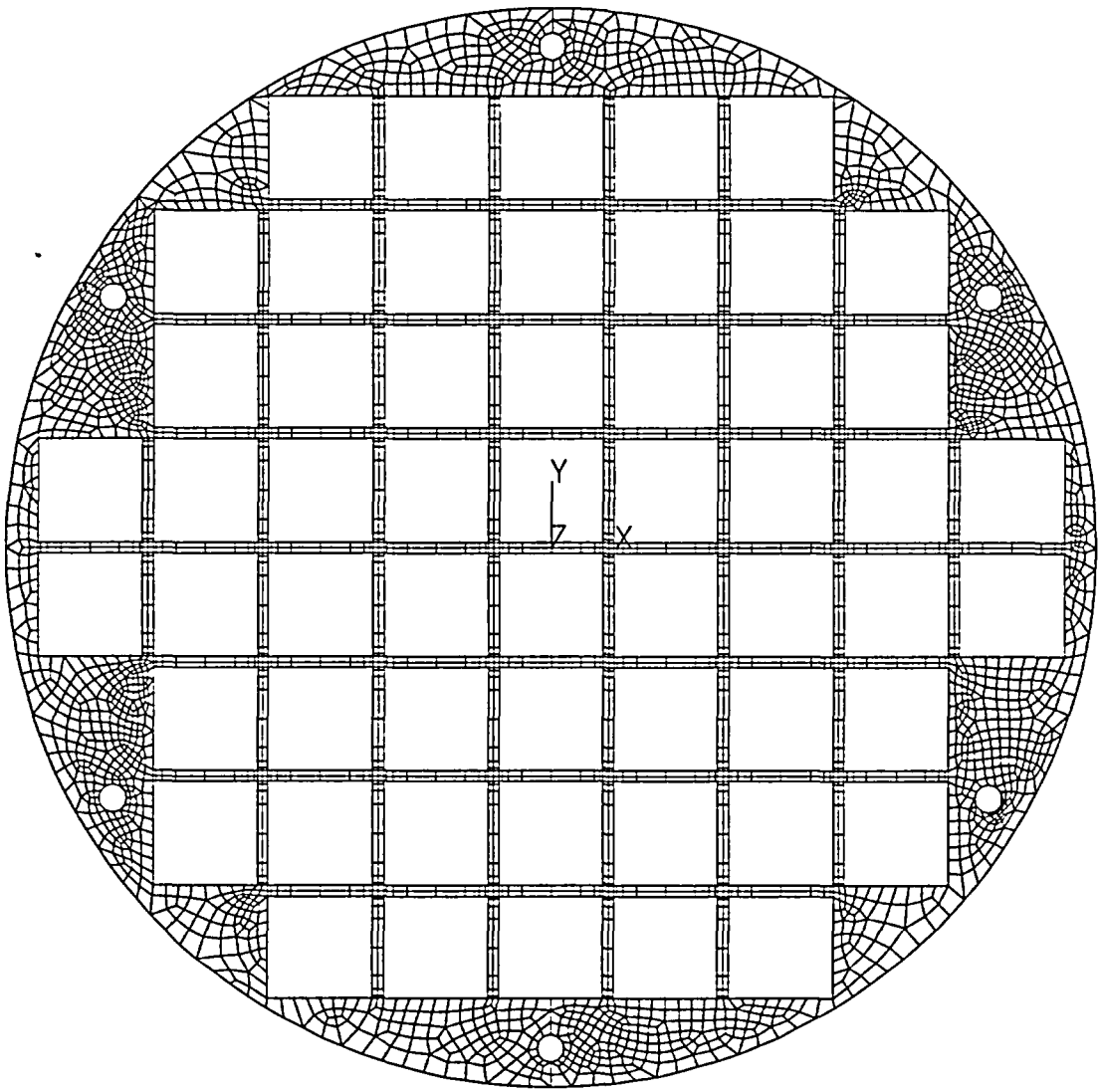

Figure 3.4.4.1-13 BWR Fuel Basket Support Disk Sections for Stress Evaluation (Quadrant I)

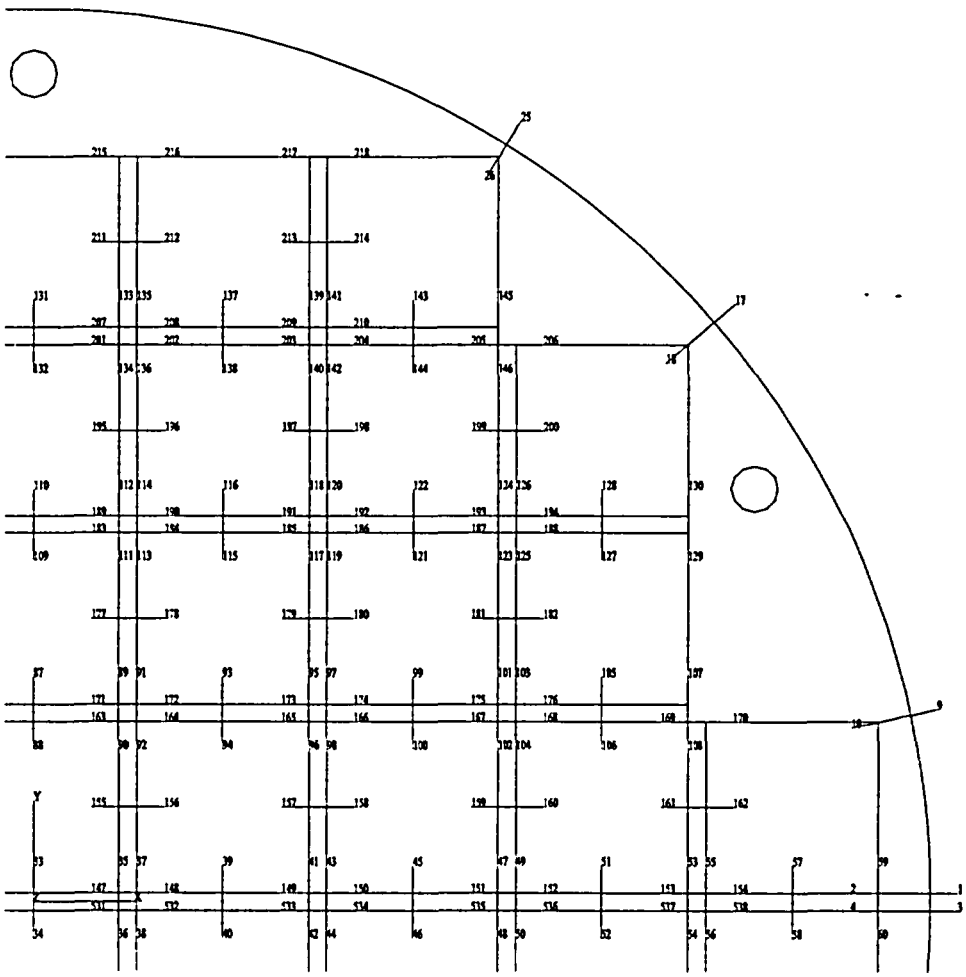

Figure 3.4.4.1-14 BWR Fuel Basket Support Disk Sections for Stress Evaluation (Quadrant II)

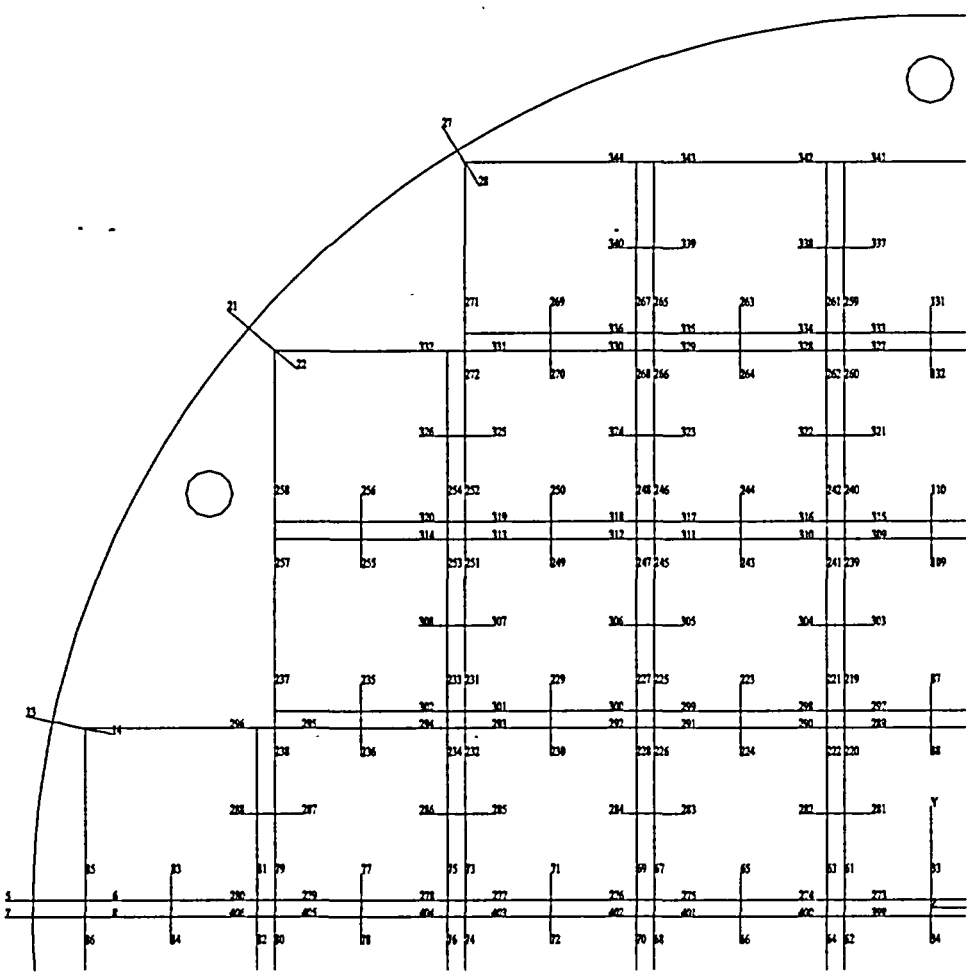

Figure 3.4.4.1-15 BWR Fuel Basket Support Disk Sections for Stress Evaluation (Quadrant III)

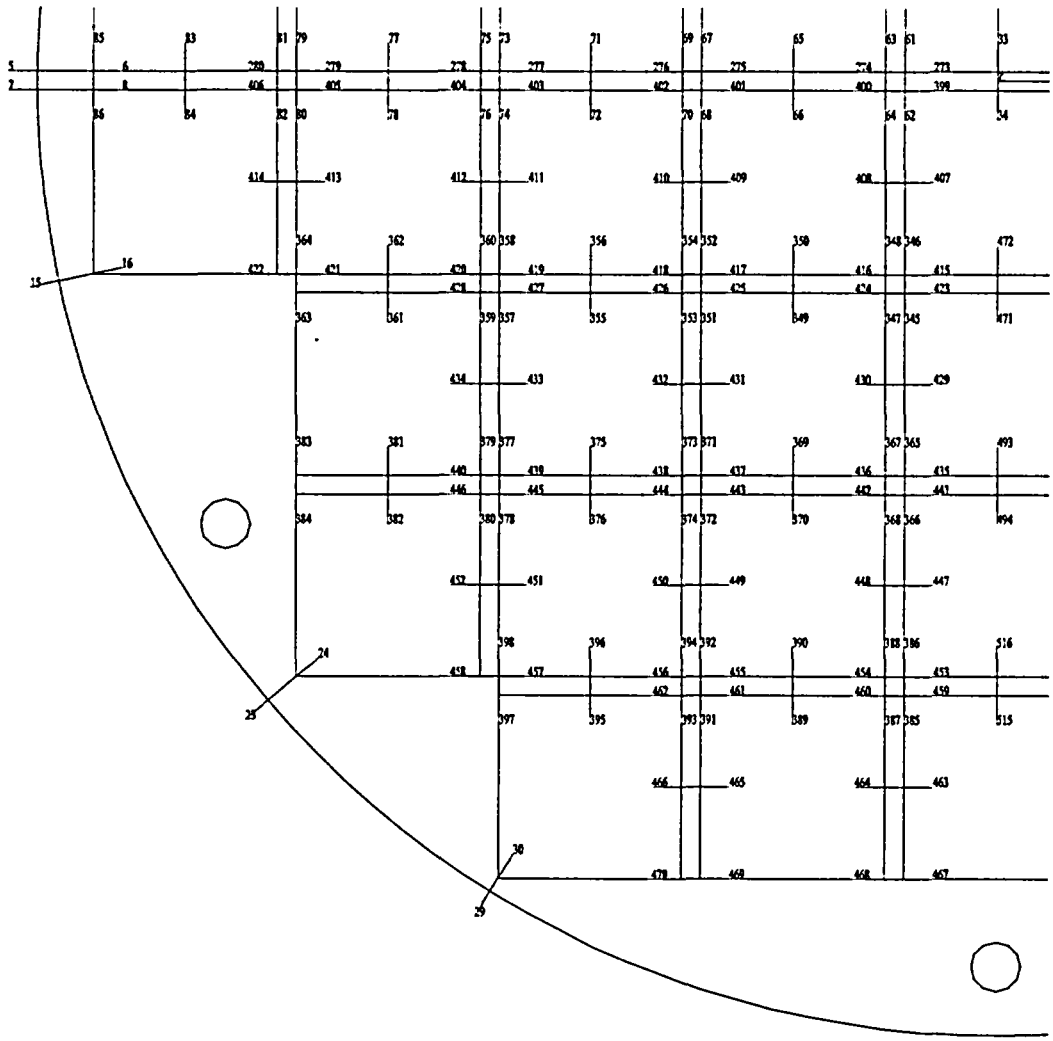

Figure 3.4.4.1-16 BWR Fuel Basket Support Disk Sections for Stress Evaluation (Quadrant IV)

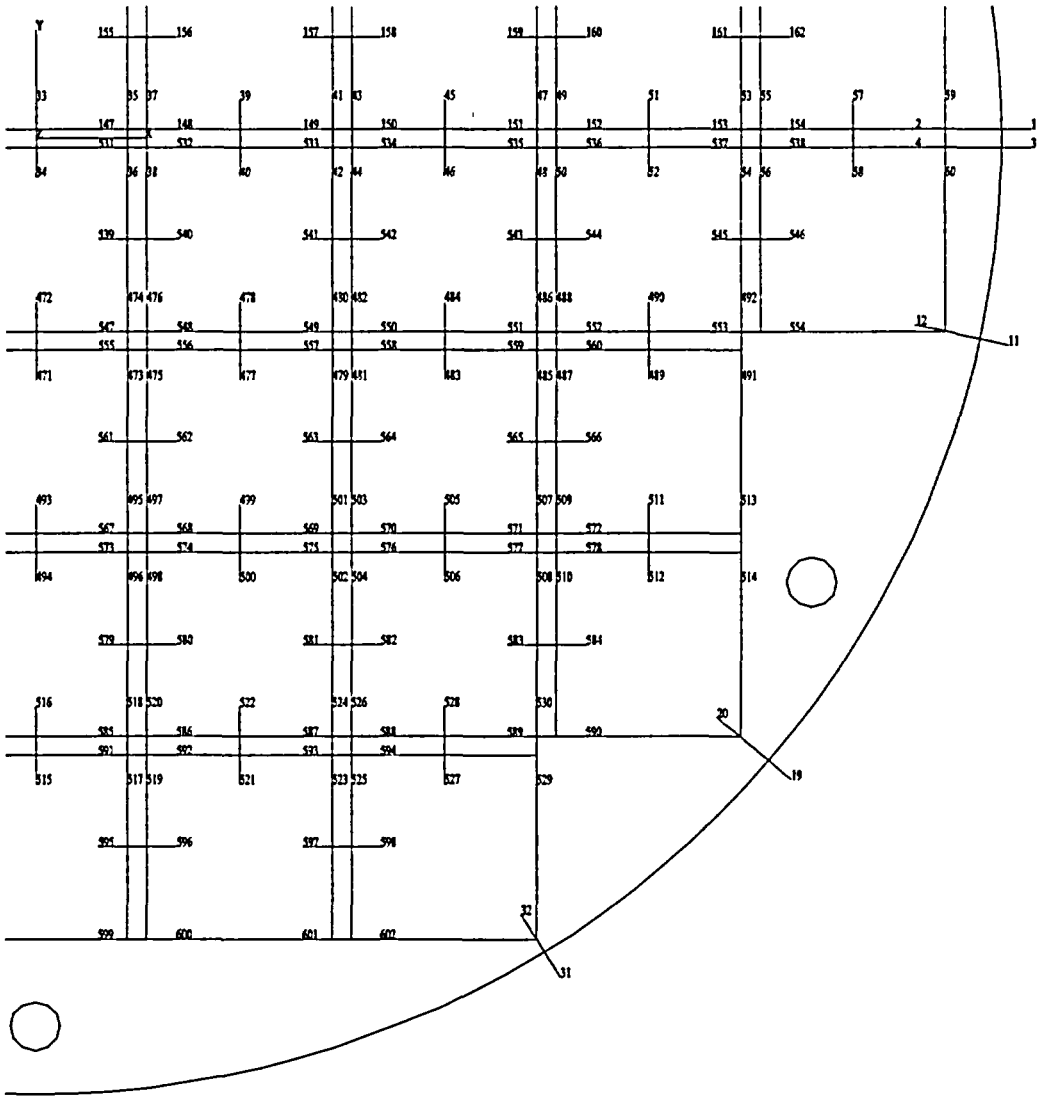

Figure 3.4.4.1-17 BWR Class 5 Fuel Tube Configuration

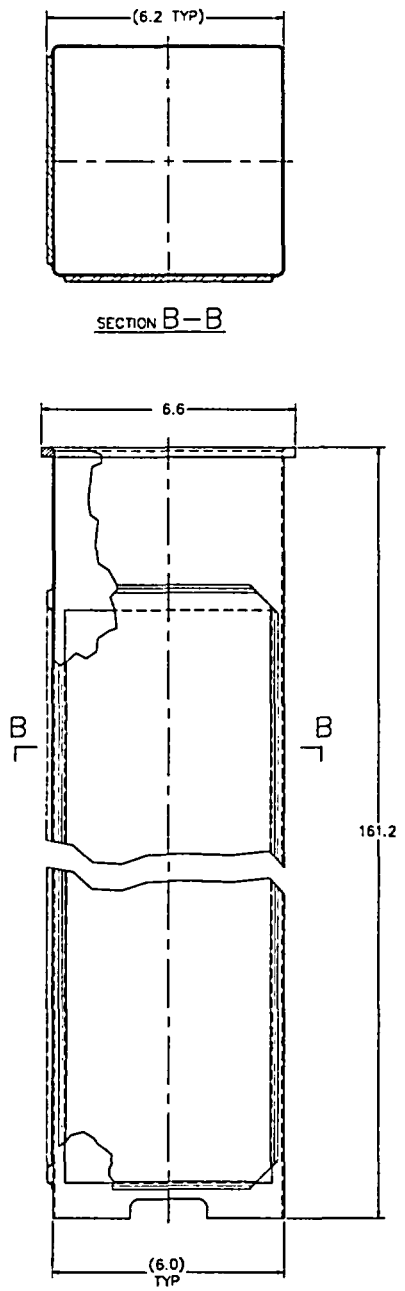

Figure 3.4.4.1-18 BWR Top Weldment Plate Finite Element Model

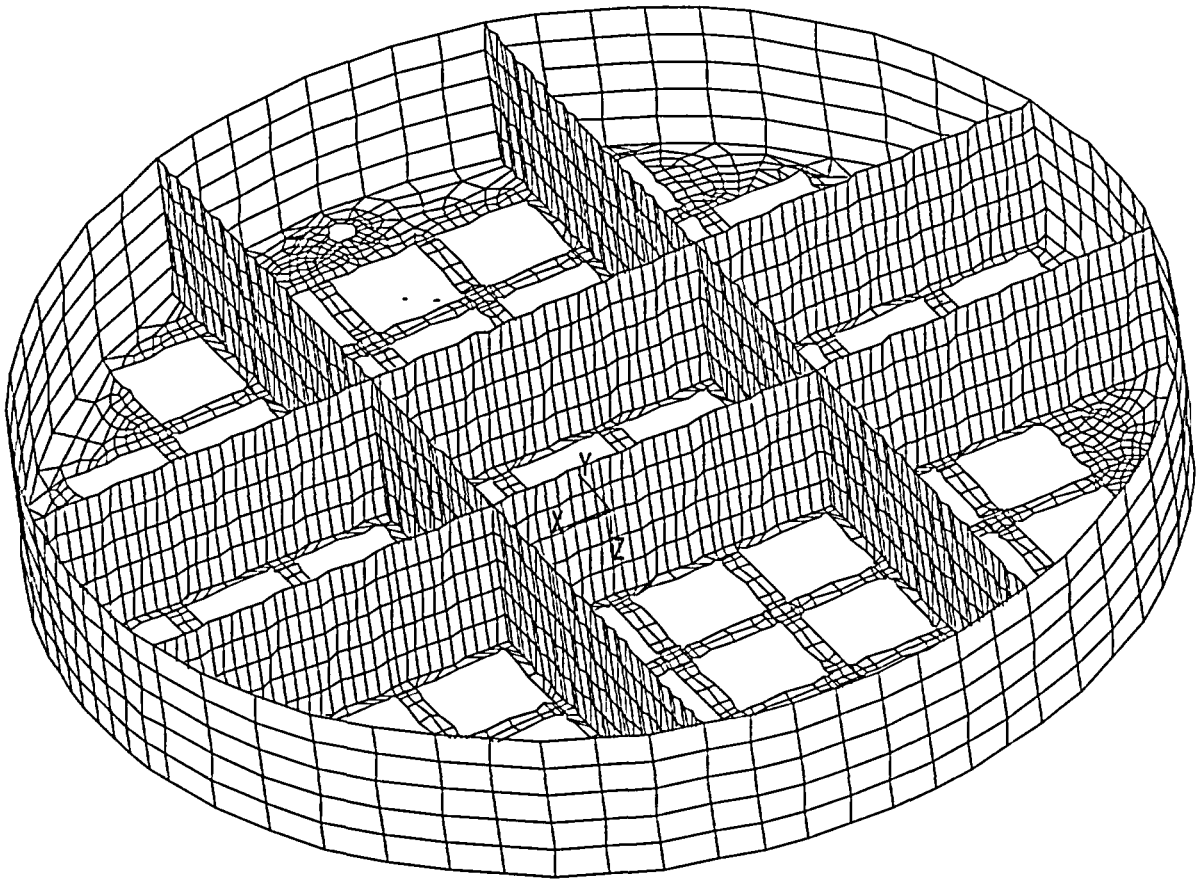

Figure 3.4.4.1-19 BWR Bottom Weldment Plate Finite Element Model

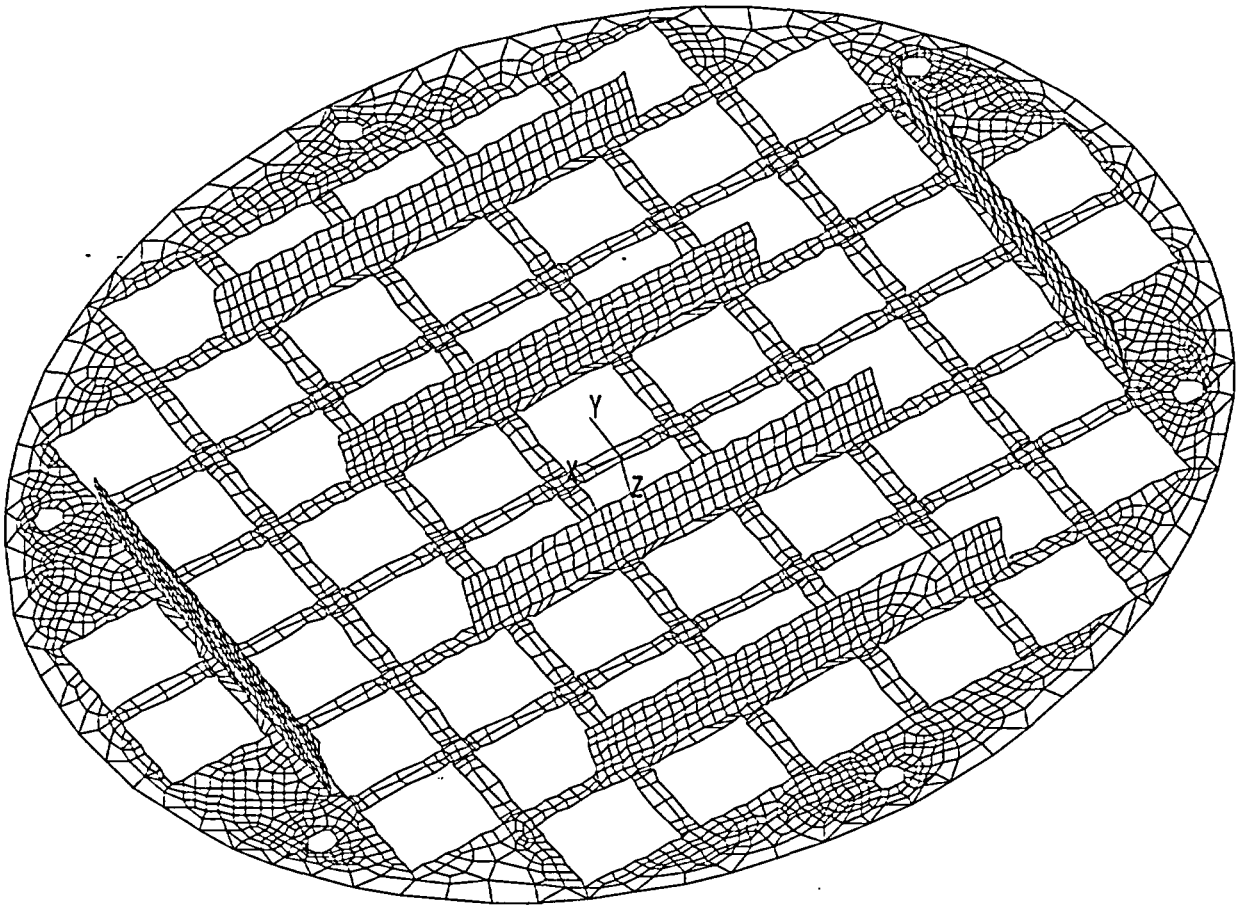

(Figure Inverted to Show Weldment Stiffeners)

Table 3.4.4.1-1 Canister Secondary (Thermal) Stresses (ksi)

Section No. [1]	S_X	S_Y	S_Z	S_{XY}	S_{YZ}	S_{XZ}	Stress Intensity
1	-0.29	1.18	0.05	-0.13	-0.03	-0.10	1.52
2	0.16	0.48	-2.23	-0.03	-0.03	-0.18	2.72
3	-0.27	1.43	3.09	-0.14	0.02	0.07	3.37
4	0.00	0.00	-0.02	0.00	0.01	0.00	0.03
5	0.00	-0.05	0.09	0.00	-0.01	-0.01	0.14
6	0.00	-0.06	0.19	0.00	0.01	0.01	0.24
7	0.00	0.00	0.01	0.00	-0.01	0.00	0.03
8	0.00	-0.01	0.08	0.00	-0.01	0.00	0.10
9	3.58	1.49	1.59	0.03	0.15	1.31	3.31
10	-6.18	-2.32	-0.84	-0.22	-0.03	-0.87	5.63
11	1.80	-1.80	-8.02	-0.27	-0.09	0.74	9.96
12	-6.18	-2.32	-0.84	-0.22	-0.03	-0.87	5.63
13	-4.26	-0.79	1.43	0.27	-0.06	0.53	5.82
14	-23.43	-22.06	-14.19	0.72	1.42	-0.10	9.85
15	-7.92	-7.44	-6.62	0.20	0.49	0.00	1.64
16	0.28	0.29	-0.08	0.00	0.00	0.00	0.37

1. See Figure 3.4.4.1-4 for definition of locations of stress sections.

Table 3.4.4.1-2 Canister Dead Weight Primary Membrane (P_m) Stresses (ksi), $P_{internal}$ = 0 psig

Section No. [1]	S_X	S_Y	S_Z	S_{XY}	S_{YZ}	S_{XZ}	Stress Intensity
1	0.00	-0.01	-0.05	0.00	0.00	-0.01	0.05
2	0.01	-0.02	-0.11	0.00	0.00	-0.01	0.12
3	0.00	-0.03	-0.13	0.00	0.00	0.00	0.12
4	0.00	0.00	-0.12	0.00	0.00	0.00	0.12
5	0.00	0.00	-0.11	0.00	0.00	0.00	0.11
6	0.00	0.00	-0.10	0.00	0.00	0.00	0.10
7	0.00	0.00	-0.09	0.00	0.00	0.00	0.09
8	0.00	0.01	-0.07	0.00	0.00	0.00	0.08
9	-0.01	-0.04	-0.04	0.00	0.00	-0.01	0.03
10	0.03	-0.02	-0.02	0.00	0.00	0.00	0.05
11	-0.03	-0.02	0.01	0.00	0.00	-0.01	0.04
12	0.01	-0.01	0.03	0.00	0.00	0.01	0.04
13	0.01	-0.02	-0.03	0.00	0.00	0.00	0.04
14	0.00	0.00	-0.02	0.00	0.00	0.00	0.02
15	0.00	0.00	0.00	0.00	0.00	0.00	0.01
16	0.00	0.00	0.00	0.00	0.00	0.00	0.00

1. See Figure 3.4.4.1-4 for definition of locations of stress sections.

Table 3.4.4.1-3 Canister Dead Weight Primary Membrane plus Bending ($P_m + P_b$) Stresses (ksi), $P_{internal} = 0$ psig

Section No. [1]	S_X	S_Y	S_Z	S_{XY}	S_{YZ}	S_{XZ}	Stress Intensity
1	0.01	-0.01	-0.06	0.00	0.00	-0.01	0.07
2	0.01	-0.03	-0.14	0.00	0.00	0.00	0.15
3	0.00	-0.03	-0.13	0.00	0.00	0.00	0.13
4	0.00	0.00	-0.12	0.00	0.00	0.00	0.12
5	0.00	0.00	-0.11	0.00	0.00	0.00	0.11
6	0.00	0.00	-0.10	0.00	0.00	0.00	0.10
7	0.00	0.00	-0.09	0.00	0.00	0.00	0.09
8	0.00	0.00	-0.09	0.00	0.00	0.00	0.09
9	-0.01	-0.05	-0.08	0.00	0.00	-0.01	0.08
10	0.02	-0.05	-0.10	0.00	0.00	-0.01	0.11
11	-0.02	0.01	0.08	0.00	0.00	-0.01	0.11
12	0.05	0.01	0.05	0.00	0.00	0.02	0.06
13	0.05	0.00	-0.01	0.00	0.00	-0.01	0.07
14	0.00	0.00	-0.02	0.00	0.00	0.00	0.02
15	0.07	0.07	0.00	0.00	0.00	0.00	0.07
16	-0.03	-0.03	0.00	0.00	0.00	0.00	0.03

1. See Figure 3.4.4.1-4 for definition of locations of stress sections.

Table 3.4.4.1-4 Canister Normal Handling With No Internal Pressure Primary Membrane (P_m) Stresses, (ksi)

Section No. [1]	S_X	S_Y	S_Z	S_{XY}	S_{YZ}	S_{XZ}	Stress Intensity
1	0.12	0.70	1.80	-0.05	-0.01	-0.26	1.76
2	1.17	-1.69	-1.15	0.22	-0.02	-0.27	2.92
3	-0.20	-2.63	0.53	0.22	0.04	0.48	3.42
4	0.00	0.01	0.51	0.00	0.00	0.00	0.51
5	0.00	0.00	0.55	0.00	0.00	0.00	0.55
6	0.01	-0.01	0.62	0.00	-0.01	0.00	0.62
7	0.01	-0.01	0.73	0.00	-0.01	0.00	0.74
8	0.02	-0.03	1.11	0.00	-0.07	0.00	1.15
9	0.05	0.40	1.56	-0.03	-0.15	0.07	1.53
10	-0.29	0.36	1.93	-0.07	-0.21	0.09	2.26
11	-0.68	0.74	1.05	-0.11	-0.13	-0.58	2.10
12	-0.13	0.52	2.01	-0.10	-0.10	0.17	2.19
13	0.34	0.99	-0.40	-0.16	-0.03	-0.61	1.79
14	0.29	0.29	-0.01	0.00	0.14	-0.02	0.41
15	-0.01	-0.01	-0.03	0.00	0.00	0.00	0.02
16	0.00	0.01	-0.05	0.00	-0.01	-0.01	0.06

1. See Figure 3.4.4.1-4 for definition of locations of stress sections.

Table 3.4.4.1-5 Canister Normal Handling With No Internal Pressure Primary Membrane plus Bending ($P_m + P_b$) Stresses (ksi)

Section No. [1]	S_X	S_Y	S_Z	S_{XY}	S_{YZ}	S_{XZ}	Stress Intensity
1	1.32	-0.05	4.36	0.07	-0.02	-0.02	4.42
2	0.57	-3.98	-8.37	0.38	-0.04	-0.60	9.05
3	-0.85	0.53	11.91	-0.08	0.04	0.62	12.82
4	0.00	-0.05	0.50	-0.01	0.00	0.00	0.56
5	0.00	-0.14	0.51	0.01	-0.01	0.00	0.65
6	0.01	-0.19	0.56	0.02	-0.01	0.00	0.75
7	0.01	-0.21	0.66	0.02	-0.01	0.00	0.88
8	0.03	-0.16	1.06	0.01	-0.05	0.00	1.23
9	-0.09	0.34	1.69	0.00	-0.21	-0.02	1.81
10	-0.46	0.64	2.87	-0.13	-0.13	0.20	3.38
11	-1.00	0.69	1.11	-0.12	-0.20	-1.02	2.98
12	-0.50	0.57	2.66	0.00	0.00	0.18	3.19
13	1.55	1.54	-0.83	-0.25	0.07	-0.25	2.67
14	6.60	6.61	0.18	0.00	0.13	-0.03	6.43
15	0.10	0.11	-0.06	0.00	0.01	0.00	0.17
16	0.25	0.27	-0.06	-0.02	-0.01	0.00	0.34

1. See Figure 3.4.4.1-4 for definition of locations of stress sections.

Table 3.4.4.1-6 Summary of Canister Normal Handling plus Normal Internal Pressure Primary Membrane (P_m) Stresses (ksi)

Section No. [1]	S_X	S_Y	S_Z	S_{XY}	S_{YZ}	S_{XZ}	Stress Intensity	Stress Allowable[2]	Margin of Safety
1	0.22	1.27	3.26	-0.09	-0.03	-0.47	3.19	16.70	4.2
2	2.15	-2.90	-2.11	0.38	-0.04	-0.48	5.16	16.70	2.2
3	-0.38	-4.49	0.95	0.38	0.08	0.90	5.94	16.70	1.8
4	0.00	0.80	0.90	-0.07	0.00	0.00	0.91	16.15	16.7
5	0.00	0.78	0.94	-0.07	0.00	0.00	0.94	14.94	14.8
6	0.01	0.78	1.01	-0.07	-0.01	0.00	1.01	14.81	13.7
7	0.01	0.78	1.12	-0.07	-0.01	0.00	1.12	15.93	13.2
8	0.02	0.49	1.49	-0.05	-0.07	-0.01	1.48	16.70	10.3
9	0.02	0.52	1.81	-0.04	-0.15	0.05	1.81	16.70	8.2
10	-0.33	0.46	2.10	-0.08	-0.21	0.02	2.47	16.70	5.8
11	-0.42	1.00	0.97	-0.12	-0.12	-0.51	1.77	16.70	8.5
12	-0.18	0.57	2.04	-0.11	-0.10	0.09	2.25	16.70	6.4
13	0.26	1.36	-0.05	-0.21	0.00	-0.57	1.90	16.70	7.8
14	0.53	0.53	-0.01	0.00	0.25	-0.04	0.74	16.70	21.6
15	-0.05	-0.05	-0.01	0.00	0.00	0.00	0.04	16.70	371.4
16	0.04	0.04	0.00	0.00	-0.01	0.00	0.04	16.70	418.2

1. See Figure 3.4.4.1-4 for definition of locations of stress sections.
2. ASME Code Service Level A is used for material allowable stresses.

Table 3.4.4.1-7 Summary of Canister Normal Handling, Plus Normal Pressure Primary Membrane plus Bending ($P_m + P_b$) Stresses (ksi)

Section No. [1]	S_X	S_Y	S_Z	S_{XY}	S_{YZ}	S_{XZ}	Stress Intensity	Stress Allowable[2]	Margin of Safety
1	2.44	0.07	7.90	0.12	-0.04	-0.04	7.83	25.05	2.2
2	1.04	-7.06	-15.17	0.67	-0.07	-1.08	16.41	25.05	0.5
3	-1.56	1.19	21.42	-0.17	0.08	1.14	23.10	25.05	0.1
4	0.00	0.87	0.96	-0.08	0.00	0.00	0.96	24.23	24.2
5	0.01	0.90	0.98	-0.08	0.00	0.00	0.98	22.41	21.9
6	0.01	0.95	1.07	-0.08	0.00	0.00	1.07	22.22	19.8
7	0.01	0.97	1.20	-0.09	-0.01	0.00	1.19	23.90	19.0
8	0.01	0.63	1.60	-0.06	-0.08	-0.01	1.60	25.05	14.7
9	-0.08	0.52	2.12	-0.02	-0.21	0.01	2.23	25.05	10.2
10	-0.48	0.72	2.93	-0.14	-0.13	0.10	3.44	25.05	6.3
11	-0.68	1.22	1.89	-0.15	-0.19	-1.00	3.29	25.05	6.6
12	-0.52	0.63	2.65	-0.14	-0.12	0.08	3.21	25.05	6.8
13	1.08	1.80	-0.72	-0.31	0.12	-0.19	2.67	25.05	8.4
14	11.68	11.70	0.33	0.00	0.22	-0.05	11.38	25.05	1.2
15	-0.25	-0.25	-0.02	0.00	0.00	0.00	0.24	25.05	103.2
16	0.82	0.81	0.02	0.01	-0.01	0.00	0.80	25.05	30.2

1. See Figure 3.4.4.1-4 for definition of locations of stress sections.
2. ASME Code Service Level A is used for material allowable stresses.

Table 3.4.4.1-8 Summary of Maximum Canister Normal Handling, plus Normal Pressure, plus Secondary (P + Q) Stresses (ksi)

Section No. [1]	S_X	S_Y	S_Z	S_{XY}	S_{YZ}	S_{XZ}	Stress Intensity	Stress Allowable[2]	Margin of Safety
1	3.73	2.84	11.32	-0.02	-0.05	0.12	8.48	50.10	4.9
2	1.25	-6.84	-18.35	0.67	-0.11	-1.23	19.81	50.10	1.5
3	-1.82	2.83	25.12	-0.33	0.10	1.22	27.07	50.10	0.9
4	0.00	0.87	0.97	-0.08	-0.01	0.00	0.98	48.46	48.7
5	-0.01	0.88	1.01	0.08	-0.02	-0.01	1.03	44.83	42.7
6	0.00	0.55	1.14	-0.05	-0.02	0.01	1.14	44.44	38.0
7	0.01	0.98	1.21	-0.09	0.00	0.00	1.21	47.79	38.6
8	0.01	0.62	1.68	-0.06	-0.07	-0.01	1.67	50.10	29.0
9	1.12	1.23	3.64	-0.02	-0.07	1.29	3.61	50.10	12.9
10	-6.72	-1.69	1.79	-0.36	-0.15	-0.79	8.69	50.10	4.8
11	2.15	-2.10	-9.58	-0.31	-0.14	0.89	11.89	50.10	3.2
12	-6.72	-1.69	1.79	-0.36	-0.15	-0.79	8.69	50.10	4.8
13	-5.08	-0.78	1.71	0.34	-0.09	0.62	6.93	50.10	6.2
14	-13.21	-12.96	-0.16	0.20	-0.05	-0.02	13.16	50.10	2.8
15	-8.25	-7.78	-6.63	0.20	0.49	0.00	1.90	50.10	25.4
16	0.01	0.06	-0.52	0.02	-0.05	0.00	0.59	50.10	83.3

1. See Figure 3.4.4.1-4 for definition of locations of stress sections.
2. ASME Code Service Level A is used for material allowable stresses.

Table 3.4.4.1-9 Canister Normal Internal Pressure Primary Membrane (P_m) Stresses (ksi)

Section No. [1]	S_X	S_Y	S_Z	S_{XY}	S_{YZ}	S_{XZ}	Stress Intensity
1	0.12	0.70	1.80	-0.05	-0.01	-0.26	1.76
2	1.17	-1.69	-1.15	0.22	-0.02	-0.27	2.92
3	-0.20	-2.63	0.53	0.22	0.04	0.48	3.42
4	0.00	0.01	0.51	0.00	0.00	0.00	0.51
5	0.00	0.00	0.55	0.00	0.00	0.00	0.55
6	0.01	-0.01	0.62	0.00	-0.01	0.00	0.62
7	0.01	-0.01	0.73	0.00	-0.01	0.00	0.74
8	0.02	-0.03	1.11	0.00	-0.07	0.00	1.15
9	0.05	0.40	1.56	-0.03	-0.15	0.07	1.53
10	-0.29	0.36	1.93	-0.07	-0.21	0.09	2.26
11	-0.68	0.74	1.05	-0.11	-0.13	-0.58	2.10
12	-0.13	0.52	2.01	-0.10	-0.10	0.17	2.19
13	0.34	0.99	-0.40	-0.16	-0.03	-0.61	1.79
14	0.29	0.29	-0.01	0.00	0.14	-0.02	0.41
15	-0.01	-0.01	-0.03	0.00	0.00	0.00	0.02
16	0.00	0.01	-0.05	0.00	-0.01	-0.01	0.06

1. See Figure 3.4.4.1-4 for definition of locations of stress sections.

Table 3.4.4.1-10 Canister Normal Internal Pressure Primary Membrane plus Bending ($P_m + P_b$) Stresses (ksi)

Section No. [1]	S_X	S_Y	S_Z	S_{XY}	S_{YZ}	S_{XZ}	Stress Intensity
1	1.32	-0.05	4.36	0.07	-0.02	-0.02	4.42
2	0.57	-3.98	-8.37	0.38	-0.04	-0.60	9.05
3	-0.85	0.53	11.91	-0.08	0.04	0.62	12.82
4	0.00	-0.05	0.50	-0.01	0.00	0.00	0.56
5	0.00	-0.14	0.51	0.01	-0.01	0.00	0.65
6	0.01	-0.19	0.56	0.02	-0.01	0.00	0.75
7	0.01	-0.21	0.66	0.02	-0.01	0.00	0.88
8	0.03	-0.16	1.06	0.01	-0.05	0.00	1.23
9	-0.09	0.34	1.69	0.00	-0.21	-0.02	1.81
10	-0.46	0.64	2.87	-0.13	-0.13	0.20	3.38
11	-1.00	0.69	1.11	-0.12	-0.20	-1.02	2.98
12	-0.50	0.57	2.66	0.00	0.00	0.18	3.19
13	1.55	1.54	-0.83	-0.25	0.07	-0.25	2.67
14	6.60	6.61	0.18	0.00	0.13	-0.03	6.43
15	0.10	0.11	-0.06	0.00	0.01	0.00	0.17
16	0.25	0.27	-0.06	-0.02	-0.01	0.00	0.34

1. See Figure 3.4.4.1-4 for definition of locations of stress sections.

Table 3.4.4.1-11 Listing of Sections for Stress Evaluation of PWR Support Disk

Section Number[1]	Point 1	Point 2	Point 1		Point 2	
			X	Y	X	Y
1	1	2	0.75	0.75	0.75	-0.75
2	3	4	0.75	0.75	-0.75	0.75
3	5	6	-0.75	0.75	-0.75	-0.75
4	7	8	-0.75	-0.75	0.75	-0.75
5	9	10	0.75	5.39	-0.75	5.39
6	11	12	0.75	10.02	-0.75	10.02
7	13	14	0.75	10.02	0.75	11.02
8	15	16	0.75	11.02	-0.75	11.02
9	17	18	-0.75	10.02	-0.75	11.02
10	19	20	0.75	15.66	-0.75	15.66
11	21	22	0.75	20.29	-0.75	20.29
12	23	24	0.75	20.29	0.75	21.17
13	25	26	0.75	21.17	-0.75	21.17
14	27	28	-0.75	20.29	-0.75	21.17
15	29	30	0.75	25.81	-0.75	25.81
16	31	32	0.75	30.44	-0.75	30.44
17	33	34	0.75	30.44	0.75	32.74
18	35	36	-0.75	30.44	-0.75	32.74
19	37	38	0.75	-5.39	-0.75	-5.39
20	39	40	0.75	-10.02	-0.75	-10.02
21	41	42	0.75	-10.02	0.75	-11.02
22	43	44	0.75	-11.02	-0.75	-11.02
23	45	46	-0.75	-10.02	-0.75	-11.02
24	47	48	0.75	-15.66	-0.75	-15.66
25	49	50	0.75	-20.29	-0.75	-20.29
26	51	52	0.75	-20.29	0.75	-21.17
27	53	54	0.75	-21.17	-0.75	-21.17
28	55	56	-0.75	-20.29	-0.75	-21.17
29	57	58	0.75	-25.81	-0.75	-25.81
30	59	60	0.75	-30.44	-0.75	-30.44
31	61	62	0.75	-30.44	0.75	-32.74
32	63	64	-0.75	-30.44	-0.75	-32.74
33	65	66	5.39	0.75	5.39	-0.75
34	67	68	10.02	0.75	10.02	-0.75
35	69	70	10.02	0.75	11.02	0.75
36	71	72	11.02	0.75	11.02	-0.75
37	73	74	10.02	-0.75	11.02	-0.75
38	75	76	15.66	0.75	15.66	-0.75
39	77	78	20.29	0.75	20.29	-0.75
40	79	80	20.29	0.75	21.17	0.75
41	81	82	21.17	0.75	21.17	-0.75
42	83	84	20.29	-0.75	21.17	-0.75
43	85	86	25.81	0.75	25.81	-0.75
44	87	88	30.44	0.75	30.44	-0.75
45	89	90	30.44	0.75	32.74	0.75

1. Section locations are shown in Figures 3.4.4.1-7 and 3.4.4.1-8.

Table 3.4.4.1-11 Listing of Sections for Stress Evaluation of PWR Support Disk (Continued)

Section Number[1]	Point 1	Point 2	Point 1		Point 2	
			X	Y	X	Y
46	91	92	30.44	-0.75	32.74	-0.75
47	93	94	-5.39	0.75	-5.39	-0.75
48	95	96	-10.02	0.75	-10.02	-0.75
49	97	98	-10.02	0.75	-11.02	0.75
50	99	100	-11.02	0.75	-11.02	-0.75
51	101	102	-10.02	-0.75	-11.02	-0.75
52	103	104	-15.66	0.75	-15.66	-0.75
53	105	106	-20.29	0.75	-20.29	-0.75
54	107	108	-20.29	0.75	-21.17	0.75
55	109	110	-21.17	0.75	-21.17	-0.75
56	111	112	-20.29	-0.75	-21.17	-0.75
57	113	114	-25.81	0.75	-25.81	-0.75
58	115	116	-30.44	0.75	-30.44	-0.75
59	117	118	-30.44	0.75	-32.74	0.75
60	119	120	-30.44	-0.75	-32.74	-0.75
61	121	122	5.39	11.02	5.39	10.02
62	123	124	5.39	20.29	5.39	21.17
63	125	126	10.02	11.02	10.02	10.02
64	127	128	10.02	10.02	11.02	10.02
65	129	130	10.02	11.52	11.52	11.52
66	131	132	10.02	20.29	10.02	21.17
67	133	134	10.02	20.29	11.52	20.29
68	135	136	10.02	5.39	11.02	5.39
69	137	138	11.52	10.02	11.52	11.52
70	139	140	16.16	10.02	16.16	11.52
71	141	142	20.29	5.39	21.17	5.39
72	143	144	20.29	10.02	21.17	10.02
73	145	146	10.02	16.16	11.52	16.16
74	147	148	20.29	10.02	20.29	11.52
75	149	150	10.24	31.11	10.02	30.44
76	151	152	31.11	10.24	30.44	10.02
77	153	154	-5.39	11.02	-5.39	10.02
78	155	156	-5.39	20.29	-5.39	21.17
79	157	158	-10.02	11.02	-10.02	10.02
80	159	160	-10.02	10.02	-11.02	10.02
81	161	162	-10.02	11.52	-11.52	11.52
82	163	164	-10.02	20.29	-10.02	21.17
83	165	166	-10.02	20.29	-11.52	20.29
84	167	168	-10.02	5.39	-11.02	5.39
85	169	170	-11.52	10.02	-11.52	11.52
86	171	172	-16.16	10.02	-16.16	11.52
87	173	174	-20.29	5.39	-21.17	5.39
88	175	176	-20.29	10.02	-21.17	10.02
89	177	178	-10.02	16.16	-11.52	16.16
90	179	180	-20.29	10.02	-20.29	11.52

1. Section locations are shown in Figures 3.4.4.1-7 and 3.4.4.1-8.

Table 3.4.4.1-11 Listing of Sections for Stress Evaluation of PWR Support Disk (Continued)

Section Number[1]	Point 1	Point 2	Point 1		Point 2	
			X	Y	X	Y
91	181	182	-10.24	31.11	-10.02	30.44
92	183	184	-31.11	10.24	-30.44	10.02
93	185	186	-5.39	-11.02	-5.39	-10.02
94	187	188	-5.39	-20.29	-5.39	-21.17
95	189	190	-10.02	-11.02	-10.02	-10.02
96	191	192	-10.02	-10.02	-11.02	-10.02
97	193	194	-10.02	-11.52	-11.52	-11.52
98	195	196	-10.02	-20.29	-10.02	-21.17
99	197	198	-10.02	-20.29	-11.52	-20.29
100	199	200	-10.02	-5.39	-11.02	-5.39
101	201	202	-11.52	-10.02	-11.52	-11.52
102	203	204	-16.16	-10.02	-16.16	-11.52
103	205	206	-20.29	-5.39	-21.17	-5.39
104	207	208	-20.29	-10.02	-21.17	-10.02
105	209	210	-10.02	-16.16	-11.52	-16.16
106	211	212	-20.29	-10.02	-20.29	-11.52
107	213	214	-10.24	-31.11	-10.02	-30.44
108	215	216	-31.11	-10.24	-30.44	-10.02
109	217	218	5.39	-11.02	5.39	-10.02
110	219	220	5.39	-20.29	5.39	-21.17
111	221	222	10.02	-11.02	10.02	-10.02
112	223	224	10.02	-10.02	11.02	-10.02
113	225	226	10.02	-11.52	11.52	-11.52
114	227	228	10.02	-20.29	10.02	-21.17
115	229	230	10.02	-20.29	11.52	-20.29
116	231	232	10.02	-5.39	11.02	-5.39
117	233	234	11.52	-10.02	11.52	-11.52
118	235	236	16.16	-10.02	16.16	-11.52
119	237	238	20.29	-5.39	21.17	-5.39
120	239	240	20.29	-10.02	21.17	-10.02
121	241	242	10.02	-16.16	11.52	-16.16
122	243	244	20.29	-10.02	20.29	-11.52
123	245	246	10.24	-31.11	10.02	-30.44
124	247	248	31.11	-10.24	30.44	-10.02

1. Section locations are shown in Figures 3.4.4.1-7 and 3.4.4.1-8.

Table 3.4.4.1-12 $P_m + P_b$ Stresses for PWR Support Disk - Normal Conditions (ksi)

Section[1]	Sx	Sy	Sxy	Stress Intensity	Allow. Stress[2]	Margin of Safety
66	0.7	0.3	0.3	0.8	52.7	64.8
72	0.3	0.7	0.3	0.8	52.7	64.8
120	0.3	0.7	-0.3	0.8	52.7	64.8
82	0.7	0.3	-0.3	0.8	52.7	64.8
12	-0.4	0.2	0.0	0.6	52.7	86.8
28	-0.4	0.2	0.0	0.6	52.7	86.8
26	-0.4	0.2	0.0	0.6	52.7	86.8
54	0.2	-0.4	0.0	0.6	52.7	86.8
14	-0.4	0.2	0.0	0.6	52.7	86.8
42	0.2	-0.4	0.0	0.6	52.7	86.8
40	0.2	-0.4	0.0	0.6	52.7	86.8
56	0.2	-0.4	0.0	0.6	52.7	86.8
90	0.4	0.1	-0.2	0.5	52.7	104.3
67	0.1	0.4	0.2	0.5	52.7	104.3
99	0.1	0.4	0.2	0.5	52.7	104.3
106	0.4	0.1	0.2	0.5	52.7	104.3
122	0.4	0.1	-0.2	0.5	52.7	104.3
74	0.4	0.1	0.2	0.5	52.7	104.3
83	0.1	0.4	-0.2	0.5	52.7	104.3
115	0.1	0.4	-0.2	0.5	52.7	104.3
88	0.2	0.2	-0.3	0.5	52.7	104.3
114	0.2	0.2	-0.3	0.5	52.7	104.3
104	0.2	0.2	0.2	0.5	52.7	104.3
98	0.2	0.2	0.2	0.5	52.7	104.3
4	-0.2	-0.4	-0.1	0.4	52.7	130.6
2	-0.2	-0.4	-0.1	0.4	52.7	130.6
3	-0.4	-0.2	-0.1	0.4	52.7	130.6
1	-0.4	-0.2	-0.1	0.4	52.7	130.6
37	-0.1	-0.4	0.1	0.4	52.7	130.6
35	-0.1	-0.4	-0.1	0.4	52.7	130.6
7	-0.4	-0.1	-0.1	0.4	52.7	130.6
49	-0.1	-0.4	0.1	0.4	52.7	130.6
51	-0.1	-0.4	-0.1	0.4	52.7	130.6
23	-0.4	-0.1	-0.1	0.4	52.7	130.6
21	-0.4	-0.1	0.1	0.4	52.7	130.6
9	-0.4	-0.1	0.1	0.4	52.7	130.6
11	-0.2	0.2	-0.1	0.4	52.7	130.6
25	-0.2	0.2	-0.1	0.4	52.7	130.6
53	0.2	-0.2	0.1	0.4	52.7	130.6
39	0.2	-0.2	0.1	0.4	52.7	130.6

1. Section locations are shown in Figures 3.4.4.1-7 and 3.4.4.1-8.
2. Stress allowables are taken at 800°F.

Table 3.4.4.1-13 $P_m + P_b + Q$ Stresses for the PWR Support Disk - Normal Conditions (ksi)

Section[1]	Sx	Sy	Sxy	Stress Intensity	Allow. Stress[2]	Margin of Safety
44	-6.9	-29.3	6.1	30.8	105.3	2.42
58	-6.9	-29.3	6.1	30.8	105.3	2.42
75	23.5	2.2	-4.3	24.3	105.3	3.33
107	23.5	2.2	-4.2	24.3	105.3	3.33
108	2.1	23.3	-4.2	24.1	105.3	3.37
76	2.1	23.2	-4.1	24.0	105.3	3.39
123	20.6	2.0	5.4	22.1	105.3	3.76
124	1.9	20.6	5.4	22.1	105.3	3.76
92	1.8	20.6	5.3	22.0	105.3	3.79
91	20.5	1.9	5.4	22.0	105.3	3.79
7	-20.1	-6.7	-2.3	20.5	105.3	4.14
23	-20.1	-6.7	-2.3	20.5	105.3	4.14
49	-6.6	-20.0	2.3	20.4	105.3	4.16
37	-6.6	-20.0	2.3	20.4	105.3	4.16
9	-20.0	-6.7	2.3	20.4	105.3	4.16
21	-20.0	-6.7	2.3	20.4	105.3	4.16
35	-6.7	-20.0	-2.3	20.4	105.3	4.16
51	-6.7	-20.0	-2.3	20.4	105.3	4.16
17	20.6	-0.4	-1.2	21.1	105.3	3.99
32	20.6	-0.4	-1.2	21.1	105.3	3.99
45	-0.5	19.9	-1.4	20.7	105.3	4.09
60	-0.5	19.9	-1.4	20.7	105.3	4.09
80	-7.7	-19.5	2.4	19.9	105.3	4.29
112	-7.7	-19.5	2.4	19.9	105.3	4.29
31	19.6	-0.4	1.6	20.3	105.3	4.19
18	19.6	-0.4	1.6	20.3	105.3	4.19
79	-19.4	-7.6	2.3	19.9	105.3	4.29
111	-19.4	-7.6	2.3	19.9	105.3	4.29
95	-19.0	-7.7	-2.2	19.4	105.3	4.43
63	-19.0	-7.7	-2.2	19.4	105.3	4.43
96	-7.7	-18.8	-2.2	19.3	105.3	4.46
64	-7.7	-18.8	-2.2	19.3	105.3	4.46
59	-2.0	16.6	0.4	18.6	105.3	4.66
46	-2.0	16.6	0.4	18.6	105.3	4.66
30	-10.5	-11.3	4.5	15.3	105.3	5.88
16	-10.5	-11.3	4.5	15.3	105.3	5.88
6	-11.1	-9.3	-4.1	14.4	105.3	6.31
20	-11.1	-9.3	-4.1	14.4	105.3	6.31
48	-9.3	-11.0	-4.1	14.3	105.3	6.36
34	-9.3	-11.0	-4.1	14.3	105.3	6.36

1. Section locations are shown in Figures 3.4.4.1-7 and 3.4.4.1-8.
2. Stress allowables are taken at 800°F.

Table 3.4.4.1-14 Listing of Sections for Stress Evaluation of BWR Support Disk

Section Number[1]	Point 1	Point 2	Point 1		Point 2	
			X	Y	X	Y
1	1	2	32.74	0.33	30.85	0.33
2	3	4	32.74	-0.33	30.85	-0.33
3	5	6	-32.74	0.33	-30.85	0.33
4	7	8	-32.74	-0.33	-30.85	-0.33
5	9	10	32.03	6.85	30.85	6.6
6	11	12	32.03	-6.85	30.85	-6.6
7	13	14	-32.03	6.85	-30.85	6.6
8	15	16	-32.03	-6.85	-30.85	-6.6
9	17	18	24.87	21.30	23.89	20.46
10	19	20	24.87	-21.30	23.89	-20.46
11	21	22	-24.87	21.30	-23.89	20.46
12	23	24	-24.87	-21.30	-23.89	-20.46
13	25	26	17.27	27.83	17.00	27.39
14	27	28	-17.27	27.83	-17.00	27.39
15	29	30	-17.27	-27.83	-17.00	-27.39
16	31	32	17.27	-27.83	17.00	-27.39
17	33	34	0	0.33	0	-0.33
18	35	36	3.14	0.33	3.14	-0.33
19	37	38	3.79	0.33	3.79	-0.33
20	39	40	6.93	0.33	6.93	-0.33
21	41	42	10.07	0.33	10.07	-0.33
22	43	44	10.72	0.33	10.72	-0.33
23	45	46	13.86	0.33	13.86	-0.33
24	47	48	17	0.33	17	-0.33
25	49	50	17.65	0.33	17.65	-0.33
26	51	52	20.78	0.33	20.78	-0.33
27	53	54	23.92	0.33	23.92	-0.33
28	55	56	24.57	0.33	24.57	-0.33
29	57	58	27.71	0.33	27.71	-0.33
30	59	60	30.85	0.33	30.85	-0.33
31	61	62	-3.14	0.33	-3.14	-0.33
32	63	64	-3.79	0.33	-3.79	-0.33
33	65	66	-6.93	0.33	-6.93	-0.33
34	67	68	-10.07	0.33	-10.07	-0.33
35	69	70	-10.72	0.33	-10.72	-0.33
36	71	72	-13.86	0.33	-13.86	-0.33
37	73	74	-17	0.33	-17	-0.33
38	75	76	-17.65	0.33	-17.65	-0.33
39	77	78	-20.78	0.33	-20.78	-0.33
40	79	80	-23.92	0.33	-23.92	-0.33
41	81	82	-24.57	0.33	-24.57	-0.33
42	83	84	-27.71	0.33	-27.71	-0.33
43	85	86	-30.85	0.33	-30.85	-0.33
44	87	88	0	7.25	0	6.6
45	89	90	3.14	7.25	3.14	6.6
46	91	92	3.79	7.25	3.79	6.6
47	93	94	6.93	7.25	6.93	6.6
48	95	96	10.07	7.25	10.07	6.6
49	97	98	10.72	7.25	10.72	6.6
50	99	100	13.86	7.25	13.86	6.6

1. Section locations are shown in Figures 3.4.4.1-13 through 3.4.4.1-16.

Table 3.4.4.1-14 Listing of Sections for Stress Evaluation of BWR Support Disk (Continued)

Section Number[1]	Point 1	Point 2	Point 1		Point 2	
			X	Y	X	Y
51	101	102	17	7.25	17	6.6
52	103	104	17.65	7.25	17.65	6.6
53	105	106	20.78	7.25	20.78	6.6
54	107	108	23.92	7.25	23.92	6.6
55	109	110	0	13.53	0	14.18
56	111	112	3.14	13.53	3.14	14.18
57	113	114	3.79	13.53	3.79	14.18
58	115	116	6.93	13.53	6.93	14.18
59	117	118	10.07	13.53	10.07	14.18
60	119	120	10.72	13.53	10.72	14.18
61	121	122	13.86	13.53	13.86	14.18
62	123	124	17	13.53	17	14.18
63	125	126	17.65	13.53	17.65	14.18
64	127	128	20.78	13.53	20.78	14.18
65	129	130	23.92	13.53	23.92	14.18
66	131	132	0	21.11	0	20.46
67	133	134	3.14	21.11	3.14	20.46
68	135	136	3.79	21.11	3.79	20.46
69	137	138	6.93	21.11	6.93	20.46
70	139	140	10.07	21.11	10.07	20.46
71	141	142	10.72	21.11	10.72	20.46
72	143	144	13.86	21.11	13.86	20.46
73	145	146	17	21.11	17	20.46
74	147	148	3.14	0.33	3.79	0.33
75	149	150	10.07	0.33	10.72	0.33
76	151	152	17	0.33	17.65	0.33
77	153	154	23.92	0.33	24.57	0.33
78	155	156	3.14	3.46	3.79	3.46
79	157	158	10.07	3.46	10.72	3.46
80	159	160	17	3.46	17.65	3.46
81	161	162	23.92	3.46	24.57	3.46
82	163	164	3.14	6.6	3.79	6.6
83	165	166	10.07	6.6	10.72	6.6
84	167	168	17	6.6	17.65	6.6
85	169	170	23.92	6.6	24.57	6.6
86	171	172	3.14	7.25	3.79	7.25
87	173	174	10.07	7.25	10.72	7.25
88	175	176	17	7.25	17.65	7.25
89	177	178	3.14	10.39	3.79	10.39
90	179	180	10.07	10.39	10.72	10.39
91	181	182	17	10.39	17.65	10.39
92	183	184	3.14	13.53	3.79	13.53
93	185	186	10.07	13.53	10.72	13.53
94	187	188	17	13.53	17.65	13.53
95	189	190	3.14	14.18	3.79	14.18
96	191	192	10.07	14.18	10.72	14.18
97	193	194	17	14.18	17.65	14.18
98	195	196	3.14	17.32	3.79	17.32
99	197	198	10.07	17.32	10.72	17.32
100	199	200	17	17.32	17.65	17.32

1. Section locations are shown in Figures 3.4.4.1-13 through 3.4.4.1-16.

Table 3.4.4.1-14 Listing of Sections for Stress Evaluation of BWR Support Disk (Continued)

Section Number[1]	Point 1	Point 2	Point 1		Point 2	
			X	Y	X	Y
101	201	202	3.14	20.46	3.79	20.46
102	203	204	10.07	20.46	10.72	20.46
103	205	206	17	20.46	17.65	20.46
104	207	208	3.14	21.11	3.79	21.11
105	209	210	10.07	21.11	10.72	21.11
106	211	212	3.14	24.25	3.79	24.25
107	213	214	10.07	24.25	10.72	24.25
108	215	216	3.14	27.39	3.79	27.39
109	217	218	10.07	27.39	10.72	27.39
110	219	220	-3.14	7.25	-3.14	6.6
111	221	222	-3.79	7.25	-3.79	6.6
112	223	224	-6.93	7.25	-6.93	6.6
113	225	226	-10.07	7.25	-10.07	6.6
114	227	228	-10.72	7.25	-10.72	6.6
115	229	230	-13.86	7.25	-13.86	6.6
116	231	232	-17	7.25	-17	6.6
117	233	234	-17.65	7.25	-17.65	6.6
118	235	236	-20.78	7.25	-20.78	6.6
119	237	238	-23.92	7.25	-23.92	6.6
120	239	240	-3.14	13.53	-3.14	14.18
121	241	242	-3.79	13.53	-3.79	14.18
122	243	244	-6.93	13.53	-6.93	14.18
123	245	246	-10.07	13.53	-10.07	14.18
124	247	248	-10.72	13.53	-10.72	14.18
125	249	250	-13.86	13.53	-13.86	14.18
126	251	252	-17	13.53	-17	14.18
127	253	254	-17.65	13.53	-17.65	14.18
128	255	256	-20.78	13.53	-20.78	14.18
129	257	258	-23.92	13.53	-23.92	14.18
130	259	260	-3.14	21.11	-3.14	20.46
131	261	262	-3.79	21.11	-3.79	20.46
132	263	264	-6.93	21.11	-6.93	20.46
133	265	266	-10.07	21.11	-10.07	20.46
134	267	268	-10.72	21.11	-10.72	20.46
135	269	270	-13.86	21.11	-13.86	20.46
136	271	272	-17	21.11	-17	20.46
137	273	274	-3.14	0.33	-3.79	0.33
138	275	276	-10.07	0.33	-10.72	0.33
139	277	278	-17	0.33	-17.65	0.33
140	279	280	-23.92	0.33	-24.57	0.33
141	281	282	-3.14	3.46	-3.79	3.46
142	283	284	-10.07	3.46	-10.72	3.46
143	285	286	-17	3.46	-17.65	3.46
144	287	288	-23.92	3.46	-24.57	3.46
145	289	290	-3.14	6.6	-3.79	6.6
146	291	292	-10.07	6.6	-10.72	6.6
147	293	294	-17	6.6	-17.65	6.6
148	295	296	-23.92	6.6	-24.57	6.6
149	297	298	-3.14	7.25	-3.79	7.25
150	299	300	-10.07	7.25	-10.72	7.25

1. Section locations are shown in Figures 3.4.4.1-13 through 3.4.4.1-16.

Table 3.4.4.1-14 Listing of Sections for Stress Evaluation of BWR Support Disk (Continued)

Section Number[1]	Point 1	Point 2	Point 1		Point 2	
			X	Y	X	Y
151	301	302	-17	7.25	-17.65	7.25
152	303	304	-3.14	10.39	-3.79	10.39
153	305	306	-10.07	10.39	-10.72	10.39
154	307	308	-17	10.39	-17.65	10.39
155	309	310	-3.14	13.53	-3.79	13.53
156	311	312	-10.07	13.53	-10.72	13.53
157	313	314	-17	13.53	-17.65	13.53
158	315	316	-3.14	14.18	-3.79	14.18
159	317	318	-10.07	14.18	-10.72	14.18
160	319	320	-17	14.18	-17.65	14.18
161	321	322	-3.14	17.32	-3.79	17.32
162	323	324	-10.07	17.32	-10.72	17.32
163	325	326	-17	17.32	-17.65	17.32
164	327	328	-3.14	20.46	-3.79	20.46
165	329	330	-10.07	20.46	-10.72	20.46
166	331	332	-17	20.46	-17.65	20.46
167	333	334	-3.14	21.11	-3.79	21.11
168	335	336	-10.07	21.11	-10.72	21.11
169	337	338	-3.14	24.25	-3.79	24.25
170	339	340	-10.07	24.25	-10.72	24.25
171	341	342	-3.14	27.39	-3.79	27.39
172	343	344	-10.07	27.39	-10.72	27.39
173	345	346	-3.14	-7.25	-3.14	-6.6
174	347	348	-3.79	-7.25	-3.79	-6.6
175	349	350	-6.93	-7.25	-6.93	-6.6
176	351	352	-10.07	-7.25	-10.07	-6.6
177	353	354	-10.72	-7.25	-10.72	-6.6
178	355	356	-13.86	-7.25	-13.86	-6.6
179	357	358	-17	-7.25	-17	-6.6
180	359	360	-17.65	-7.25	-17.65	-6.6
181	361	362	-20.78	-7.25	-20.78	-6.6
182	363	364	-23.92	-7.25	-23.92	-6.6
183	365	366	-3.14	-13.53	-3.14	-14.18
184	367	368	-3.79	-13.53	-3.79	-14.18
185	369	370	-6.93	-13.53	-6.93	-14.18
186	371	372	-10.07	-13.53	-10.07	-14.18
187	373	374	-10.72	-13.53	-10.72	-14.18
188	375	376	-13.86	-13.53	-13.86	-14.18
189	377	378	-17	-13.53	-17	-14.18
190	379	380	-17.65	-13.53	-17.65	-14.18
191	381	382	-20.78	-13.53	-20.78	-14.18
192	383	384	-23.92	-13.53	-23.92	-14.18
193	385	386	-3.14	-21.11	-3.14	-20.46
194	387	388	-3.79	-21.11	-3.79	-20.46
195	389	390	-6.93	-21.11	-6.93	-20.46
196	391	392	-10.07	-21.11	-10.07	-20.46
197	393	394	-10.72	-21.11	-10.72	-20.46
198	395	396	-13.86	-21.11	-13.86	-20.46
199	397	398	-17	-21.11	-17	-20.46
200	399	400	-3.14	-0.33	-3.79	-0.33

1. Section locations are shown in Figures 3.4.4.1-13 through 3.4.4.1-16.

Table 3.4.4.1-14 Listing of Sections for Stress Evaluation of BWR Support Disk (Continued)

Section Number[1]	Point 1	Point 2	Point 1		Point 2	
			X	Y	X	Y
201	401	402	-10.07	-0.33	-10.72	-0.33
202	403	404	-17	-0.33	-17.65	-0.33
203	405	406	-23.92	-0.33	-24.57	-0.33
204	407	408	-3.14	-3.46	-3.79	-3.46
205	409	410	-10.07	-3.46	-10.72	-3.46
206	411	412	-17	-3.46	-17.65	-3.46
207	413	414	-23.92	-3.46	-24.57	-3.46
208	415	416	-3.14	-6.6	-3.79	-6.6
209	417	418	-10.07	-6.6	-10.72	-6.6
210	419	420	-17	-6.6	-17.65	-6.6
211	421	422	-23.92	-6.6	-24.57	-6.6
212	423	424	-3.14	-7.25	-3.79	-7.25
213	425	426	-10.07	-7.25	-10.72	-7.25
214	427	428	-17	-7.25	-17.65	-7.25
215	429	430	-3.14	-10.39	-3.79	-10.39
216	431	432	-10.07	-10.39	-10.72	-10.39
217	433	434	-17	-10.39	-17.65	-10.39
218	435	436	-3.14	-13.53	-3.79	-13.53
219	437	438	-10.07	-13.53	-10.72	-13.53
220	439	440	-17	-13.53	-17.65	-13.53
221	441	442	-3.14	-14.18	-3.79	-14.18
222	443	444	-10.07	-14.18	-10.72	-14.18
223	445	446	-17	-14.18	-17.65	-14.18
224	447	448	-3.14	-17.32	-3.79	-17.32
225	449	450	-10.07	-17.32	-10.72	-17.32
226	451	452	-17	-17.32	-17.65	-17.32
227	453	454	-3.14	-20.46	-3.79	-20.46
228	455	456	-10.07	-20.46	-10.72	-20.46
229	457	458	-17	-20.46	-17.65	-20.46
230	459	460	-3.14	-21.11	-3.79	-21.11
231	461	462	-10.07	-21.11	-10.72	-21.11
232	463	464	-3.14	-24.25	-3.79	-24.25
233	465	466	-10.07	-24.25	-10.72	-24.25
234	467	468	-3.14	-27.39	-3.79	-27.39
235	469	470	-10.07	-27.39	-10.72	-27.39
236	471	472	0	-7.25	0	-6.6
237	473	474	3.14	-7.25	3.14	-6.6
238	475	476	3.79	-7.25	3.79	-6.6
239	477	478	6.93	-7.25	6.93	-6.6
240	479	480	10.07	-7.25	10.07	-6.6
241	481	482	10.72	-7.25	10.72	-6.6
242	483	484	13.86	-7.25	13.86	-6.6
243	485	486	17	-7.25	17	-6.6
244	487	488	17.65	-7.25	17.65	-6.6
245	489	490	20.78	-7.25	20.78	-6.6
246	491	492	23.92	-7.25	23.92	-6.6
247	493	494	0	-13.53	0	-14.18
248	495	496	3.14	-13.53	3.14	-14.18
249	497	498	3.79	-13.53	3.79	-14.18
250	499	500	6.93	-13.53	6.93	-14.18

1. Section locations are shown in Figures 3.4.4.1-13 through 3.4.4.1-16.

Table 3.4.4.1-14 Listing of Sections for Stress Evaluation of BWR Support Disk (Continued)

Section Number[1]	Point 1	Point 2	Point 1		Point 2	
			X	Y	X	Y
251	501	502	10.07	-13.53	10.07	-14.18
252	503	504	10.72	-13.53	10.72	-14.18
253	505	506	13.86	-13.53	13.86	-14.18
254	507	508	17	-13.53	17	-14.18
255	509	510	17.65	-13.53	17.65	-14.18
256	511	512	20.78	-13.53	20.78	-14.18
257	513	514	23.92	-13.53	23.92	-14.18
258	515	516	0	-21.11	0	-20.46
259	517	518	3.14	-21.11	3.14	-20.46
260	519	520	3.79	-21.11	3.79	-20.46
261	521	522	6.93	-21.11	6.93	-20.46
262	523	524	10.07	-21.11	10.07	-20.46
263	525	526	10.72	-21.11	10.72	-20.46
264	527	528	13.86	-21.11	13.86	-20.46
265	529	530	17	-21.11	17	-20.46
266	531	532	3.14	-0.33	3.79	-0.33
267	533	534	10.07	-0.33	10.72	-0.33
268	535	536	17	-0.33	17.65	-0.33
269	537	538	23.92	-0.33	24.57	-0.33
270	539	540	3.14	-3.46	3.79	-3.46
271	541	542	10.07	-3.46	10.72	-3.46
272	543	544	17	-3.46	17.65	-3.46
273	545	546	23.92	-3.46	24.57	-3.46
274	547	548	3.14	-6.6	3.79	-6.6
275	549	550	10.07	-6.6	10.72	-6.6
276	551	552	17	-6.6	17.65	-6.6
277	553	554	23.92	-6.6	24.57	-6.6
278	555	556	3.14	-7.25	3.79	-7.25
279	557	558	10.07	-7.25	10.72	-7.25
280	559	560	17	-7.25	17.65	-7.25
281	561	562	3.14	-10.39	3.79	-10.39
282	563	564	10.07	-10.39	10.72	-10.39
283	565	566	17	-10.39	17.65	-10.39
284	567	568	3.14	-13.53	3.79	-13.53
285	569	570	10.07	-13.53	10.72	-13.53
286	571	572	17	-13.53	17.65	-13.53
287	573	574	3.14	-14.18	3.79	-14.18
288	575	576	10.07	-14.18	10.72	-14.18
289	577	578	17	-14.18	17.65	-14.18
290	579	580	3.14	-17.32	3.79	-17.32
291	581	582	10.07	-17.32	10.72	-17.32
292	583	584	17	-17.32	17.65	-17.32
293	585	586	3.14	-20.46	3.79	-20.46
294	587	588	10.07	-20.46	10.72	-20.46
295	589	590	17	-20.46	17.65	-20.46
296	591	592	3.14	-21.11	3.79	-21.11
297	593	594	10.07	-21.11	10.72	-21.11
298	595	596	3.14	-24.25	3.79	-24.25
299	597	598	10.07	-24.25	10.72	-24.25
300	599	600	3.14	-27.39	3.79	-27.39
301	601	602	10.07	-27.39	10.72	-27.39

1. Section locations are shown in Figures 3.4.4.1-13 through 3.4.4.1-16.

Table 3.4.4.1-15 $P_m + P_b$ Stresses for BWR Support Disk - Normal Conditions (ksi)

Section[1]	Sx	Sy	Sxy	Stress Intensity	Allow. Stress[2]	Margin of Safety
129	1.0	0.3	0.2	1.0	40.5	39.5
54	1.0	0.2	0.2	1.0	40.5	39.5
171	0.2	1.0	0.1	1.0	40.5	39.5
300	0.2	1.0	0.1	1.0	40.5	39.5
65	0.9	0.3	-0.2	1.0	40.5	39.5
192	0.9	0.3	-0.2	1.0	40.5	39.5
257	0.8	0.4	-0.3	1.0	40.5	39.5
234	0.2	0.9	-0.1	1.0	40.5	39.5
108	0.2	0.9	-0.1	1.0	40.5	39.5
119	0.9	0.2	-0.2	1.0	40.5	39.5
246	0.9	0.2	-0.2	0.9	40.5	44.0
182	0.9	0.2	0.2	0.9	40.5	44.0
103	0.3	0.3	0.2	0.5	40.5	80.0
229	0.2	0.3	0.2	0.5	40.5	80.0
109	-0.1	0.4	0.0	0.5	40.5	80.0
77	0.2	-0.3	0.1	0.5	40.5	80.0
203	0.2	-0.3	0.1	0.5	40.5	80.0
140	0.2	-0.3	-0.1	0.5	40.5	80.0
295	0.2	0.3	-0.2	0.5	40.5	80.0
269	0.2	-0.3	-0.1	0.5	40.5	80.0
166	0.2	0.3	-0.2	0.5	40.5	80.0
301	-0.1	0.4	0.0	0.5	40.5	80.0
172	-0.1	0.4	0.0	0.5	40.5	80.0
134	0.0	0.2	-0.2	0.5	40.5	80.0
263	0.0	0.2	-0.2	0.5	40.5	80.0
197	0.0	0.2	0.2	0.5	40.5	80.0
71	0.0	0.2	0.2	0.5	40.5	80.0
235	-0.1	0.4	0.0	0.5	40.5	80.0
27	0.3	-0.2	-0.1	0.5	40.5	80.0
165	-0.2	-0.1	-0.2	0.5	40.5	80.0
228	-0.2	-0.1	0.2	0.5	40.5	80.0
294	-0.2	-0.1	-0.2	0.5	40.5	80.0
40	0.3	-0.2	0.1	0.5	40.5	80.0
102	-0.2	-0.1	0.2	0.5	40.5	80.0
73	0.1	0.3	0.2	0.5	40.5	80.0
199	0.1	0.3	0.2	0.5	40.5	80.0
124	-0.4	-0.1	-0.2	0.4	40.5	100.3
252	-0.4	-0.1	-0.2	0.4	40.5	100.3
60	-0.4	-0.1	0.2	0.4	40.5	100.3
187	-0.4	-0.1	0.2	0.4	40.5	100.3

1. Section locations are shown in Figures 3.4.4.1-13 through 3.4.4.1-16.
2. Stress allowables are taken at 800°F.

Table 3.4.4.1-16 $P_m + P_b + Q$ Stresses for BWR Support Disk - Normal Conditions (ksi)

Section[1]	Sx	Sy	Sxy	Stress Intensity	Allow. Stress[2]	Margin of Safety
30	-8.8	-16.9	2.7	17.7	81.0	3.58
15	14.2	5.0	-6.4	17.4	81.0	3.66
43	-9.0	-16.6	2.7	17.4	81.0	3.66
13	14.0	5.1	-6.4	17.4	81.0	3.66
16	15.1	4.2	5.1	17.1	81.0	3.74
14	15.0	4.3	5.1	17.1	81.0	3.74
1	-1.8	14.0	-1.0	15.8	81.0	4.13
2	-1.8	14.0	-1.0	15.8	81.0	4.13
3	-1.8	13.9	-0.9	15.7	81.0	4.16
4	-1.8	13.9	-0.9	15.7	81.0	4.16
268	-7.4	-15.3	1.9	15.7	81.0	4.16
139	-7.4	-15.2	1.9	15.6	81.0	4.19
202	-7.4	-15.2	-1.9	15.6	81.0	4.19
76	-7.4	-15.2	-1.9	15.6	81.0	4.19
295	-0.6	-15.5	1.0	15.6	81.0	4.19
166	-0.5	-15.5	0.9	15.5	81.0	4.23
229	-0.8	-15.3	-1.0	15.4	81.0	4.26
103	-0.8	-15.3	-0.9	15.3	81.0	4.29
289	-4.4	-14.5	1.2	14.6	81.0	4.55
223	-4.5	-14.4	-1.2	14.6	81.0	4.55
160	-4.4	-14.4	1.2	14.5	81.0	4.59
97	-4.5	-14.4	-1.2	14.5	81.0	4.59
276	-5.6	-14.0	1.3	14.2	81.0	4.70
147	-5.6	-14.0	1.3	14.2	81.0	4.70
210	-5.5	-13.9	-1.3	14.1	81.0	4.74
84	-5.5	-13.9	-1.3	14.1	81.0	4.74
269	-6.7	-13.5	1.7	13.8	81.0	4.87
77	-6.5	-13.5	-1.6	13.8	81.0	4.87
140	-6.7	-13.5	1.7	13.8	81.0	4.87
203	-6.6	-13.5	-1.6	13.8	81.0	4.87
266	-8.3	-12.9	2.0	13.7	81.0	4.91
137	-8.3	-12.9	2.0	13.7	81.0	4.91
74	-8.2	-12.8	-2.0	13.6	81.0	4.96
18	-12.6	-7.2	2.4	13.6	81.0	4.96
200	-8.2	-12.8	-2.0	13.5	81.0	5.00
31	-12.6	-7.2	2.4	13.5	81.0	5.00
199	-13.0	-6.4	-1.5	13.3	81.0	5.09
73	-12.9	-6.3	-1.5	13.2	81.0	5.14
34	-12.4	-6.2	2.2	13.1	81.0	5.18
21	-12.4	-6.2	2.2	13.1	81.0	5.18

1. Section locations are shown in Figures 3.4.4.1-13 through 3.4.4.1-16.
2. Stress allowables are taken at 800°F.

Table 3.4.4.1-17 Summary of Maximum Stresses for PWR and BWR Fuel Basket Weldments - Normal Conditions (ksi)

Component	Stress Category	Maximum Stress Intensity[1]	Node Temperature (°F)	Stress Allowable[2]	Margin of Safety
PWR Top Weldment	$P_m + P_b$	0.5	297	28.1	+Large
	$P_m + P_b + Q$	52.4	292	56.1	0.07
PWR Bottom Weldment	$P_m + P_b$	0.6	179	30.0	+Large
	$P_m + P_b + Q$	20.9	175	60.0	+1.87
BWR Top Weldment	$P_m + P_b$	0.8	226	26.3	+Large
	$P_m + P_b + Q$	14.2	383	52.5	+Large
BWR Bottom Weldment	$P_m + P_b$	0.9	269	26.7	+Large
	$P_m + P_b + Q$	36.6	203	53.4	0.64

1. Nodal stresses are from the finite element analysis.
2. Conservatively, stress allowables are taken at 400°F for the PWR top weldment, 300°F for the PWR bottom weldment, 500°F for the BWR top weldment, and 300°F for the BWR bottom weldment.

3.4.4.2 Vertical Concrete Cask Analyses

The stresses in the concrete cask are evaluated in this section for normal conditions of storage. The evaluation for the steel base plate at the bottom of the cask is presented in Section 3.4.3.1. The stresses in the concrete due to dead load, live load, and thermal load are calculated in this section. The evaluations for off-normal and accident loading conditions are presented in Chapter 11.0. The radial dimensions of the concrete cask are the same for all cask configurations, only the height of the cask varies. Thus, the temperature differences through the concrete for all cask configurations vary only as a function of the heat source. Using the model described in this section, thermal analyses were run for both the maximum BWR and PWR heat loads for normal, off-normal, and accident conditions. The results of these analyses showed that the maximum temperature differences across the concrete cask wall occurred under normal operating conditions (76°F, with a 1.275 load factor) for the BWR casks and under accident conditions (133°F, with a load factor of 1.0) for the PWR casks. Thus, the structural analyses in this chapter use the temperature gradients from the BWR cask at 76°F and the analyses in Chapter 11 use the temperature differences for the PWR cask at 133°F. A summary of calculated stresses for the load combinations defined in Table 2.2-1 is presented in Table 3.4.4.2-1. As shown in Table 3.4.4.2-2, the concrete cask meets the structural requirements of ACI-349-85 [4].

The structural evaluation of the Universal Storage System is based on consideration of the bounding conditions for each aspect of the analysis. Generally, the bounding condition is represented by the component, or combination of components, of each configuration that is the heaviest. For reference, the bounding case used in each of the structural evaluations is presented in the following table.

Section	Aspect Evaluated	Bounding Condition	Configuration
3.4.4.2.1	Dead Load	Heaviest concrete cask	PWR Class 3
3.4.4.2.2	Live Load	Heaviest loaded transfer cask	BWR Class 5
	Snow Load	Same for all configurations	Not Applicable
3.4.4.2.3	Thermal Load	Highest temperature gradient under normal conditions	BWR Class 4

3.4.4.2.1 Dead Load

The concrete cask dead load evaluation is based on the PWR Class 3 concrete cask, which is the heaviest concrete cask. The weight used in this analysis bounds the calculated weight of the PWR Class 3 concrete cask, as shown in Tables 3.2-1 and 3.2-2. The dead load of the cask concrete is resisted by the lower concrete surface only. The concrete compression stress due to the weight of the concrete cask is:

$\sigma_v = -W/A = -26.1$ psi (compression)
(30.0 psi conservatively used in the loading combination, Table 3.4.4.2-1)

where:

W = 250,000 lb concrete cask bounding dead weight (maximum calculated weight = 249,400 lb)
OD = 136 in. concrete exterior diameter
ID = 79.5 in. concrete interior diameter
A $= \pi (OD^2 - ID^{2)} / 4 = 9{,}563$ in.^{2}

This evaluation of stress at the base of the concrete conservatively considers the weight of the empty concrete cask, rather than the concrete alone. The weight of the canister is not supported by the concrete.

3.4.4.2.2 Live Load

The concrete cask is subjected to two live loads: the snow load and the weight of the fully loaded transfer cask resting atop the concrete cask. These loads are conservatively assumed to be applied to the concrete portion of the cask. No loads are assumed to be taken by the concrete cask's steel liner. The loads from the canister and its contents are transferred to the steel support inside the concrete cask and are not applied to the concrete. The stress in the steel support is evaluated in Section 3.4.3.1. Under these conditions, the only stress component is the vertical compression stress.

Snow Load

The calculated snow load and the resulting stresses are the same for all five of the concrete cask configurations because the top surface areas are the same for all configurations. The snow load on the concrete cask is determined in accordance with ANSI/ASCE 7-93 [30].

The uniformly distributed snow load on the top of the concrete cask, P_f, is

$$P_f = 0.70\ C_e\ C_t\ I\ P_g = 101\ \text{lbf/ft}^2$$

The concrete cask top area,

$$A_{top} = \pi\ (D/2)^2 = 14{,}527\ \text{in.}^2 = 101\ \text{ft}^2$$

The maximum snow load, F_s, is,

$$F_s = P_f \times A_{top} = 101\ \text{lbf/ft}^2 \times (101\ \text{ft}^2) = 10{,}201\ \text{lbf.}$$

The snow load is uniformly distributed over the top surface of the concrete cask. This load is negligible.

Transfer Cask Load

The live load of the heaviest loaded transfer cask is bounded by the weight used in this analysis, which is much greater than the weight of the maximum postulated snow load. Consequently, the stress due to the snow load is bounded by the stress due to the weight of the heaviest transfer

cask. As with the snow load, the calculated transfer cask load, and the resulting stresses, are the same for all five of the concrete cask configurations because the top surface areas are the same for all configurations.

W $\approx$ 215,000 lb-bounding transfer cask weight (fully loaded)
D = 136 in.-concrete exterior diameter
ID = 79.5 in.-concrete interior diameter
A $= \pi (D^2 - ID^2)/4 = 9563$ in.^{2}

Compression stress at the base of the concrete is:

$\sigma_v = W/A = -22.5$ psi ≈ -25.0 psi (compressive)
(25.0 psi conservatively used in loading combination, Table 3.4.4.2-1)

3.4.4.2.3 Thermal Load

A three dimensional finite element model, shown in Figure 3.4.4.2-1, comprised of SOLID45, LINK8 (elements which support uniaxial loads only—no bending), and CONTAC52 elements was used to determine the stresses in the concrete cask due to thermal expansion. The SOLID45 elements represented the concrete while the LINK8 elements were used to represent the hoop and the vertical reinforcement bars. The model of the reinforcement bars is shown in Figure 3.4.4.2-2. The concrete cask has two sets of vertical reinforcement. At the inner radius of the concrete cask, there are 36 sets of vertical reinforcement, while at the outer radius, 56 sets of vertical reinforcement are used. The finite element model is a 1/56th circumferential model (or 360/56 = 6.42°), and the vertical reinforcement is modeled at the angular center of the model. To compensate for the smaller number of reinforcement elements at the inner radial location, the cross sectional area of the LINK8 elements were factored by 36/56. The cross sectional area of the LINK8s at the outer radial location corresponds to a Number 6 reinforcement bar, which has a 0.75-in. diameter and a cross sectional area of 0.44 in^2. LINK8s are also employed for the hoop reinforcements. The hoop reinforcements at the inner radial location are modeled 8-in. on center, while the outer hoop reinforcements are modeled on 4-in. centers. The nodal locations of the SOLID45 elements also correspond to the reinforcement locations to allow for the correct placement of the LINK8 elements in the model.

To allow the reinforcement to contain the tension stiffness of the concrete, the SOLID45 elements having nodes at a specified horizontal plane were separated by a small vertical distance

(0.1 in.) and were connected by CONTAC52 elements. The model contains three horizontal planes located at points ¼, ½, and ¾ of the axial length of the model. The CONTAC52 elements transmit compression across the horizontal planes, which allows the concrete elements to be subjected to compression. The LINK8 elements maintain a continuous connection from top to bottom. The structural boundary conditions are shown in Figure 3.4.4.2-3. The side of the model at 0° is restrained from translation in the circumferential direction. At 6.4°, the circumferential reinforcing bar (LINK8) elements extend beyond the model boundary and are also restrained at their ends from circumferential translation. The remaining nodes at 6.4° are attached to the CONTAC52 elements that only support compressive loading. The steel inner liner is radially coupled to the concrete, since for the thermal conditions analyzed, the steel will expand more than the concrete. The boundary conditions used simulate a complete fracture of the concrete at the 6.4° plane and between each of the axial sections of the model.

Analysis of the thermal loads and conditions for all cask configurations showed that maximum temperature gradient across the concrete wall of the cask under normal conditions, 62.42°F, occurs for the BWR configuration. Thus, the steady-state, three-dimensional thermal conduction analysis used the surface temperature boundary conditions for the 76°F normal operating condition to determine the temperature field throughout the model. These temperatures were applied with a load factor of 1.275 along the steel liner interior and concrete shell.

After the thermal solution was obtained, the thermal model was converted to a structural model. The nodal temperatures developed from the heat transfer analysis became the thermal load boundary conditions for the structural model.

The membrane stresses occurring in each individual circumferential reinforcement bar (rebar) varied on the basis of the rebar location along the longitudinal axis of the cask. The maximum circumferential tensile stress, 6,423 psi, occurred in the outer rebar, 56.4 in. from the base of the concrete cask.

The membrane stresses occurring in the vertical rebar varied on the basis of the radial location within the concrete shell. The maximum vertical tensile stress, 5,338 psi, occurred in the outer rebar 140.3 in. from the base of the cask.

The maximum allowable stress in the ASTM A-706 rebar material is:

$F_c = 60{,}000$ psi

The maximum allowable stress for the rebar assembly in the concrete cask shell is:

$$\sigma_{rebar} = \phi F_c = (0.9)(60{,}000 \text{ psi}) = 54{,}000 \text{ psi}$$

where:

F_c = 60,000 psi, the allowable stress on the rebar, and

ϕ = 0.90, a load reduction factor based on the rebar configuration.

Thus, the margin of safety of the rebar in the BWR cask under normal operating conditions is

$$MS = \frac{54{,}000\text{psi}}{6{,}423\text{psi}} - 1 = +7.4$$

The concrete component of the shell carries the compressive loads in both the circumferential and the vertical direction. The maximum calculated compressive stress, which occurs 144 in. from the base of the cask, is 116 psi in the circumferential direction. The maximum compressive concrete stress in the vertical direction is 653 psi, which occurs 136.34 in. from the base of the cask.

Tensile stresses were examined in both the axial and circumferential directions. Two vertical planes (at 0° and at 6.4° for circumferential stress) and three horizontal planes (bottom, middle and top, for axial stress) were examined at each of the four concrete sections modeled. The locations of the planes where the stress evaluations are performed are shown in Figures 3.4.4.2-4 and 3.4.4.2-5. The appropriate element stress is examined at each plane to determine if the stress is tensile or compressive. If the stress is tensile, the component stress and face area of that element are used to calculate an average concrete stress on the plane. If compressive, the element results are excluded from the calculation. Experimental studies show that the tensile strength of concrete is 8% to 15% of the concrete compressive strength [35]. Using a compressive strength of 4,000 psi and an 8% factor, an allowable tensile strength of 320 psi is used in the evaluation.

The results of the evaluation, presented in Tables 3.4.4.2-3 and 3.4.4.2-4, show that maximum tensile stress in the concrete is 143 psi and 243 psi, for the normal and accident conditions, respectively. These maximum stresses are less than the allowable stress (320 psi). Consequently, no cracking of the concrete will occur.

Applying the ACI 349-85 load reduction factor, the allowable bearing stress on the concrete shell is,

$$\sigma_{bearing} = \phi f_c' = (0.70)(4{,}000) = 2{,}800 \text{ psi}$$

where:

ϕ, the strength reduction factor for the concrete shell = 0.70

f_c', the nominal concrete compressive strength = 4,000 psi

The maximum 76°F normal operating thermally induced stress of 653 psi represents a margin of safety of

$$MS = \frac{2{,}800\text{psi}}{653\text{psi}} - 1 = +3.3$$

Figure 3.4.4.2-1 Concrete Cask Thermal Stress Model

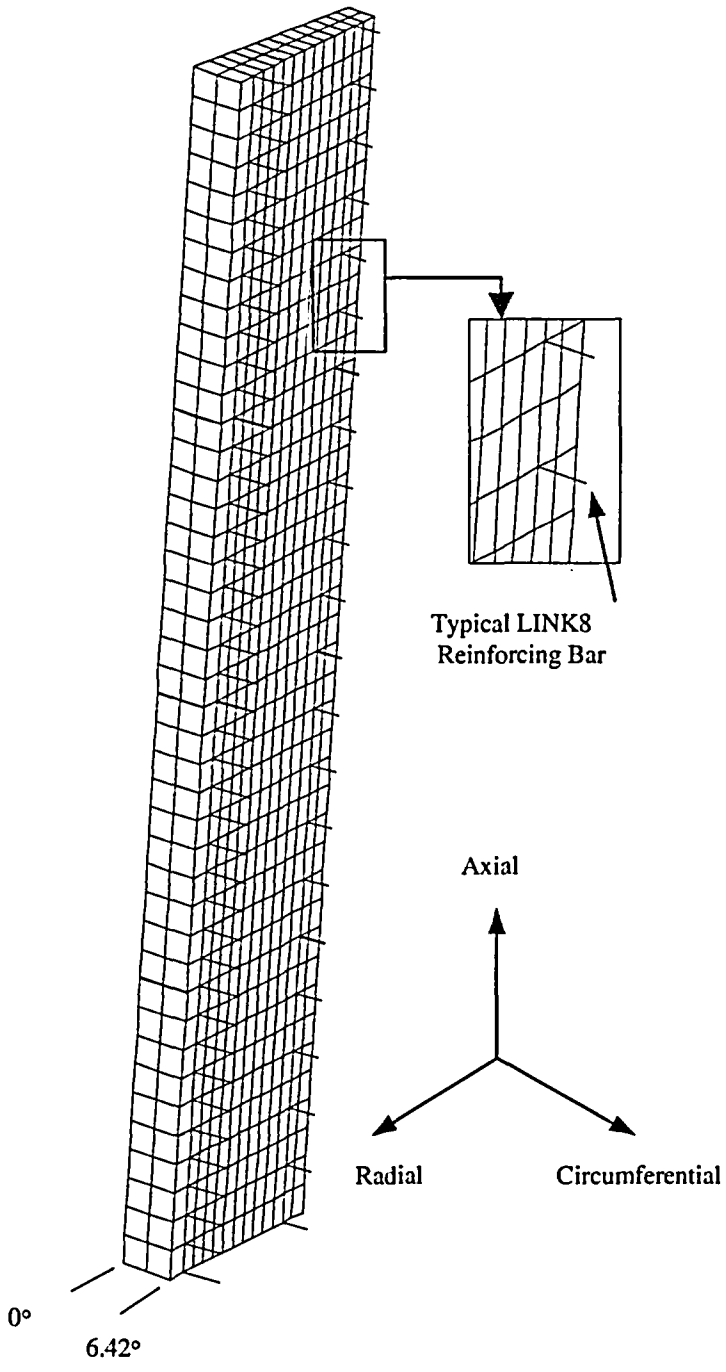

Figure 3.4.4.2-2 Concrete Cask Thermal Stress Model - Vertical and Horizontal Rebar Detail

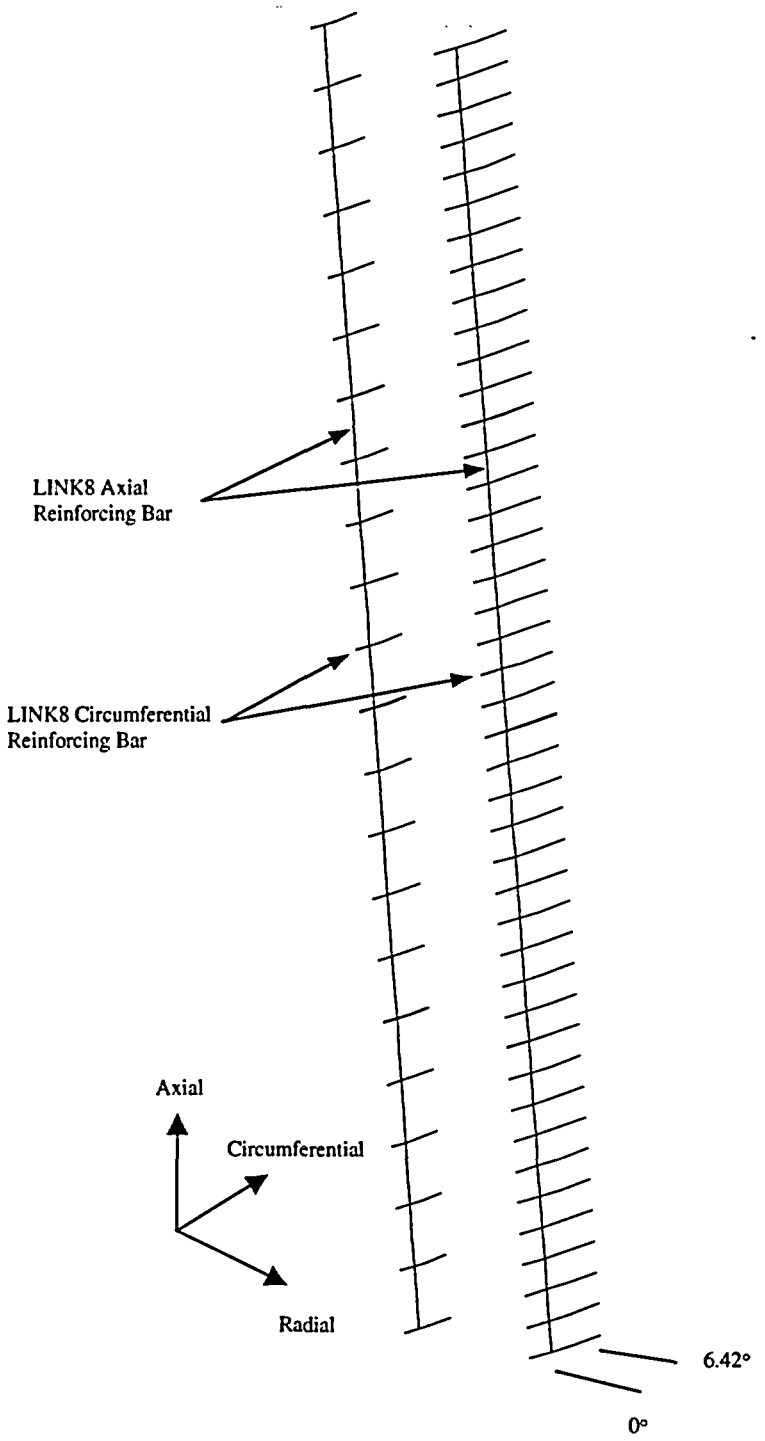

Figure 3.4.4.2-3 Concrete Cask Thermal Model Boundary Conditions

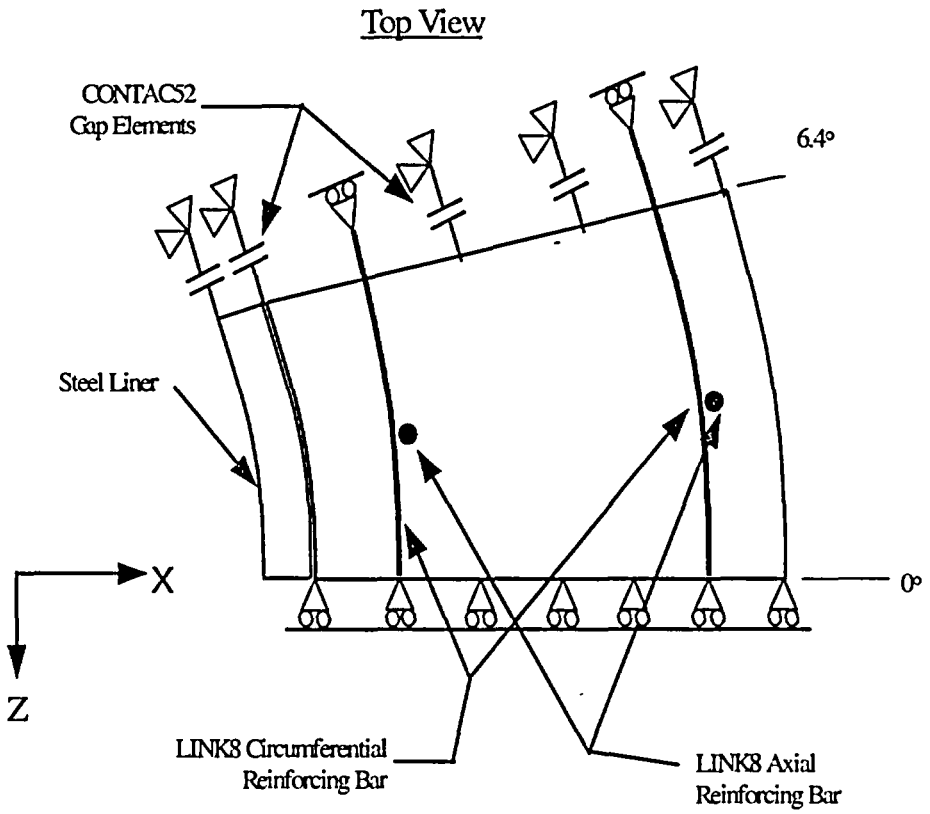

Note: CONTAC52 GAP Elements allow radial translation but don't transmit tensile loading

Figure 3.4.4.2-4 Concrete Cask Thermal Model Axial Stress Evaluation Locations

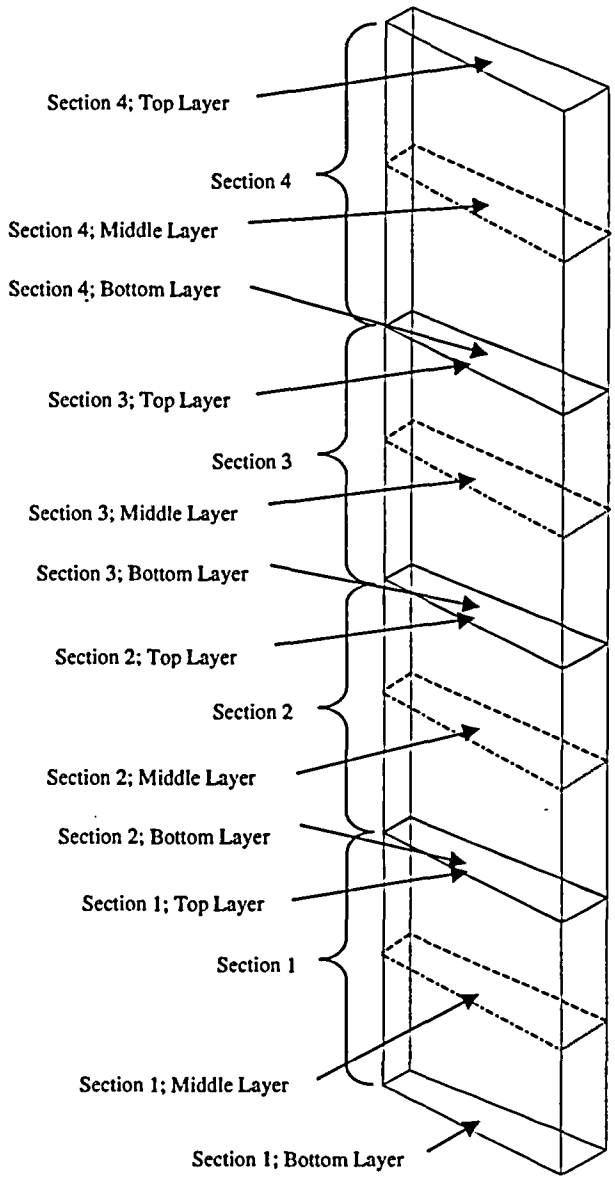

Figure 3.4.4.2-5 Concrete Cask Thermal Model Circumferential Stress Evaluation Locations

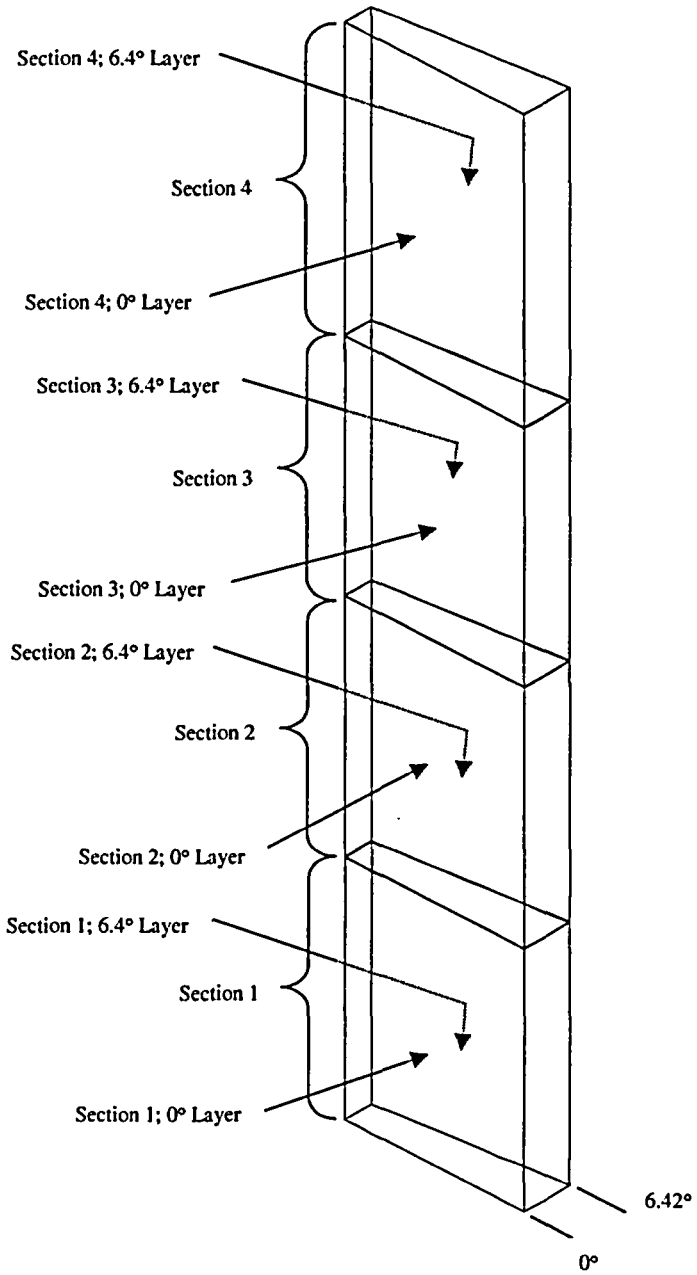

Table 3.4.4.2-1 Summary of Maximum Stresses for Vertical Concrete Cask Load Combinations

Load Comb[a]	Stress Direction	Stress[b] (psi) Dead	Live	Wind[c]	Thermal[d]	Seismic[e]	Tornado[f]	Flood[g]	Total
Concrete Outside Surface:									
1	Vertical	-42.0	-43.0	—	—	—	—	—	-85.0
2	Vertical	-32.0	-32.0	—	—	—	—	—	-64.0
3	Vertical	-32.0	-32.0	-26.0	—	—	—	—	-90.0
4	Vertical	-30.0	-25.0	—	—	—	—	—	-55.0
5	Vertical	-30.0	-25.0	—	—	-135.0	—	—	-190.0
7	Vertical	-30.0	-25.0	—	—	—	—	-20.0	-75.0
8	Vertical	-30.0	-25.0	—	—	—	-20.0	—	-75.0
Concrete Inside Surface:									
1	Vertical	-42.0	-43.0	—	—	—	—	—	-85.0
	Circumferential	0.0	0.0	—	—	—	—	—	0.0
2	Vertical	-32.0	-32.0	—	-833.0	—	—	—	-897.0
	Circumferential	0.0	0.0	—	-147.0	—	—	—	-147.0
3	Vertical	-32.0	-32.0	-26.0	-833.0	—	—	—	-923.0
	Circumferential	0.0	0.0	0.0	-143.0	—	—	—	-143.0
4	Vertical	-30.0	-.30.0	—	-.721.0	—	—	—	-776.0
	Circumferential	0.0	0.0	—	-103.0	—	—	—	-103.0
5	Vertical	-.30.0	-30.0	—	-.653.0	-100.0	—	—	-808.0
	Circumferential	0.0	0.0	—	-116.0	—	—	—	-116.0
7	Vertical	-30.0	-30.0	—	-653.0	—	—	-20.0	-728.0
	Circumferential	0.0	0.0	—	-116.0	—	—	—	-116.0
8	Vertical	-30.0	-30.0	—	-653.0	—	-20.0	—	-728.0
	Circumferential	0.0	0.0	—	-116.0	—	—	—	-116.0

[a] Load combinations are defined in Table 2.2-1. See Sections 11.2.4 and 11.2.12 for evaluations of drop/impact and tipover conditions for load combination No. 6.

[b] Positive stress values indicate tensile stresses and negative values indicate compressive stresses.

[c] Stress results from Section 11.2.11 (tornado) are conservatively used with a load factor of 1.275.

[d] Tensile stresses (at concrete outside surface) are taken by the steel reinforcing bars and therefore are not shown in this Table. Stress Results for T_a (load combination #4) are obtained from Section 11.2.7.

[e] Stress results are obtained from Section 11.2.8.

[f] Stress results are obtained from Section 11.2.11 (tornado wind).

[g] Stress results are obtained from Section 11.2.9.

Table 3.4.4.2-2 Maximum Concrete and Reinforcing Bar Stresses

	Calculated (psi)	Allowable[1] (psi)	Margin of Safety
Concrete	923	2,800	+2.03
Reinforcing Bar			
Normal - vertical	5,338	54,000	+9.1
- hoop	6,423	54,000	+7.4
Accident[2] - vertical	6,619	54,000	+7.2
- hoop	7,869	54,000	+5.9

1 Allowable compressive stress for concrete is (0.7)(4,000 psi)=2,800 psi, where 0.7 is the strength reduction factor per ACI-349-85, Section 9.3; 4,000 psi is the nominal concrete strength. Allowable stress for reinforcing bar is determined in the calculation in this ACI Section.

2 Results are obtained from Section 11.2.7.

Table 3.4.4.2-3 Concrete Cask Average Concrete Axial Tensile Stresses

Stress Location	Normal Conditions			Accident Conditions		
	Calculated Stress (psi)	Allowable Stress (psi)	M.S.	Calculated Stress (psi)	Allowable Stress (psi)	M.S.
Section 1; Bottom Layer	38	320	7.4	149	320	1.1
Section 1; Middle Layer	27	320	10.8	46	320	6.0
Section 1; Top Layer	10	320	+Large	6	320	+Large
Section 2; Bottom Layer	85	320	2.7	133	320	1.4
Section 2; Middle Layer	42	320	6.6	90	320	2.6
Section 2; Top Layer	19	320	15.8	44	320	6.3
Section 3; Bottom Layer	77	320	3.2	120	320	1.7
Section 3; Middle Layer	66	320	3.8	136	320	1.4
Section 3; Top Layer	72	320	3.4	119	320	1.7
Section 4; Bottom Layer	37	320	7.6	65	320	3.9
Section 4; Middle Layer	59	320	4.4	116	320	1.8
Section 4; Top Layer	143	320	1.2	244	320	0.31

Table 3.4.4.2-4 Concrete Cask Average Concrete Hoop Tensile Stresses

Stress Location	Normal Conditions			Accident Conditions		
	Calculated Stress (psi)	Allowable Stress (psi)	M.S.	Calculated Stress (psi)	Allowable Stress (psi)	M.S.
Section 1; 0° Layer	29	320	10.0	50	320	5.4
Section 1; 6.42° Layer	28	320	10.4	43	320	6.4
Section 2; 0° Layer	57	320	4.6	89	320	2.6
Section 2; 6.42° Layer	59	320	4.4	85	320	2.8
Section 3; 0° Layer	87	320	2.7	114	320	1.8
Section 3; 6.42° Layer	85	320	2.8	108	320	2.0
Section 4; 0° Layer	61	320	4.2	80	320	3.0
Section 4; 6.42° Layer	58	320	4.5	74	320	3.3

THIS PAGE INTENTIONALLY LEFT BLANK

3.4.5 Cold

Severe cold environments are evaluated in Section 11.1.1. Stress intensities corresponding to thermal loads in the canister are evaluated by using a finite element model as described in Section 3.4.4.1. The thermal stresses that occur in the canister as a result of the maximum off-normal temperature gradients in the canister are bounded by the analysis of extreme cold in Section 11.1.1.

The PWR canister and basket are fabricated from stainless steel and aluminum, which are not subject to a ductile-to-brittle transition in the temperature range of interest. The BWR canister and basket are fabricated from stainless steel, aluminum, with carbon steel support disks. The carbon steel support disk thickness, 5/8 in., is selected to preclude brittle fracture at the design basis low temperature (-40°F). However, low temperature handling limits do apply to the transfer cask.

THIS PAGE INTENTIONALLY LEFT BLANK

3.5 Fuel Rods

The Universal Storage System is designed to limit fuel cladding temperatures to levels below those where Zircaloy degradation is expected to lead to fuel clad failure. As shown in Chapter 4, fuel cladding temperature limits for PWR and BWR fuel have been established at 380°C based on 5-year cooled fuel for normal conditions of storage and 570°C for short term off-normal and accident conditions.

As shown in Table 4.1-4 and 4.1-5, the calculated maximum fuel cladding temperatures are well below the temperature limits for all design conditions of storage.

THIS PAGE INTENTIONALLY LEFT BLANK

3.6 Structural Evaluation of Site Specific Spent Fuel

This section presents the structural evaluation of fuel assemblies or configurations, which are unique to specific reactor sites or which differ from the UMS® Storage System design basis fuel. These site specific configurations result from conditions that occurred during reactor operations, participation in research and development programs, and from testing programs intended to improve reactor operations. Site specific fuel includes fuel assemblies that are uniquely designed to accommodate reactor physics, such as axial fuel blanket and variable enrichment assemblies, and fuel that is classified as damaged. Damaged fuel includes fuel rods with cladding that exhibit defects greater than pinhole leaks or hairline cracks.

Site specific fuel assembly configurations are either shown to be bounded by the analysis of the standard design basis fuel assembly configuration of the same type (PWR or BWR), or are shown to be acceptable contents by specific evaluation.

3.6.1 Structural Evaluation of Maine Yankee Site Specific Spent Fuel for Normal Operating Conditions

This section describes the structural evaluation for site specific spent fuel configurations. As described in Sections 1.3.2.1 and 2.1.3.1, the inventory of site specific spent fuel configurations includes fuel classified as intact, intact with additional fuel and non fuel-bearing hardware, consolidated fuel and fuel classified as damaged. Damaged fuel is separately containerized in one of the two configurations of the Maine Yankee Fuel Can.

3.6.1.1 Maine Yankee Intact Spent Fuel

The description for Maine Yankee site specific fuel is in Section 1.3.2.1. The standard spent fuel assembly for the Maine Yankee site is the Combustion Engineering (CE) 14×14fuel assembly. Fuel of the same design has also been supplied by Westinghouse and by Exxon. The standard 14×14 fuel assemblies are included in the population of the design basis PWR fuel assemblies for the UMS® Storage System (see Table 2.1.1-1). The structural evaluation for the UMS® transport system loaded with the standard Maine Yankee fuels is bounded by the structural evaluations in Chapter 3 for normal conditions of storage and Chapter 11 for off-normal and accident conditions of storage.

With the Control Element Assembly (CEA) inserted, the weight of a standard CE 14x14 fuel assembly is 1,360 pounds. This weight is bounded by the weight of the design basis PWR fuel assembly (37,608/24 = 1,567 lbs) used in the structural evaluations (Table 3.2-1). The fuel configurations with removed fuel rods, with fuel rods replaced by solid stainless steel or Zircaloy rods, or with poison rods replaced by hollow Zircaloy rods, all weigh less than the standard CE 14x14 fuel assembly. The configuration with instrument thimbles installed in the center guide tube position weighs less than the standard assembly with the installed control element assembly. Consequently, this configuration is also bounded by the weight of the design basis fuel assembly. Since the weight of any of these fuel assembly configurations is bounded by the design basis fuel assembly weight, no additional analysis of these configurations is required.

The two consolidated fuel lattices are each constructed of 17x17 stainless steel fuel grids and stainless steel end fittings, which are connected by 4 stainless steel support rods. One of the consolidated fuel lattices has 283 fuel rods with 2 empty positions. The other has 172 fuel rods, with the remaining positions either empty or holding stainless steel rods. The calculated weight for the heaviest of the two consolidated fuel lattices is 2,100 pounds. Only one consolidated fuel lattice can be loaded into any one canister. The weight of the site specific 14x14 fuel assembly plus the CEA is approximately 1,360 lbs. Twenty-three (23) assemblies (at 1,360 lbs each) in addition to the consolidated fuel assembly (at approximately 2,100 lbs) would result in a total weight of 33,380 pounds.

Therefore, the design basis UMS® PWR fuel weight of 37,608 lbs bounds the site specific fuel and consolidated fuel by 12%. The evaluations for the Margin of Safety for the dead weight load of the fuel and the lifting evaluations in Section 3.4.4 bound the Margins of Safety for the Maine Yankee site specific fuel.

3.6.1.2 Maine Yankee Damaged Spent Fuel

The Maine Yankee fuel can, shown in Drawings 412-501 and 412-502, is provided to accommodate Maine Yankee damaged fuel. The fuel can fits within a standard PWR basket fuel tube. The primary function of the Maine Yankee fuel can is to confine the fuel material within the can to minimize the potential for dispersal of the fuel material into the canister cavity volume.

The Maine Yankee fuel can is designed to hold an intact fuel assembly, a damaged fuel assembly, a fuel assembly with a burnup between 45,000 and 50,000 MWD/MTU and having a cladding oxidation layer thickness greater than 80 microns, or consolidated fuel in the Maine Yankee fuel inventory.

The fuel can is provided in two configurations that differ only in the square cross-section of the body of the fuel can. Both fuel can configurations have walls made of 0.048-inch thick Type 304 stainless steel sheet (18 gauge), have a total length of 162.8 inches and both have a bottom plate that is 0.63 inches thick. Four holes in the plates, screened with a Type 304 stainless steel wire screen (250 openings/inch × 250 openings/inch mesh), permit water to be drained from the can during loading operations. Since the bottom surface of the fuel can rests on the canister bottom plate, additional slots are machined in the fuel can (extending from the holes to the side of the bottom assembly) to allow the water to be drained from the can. At the top of the can, the wall thickness is increased to 0.15-inches to permit the can to be handled. Slots in the top assembly side plates allow the use of a handling tool to lift the can and contents. To confine the contents within the can, the top assembly consists of a 0.88-inch thick plate with screened drain holes identical to those in the bottom plate. Once the can is loaded, the can and contents are inserted into the basket, where the can may be supported by the sides of the fuel assembly tube, which are backed by the structural support disks. Alternately, the empty fuel can may be placed in the basket prior to having the designated contents inserted in the fuel can. The two configurations have different cross-sections in the can body. The first configuration has a square minimum internal width of 8.52 inches. The second has a square minimum internal width of 8.3 inches. This smaller internal width is conservatively used in the load handling analysis.

In normal operation, the can is in a vertical position. The weight of the fuel can contents is transferred through the bottom plate of the can to the canister bottom plate, which is the identical load path for intact fuel. The only loading in the vertical direction is the weight of the can and the top assembly. The lifting of the can with its contents is also in the vertical direction.

Classical hand calculations are used to qualify the stresses in the Maine Yankee fuel can.

A conservative bounding temperature of 600°F is used for the evaluation of the fuel can for normal conditions of storage. A temperature of 300°F is used for the lifting components at the top of the fuel can and for the lifting tool.

Calculated stresses are compared to allowable stresses in accordance with ASME Code, Section III, Subsection NG. The ASME Code, Section III, Subsection NG allowable stresses used for stress analysis are:

Property	600°F	300°F
S_u	63.3 ksi	66.0 ksi
S_y	18.6 ksi	22.5 ksi
S_m	16.7 ksi	20.0 ksi
E	25.2×10^3 ksi	27.0×10^3 ksi

The Maine Yankee fuel can is evaluated for dead weight and handling loads for normal conditions of storage. Since the can is not restrained, it is free to expand. Therefore, the thermal stress is considered to be negligible.

The Maine Yankee fuel can lifting components and handling tools are designed with a safety factor of 3.0 on material yield strength.

3.6.1.2.1 Dead Weight and Handling Loading Evaluation

The weight of the Maine Yankee fuel can is 130 pounds. The maximum compressive stress acting in the tube of the fuel can is due to its own weight in addition to that of the top assembly. A 10% dynamic load factor is applied to the fuel can weight for an applied load of 143 pounds to account for loads due to handling. Based on the minimum cross-sectional area of $(8.42)^2 - (8.32)^2 = 1.674$ in^2, the margin of safety at 300°F is:

$$\text{M.S.} = 20{,}000/(143/1.674) - 1$$
$$\text{M.S.} = +\text{Large}$$

3.6.1.2.2 Lifting Evaluation

Based on the loaded weight of the fuel can, the lift evaluation does not require the use of the design criteria of ANSI N14.6 or NUREG-0612. However, for purposes of conservatism and good engineering practice, a factor of safety of three on material yield strength is used for the stress evaluations for the lift condition. Since a combined stress state results from the loading and the calculated stresses are compared to material yield strength, the Von Mises stress is computed.

Side Plates

The side plates will be subjected to bending, shear, and bearing stresses because of interaction with the lifting tool during handling operations. The lifting tool engages the 1.875-inch × 0.38-inch lifting slots with lugs that are 1-inch wide and lock into the four lifting slots. For this evaluation, the handling load is the weight of the consolidated fuel assembly (2,100 lbs design weight) plus the Maine Yankee fuel can weight (130 lbs), amplified by a dynamic load factor of 10%. Although the four slots are used to lift the can, the analysis assumes that the entire design load is shared by only two lift slots.

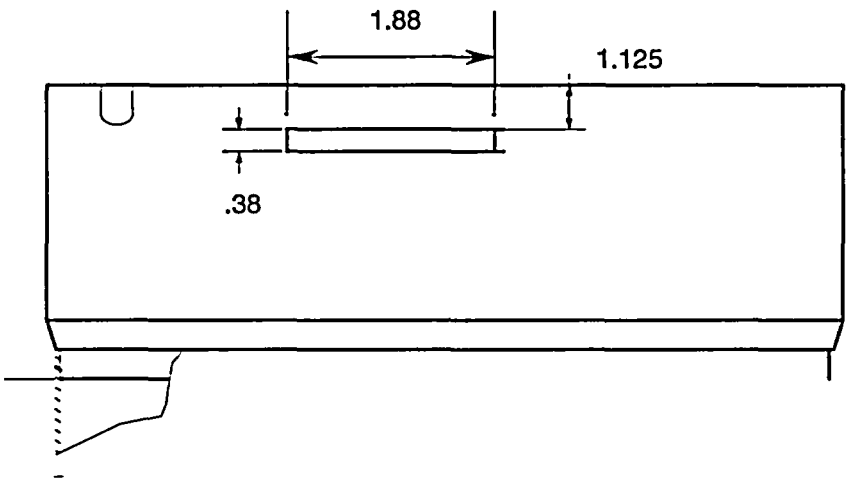

The stress in the side plate above the slot is determined by analyzing the section above the slot as a 0.15-inch wide × 1.875-inch long × 1.125-inch deep beam that is fixed at both ends. The lifting tool lug is 1 inch wide and engages the last 1 inch of the slot. The following figure represents the configuration to be evaluated:

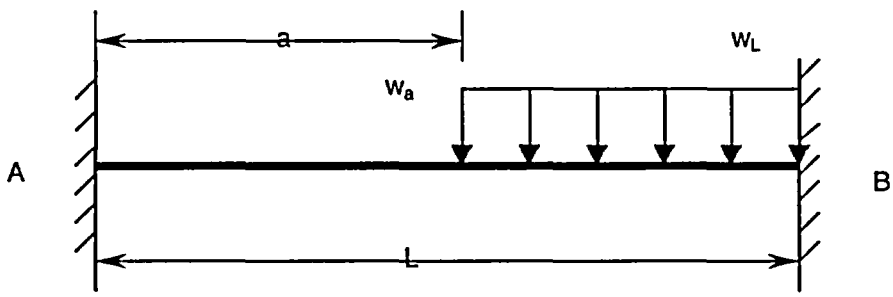

where:

$a = 0.875$ in.
$L = 1.875$ in.
$w_a = w_L = (2{,}230 \text{ lbs}/2)(1.10)/1.0 \text{ in.} = 613.3$ lbs/in, use 620 lbs/in.

Reactions and moments at the fixed ends of the beam are calculated per Roark's Formula, Table 3, Case 2d.

The reaction at the left end of the beam (R_A) is:

$$R_A = \frac{w_a}{2L^3}(L-a)^3(L+a)$$

$$= \frac{620}{2(1.875)^3}(1.875-0.875)^3(1.875+0.875) = 129.3 \text{ lbs}$$

The moment at the left end of the beam (M_A) is:

$$M_A = \frac{-w_a}{12L^2}(L-a)^3(L+3a)$$
$$= \frac{-620}{12(1.875)^2}(1.875-0.875)^3(1.875+3(0.875)) = -66.1 \text{ lbs}\cdot\text{in.}$$

The reaction at the right end of the beam (R_B) is:

$$R_B = w_a(L-a) - R_A = 620(1.875-0.875) - 164.2 = 490.7 \text{ lbs}$$

The moment at the right end of the beam (M_B) is:

$$M_B = R_A L + M_A - \frac{w_a}{2}(L-a)^2$$
$$= 129.3(1.875) + (-66.1) - \frac{620}{2}(1.875-0.875)^2 = -133.7 \text{ lbs}\cdot\text{in.}$$

The maximum bending stress (σ_b) in the side plate is:

$$\sigma_b = \frac{Mc}{I} = \frac{133.7(0.5625)}{0.0178} = 4{,}224 \text{ psi}$$

The maximum shear stress (τ) occurs at the right end of the slot:

$$\tau = \frac{R_B}{A} = \frac{490.7}{1.125(0.15)} = 2{,}908 \text{ psi}$$

The Von Mises stress (σ_{max}) is:

$$\sigma_{max} = \sqrt{\sigma_b^2 + 3\tau^2} = \sqrt{4{,}224^2 + 3(2{,}908)^2} = 6{,}573 \text{ psi}$$

The yield strength (S_y) for Type 304 stainless steel is 22,500 psi at 300°F. The factor of safety is calculated as:

$$FS = \frac{22{,}500}{6{,}573} = 3.4 > 3$$

The design condition requiring a safety factor of 3 on material yield strength is satisfied.

Tensile Stress

The tube body will be subjected to tensile loads during lifting operations. The load (P) includes the can contents (2,100 lbs design weight), the tube body weight (78.77 lbs), and the bottom assembly weight (12.98 lbs) for a total of 2,191.8 pounds. A load of 2,200 lbs with a 10% dynamic load factor is used for the analysis.

The tensile stress (σ_t) is then:

$$\sigma_t = \frac{1.1P}{A} = \frac{1.1(2{,}200 \text{ lb})}{1.674 \text{ in.}^2} = 1{,}446 \text{ psi}$$

where:

A = tube cross-section area = $8.42^2 - 8.32^2 = 1.674\ in^2$

The factor of safety (FS) based on the yield strength at 600°F (18,600 psi) is:

$$FS = \frac{18{,}600\ psi}{1{,}446} = 12.9 > 3$$

Weld Evaluation

The welds joining the tube body to the bottom weldment and to the side plates are full penetration welds (Type III, paragraph NG-3352.3). In accordance with NG-3352-1, the weld quality factor (n) for a Type III weld with visual surface inspection is 0.5.

The weld stress (σ_w) is:

$$\sigma_w = \frac{1.1(P)}{A} = \frac{1.1(2{,}200)}{1.674} = 1{,}446\ psi$$

where:

P = the combined weight of the tube body, bottom weldment, and can contents
A = cross sectional area of thinner member joined

The factor of safety (FS) is:

$$FS = \frac{n \cdot S_y}{\sigma_w} = \frac{0.5(18{,}600\ psi)}{1{,}446\ psi} = +6.4 > 3$$

3.7 References

1. 10 CFR 72, Code of Federal Regulations, "Licensing Requirements for the Independent Storage of Spent Fuel and High Level Radioactive Waste," January 1996.

2. "Safety Analysis Report for the UMS® Safety Analysis Report for the UMS® Universal Transport Cask," EA790-SAR-001, Docket No. 71-9270, NAC International, Atlanta, GA, April 1997.

3. ANSI/ANS 57.9-1992, "Design Criteria for an Independent Spent Fuel Storage Installation (Dry Type)," American National Standards Institute, May 1992.

4. American Concrete Institute, "Code Requirements for Nuclear Safety Related Concrete Structures (ACI-349-85) and Commentary (ACI 349R-85)," March 1986.

5. ASME Boiler and Pressure Vessel Code, Section III, Division I, Subsection NB, "Class 1 Components," 1995 Edition with 1995 Addenda.

6. ASME Boiler and Pressure Vessel Code, Section III, Division I, Subsection NG, "Core Support Structures," 1995 Edition with 1995 Addenda.

7. NUREG/CR 6322, "Buckling Analysis of Spent Fuel Baskets," U.S. Nuclear Regulatory Commission, May 1995.

8. NUREG-0612, "Control of Heavy Loads at Nuclear Power Plants," U.S. Nuclear Regulatory Commission, July 1980.

9. American National Standards Institute, "Radioactive Materials - Special Lifting Devices for Shipping Containers Weighing 10,000 Pounds (4,500 kg) or More," ANSI N14.6-1993, 1993.

10. ASME Boiler and Pressure Vessel Code, Section II, Part D, "Material Properties," 1995 Edition, with 1995 Addenda.

11. ASME Boiler and Pressure Vessel Code, Division I, Section III, Appendices, 1995 Edition, with 1995 Addenda.

12. "Metallic Materials Specification Handbook," 4th Edition, R. B. Ross, London, Chapman and Hall, 1992.

13. ASME Boiler and Pressure Vessel Code, Code Cases-Nuclear Components, 1995 Edition with 1995 Addenda.

14. ASTM A 615- 95b, Standard Specification for Deformed and Plain Billet-Steel Bars for Concrete Reinforcement, Annual Book of ASTM Standards, Vol. 01.04, American Society for Testing and Materials, Conshohocken, PA, 1996.

15. Metallic Materials and Elements for Aerospace Vehicle Structures, Military Handbook MIL-HDBK-5G, U.S. Department of Defense, November 1994.

16. Handbook of Concrete Engineering, 2nd Edition, M. Fintel, Van Nosttrand Reinhold Co., New York.

17. "NS-4-FR Fire Resistant Neutron and/or Gamma Shielding Material," GESC Product Data, Genden Engineering Services & Construction Co., Tokyo, Japan.

18. NRC Bulletin 96-04, "Chemical, Galvanic, or Other Reactions in Spent Fuel Storage and Transportation Casks," U.S. Nuclear Regulatory Commission, July 5, 1996.

19. ASM Handbook, Corrosion, Vol. 13, ASM International, 1987.

20. "Guidelines for the use of Aluminum with Food and Chemicals (Compatibility Data on Aluminum in the Food and Chemical Process Industries," Aluminum Association, Inc., Washington, DC, April 1984.

21. TRW, Nelson Division, "Embedment Properties of Headed Studs," Design Data 10, 1975.

22. "Design of Weldments, Omer Blodgett, The Lincoln Arc Welding Foundation, Cleveland, OH, August 1976.

23. "Manual of Steel Construction, Allowable Stress Design," American Institute of Steel Construction, Inc., Ninth Edition, Chicago, Illinois, 1991.

24. "Machinery's Handbook," 22nd Edition, Erik Oberg, et. al, First Printing, Industrial Press, Inc., New York, 1984.

25. NUREG/CR-1815, "Recommendations for Protecting Against Failure by Brittle Fracture in Ferritic Steel Shipping Containers Up to Four Inches Thick," U.S. Nuclear Regulatory Commission, Washington, DC, 1981.

26. "Roark's Formulas for Stress and Strain," Sixth Edition, Warren C. Young, McGraw-Hill, Inc., New York, 1989.

27. "Machinery's Handbook," 23rd Edition, Erik Oberg, Fourth Printing, Industrial Press, Inc., New York, 1990.

28. NUREG/CR-1815, "Recommendations for Protecting Against Failure by Brittle Fracture in Ferritic Steel Shipping Containers Up to Four Inches Thick," U. S. Nuclear Regulatory Commission, Washington, DC, 1981.

29. ASME Boiler and Pressure Vessel Code, Section II, Part C, "Specifications for Welding Rods, Electrodes, and Filler Metals," 1995 Edition, American Society of Mechanical Engineers, New York, July 1995.

30. American Society of Civil Engineers, "Minimum Design Loads for Buildings and Other Structures," ANSI/ASCE 7-93, May 1994.

31. ASME Boiler and Pressure Vessel Code, Section III-A, "Appendices," 1995 Edition, American Society of Mechanical Engineers, New York, July 1995.

32. Maddux, Gene E., "Stress Analysis Manual," AFFDL-TR-69-42, Air Force Flight Dynamics Laboratory, August 1969.

33. Avallone, Eugene A. and Baumeister III, Theodore, "Marks' Standard Handbook for Mechanical Engineers," Ninth Edition, McGraw-Hill Book Company, New York, New York, 1987.

34. "Code Requirements for Nuclear Safety Related Concrete Structures," ACI-349-90, American Concrete Institute, 1990.

35. Leet, Kenneth, "Reinforced Concrete Design," 2nd Edition, McGraw-Hill, 1991.

36. "Coating Handbook for Nuclear Power Plants," EPRI TR 106160, Electric Power Research Institute, June 1996.

37. ASTM B733-97, "Standard Specification for Autocatalytic (Electroless) Nickel-Phosphorus Coatings on Metal," Annual Book of ASTM Standards, Vol. 02.05, American Society for Testing and Materials, Conshohocken, PA, 1996.

38. American Society for Metals, "Metals Handbook," 1985.

39. Duncan, R.N., "Corrosion Resistance of High-Phosphorus Electroless Nickel Coatings," Plating and Surface Finishing, July 1986, pages 52-56.

40. "Machinery's Handbook," 25th Edition, Robert E. Green, Industrial Press, Inc., New York, 1996.

41. American Concrete Institute, "Building Code Requirements for Structural Concrete," ACI 318-95, 1999.

THIS PAGE INTENTIONALLY LEFT BLANK

3.8 Carbon Steel Coatings Technical Data

This section presents the technical data sheets for Carboline 890, Keeler & Long E-Series Epoxy Enamel, Keeler & Long Kolor-Poxy Primer No. 3200, and Acrythane Enamel Y-1 Series top coating. These coatings are applied to protect exposed carbon steel surfaces of the transfer cask and the vertical concrete cask. Also provided is a description of the electroless nickel coating that is applied to the BWR support disks. Each coating meets the service and performance requirements that are established for the coating by the design and service environment of the component to be covered.

The service and performance requirements for the coatings of the carbon steel components of the transfer cask, the vertical concrete cask, and the BWR support disks are similar and require that the coating:

- be applied to carbon steel
- be submersible for up to a week in clean water
- is rated Service Level 1 or 2 (EPRI TR-106160 for paints)
- does not contain Zinc
- have a service temperature of at least 200°F in water and 600°F in a dry environment
- generate no hydrogen, or minimal hydrogen, when submersed in water
- have no, or limited, special processes required for proper application or curing
- have a service environment in a high radiation field.

Either Carboline 890 or Keeler & Long E-Series Epoxy Enamel may be used on the exposed carbon steel surfaces of the transfer cask and the transfer cask extension. These coatings are listed in EPRI TR 106160, "Coating Handbook for Nuclear Power Plants," June 1996 [36], as meeting the requirements for Service Level 1 or 2.

Electroless nickel coating is used on the carbon steel BWR support disks to provide a submersible, passive protective finish. This coating has a history of acceptance and successful performance in similar service conditions.

No coating characteristics that may enhance the performance of the coated components (such as better emissivity) are considered in the analyses of these components. Therefore, no adverse effect on system performance results from incidental scratching or flaking of the coating, and no touchup of the coating on the BWR support disks or the storage cask liner is required.

3.8.1 Carboline 890

product data sheet

carboline

CARBOLINE® 890

VOC

SELECTION DATA

GENERIC TYPE: Two component, cross-linked epoxy.

GENERAL PROPERTIES: CARBOLINE 890 is a high solids, high gloss, high build epoxy topcoat that can be applied by spray, brush, or roller. The cured film provides a tough, cleanable and esthetically pleasing surface. Available in a wide variety of clean, bright colors. Features include:

- Good flexibility and lower stress upon curing than most epoxy coatings.
- Very good weathering resistance for a high gloss epoxy.
- Very good abrasion resistance.
- Excellent performance in wet exposures.
- Meets the most stringent VOC (Volatile Organic Content) regulations.

RECOMMENDED USES: Recommended where a high performance, attractive, chemically resistant epoxy topcoat is desired. Offers outstanding protection for interior floors, walls, piping, equipment and structural steel or as an exterior coating for tank farms, railcars, structural steel and equipment in various corrosive environments. Recommended industrial environments include Chemical Processing, Offshore Oil and Gas, Food Processing and Pharmaceutical, Water and Waste Water Treatment, Pulp and Paper, Power Generation among others. May be used as a two coat system direct to metal or concrete for Water and Municipal Waste Water immersion. CARBOLINE 890 has been accepted for use in areas controlled by USDA regulations for incidental food contact. Consult Carboline Technical Service Department for other specific uses.

NOT RECOMMENDED FOR: Strong acid or solvent exposures, or immersion service other than recommended.

TYPICAL CHEMICAL RESISTANCE:

Exposure	Immersion	Splash and Spillage	Fumes
Acids	NR	Very Good	Very Good
Alkalies	NR	Excellent	Excellent
Solvents	NR	Very Good	Excellent
Salt Solutions	Excellent	Excellent	Excellent
Water	Excellent	Excellent	Excellent

*NR = Not recommended

TEMPERATURE RESISTANCE:
Continuous: 200° F (93° C)
Non-continuous: 250° F (121° C)

At 300° F, coating discoloration and loss of gloss is observed, without loss of film integrity.

SUBSTRATES: Apply over suitably prepared metal, concrete, or other surfaces as recommended.

COMPATIBLE COATINGS: May be applied directly over inorganic zincs, weathered galvanizing, catalyzed epoxies, phenolics or other coatings as instructed. A test patch is recommended before use over existing coatings. May be used as a tiecoat over inorganic zincs. A mist coat of CARBOLINE 890 is required when applied over inorganic zincs to minimize bubbling. May be topcoated to upgrade weathering resistance. Not recommended over chlorinated rubber or latex coatings. Consult Carboline Technical Service Department for specific recommendations.

April 91 Replaces Oct. 90

SPECIFICATION DATA

THEORETICAL SOLIDS CONTENT OF MIXED MATERIAL:*

	By Volume
CARBOLINE 890	75% ± 2%

VOLATILE ORGANIC CONTENT:*
As Supplied: 1.78 lbs./gal.(214 gm/liter)
Thinned: The following are nominal values utilizing:

% Thinned	Fluid Ounces/Gal.	Pounds/ Gallon	Grams/ Liter
CARBOLINE Thinner # 2 (spray application)			
10%	12.8	2.26	271
CARBOLINE Thinner #33 (brush & roller application)			
12%	16	2.38	285

*Varies with color

RECOMMENDED DRY FILM THICKNESS PER COAT:
4-6 mils(100-150 microns).

5-7 mils (125-175 microns) DFT for a more uniform gloss over inorganic zincs.

Dry film thicknesses in excess of 10 mils(250 microns) per coat are not recommended. Excessive film thickness over inorganic zinc may increase damage during shipping or erection.

THEORETICAL COVERAGE PER MIXED GALLON:
1203 mil sq. ft. (30 sq. m/l at 25 microns)
241 sq. ft. at 5 mils(6.0 sq. m/l at 125 microns)
Mixing and application losses will vary and must be taken into consideration when estimating job requirements.

STORAGE CONDITIONS: Store Indoors
Temperature: 40-110° F (4-43° C)
Humidity: 0-100%

SHELF LIFE: Twenty-four months minimum when stored at 75° F (24° C).

COLORS: Available in Carboline Color Chart colors. Some colors may require two coats for adequate hiding. Colors containing lead or chrome pigments are not USDA acceptable. Consult your local Carboline representative or Carboline Customer Service for availability.

* See notice under DRYING TIMES.

GLOSS: High gloss (Epoxies lose gloss and eventually chalk in sunlight exposure).

ORDERING INFORMATION

Prices may be obtained from your local Carboline Sales Representative or Carboline Customer Service Department.

APPROXIMATE SHIPPING WEIGHT:

	2 Gal. Kit	10 Gal. Kit
CARBOLINE 890	29 lbs. (13 kg)	145 lbs. (66 kg)
THINNER #2	8 lbs. in 1's (4 kg)	39 lbs. in 5's (18 kg)
THINNER #33	9 lbs. in 1's (4 kg)	45 lbs. in 5's (20 kg)

FLASHPOINT: (Pensky-Martens Closed Cup)

CARBOLINE 890 Part A	73° F (23° C)
CARBOLINE 890 Part B	71° F (22° C)
THINNER #2	24° F (– 5° C)
THINNER #33	96° F (37° C)

To the best of our knowledge the technical data contained herein are true and accurate at the date of issuance and are subject to change without prior notice. User must contact Carboline Company to verify correctness before specifying or ordering. No guarantee of accuracy is given or implied. We guarantee our products to conform to Carboline quality control. We assume no responsibility for coverage, performance or injuries resulting from use. Liability, if any, is limited to replacement of products. Prices and cost data if shown, are subject to change without prior notice. NO OTHER WARRANTY OR GUARANTEE OF ANY KIND IS MADE BY Carboline, EXPRESS OR IMPLIED, STATUTORY, BY OPERATION OF LAW, OR OTHERWISE, INCLUDING MERCHANTABILITY AND FITNESS FOR A PARTICULAR PURPOSE.

APPLICATION INSTRUCTIONS
CARBOLINE® 890

These instructions are not intended to show product recommendations for specific service. They are issued as an aid in determining correct surface preparation, mixing instructions and application procedure. It is assumed that the proper product recommendations have been made. These instructions should be followed closely to obtain the maximum service from the materials.

0986

SURFACE PREPARATION: Remove oil or grease from surface to be coated with clean rags soaked in CARBOLINE Thinner #2 or Surface Cleaner #3 (refer to Surface Cleaner #3 Instructions) in accordance with SSPC-SP 1.

Steel: Normally applied over clean, dry recommended primers. May be applied directly to metal. For immersion service, abrasive blast to a minimum Near White Metal Finish in accordance with SSPC-SP10, to a degree of cleanliness in accordance with NACE #2 to obtain a 1.5-3 mil (40-75 micron) blast profile. For non-immersion, abrasive blast to a Commercial Grade Finish in accordance with SSPC-SP6, to a degree of cleanliness in accordance with NACE #3 to obtain a 1.5-3 mil (40-75 micron) blast profile.

Concrete: Apply over clean, dry recommended surfacer or primer. Can be applied directly to damp(not visibly wet) or dry concrete where an uneven surface can be tolerated. Remove laitance by abrasive blasting or other means.

Do not coat concrete treated with hardening solutions unless test patches indicate satisfactory adhesion. Do not apply coating unless concrete has cured at least 28 days at 70° F (21° C) and 50% RH or equivalent time.

MIXING: Mix separately, then combine and mix in the following proportions:

	2 Gal. Kit	10 Gal. Kit
CARBOLINE 890 Part A	1 gallon	5 gallons
CARBOLINE 890 Part B	1 gallon	5 gallons

THINNING: For spray applications, may be thinned up to 10% (12.8 fl. oz./gal.) by volume with CARBOLINE Thinner #2.

For brush and roller application may be thinned up to 12 % (16 fl. oz./gal.) by volume with CARBOLINE Thinner #33.

Refer to Specification Data for VOC information.

Use of thinners other than those supplied or approved by Carboline may adversely affect product performance and void product warranty, whether express or implied.

POT LIFE: Three hours at 75° F (24° C) and less at higher temperatures. Pot life ends when material loses film build.

APPLICATION CONDITIONS:

	Material	Surfaces	Ambient	Humidity
Normal	60-85° F (16-29° C)	60-85° F (16-29° C)	60-90° F (16-32° C)	0-80%
Minimum	50° F (10° C)	50° F (10° C)	50° F (10° C)	0%
Maximum	90° F (32° C)	125° F (52° C)	110° F (43° C)	80%

Do not apply when the surface temperature is less than 5° F (or 3° C) above the dew point.

Special thinning and application techniques may be required above or below normal conditions.

SPRAY: This is a high solids coating and may require slight adjustments in spray techniques. Wet film thicknesses are easily and quickly achieved. The following spray equipment has been found suitable and is available from manufacturers such as Binks, DeVilbiss and Graco.

Conventional: Pressure pot equipped with dual regulators, 3/8" I.D. minimum material hose, .070" I.D. fluid tip and appropriate air cap.

Airless:
Pump Ratio: 30:1 (min.)*
GPM Output: 3.0 (min.)
Material Hose: 3/8" I.D. (min.)
Tip Size: .017-.021"
Output psi: 2100-2300
Filter Size: 60 mesh

*Teflon packings are recommended and are available from the pump manufacturer.

BRUSH OR ROLLER: Use medium bristle brush, or good quality short nap roller, avoid excessive rebrushing and rerolling. Two coats may be required to obtain desired appearance, hiding and recommended DFT. For best results, tie-in within 10 minutes at 75° F (24° C).

DRYING TIMES: These times are at 5 mils (125 microns) dry film thickness. Higher film thicknesses will lengthen cure times.

Dry to Touch 2 1/2 hours at 75° F (24° C)
Dry to Handle 6 1/2 hours at 75° F (24° C)

Temperature	Dry to Topcoat**	Final Cure
50° F (10° C)	24 hours	3 days
60° F (16° C)	16 hours	2 days
75° F (24° C)	8 hours	1 day
90° F (32° C)	4 hours	16 hours

**When recoating with CARBOLINE 890, recoat times will be drastically reduced. Contact Carboline Technical Service for specific recommendation.

Recommended minimum cure before immersion service is 5 days at 75° F (24° C).

EXCESSIVE HUMIDITY OR CONDENSATION ON THE SURFACE DURING CURING MAY RESULT IN SURFACE HAZE OR BLUSH; ANY HAZE OR BLUSH MUST BE REMOVED BY WATER WASHING BEFORE RECOATING.

CLEANUP: Use CARBOLINE Thinner #2.

CAUTION: READ AND FOLLOW ALL CAUTION STATEMENTS ON THIS PRODUCT DATA SHEET AND ON THE MATERIAL SAFETY DATA SHEET FOR THIS PRODUCT.

CAUTION: CONTAINS FLAMMABLE SOLVENTS. KEEP AWAY FROM SPARKS AND OPEN FLAMES. IN CONFINED AREAS WORKMEN MUST WEAR FRESH AIRLINE RESPIRATORS. HYPERSENSITIVE PERSONS SHOULD WEAR GLOVES OR USE PROTECTIVE CREAM. ALL ELECTRIC EQUIPMENT AND INSTALLATIONS SHOULD BE MADE AND GROUNDED IN ACCORDANCE WITH THE NATIONAL ELECTRICAL CODE. IN AREAS WHERE EXPLOSION HAZARDS EXIST, WORKMEN SHOULD BE REQUIRED TO USE NONFERROUS TOOLS AND TO WEAR CONDUCTIVE AND NONSPARKING SHOES

carboline

350 Hanley Industrial Ct • St. Louis, MO 63144-1599
an RPM company • 314-644-1000

3.8.2 Keeler & Long E-Series Epoxy Enamel

March, 1995 SSU-1

KEELER & LONG INC

HEADQUARTERS:
P. O. Box 460
856 Echo Lake Road
Watertown, CT 06795
Tel (860) 274-6701
Fax (860) 274-5857

PROTECTIVE COATING SYSTEMS FOR NUCLEAR POWER PLANTS

INTRODUCTION

In the 1960's Keeler & Long made the commitment to develop Protective Coating Systems for Nuclear Power Plants. Coating Systems were developed and qualified in accordance with accepted standards, with emphasis upon their usage and specification for NEW construction projects. These systems were applied directly to either concrete or carbon steel substrates utilizing ideal surface preparation.

Presently, there is a necessity to apply these same coating systems or newly formulated systems over the original systems or over substrates which cannot be ideally prepared. Several years ago, Keeler & Long initiated a test program in order to test and qualify systems in conjunction with competitors products and/or with methods of preparation which are considered less than ideal. This test program provides OPERATING Nuclear Plants with qualified methods of preparation and a variety of qualified mixed coating systems.

HISTORY

In 1967, we embarked upon a testing program in order to comply with standards being prepared by the experts in the field and under the jurisdiction of The American National Standards Institute (ANSI). Earlier testing had involved research in order to determine the radiation tolerance and the decontamination properties of a variety of generic coating types including zinc rich, alkyds, chlorinated rubbers, vinyls, latex emulsions, and epoxies. This testing was conducted by various independent laboratories, such as Oak Ridge National Laboratory, Idaho Nuclear, and The Western New York Nuclear Research Center. It was concluded from these tests that almost any generic coating type would produce satisfactory radiation resistance and decontaminability.

Upon completion of the first ANSI Standards, however, it became evident that only Epoxy Coatings would meet the specific minimum acceptance criteria set forth in these standards. The single most important change from the earlier testing was the inclusion of a test which simulates the operation of the emergency core cooling system. This test is referred to as the Loss of Coolant Accident (LOCA) or the Design Basis Accident Condition (DBA). The test involves a high pressure, high temperature, alkaline, immersion environment.

Simultaneous with the preparation of these standards, we prepared to test Epoxy Systems in order to comply with the requirements. First hand knowledge of these standards was available since our personnel assisted in the development of these documents. Equipment was designed and built by our laboratory in order to conduct in-house DBA tests. The required physical and chemical tests were either conducted by us or by universities through research grants.

In 1972, the testing program was taken a step further in order to establish more credibility. The Franklin Institute of Philadelphia constructed an apparatus in order to simulate various Design Basis Accident Conditions and we prepared blocks and panels for an independent evaluation. The test results were among the "First" from an independent source, and these tests substantiated more than two years of in-house testing.

The Franklin Institute tests, along with our in-house testing program, were used as a basis for qualification until 1976. During this period also the following ANSI standards were revised and/or developed:

ANSI N5.9-1967 "Protective Coatings (Paints) for the Nuclear Industry" (Rev. ANSI N512-1974)

ANSI N101.2-1972 "Protective Coatings (Paints) for Light Water Nuclear Reactor Containment Facilities"

ANSI N101.4-1972 "Quality Assurance for Protective Coatings Applied to Nuclear Facilities"

Simultaneously, we developed a written Quality Assurance Program in compliance with ANSI N101.4 - 1972, Appendix B 10CFR50 of the Federal Register, and ANSI N45.2-1971 "Quality Assurance Program Requirements For Nuclear Power Plants".

In 1976, Oak Ridge national Laboratory (ORNL) established a testing program in order to conduct Radiation, Decontamination, and DBA tests under one roof. Keeler & Long, under contract with ORNL, conducted a series of tests in compliance with the parameters established by a major engineering firm and the ANSI standards. These tests, and similar series of tests conducted two years later in 1978, became the basis for the qualification of several of our concrete and carbon steel coating systems. From 1978 to the present day we have continued to qualify through ORNL and several other independent testing agencies any modifications to existing formulas and any changes in surface preparation or application requirements. We have also maintained an in-house testing program used to screen new products as well as modifications of existing systems. Furthermore, progress has continued in the revision of the ANSI standards during this time frame. Revision of these documents is presently under the jurisdiction of the American Society for Testing and Materials (ASTM) as outlined in D3842-80 "Standard Guide for Selection of Test Methods for Coatings Used in Light-Water Nuclear Power Plants".

The future dictates significantly less construction of new Nuclear Plants and much more emphasis upon the repair and maintenance of existing facilities. Our commitment remains the same as it was in 1965; that is, to meet the coating requirements of Nuclear Power Plants.

NUCLEAR COATINGS

SSU-1

Level One Coating Systems

The following Coating Systems are qualified for Coating Service Level One of a Nuclear Power Plant. "Coating Service Level One pertains to those systems applied to structures, systems and other safety related components which are essential to the prevention of, or the mitigation of the consequences of postulated accidents that could cause undue risk to the health and safety of the public."

SYSTEM IDENTIFICATION	COATING SYSTEMS	DRY FILM THICKNESS RANGE
CARBON STEEL COATING SYSTEMS		
System S-1		
Primer	No. 6548/7107 EPOXY WHITE PRIMER	3.0 - 14.0 mils DFT
Finish	No. E-1 SERIES EPOXY ENAMEL	2.5 - 6.0 mils DFT
System S-10		
Primer	No. 6548/7107 EPOXY WHITE PRIMER	5.0 - 12.0 mils DFT
Finish	No. D-1 SERIES EPOXY HI-BUILD ENAMEL	3.0 - 6.0 mils DFT
System S-11		
Primer/Finish	No. 6548/7107 EPOXY WHITE PRIMER	8.0 - 18.0 mils DFT
System S-12		
Primer/Finish	No. 4500 EPOXY SELF-PRIMING SURFACING ENAMEL	5.0 - 18.0 mils DFT
System S-14 (FLOORS ONLY)		
Finish	No. 5000 EPOXY SELF-LEVELING FLOOR COATING	10.0 - 25.0 mils DFT
System S-15		
Primer	No. 6548/7107 EPOXY WHITE PRIMER	2.5 - 6.0 mils DFT
Finish	No. 9600 N KEELOCK	5.0 - 8.0 mils DFT
CONCRETE COATING SYSTEMS		
System KL-2		
Curing Compound/Sealer	No. 4129 EPOXY CLEAR CURING COMPOUND	0.5 - 1.75 mils DFT
Surfacer	No. 6548-S EPOXY SURFACER	Flush - 50.0 mils DFT
Finish	No. E-1 SERIES EPOXY ENAMEL	2.5 - 6.0 mils DFT
System KL-8		
Curing Compound/Sealer	No. 4129 EPOXY CLEAR CURING COMPOUND	0.5 - 1.75 mils DFT
Surfacer	No. 6548-S EPOXY SURFACER	Flush - 50.0 mils DFT
Finish	No. D-1 SERIES EPOXY HI-BUILD ENAMEL	4.0 - 8.0 mils DFT
System KL-9		
Curing Compound/Sealer	No. 4129 EPOXY CLEAR CURING COMPOUND	0.5 - 1.75 mils DFT
Surfacer	No. 6548/7107 EPOXY WHITE PRIMER	5.0 - 10.0 mils DFT
Finish	No. D-1 SERIES EPOXY HI-BUILD ENAMEL	3.0 - 8.0 mils DFT
System KL-10		
Curing Compound/Sealer	No. 4129 EPOXY CLEAR CURING COMPOUND	0.5 - 1.75 mils DFT
Surfacer	No. 4000 EPOXY SURFACER	Flush - 50.0 mils DFT
Finish	No. D-1 SERIES EPOXY HI-BUILD ENAMEL	3.0 - 6.0 mils DFT
System KL-12		
Curing Compound/Sealer	No. 4129 EPOXY CLEAR CURING COMPOUND	0.5 - 1.75 mils DFT
Surfacer/Finish	No. 4500 EPOXY SELF-PRIMING SURFACING ENAMEL	10.0 - 50.0 mils DFT
System KL-14 (FLOORS ONLY)		
Primer/Sealer	No. 6129 EPOXY CLEAR PRIMER/SEALER	1.5 - 2.5 mils DFT
Finish	No. 5000 EPOXY SELF-LEVELING FLOOR COATING	35.0 - 50.0 mils DFT

SUMMARY OF QUALIFICATION TEST RESULTS

KEELER & LONG maintains a complete file of Nuclear Test Reports which substantiate the specification of the carbon steel and concrete coating systems listed in this bulletin. This file was initiated in the early 1970's and provides complete qualification in accordance with ANSI Standards N512 and N101.2. Results for radiation tolerance, decontamination, and the Design Basis Accident Condition are reported as performed by Independent Laboratories. Also reported are the chemical and physical tests which were conducted by the Keeler & Long Laboratory in compliance with the ANSI Standards.

TEST REPORT REFERENCE

K&L COATING SYSTEM	SUBSTRATE	KEELER & LONG TEST REPORT NO. 76-0728-1	78-0610-1	85-0404	85-0524	90-0227	93-0818	93-0601
S-1	Steel	•	•					
S-10	Steel		•					
S-11	Steel		•					
S-12	Steel			•				
S-14	Steel					•		
S-15	Steel						•	
KL-2	Concrete	•	•					
KL-8	Concrete	•						
KL-9	Concrete	•	•					
KL-10	Concrete		•					
KL-12	Concrete				•			
KL-14	Concrete					•		•

This information is presented as accurate and correct, in good faith, to assist the user in application. No warranty is expressed or implied. No liability is assumed.

KOLORS KEELER & LONG INC. SSPC SUSTAINING MEMBER

E.340

KEELER & LUGHT INC.

HEADQUARTERS:
P. O. Box 460
856 Echo Lake Road
Watertown, CT 06795
Tel (860) 274-6701
Fax (860) 274-5857

EPOXY ENAMEL
E-SERIES

GENERIC TYPE: POLYAMIDE EPOXY

PRODUCT DESCRIPTION: A two component, polyamide epoxy enamel formulated to provide excellent chemical resistance, as well as being extremely resistant to abrasion and direct impact, for interior exposures.

RECOMMENDED USES: As a topcoat for concrete and steel surfaces subject to radiation, decontamination, and loss-of-coolant accidents in Coating Service Level I Areas of nuclear power plants.

NOT RECOMMENDED FOR: Areas other than the above, as the J-SERIES can be utilized in Coating Service Level II and III Areas, as well as Balance of Plant, of nuclear power plants, with attendant cost savings.

COMPATIBLE UNDERCOATS: Epoxy White Primer
Epoxy Surfacer

PRODUCT CHARACTERISTICS:

Solids by Volume:	53% ± 3%
Solids by Weight:	66% ± 3%
Recommended Dry Film Thickness:	2.0 - 2.5 mils
Theoretical Coverage:	425 Sq. Ft./Gallon @ 2.0 mils DFT
Finish:	Full Gloss (E-1), Semi-Gloss (E-2)
Available Colors:	White, light tints, and dark red
Drying Time @ 72°F	
To Touch:	4 Hours
To Handle:	8 Hours
To Recoat:	48 Hours
VOC Content:	3.4 Pounds/Gallon 407 Grams/Liter

June, 1994

TECHNICAL BULLETIN

E-SERIES E 340

TECHNICAL DATA

PHYSICAL DATA:	Weight per gallon:	10.2 ± 0.5 (pounds)
	Flash Point (Pensky-Martens):	85°F± 2°
	Shelf Life:	1 Year
	Pot Life @ 72°F:	8 Hours
	Temperature Resistance:	350°F
	Viscosity @ 77°F:	85 ± 5 (Krebs Units)
	Gloss (60° meter):	95 ± 5 (E-1)
	Storage Temperature:	55 - 95°F
	Mixing Ratio (Approx. by Volume):	4:1
APPLICATION DATA:	Application Procedure Guide:	APG-2
	Wet Film Thickness Range:	4.0 - 5.0 mils
	Dry Film Thickness Range:	2.0 - 2.5 mils
	Temperature Range:	55 - 120°F
	Relative Humidity:	80% Maximum
	Substrate Temperature:	Dew Point + 5°F
	Minimum Surface Preparation:	Primed
	Induction Time @ 72°F:	1 Hour
	Recommended Solvent	
	@ 50 - 85°F:	No. 4093
	@ 86 - 120°F:	No. 2200

Application Methods

Air Spray	
Tip Size:	.055"
Pressure:	30 - 60 PSIG
Thin:	1.0 - 2.0 Pts/Gal
Airless Spray	
Tip Size:	.011" - .017"
Pressure:	2500 - 3000 PSIG
Thin:	0.5 - 1.5 Pts/Gal
Brush or Roller	
Thin:	1.0 - 2.0 Pts/Gal

KEELER & LONG INC.

KOLORS

P. O. Box 460, 856 Echo Lake Road
Watertown, CT 06795
Tel: (860) 274-6701 Fax: (860) 274-5857

This information is presented as accurate and correct, in good faith, to assist the user in specification and application. No warranty is expressed or implied. No liability is assumed. Product specifications are subject to change without notice. Data listed above is for white or base color of the product. Data for other colors may differ.

SSPC SUSTAINING MEMBER

3.8.3 Description of Electroless Nickel Coating

This section provides a description of the electroless Nickel coating process as prepared by the ASM Committee on Nickel Plating. The electroless Nickel coating is used to provide corrosion protection of the BWR carbon steel support disks during the short time period from placement of the BWR canister in the spent fuel pool to the time of completion of vacuum drying and inerting with helium. The coating is applied in accordance with ASTM B733-SC3, Type V, Class 1 [37].

Electroless nickel is a nickel/phosphorus alloy that is produced by the use of a chemical reducing agent a hot aqueous solution to deposit nickel on a catalytic surface without the use of an electric current. The chemical reduction process produces a uniform, predicable coating thickness. Adhesion of the nickel coating to properly cleaned carbon steel is excellent with reported bond strength in the range of 40 to 60 ksi [38].

Electroless nickel coating is highly corrosion resistant because of its non-porous structure that seals off the coated surface from the environment. During the time following completion of the coating of the UMS BWR support disk until actual use, the nickel surface bonds with oxygen atoms in the air to create a passive nickel oxide layer on the surfaces of the support disk. Thus, very few free electrons are available on the surface to cathodically react with water and produce hydrogen gas. Test data for electroless nickel coated steel have been reported to show corrosion rates from 1 to 2 μm per year in water [39].

The coating classification of SC3 provides a minimum thickness of 25 μm (0.001 inch).

Nonelectrolytic Nickel Plating

*By the ASM Committee on Nickel Plating**

THREE METHODS may be employed for depositing nickel coatings without the use of electric current:

1 Immersion plating
2 Chemical reduction of nickelous oxide at 1600 to 2000 F
3 Autocatalytic chemical reduction of nickel salts by hypophosphite anions in an aqueous bath at 190 to 205 F ("electroless" nickel plating).

All three methods are, under certain limited conditions, useful substitutes for nickel electroplating; they are particularly useful in applications in which electroplating is impracticable or impossible because of cost or technical difficulties. Of the three methods, electroless nickel plating is in widest use, and is the method to which the most attention is devoted in this article.

Immersion Plating

The composition and operating conditions of an aqueous immersion plating bath are as follows:

Nickel chloride ($NiCl_2 \cdot 6H_2O$)	30 oz per gal
Boric acid (H_3BO_3)	4 oz per gal
pH	3.5 to 4.5
Temperature	160 F

When using this bath, it is desirable, but not mandatory, to move the work at a rate of about 16 ft per min.

This solution is capable of depositing a very thin (about 0.025 mil) and uniform coating of nickel on steel in periods of up to 30 min. The coating is porous and possesses only moderate adhesion, but these conditions can be improved by heating the coated part at 1200 F for 45 min in a nonoxidizing atmosphere. (Higher temperatures will promote diffusion of the coating.)

High-Temperature Chemical-Reduction Coating

By the reduction of a mixture of nickelous oxide and dibasic ammonium phosphate in hydrogen or other reducing atmosphere at 1600 to 2000 F, a nickel coating can be deposited without the use of electric current. This method (U. S. Patent 2,633,631) consists of applying a slurry of the two chemicals to all or selected surfaces of the workpiece, drying the slurry in air, and performing the chemical reduction at elevated temperature. No special tanks or other plating facilities are required. Some diffusion of nickel and phosphorus into the basis metal occurs at elevated temperature; when the coating is applied to steel, it will consist of nickel, iron, and about 3% phosphorus. The slurry may be used for brazing.

Electroless Nickel Plating

The electroless nickel plating process employs a chemical reducing agent (sodium hypophosphite) to reduce a nickel salt (such as nickel chloride) in hot aqueous solution and to deposit nickel on a catalytic surface. The deposit obtained from an electroless nickel solution is an alloy containing from 4 to 12% phosphorus and is quite hard. (As indicated later in this article, the hardness of the as-plated deposit can be increased by heat treatment.) Because the deposit is not dependent on current distribution, it is uniform in thickness, regardless of the shape or size of the plated surface.

Electroless nickel deposits may be applied to provide the basis metal with resistance to corrosion or wear, or for the buildup of worn areas. Typical applications of electroless nickel for these purposes are given in Table 1, which also indicates plate thicknesses and postplating heat treatments.

Surface Cleaning. In general, the methods employed for cleaning and preparing metal surfaces for electroless nickel plating are the same as those used for conventional electroplating. Heavy oxides are removed mechanically, and oils and grease are removed by vapor degreasing. A typical precleaning cycle might consist of alkaline cleaning (either agitated soak or anodic) and acid pickling, both followed by water rinsing.

Prior to electroless plating, the surfaces of all stainless steel parts must be chemically activated in order to obtain satisfactory adhesion of the plate. One activating treatment consists of immersing the work for about 3 min in a hot (200 F) solution containing equal volumes of water and concentrated sulfuric acid. Another treatment consists of immersing the work for 2 to 3 min in the following solution at 160 F:

Sulfuric acid (66° Bé)	25% by volume
Hydrochloric acid (18° Bé)	5% by volume
Ferric chloride hexahydrate	0.83 oz per gal

Pretreatments that are unique to electroless nickel plating include:

1 A strike copper plate must be applied to parts made of or containing lead, tin, cadmium or zinc, to insure adequate coverage and to prevent contamination of the electroless solution.
2 Massive parts are preheated to bath temperature to avoid delay in the deposition of nickel from the hot electroless bath.

Bath Characteristics. A simplified equation that describes the formation of electroless nickel deposits is:

$$NiSO_4 + NaH_2PO_2 + H_2O \xrightarrow[\text{catalyst}]{\text{heat}} Ni + NaH_2PO_3 + H_2SO_4$$

The essential requirements for any electroless nickel solution are:

1 A salt to supply the nickel
2 A hypophosphite salt to provide chemical reduction
3 Water
4 A complexing agent
5 A buffer to control pH
6 Heat
7 A catalytic surface to be plated.

Detailed discussions of the chemical characteristics of electroless baths, and of the critical concentration limits of the various reactants, can be found in several of the references listed at the end of this article.

Both alkaline (pH, 7.5 to 10) and acid (pH, 4.5 to 6) electroless nickel baths are used in industrial production. Although the acid baths are easier to maintain and are more widely used, the alkaline baths are reported to have greater compatibility with sensitive substrates (such as magnesium, silicon and aluminum).

Catalysis. Nickel and hypophosphite ions can exist together in a dilute solution without interaction, but will react on a catalytic surface to form a deposit. Furthermore, the surface of the deposit is also catalytic to the reaction, so that the catalytic process continues until any reasonable plate thickness is applied. This autocatalytic effect is the principle upon which all electroless nickel solutions are based.

Metals that catalyze the plating reaction are members of group VIII in the periodic table, which group includes nickel, cobalt and palladium. A deposit will begin to form on surfaces of these metals by simple contact with the solution. Other metals, such as aluminum or low-alloy steel, first form an

* See page 432 for committee list.

Table 1. Typical Applications of Electroless Nickel Plating

Part and basis metal	Typical plate thickness, mils	Postplating heat treatment(a)
Plate Applied for Corrosion Resistance		
Valve body, cast iron	5.0	None
Printing rolls, cast iron	1.0	None
Electronic chassis, 1010 steel	1.0	None
Railroad tank cars, 1020 steel	3.5	1 hr at 1150 F
Reactor vessels, 1020 steel	4.0	1 hr at 1150 F
Pressure vessel, 4130 steel	1.5	3 hr at 350 F
Tubular shaft, 4340 steel	1.5	3 hr at 375 F
Plate Applied for Wear Resistance		
Centrifugal pump, steel	1.0	2 hr at 400 F
Plastic extrusion dies, steel	2.0	2 hr at 375 F
Printing-press bed, steel	1.0	None
Valve inserts, steel	0.5	2 hr at 1150 F
Hydraulic pistons, 4340 steel	1.0	1 hr at 750 F
Screws, 410 stainless	0.2	None
Stator and rotor blades, 410 stainless	0.8 to 1.0	1 hr at 750 F
Spray nozzles, brass	0.3	None
Plate Applied for Buildup of Worn Areas		
Carburized gear (bearing journal)	0.8 to 1.0	5 hr at 275 F
Splined shaft (ID spline), 16-25-6 stainless	0.5	1 hr at 750 F
Connecting arm (dowel-pin holes), type 410	5.0	1 hr at 750 F

(a) Heat treatments above 450 F should be carried out in an inert or reducing atmosphere.

immersion deposit of nickel on their surfaces, which then catalyzes the reaction; still others, such as copper, require a galvanic nickel deposit in order to be plated. Such a galvanic nickel deposit can be formed by the plating solution itself, if the copper is in contact with steel or aluminum.

Plastics, glass, ceramics and other nonmetallics also can be plated, if their surfaces can be made catalytic. This usually is done by the application of traces of a strongly catalytic metal to the nonmetallic surface by chemical or mechanical means.

There is, however, a group of metals that not only do not display any catalytic action, but also interfere with all plating activity. The salts of these metals, if dissolved in a solution even in comparatively small amounts, are poisons and stop the plating reaction on all metals, thus necessitating the discarding of the solution and the formulation of a new one. Examples of these anticatalysts are Pb, Sn, Zn, Cd, Sb, As and Mo.

Paradoxically, the deliberate introduction of extremely minute traces of poisons has been practiced by a number of users of electroless nickel, with the intent of stabilizing the solution. Being an inherently metastable mixture, electroless nickel solutions are likely to decompose spontaneously, with the nickel and hypophosphite reacting on trace amounts of solid impurities present in any plating bath. In order to minimize this problem, a poisoning element is added in trace concentrations of parts per million (or per trillion) to the original make-up of the solution. The poison is adsorbed on the solid impurities in quantities large enough to destroy their catalytic nature. This selective adsorption on catalytic centers decreases the concentration of the catalytic poison to a level below the critical threshold, so that normal deposition of nickel is not impeded, although the rate of deposition is somewhat reduced. The deliberate introduction of catalytic poisons for the purpose of stabilization is covered by several patents, including U. S. Patents 2,762,723 and 2,847,327.

Table 2. Alkaline Electroless Nickel Baths

Constituent or condition	Bath 1	Bath 2	Bath 3
Composition, Grams per Liter			
Nickel chloride	30	45	30
Sodium hypophosphite	10	11	10
Ammonium chloride	50	50	50
Sodium citrate	..	100	..
Ammonium citrate	..	..	65
Ammonium hydroxide	to pH	to pH	to pH
Operating Conditions			
pH	8 to 10	8.5 to 10	8 to 10
Temperature, F	195 to 205	195 to 205	195 to 205
Plating rate (approx), mil per hr	0.3	0.4	0.3

Alkaline Baths. Most alkaline baths in commercial use today are based on the original formulations developed by Brenner and Riddell. They contain a nickel salt, sodium hypophosphite, ammonium hydroxide, and an ammonium salt; they may also contain sodium citrate or ammonium citrate. The ammonium salt serves to complex the nickel and buffer the solution. Ammonium hydroxide is used to maintain the pH between 7.5 and 10. Table 2 gives the compositions and operating conditions of three alkaline electroless baths.

At the operating temperatures of these baths (about 200 F), ammonia losses are considerable. Thorough ventilation and frequent adjustment of pH are required. The alkaline solutions are inherently unstable and are particularly sensitive to the poisoning effects of anticatalysts such as lead, tin, zinc, cadmium, antimony, arsenic and molybdenum — even when these elements are present in only trace quantities. However, when depletion occurs, these solutions undergo a definite color change from blue to green, indicating the need for addition of ammonium hydroxide.

Acid baths are more widely used in commercial installations than alkaline baths. Essentially, acid baths contain a nickel salt, a hypophosphite salt, and a buffer; some solutions also contain a chelating agent. Frequently, wetting agents and stabilizers also are added.

These baths are more stable than alkaline solutions, are easier to control, and usually provide a higher plating rate. Except for the evaporation of water, there is no loss of chemicals when acid baths are heated to their operating range. Table 3 gives the compositions and operating conditions of several acid electroless baths.

Solution Control. In order to assure optimum results and consistent plating rates, the composition of the plating solution should be kept relatively constant; this requires periodic analyses for the determination of pH, nickel content, and phosphite and hypophosphite concentrations. The rate at which these analyses should be made depends on the quantity of work being plated and the volume and type of solution being used. The following methods have been employed:

pH — Standard electrometric method

Nickel — Any one of the colorimetric, gravimetric or volumetric methods is satisfactory; the cyanide method is probably the most popular.

Phosphite — A 10-ml sample of the plating solution is combined with 20 ml of a 5% solution of sodium bicarbonate and cooled in an ice bath. Next, 50 ml of 0.1*N* iodine solution is added and the flask containing this mixture is stoppered and permitted to stand for 2 hr at room temperature. Then the flask is cooled for 15 min in ice water, after which it is unstoppered, the mixture is acidified with acetic acid, and the excess iodine is titrated with 0.1*N* sodium thiosulfate, with starch as an indicator. Determination is then made as follows:

$$NaH_2PO_2 \text{ per liter} = \frac{\text{net ml of } 0.1N \text{ iodine} \times 6.3}{\text{ml of plating solution}}$$

Hypophosphite (U. S. Patent 2,697,651) — A 25-ml sample of the plating solution is diluted to 1 liter. A 5-ml aliquot of the

Table 3. Acid Electroless Nickel Plating Baths(a)

Constituent or condition	Bath 4	Bath 5	Bath 6	Bath 7	Bath 8	Bath 9
Composition, Grams per Liter						
Nickel chloride	30	..	..	30	..	30
Nickel sulfate	..	21	20	..	15	..
Sodium hypophosphite	10	24	27	10	14	12
Sodium acetate	..	..	..	..	13	..
Sodium hydroxyacetate	50	..	..	10	..	..
Sodium succinate	..	..	16	..	..	..
Lactic acid (80%)	..	34 ml	..	..	..	..
Propionic acid (100%)	..	2.2 ml	..	..	..	10
Operating Conditions						
pH	4 to 6	4.3 to 4.6	4.5 to 5.5	4 to 6	5 to 6	4.5 to 5.5
Temperature, F	190 to 210	203	200 to 210	190 to 210	190 to 210	190 to 210
Plating rate (approx), mil per hr	0.5	1.0	1.0	0.4	0.7	0.6

(a) Baths 4 and 7 are covered by U. S. Patent 2,532,283 (a public patent assigned to the National Bureau of Standards); bath 5, by U. S. Patents 2,822,293 and 2,822,294, and bath 6 by U. S. Patents 2,658,841 and 2,658,842.

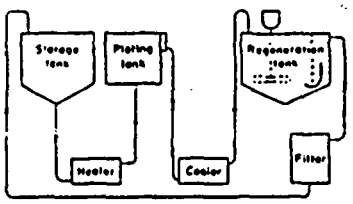

Fig. 1. Schematic of continuous-type system for electroless nickel plating. See text.

dilution is combined with 10 ml of a 10% solution of ammonium molybdate and 10 ml of fresh 6% sulfurous acid. The sample is covered and heated to boiling, and a deep blue color develops. The sample is cooled and diluted to 100 ml, and transmittance at a wave length of 440 microns is determined. The calibration curve on semilog paper is linear.

Hypophosphite (alternative method) — A 5-ml sample of the plating solution is mixed in a beaker with 5 ml of methyl orange solution made up of 1 gram of methyl orange in 1 liter of water. In another beaker is placed 15 ml of an acid solution made up by (a) dissolving 40 grams of sodium metabisulfate in 200 ml of water, (b) slowly adding the sodium metabisulfate solution to a cold solution of 82 ml of sulfuric acid in 650 ml of water, and then (c) diluting this mixture with water to 1 liter. When the acid solution and the solution containing the sample and methyl orange reach a temperature of 77 F in a thermostat, the two solutions are mixed. The time between mixing and the disappearance of the red color is recorded. The hypophosphite concentration is a function of this time and is read from a concentration-time curve made from known standards.

Equipment Requirements. The precleaning and post-treating equipment for an electroless nickel line is comparable to that employed in conventional electrodeposition. The plating tank itself, however, is unique.

The preferred plating tank for batch operations is constructed of stainless steel or aluminum and is lined with a coating of an inert material, such as tetrafluoroethylene or a phenolic-base organic. The size and shape of the tank are usually dictated by the parts to be plated, but the surface area of the plating solution should not be so large that excessive heat loss occurs as a result of evaporation.

A large heat-transfer area and a low temperature gradient are necessary between the heating medium and the plating solution. This combination provides for a reasonable heat-up time without local hot spots that could decompose the solution. It is accepted practice to surround the plating tank with a hot-water jacket or to immerse it in a tank containing hot water. Heating jackets using low-pressure steam also have been used successfully. The use of immersed steam coils is not favored, however, because it entails the sacrifice of a large amount of working area in the tank.

Accessory equipment required or recommended for the tank includes:

1 An accurate temperature controller
2 A filter to remove any suspended solids
3 A pH meter
4 An agitator to prevent gas streaking
5 On small tanks, a cover, to minimize heat loss and exclude foreign particles.
6 On large tanks, a separate small tank to dissolve and filter additives before they are put into the plating tank.

Considerably more equipment is required for a continuous-type system, such as that shown in Fig. 1. The bath is prepared and stored in a separate tank and flows through a heater (which raises its temperature to 205 F) into the plating tank. From the plating tank, the solution is pumped through a cooler, which decreases its temperature to 175 F or below, and then to an agitated regeneration tank, where reagents are added in controlled amounts to restore the solution to its original composition. The solution is then directed past a vertical underflow baffle and out of the regeneration tank to a filter, and then returned to storage.

In externally heated continuous-type systems such as the one shown in Fig. 1, the plating tank and other components of the system that come in contact with the plating solution are constructed of type 304 stainless steel and are not lined or coated; these components are periodically deactivated by chemical treatment. Details of this type of system are covered by several patents, including U. S. Patents 2,941,902; 2,858,839 and 2,874,073.

Properties of the Deposit. Electroless nickel is a hard, lamellar, brittle, uniform deposit. As plated, the hardness

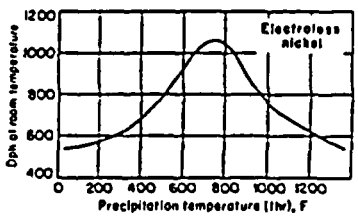

Effect of temperature of 1-hr precipitation heat treatment on room-temperature hardness of a typical electroless nickel deposit (Eberbach tester, 100-gram load). Above 450 F, heat treatment was in an inert atmosphere.

Fig. 2. Heat treatment of coating

varies over a considerable range (425 to 575 dph), depending primarily on phosphorus content, which ranges from 4 to 12%. This hardness can be increased by a precipitation heat treatment. As indicated in Fig. 2, which shows temperature-hardness relationships for a typical deposit, by heating at 750 F for ½ to 1 hr, hardness can be increased to about 1000 dph.

The corrosion resistance of electroless nickel deposits is superior to that of electrodeposited nickel of comparable thickness, but this superiority varies with exposure conditions. Outdoor exposure and salt spray corrosion data indicate that about 25% more resistance is given a steel panel by electroless nickel than by electrolytic.

Table 4. Physical Properties of Electroless Nickel Deposits

Property	Value
Specific gravity	7.8 to 8.5
Melting point	1638 to 1850 F
Electrical resistivity	60 microhm-cm
Thermal expansion	13 × 10^{-6} per °C
Thermal conductivity	0.0105 to 0.0135 cal/cm sec/°C

Table 5. Costs for Electroless Nickel Plating (Example 2) (a)

Cost factor	Cost per year (b)
Original investment	$18,000
Fixed costs:	
Depreciation (10 years)	$ 1,800
Insurance	450
Floor space (200 sq ft)	192
Repairs and maintenance	450
Variable costs:	
Raw material	6,100
Utilities	740
Labor costs:	
Direct	10,400
Indirect	2,630
Total	$22,762
Total cost per hr	$9.48
Total cost per sq ft coated to 1 mil	$1.00

(a) Exclusive of costs for: overhead and administration; racking, cleaning and unracking; and preplating and postplating processes. (b) Based on deposition of 1 mil on 0.1-sq-ft parts at rate of 0.8 mil per hr (capacity: 117 pieces, or 9.4 sq-ft/mil, per hr), on a schedule of 10 hr per day, 20 days per month, 2400 hr per year.

Some of the physical properties of electroless nickel are listed in Table 4.

Advantages and Limitations. Some advantages of electroless nickel are:

1 Good resistance to corrosion and wear
2 Excellent uniformity
3 Solderability and brazability
4 Good oxidation resistance.

Limitations of electroless nickel are:

1 High cost
2 Brittleness
3 Poor welding characteristics
4 Lead, tin, cadmium and zinc must be copper strike plated before electroless nickel can be applied
5 Slower plating rate (in general), as compared to electrolytic methods
6 Full brightness in deposit cannot be obtained without extreme brittleness.

Cost. Electroless nickel is considerably more expensive than electrodeposited nickel. Actual costs for electroless nickel plating, as reported by two users, are given in the following examples.

Example 1. Based on the experience of one manufacturing plant, it costs $1.20 to deposit an electroless nickel coating 1 mil thick on a square foot of surface area: 37¢ for chemicals, 59¢ for labor, and 24¢ for equipment and maintenance.

Example 2. Another manufacturing plant reports that it costs $1 per sq ft to plate a 1-mil thickness of electroless nickel on specific parts with a surface area of 0.1 sq ft, on the basis of data obtained over a one-year period (2400 working hours). An analysis of their costs is given in Table 5.

Selected References

A. Brenner, Electroless Plating Comes of Age, *Metal Finishing*, November 1954, p 60-70; December 1954, p 61-68

A. Brenner and G. Riddell, Nickel Plating on Steel by Chemical Reduction, *J Res Nat Bur Stds*, July 1946, p 31-34, and *Proc Am Electroplaters' Soc*, 1946, p 23-29; Deposition of Nickel and Cobalt by Chemical Reduction, *J Res Nat Bur Stds*, Nov 1947, p 385-393, and *Proc Am Electroplaters' Soc*, 1948, p 156-168

G. Gutzeit, Industrial Nickel Coating by Chemical Catalytic Reduction, *Trans Inst Metal Finishing*, 33, 383-412 (1955-1956), and *Corrosion Technol*, 3, 208 (1956)

G. Gutzeit, An Outline of the Chemistry Involved in the Process of Catalytic Nickel Deposition from Aqueous Solution, *Plating*, Oct 1959, p 1156-1164; Nov 1959, p 1275-1278; Dec 1959, p 1377-1378; Jan 1960, p 63-70

C. H. de Minjer and A. Brenner, Studies on Electroless Nickel Plating, *Plating*, December 1957, p 1297-1305

Symposium on Electroless Nickel Plating (Catalytic Deposition of Nickel-Phosphorus Alloys by Chemical Reduction in Aqueous Solution), *ASTM STP No. 265* (1959)

3.8.4 Keeler & Long Kolor-Poxy Primer No. 3200

E.140

KEELER & LONG INC.

HEADQUARTERS:
P. O. Box 460
856 Echo Lake Road
Watertown, CT 06795
Tel (860) 274-6701
Fax (860) 274-5857

KOLOR-POXY PRIMER
No. 3200

GENERIC TYPE: POLYAMIDE EPOXY

PRODUCT DESCRIPTION: A two component, high solids, polyamide epoxy primer/topcoat formulated to provide a high-build; abrasion, impact and chemical resistant coating.

RECOMMENDED USES: As a high-build primer for steel and concrete surfaces exposed to a wide range of conditions. No. 3200 is certified by the National Sanitation Foundation (NSF) and Ministry of Environment (Ontario and Saskatchewan, CN)** for application to the interior of potable water tanks.* No. 3200 is also accepted by the USDA for application to incidental food contact surfaces.

NOT RECOMMENDED FOR: Immersion in strong acids.

COMPATIBLE TOPCOATS:

Kolor-Poxy Primers and Enamels	Kolor-Sil Enamels
Kolor-Poxy Hi-Solids Primer	Acrythane Enamels
Kolor-Poxy Hi-Build Enamels	Kolorane Enamels
Poly-Silicone Enamels	Tri-Polar Silicone Enamels
Hydro-Poxy Enamels	

PRODUCT CHARACTERISTICS:

Solids by Volume:	66% ± 3%
Solids by Weight:	82% ± 3%
Recommended Dry Film Thickness:	2.5 - 6.0 mils
Theoretical Coverage:	350 Sq. Ft./Gallon @ 3.0 mils DFT
Finish:	Flat
Available Colors:	White and tints
Drying Time @ 72°F	
To Touch:	4 Hours
To Handle:	8 Hours
To Recoat:	24 Hours
To Immersion:	10 Days
VOC Content:	2.52 Pounds/Gallon 302 Grams/Liter

*
White or light gray only
5000 gallon tanks or larger
Up to four coats - Total DFT 24 mils maximum
Use No. 3700 Thinner up to 25% by volume

** Substrate temperature; 45°F (70°C) minimum during cure. Thorough rinse required after final cure.

June, 1994

TECHNICAL BULLETIN

No. 3200 E-140

TECHNICAL DATA

PHYSICAL DATA:	Weight per gallon:	13.6 ± 0.5 (pounds)
	Flash Point (Pensky-Martens):	85°F
	Shelf Life:	2 Years
	Pot Life @ 72°F:	8 Hours
	Temperature Resistance:	350°F
	Viscosity @ 77°F:	87 ± 5 (Krebs Units)
	Gloss (60° meter):	6 ± 5
	Storage Temperature:	50 - 95°F
	Mixing Ratio (Approx. by Volume):	4:1
APPLICATION DATA:	Application Procedure Guide:	APG-3
	Wet Film Thickness Range:	3.8 - 9.1 mils
	Dry Film Thickness Range:	2.5 - 6.0 mils
	Temperature Range:	50 - 120°F
	Relative Humidity:	80% Maximum
	Substrate Temperature:	Dew Point + 5°F
	Minimum Surface Preparation:	SSPC-SP6, SP10, SP5
	Induction Time @ 72°F:	45 Minutes
	Recommended Solvent	
	@ 50 - 85°F:	No. 3700
	@ 86 - 120°F:	No. 2200
	Application Methods	
	Air Spray	
	Tip Size:	.055" - .073"
	Pressure:	30 - 60 PSIG
	Thin:	1.0 - 2.0 Pts/Gal
	Airless Spray	
	Tip Size:	.015" - .019"
	Pressure:	2500 PSIG
	Thin:	0.5 - 1.5 Pts/Gal
	Brush or Roller	
	Thin:	0.5 - 1.5 Pts/Gal

KEELER & LONG INC.

P. O. Box 460, 856 Echo Lake Road
Watertown, CT 06795
Tel: (860) 274-6701 Fax: (860) 274-5857

This information is presented as accurate and correct, in good faith, to assist the user in specification and application. No warranty is expressed or implied. No liability is assumed. Product specifications are subject to change without notice. Data listed above is for white or base color of the product. Data for other colors may differ.

SUSTAINING MEMBER

3.8.5 Acrythane Enamel Y-1 Series Top Coating

U.150

KEELER & EDWARDS INC.

HEADQUARTERS:
P. O. Box 460
856 Echo Lake Road
Watertown, CT 06795
Tel (860) 274-6701
Fax (860) 274-5857

ACRYTHANE ENAMEL
Y-1-SERIES

GENERIC TYPE: ACRYLIC URETHANE

PRODUCT DESCRIPTION: A two component, acrylic urethane high-gloss enamel formulated to provide maximum appearance and protective qualities when exposed to an exterior environment. It produces the ultimate in long term color and gloss retention.

RECOMMENDED USES: As a topcoat for exterior structural steel, tanks, piping, conveyors, equipment, and other similar surfaces, as well as interior and exterior concrete surfaces.

NOT RECOMMENDED FOR: Immersion service; splash and spillage of strong acids and alkalies.

COMPATIBLE UNDERCOATS:
Kolorane Aluminum Primer
Kolorane Zinc Rich Primer
Kolor-Poxy Primers and Enamels
Kolor-Poxy Hi-Solids Primer
Acrythane Intermediate Primer
Kolor-Poxy Surfacer

PRODUCT CHARACTERISTICS:

Solids by Volume:	52% ± 5%
Solids by Weight:	67% ± 5%
Recommended Dry Film Thickness:	2.0 - 4.0 mils
Theoretical Coverage:	278 Sq. Ft./Gallon @ 3.0 mils DFT
Finish:	Full Gloss
Available Colors:	Unlimited
Drying Time @ 72°F	
To Touch:	6 Hours
To Handle:	12 Hours
To Recoat:	24 Hours
VOC Content:	< 3.5 Pounds/Gallon < 420 Grams/Liter

June, 1995

TECHNICAL BULLETIN

Y-SERIES U-150

TECHNICAL DATA

PHYSICAL DATA:	Weight per gallon:	10.5 ± 0.5 (pounds)
	Flash Point (Pensky-Martens):	85°F
	Shelf Life:	1 Year
	Pot Life @ 72°F:	6 Hours
	Temperature Resistance:	250°F
	Viscosity @ 77°F:	75 ± 5 (Krebs Units)
	Gloss (60° meter):	90 ± 5 (Y-1)
	Storage Temperature:	45 - 95°F
	Mixing Ratio (Approx. by Volume):	4.2:1 (White only)
APPLICATION DATA:	Application Procedure Guide:	APG-5
	Wet Film Thickness Range:	3.5 - 7.0 mils
	Dry Film Thickness Range:	2.0 - 4.0 mils
	Temperature Range:	45 - 100°F
	Relative Humidity:	80% Maximum
	Substrate Temperature:	Dew Point + 5°F
	Minimum Surface Preparation:	Primed
	Induction Time @ 72°F:	None
	Recommended Solvent	
	@ 45 - 85°F:	No. 1200
	@ 86 - 100°F:	No. 0700
	Application Methods	
	Air Spray	
	Tip Size:	.055"
	Pressure:	30 - 60 PSIG
	Thin:	0.5 - 2.0 Pts/Gal
	Airless Spray	
	Tip Size:	.011" - .015"
	Pressure:	2000 - 2500 PSIG
	Thin:	0.0 - 1.5 Pts/Gal
	Brush or Roller	Recommended only with limitations
	Thin (No. 0700):	0.5 - 1.5 Pts/Gal

KEELER & LONG INC.

P. O. Box 460, 856 Echo Lake Road
Watertown, CT 06795
Tel: (860) 274-6701 Fax: (860) 274-5857

This information is presented as accurate and correct, in good faith, to assist the user in specification and application. No warranty is expressed or implied. No liability is assumed. Product specifications are subject to change without notice. Data listed above is for white or base color of the product. Data for other colors may differ.

SSPC SUSTAINING MEMBER

THIS PAGE INTENTIONALLY LEFT BLANK

Table of Contents

4.0 THERMAL EVALUATION 4.1-1

4.1 Discussion 4.1-1

4.2 Summary of Thermal Properties of Materials 4.2-1

4.3 Technical Specifications for Components 4.3-1

4.4 Thermal Evaluation for Normal Conditions of Storage 4.4-1

4.4.1 Thermal Models 4.4.1-1

4.4.1.1 Two-Dimensional Axisymmetric Air Flow and Concrete Cask Models 4.4.1-3

4.4.1.2 Three-Dimensional Canister Models 4.4.1-14

4.4.1.3 Three-Dimensional Transfer Cask and Canister Models 4.4.1-27

4.4.1.4 Three-Dimensional Periodic Canister Internal Models 4.4.1-31

4.4.1.5 Two-Dimensional Fuel Models 4.4.1-35

4.4.1.6 Two-Dimensional Fuel Tube Models 4.4.1-38

4.4.1.7 Two-Dimensional Forced Air Flow Model for Transfer Cask Cooling 4.4.1-44

4.4.2 Test Model 4.4.2-1

4.4.3 Maximum Temperatures for PWR and BWR Fuel 4.4.3-1

4.4.3.1 Maximum Temperatures at Reduced Total Heat Loads 4.4.3-2

4.4.4 Minimum Temperatures 4.4.4-1

4.4.5 Maximum Internal Pressures 4.4.5-1

4.4.5.1 Maximum Internal Pressure for PWR Fuel Canister 4.4.5-1

4.4.5.2 Maximum Internal Pressure for BWR Fuel Canister 4.4.5-3

4.4.6 Maximum Thermal Stresses 4.4.6-1

4.4.7 Evaluation of System Performance for Normal Conditions of Storage 4.4.7-1

Table of Contents (Continued)

4.5 Thermal Evaluation for Site Specific Spent Fuel 4.5-1
4.5.1 Maine Yankee Site Specific Spent Fuel 4.5-1
4.5.1.1 Thermal Evaluation for Maine Yankee Site Specific Spent Fuel 4.5-3
4.5.1.2 Preferential Loading with Higher Heat Load (1.05 kW) at the Basket Periphery 4.5-17

4.6 References 4.6-1

List of Figures

Figure 4.3-1 PWR Heat Transfer Disk Model for Normal Handling Condition 4.3-2
Figure 4.3-2 BWR Heat Transfer Disk Model for Normal Handling Condition 4.3-3
Figure 4.4.1.1-1 Two-Dimensional Axisymmetric Air Flow and Concrete Cask Model: PWR 4.4.1-10
Figure 4.4.1.1-2 Two-Dimensional Axisymmetric Air Flow and Concrete Cask Finite Element Model: PWR 4.4.1-11
Figure 4.4.1.1-3 Axial Power Distribution for PWR Fuel 4.4.1-12
Figure 4.4.1.1-4 Axial Power Distribution for BWR Fuel 4.4.1-13
Figure 4.4.1.2-1 Three-Dimensional Canister Model for PWR Fuel 4.4.1-19
Figure 4.4.1.2-2 Three-Dimensional Canister Model for PWR Fuel - Cross Section 4.4.1-20
Figure 4.4.1.2-3 Three-Dimensional Canister Model for BWR Fuel 4.4.1-21
Figure 4.4.1.2-4 Three-Dimensional Canister Model for BWR Fuel - Cross Section 4.4.1-22
Figure 4.4.1.3-1 Three-Dimensional Transfer Cask and Canister Model - PWR 4.4.1-29
Figure 4.4.1.3-2 Three-Dimensional Transfer Cask and Canister Model - BWR 4.4.1-30
Figure 4.4.1.4-1 Three-Dimensional Periodic Canister Internal Model - PWR 4.4.1-33
Figure 4.4.1.4-2 Three-Dimensional Periodic Canister Internal Model - BWR 4.4.1-34
Figure 4.4.1.5-1 Two-Dimensional PWR (17 × 17) Fuel Model 4.4.1-37
Figure 4.4.1.6-1 Two-Dimensional Fuel Tube Model: PWR Fuel 4.4.1-41
Figure 4.4.1.6-2 Two-Dimensional Fuel Tube Model: BWR Fuel Tube with Neutron Absorber 4.4.1-42
Figure 4.4.1.6-3 Two-Dimensional Fuel Tube Model: BWR Fuel Tube without Neutron Absorber 4.4.1-43
Figure 4.4.1.7-1 Two-Dimensional Axisymmetric Finite Element Model for Transfer Cask Forced Air Cooling 4.4.1-45
Figure 4.4.1.7-2 Two-Dimensional Axisymmetric Outlet Air Flow Model for Transfer Cask Cooling 4.4.1-46
Figure 4.4.1.7-3 Two-Dimensional Axisymmetric Inlet Air Flow Model for Transfer Cask Cooling 4.4.1-47
Figure 4.4.1.7-4 Non-Uniform Heat Load from Canister Contents 4.4.1-48

List of Figures (continued)

Figure 4.4.1.7-5 Maximum Canister Temperature Versus Air Volume Flow Rate 4.4.1-49

Figure 4.4.3-1 Temperature Distribution (°F) for the Normal Storage Condition: PWR Fuel 4.4.3-6
Figure 4.4.3-2 Air Flow Pattern in the Concrete Cask in the Normal Storage Condition: PWR Fuel 4.4.3-7
Figure 4.4.3-3 Air Temperature (°F) Distribution in the Concrete Cask During the Normal Storage Condition: PWR Fuel 4.4.3-8
Figure 4.4.3-4 Concrete Temperature (°F) Distribution During the Normal Storage Condition: PWR Fuel 4.4.3-9
Figure 4.4.3-5 History of Maximum Component Temperature (°F) for Transfer Conditions for PWR Fuel with Design Basis 23 kW Uniformly Distributed Heat Load 4.4.3-10
Figure 4.4.3-6 History of Maximum Component Temperature (°F) for Transfer Conditions for BWR Fuel with Design Basis 23 kW Uniformly Distributed Heat Load 4.4.3-11
Figure 4.4.3-7 Basket Location for the Thermal Analysis of PWR Reduced Heat Load Cases 4.4.3-12
Figure 4.4.3-8 BWR Fuel Basket Location Numbers 4.4.3-13

Figure 4.5.1.1-1 Quarter Symmetry Model for Maine Yankee Consolidated Fuel 4.5-12
Figure 4.5.1.1-2 Maine Yankee Three-Dimensional Periodic Canister Internal Model 4.5-13
Figure 4.5.1.1-3 Evaluated Locations for the Maine Yankee Consolidated Fuel Lattice in the PWR Fuel Basket 4.5-14
Figure 4.5.1.1-4 Active Fuel Region in the Three-Dimensional Canister Model 4.5-15
Figure 4.5.1.1-5 Fuel Debris and Damaged Fuel Regions in the Three-Dimensional Canister Model 4.5-16
Figure 4.5.1.2-1 Canister Basket Preferential Loading Plan 4.5-19

List of Tables

Table 4.1-1 Summary of Thermal Design Conditions for Storage 4.1-4
Table 4.1-2 Summary of Thermal Design Conditions for Transfer 4.1-5
Table 4.1-3 Maximum Allowable Material Temperatures 4.1-6
Table 4.1-4 Summary of Thermal Evaluation Results for the Universal Storage System: PWR Fuel 4.1-7
Table 4.1-5 Summary of Thermal Evaluation Results for the Universal Storage System: BWR Fuel 4.1-8
Table 4.2-1 Thermal Properties of Solid Neutron Shield (NS-4-FR and NS-3) 4.2-2
Table 4.2-2 Thermal Properties of Stainless Steel 4.2-2
Table 4.2-3 Thermal Properties of Carbon Steel 4.2-3
Table 4.2-4 Thermal Properties of Chemical Copper Lead 4.2-3
Table 4.2-5 Thermal Properties of Type 6061-T651 Aluminum Alloy 4.2-3
Table 4.2-6 Thermal Properties of Helium 4.2-4
Table 4.2-7 Thermal Properties of Dry Air 4.2-4
Table 4.2-8 Thermal Properties of Zircaloy and Zircaloy-4 Cladding 4.2-5
Table 4.2-9 Thermal Properties of Fuel (UO_2) 4.2-5
Table 4.2-10 Thermal Properties of BORAL Composite Sheet 4.2-6
Table 4.2-11 Thermal Properties of Concrete 4.2-6
Table 4.2-12 Thermal Properties of Water 4.2-7
Table 4.2-13 Thermal Properties of METAMIC 4.2-7
Table 4.4.1.2-1 Effective Thermal Conductivities for PWR Fuel Assemblies 4.4.1-23
Table 4.4.1.2-2 Effective Thermal Conductivities for BWR Fuel Assemblies 4.4.1-24
Table 4.4.1.2-3 Effective Thermal Conductivities for PWR Fuel Tubes 4.4.1-25
Table 4.4.1.2-4 Effective Thermal Conductivities for BWR Fuel Tubes 4.4.1-26

Table 4.4.3-1 Maximum Component Temperatures for the Normal Storage Condition - PWR 4.4.3-14
Table 4.4.3-2 Maximum Component Temperatures for the Normal Storage Condition - BWR 4.4.3-15
Table 4.4.3-3 Maximum Component Temperatures for the Transfer Condition – PWR Fuel with Design Basis 23 kW Uniformly Distributed Heat Load 4.4.3-16

List of Tables (continued)

Table 4.4.3-4 Maximum Component Temperatures for the Transfer Condition – BWR Fuel with Design Basis 23 kW Uniformly Distributed Heat Load 4.4.3-16
Table 4.4.3-5 Maximum Limiting Component Temperatures in Transient Operations for the Reduced Heat Load Cases for PWR Fuel 4.4.3-17
Table 4.4.3-6 Maximum Limiting Component Temperatures in Transient Operations for the Reduced Heat Load Cases for PWR Fuel after In-Pool Cooling 4.4.3-18
Table 4.4.3-7 Maximum Limiting Component Temperatures in Transient Operations for the Reduced Heat Load Cases for PWR Fuel after Forced-Air Cooling 4.4.3-18
Table 4.4.3-8 Maximum Limiting Component Temperatures in Transient Operations for BWR Fuel 4.4.3-19
Table 4.4.3-9 Maximum Limiting Component Temperatures in Transient Operations after Vacuum for BWR Fuel after In-Pool Cooling 4.4.3-20
Table 4.4.3-10 Maximum Limiting Component Temperatures in Transient Operations after Vacuum for BWR Fuel after Forced-Air Cooling. 4.4.3-20
Table 4.4.3-11 Maximum Limiting Component Temperatures in Transient Operations after Helium for BWR Fuel after In-Pool Cooling..... 4.4.3-21
Table 4.4.3-12 Maximum Limiting Component Temperatures in Transient Operations after Helium for BWR Fuel after Forced-Air Cooling.. 4.4.3-21
Table 4.4.3-13 Maximum Limiting Component Temperatures in Transient Operations after Helium for PWR Fuel after In-Pool Cooling 4.4.3-21
Table 4.4.3-14 Maximum Limiting Component Temperatures in Transient Operations after Helium for PWR Fuel after Forced-Air Cooling .. 4.4.3-22
Table 4.4.5-1 PWR Per Assembly Fuel Generated Gas Inventory..... 4.4.5-4
Table 4.4.5-2 PWR Canister Free Volume (No Fuel or Inserts) 4.4.5-4
Table 4.4.5-3 PWR Maximum Normal Condition Pressure Summary..... 4.4.5-4
Table 4.4.5-4 BWR Per Assembly Fuel Generated Gas Inventory 4.4.5-5
Table 4.4.5-5 BWR Canister Free Volume (No Fuel or Inserts)..... 4.4.5-5
Table 4.4.5-6 BWR Maximum Normal Condition Pressure Summary 4.4.5-5

4.0 THERMAL EVALUATION

This section presents the thermal design and analyses of the Universal Storage System for normal conditions of storage of spent nuclear fuel. The analyses include consideration of design basis PWR and BWR fuel. Results of the analyses demonstrate that with the design basis contents, the Universal Storage System meets the thermal performance requirements of 10 CFR 72 [1].

4.1 Discussion

The Universal Storage System consists of a Transportable Storage Canister, Vertical Concrete Cask, and a transfer cask. In long-term storage, the canister is installed in the concrete cask, which provides passive radiation shielding and natural convection cooling. The fuel is loaded in a basket structure positioned within the canister. The transfer cask is used for the handling of the canister. The thermal performance of the concrete cask containing the design basis fuel (during storage) and the performance of the transfer cask containing design basis fuel (during handling) are evaluated herein.

The significant thermal design feature of the Vertical Concrete Cask is the passive convective air flow up along the side of the canister. Cool (ambient) air enters at the bottom of the concrete cask through four inlet vents. Heated air exits through the four outlets at the top of the cask. Radiant heat transfer occurs from the canister shell to the concrete cask liner, which also transmits heat to the adjoining air flow. Conduction does not play a substantial role in heat removal from the canister surface. Natural circulation of air inside the Vertical Concrete Cask, in conjunction with radiation from the canister surface, maintains the fuel cladding temperature and all of the concrete cask component temperatures below their design limits.

The UMS® Storage System design basis heat load is 23.0 kW for up to 24 PWR (0.958 kW per assembly) or up to 56 BWR (0.411 kW per assembly) fuel assemblies, except in cases where preferential loading patterns are employed.

The thermal evaluation considers normal, off-normal, and accident conditions of storage. Each of these conditions can be described in terms of the environmental temperature, use of solar insolation, and the condition of the air inlets and outlets, as shown in Table 4.1-1. The design conditions for transfer are defined in Table 4.1-2. The transfer conditions consider the transient effect for PWR and BWR fuel, starting from the removal of the transfer cask/canister from the spent fuel pool. The canister is considered under normal operation to be inside the transfer cask and initially filled with water. The canister is vacuum dried, back-filled with helium and then transferred into the Vertical Concrete Cask. As shown in Section 4.4.3, the time duration of the spent fuel in the water and vacuum conditions is administratively controlled to prevent general boiling of the water and to ensure that the allowable temperatures of the limiting components (fuel cladding, structural disks and heat transfer disks) are not exceeded.

This evaluation applies different component temperature limits and different material stress limits for long-term conditions and short-term conditions. Normal storage is considered to be a long-term condition. Off-normal and accident events, as well as the transfer condition that temporarily occurs during the preparation of the canister while it is in the transfer cask, are considered as short-term conditions. Thermal evaluations are performed for the design basis PWR and BWR fuels for all design conditions. The maximum allowable material temperatures for long-term and short-term conditions are provided in Table 4.1-3.

During normal conditions of storage and hypothetical accident conditions, the concrete cask must reject the fuel decay heat to the environment without exceeding the operational temperature ranges of the components important to safety. In addition, to maintain fuel rod integrity for normal conditions of storage the fuel must be maintained at a sufficiently low temperature in an inert atmosphere to preclude thermally induced fuel rod cladding deterioration. To preclude fuel degradation, the maximum allowable cladding temperature under normal conditions of storage and transfer for PWR fuel and BWR fuel is 752°F (400°C) in accordance with ISG-11, Rev 2 [38]. For either of these fuel types, the maximum cladding temperature under off-normal and accident conditions must remain below 1,058°F (570°C). Finally, for the structural components of the storage system, the thermally induced stresses, in combination with pressure and mechanical load stresses, must be below material allowable stress levels.

Thermal evaluations for normal conditions of storage and transfer (canister handling) condition operations are presented in Section 4.4. The finite element method is used to calculate the temperatures for the various components of the concrete cask, canister, basket, fuel cladding and transfer cask. Thermal models used in evaluation of normal and transfer conditions are described in Section 4.4.1.

A summary of the thermal evaluation results for the Universal Storage System are provided in Tables 4.1-4 and 4.1-5 for the PWR and BWR cases, respectively. Evaluation results for accident conditions of "All air inlets and outlets blocked" and "Fire" are presented in Chapter 11. The results demonstrate that the calculated temperatures are below the allowable component temperatures for all normal (long-term) storage conditions and for short-term events. The thermally induced stresses, combined with pressure and mechanical load stresses, are also within the allowable levels, as demonstrated in Chapter 3.

Table 4.1-1 Summary of Thermal Design Conditions for Storage

Condition[1]		Environmental Temperature (°F)	Solar Insolation[2]	Condition of Concrete Cask Inlets and Outlets
Normal		76	Yes	All inlets and outlets open
Off-Normal - Half Air Inlets Blocked		76	Yes	Half inlets blocked and all outlets open
Off-Normal - Severe Heat		106	Yes	All inlets and outlets open
Off-Normal - Severe Cold		-40	No	All inlets and outlets open
Accident - Extreme Heat		133	Yes	All inlets and outlets open
Accident - All Air Inlets and Outlets Blocked[3]		76	Yes	All inlets and outlets blocked
Accident - Fire[4]	During Fire	1475	Yes	All inlets and outlets open
	Before and After Fire	76	Yes	All inlets and outlets open

1. Off-normal and accident condition analyses are presented in Chapter 11.
2. Solar Insolation per 10 CFR 71:
   Curved Surface: 400 g cal/cm^2 (1475 Btu/ft^2) for a 12-hour period.
   Flat Horizontal Surface: 800 g cal/cm^2 (2950 Btu/ft^2) for a 12-hour period.
3. This condition bounds the case in which all inlets are blocked, with all outlets open.
4. The evaluated fire accident is the described in Section 11.2.6.

Table 4.1-2 Summary of Thermal Design Conditions for Transfer

Condition[1,2]	Maximum Duration (Hours)[3]	
	PWR	BWR
Canister Filled with Water[4]	17	17
Vacuum Drying	27	25
Canister Filled with Helium	20	16

(1) The canister is inside the transfer cask, with an ambient temperature of 76°F.

(2) See Section 8.1 for description of limiting conditions.

(3) Maximum durations based on 23 kW heat load.

(4) The initial water temperature is considered to be 100°F.

Table 4.1-3 Maximum Allowable Material Temperatures

Material	Temperature Limits (°F)		Reference
	Long Term	Short Term	
Concrete	150(B)/300(L)(1)	350	ACI-349 [4]
Fuel Clad PWR Fuel (5-year cooled) BWR Fuel (5-year cooled)	 752 752	 752/1,058(2) 752/1,058(2)	ISG-11 [38] and PNL-4835 [2]
Aluminum 6061-T651	650	750	MIL-HDBK-5G [7]
NS-4-FR	300	300	GESC [8]
Chemical Copper Lead	600	600	Baumeister [9]
SA693 17-4PH Type 630 Stainless Steel	650	800	ASME Code [13] ARMCO [11]
SA240 Type 304 Stainless Steel	800	800	ASME Code [13]
SA240 Type 304L Stainless Steel	800	800	ASME Code [13]
ASTM A533 Type B Carbon Steel	700	700	ASME Code [13]
ASME SA588 Carbon Steel	700	700	ASME Code Case N-71-17 [12]
ASTM A36 Carbon Steel	700	700	ASME Code Case N-71-17 [12]

(1) B and L refer to bulk temperatures and local temperatures, respectively. The local temperature allowable applies to a restricted region where the bulk temperature allowable may be exceeded.

(2) The temperature limit of the fuel cladding is 400°C (752°F) for storage (long-term) and transfer (short-term) conditions. The temperature limit of the fuel cladding is 570°C (1,058°F) for off-normal and accident (short-term) conditions.

Table 4.1-4 Summary of Thermal Evaluation Results for the Universal Storage System: PWR Fuel

Long-Term Condition:						
	Maximum Temperatures (°F)					
Design Condition	Concrete Bulk	Concrete Local	Heat Transfer Disks	Support Disks[1]	Canister[2]	Fuel Clad
Normal (76°F Ambient)	135	186	599	601	351	648
Allowable	150	300	650	650	800	752
Short-Term Condition:						
	Maximum Temperatures (°F)					
Design Condition	Concrete		Heat Transfer Disks	Support Disks[1]	Canister[2]	Fuel Clad
Off-Normal - Half Inlets Blocked (76°F Ambient)	191		600	603	350	649
Off-Normal - Severe Heat (106°F Ambient)	228		626	628	381	672
Off-Normal - Severe Cold (-40°F Ambient	17		502	505	226	561
Accident - Extreme Heat (133°F Ambient)	262		648	650	408	693
Accident - Fire	244		639	641	391	688
Allowable	350		750	800	800	1058
	Maximum Temperatures (°F)					
Transfer - Vacuum Drying	N/A		641	644	304	732
Transfer - Backfilled with Helium	N/A		680	683	455	732
Allowable	350		750	800	800	752

1. SA 693, 17-4PH Type 630 SS.
2. SA240, Type 304L SS (including canister shell, lid and bottom plate).

Table 4.1-5 Summary of Thermal Evaluation Results for the Universal Storage System: BWR Fuel

Long-Term Condition:						
	Maximum Temperatures (°F)					
Design Condition	Concrete Bulk	Concrete Local	Heat Transfer Disks	Support Disks[1]	Canister[2]	Fuel Clad
Normal (76°F Ambient)	136	192	612	614	376	642
Allowable	150	300	650	700	800	752

Short-Term Condition:					
	Maximum Temperatures (°F)				
Design Condition	Concrete	Heat Transfer Disks	Support Disks[1]	Canister[2]	Fuel Clad
Off-Normal - Half Inlets Blocked (76°F Ambient)	195	612	614	373	642
Off-Normal - Severe Heat (106°F Ambient)	231	638	640	405	667
Off-Normal - Severe Cold (-40°F Ambient)	20	504	505	252	540
Accident - Extreme Heat (133°F Ambient)	266	662	664	432	690
Accident - Fire	244	652	654	416	682
Allowable	350	750	700	800	1058
	Maximum Temperatures (°F)				
Transfer - Vacuum Drying	N/A	653	659	267	733
Transfer - Backfilled with Helium	N/A	683	686	462	733
Allowable	350	750	700	800	752

1. SA 533, Type B, CS.
2. SA240, Type 304L SS (including canister shell, lid and bottom plate).

4.2 Summary of Thermal Properties of Materials

The material thermal properties used in the thermal analyses are shown in Tables 4.2-1 through 4.2-13. Derivation of effective conductivities is described in Section 4.4.1. Tables 4.2-1 through 4.2-13 include only the materials that form the heat transfer pathways employed in the thermal analysis models. Materials for small components, which are not directly modeled are not included in the property tabulation.

Table 4.2-1 Thermal Properties of Solid Neutron Shield (NS-4-FR and NS-3)

Property (units) [8]	NS-4-FR	NS-3
Conductivity (Btu/hr-in-°F)	0.0311	0.0407
Density (borated) (lbm/in^3)	0.0589	0.0621
Density (nonborated) (lbm/in^3)	0.0607	0.0640
Specific Heat (Btu/lbm-°F)	0.319	0.149

Table 4.2-2 Thermal Properties of Stainless Steel

Type 304 and 304L

Property (units)	Value at Temperature				
	100°F	200°F	400°F	550°F	750°F
Conductivity (Btu/hr-in-°F) [13]	0.7250	0.7750	0.8667	0.9250	1.0000
Density (lb/in^3) [14]	0.2896	0.2888	0.2872	0.2857	0.2839
Specific Heat (Btu/lbm-°F) [14]	0.1156	0.1202	0.1274	0.1314	0.1355
Emissivity [14]	← 0.36 →				

17-4PH, Type 630

Property (units)	Value at Temperature			
	70°F	200°F	400°F	650°F
Conductivity (Btu/hr-in-°F) [13]	0.824	0.883	0.975	1.083
Density (lb/in^3) [13]	← 0.291 →			
Specific Heat (Btu/lbm-°F) [11]	← 0.11 →			
Emissivity [15]	← 0.58 →			

Table 4.2-3 Thermal Properties of Carbon Steel

Material[1] Property (units)	Value at Temperature					
	100°F	200°F	400°F	500°F	700°F	800°F
Conductivity (Btu/hr-in-°F) [13]	1.992	2.033	2.017	1.975	1.867	1.808
Density (lb/in^3) [16]	← 0.284 →					
Specific Heat (Btu/lbm-°F) [17]	← 0.113 →					
Emissivity [9]	← 0.80 →					

1. A-36, SA-533, A-588 and SA-350.

Table 4.2-4 Thermal Properties of Chemical Copper Lead

Property (units)	Value at Temperature			
	209°F	400°F	581°F	630°F
Conductivity (Btu/hr-in-°F) [18]	1.6308	1.5260	1.2095	1.0079
Density (lb/in^3) [18]	← 0.411 →			
Specific Heat (Btu/lbm-°F) [18]	← 0.03 →			
Emissivity [9]	← 0.28 (75°F) →			

Table 4.2-5 Thermal Properties of Type 6061-T651 Aluminum Alloy

Property (units)	Value at Temperature					
	200°F	300°F	400°F	500°F	600°F	750°F
Conductivity (Btu/hr-in-°F) [7,13]	8.25	8.38	8.49	8.49	8.49	8.49
Specific Heat (Btu/hr-in-°F) [13]	← 0.23 →					
Emissivity [15]	← 0.22 →					

Table 4.2-6 Thermal Properties of Helium

Property (units)	Value at Temperature			
	80°F	260°F	440°F	800°F
Conductivity (Btu/hr-in-°F) [20]	0.00751	0.00915	0.01068	0.01355

Property (units)	Value at Temperature			
	200°F	400°F	600°F	800°F
Density (lb/in^3) [19]	4.83E-06	3.70E-06	3.01E-06	2.52E-06
Specific Heat (Btu/lbm-°F) [19]	← 1.24 →			

Table 4.2-7 Thermal Properties of Dry Air

Property (units)	Value at Temperature			
	100°F	300°F	500°F	700°F
Conductivity (Btu/hr-in-°F) [19]	0.00128	0.00161	0.00193	0.00223
Density (lb/in^3) [19]	4.11E-05	3.01E-05	2.38E-05	1.97E-05
Specific Heat (Btu/lbm-°F) [19]	0.240	0.244	0.247	0.253

Table 4.2-8 Thermal Properties of Zircaloy and Zircaloy-4 Cladding

Property (units)	Value at Temperature			
	392°F	572°F	752°F	932°F
Conductivity (Btu/hr-in-°F) [22]	0.69	0.73	0.80	0.87
Density (lb/in^3) [23]	← 0.237 →			
Specific Heat (Btu/lbm-°F) [22]	0.072	0.074	0.076	0.079
Emissivity [22]	← 0.75 →			

Table 4.2-9 Thermal Properties of Fuel (UO_2)

Property (units)	Value at Temperature				
	100°F	257°F	482°F	707°F	932°F
Conductivity (Btu/hr-in-°F) [22]	0.38	0.347	0.277	0.236	0.212
Specific Heat (Btu/lbm-°F) [22]	0.057	0.062	0.067	0.071	0.073
Density (lbm/in^3) [23]	← 0.396 →				
Emissivity [22]	← 0.85 →				

Table 4.2-10 Thermal Properties of BORAL Composite Sheet

Property (units)	Value at Temperature	
	100°F	500°F
Conductivity (Btu/hr-in-°F)		
Aluminum Clad [24]	7.805	8.976
Core Matrix		
PWR (calculated)	3.45	3.05
BWR (calculated)	6.60	7.23
Emissivity[1] [25]	← 0.15 →	

[1] The emissivity of the aluminum clad of the BORAL sheet ranges from 0.10 to 0.19. An averaged value of 0.15 is used.

Table 4.2-11 Thermal Properties of Concrete

Property (units)	Value at Temperature		
	100°F	200°F	300°F
Conductivity (Btu/hr-in-°F) [26]	0.091	0.089	0.086
Density (lbm/in^3) [27]	← 140 →		
Specific Heat (Btu/lbm-°F) [17]	← 0.20 →		
Emissivity [1] [17,28]	← 0.90 →		
Absorptivity [29]	← 0.60 →		

[1] Emissivity = 0.93 for masonry, 0.94 for rough concrete; 0.9 is used.

Table 4.2-12 Thermal Properties of Water

Property (units)	Value at Temperature		
	70°F	200°F	300°F
Conductivity (Btu/hr-in-°F) [32]	0.029	0.033	0.033
Specific Heat (Btu/lbm-°F) [32]	0.998	1.00	1.03
Density (lbm/in³) [32]	0.036	0.035	0.033

Table 4.2-13 Thermal Properties of METAMIC

Property (units)	Value at Temperature		
	77°F	212°F	482°F
Conductivity (Btu/hr-in-°F) [37]	4.54	4.42	4.64
Specific Heat (Btu/lbm-°F) [37]	0.2207	0.2412	0.2938
Density (lbm/in^3) [37]	← 0.094 →		

THIS PAGE INTENTIONALLY LEFT BLANK

4.3 Technical Specifications for Components

Five major components of the Universal Storage System must be maintained within their safe operating temperature ranges: the concrete, the lead gamma shield, the NS-4-FR solid neutron shield in the transfer cask, the aluminum heat transfer disks and steel (17-4PH and ASTM A533) support disks in the basket structure inside the canister. The safe operating ranges for these components are from a minimum temperature of -40°F to the maximum temperatures as shown in Table 4.1-3.

The criterion for the safe operating range of the lead gamma shield is the prevention of the lead from reaching its melting point of 620°F [9]. The maximum operating temperature limit of the NS-4-FR solid neutron shield material, determined by the manufacturer, is to ensure sufficient neutron shielding capacity.

The primary consideration in establishing the safe operating range of the aluminum heat transfer disks and steel support disks is maintaining the integrity of the aluminum and steel.

The temperature limit for the aluminum heat transfer disks is 650°F and 750°F for the long-term and short-term conditions, respectively, based on data from MIL-HDBK-5G. Note that the heat transfer disk is not a structural component. During the limiting condition (short term) of canister transfer, the heat transfer disk is subjected to a maximum loading of 1.1 g (normal handling). An evaluation is performed for the heat transfer disks for both PWR and BWR configurations to the stresses for this condition. Two quarter-symmetry models were generated using ANSYS SHELL63 elements for the evaluation, as shown in Figures 4.3-1 and 4.3-2. The disks are supported at the basket tie-rod locations in the canister axial direction. Symmetry boundary conditions are applied at the planes of symmetry. An inertia load of 1.1 g is applied to the disk in the out-of-plane direction.

The analysis results indicate that the stress is less than 0.13 ksi at the central region of the basket where maximum temperature occurs for both the PWR and BWR configuration. The corresponding margin of safety is + 9.8 based on the yield stress of 1.4 ksi at 750°F. Therefore, the aluminum heat transfer disk will maintain its integrity as long as it does not exceed the temperature limits.

Figure 4.3-1 PWR Heat Transfer Disk Model for Normal Handling Condition

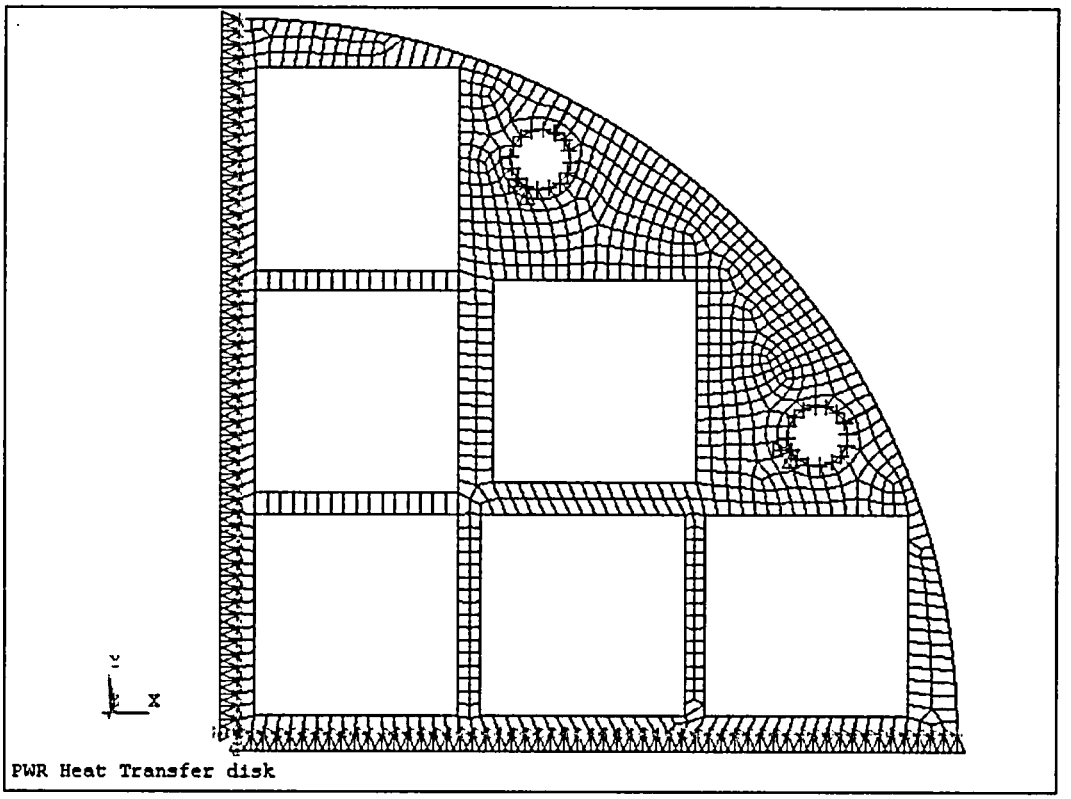

Figure 4.3-2 BWR Heat Transfer Disk Model for Normal Handling Condition

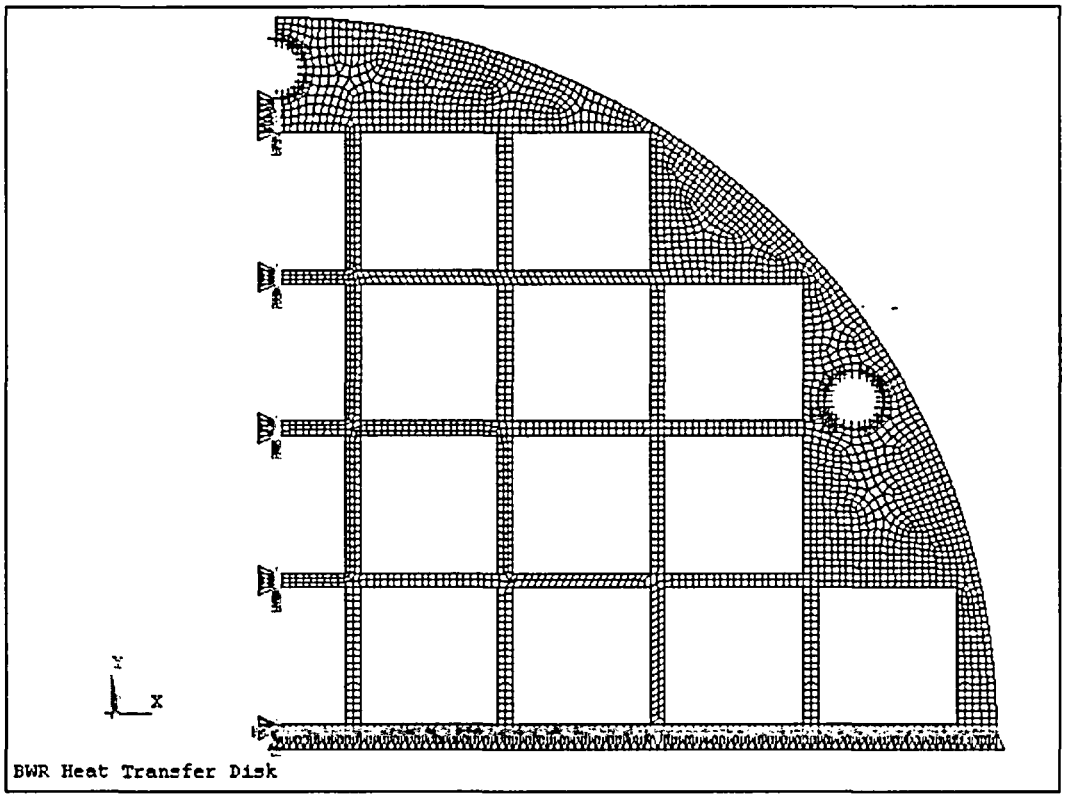

THIS PAGE INTENTIONALLY LEFT BLANK

4.4 Thermal Evaluation for Normal Conditions of Storage

The finite element method is used to evaluate the thermal performance of the Universal Storage System for normal conditions of storage. The general-purpose finite element analysis program ANSYS Revisions 5.2 and 5.5 [6] are used to perform the finite element evaluations.

THIS PAGE INTENTIONALLY LEFT BLANK

4.4.1 Thermal Models

Finite element models are utilized for the thermal evaluation of the Universal Storage System, as shown below. These models are used separately to evaluate the system for the storage of PWR or BWR fuel.

1. Two-Dimensional Axisymmetric Air Flow and Concrete Cask Models
2. Three-Dimensional Canister Models
3. Three-Dimensional Transfer Cask and Canister Models
4. Three-Dimensional Periodic Canister Internal Models
5. Two-Dimensional Fuel Models
6. Two-Dimensional Fuel Tube Models
7. Two-Dimensional Forced Air Flow Model for Transfer Cask Cooling

The two-dimensional axisymmetric air flow and concrete cask model includes the concrete cask, air in the air inlets, annulus and the air outlets, the canister and the canister internals, which are modeled as homogeneous regions with effective thermal conductivities. The effective thermal conductivities for the canister internals in the radial direction are determined using the three-dimensional periodic canister internal models. The effective conductivities in the canister axial direction are calculated using classical methods. The two-dimensional axisymmetric air flow and concrete cask model is used to perform computational fluid dynamic analyses to determine the mass flow rate, velocity and temperature of the air flow, as well as the temperature distribution of the concrete, concrete cask steel liner and the canister. Two models are generated for the evaluations of the PWR and the BWR systems, respectively. These models are essentially identical, but have slight differences in dimensions and the effective properties of the canister internals.

The three-dimensional canister model comprises the fuel assemblies, fuel tubes, stainless steel or carbon steel support disks, aluminum heat transfer disks, top and bottom weldments, the canister shell, lids and bottom plate. The canister model is employed to evaluate the temperature distribution of the fuel cladding and basket components. The fuel assemblies and the fuel tubes in the three-dimensional canister model are modeled using effective conductivities. The effective conductivities for the fuel assemblies are determined using the two-dimensional fuel models. The effective conductivities for the fuel tubes are determined using the two-dimensional fuel tube

models. Two three-dimensional canister models are generated for the PWR and BWR canisters, respectively.

The three-dimensional transfer cask model includes the transfer cask and the canister with its internals. This model is used to perform transient and steady state analyses for the transfer condition, starting from removing the transfer cask/canister from the spent fuel pool, vacuum drying and finally back-filling the canister with helium. Separate transfer cask models are required for PWR and BWR systems.

The three-dimensional canister internal model consists of a periodic section of the canister internals. For the PWR canister, the model contains one support disk with two heat transfer disks (half thickness) on its top and bottom, fuel assemblies, fuel tubes and the media in the canister. For the BWR canister, two models are required. The first model, for the central region of the BWR canister, contains one heat transfer disk with two support disks (half thickness) on its top and bottom, fuel assemblies, fuel tubes and the media in the canister. The other model, for the region without heat transfer disks, contains two support disks (half thickness), fuel assemblies, fuel tubes and the media in the canister. The purpose of the three-dimensional periodic canister internal model is to determine the effective thermal conductivity of the canister internals in the canister radial direction. The effective conductivities are used in the two-dimensional axisymmetric air flow and concrete cask models. The media in the canister is considered to be helium. The fuel assemblies and fuel tubes in this model are modeled as homogeneous regions with effective thermal properties, which are determined by the two-dimensional fuel models and the two-dimensional fuel tube models.

The two-dimensional fuel model includes the fuel pellets, cladding and the media occupying the space between fuel rods. The media is considered to be helium for storage conditions and water, vacuum or helium for transfer conditions. The model is used to determine the effective thermal conductivities of the fuel assembly. In order to account for various types of fuel assemblies, a total of seven fuel models are generated: Four models for the 14×14, 15×15, 16×16 and 17×17 PWR fuel assemblies and three models for the 7×7, 8×8 and 9×9 BWR fuel assemblies. The effective properties are used in the three-dimensional canister models, the three-dimensional periodic canister internal models and the three-dimensional transfer cask and canister model.

The two-dimensional fuel tube model is used to determine the effective conductivities of the fuel tube wall and neutron absorber. BORAL effective conductivity is considered in the model for the neutron absorber. The effective conductivity of METAMIC is essentially identical to that of BORAL. The effective conductivities are used in the three-dimensional canister models, the three-dimensional periodic canister internal models and the three-dimensional transfer cask and canister model.

The two-dimensional axisymmetric air flow model is used to determine the air flow rate needed for the forced air cooling of the canister inside the transfer cask.

Detailed description of the finite element models are presented in Sections 4.4.1.1 through 4.4.1.7.

4.4.1.1 Two-Dimensional Axisymmetric Air Flow and Concrete Cask Models

This section describes the finite element models used to evaluate the thermal performance of the vertical concrete cask for the PWR and BWR configurations. The model includes the concrete cask, the air in the air inlets, the annulus and the air outlets, the canister and the canister internals, which are modeled as homogeneous regions with effective thermal conductivities. Two separate two-dimensional axisymmetric models are used for the PWR and BWR configurations, respectively. The PWR model is shown in Figures 4.4.1.1-1 and 4.4.1.1-2. The BWR model is essentially identical to the PWR model, but it incorporates different effective thermal properties of the canister internals, and slight differences in dimensions.

The fuel canister is cooled by (1) natural/free convection of air through the lower vents (the air inlets), the vertical air annulus, and the upper vents (the air outlets); and (2) radiation heat transfer between the surfaces of the canister shell and the steel liner. The heat transferred to the liner is rejected by air convection in the annulus and by conduction through the concrete. The heat flow through the concrete is dissipated to the surroundings by natural convection and radiation heat transfer. The temperature in the concrete region is controlled by radiation heat transfer between the vertical annulus surfaces (the canister shell outer surface and the steel liner inner surface), natural convection of air in the annulus, and boundary conditions applicable to the concrete cask outer surfaces—e.g., natural convection and radiation heat transfer between the outer surfaces and the environment, including consideration of incident solar energy. These heat transfer modes are combined in the air flow and concrete cask model. The entire thermal system,

including mass, momentum, and energy, is analyzed using the two-dimensional axisymmetric air flow and concrete cask models. The temperature distributions of the concrete cask, the air region and the canister are determined by these models. Detailed thermal evaluations for the canister internals (fuel cladding, basket, etc.) are performed using the three-dimensional canister models as described in Section 4.4.1.2.

The concrete cask has four air inlets at the bottom and four air outlets at the top that extend through the concrete. Since the configuration is symmetrical, it can be simplified into a two-dimensional axisymmetric model by using equivalent dimensions for the air inlets and outlets, which are assumed to extend around the concrete cask periphery. The canister internals are modeled as three homogeneous regions using effective thermal conductivities - the active fuel region and the regions above and below the active fuel region. The two-dimensional axisymmetric model is shown schematically in Figure 4.4.1.1-1. Determination of the effective properties is described in Section 4.4.1.4.

ANSYS FLOTRAN FLUID141 fluid thermal elements are used to construct the two-dimensional axisymmetric finite element models, as shown in Figure 4.4.1.1-2. In the air region (including the air inlet, outlet and annulus regions), only quadrilateral elements are used and the element sizes are nonuniform with much smaller element sizes close to the walls. In other regions, to simulate conduction, a mix of quadrilateral elements and triangular elements are used. Radiation heat transfer that occurs in the following regions is included in the model:

1. From the concrete outer surfaces to the ambient
2. Across the vertical air annulus (from the canister shell to the concrete cask liner)
3. From the top of the active fuel region to the bottom of the canister shield lid
4. From the bottom of the active fuel region to the top of the canister bottom plate
5. From the canister structural lid to the shield plug
6. From the shield plug to the concrete cask lid

Loads and Boundary Conditions

1. Heat generation in the active fuel region.

The distribution of the heat generation is based on the axial power distribution shown in Figures 4.4.1.1-3 and 4.4.1.1-4 for PWR and BWR fuels, respectively (see description in Chapter 5, Section 5.2.6, for the design-basis fuel).

2. Solar insolation to the outer surfaces of the concrete cask.

The solar insolation to the concrete cask outer surfaces is considered in the model. The incident solar energy is applied based on 24-hour averages as shown below.

Side surface: $$\frac{1475 Btu / ft^2}{24 hrs} = 61.46 Btu / hr \cdot ft^2$$

Top surface: $$\frac{2950 Btu / ft^2}{24 hrs} = 122.92 Btu / hr \cdot ft^2$$

3. Natural convection heat transfer at the outer surfaces of the concrete cask.

Natural convection heat transfer at the outer surfaces of the concrete cask is evaluated by using the heat transfer correlation for vertical and horizontal plates [17, 29]. This method assumes a surface temperature and then estimates Grashof (Gr) or Rayleigh (Ra) numbers to determine whether a heat transfer correlation for a laminar flow model or for a turbulent flow model should be used. Since Grashof or Rayleigh numbers are much higher than the critical values, correlation for the turbulent flow model is used as shown in the following.

Side surface [17]:

$$Nu = 0.13(Gr \cdot Pr)^{1/3}$$
$$h_c = Nu \cdot k_f / H_{VCC} \qquad \text{for } Gr > 10^9$$

Top surface [29]:

$$Nu = 0.15 Ra^{1/3}$$
$$h_c = Nu \cdot k_f / L \qquad \text{for } Ra > 10^7$$

where:

Gr	Grashof number
h_c	Average natural convection heat transfer coefficient
H_{vcc}	Height of the vertical concrete cask
k_f	Conductivity
L	Top surface characteristic length, L = area / perimeter
Nu	Average Nusselt number
Pr	Prandtl number
Ra	Rayleigh number

All material properties required in the above equations are evaluated based on the film temperature, that is, the average value of the surface temperature and the ambient temperature.

4. Radiation heat transfer at the concrete cask outer surfaces.

The radiation heat transfer between the outer surfaces and the ambient is evaluated in the model by calculating an equivalent radiation heat transfer coefficient.

$$h_{rad} = \frac{\sigma(T_1^2 + T_2^2)(T_1 + T_2)}{1/\varepsilon_1 + 1/\varepsilon_2 + 1/F_{12} - 2}$$

where:

h_{rad}	Equivalent radiation heat transfer coefficient
F_{12}	View factor
T_1 & T_2	Surface (T_1) and ambient (T_2) temperatures
ε_1 & ε_2	Surface (ε_1) and ambient (ε_2=1) emissivities
σ	Stefan-Boltzmann Constant

At the concrete cask side, an emissivity for a concrete surface of $\varepsilon_1 = 0.9$ is used and a calculated view factor (F_{12}) = 0.182 [29] is applied. The view factor is determined by conservatively assuming that the cask is surrounded by eight casks.

At the cask top, an emissivity, ε_1, of 0.8 is conservatively used (emissivity for concrete is 0.9), and a view factor, F_{12}, of 1 is applied.

Accuracy Check of the Numerical Simulation

To ensure the accuracy of the numerical simulation of the air flow in the concrete cask, and to ensure reliable numerical results, the following checks and confirmations are performed.

1. Global convergence of the iteration process for the nonlinear system.

The system controlling air flow through the cask and, therefore, the temperature field is nonlinear and is solved iteratively.

The global iteration process is monitored by checking the variation of parameters with the global iteration—e.g., the maximum air temperature, the mass flow rate, and the net heat carried out of the concrete cask by air convection. All of the results presented are at the converged state.

2. Overall energy balance and mass balance.

This step validates the overall energy balance and mass balance. The mass balance is also shown in Figure 4.4.1.1-5. At the converged state, the mass flow rate at the air inlets matches the mass flow rate at the air outlets, showing that an excellent mass balance has been obtained.

The overall energy balance is checked by computing the total heat input (Q_{in}) and total heat output (Q_{out}). The total heat input includes the total heat from the fuel (Q_{fuel}) and the total absorbed solar energy (Q_{sun}) incident on the concrete cask outer surfaces. The total heat output is the sum of the net heat carried out of the cask by air (Q_{air}) and by convection and radiation heat loss at the concrete cask outer surfaces (Q_{con}).

For the normal storage condition with the PWR design heat load of 23.0 kW:

$$Q_{in} = Q_{fuel} + Q_{sun} = 23.0\text{ kW} + 9.18\text{ kW} = 32.18\text{ kW}$$
$$Q_{out} = Q_{air} + Q_{con} = 20.97\text{ kW} + 11.72\text{ kW} = 32.69\text{ kW}$$
$$Q_{out}/Q_{in} = 1.016$$

For the normal storage condition with the BWR design heat load of 23.0 kW:

$$Q_{in} = Q_{fuel} + Q_{sun} = 23.0\ kW + 9.52\ kW = 32.52\ kW$$
$$Q_{out} = Q_{air} + Q_{con} = 20.70\ kW + 12.12\ kW = 32.82\ kW$$
$$Q_{out}/Q_{in} = 1.009$$

The overall energy balance is demonstrated to be within 2 percent for all design conditions.

3. Finite Element Mesh Adequacy Study.

A sensitivity evaluation is performed to assess the effect of the number of elements used in the Two-dimensional Axisymmetric Air Flow and Concrete Cask Models. The sensitivity evaluation is performed with a reduced element model based on the model for the PWR fuel configuration. The total number of elements in the reduced-element model (13,371 elements) is 21% less than the number of elements used in the axisymmetric air flow and concrete cask model described above. The reduction in the number of elements occurs in the air flow region in the radial direction, which has the largest gradients in velocity and temperature. As shown below, the temperatures calculated by the reduced element model (Case ES1) are essentially the same as the temperatures calculated by the axisymmetric air flow and concrete cask model (Case ES2).

Case	Number of Elements in Model	Max. Air Temp. in Annular Region (Canister Surface)	Maximum Concrete Temp.	Average Air Temp. at the Outlet	Maximum Canister Shell Temp.
ES1	13,371	451 K	360 K	335 K	452 K
ES2	16,835	448 K	359 K	339 K	449 K
ES1/ES2	0.79	1.01	1.00	0.99	1.01

A comparison of the two models (Case ES1/ES2) shows that the maximum difference is 1%. Therefore, the number of elements used in the Two-dimensional Axisymmetric Air Flow and Concrete Cask Model (16,835) is adequate.

Supplemental Shielding Fixture Evaluation

The effect of the installation of an optional supplemental shielding fixture, shown in Drawing 790-613, installed in the air inlet is evaluated based on one-half of the air inlets blocked. The analysis results show that the maximum temperature increase is 5°F, which remains well below normal condition allowables. The pipes in the shielding fixture are offset to block (gamma) radiation, but allow air flow.

Off-Center Canister Evaluation

The analysis assumes that the canister is centered in the concrete cask. However, the potential exists for the canister to be placed off-center when it is installed in the storage cask. Placing the canister within the boundary of the support ring limits the extent of off-center positioning, which precludes the canister from being placed closer than 1 inch to the concrete cask liner. This placement reduces the area of the air flow path in an arc established by the canister shell and concrete cask liner. An air flow analysis is performed to evaluate the effects of the off-center positioning of the canister. The analysis results show an increase in air mass flow rate occurs in the annulus, which results in a temperature reduction in the canister shell and concrete cask liner. Consequently, the off-center canister placement condition is bounded by the condition that the canister is at the center of the concrete cask, as considered in the two-dimensional axisymmetric finite element model described in this section.

Figure 4.4.1.1-1 Two-Dimensional Axisymmetric Air Flow and Concrete Cask Model: PWR

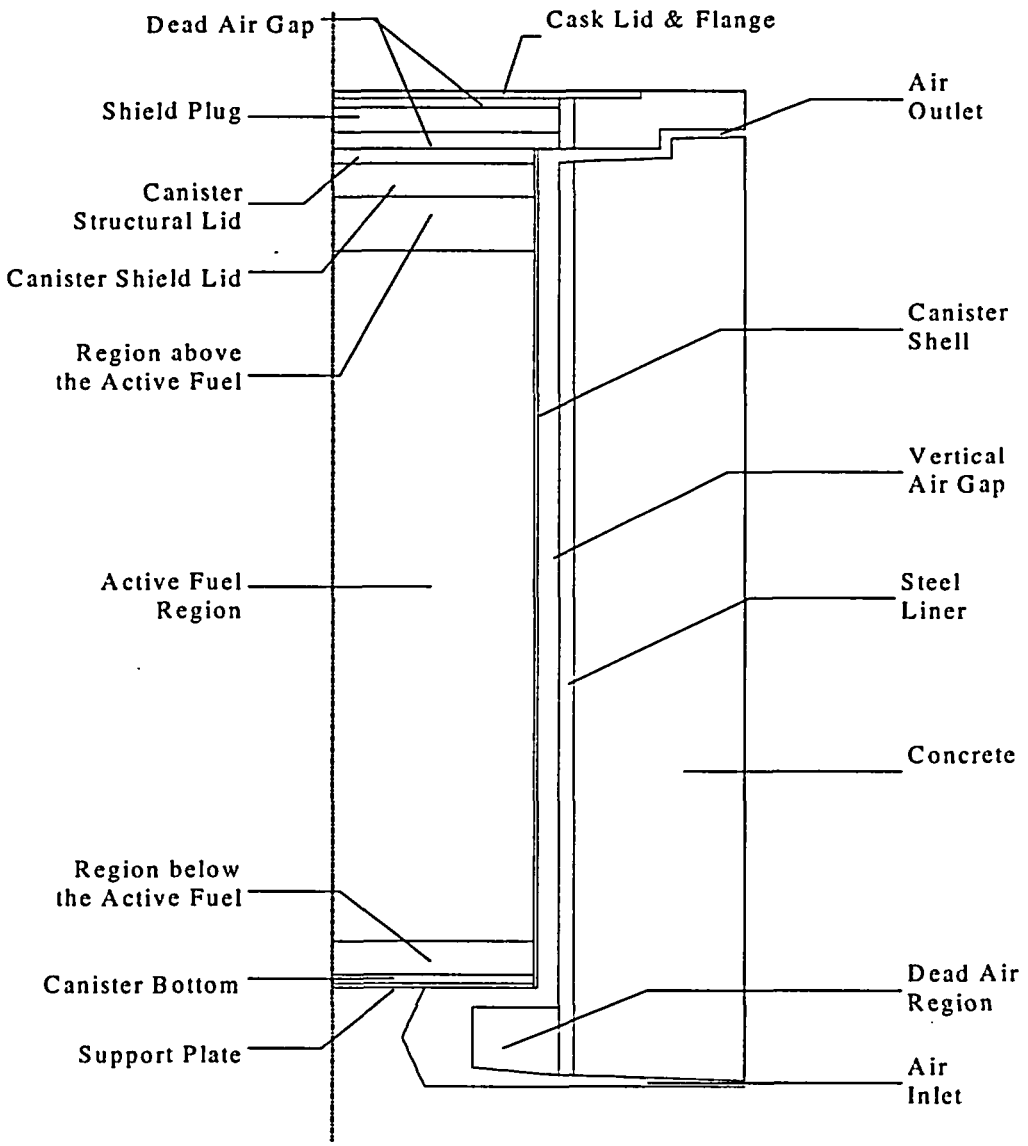

Figure 4.4.1.1-2 Two-Dimensional Axisymmetric Air Flow and Concrete Cask Finite Element Model: PWR

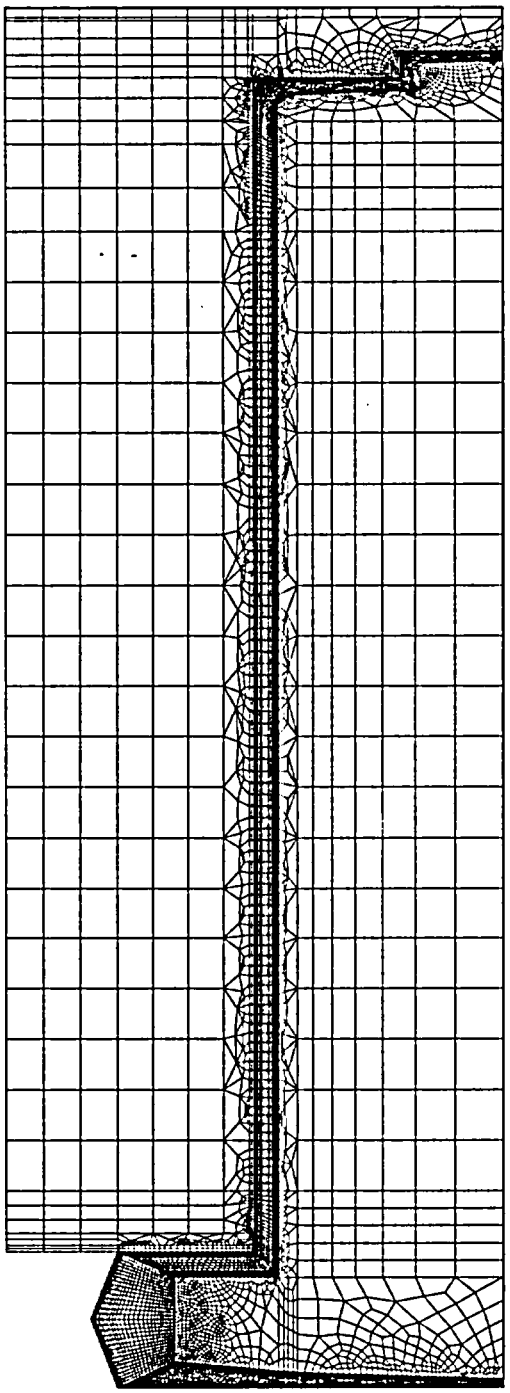

Figure 4.4.1.1-3 Axial Power Distribution for PWR Fuel

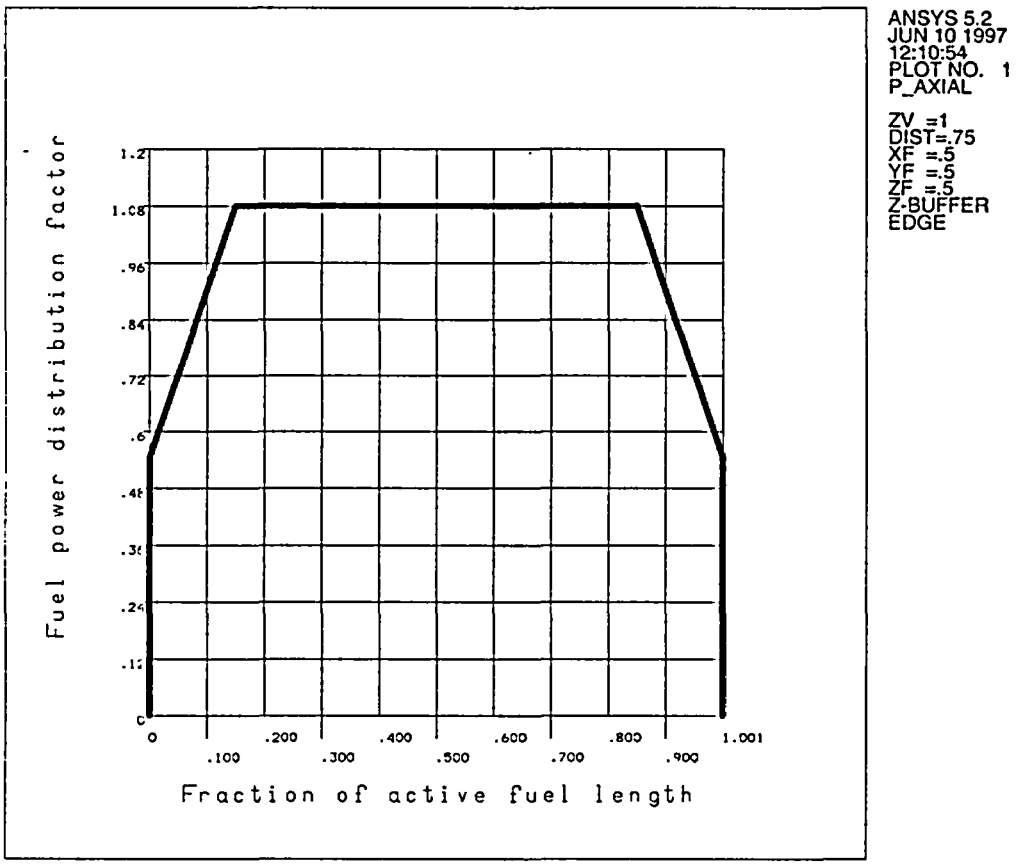

Figure 4.4.1.1-4 Axial Power Distribution for BWR Fuel

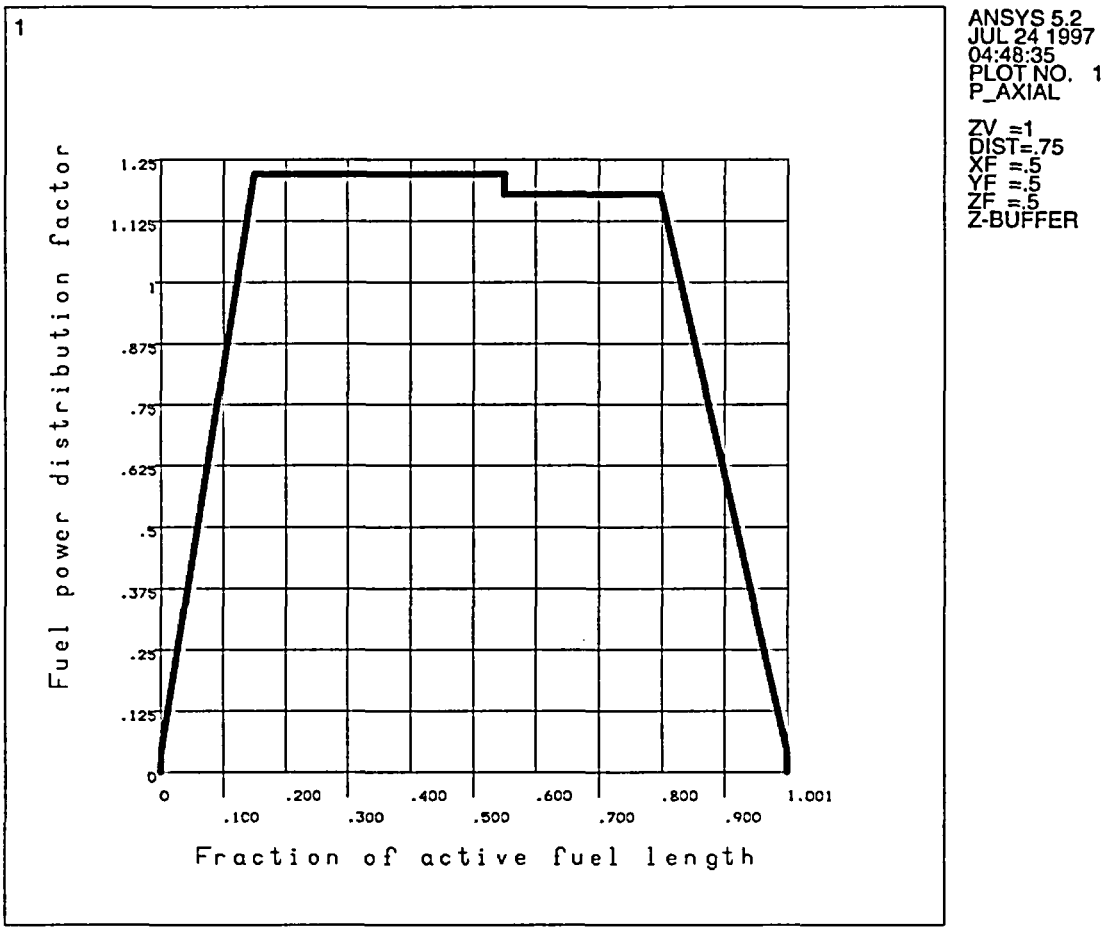

4.4.1.2 Three-Dimensional Canister Models

Two three-dimensional canister models are used to evaluate the temperature distribution of the fuel cladding and basket components inside the canister for the PWR and BWR configurations, respectively. The model for PWR fuel is shown in Figures 4.4.1.2-1 and 4.4.1.2-2. The model for BWR fuel is shown in Figures 4.4.1.2-3 and 4.4.1.2-4.

ANSYS SOLID70 three-dimensional conduction elements and LINK31 radiation elements are used to construct the model. The model includes the fuel assemblies, fuel tubes, support disks, heat transfer disks, top and bottom weldments, canister shell, lids, bottom plate and gas inside the canister (helium). Based on symmetry, only half of the canister is modeled. The plane of symmetry is considered to be adiabatic.

The canister outer surface temperatures obtained from the two-dimensional axisymmetric air flow and concrete cask model (Section 4.4.1.1) are applied at the canister surfaces in the model as boundary conditions. In the model, the fuel assemblies are considered to be centered in the fuel tubes. The fuel tubes are centered in the slots of the support disks and heat transfer disks. The basket is centered in the canister. These assumptions are conservative, since any contact between components will provide a more efficient path to reject the heat.

The gaps used in the three-dimensional canister model between the support disks and canister shell, as well as between the heat transfer disk and the canister shell, are shown in the following table.

		Nominal Gap At Room Temperature (inch)	Gap Used in the 3-D Thermal Model (inch)	
			At Room Temperature	At Elevated Temperature
PWR	Gap between Support Disk and Canister Shell	0.120	0.155	0.165
	Gap between Heat Transfer Disk and Canister Shell	0.245	0.280	0.195
BWR	Gap between Support Disk and Canister Shell	0.120	0.155	0.165
	Gap between Heat Transfer Disk and Canister Shell	0.280	0.315	0.232

The gaps at room temperature are first used in the model to calculate preliminary temperature distribution and to determine the differential thermal expansion of the disks and canister shell at the elevated temperatures. The gaps at elevated temperature are then established, based on the differential thermal expansions between components, and used in the model for final solution. As shown above, the room temperature gaps used in the thermal model bound the actual nominal gaps at room temperature.

These gap sizes are adjusted in the model to account for differential thermal expansion of the disks and canister shell based on thermal conditions. The gaps used in the model are shown to be larger than the actual gap size based on thermal expansion calculation using the thermal analysis results; therefore, the model is conservative.

A sensitivity study was performed to assess the effect of gap sizes on temperature results, with consideration of fabrication tolerance of the canister and basket. The ANSYS three-dimensional canister model for the PWR fuel is used for the study. The gaps between the disks and canister shell are increased to account for the worst case fabrication tolerance of the canister and basket. The gaps are also adjusted based on the differential thermal expansion of the canister and basket at elevated temperature. Compared to the gaps used in the original three-dimensional thermal model, the gap between the support disk and the canister shell is increased by 27% and the gap between the heat transfer disk and the canister shell is increased by 24%. The results of the sensitivity study indicate that the increase in the maximum fuel cladding and basket temperatures is less than 9°F, which is less than 3% of the temperature difference between the maximum temperature of the fuel cladding/basket and the canister shell. Therefore, the effect of the thermal model gap size on the maximum temperature of the basket and fuel cladding is not significant.

The structural lid and the shield lid are expected to be in full contact due to the weight of the structural lid. The thermal resistance across the contact surface is considered to be negligible and, therefore, no gap is modeled between the lids.

All material properties used in the model, except the effective properties discussed below, are shown in Tables 4.2-1 through 4.2-13.

The fuel assemblies and fuel tubes are modeled as homogenous regions with effective conductivities, determined by the two-dimensional fuel models (Section 4.4.1.5) and the

two-dimensional fuel tube models (Section 4.4.1.6), respectively. The effective properties are listed in Tables 4.4.1.2-1 through 4.4.1.2-4. The properties corresponding to the PWR 14 × 14 assemblies are used for the PWR model, since the 14 × 14 assemblies have lower conductivities as compared to other PWR assemblies. For the same reason, the properties corresponding to the BWR 9 × 9 assemblies are used in the BWR model.

In the model, radiation heat transfer is taken into account in the following locations:

1. From the top of the fuel region to the bottom surface of the canister shield lid.
2. From the bottom of the fuel region to the top surface of the canister bottom plate.
3. From the exterior surfaces of the fuel tubes (surface between disks) to the inner surface of the canister shell.
4. From the edge of the PWR support disks to the inner surface of the canister shell.
5. From the edge of heat transfer disks to the inner surface of the canister shell.
6. Between disks in the PWR model in the canister axial direction.

The radiation heat transfer from the BWR support disk is conservatively neglected by using an emissivity value of 0.0001 for the BWR support disk in the model. An emissivity of 0.22 is used for the heat transfer disk, except the water-jet cut surfaces (the circumferential surfaces at the edges of the disks facing the canister shell and the inner surfaces of each slot). The surface condition of the water-jet cut surfaces is similar to that of the sandblasted surface and, therefore, an emissivity of 0.4 is used.

Radiation elements (LINK31) are used to model the radiation effect for the first three locations. Radiation across the gaps (Locations No. 4 through 6) is accounted for by establishing effective conductivities for the gas in the gap, as shown below. The gaps are small compared to the surfaces separated by the gaps.

Radiation heat transfer between two nodes i (hotter node) and j (colder node) is accounted for by the expression:

$$q_r = \sigma \varepsilon A F \left(T_i^4 - T_j^4\right)$$

where:

σ = the Stefan-Boltzman constant
ε = effective emissivity between two surfaces
A = surface area

F = the gray body shape factor for the surfaces
T_i = temperature of the i th node
T_j = temperature of the j th node

The total heat transfer can be expressed as the sum of the radiation and the conduction processes:

$$Q_t = q_r + q_k$$

where q_r is specified above for the radiation heat transfer and q_k, which is the heat transfer by conduction is expressed as:

$$q_k = \frac{KA}{g}(T_i - T_j)$$

where:

T_i = temperature of the i th node
T_j = temperature of the j th node
g = gap distance (between the two surfaces defined by node i and node j)
K = conductivity of the gas in the gap
A = area of gap surface

By combining the two expressions (for q_k and q_r) and factoring out the term $A(T_i - T_j)/g$,

$$Q_t = [g\sigma\varepsilon F(T_i^2 + T_j^2)(T_i+T_j) + K][A(T_i - T_j)/g]$$

or

$$Q_t = K_{eff}A(T_i - T_j)/g$$

where:

$$K_{eff} = g\sigma\varepsilon F(T_i^2 + T_j^2)(T_i+T_j) + K$$

The material conductivity used in the analysis for the elements comprising the gap includes the heat transfer by both conduction and radiation.

Effective emissivities (ε) are used for all radiation calculations, based on the formula below [17]. The view factor is taken to be unity.

$$\varepsilon = 1/(1/\varepsilon_1 + 1/\varepsilon_2 - 1)$$

where ε_1 & ε_2 are the emissivities of two parallel plates

Radiation between the exterior surfaces of the fuel tubes is conservatively ignored in the model.

Volumetric heat generation (Btu/hr-in^3) is applied to the active fuel region based on design heat load, active fuel length of 144 inches and an axial power distribution as shown in Figures 4.4.1.1-3 and 4.4.1.1-4 for PWR and BWR fuel, respectively.

Figure 4.4.1.2-1 Three-Dimensional Canister Model for PWR Fuel

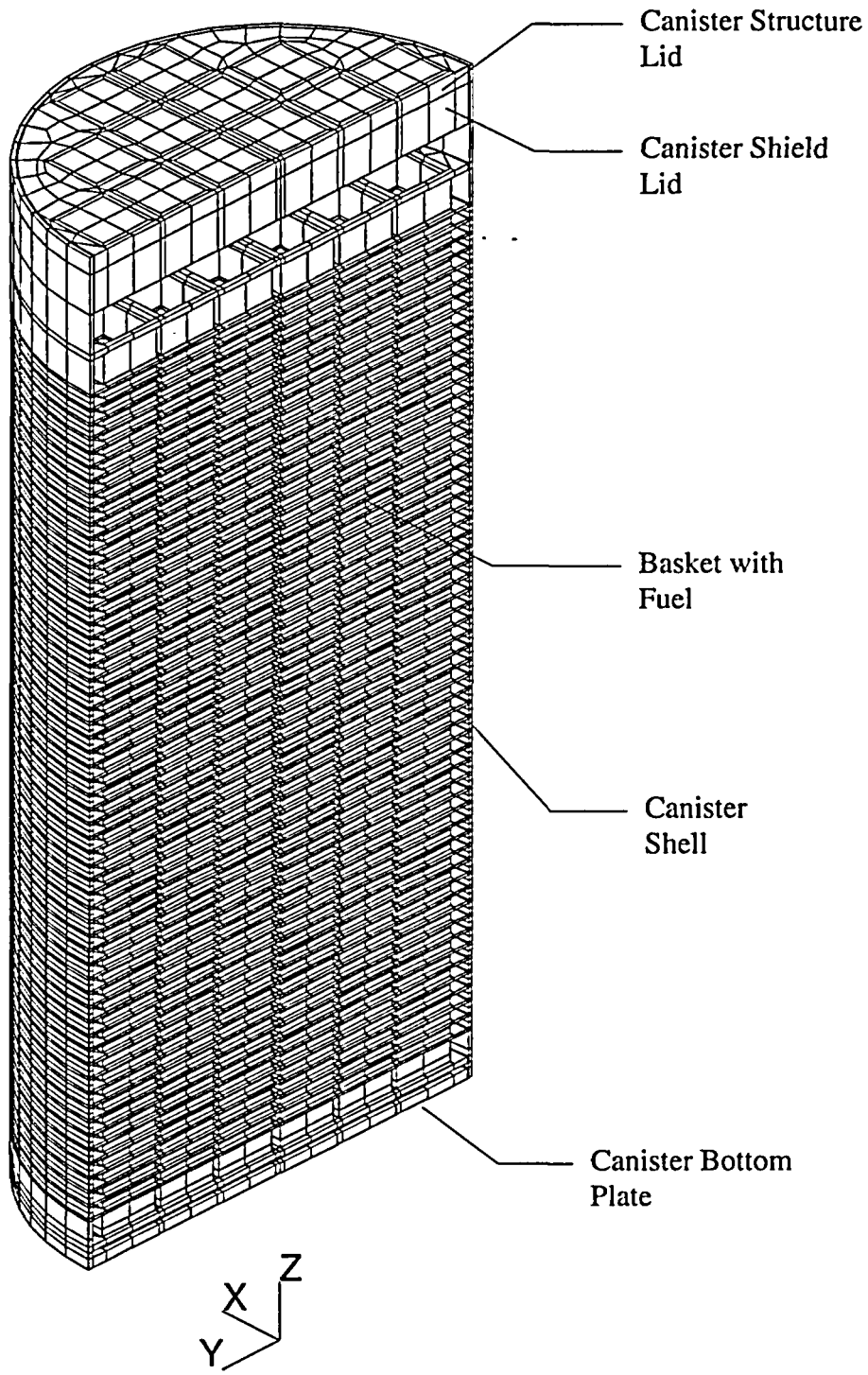

Figure 4.4.1.2-2 Three-Dimensional Canister Model for PWR Fuel – Cross Section

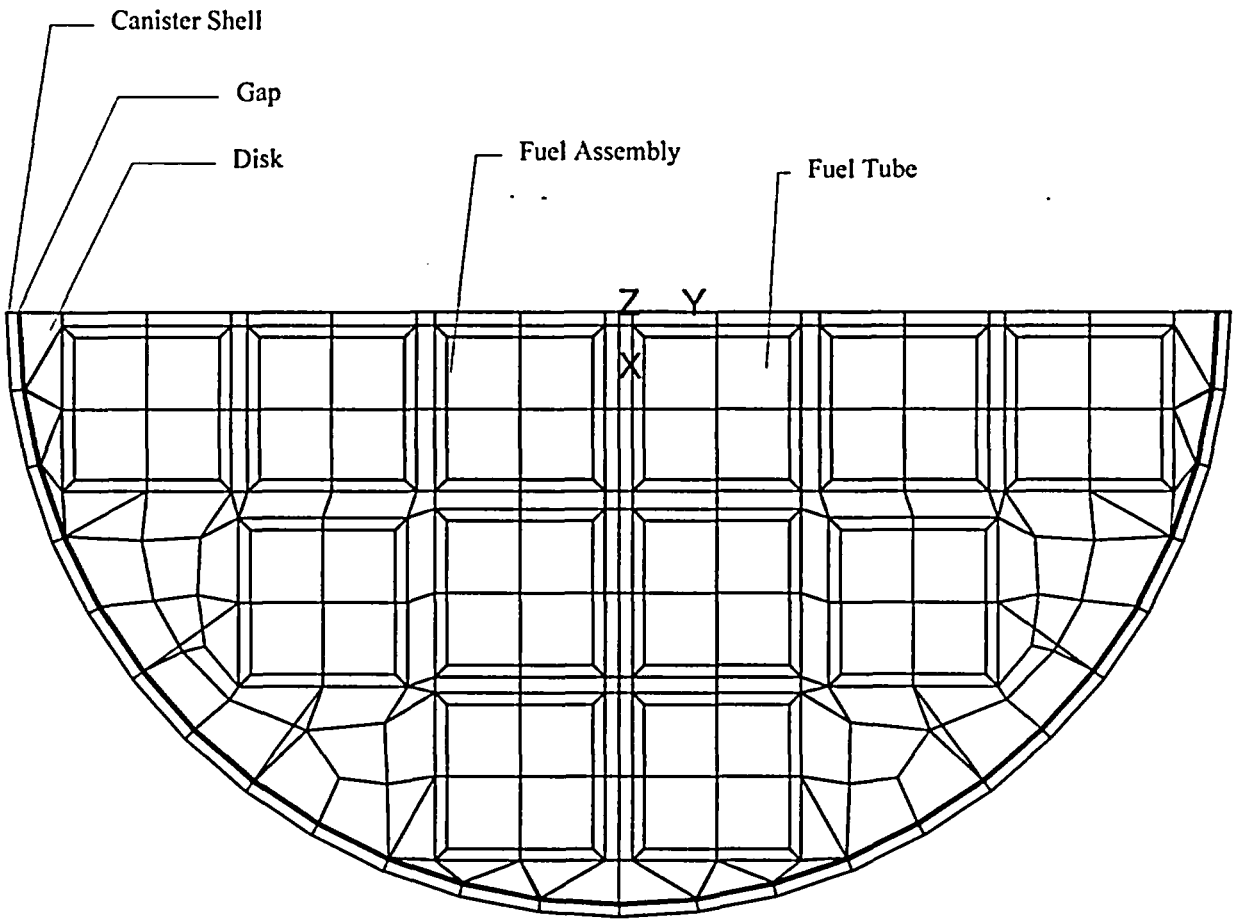

Figure 4.4.1.2-3 Three-Dimensional Canister Model for BWR Fuel

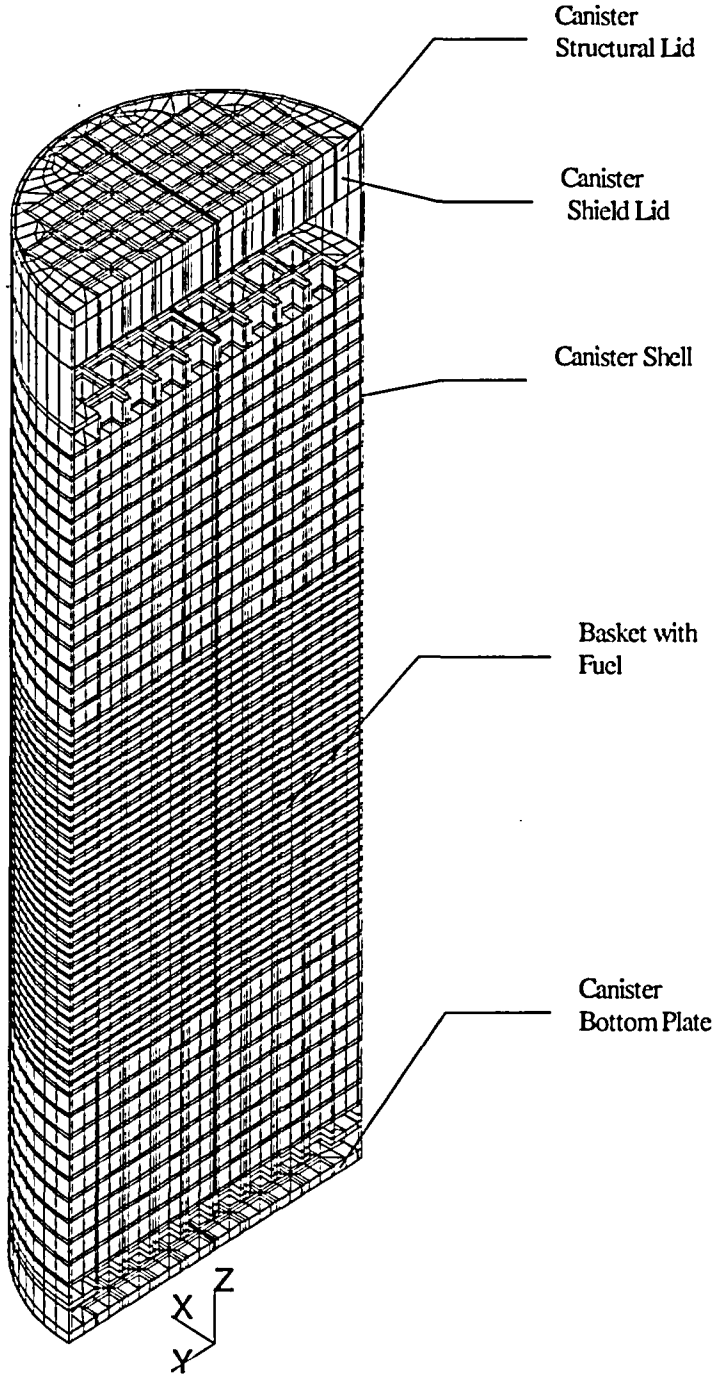

Figure 4.4.1.2-4 Three-Dimensional Canister Model for BWR Fuel – Cross Section

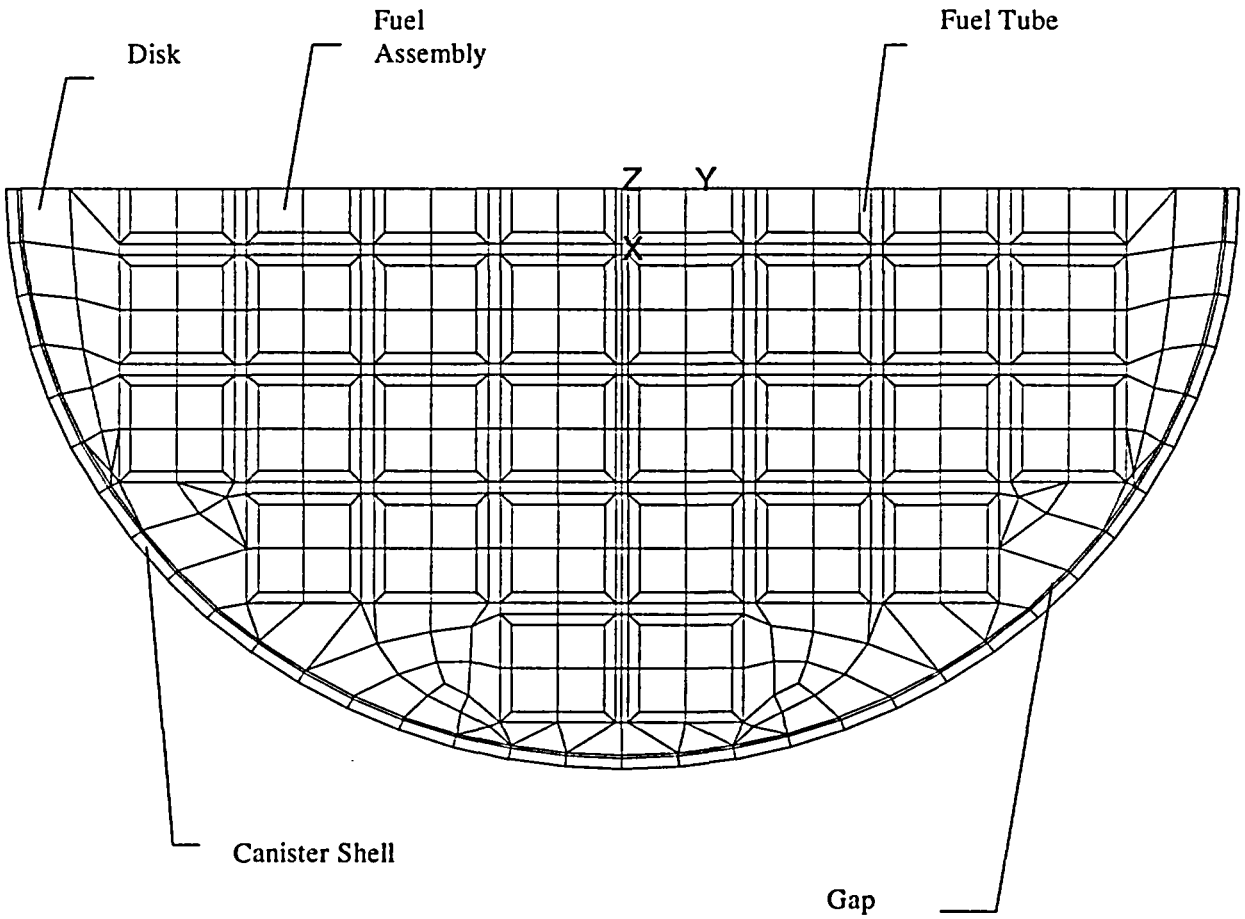

Table 4.4.1.2-1 Effective Thermal Conductivities for PWR Fuel Assemblies

Conductivity (Btu/hr-in-°F)	Temperature (°F)			
	220	414	611	812
Kxx	0.020	0.027	0.037	0.049
Kyy	0.020	0.027	0.037	0.049
Kzz	0.171	0.154	0.145	0.142

Note: x, y and z are in the coordinate system shown in Figure 4.4.1.2-1.

Table 4.4.1.2-2 Effective Thermal Conductivities for BWR Fuel Assemblies

Conductivity (Btu/hr-in-°F)	Temperature (°F)			
	186	389	593	799
Kxx	0.021	0.029	0.041	0.056
Kyy	0.021	0.029	0.041	0.056
Kzz	0.181	0.165	0.157	0.156

Note: x, y and z are in the coordinate system shown in Figure 4.4.1.2-3.

Table 4.4.1.2-3 Effective Thermal Conductivities for PWR Fuel Tubes

Fuel Assembly Group	Conductivity (Btu/hr-in-°F)	Temperature (°F)			
		206	405	604	803
In SS disk region					
	Kxx	0.022	0.028	0.033	0.040
	Kyy	1.54	1.57	1.59	1.61
	Kzz	1.54	1.57	1.59	1.61
In AL disk region					
	Kxx	0.022	0.027	0.032	0.038
	Kyy	1.54	1.57	1.59	1.61
	Kzz	1.54	1.57	1.59	1.61

Note: Kxx is in the direction across the thickness of the fuel tube wall.
Kyy is in the direction parallel to the fuel tube wall.
Kzz is in the canister axial direction.

Table 4.4.1.2-4 Effective Thermal Conductivities for BWR Fuel Tubes

	Conductivity	Temperature (°F)			
Tubes with Neutron Absorber	**(Btu/hr-in-°F)**	**200**	**400**	**600**	**800**
In CS disk region					
	Kxx	0.017	0.022	0.027	0.032
	Kyy	1.665	1.759	1.815	1.830
	Kzz	1.665	1.759	1.815	1.830
In AL disk region					
	Kxx	0.017	0.022	0.027	0.033
	Kyy	1.665	1.759	1.815	1.830
	Kzz	1.665	1.759	1.815	1.830
Tubes without Neutron Absorber		**200**	**400**	**600**	**800**
In CS disk region					
	Kxx	0.012	0.015	0.018	0.021
	Kyy	0.191	0.202	0.218	0.236
	Kzz	0.191	0.202	0.218	0.236
In AL disk region					
	Kxx	0.012	0.015	0.019	0.023
	Kyy	0.191	0.202	0.218	0.236
	Kzz	0.191	0.202	0.218	0.236

Note: Kxx is in the direction across the thickness of fuel tube wall.
Kyy is in the direction parallel to fuel tube wall.
Kzz is in the canister axial direction.

4.4.1.3 Three-Dimensional Transfer Cask and Canister Models

The three-dimensional quarter-symmetry transfer cask model is a representation of the PWR canister and transfer cask assembly. A half-symmetry model is used for the BWR canister and transfer cask. The model is used to perform a transient thermal analysis to determine the maximum water temperature in the canister for the period beginning immediately after removing the transfer cask and canister from the spent fuel pool. The model is also used to calculate the maximum temperature of the fuel cladding, the transfer cask and canister components during the vacuum drying condition and after the canister is backfilled with helium. The transfer cask is evaluated separately for PWR or BWR fuel using two models. For each fuel type, the class of fuel with the shortest associated canister and transfer cask is modeled in order to maximize the contents heat generation rate per unit volume and minimize the heat rejection from the external surfaces. The models for PWR and BWR fuel are shown in Figures 4.4.1.3-1 and 4.4.1.3-2, respectively. ANSYS SOLID70 three-dimensional conduction elements, LINK31 (PWR model) and MATRIX50 (BWR model) radiation elements are used. The model includes the transfer cask and the canister and its internals. The details of the canister and contents are modeled using the same methodology as that presented in Section 4.4.1.2 (Three-Dimensional Canister Models). Effective thermal properties for the fuel regions and the fuel tube regions are established using the fuel models and fuel tube models presented in Sections 4.4.1.5 and 4.4.1.6, respectively. The effective specific heat and density are calculated on the basis of material mass and volume ratio, respectively.

Radiation across the gaps was represented by the LINK31 elements or the MATRIX50 elements, which used the gray body emissivities for stainless and carbon steels. Convection is considered at the top of the canister lid, the exterior surfaces of the transfer cask, as well as at the annulus between the canister and the inner surface of the transfer cask. The combination of radiation and convection at the transfer cask exterior vertical surfaces and canister lid top surface is taken into account in the model using the same method described in Section 4.4.1.2 for the three-dimensional canister models. The bottom of the transfer cask is modeled as being in contact with the concrete floor. Volumetric heat generation (Btu/hr-in^3) is applied to the active fuel region based on a total heat load of 23 kW for both PWR and BWR fuel. The model considers the active fuel length of 144 inches and an axial power distribution, as shown in Figures 4.4.1.1-3 and 4.4.1.1-4 for PWR and BWR fuel, respectively.

An initial temperature of 100°F is considered in the model on the basis of typical maximum average water temperature in the spent fuel pool. For the design basis heat loads, the water inside the canister is drained within 17 hours and the canister is backfilled with helium immediately after the vacuum drying and transferred to the concrete cask. The design basis heat load transient analysis is performed for 17 hours with the water inside the canister, 27 hours (PWR) and 25 hours (BWR) for the vacuum condition, and 20 hours (PWR) and 16 hours (BWR) for the helium condition, followed by a steady state analysis (in helium condition). Different time durations are used for the transient analyses for the reduced heat load cases, as specified in Section 4.4.3.1. The temperature history of the fuel cladding and the basket components, as well as the transfer cask components, is determined and compared with the short-term temperature limits presented in Tables 4.4.3-3 and 4.4.3-4.

Figure 4.4.1.3-1 Three-Dimensional Transfer Cask and Canister Model - PWR

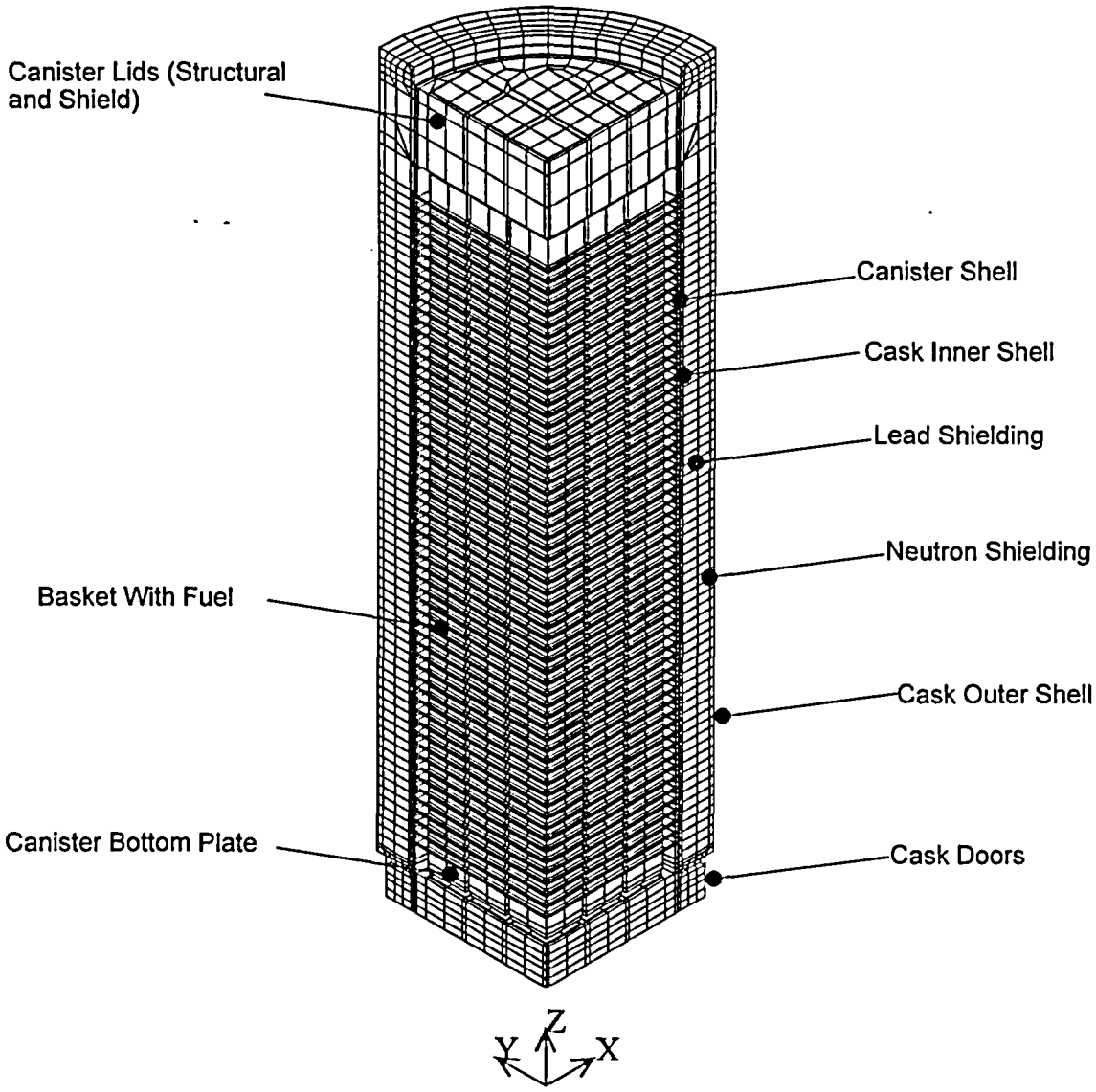

Note: Canister and transfer cask media not shown for clarity.

Figure 4.4.1.3-2 Three-Dimensional Transfer Cask and Canister Model - BWR

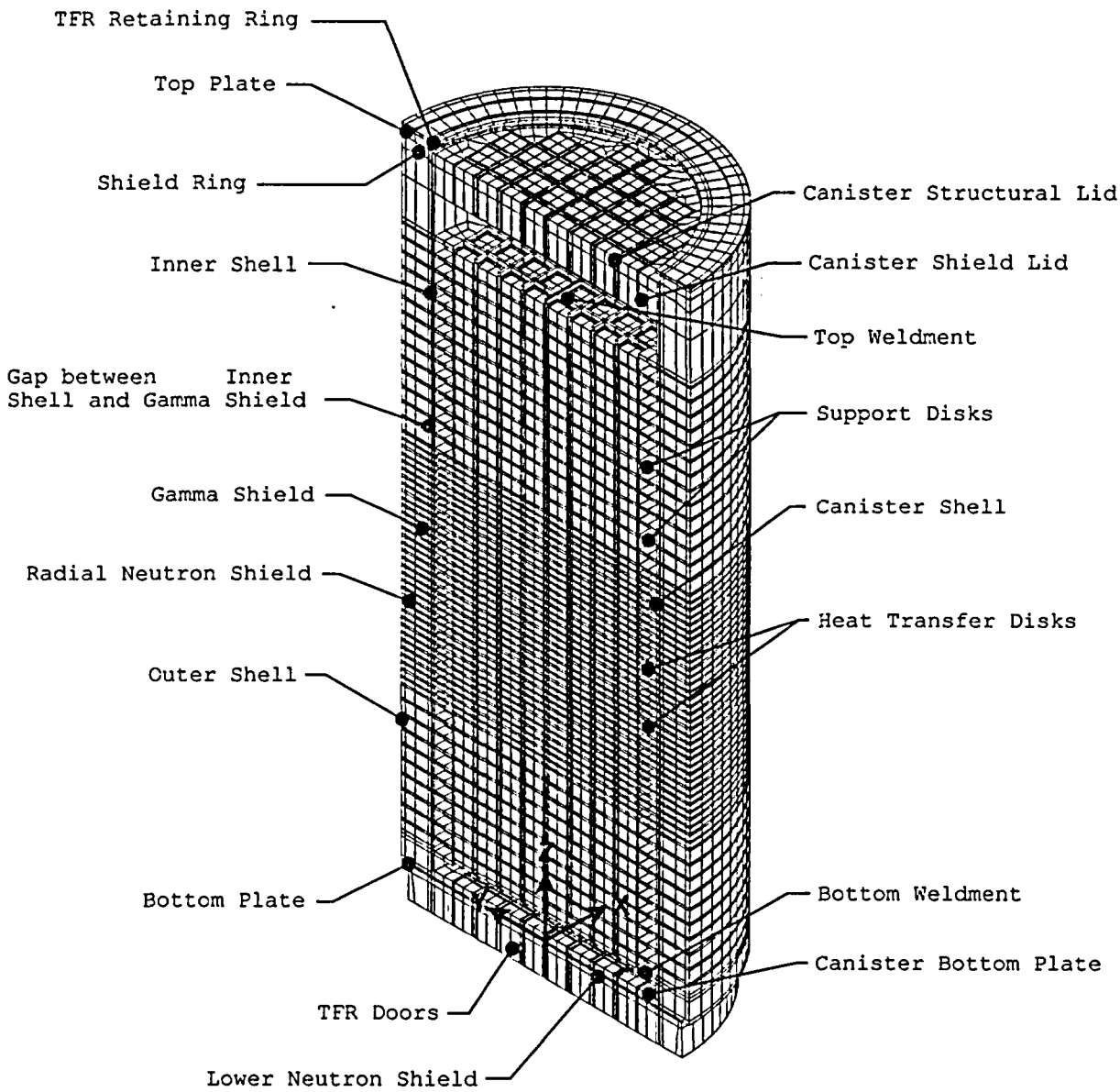

Canister and transfer cask media (water/helium) not shown for clarity.

4.4.1.4 Three-Dimensional Periodic Canister Internal Models

The three-dimensional periodic canister internal model consists of a periodic section of the canister internals. A total of three models are used: one for PWR fuel and two for BWR fuel. For the PWR canister, the model contains one support disk with two heat transfer disks (half thickness) on its top and bottom, the fuel assemblies, the fuel tubes and the media in the canister, as shown in Figure 4.4.1.4-1. The first BWR model, shown in Figure 4.4.1.4-2, represents the central region of the BWR canister, which contains one heat transfer disk with two support disks (half thickness) on its top and bottom, the fuel assemblies, the fuel tubes and the media in the canister. The second BWR model (not shown), for the region without heat transfer disks, contains two support disks (half thickness), the fuel assemblies, the fuel tubes and the media in the canister. The difference between the two BWR models is that the second model does not have the heat transfer disk. The purpose of these models is to determine the effective thermal conductivity of the canister internals in the canister radial direction. The effective conductivities are used in the two-dimensional axisymmetric air flow and concrete cask models. The media in the canister is considered to be helium. The fuel assemblies and fuel tubes in this model are represented by homogeneous regions with effective thermal properties. The effective conductivities for the fuel assemblies and the fuel tubes are determined by the two-dimensional fuel models (Section 4.4.1.5) and the two-dimensional fuel tube models (Section 4.4.1.6) respectively. The properties corresponding to the PWR 14 × 14 assemblies are used for the PWR model, since the 14 × 14 assemblies have the lowest conductivities as compared to other PWR assemblies. For the same reason, the properties corresponding to the BWR 9 × 9 assemblies are used for the BWR models.

The effective thermal conductivity (k_{eff}) of the fuel region in the radial direction is determined by considering the canister internals as a solid cylinder with heat generation. The temperature distribution in the cylinder may be expressed as [17]:

$$T - T_o = \frac{q''' R^2}{4k_{eff}}[1 - (\frac{r}{R})^2]$$

where:

T_o = the surface temperature of the cylinder
T = temperature at radius "r" of the cylinder
R = the outer radius of the cylinder,
r = radius
q''' = the heat generation rate = $\frac{Q}{\pi R^2 H}$

where: Q = total heat generated in the cylinder
H = length of the cylinder

Considering the temperature at the center of the canister to be T_{max}, the above equation can be simplified and used to compute the effective thermal conductivity (k_{eff}):

$$k_{eff} = \frac{Q}{4\pi H(T_{max} - T_o)} = \frac{Q}{4\pi H \Delta T}$$

where:

Q = total heat generated by the fuel
H = length of the active fuel region
T_o = temperature at outer surface internals (inside surface of the canister)
$\Delta T = T_{max} - T_o$

The value of ΔT is obtained from thermal analysis using the three-dimensional periodic canister internal model with the boundary temperature constrained to be T_o. The effective conductivity (k_{eff}) is then determined by using the above formula. Analysis is repeated by applying different boundary temperatures so that temperature-dependent conductivities can be determined.

Figure 4.4.1.4-1 Three-Dimensional Periodic Canister Internal Model - PWR

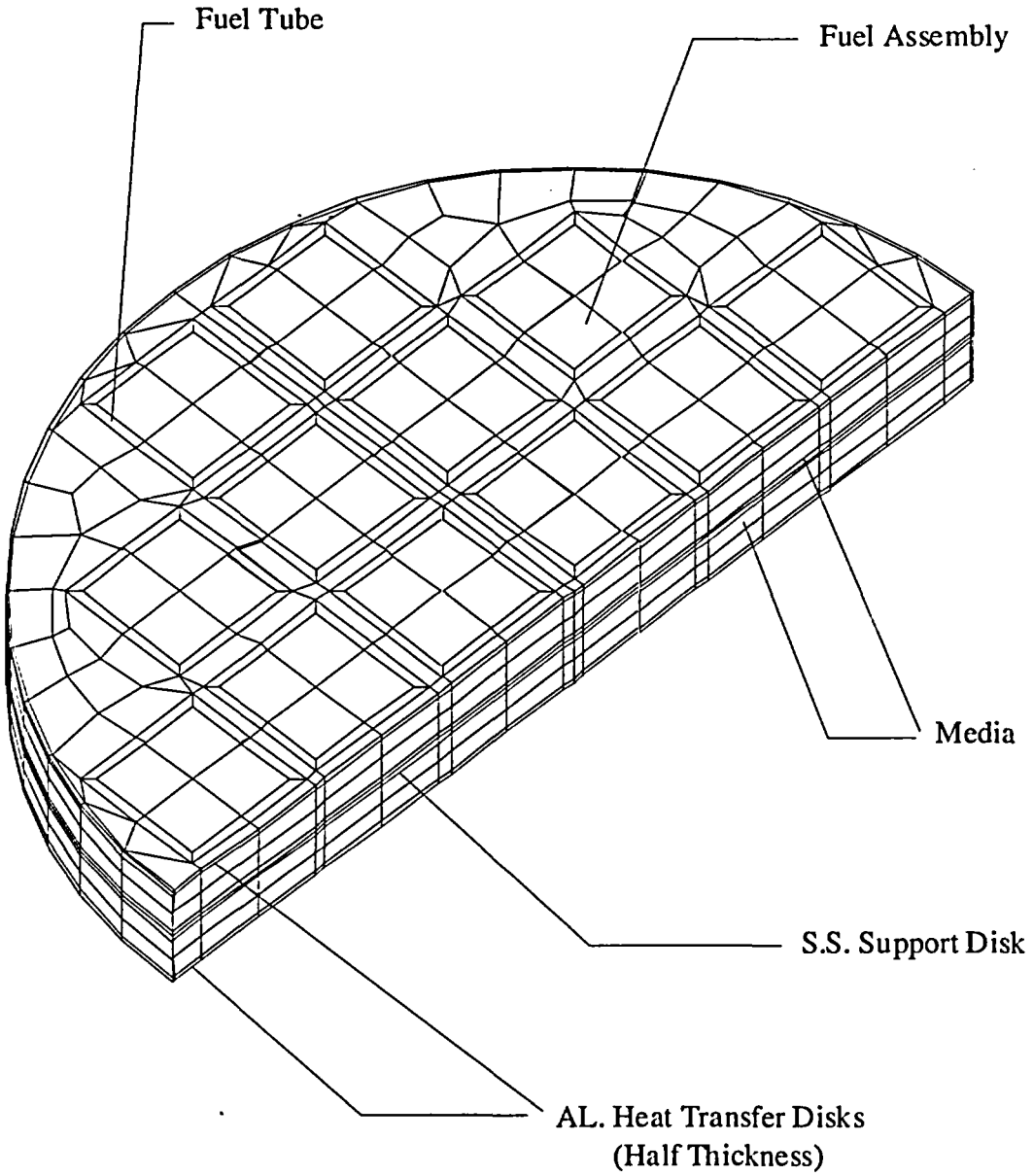

Figure 4.4.1.4-2 Three-Dimensional Periodic Canister Internal Model - BWR

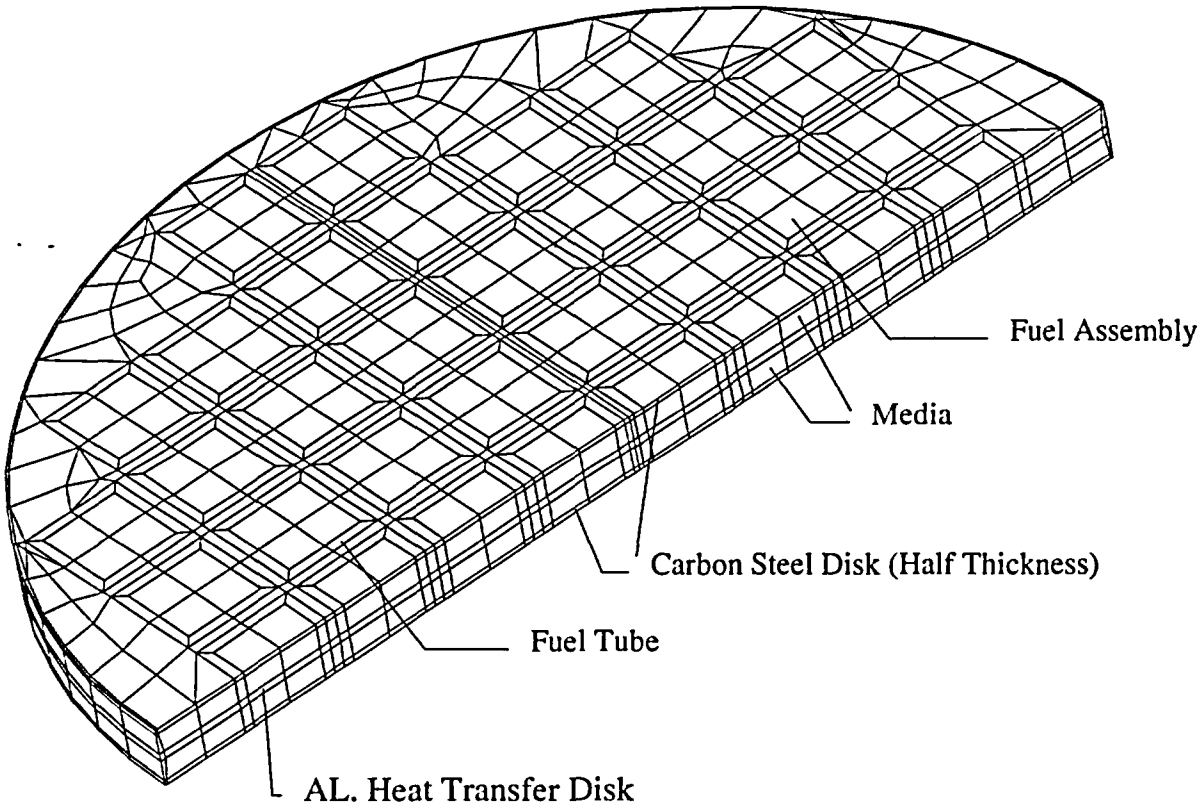

4.4.1.5 Two-Dimensional Fuel Models

The effective conductivity of the fuel is determined by the two-dimensional finite element model of the fuel assembly. The effective conductivity is used in the three-dimensional canister models (Section 4.4.1.2) and the three-dimensional periodic canister internal models (Section 4.4.1.4). A total of seven models are required: four models for the 14×14, 15×15, 16×16 and 17×17 PWR fuels and three models for the 7×7, 8×8 and 9×9 BWR fuels. Because of similarity, only the figure for the PWR 17×17 model is shown in this section (Figure 4.4.1.5-1). All models contain a full cross-section of an assembly to accommodate the radiation elements.

The model includes the fuel pellets, cladding, media between fuel rods, media between the fuel rods and the inner surface of the fuel tube (PWR) or fuel channel (BWR), and helium at the gap between the fuel pellets and cladding. Three types of media are considered: helium, water and a vacuum. Modes of heat transfer modeled include conduction and radiation between individual fuel rods for the steady-state condition. ANSYS PLANE55 conduction elements and MATRIX50 radiation elements are used to model conduction and radiation. Radiation elements are defined between fuel rods and from rods to the wall. Radiation at the gap between the pellets and the cladding is conservatively ignored.

The effective conductivity for the fuel is determined by using an equation defined in a Sandia National Laboratory Report [30]. The equation is used to determine the maximum temperature of a square cross-section of an isotropic homogeneous fuel with a uniform volumetric heat generation. At the boundary of the square cross-section, the temperature is constrained to be uniform. The expression for the temperature at the center of the fuel is given by:

$$T_c = T_e + 0.29468\,(Qa^2 / K_{eff})$$

where: T_c = the temperature at the center of the fuel (°F)
T_e = the temperature applied to the exterior of the fuel (°F)
Q = volumetric heat generation rate (Btu/hr-in^3)
a = half length of the square cross-section of the fuel (inch)
K_{eff} = effective thermal conductivity for the isotropic homogeneous fuel material (Btu/hr-in-°F)

Volumetric heat generation (Btu/hr-in^3) based on the design heat load is applied to the pellets. The effective conductivity is determined based on the heat generated and the temperature difference from the center of the model to the edge of the model. Temperature-dependent effective properties are established by performing multiple analyses using different boundary temperatures. The effective conductivity in the axial direction of the fuel assembly is calculated on the basis of the material area ratio.

Figure 4.4.1.5-1 Two-Dimensional PWR (17×17) Fuel Model

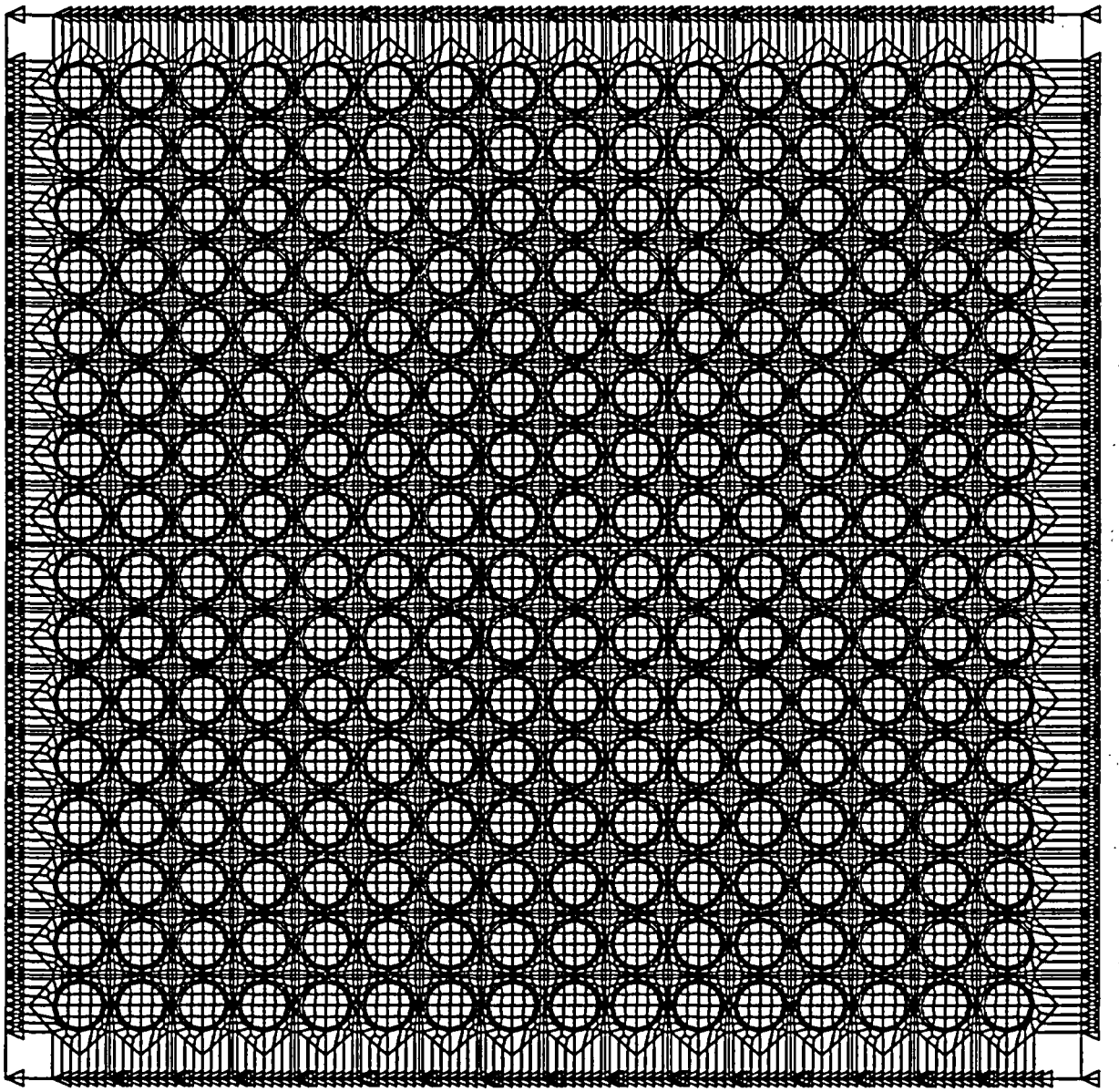

4.4.1.6 Two-Dimensional Fuel Tube Models

The two-dimensional fuel tube model is used to calculate the effective conductivities of the fuel tube wall and BORAL plate. These effective conductivities are used in the three-dimensional canister models (Section 4.4.1.2), the three-dimensional transfer cask and canister models (Section 4.4.1.3) and the three-dimensional periodic canister internal models (Section 4.4.1.4). A total of three models is required: one PWR model and two BWR models (one with the neutron absorber plate, one without the neutron absorber plate), corresponding to the enveloping configurations of the 7×7, 8×8 and 9×9 BWR fuels.

Two forms of the neutron absorber plates are evaluated. The configuration shown in the fuel tube models in Figures 4.4.1.6-1 and 4.4.1.6-2 (for PWR and BWR fuel, respectively) incorporates the BORAL core matrix sandwiched between two layers of aluminum cladding. An alternate design substitutes a single layer of METAMIC for the BORAL. The thermal properties of these materials are presented in Tables 4.2-10 (BORAL) and 4.2-13 (METAMIC). The difference in thermal performance between the two neutron absorber materials is considered to be insignificant, since the primary thermal resistance in the fuel tube design is not the neutron absorber material, but rather the gaps between the fuel tube and the disks.

As shown in Figure 4.4.1.6-1, the PWR model includes the fuel tube, the BORAL plate (including the core matrix sandwiched by aluminum cladding), the stainless steel cladding and the gap between the stainless steel cladding and the support disk or heat transfer disk. Three conditions of media are considered in the gaps: helium, water and a vacuum.

ANSYS PLANE55 conduction elements and LINK31 radiation elements are used to construct the model. The model consists of six layers of conduction elements and two radiation elements (radiation elements are not used for water condition) that are defined at the gaps (two for each gap). The thickness of the model (x-direction) is the distance measured from the outside face of the fuel assembly to the inside face of the slot in the support disk (assuming the fuel tube is centered in the hole in the disk). The gap size between the neutron absorber plate and the stainless steel cladding is 0.003 inch. The height of the model is defined as equal to the width of the model.

The fuel tubes in the BWR fuel basket differ from those in the PWR fuel basket in that not all sides of the fuel tubes contain neutron absorber. In addition, the BWR fuel assembly is contained in a fuel channel. Therefore, two effective conductivity models are necessary, one fuel tube model with the neutron absorber plate (a total of eight layers of materials) and another fuel tube model with a gap replacing the neutron absorber plate (a total of four layers of materials).

As shown in Figure 4.4.1.6-2, the BWR fuel tube model with neutron absorber includes the fuel channel, the gap between the fuel channel and fuel tube, the fuel tube, the neutron absorber plate (including the core matrix sandwiched by aluminum claddings), and a gap between the stainless steel cladding for the neutron absorber plate and the support disk or heat transfer disk. The effective conductivity of the fuel tube without the neutron absorber plate is determined using the second BWR fuel tube model. As shown in Figure 4.4.1.6-3, this model includes the gap between fuel assembly and the fuel channel, the fuel channel, gap between the fuel channel and stainless steel fuel tube, the fuel tube, and a gap between the fuel tube and the support disk or heat transfer disk. An emissivity value of 0.0001 is conservatively used for the BWR support disk in the model.

Heat flux is applied at the left side of the model (fuel tube for PWR models and fuel channel for BWR models), and the temperature at the right boundary of the model is constrained. The heat flux is determined based on the design heat load. The maximum temperature of the model (at the left boundary) and the temperature difference (ΔT) across the model are calculated by the ANSYS model. The effective conductivity (K_{xx}) is determined using the following formula:

$$q = K_{xx} (A/L) \Delta T$$

or

$$K_{xx} = q \ L / (A \ \Delta T)$$

where:

K_{xx} = effective conductivity (Btu/hr-in-°F) in X direction in Figure 4.4.1.6-1.
q = heat rate (Btu/hr)
A= area (in^2)
L= length (thickness) of model (in)
ΔT = temperature difference across the model (°F)

The temperature-dependent conductivity is determined by varying the temperature constraints at one boundary of the model and resolving for the heat rate (q) and temperature difference. The effective conductivity for the parallel path (the Y direction in Figure 4.4.1.6-1) is calculated by:

$$K_{yy} = \frac{\sum K_i t_i}{L}$$

where:

K_i = thermal conductivity of each layer
t_i = thickness of each layer
L = total length (thickness) of the model

Figure 4.4.1.6-1 Two-Dimensional Fuel Tube Model: PWR Fuel

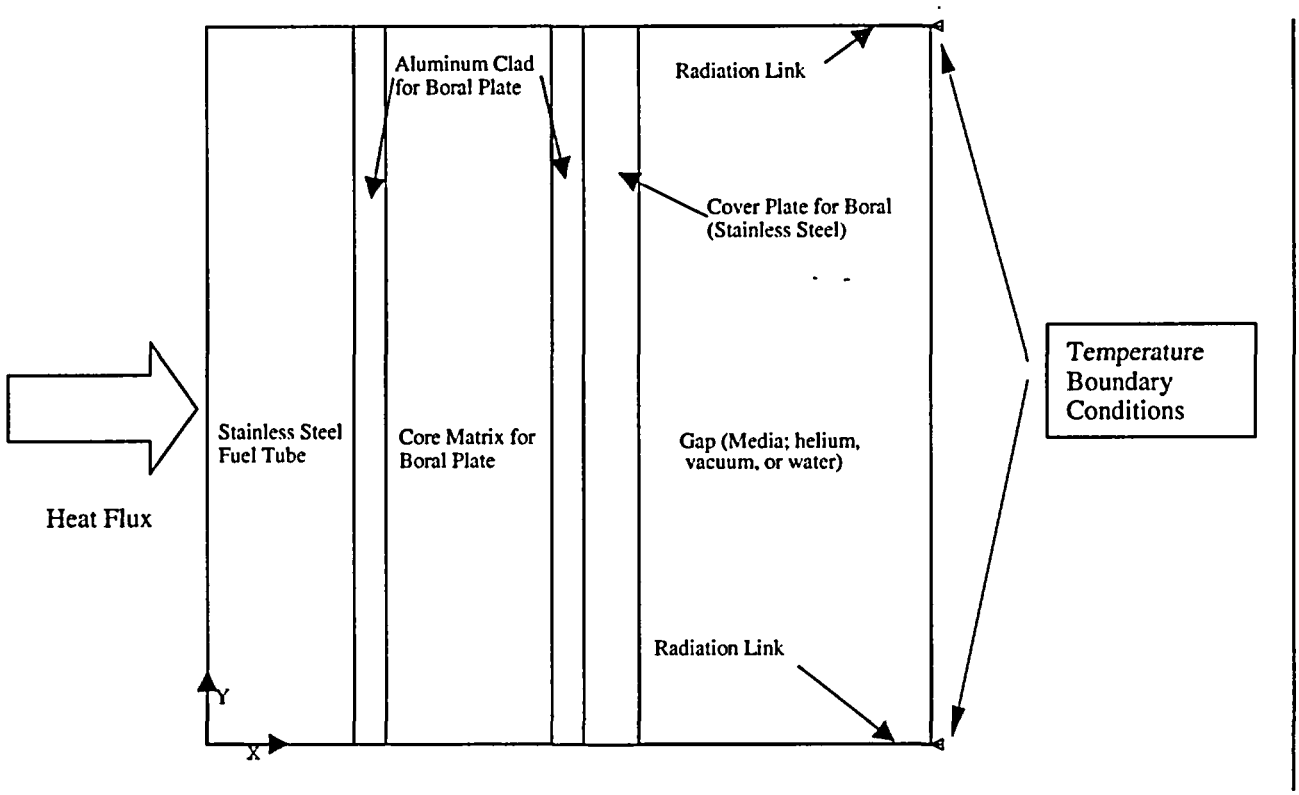

*Media can be water, vacuum, or helium.

Figure 4.4.1.6-2 Two-Dimensional Fuel Tube Model: BWR Fuel Tube with Neutron Absorber

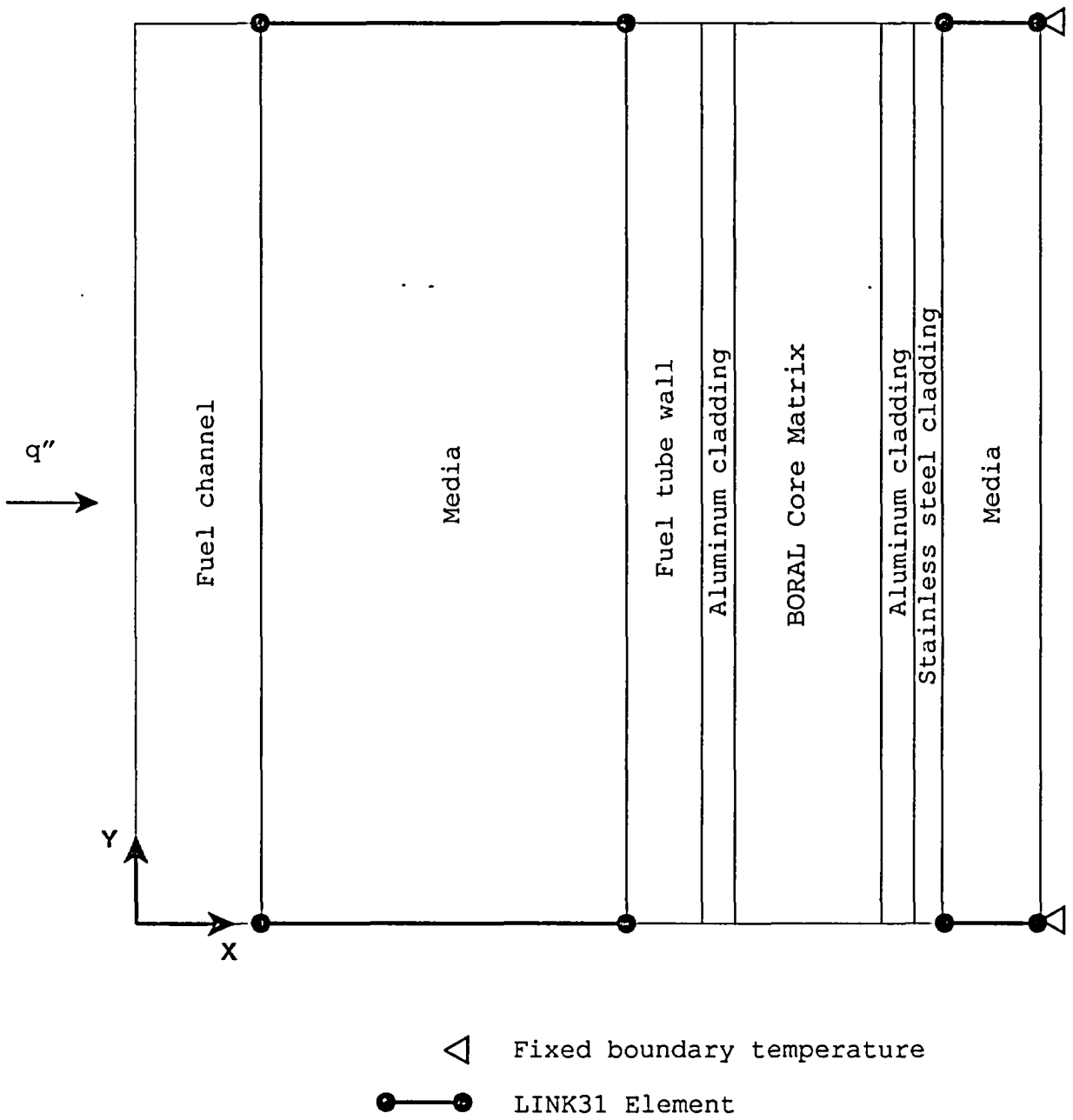

*Media can be water, vacuum, or helium.

Figure 4.4.1.6-3 Two-Dimensional Fuel Tube Model: BWR Fuel Tube without Neutron Absorber

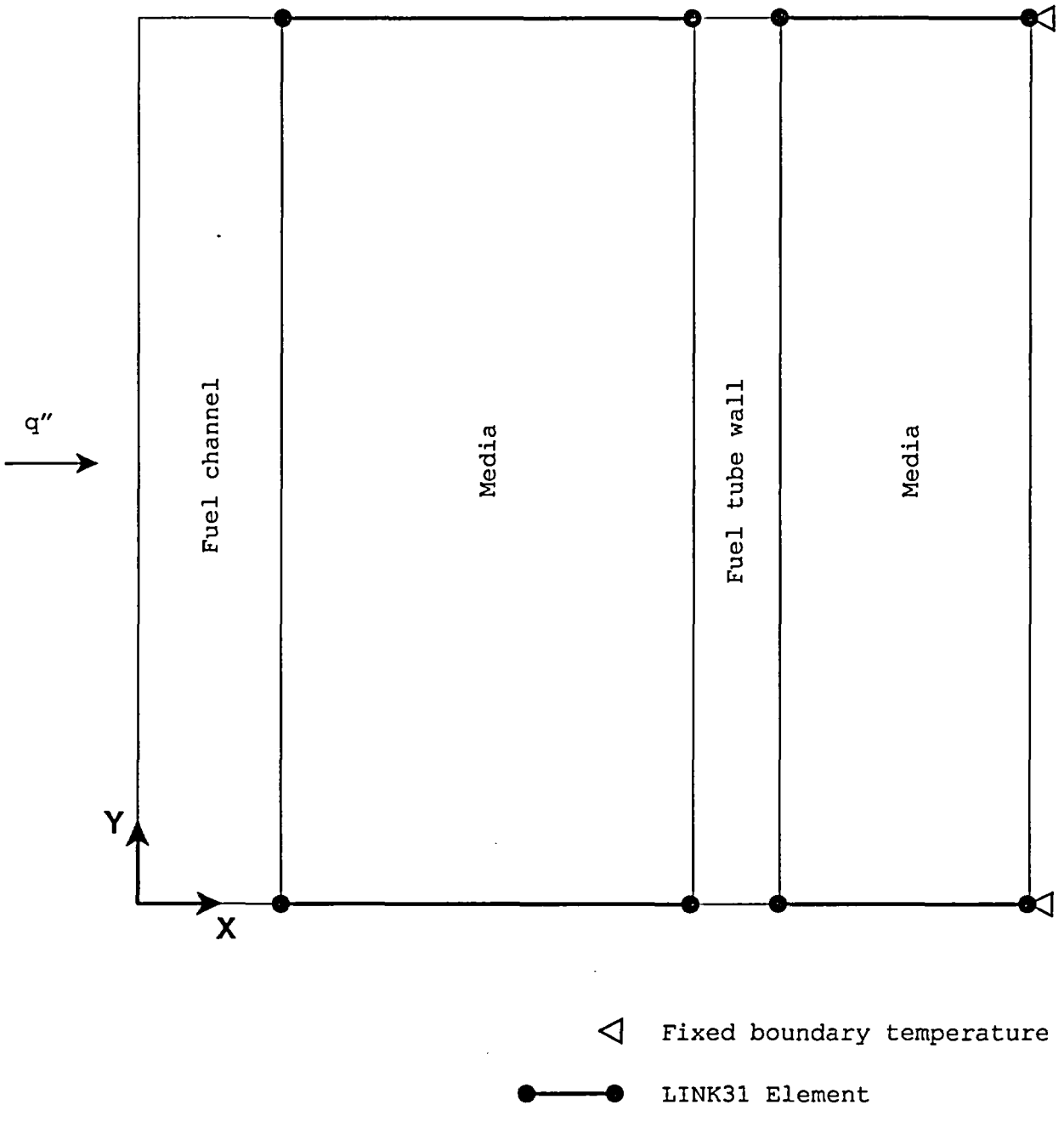

*Media can be water, vacuum, or helium.

4.4.1.7 Two-Dimensional Forced Air Flow Model for Transfer Cask Cooling

A two-dimensional axisymmetric air flow model is used to determine the air flow rate needed to ensure that the maximum temperature of the canister shell and canister components inside the transfer cask do not exceed those presented in Tables 4.4.3-3 and 4.4.3-4 for the helium condition. This air flow model considers a 0.34-inch air annulus between the outer surface of the canister shell and the inner surface of the transfer cask, and has a total length of 191-inches. The fuel canister is cooled by forced convection in the air annulus resulting from air pumped in through fill/drain ports in the body of the transfer cask. The radiation heat transfer between the vertical annulus surfaces (the canister shell outer surface and the transfer cask inner surface) is conservatively neglected. All heat is considered to be removed by the air flow.

ANSYS FLOTRAN FLUID141 fluid thermal elements are used to construct the two-dimensional axisymmetric air flow finite element model for transfer cask cooling. The model and the boundary conditions applied to the model, are shown in Figures 4.4.1.7-1, 4.4.1.7-2 and 4.4.1.7-3.

As shown in Tables 4.4.3-3 and 4.4.3-4, the temperature margin of the governing component (the heat transfer disk) for the PWR fuel configuration is lower than the margin for the BWR fuel configuration; therefore, the thermal loading for the PWR configuration is used. The non-uniform heat generation applied in the model, shown in Figure 4.4.1.7-4, is based on the axial power distribution shown in Figure 4.4.1.1-3 for PWR fuel.

The inlet air velocity is specified based on the volume flow rate. Room temperature (76°F) is applied to the inlet nodes, while zero air velocity, in both the X and Y directions, is defined as the boundary condition for the vertical solid sides.

Results of the analyses of forced air cooling of the canister inside the transfer cask are shown in Figure 4.4.1.7-5. As shown in the figure, the maximum canister shell temperature is less than 416°F for a forced air flow rate of 275 ft^3/minute, or higher, where 416°F is the calculated maximum canister shell temperature for the typical transfer operation for the PWR configuration (Table 4.4.3-3). A forced air volume flow rate of 375 ft^3/minute is conservatively specified for cooling the canister in the event that forced air cooling is required. Evaluation of a forced air volume flow rate of 375 ft^3/minute, results in a maximum canister shell temperature of 321°F, which is significantly less than the design basis temperature of 416°F.

Figure 4.4.1.7-1 Two-Dimensional Axisymmetric Finite Element Model for Transfer Cask Forced Air Cooling

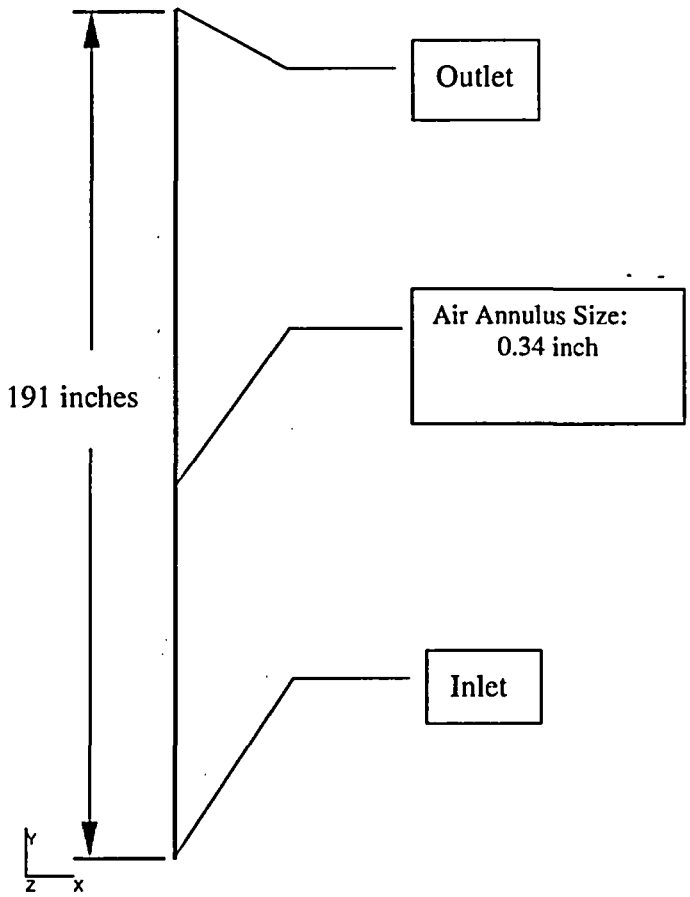

Figure 4.4.1.7-2 Two-Dimensional Axisymmetric Outlet Air Flow Model for Transfer Cask Cooling

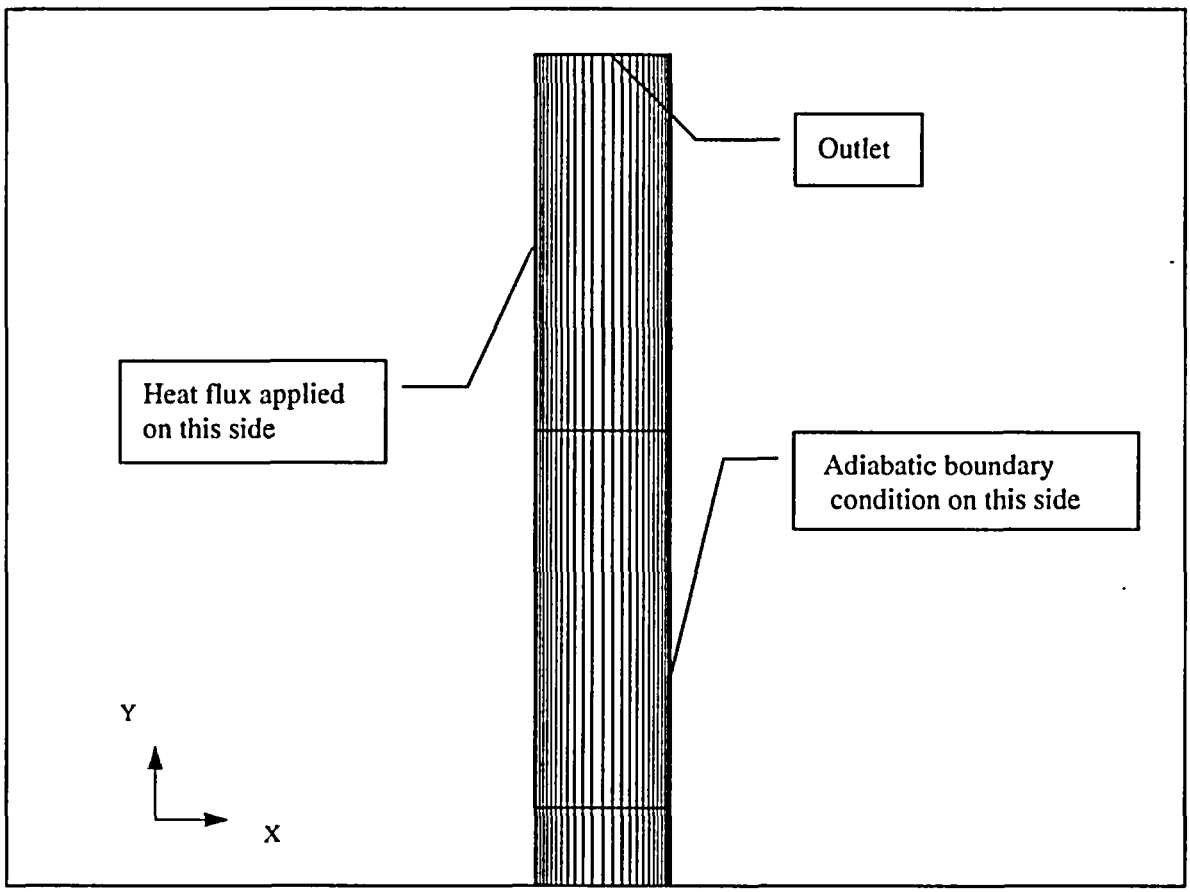

Figure 4.4.1.7-3 Two-Dimensional Axisymmetric Inlet Air Flow Model for Transfer Cask Cooling

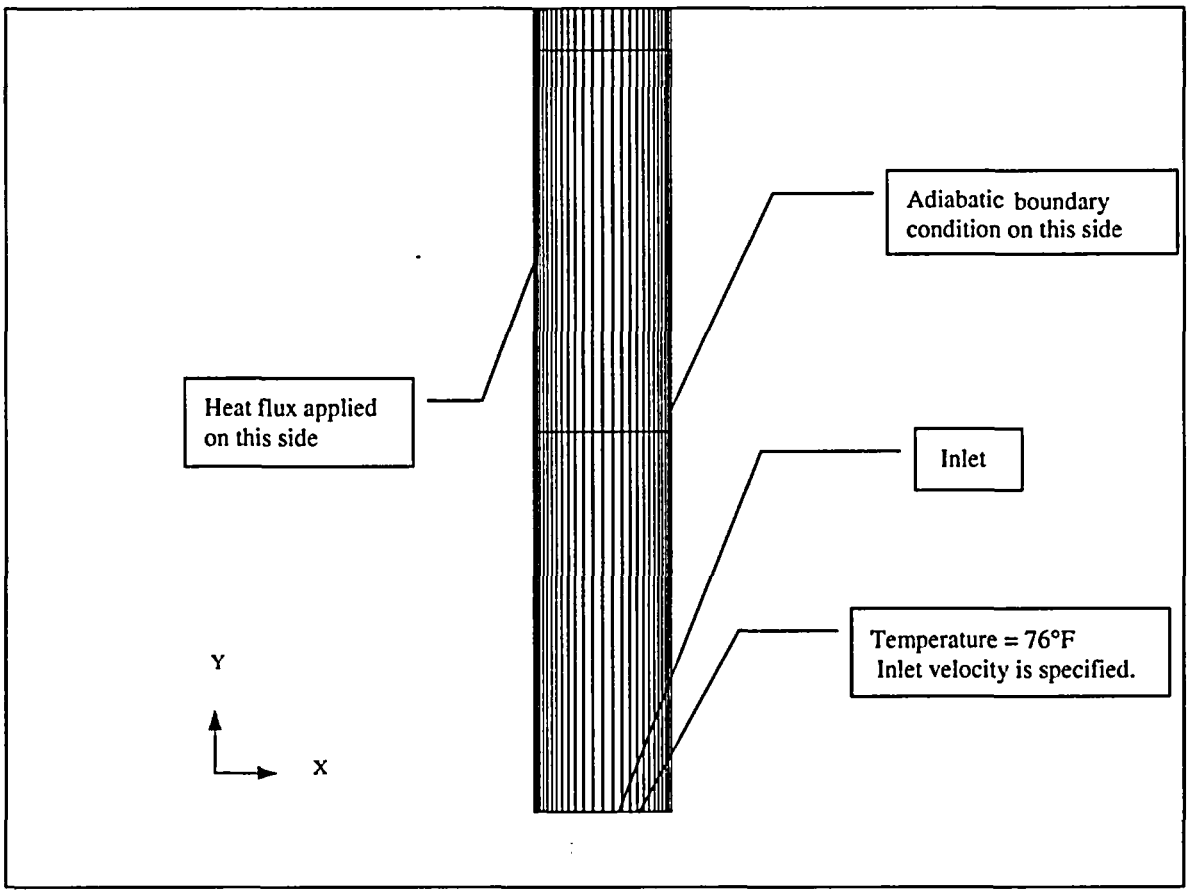

Figure 4.4.1.7-4 Non-Uniform Heat Load from Canister Contents

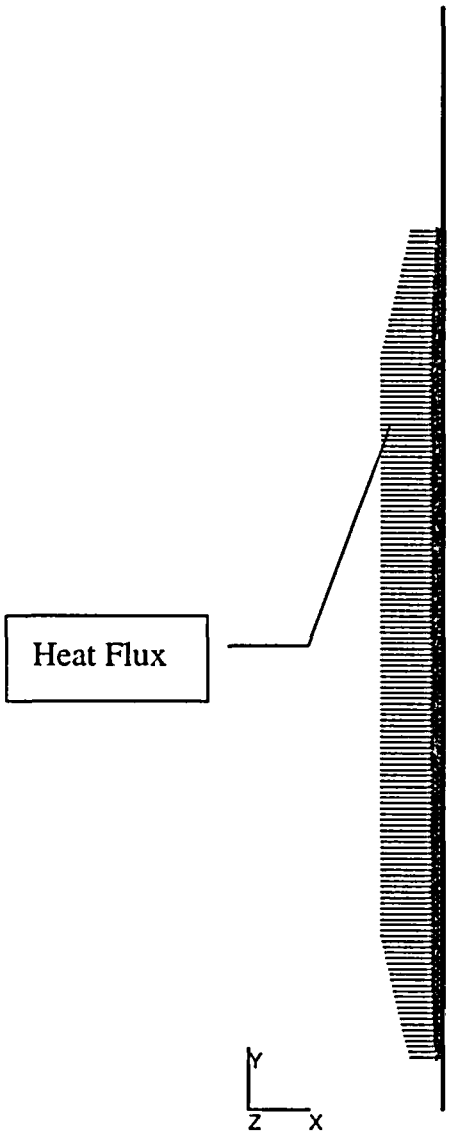

Figure 4.4.1.7-5 Maximum Canister Temperature Versus Air Volume Flow Rate

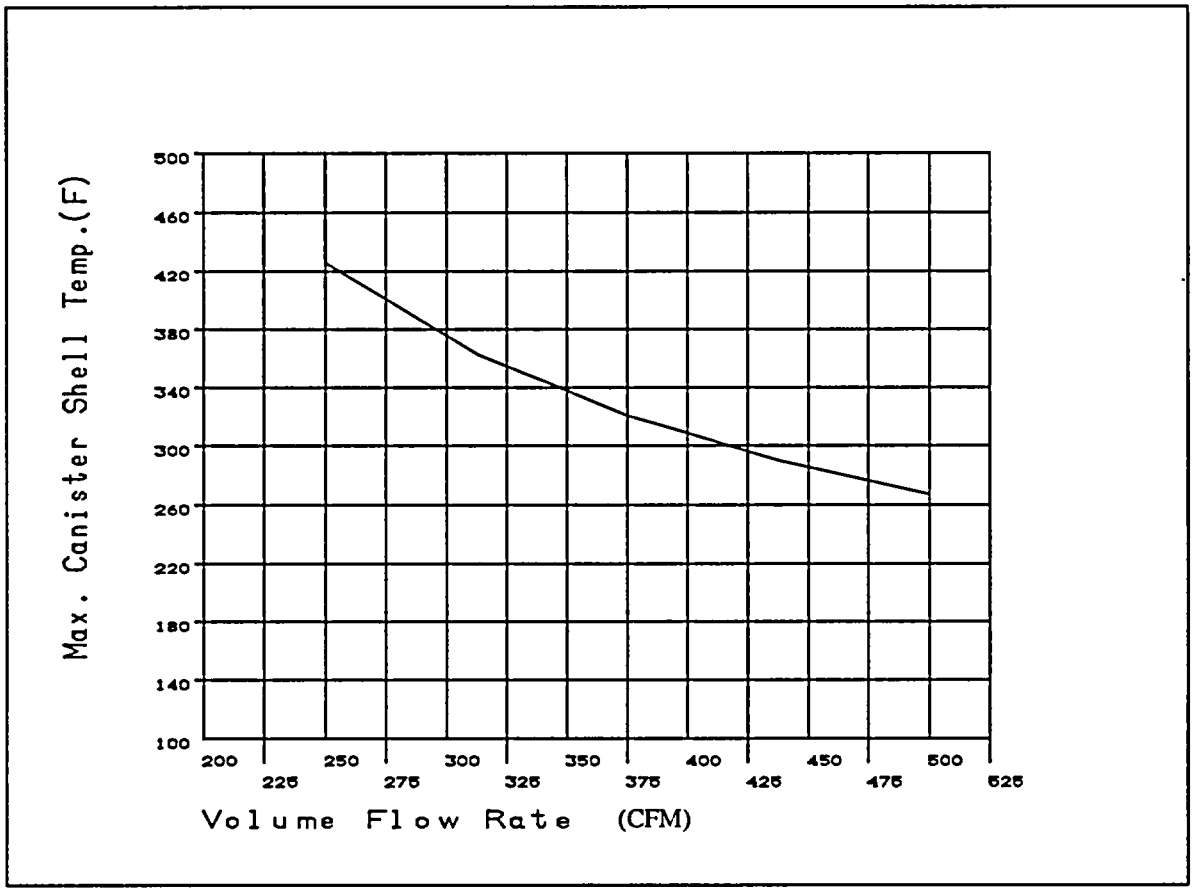

THIS PAGE INTENTIONALLLY LEFT BLANK

4.4.2 Test Model

The Universal Storage System is conservatively designed by analysis. Therefore, no physical model is employed for thermal analysis.

THIS PAGE INTENTIONALLY LEFT BLANK

4.4.3 Maximum Temperatures for PWR and BWR Fuel

Temperature distribution and maximum component temperatures for the Universal Storage System under the normal conditions of storage and transfer, based on the use of the transfer cask, are provided in this section. Components of the Universal Storage System containing PWR and BWR fuels are addressed separately. Temperature distributions for the evaluated off-normal and accident conditions are presented in Sections 11.1 and 11.2.

Figure 4.4.3-1 shows the temperature distribution of the Vertical Concrete Cask and the canister containing the PWR design basis fuel for the normal, long-term storage condition. The air flow pattern and air temperatures in the annulus between the PWR canister and the concrete cask liner for the normal condition of storage are shown in Figures 4.4.3-2 and 4.4.3-3, respectively. The temperature distribution in the concrete portion of the concrete cask for the PWR assembly is shown in Figure 4.4.3-4. The temperature distribution for the BWR design basis fuel is similar to that of the PWR fuel and is, therefore, not presented. Table 4.4.3-1 shows the maximum component temperatures for the normal condition of storage for the PWR design basis fuel. The maximum component temperatures for the normal condition of storage for the BWR design basis fuel are shown in Table 4.4.3-2.

As shown in Figure 4.4.3-3, a high-temperature gradient exists near the wall of the canister and the liner of the concrete cask, while the air in the center of the annulus exhibits a much lower temperature gradient, indicating significant boundary layer features of the air flow. The temperatures at the concrete cask steel liner surface are higher than the air temperature, which indicates that salient radiation heat transfer occurs across the annulus. As shown in Figure 4.4.3-4, the local temperature in the concrete, directly affected by the radiation heat transfer across the annulus, can reach 186°F (less than the 200°F allowable temperature). The bulk temperature in the concrete, as determined using volume average of the temperatures in the concrete region, is 135°F, less than the allowable value of 150°F.

Under typical operations, the transient history of maximum component temperatures for the transfer conditions (canister, inside the transfer cask, containing water for 17 hours, vacuum for 27 hours for PWR and 25 hours for BWR and for 20 hours in helium for PWR and 16 hours in helium for BWR) is shown in Figures 4.4.3-5 and 4.4.3-6 for PWR and BWR fuels, respectively. The maximum component temperatures for the transfer conditions (vacuum and helium conditions) are shown in Tables 4.4.3-3 and 4.4.3-4, for PWR and BWR fuels, respectively.

The maximum calculated water temperature is 203°F for both the PWR and BWR fuels at the end of 17 hours based on an initial water temperature of 100°F.

4.4.3.1 Maximum Temperatures at Reduced Total Heat Loads

This section provides the evaluation of component temperatures for fuel heat loads less than the design basis heat load of 23 kW. Transient thermal analyses are performed for PWR fuel heat loads of 20, 17.6, 14, 11 and 8 kW to establish the allowable time limits for the vacuum condition in the canister as described in the Technical Specifications for the Limiting Conditions of Operation (LCO), LCOs 3.1.1 and 3.1.4. The time limits ensure that the allowable temperatures of the limiting components — the heat transfer disks and the fuel cladding — are not exceeded. A steady-state evaluation is also performed for all the heat load cases in the vacuum condition and all the heat load cases in the helium condition. If the steady-state temperature calculated is less than the limiting component allowable temperature, then the allowable time duration in the vacuum or helium conditions is defined to be 600 hours (25 days) based on the 30 day time test for abnormal regimes as described in PNL-4835 [34].

The three-dimensional transfer cask and canister model for the PWR fuel configuration, described in Section 4.4.1.3, is used for the transient and steady-state thermal analysis for the reduced heat load cases. To obtain the bounding temperatures for all possible loading configurations, thermal analyses are performed for a total of 14 cases as tabulated in the following table. The basket locations are shown in Figure 4.4.3-7. Since the maximum temperature for the limiting components (fuel cladding and heat transfer disk) always occurs at the central region of the basket, hotter fuels (maximum allowable heat load for 5-year cooled fuel: 0.958 kW = 23 kW/24) are specified at the central basket locations. The bounding cases for each heat load condition are noted with an asterisk (*) in the tabulation which follows. Six cases (cases 3 through 8) are evaluated for the 17.6 kW heat load condition. The first four cases (cases 3 through 6) represent standard UMS® system fuel loadings. The remaining two cases (cases 7 and 8) account for the preferential loading configuration for Maine Yankee site-specific fuel (Section 4.5.1.2), with case 8 being the bounding case for the Maine Yankee fuel. Based on the analysis results of the 17.6 kW heat load cases, only two loading cases are required to establish the bounding condition for the 20, 14, 11 and 8 kW heat loads.

Canister Heat Load (kW)	Heat Load Case	Heat Load (kW) Evaluated in Each Basket Location (See Figure 4.4.3-7)					
		1	2	3	4	5	6
20	1	0.958	0.958	0.709	0.958	0.709	0.709
20*	2	0.958	0.958	0.958	0.958	0.958	0.210
17.6	3	0.958	0.958	0.509	0.958	0.509	0.509
17.6*	4	0.958	0.958	0.568	0.958	0.958	0.000
17.6	5	0.958	0.958	0.958	0.958	0.568	0.000
17.6	6	0.958	0.958	0.284	0.958	0.958	0.284
17.6	7	0.958	0.146	1.050	0.146	1.050	1.050
17.6	8	0.958	0.958	1.050	0.384	1.050	0.000
14	9	0.958	0.958	0.209	0.958	0.209	0.209
14*	10	0.958	0.958	0.000	0.958	0.626	0.000
11	11	0.958	0.896	0.000	0.896	0.000	0.000
11*	12	0.958	0.958	0.000	0.834	0.000	0.000
8	13	0.958	0.521	0.000	0.521	0.000	0.000
8*	14	0.958	0.958	0.000	0.084	0.000	0.000

The heat load (23 kW/24 Assemblies = 0.958 kW) at the four (4) central basket locations corresponds to the maximum allowable canister heat load for 5-year cooled fuel (Table 4.4.7-8). The non-uniform heat loads evaluated in this section bound the equivalent uniform heat loads, since they result in higher maximum temperatures of the fuel cladding and heat transfer disk.

Volumetric heat generation (Btu/hr-in^3) is applied to the active fuel region in each fuel assembly location of the model using the axial power distribution for PWR fuel (Figure 4.4.1.1-3) in the axial direction.

The thermal analysis results for the closure and transfer of a loaded PWR fuel canister in the transfer cask for the reduced heat load cases are shown in Table 4.4.3-5, with a comparison to the results for the design basis heat load case. The temperatures shown are the maximum temperatures for the limiting components (fuel cladding and heat transfer disk). The maximum temperatures of the fuel cladding and the heat transfer disk are less than the allowable temperatures (Table 4.1-3) of these components for the short-term conditions of vacuum drying and helium backfill. As shown in Table 4.4.3-5, a time limit of 600 hours is specified for moving the canister out of the transfer cask after the canister is filled with helium. This time limit is for the heat load cases where the maximum fuel cladding/heat transfer disk temperatures for the steady-state condition are below the short-term allowable temperatures. Note that the maximum water temperature at the end of the "water period" is considered to be the volumetric average temperature of the calculated cladding temperatures in the active fuel region of the hottest fuel assembly. The

results indicate that the volumetric average water temperature is below 212°F for all cases evaluated. This is consistent with the thermal model that only considers conduction in the fuel assembly region and between the disks. This approach does not include consideration of convection of the water or the energy absorbed by latent heat of vaporization.

The Technical Specifications specify the remedial actions, either in-pool or forced air cooling, required to ensure that the fuel cladding and basket component temperatures do not exceed their short-term allowable temperatures, if the time limits are not met. LCOs 3.1.1 and 3.1.4 incorporate the operating times for heat loads that are less than the design basis heat loads as evaluated in this section.

Using the same three-dimensional transfer cask/canister models, analysis is performed for the conditions of in-pool cooling and forced air cooling followed by the vacuum drying and helium backfill operation (LCO 3.1.1). The conditions at the end of the vacuum drying as shown in Tables 4.4.3-5 (PWR) and 4.4.3-8 (BWR) are used as the initial conditions of the analyses. The LCO 3.1.1 "Action" analysis results are shown in Tables 4.4.3-6 and 4.4.3-7 for the PWR configuration and Tables 4.4.3-9 and 4.4.3-10 for the BWR configuration. Note that the duration of the second vacuum (after completion of the in-pool or forced air cooling) is limited (calculated based on the heat-up rate of the first vacuum), so the maximum temperatures at the end of the second vacuum cycle will not exceed those at the end of the first vacuum cycle. The maximum temperatures at the end of the first vacuum (Table 4.4.3-5 for PWR and Table 4.4.3-8 for BWR) are conservatively presented as the maximum temperatures for the second vacuum condition. The maximum temperatures for the fuel cladding and the heat transfer disk are below the short-term allowable temperatures.

The in-pool cooling and the forced-air cooling followed by the helium backfill operation in LCO 3.1.4 are also evaluated for the PWR configuration for the 23 kW case and the BWR configuration for the 23 kW and 20 kW cases. The temperature profiles at the end of the helium condition, as shown in Table 4.4.3-5 for PWR and Table 4.4.3-8 for BWR, are used as the initial condition. The results for the BWR are shown in Tables 4.4.3-11 and 4.4.3-12 for the in-pool cooling and forced-air cooling, respectively. The results for the PWR are shown in Tables 4.4.3-13 and 4.4.3-14 for the in-pool cooling and forced-air cooling, respectively. Note that the time limit for the first helium backfill condition is used for the second helium backfill condition (after completion of the in-pool or forced-air cooling). Based on the heat-up rate of the first helium condition, the maximum component temperatures at the end of the second helium condition are well below the maximum temperatures at the end of the first helium condition. The maximum

temperatures at the end of the first helium condition (Table 4.4.3-5 for PWR and Table 4.4.3-8 for BWR) are conservatively presented as the maximum temperatures for the second helium backfill condition, as shown in Tables 4.4.3-11 and 4.4.3-12 for the BWR configuration and Tables 4.4.3-13 and 4.4.3-14 for the PWR configuration.

Figure 4.4.3-1 Temperature Distribution (°F) for the Normal Storage Condition: PWR Fuel

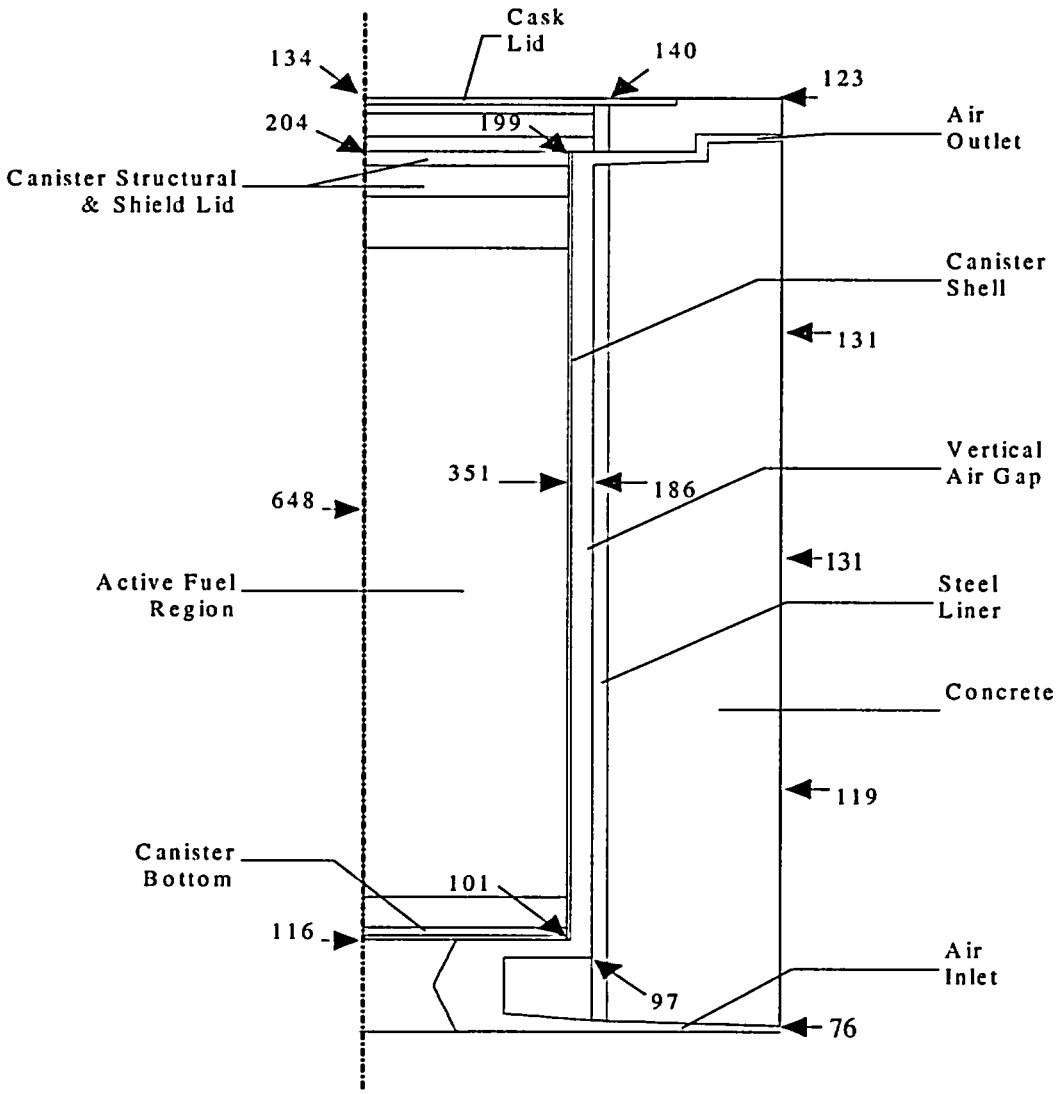

Figure 4.4.3-2 Air Flow Pattern in the Concrete Cask in the Normal Storage Condition: PWR Fuel

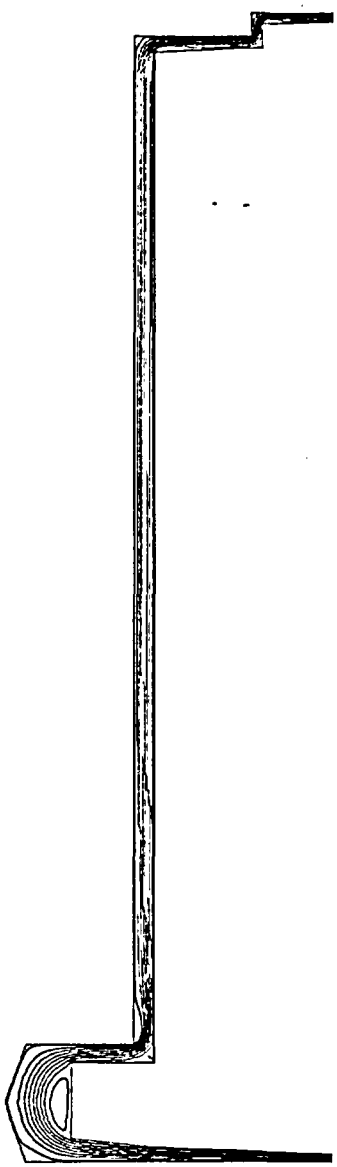

Figure 4.4.3-3 Air Temperature (°F) Distribution in the Concrete Cask During the Normal Storage Condition: PWR Fuel

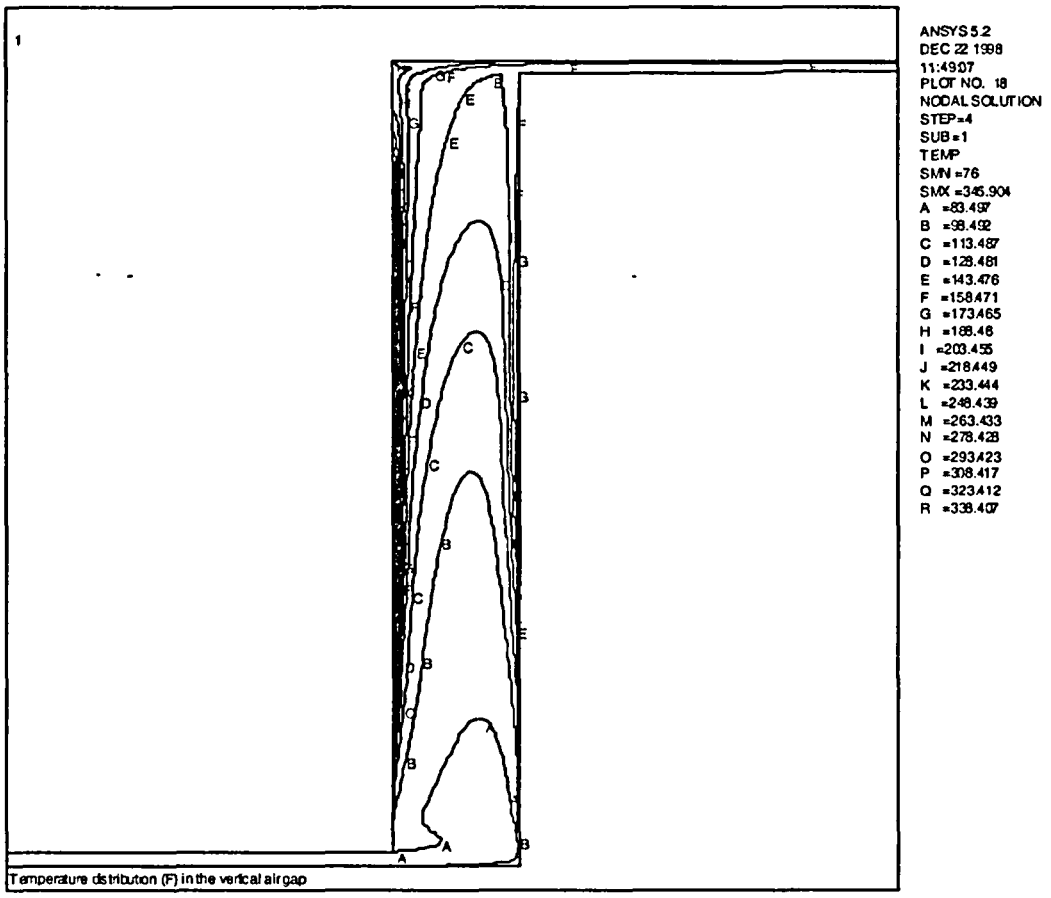

Figure 4.4.3-4 Concrete Temperature (°F) Distribution During the Normal Storage Condition: PWR Fuel

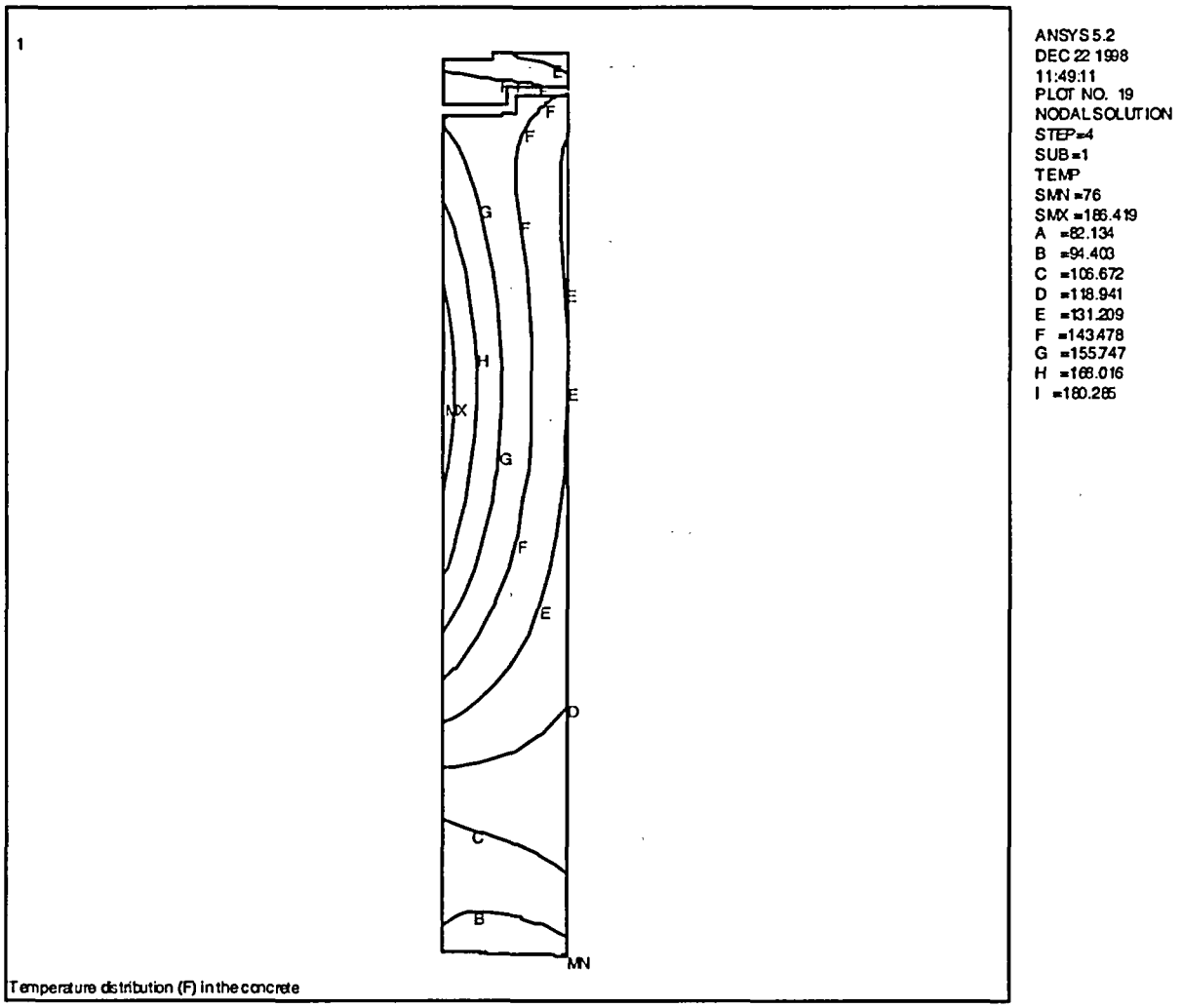

Figure 4.4.3-5 History of Maximum Component Temperature (°F) for Transfer Conditions for PWR Fuel with Design Basis 23 kW Uniformly Distributed Heat Load

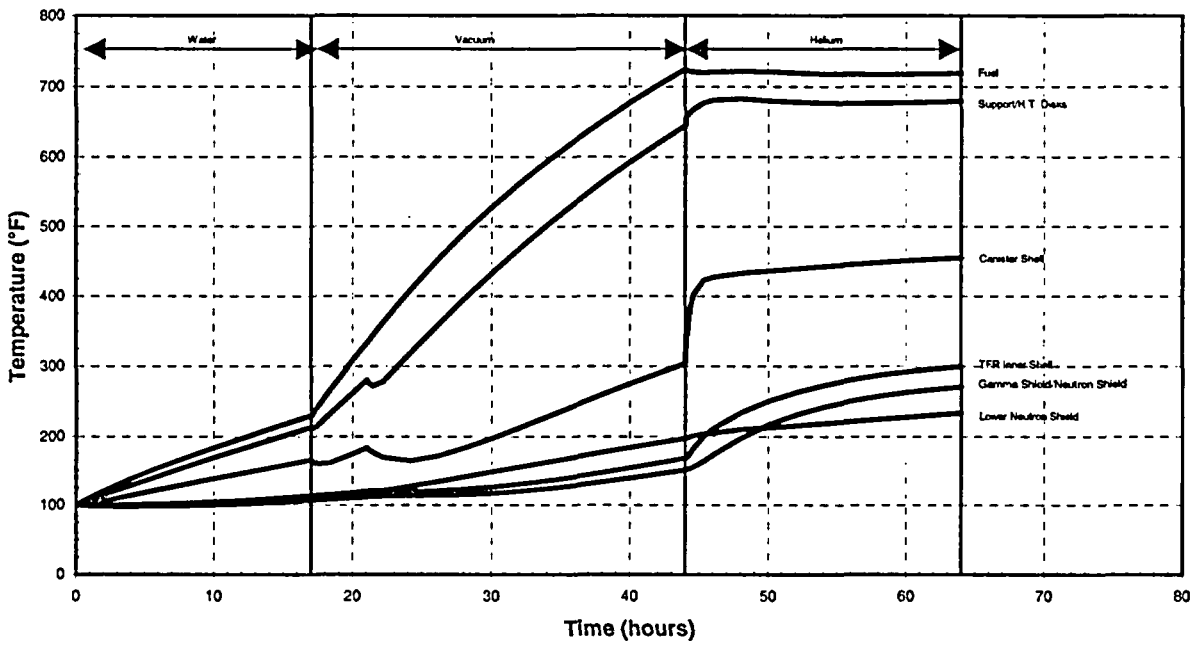

Notes:

1. This graph corresponds to a canister containing water for 17 hours, vacuum for 27 hours and 20 hours in the helium condition. The results correspond to a uniformly distributed decay heat load of 23 kW.
2. "TFR" refers to the transfer cask.

Figure 4.4.3-6 History of Maximum Component Temperature (°F) for Transfer Conditions for BWR Fuel with Design Basis 23 kW Uniformly Distributed Heat Load

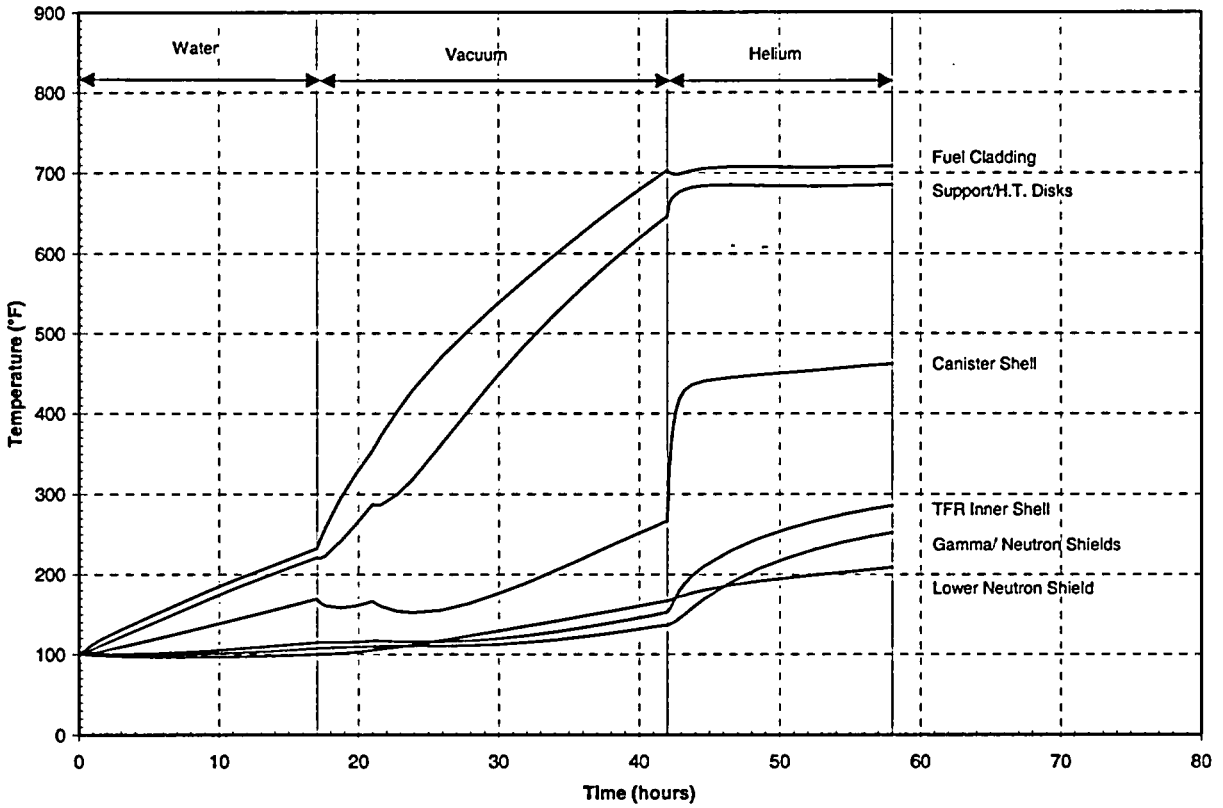

Notes:

1. This graph corresponds to a canister containing water for 17 hours, vacuum for 25 hours and 16 hours in the helium condition. The results correspond to a uniformly distributed decay heat load of 23 kW.
2. "TFR" refers to the transfer cask.

Figure 4.4.3-7 Basket Location for the Thermal Analysis of PWR Reduced Heat Load Cases

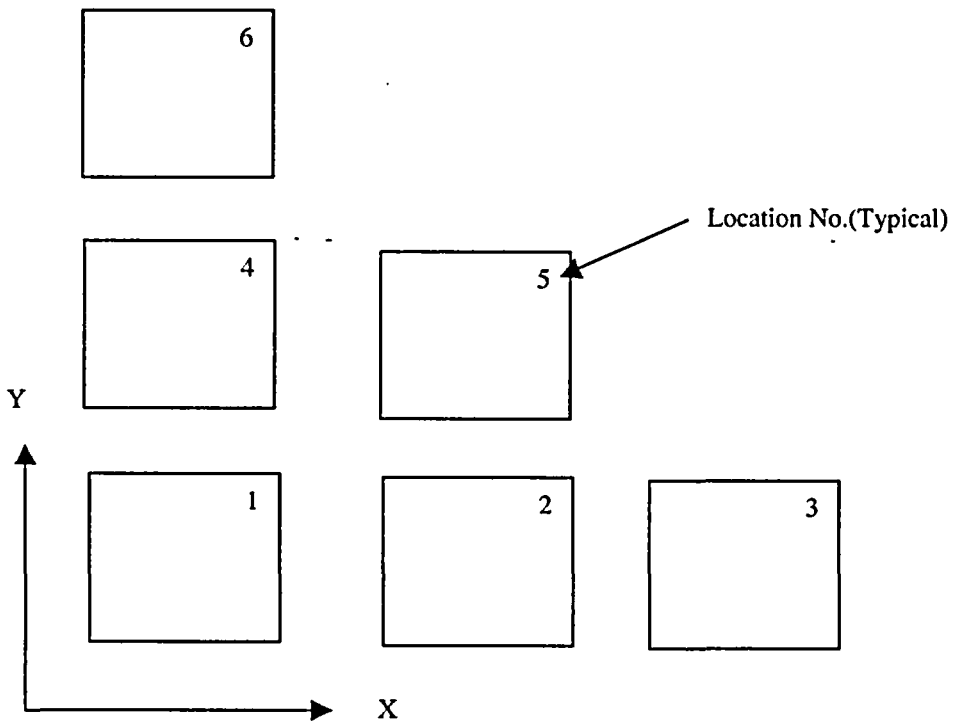

A quarter symmetry configuration is considered. X and Y axes are at the centerlines of the basket.

Figure 4.4.3-8 BWR Fuel Basket Location Numbers

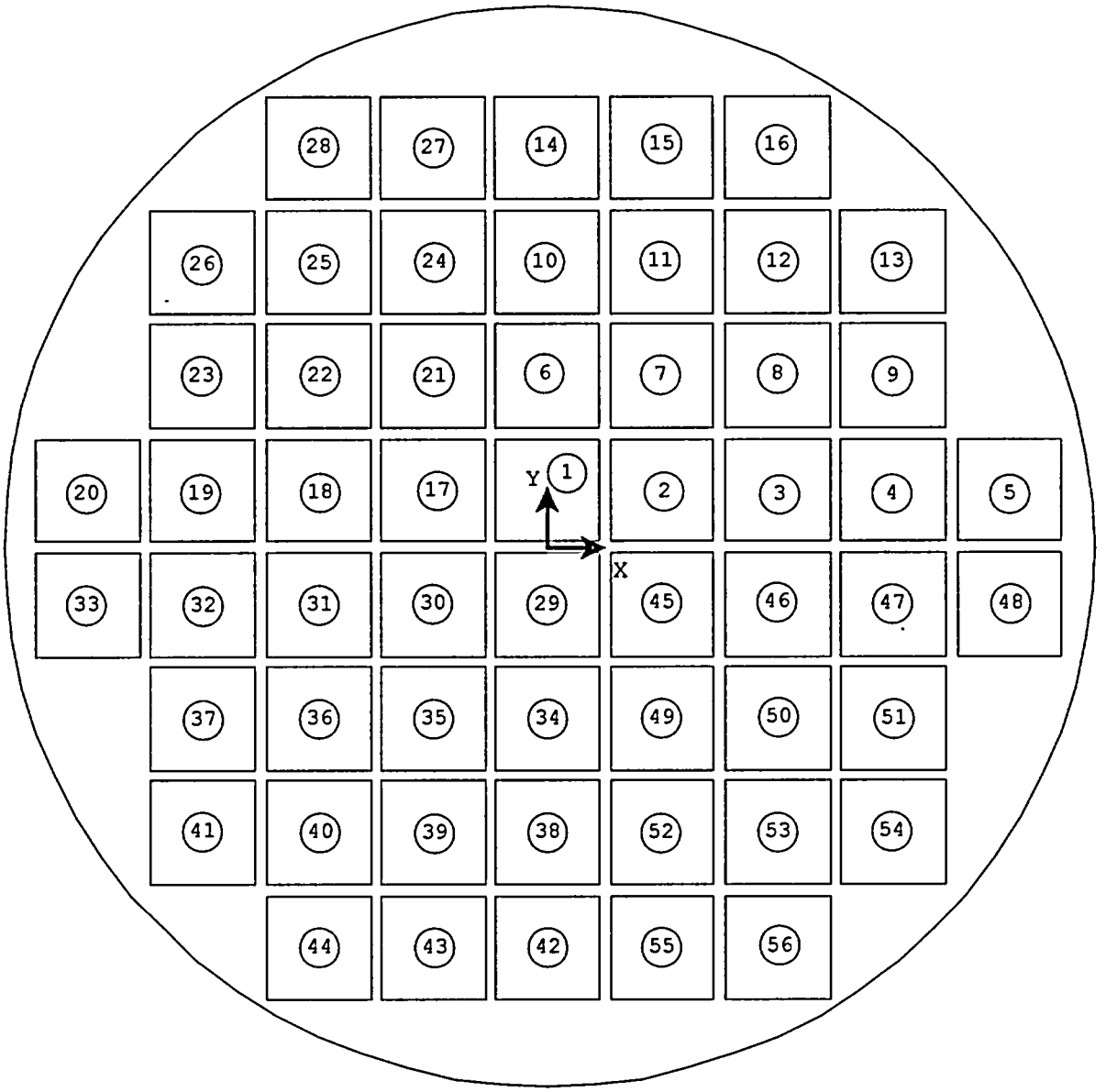

Table 4.4.3-1 Maximum Component Temperatures for the Normal Storage Condition - PWR

Component	Maximum Temperature (°F)	Allowable Temperatures (°F)
Fuel Cladding	648	752
Heat Transfer Disk	599	650
Support Disk	601	650
Top Weldment	399	800
Bottom Weldment	159	800
Canister Shell	351	800
Canister Structural Lid	204	800
Canister Shield Lid	212	800
Concrete	186 (local) 135 (bulk*)	300 (local) 150 (bulk)

* The volume average temperature of the concrete region is used as the bulk concrete temperature.

Table 4.4.3-2 Maximum Component Temperatures for the Normal Storage Condition - BWR

Component	Maximum Temperature (°F)	Allowable Temperatures (°F)
Fuel Cladding	642	752
Heat Transfer Disk	612	650
Support Disk	614	700
Top Weldment	361	800
Bottom Weldment	276	800
Canister Shell	376	800
Canister Structural Lid	180	800
Canister Shield Lid	185	800
Concrete	192 (local) 136 (bulk*)	300 (local) 150 (bulk)

*The volume average temperature of the concrete region is used as the bulk concrete temperature.

Table 4.4.3-3 Maximum Component Temperatures for the Transfer Condition – PWR Fuel with Design Basis 23 kW Uniformly Distributed Heat Load

Component	Maximum Temperature (°F)		Allowable Temperature (°F)
	Vacuum[1]	Helium[1]	
Fuel	724	724	752
Lead	151	271	600
Neutron Shield	149	267	300
Heat Transfer Disk	641	680	750
Support Disk	644	683	800
Canister	304	455	800
Transfer Cask Shells	168	300	700

1. See Figure 4.4.3-5 for history of maximum component temperatures.

Table 4.4.3-4 Maximum Component Temperatures for the Transfer Condition – BWR Fuel with Design Basis 23 kW Uniformly Distributed Heat Load

Component	Maximum Temperature (°F)		Allowable Temperature (°F)
	Vacuum[1]	Helium[1]	
Fuel	703	708	752
Lead	137	252	600
Neutron Shield	135	249	300
Heat Transfer Disk	645	683	750
Support Disk	646	686	700
Canister	267	462	800
Transfer Cask Shells	153	286	700

1. See Figure 4.4.3-6 for history of maximum component temperatures.

Table 4.4.3-5 Maximum Limiting Component Temperatures in Transient Operations for the Reduced Heat Load Cases for PWR Fuel

Heat Load (kW)	Water			Vacuum			Helium		
	Duration (hours)	Maximum Temperature (°F)		Duration (hours)	Maximum Temperature (°F)		Duration (hours)	Max. Temp. / Temp. at Steady-state (°F)	
		Fuel	Heat Transfer Disk		Fuel	Heat Transfer Disk		Fuel	Heat Transfer Disk
23.0	17	230	213	27	724	641	20	724[3]	680[3]
20.0	18	232	214	30	728	628	600[2]	728/708	664/664
17.6	20	239	219	33	731	617	600[2]	731/672	651/624
17.6[1]	20	231	214	33	722	604	600[2]	722/657	635/609
14.0	22	240	219	40	732	596	600[2]	732/613	630/559
11.0	24	237	215	52	730	575	600[2]	730/555	611/495
8.0	37	247	221	103	731	557	600[2]	731/483	595/412

1. Preferential loading configuration, site specific case for Maine Yankee.
2. Duration is defined based on a test time of 30 days for abnormal regimes as described in PNL-4835 [34].
3. Since the time in helium is limited for the 23 kW configuration, only the maximum temperatures are listed.

Table 4.4.3-6 Maximum Limiting Component Temperatures in Transient Operations for the Reduced Heat Load Cases for PWR Fuel after In-Pool Cooling

Heat Load (kW)	In-Pool (helium)			Vacuum			Helium		
	Duration (hours)	End Temperature (°F)		Duration[1] (hours)	Maximum Temperature (°F)[2]		Duration (hours)	Max. Temp. / Temp. at Steady-state (°F)	
		Fuel	Heat Transfer Disk		Fuel	Heat Transfer Disk		Fuel	Heat Transfer Disk
23.0	24	491	415	14	724	641	20	724[4]	680[4]
20.0	24	477	397	17	728	628	600[3]	728/708	664/664
17.6	24	465	383	20	731	617	600[3]	731/672	651/624
14.0	24	445	360	26	732	596	600[3]	732/613	630/559
11	24	422	334	38	730	575	600[3]	730/555	611/495
8	24	390	293	89	731	557	600[3]	731/483	595/412

1. The maximum allowable time in the Technical Specification for this condition is equal to 2 hours less than the maximum allowable time shown in this table. This 2-hour reduction allows the handling time required to enter the next stage.
2. The maximum temperatures at the end of the first vacuum (Table 4.4.3-5) are conservatively presented.
3. Duration is defined based on a test time of 30 days for abnormal regimes as described in PNL-4835.
4. Since the time in helium is limited for the 23 kW configuration, only the maximum temperatures are listed.

Table 4.4.3-7 Maximum Limiting Component Temperatures in Transient Operations for the Reduced Heat Load Cases for PWR Fuel after Forced-Air Cooling

Heat Load (kW)	Forced-Air (helium)			Vacuum			Helium		
	Duration (hours)	End Temperature (°F)		Duration[1] (hours)	Maximum Temperature (°F)[2]		Duration (hours)	Max. Temp. / Temp. at Steady-state (°F)	
		Fuel	Heat Transfer Disk		Fuel	Heat Transfer Disk		Fuel	Heat Transfer Disk
23.0	24	621	564	5	724	641	20	724[4]	680[4]
20.0	24	591	530	8	728	628	600[3]	728/708	664/664
17.6	24	567	502	11	731	617	600[3]	731/672	651/624
14.0	24	530	458	18	732	596	600[3]	732/613	630/559
11	24	493	415	29	730	575	600[3]	730/555	611/495
8	24	450	363	80	731	557	600[3]	731/483	595/412

1. The maximum allowable time in the Technical Specification for this condition is equal to 2 hours less than the maximum allowable time shown in this table. This 2-hour reduction allows the handling time required to enter the next stage.
2. The maximum temperatures at the end of the first vacuum (Table 4.4.3-5) are conservatively presented.
3. Duration is defined based on a test time of 30 days for abnormal regimes as described in PNL-4835.
4. Since the time in helium is limited for the 23 kW configuration, only the maximum temperatures are listed.

Table 4.4.3-8 Maximum Limiting Component Temperatures in Transient Operations for BWR Fuel

Heat Load (kW)	Water			Vacuum			Helium		
	Duration (hours)	Maximum Temperature (°F)		Duration (hours)	Maximum Temperature (°F)		Duration (hours)	Max. Temp. / Temp. at Steady-state (°F)	
		Fuel	Heat Transfer Disk		Fuel	Heat Transfer Disk		Fuel	Heat Transfer Disk
23	17	232	221	25	703	645	16	708[2]	683[2]
20	18	234	222	27	694	627	30	694[2]	661[2]
17	19	234	221	33	701	629	600[1]	701/660	659/631
14	20	232	219	45	719	643	600[1]	719/606	671/574
11	23	234	220	72	733	653	600[1]	733/543	679/508
8	31	236	220	600[1]	724	639	600[1]	724/467	639/427

1. Duration is defined based on a test time of 30 days for abnormal regimes as described in PNL-4835.
2. Since the time in helium is limited for the 23 kW and 20 kW cases, only the maximum temperatures are listed.

Table 4.4.3-9 Maximum Limiting Component Temperatures in Transient Operations after Vacuum for BWR Fuel after In-Pool Cooling

Heat Load (kW)	In-Pool (helium)			Vacuum			Helium		
	Duration (hours)	End Temperature (°F)		Duration[1] (hours)	Maximum Temperature (°F)[2]		Duration (hours)	Max. Temp. / Temp. at Steady-state (°F)	
		Fuel	Heat Transfer Disk		Fuel	Heat Transfer Disk		Fuel	Heat Transfer Disk
23	24	488	444	12	703	645	16	708[4]	683[4]
20	24	476	431	13	694	627	30	694[4]	661[4]
17	24	467	419	19	701	629	600[3]	701/660	659/631
14	24	455	404	28	719	643	600[3]	719/606	671/574
11	24	439	383	54	733	653	600[3]	733/543	679/508

1. The maximum allowable time in the Technical Specification for this condition is equal to 2 hours less than the maximum allowable time shown in this table. This 2-hour reduction allows the handling time required to enter the next stage.
2. The maximum temperatures at the end of the first vacuum (Table 4.4.3-8) are conservatively presented.
3. Duration is defined based on a test time of 30 days for abnormal regimes as described in PNL-4835.
4. Since the time in helium is limited for the 23 kW and 20 kW cases, only the maximum temperatures are listed.

Table 4.4.3-10 Maximum Limiting Component Temperatures in Transient Operations after Vacuum for BWR Fuel after Forced-Air Cooling

Heat Load (kW)	Forced-Air (helium)			Vacuum			Helium		
	Duration (hours)	End Temperature (°F)		Duration[1] (hours)	Maximum Temperature (°F)[2]		Duration (hours)	Max. Temp. / Temp. at Steady-state (°F)	
		Fuel	Heat Transfer Disk		Fuel	Heat Transfer Disk		Fuel	Heat Transfer Disk
23	24	623	591	4	703	645	16	708[4]	683[4]
20	24	592	558	5	694	627	30	694[4]	661[4]
17	24	565	528	10	701	629	600[3]	701/660	659/631
14	24	541	503	20	719	643	600[3]	719/606	671/574
11	24	519	477	43	733	653	600[3]	733/543	679/508

1. The maximum allowable time in the Technical Specification for this condition is equal to 2 hours less than the maximum allowable time shown in this table. This 2-hour reduction allows the handling time required to enter the next stage.
2. The maximum temperatures at the end of the first vacuum (Table 4.4.3-8) are conservatively presented.
3. Duration is defined based on a test time of 30 days for abnormal regimes as described in PNL-4835.
4. Since the time in helium is limited for the 23 kW and 20 kW cases, only the maximum temperatures are listed.

Table 4.4.3-11 Maximum Limiting Component Temperatures in Transient Operations after Helium for BWR Fuel after In-Pool Cooling

Heat Load (kW)	In-Pool (helium)			Helium		
	Duration (hours)	End Temperature (°F)		Duration (hours)	Max. Temp. (°F)[1]	
		Fuel	Heat Transfer Disk		Fuel	Heat Transfer Disk
23	24	489	444	16	708	683
20	24	477	431	30	694	661

1. The maximum temperatures at the end of helium in Table 4.4.3-8 are conservatively used.

Table 4.4.3-12 Maximum Limiting Component Temperatures in Transient Operations after Helium for BWR Fuel after Forced-Air Cooling

Heat Load (kW)	Forced-Air (helium)			Helium		
	Duration (hours)	End Temperature (°F)		Duration (hours)	Max. Temp. (°F)[1]	
		Fuel	Heat Transfer Disk		Fuel	Heat Transfer Disk
23	24	630	598	16	708	683
20	24	601	566	30	694	661

1. The maximum temperatures at the end of helium in Table 4.4.3-8 are conservatively used.

Table 4.4.3-13 Maximum Limiting Component Temperatures in Transient Operations after Helium for PWR Fuel after In-Pool Cooling

Heat Load (kW)	In-Pool (helium)			Helium		
	Duration (hours)	End Temperature (°F)		Duration (hours)	Max. Temp. (°F)[1]	
		Fuel	Heat Transfer Disk		Fuel	Heat Transfer Disk
23	24	489	413	20	724	680

1. The maximum temperatures at the end of helium in Table 4.4.3-5 are conservatively used.

Table 4.4.3-14 Maximum Limiting Component Temperatures in Transient Operations after Helium for PWR Fuel after Forced-Air Cooling

Heat Load (kW)	Forced-Air (helium)			Helium		
	Duration (hours)	End Temperature (°F)		Duration (hours)	Max. Temp. (°F)[1]	
		Fuel	Heat Transfer Disk		Fuel	Heat Transfer Disk
23	24	626	569	20	724	680

1. The maximum temperatures at the end of helium in Table 4.4.3-5 are conservatively used.

4.4.4 Minimum Temperatures

The minimum temperatures of the Vertical Concrete Cask and components occur at -40°F with no heat load. The temperature distribution for this off-normal environmental condition is provided in Section 11.1. At this extreme condition, the component temperatures are above their minimum material limits.

THIS PAGE INTENTIONALLY LEFT BLANK

4.4.5 Maximum Internal Pressures

The maximum internal operating pressures for normal conditions of storage are calculated in the following sections for the PWR and BWR Transportable Storage Canisters.

4.4.5.1 Maximum Internal Pressure for PWR Fuel Canister

The internal pressures within the PWR fuel canister are a function of fuel type, fuel condition (failure fraction), burnup, UMS® canister type, and the backfill gases in the canister cavity. Gases included in the canister pressure evaluation include rod-fill, rod fission and rod backfill gases, canister backfill gases and burnable poison generated gases. Each of the fuel types expected to be loaded into the UMS® canister system is separately evaluated to arrive at a bounding canister pressure.

Fission gases include all fuel material generated gases including long-term actinide decay generated helium. Based on detailed SAS2H calculations of the maximum fissile material mass assemblies in each canister class, the quantity of gas generated by the fuel rods rises as burnup and cool time is increased and enrichment is decreased. To assure the maximum gas is available for release, the PWR inventories are extracted from 60,000 MWD/MTU burnup cases at an enrichment of 1.9 wt. % ^{235}U and a cool time of 40 years. Gas inventories at 60,000 MWD/MTU bound those calculated at 45,000 MWD/MTU, the maximum allowable burnup. Gases included are all krypton, iodine, and xenon isotopes in addition to helium and tritium (^{3}H). Molar quantities for each of the maximum fissile mass assemblies are summarized in Table 4.4.5-1. Fuel generated gases are scaled by fissile mass to arrive at molar contents of other UMS® fuel types.

Fuel rod backfill pressure varies significantly between the PWR fuel types. The maximum reported backfill pressure is listed for the Westinghouse 17×17 fuel assembly at 500 psig. With the exception of the B&W fuel assemblies, which are limited to 435 psig, all fuel assemblies evaluated are set to the maximum 500 psig backfill reported for the Westinghouse assembly. Backfill quantities are based on the free volume between the pellet and the clad and the plenum volume. The fuel rod backfill gas temperature is conservatively assumed to have an initial temperature of 68°F.

Burnable poison rod assemblies (BPRAs) placed within the UMS® storage canister may contribute additional molar gas quantities due to (n,alpha) reactions of fission generated neutrons with ^{10}B during in-core operation. ^{10}B forms the basis of a portion of the neutron poison population. Other neutron poisons, such as gadolinium and erbium, do not produce a significant amount of helium nuclides (alpha particles) as part of their activation chain. Primary BPRAs in existence include Westinghouse Pyrex (borosilicate glass) and WABA (wet annular burnable absorber) configurations, as well as B&W BPRAs and shim rods employed in CE cores. The CE shim rods replace standard fuel rods to form a complete assembly array. The quantity of helium available for release from the BPRAs is directly related to the initial boron content of the rods and the release fraction of gas from the matrix material in question. Release from either of the low temperature, solid matrix materials is likely to be limited, but no release fractions were available in open literature. As such, a 100% release fraction is assumed based on a boron content of 0.0063 g/cm ^{10}B per rod, with the maximum number of rods per assembly. The maximum number of rods is 16 for Westinghouse core 14×14 assemblies, 20 rods for Westinghouse and B&W 15×15 assemblies, and 24 rods for Westinghouse and B&W 17×17 assemblies. The length of the absorber is conservatively taken as the active fuel length. CE core shim rods are modeled at 0.0126 g/cm ^{10}B for 16, 12, and 12 rods applied to CE manufactured 14×14, 15×15 and 16×16 cores, respectively.

The canister backfill gases are conservatively assumed to be at 250°F, which is significantly below the canister shell maximum initial temperature of 304°F at the end of vacuum drying. The initial pressure of the canister backfill gas is 1 atm (0.0 psig). Free volume inside each PWR canister class is listed in Table 4.4.5-2. The listed free volumes do not include fuel assembly components since these components vary for each assembly type and fuel insert. Subtracting out the rod and guide tube volumes and all hardware components arrives at free volume of the canisters including fuel assemblies and a load of 24 BPRAs. For the Westinghouse BPRAs, the Pyrex volume is employed since it displaces more volume than the WABA rods.

The total pressure for each of the UMS® payloads is found by calculating the releasable molar quantity of each gas (30% of the fission gas and 100% of the rod backfill adjusted for the 1% fuel failure fraction), and summing the quantities directly. The quantity of gas is then employed in the ideal gas equation in conjunction with the average gas temperature at normal operating conditions to arrive at system pressures. The normal condition average temperature of the gas within the PWR canister is conservatively considered to be 420°F. This temperature bounds the

calculated gas temperature (418°F) for normal conditions of storage using the three-dimensional canister models. Each of the UMS® PWR fuel types is individually evaluated for normal condition pressure, and sets the maximum normal condition pressure at 4.21 psig. A summary of the maximum pressure in each PWR canister class is shown in Table 4.4.5-3. The table also includes the fuel type producing the listed maximum pressures.

4.4.5.2 Maximum Internal Pressure for BWR Fuel Canister

BWR canister maximum pressures are determined in the same manner as those documented for the PWR canister cases. Primary differences between PWR and BWR analysis include a maximum normal condition average gas temperature of 410°F, rod backfill gas pressures of 132 psig, and limits pressurizing gases to fission gases (including helium actinide decay gas), rod backfill gases, and canister backfill gas. The 132 psig employed in this analysis is significantly higher than the 6 atmosphere maximum pressure reported in open literature. BWR assemblies do not contain an equivalent to the PWR BPRAs and, therefore, do not require ^{10}B helium generated gases to be added. Fissile gas inventories for the maximum fissile material assemblies in each of the three BWR lattices configurations (7×7, 8×8, and 9×9) are shown in Table 4.4.5-4. Free volumes, without fuel components, in UMS® canister classes 4 and 5 are shown in Table 4.4.5-5. Maximum pressures for each canister class are listed in Table 4.4.5-6. The maximum normal condition pressure of 3.97 psig is based on a GE 7×7 assembly, designed for a BWR/2-3 reactor, with gas inventories conservatively taken from a 60,000 MWD/MTU source term. The normal condition pressure for a UMS® storage canister containing the GE 9×9 fuel assembly with 79 fuel rods is 3.96 psig. Similar fuel masses and displaced volume account for similar canister pressures.

Table 4.4.5-1 PWR Per Assembly Fuel Generated Gas Inventory

Array	Assy Type	MTU	Moles
14×14	WE Standard	0.4144	35.52
15×15	B&W	0.4807	41.32
16×16	CE (System 80)	0.4417	38.10
17×17	WE Standard	0.4671	40.18

Table 4.4.5-2 PWR Canister Free Volume (No Fuel or Inserts)

Canister Class	1	2	3
Basket Volume (in^3)	69800	74490	77460
Canister Height (inch)	175.05	184.15	191.75
Canister Free Volume w/o Fuel (liter)	7970	8400	8770

Table 4.4.5-3 PWR Maximum Normal Condition Pressure Summary

Canister Class	Fuel Type	Pressure (psig)
Class 1	WE 17×17 Standard	4.20
Class 2	B&W 17×17 Mark C	4.21
Class 3	CE 16×16 System 80	4.11

Table 4.4.5-4 BWR Per Assembly Fuel Generated Gas Inventory

Array	Assy Type	MTU	Moles
7×7	GE 7×7 (49 Rods)	0.1985	16.78
8×8	GE 8×8 (63 Rods)	0.1880	16.07
9×9	GE 9×9 (79 Rods)	0.1979	16.86

Table 4.4.5-5 BWR Canister Free Volume (No Fuel or Inserts)

Canister Class	4	5
Basket Volume (in^3)	73110	74680
Canister Height (inch)	185.55	190.35
Canister Free Volume w/o Fuel (liter)	8500	8740

Table 4.4.5-6 BWR Maximum Normal Condition Pressure Summary

Canister Class	Fuel Type	Pressure (psig)
Class 4	GE 7×7	3.97
Class 5	GE 9×9	3.96

THIS PAGE INTENTIONALLY LEFT BLANK

4.4.6 Maximum Thermal Stresses

The results of thermal stress calculations for normal conditions of storage are reported in Section 3.4.4.

THIS PAGE INTENTIONALLY LEFT BLANK

4.4.7 Evaluation of System Performance for Normal Conditions of Storage

Results of thermal analysis of the Universal Storage System containing PWR or BWR fuel under normal conditions of storage are summarized in Tables 4.4.3-1 through 4.4.3-4. The maximum PWR and BWR fuel rod cladding temperatures are below the allowable temperatures; temperatures of safety-related components during storage and transfer operations under normal conditions are maintained within their safe operating ranges; and thermally induced stresses in combination with pressure and mechanical load stresses are shown in the structural analysis of Chapter 3.0 to be less than the allowable stresses. Therefore, the Universal Storage System performance meets the requirements for the safe storage of design basis fuel under the normal operating conditions specified in 10 CFR 72.

THIS PAGE INTENTIONALLY LEFT BLANK

4.5 Thermal Evaluation for Site Specific Spent Fuel

This section presents the thermal evaluation of fuel assemblies or configurations, which are unique to specific reactor sites or which differ from the UMS® Storage System design basis fuel. These site specific configurations result from conditions that occurred during reactor operations, participation in research and development programs, and from testing programs intended to improve reactor operations. Site specific fuel includes fuel assemblies that are uniquely designed to accommodate reactor physics, such as axial fuel blanket and variable enrichment assemblies, and fuel that is classified as damaged. Damaged fuel includes fuel rods with cladding that exhibit defects greater than pinhole leaks or hairline cracks.

Site specific fuel assembly configurations are either shown to be bounded by the analysis of the standard design basis fuel assembly configuration of the same type (PWR or BWR), or are shown to be acceptable contents by specific evaluation.

4.5.1 Maine Yankee Site Specific Spent Fuel

The standard spent fuel assembly for the Maine Yankee site is the Combustion Engineering (CE) 14×14 fuel assembly. Fuel of the same design has also been supplied by Westinghouse and by Exxon. The standard 14×14 fuel assembly is included in the population of the design basis PWR fuel assemblies for the UMS® Storage System (See Table 2.1.1-1). The maximum decay heat for the standard Maine Yankee fuel is the design basis heat load for the PWR fuels (23 kW total, or 0.958 kW per assembly). This heat load is bounded by the thermal evaluations in Section 4.4 for the normal conditions of storage, Section 4.4.3.1 for less than design basis heat loads and Chapter 11 for off-normal and accident conditions.

Some Maine Yankee site specific fuel has a burnup greater than 45,000 MWD/MTU, but less than 50,000 MWD/MTU. As shown in Table B2-6 in Appendix B of the Amendment 3 Technical Specifications, loading of fuel assemblies in this burnup range is subject to preferential loading in designated basket positions in the Transportable Storage Canister. Certain fuel assemblies in this burnup range must be loaded in one of the two configurations of the Maine Yankee Fuel Can.

The site specific fuels included in this evaluation are:

1. Consolidated fuel rod lattices consisting of a 17 × 17 lattice fabricated with 17 × 17 grids, 4 stainless steel support rods and stainless steel end fittings. One of these

lattices contains 283 fuel rods and 2 rod position vacancies. The other contains 172 fuel rods, with the remaining rod position locations either empty or containing stainless steel dummy rods.

2. Standard fuel assemblies with a Control Element Assembly (CEA) inserted in each one.
3. Standard fuel assemblies that have been modified by removing damaged fuel rods and replacing them with stainless steel dummy rods, solid zirconium rods, or 1.95 wt % enriched fuel rods.
4. Standard fuel assemblies that have had the burnable poison rods removed and replaced with hollow Zircaloy tubes.
5. Standard fuel assemblies with in-core instrument thimbles stored in the center guide tube.
6. Standard fuel assemblies that are designed with variable enrichment (radial) and axial blankets.
7. Standard fuel assemblies that have some fuel rods removed.
8. Standard fuel assemblies that have damaged fuel rods.
9. Standard fuel assemblies that have some type of damage or physical alteration to the cage (fuel rods are not damaged).
10. Two (2) rod holders, designated CF1 and CA3. CF1 is a lattice having approximately the same dimensions as a standard fuel assembly. It is a 9×9 array of tubes, some of which contain damaged fuel rods. CA3 is a previously used fuel assembly lattice that has had all of the rods removed, and in which damaged fuel rods have been inserted.
11. Standard fuel assemblies that have damaged fuel rods stored in their guide tubes.
12. Standard fuel assemblies with inserted startup sources and other non-fuel items.

The Maine Yankee site specific fuels are also described in Section 1.3.2.1.

The thermal evaluations of these site specific fuels are provided in Section 4.5.1.1. Section 4.5.1.2 presents the evaluation of the Maine Yankee preferential loading of fuel exceeding the design basis heat load (0.958 kW) per assembly on the basket periphery.

4.5.1.1 Thermal Evaluation for Maine Yankee Site Specific Spent Fuel

The maximum heat load per assembly for site specific fuel considered in this section is limited to the design basis heat load (0.958 kW). The evaluation of fuel configurations having a greater heat load is presented in Section 4.5.1.2.

4.5.1.1.1 Consolidated Fuel

There are two (2) consolidated fuel lattices. One lattice contains 283 fuel rods and the other contains 172 fuel rods. Conservatively, only one consolidated fuel lattice is loaded in any Transportable Storage Canister.

The maximum decay heat of the consolidated fuel lattice having 283 fuel rods is 0.279 kW. This heat load is bounded by the design basis PWR fuel assembly, since it is less than one-third of the design basis heat load.

The second consolidated fuel lattice has 172 fuel rods with 76 stainless steel dummy rods at the outer periphery of the lattice. Due to the existence of the stainless steel rods, the effective thermal conductivities of this assembly may be slightly lower than those of the standard CE 14×14 fuel assembly. While the stainless steel rods provide better conductance in the axial direction, the radiation heat transfer is less effective at the surface of stainless steel rods, as compared to the standard fuel rods. The radiation is a function of surface emissivity and the emissivity for stainless steel (0.36) is less than one-half of that for Zircaloy (0.75). A parametric study is performed to demonstrate that the thermal performance of the UMS PWR basket loading configuration consisting of 23 standard CE 14×14 fuel assemblies and the consolidated fuel lattice with stainless rods is bounded by that of the configuration consisting of 24 standard CE 14×14 fuel assemblies. Two finite element models are used in the study: a two-dimensional fuel assembly model and a three-dimensional periodic canister internal model.

The two-dimensional model is used to determine the effective thermal conductivities of the consolidated fuel lattice with stainless steel rods. Considering the symmetry of the consolidated fuel, the finite element model represents a one-quarter section as shown in Figure 4.5.1.1-1. The methodology used in Section 4.4.1.5 for the two-dimensional fuel model for PWR fuel is employed in this model. The model includes the fuel pellets, cladding, helium between the fuel rods, and helium occupying the gap between the fuel pellets and cladding. In addition, the

rods at the two outer layers are modeled as solid stainless steel rods to represent the configuration of this consolidated fuel lattice. Modes of heat transfer modeled include conduction and radiation between individual rods for steady-state condition. ANSYS PLANE55 conduction elements and LINK31 radiation elements are used in the model. Radiation elements are defined between rods and from rods to the boundary of the model. The effective conductivity for the fuel is determined using the procedure described in Section 4.4.1.5.

The three-dimensional periodic canister internal model consists of a periodic section of the canister internals. The model contains one support disk with two heat transfer disks (half thickness) on its top and bottom, the fuel assemblies, the fuel tubes and the helium in the canister, as shown in Figure 4.5.1.1-2. The purpose of this model is to compare the maximum fuel cladding temperatures of the following cases:

1) Base Case: All 24 positions loaded with standard CE 14×14 fuel assemblies.
2) Case 2: 23 positions with standard fuel, with one consolidated fuel lattice in position 2.
3) Case 3: 23 positions with standard fuel, with one consolidated fuel lattice in position 3.
4) Case 4: 23 positions with standard fuel, with one consolidated fuel lattice in position 4.
5) Case 5: 23 positions with standard fuel, with one consolidated fuel lattice in position 5.

Positions 2, 3, 4, and 5 are shown in Figure 4.5.1.1-3. Based on symmetry, these locations represent all of the possible locations for consolidated fuel in the basket.

The fuel assemblies and fuel tubes are represented by homogeneous regions with effective thermal conductivities. The effective conductivities for the consolidated fuel are determined by the two-dimensional fuel assembly model discussed above. The effective conductivities for the CE 14×14 fuel assemblies are established based on the model described in Section 4.4.1.5. Effective properties for the fuel tubes are determined by the two-dimensional fuel tube model in Section 4.4.1.6. Volumetric heat generation corresponding to the design basis heat load of 0.958 kW per assembly is applied to the CE 14×14 fuel regions in the model. Similarly, a heat generation rate corresponding to 0.279 kW is applied to the consolidated fuel assembly region. The heat conduction in the axial direction is conservatively ignored by assuming that the top and

bottom surfaces of the model are adiabatic. A constant temperature of 400°F is applied to the outer surface of the model as boundary conditions. Note that the maximum canister temperature is 351°F for PWR configurations for the normal condition of storage (Table 4.1-4). Steady state thermal analysis is performed for all five cases and the calculated maximum fuel cladding temperatures in the model are:

	Base Case	Case 2	Case 3	Case 4	Case 5
Maximum Fuel Cladding Temperature (°F)	755	733	738	740	740

As shown, the maximum temperatures for Cases 2 through 5 are less than those of the Base Case. It is concluded that the thermal performance of the configuration consisting of 23 standard CE 14×14 fuel assemblies and one consolidated fuel lattice is bounded by that of the configuration consisting of 24 standard CE 14×14 fuel assemblies. This study shows that a consolidated fuel lattice can be located in any basket position. However, as shown in Table B2-6 of Appendix B, the consolidated fuel assembly must be loaded in a corner position of the fuel basket (e.g., Position 5 shown in Figure 4.5.1.1-3).

4.5.1.1.2 Standard CE 14 × 14 Fuel Assemblies with Control Element Assemblies

A Control Element Assembly (CEA) consists of five solid B_4C rods encapsulated in stainless steel tubes. The B_4C material has a conductivity of 1.375 BTU/hr-in-°F. With the CEA inserted into the guide tubes of the CE 14×14 fuel assembly, the effective conductivity in the axial direction of the fuel assembly is increased because solid material replaces helium in the guide tubes. The change in the effective conductivity in the transverse direction of the fuel assembly is negligible since the CEA is inside of the guide tubes. Note that the total heat load, including the small amount of extra heat generated by the CEA, remains below the design basis heat load. Therefore, the thermal performance of the fuel assemblies with CEAs inserted is bounded by that of the standard fuel assemblies.

4.5.1.1.3 Modified Standard Fuel Assemblies

These assemblies include those standard fuel assemblies that have been modified by removing damaged fuel rods and replacing them with stainless steel dummy rods, solid zirconium rods or 1.95 wt % enriched fuel rods.

The maximum number of fuel rods replaced by stainless steel rods is six (6) per assembly, which is about 3% of the total number of fuel rods in each assembly (176). The conductivity of the stainless steel is similar to that of Zircaloy and better than that of the UO_2. The resultant increase in effective conductivity of the modified fuel assembly in the axial direction offsets the decrease in the effective conductivity in the transverse direction (due to slight reduction of radiation heat transfer at the surface of the stainless steel rods). The maximum number of fuel rods replaced by solid Zirconium rods is five (5) per assembly. Since the solid Zirconium rod has a higher conductivity than the fuel rod (UO_2 with Zircaloy clad), the effective conductivity of the repaired fuel assembly is increased. The thermal properties for the enriched fuel rod remain the same as for standard fuel rods, so there is no change in effective conductivity of the fuel assembly results from the use of fuel rods enriched to 1.95 wt % ^{235}U. These rods replace other fuel rods in the assembly after the first or second burnup cycles were completed. Therefore, these replacement fuel rods have been burned a minimum of one cycle less than the remainder of the assembly, producing a proportionally lower per rod heat load. The heat load (on a per rod basis) of the fuel rods in a standard assembly, bounds the heat load of the 1.95 wt % ^{235}U enriched fuel rods. Consequently, the loading of modified fuel assemblies is bounded by the thermal evaluation of the standard fuel assembly.

4.5.1.1.4 Use of Hollow Zircaloy Tubes

Certain standard fuel assemblies have had the burnable poison rods removed. These rods were replaced with hollow Zircaloy tubes.

There are 16 locations where burnable poison rods were removed and hollow Zircaloy tubes were installed in their place. Since the maximum heat load for these assemblies is 0.552 kW per assembly (less than two-thirds of the design basis heat load) and the number of hollow Zircaloy rods is only about one-tenth (16/176) of the total number of the fuel rods, the thermal performance of these fuel assemblies is bounded by that of the standard fuel assemblies.

4.5.1.1.5 Standard Fuel with In-core Instrument Thimbles

Certain fuel assemblies have in-core instrument thimbles stored within the center guide tube of each fuel assembly. Storing an in-core instrument thimble assembly in the center guide tube of a fuel assembly will slightly increase the axial conductance of the fuel assembly (helium replaced by solid material). Therefore, there is no negative impact on the thermal performance of the fuel

assembly with this configuration. The thermal performance of these fuel assemblies is bounded by that of the standard fuel assemblies.

4.5.1.1.6 Standard Fuel Assemblies with Variable Enrichment and Axial Blankets

The Maine Yankee variably enriched fuel assemblies are limited to two batches of fuel, which have a maximum burnup less than 30,000 MWD/MTU. The variably enriched rods in the fuel assemblies have enrichments greater than 3.4 wt % ^{235}U, except that the axial blankets on one batch are enriched to 2.6 wt % ^{235}U. As shown in Table B2-8 of Appendix B, fuel at burnups less than or equal to 30,000 MWD/MTU with any enrichment greater than, or equal to, 1.9 wt % ^{235}U may be loaded with 5 years cool time.

The thermal conductivities of the fuel assemblies with variable enrichment (radial) and axial blankets are considered to be essentially the same as those of the standard fuel assemblies. Since the heat load per assembly is limited to the design basis heat load, there is no effect on the thermal performance of the system due to this loading configuration.

4.5.1.1.7 Standard Fuel Assemblies with Removed Fuel Rods

Except for assembly number EF0046, the maximum number of missing fuel rods from a standard fuel assembly is 14, or 8% (14/176) of the total number of rods in one fuel assembly. The maximum heat load for any one of these fuel assemblies is conservatively determined to be 0.63 kW. This heat load is 34% less than the design basis heat load of 0.958 kW. Fuel assembly EF0046 was used in the consolidated fuel demonstration program and has only 69 rods remaining in its lattice. This fuel assembly has a heat load of 70 watts, or 7% of the design basis heat load of 0.958 kW. Therefore, the thermal performance of fuel assemblies with removed fuel rods is bounded by that of the standard fuel assemblies.

4.5.1.1.8 Fuel Assemblies with Damaged Fuel Rods

Damaged fuel assemblies are standard fuel assemblies with fuel rods with known or suspected cladding defects greater than hairline cracks or pinhole leaks. Fuel, classified as damaged, will be placed in one of the two configurations of the Maine Yankee Fuel Can. The primary function of the fuel can is to confine fuel material within the can and to facilitate handling and retrievability. The Maine Yankee fuel can is shown in Drawings 412-501 and 412-502. The placement of the loaded fuel cans is restricted by the operating procedures and/or Technical

Specifications to loading into the four corner positions at the periphery of the fuel basket as shown in Figure B2-1. The heat load for each damaged fuel assembly is considered to be the design basis heat load of 0.958 kW (23 kW/24).

A steady-state thermal analysis is performed using the three-dimensional canister model described in Section 4.4.1.2 simulating 100% failure of the fuel rods, fuel cladding, and guide tubes of the damaged fuel held in the Maine Yankee fuel can. The canister is assumed to contain twenty (20) design basis PWR fuel assemblies and damaged fuel assemblies in fuel cans in each of the four corner positions.

Two debris compaction levels are considered for the 100% failure condition: (Case 1) 100% compaction of the fuel rod, fuel cladding, and guide tube debris resulting in a 52-inch debris level in the bottom of each fuel can, and (Case 2) 50% compaction of the fuel rod, fuel cladding, and guide tube debris resulting in a 104-inch debris level in the bottom of each fuel can. The entire heat generation rate for a single fuel assembly (i.e., 0.958 kW) is concentrated in the debris region with the remainder of the active fuel region having no heat generation rate applied. To ensure the analysis is bounding, the debris region is located at the lower part of the active fuel region in lieu of the bottom of the fuel can. This location is closer to the center of the basket where the maximum fuel cladding temperature occurs. The effective thermal conductivities for the design basis PWR fuel assembly (Section 4.4.1.5) are used for the debris region. This is conservative since the debris (100% failed rods) is expected to have higher density (better conduction) and more surface area (better radiation) than an intact fuel assembly. In addition, the thermal conductivity of helium is used for the remainder of the active fuel length. Boundary conditions corresponding to the normal condition of storage are used at the outer surface of the canister model (see Section 4.4.1.2). A steady-state thermal analysis is performed. The results of the thermal analyses performed for 100% fuel rod, fuel cladding, and guide tube failure are:

Description	Maximum Temperature (°F)			
	Fuel Cladding	Damaged Fuel	Support Disk	Heat Transfer Disk
Case 1 (100% Compaction)	654	672	598	594
Case 2 (50% Compaction)	674	594	620	616
Design Basis PWR Fuel	670	N/A	615	612
Allowable	752	N/A	650	650

As demonstrated, the extreme case of 100% fuel rod, fuel cladding, and guide tube failure with 50% compaction of the debris results in temperatures that are less than 1% higher than those calculated for the design basis PWR fuel. The maximum temperatures for the fuel cladding, damaged fuel assembly, support disks, and heat transfer disks remain within the allowable temperature range for both 100% failure cases. Additionally, the temperatures used in the structural analyses of the fuel basket envelop those calculated for both 100% failure cases.

Additionally, the above analysis has been repeated to consider a maximum heat load of 1.05 kW/assembly (see Section 4.5.1.2) in the Maine Yankee fuel cans. To maintain the 23 kW total heat load per canister, the model considers a heat load of 1.05 kW/assembly in the four (4) Maine Yankee fuel cans and 0.94 kW/assembly in the rest of the twenty (20) basket locations. The analysis results indicate that the maximum temperatures for the fuel cladding and basket components are slightly lower than those for the case with a heat load of 0.958 kW in the damaged fuel can, as presented above. The maximum fuel cladding temperature is 650°F (< 654°F) and 672°F (< 674°F) for 100% and 50% compaction ratio cases, respectively. Therefore, the case with 1.05 kW/assembly in the Maine Yankee fuel can is bounded by the case with 0.958 kW/assembly in the fuel cans.

4.5.1.1.9 Standard Fuel Assemblies with Damaged Lattice

Certain standard fuel assemblies may have damage or physical alteration to the lattice or cage that holds the fuel rods, but not exhibit damage to the fuel rods. Fuel assemblies with lattice damage are evaluated in Section 11.2.15. The structural analysis demonstrates that these assemblies retain their configuration in the design basis accident events and loading conditions.

The effective thermal conductivity for the fuel assembly used in the thermal analyses in Section 4.4 is determined by the two-dimensional fuel model (Section 4.4.1.5). The model conservatively ignores the conductance of the steel cage of the fuel assembly. Therefore, damage or physical alteration to the cage has no effect on the thermal conductivity of the fuel assembly used in the thermal models. The thermal performance of these fuel assemblies is bounded by that of the standard fuel assemblies.

4.5.1.1.10 Damaged Fuel Rod Holders

The Maine Yankee site specific fuel inventory includes two (2) damaged fuel rod holders designated CF1 and CA3. CF1 is a 9×9 array of tubes having roughly the same dimensions as a fuel assembly. Some of the tubes hold damaged fuel rods. CA3 is a previously used fuel assembly cage (i.e., a fuel assembly with all of the fuel rods removed), into which damaged fuel rods have been inserted.

Similar to the fuel assemblies that have damaged fuel rods, the damaged fuel rod holders will be placed in one of the two configurations of the Maine Yankee Fuel Can and their location in the basket is restricted to one of the four corner fuel tube positions of the basket. The decay heat generated by the fuel in each of these rod holders is less than one-fourth of the design basis heat load of 0.958 kW. Therefore, the thermal performance of the damaged fuel rod holders is bounded by that of the standard fuel assemblies.

4.5.1.1.11 Assemblies with Damaged Fuel Rods Inserted in Guide Tubes

Similar to fuel assemblies that have damaged fuel rods, fuel assemblies that have up to two damaged fuel rods or poison rods stored in each guide tube are placed in one of the two configurations of the Maine Yankee Fuel Can and their loading positions are restricted to the four corner fuel tubes in the basket. The rods inserted in the guide tubes can not be from a different fuel assembly (i.e., any rod in a guide tube originally occupied a rod position in the same fuel assembly). Storing fuel rods in the guide tubes of a fuel assembly slightly increases the axial conductance of the fuel assembly (helium replaced by solid material). The design basis heat load bounds the heat load for these assemblies. Therefore, the thermal performance of fuel assemblies with rods inserted in the guide tubes is bounded by that of the standard fuel assemblies.

4.5.1.1.12 Standard Fuel Assemblies with Inserted Start-up Sources and Other Non-Fuel Items

Five Control Element Assembly (CEA) fingertips and a 24-inch ICI segment may be placed into the guide tubes of a fuel assembly. In addition, four irradiated start-up neutron sources and one unirradiated source, having a combined total heat load of 15.4 watts, will be loaded into separate fuel assemblies. With the CEA fingertips and the neutron sources inserted into the guide tubes of the fuel assemblies, the effective conductivity in the axial direction of the fuel assembly is increased because solid material replaces helium in the guide tubes. The change in the effective

conductivity in the transverse direction of the fuel assembly is negligible, since the non-fuel items are inside of the guide tubes. In addition, the fuel assemblies that hold these non-fuel items are restricted to basket corner loading locations, which have an insignificant effect on the maximum fuel cladding and basket component temperatures at the center of the basket.

Note that the total heat load of the fuel assembly, including the small amount of extra heat generated by the CEA fingertips, ICI 24-inch segment, and the neutron sources, remains below the design basis heat load. Therefore, the thermal performance of the fuel assemblies with these non-fuel items inserted is bounded by that of the standard fuel assemblies.

Figure 4.5.1.1-1 Quarter Symmetry Model for Maine Yankee Consolidated Fuel

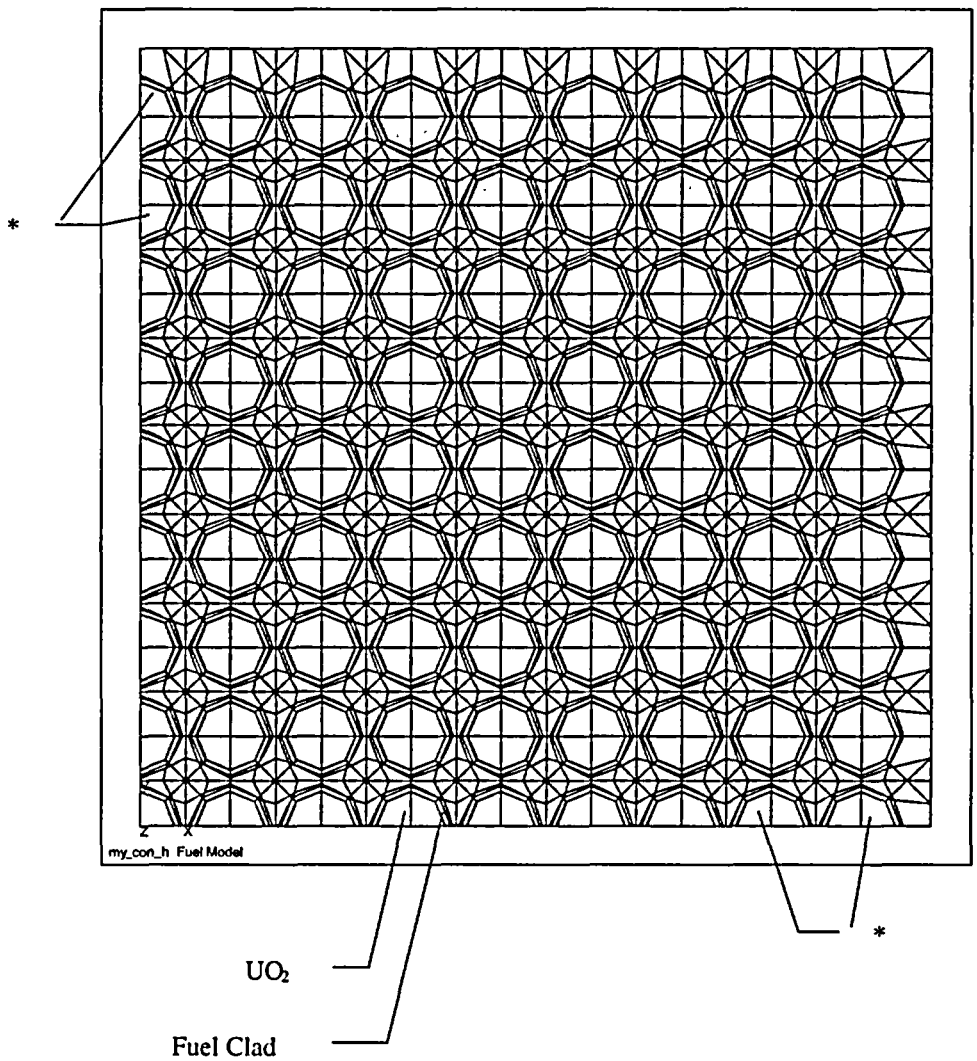

* Two outer layers (rows) of rods are modeled as stainless steel

Figure 4.5.1.1-2 Maine Yankee Three-Dimensional Periodic Canister Internal Model

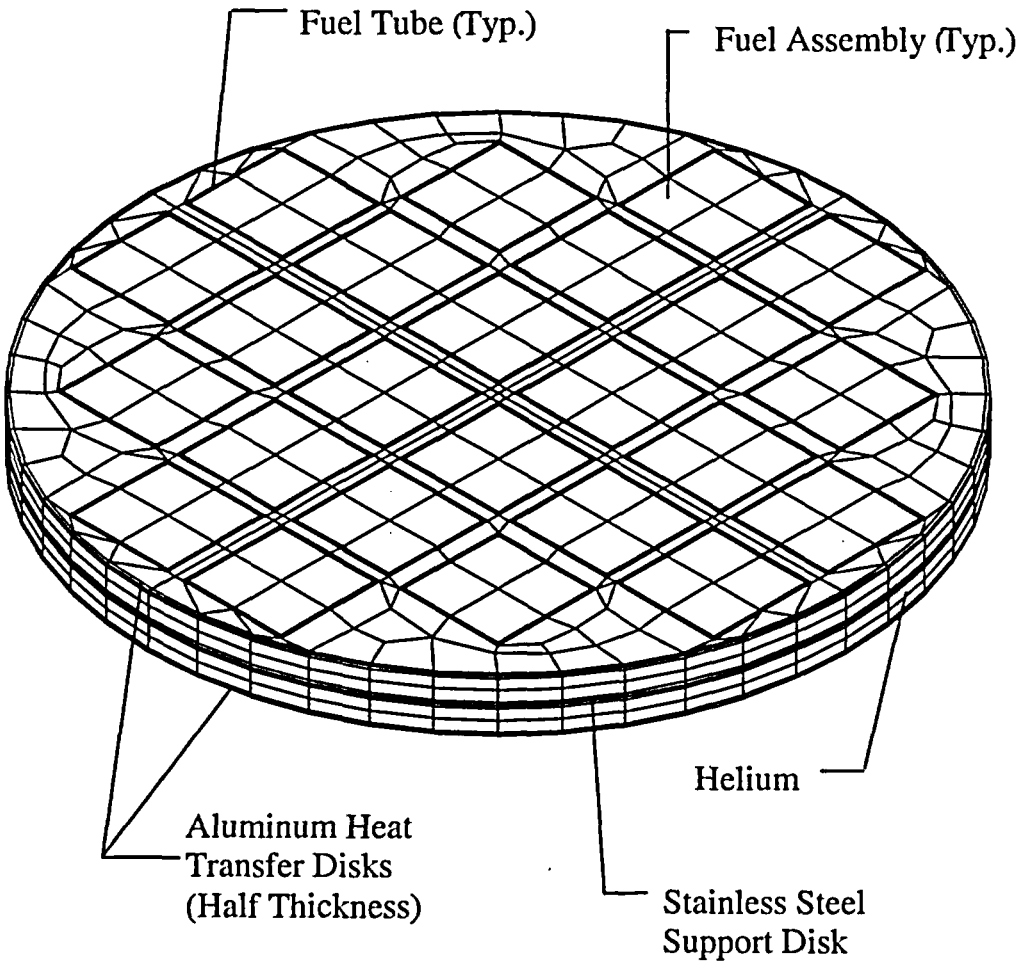

Figure 4.5.1.1-3 Evaluated Locations for the Maine Yankee Consolidated Fuel Lattice in the PWR Fuel Basket

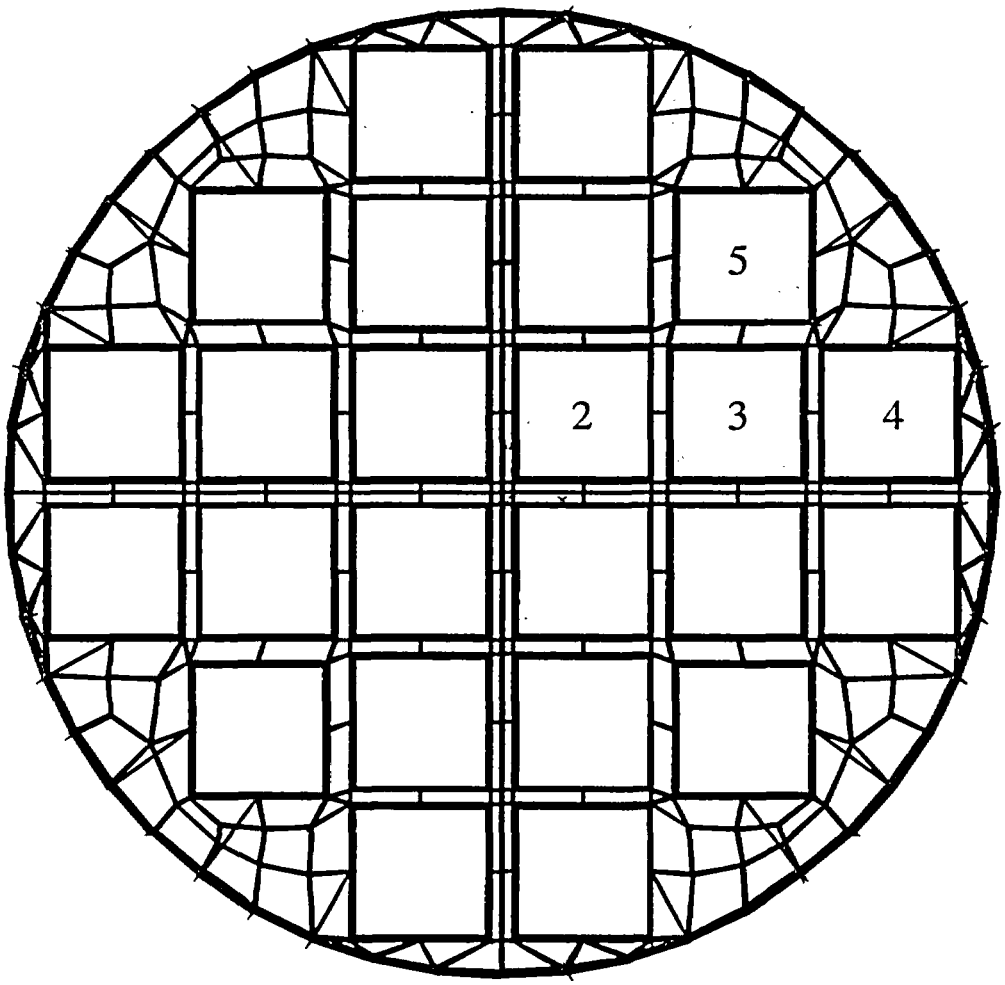

Figure 4.5.1.1-4 Active Fuel Region in the Three-Dimensional Canister Model

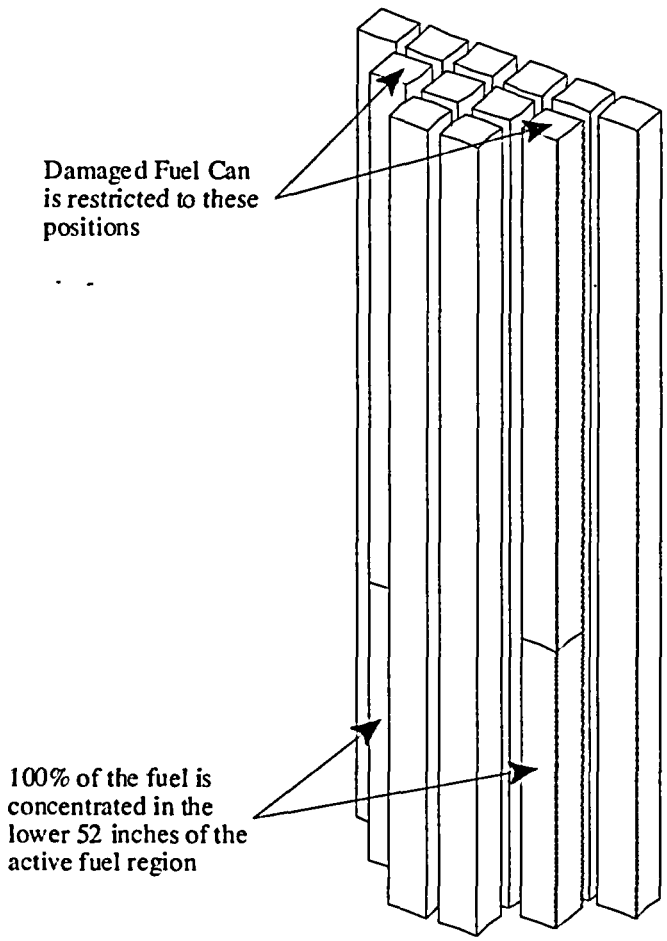

Note: Finite element mesh not shown for clarity.

Figure 4.5.1.1-5 Fuel Debris and Damaged Fuel Regions in the Three-Dimensional Canister Model

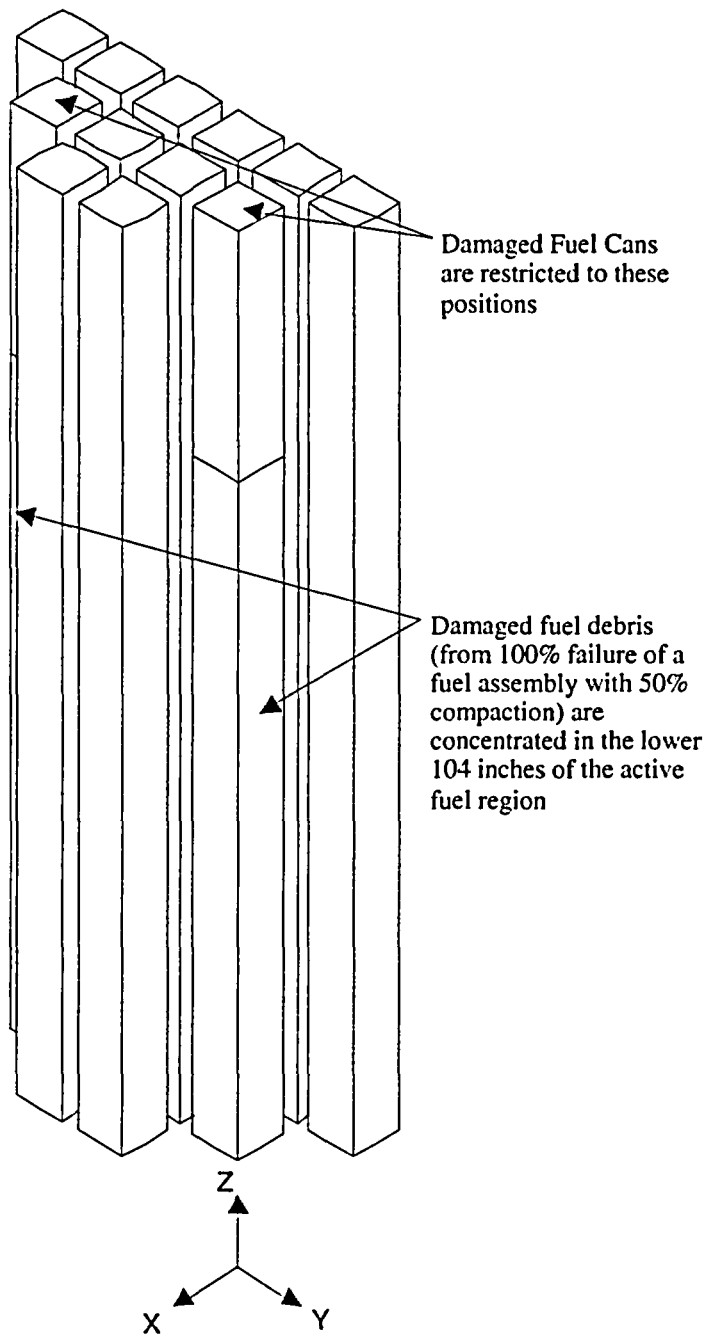

4.5.1.2 Preferential Loading with Higher Heat Load (1.05 kW) at the Basket Periphery

The Maine Yankee fuel inventory includes fuel assemblies that will exceed the initial per assembly heat load of 0.958 kW. To enable loading of these assemblies into the storage cask, a higher peripheral heat load is evaluated. The maximum heat load for peripheral assemblies is set at 1.05 kW. The maximum basket heat load for this configuration remains restricted to 23 kW.

To ensure that these fuel assemblies do not exceed their allowable cladding temperatures, a loading pattern is shown that places higher heat load assemblies at the periphery of the basket (Positions "A" in Figure 4.5.1.2-1) and compensates by placing lower heat load assemblies in the basket interior positions (Positions "B" in Figure 4.5.1.2-1). There are 12 interior basket locations and 12 peripheral basket locations in the UMS® PWR basket design. The maximum total basket heat load of 23 kW is maintained for these peripheral loading scenarios.

Given the higher than design basis heat load in peripheral basket locations, an evaluation is performed to assure that maximum cladding temperature does not exceed the allowable temperature of 400°C (752°F) per ISG-11, Revision 2 [38].

A parametric study is performed using the three-dimensional periodic model, as described in Section 4.5.1.1 (Figure 4.5.1.1-2), to demonstrate that placing a higher heat load in the peripheral locations does not result in heating of the fuel assemblies in the interior locations beyond that found in the uniform heat loading case. The side surface of the model is assumed to have a uniform temperature of 350°F.

Two cases are considered (total heat load per cask = 20 kW for both cases):

1. Uniform loading: Heat load = 0.833 (20/24) kW per assembly for all 24 assemblies
2. Non-uniform loading:
   Heat load = 0.958 (23/24) kW per assembly for 12 peripheral assemblies
   Heat load = 0.708 (17/24) kW per assembly for 12 interior assemblies

The analysis results (maximum temperatures) are:

	Case 1 Uniform Loading (°F)	Case 2 Non-Uniform Loading (°F)
Fuel (Location 1)	675	648
Fuel (Locations 2 & 4)	632	611
Fuel (Location 5)	577	588
Fuel (Locations 3 & 6)	563	576
Basket	611	592

Locations are shown in Figure 4.5.1.2-1.

The maximum fuel cladding temperature for Case 2 (non-uniform loading pattern) is well below that for Case 1 (uniform loading pattern). The comparison shows that placing hotter fuel in the peripheral locations of the basket and cooler fuel in the interior locations (while maintaining the same total heat load per basket) reduces the maximum fuel cladding temperature (which occurs in the interior assembly), as well as the maximum basket temperature.

Based on the parametric study (uniform versus non-uniform analysis) of the 20 kW basket, a 15% redistribution of heat load resulted in a maximum increase of 13°F (576-563=13) in a peripheral basket location. Changing the basket peripheral location heat load from 0.958 kW maximum to 1.05 kW is a less than 10% redistribution for the 23 kW maximum basket heat load. The highest temperature of a peripheral basket location may, therefore, be estimated by adding 13°F to 566°F (maximum temperature in peripheral assemblies for the 23 kW basket with uniform heat load distribution). The 579°F (304°C) temperature is well below the allowable cladding temperature of 400°C .

Therefore, the maximum fuel cladding temperature for the preferential loading configuration with the higher heat load of 1.05 kW at the periphery basket locations will not exceed the allowable fuel cladding temperature.

Figure 4.5.1.2-1 Canister Basket Preferential Loading Plan

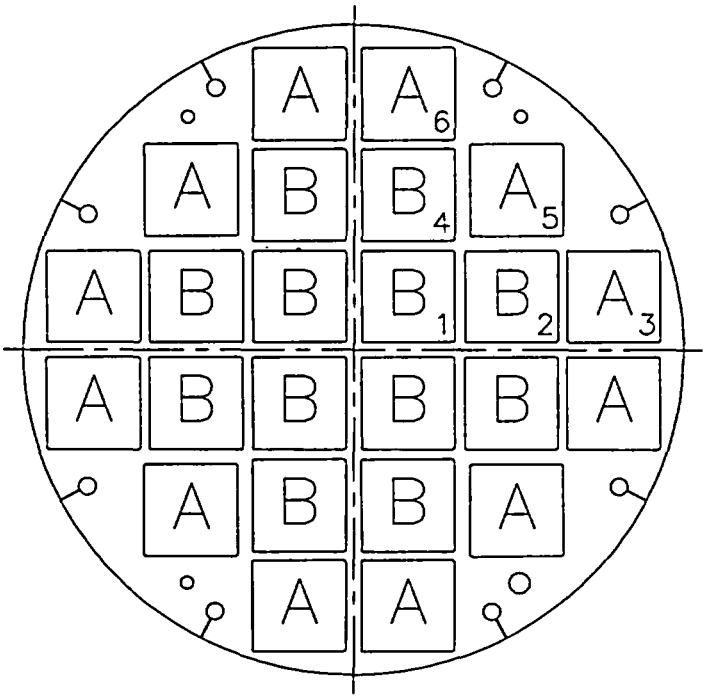

"A" indicates peripheral locations.

"B" indicates interior locations.

Numbered locations indicate positions where maximum fuel temperatures are presented.

THIS PAGE INTENTIONALLY LEFT BLANK

4.6 References

1. Code of Federal Regulations, "Licensing Requirements for the Independent Storage of Spent Nuclear Fuel and High Level Radioactive Waste," Part 72, Title 10, January 1996.

2. PNL-4835, Johnson, A.B., and Gilbert, E.R., "Technical Basis for Storage of Zircaloy-Clad Fuel in Inert Gases," 1985.

3. PNL-4555, "Results of Simulated Abnormal Heating Events for Full-Length Nuclear Fuel Rods," Gwenther, R.J., Pacific Northwest Laboratories, 1983.

4. ACI-349-85, American Concrete Institute, "Code Requirement for Nuclear Safety Related Concrete Structures and Commentary."

5. PNL-6189, Levy, et al., Pacific Northwest Laboratory, "Recommended Temperature Limits for Dry Storage of Spent Light-Water Zircalloy Clad Fuel Rods in Inert Gas," May 1987.

6. ANSYS Revision 5.2 and ANSYS Revision 5.5, Computer Program, ANSYS, Inc., Houston, PA.

7. MIL-HDBK-5G, Military Handbook, "Metallic Materials and Elements for Aerospace Vehicle Structures," U.S. Department of Defense, November 1994.

8. Genden Engineering Services & Construction Company, NS-4-FR Fire Resistant Neutron and/or Gamma Shielding Material - Product Technical Data.

9. Baumeister T. and Mark, L.S., Standard Handbook for Mechanical Engineers, 7th Edition, New York, McGraw-Hill Book Co., 1967.

10. The American Society of Mechanical Engineers, "ASME Boiler and Pressure Vessel Code," 1995, with 1995 Addenda.

11. ARMCO Product Data Bulletin No. S-22, "17-4PH, Precipitation Hardening Stainless Steel," ARMCO, Inc., 1988.

12. The American Society of Mechanical Engineers, "ASME Boiler and Pressure Vessel Code, Code Cases - Boilers and Pressure Vessels," Code Case N-71-17, 1996.

13. The American Society of Mechanical Engineers, "ASME Boiler and Pressure Vessel Code, Section II, Part D - Properties," 1995 Edition with 1995 Addenda.

14. Hanford Engineering Development Laboratory, "Nuclear Systems Materials Handbook," Volume 1, Design Data, Westinghouse Hanford Company, TID26666.

15. Bucholz, J.A., "Scoping Design Analyses for Optimized Shipping Casks Containing 1, 2-, 3-, 5-, 7-, or 10-Year-Old Spent Fuel, Oak Ridge National Library," ORNL/CSD/TM-149, 1983.

16. Ross R. B., "Metallic Specification Handbook," 4th Edition, London, Chapman and Hall, 1992.

17. Kreith, F., and Bohn, M. S., "Principles of Heat Transfer," 5th Edition, West Publishing Company, 1993.

18. Edwards, "TRUMP, A Computer Program for Transient and Steady State Temperature Distributions in Multimensional Systems," Lawrence Radiation Laboratory, Livermore, Rept, UCLR-14754, Rev. 1, May 1968.

19. Kreith, F., "Principles of Heat Transfer," 3rd Edition, New York, Intext Educational Publishers.

20. Vargaftik, Natan B., et al., "Handbook of Thermal Conductivity of Liquids and Gases," CRC Press, October 1993.

21. Chapman, A.J., "Heat Transfer," 4th Edition, MacMillan Publishing Company, New York, 1987.

22. Hagrman, D.L., Reymann, G.A., "Matpro-Version 11 A Handbook of Material Properties for Use in the Analysis of Light Water Reactor Rod Behavior," Idaho Falls, ID, EG&G Idaho, Inc., 1979.

23. Rust, J.H., "Nuclear Power Plant Engineering," Atlanta, GA, S.W., Holland Company, 1979.

24. AAR BORAL Sheet Manufacturers Data, Sheet Product Performance Report 624, Brooks & Perkins Advanced Structures Company, 1983.

25. AAR Standard Specification Sheet for BORAL™ Composite Sheet, Brooks & Perkins Advances Structures Company, BRJREVO-940107.

26. Fintel, M., "Handbook of Concrete Engineering," 2nd Edition, Van Nostrand Reinhold Co., New York.

27. ASTM C150-95a, American Society for Testing and Materials, "Standard Specification for Portland Cement."

28. Siegel, R., and Howell, J. R., "Thermal Radiation Heat Transfer," 3rd Edition, Hemisphere Publishing Co., 1992.

29. Incropera, E. P., and DeWitt, D. P., "Fundamentals of Heat and Mass Transfer," 4th Edition, 1996.

30. SAND90-2406, Sanders, T.L., et al., "A Method for Determining the Spent-Fuel Contribution to Transport Cask Containment Requirements," TTC-1019, UC-820, November 1992.

31. Olander, D. R., "Fundamental Aspects of Nuclear Reactors Fuel Elements," Technical Information Center (U. S. Department of Energy), 1985.

32. Kreith, F., "Principles of Heat Transfer," 2nd Edition, 1965.

33. PNL-6364, "Control of Degradation of Spent LWR Fuel During Dry Storage in an Inert Atmosphere," Pacific Northwest Laboratory, Richland, Washington, October 1987.

34. PNL-4835, "Technical Basis for Storage of Zircaloy-Cladding Spent Fuel in Inert Gas," September 1983.

35. Regulatory Guide 1.25, "Assumptions Used for Evaluating the Potential Radiological Consequences of a Fuel Handling Accident in the Fuel Handling and Storage Facility for Boiling and Pressurized Water Reactors (Safety Guide 25)," March 1972.

36. Pati, S.R., Garde, A. M., Clink, L.J., "Contribution of Pellet Rim Porosity to Low-Temperature Fission Gas Release at Extended Burnups," American Nuclear Society Topical Meeting on LWR Fuel Performance, April 17-20, 1988, Williamsburg, VA.

37. NET 152-03, "METAMIC Qualification Program for Nuclear Fuel Storage Applications – Final Test Results," Revision 0, Northeast Technology Corporation, September 2001.

38. Nuclear Regulatory Commission, "Cladding Considerations for Transportation and Storage of Spent Fuel," Interim Staff Guidance – 11, Revision 2.